Lecture Notes on Biodiversity

Thierry Roncalli

Université Paris-Saclay

Table of Contents

Abbreviations

AQI Air quality index.

BII Biodiversity intactness index.
BMI Body mass index.

CBD Convention on biological diversity.
CICES Common international classification of ecosystem services.
CITES Convention on international trade in endangered species of wild fauna and flora.
COP Conference of the parties.
CRF Concentration-response function.
CSR Corporate social responsibility.

DALY Disability-adjusted life years.
DEC Dietary energy consumption.
DNSH Do no significant harm.

EAR Endemics-area relationship.
EEA European environment agency.
ENCORE Exploring natural capital opportunities, risks and exposure.
EPA Environmental protection agency.
ESG Environmental, social and governance.

FAO Food and agriculture organization.
FSB Financial stability board.

GBF Kunming-Montreal global biodiversity framework.
GMO Genetically modified organism.

IAS Invasive alien species.
IASB International accounting standards board.
IBAT Integrated Biodiversity Assessment Tool.
IEA International energy agency.
IFRS International financial reporting standards.
IPBES Intergovernmental science-policy platform on biodiversity and ecosystem services.
IPCC Intergovernmental panel on climate change.
ISSB International sustainabilityÂăstandards board.
IUCN International union for conservation of nature.

LCA Life cycle assessment.
LPI Living planet index.
LULUCF Land use, land-use change, and forestry.

MDER Minimum dietary energy requirement.
MSA Mean species abundance.
MSY Maximum sustainable yield.

NCAVES Natural capital accounting and valuation of ecosystem services.
NGFS Network of central banks and supervisors for greening the financial system.
NGO Non-governmental organization.

OECD Organisation for economic cooperation and development.
OPS One planet summit.

PDF Potentially disappeared fraction.
PM Particulate matter.
POP Persistent organic pollutant.
PRI Principles for responsible investment.

QALE Quality-adjusted life expectancy.
QALY Quality-adjusted life year.

RLI Red list index.

SAC Species accumulation curve.
SAD Species abundance distribution.
SAR Species-area relationship.
SDG Sustainable development goal.
SEEA System of environmental-economic accounting.
STAR Species Threat Abatement and Restoration metric.

TCFD Task force on climate-related financial disclosures.
TEEB The economics of ecosystems and biodiversity.
TIB Theory of island biogeography.
TNFD Task force on nature-related financial disclosures.

UNDP United Nations development programme.
UNEP United Nations environment programme.

UNEP FI United Nations environment programme finance initiative.

UNFCCC UN framework convention on climate change.

VOLY Value of life year.

VSL Value of a statistical life.

VSLY Value per statistical life year.

WDPA World Database on Protected Areas.

WEF World economic forum.

WHO World health organization.

WRI World resources institute.

YLD Years lived with disability.

YLL Years of life lost.

Abstract

These lecture notes are part of the Handbook of Sustainable Finance (Roncalli, 2025). They provide the basics of biodiversity for students and professionals who want to understand this topic and the key challenges of biodiversity investing. The first three sections cover the definition of biodiversity, ecosystem functions and services, and threats to biodiversity. These correspond to material typically taught in conservation biology courses. The fourth section focuses on measuring biodiversity. Finally, the last two sections cover biodiversity governance and regulation, and biodiversity investment approaches.

In these lecture notes, we will learn that biodiversity goes far beyond the issues of species extinction and deforestation. In fact, it is much broader and includes fisheries, food security, health issues, invasive species, natural resources, pollution, and water stress, among others. However, most measures of biodiversity focus primarily on species richness, abundance, or extinction. From a financial perspective, this is unsatisfactory, and biodiversity finance requires more sophisticated metrics. In addition, new regulations and frameworks are pushing investors to become actively involved in biodiversity restoration. The concept of double materiality also underscores the importance of biodiversity to companies and implies some hidden risks in financial assets because they impact or can be impacted by biodiversity loss. Despite growing awareness, long-term investors are not yet fully equipped to integrate biodiversity risks into their investment decisions. While progress is being made, there is still a long way to go in developing robust methodologies that can effectively integrate biodiversity into sustainable investment strategies.

Keywords: Biodiversity, species, ecosystem, natural capital, pollination, food security, habitat degradation, invasive species, pollution, overexploitation, biodiversity measurement, Convention on Biodiversity, TNFD, mitigation hierarchy.

JEL Classification: Q, O1, I1, G11.

Acknowledgement

Introduction

Biodiversity has become an important issue in the ESG financial community in recent years. For example, the SFDR's mandatory principal adverse impact indicator on biodiversity (PAI 7) requires companies to disclose activities that negatively impact biodiversity sensitive areas[1], the sixth economic objective of the EU green taxonomy is the protection and restoration of biodiversity and ecosystems[2] while the ESRS E4 category of the CSRD is named biodiversity and ecosystems[3]. In this context, where biodiversity is an important issue in sustainable finance regulations, it was obvious that investors wanted to develop biodiversity products or manage investments with respect to biodiversity risks and they have done so. And this is certainly just the beginning. When we talk about biodiversity, the two words that come to mind are risk and impact. It's easy to take the shortcut that an investment that takes biodiversity into account is an investment with impact, but does that mean it falls into the category of impact investing? Generally not, because there is a significant difference between investing in assets that carry biodiversity risks and investing with the goal of having a positive impact on biodiversity. To understand this distinction between investing with impact and investing for impact, it is important to first define what biodiversity really means[4].

Box 1: Edward O. Wilson

Edward O. Wilson (1929–2021) was a renowned American biologist, naturalist, ecologist, and entomologist. He is widely regarded as one of the greatest natural scientists of our time and is often referred to as the father of biodiversity. He received his B.S. and M.S. in biology from the University of Alabama and his Ph.D. in biology from Harvard University in 1955. The author of more than 400 scientific articles from 1950 to 2005, he has written numerous influential books, including *The Theory of Island Biogeography* (1967), *Sociobiology* (1975), *On Human Nature* (1979), and *The Diversity of Life* (1992), which have had a profound impact on the fields of biology and ecology. In 1988, he co-edited the first book on biodiversity with Frances Peter.

Figure 5.B: Cover of the book *Tales from the Ant World*

---
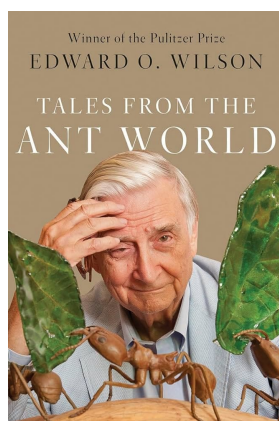
[1]See Roncalli (2025, Section 1.4.3, page 36 & Table 1.8, 38).

[2]See Roncalli (2025, Section 1.4.1, page 33).

[3]See Roncalli (2025, Section 1.4.5, page 39).

[4]This section is based on the textbook *Biodiversity: An Introduction* written by Kevin Gaston and John Spicer and the scientific book *Conservation Biology for All* edited by Navjot Sodhi and Paul Ehrlich. *Essentials of Conservation Biology* by Richard Primack is another reference book, but it is more advanced and technical.

1 Definition

Biodiversity, or biological diversity, refers to the variety and variability of life on Earth in all its many manifestations. According to Gaston and Spicer (2004), it is a broad, unifying concept that encompasses all forms, levels, and combinations of natural variation at all levels of biological organization. For example, it includes genetic diversity within species, the diversity of species in different habitats, and the diversity of ecosystems themselves. In other words, biodiversity encompasses all living organisms, from the smallest bacteria to the largest mammals, and the complex relationships and interactions among them. In addition, biodiversity is essential to the health of ecosystems, providing critical services such as air and water purification, crop pollination, climate regulation and food production.

Remark 1 *In the scientific world, biodiversity is generally associated with conservation biology, the scientific discipline dedicated to understanding and preserving biodiversity and protecting ecosystems. This field emerged in response to the rapid loss of biodiversity due to human activities such as habitat destruction, pollution, and climate change. Biodiversity and conservation biology are therefore closely related, which is why many master's programs use both the term biodiversity and conservation biology.*

1.1 Key components of biodiversity

There are several ways to assess and measure biodiversity. In general, we consider three building blocks:

1. Genetic diversity
   This refers to the variety of genes within a species, such as different varieties of rice. Genetic diversity is essential for the survival and adaptability of species, allowing them to evolve in response to changing conditions.

2. Organismal (or species) diversity
   This refers to the variety of species in a given area or ecosystem. It includes the number of different species (species richness), the relative abundance of each species (species evenness), and variation in the distribution of species in space (beta diversity or species density). A greater number of species indicates greater biodiversity and generally contributes to more resilient ecosystems that are able to maintain their functionality after environmental changes.

3. Ecological (or ecosystem) diversity
   This refers to the variety of ecosystems in a region, including different habitats, biological communities, and ecological processes. Ecosystem diversity includes forests, grasslands, wetlands, deserts, marine environments, etc. This element is essential for maintaining the range of ecological processes that support life, such as nutrient cycling, energy flow, and climate regulation.

In Table 2 we reproduce the different elements of the three building blocks, which are organized in nested hierarchies with higher and lower order elements (Gaston, 2010, pages 27-32). Some elements are specific to a given building block, *e.g.*, nucleotides belong to the genetic diversity cluster, while other elements may be shared by two or three building blocks, *e.g.*, individuals belong to both the genetic diversity and species diversity clusters. In addition to these three building blocks, we can consider other dimensions of biodiversity, such as functional diversity[5] or temporal diversity[6].

---

[5]Functional diversity refers to the range of different functions or roles that species play within an ecosystem.

[6]Temporal diversity refers to changes in biodiversity over time, including seasonal variations, successional changes in ecosystems, and long-term evolutionary processes.

Table 1: Elements of biodiversity

Ecological diversity	Genetic diversity	Organismal diversity
Biogeographic realms		Domains or Kingdoms
Biomes		Phyla
Provinces		Families
Ecoregions		Genera
Ecosystems		Species
Habitats		Subspecies
Populations	Populations	Populations
	Individuals	Individuals
	Chromosomes	
	Genes	
	Nucleotides	

Source: Heywood (1995) & Gaston (2010, Table 2.1, page 27).

1.1.1 Genetic diversity

Genetic (or genomic) diversity can be assessed at different structural levels: nucleotides, genes, or chromosomes. Thus, we can measure genetic diversity by nucleotide[7] differences, allelic diversity (average number of alleles per locus), gene diversity or polymorphism (proportion of polymorphic loci[8] across the genome), and heterozygosity[9].

Figure 1: Nucleotides, genes, and chromosomes
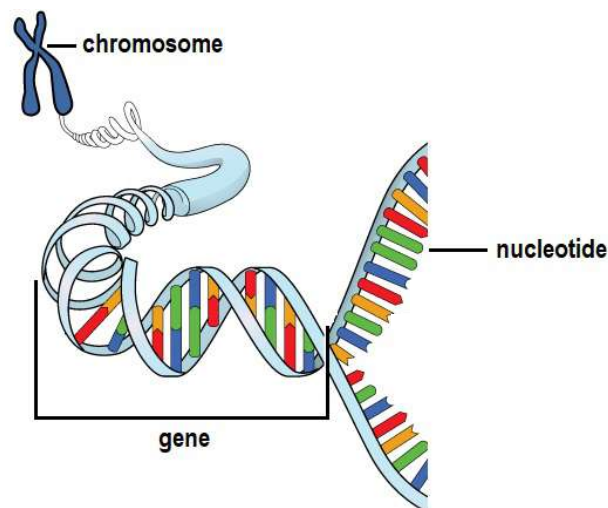
Source: blog.myheritage.com/2018/02/dna-basics-chapter-3-dna-expression.

---

[7]For example, adenine (A), cytosine (C), guanine (G), and thymine (T) are the four types of nucleotides that make up DNA.

[8]At a polymorphic locus, two or more different alleles exist within a population. For example, the ABO blood group system is determined by a polymorphic locus on chromosome 9, where multiple alleles (A, B, and O) exist, resulting in different blood types. The four basic ABO phenotypes are A, B, AB, and O.

[9]If an individual has two identical alleles at a given locus, they are said to be homozygous for that gene. If they have two different alleles, they are heterozygous.

Box 2: Ploidy and the number of chromosomes

Ploidy is the number of sets of chromosomes in the nucleus of a cell. Ploidy varies from species to species and can even vary within the same species. A haploid cell has only one set of chromosomes, while cells with two, three, four, etc. complete sets of chromosomes are called diploid, triploid, tetraploid, and so on. The haploid number of chromosomes is called n, while $2n$ and kn are the diploid and k-ploid numbers of chromosomes, respectively. For example, humans are diploid because human cells contain two copies of each chromosome. Since humans have two copies of 23 chromosomes, the haploid number of chromosomes is $n = 23$, while the diploid number of chromosomes is $2n = 46$. The total number of chromosomes is kn, where k is the ploidy of the cell. In the case of humans, the total number of chromosomes is then 46. Most organisms on Earth are diploid, so the reported number of chromosomes is generally the diploid number. There are some exceptions. For example, Mycoplasma, Escherichia coli (E. coli), and most bacteria are haploid organisms. Human gametes (sperm in males and egg in females) are also haploid because they are reproductive cells that contain half the number of chromosomes. This means that the number of chromosomes in the sperm or egg is $n = 23$, not $2n = 46$. In honey bees, the diploid queen has 32 chromosomes ($2n = 32$). The drones (male bees) are entirely derived from the queen (they are formed from unfertilized eggs), which means that the haploid drones have 16 chromosomes ($n = 16$). Female worker bees, on the other hand, are derived from the mother and a father, so they are diploid organisms with 32 chromosomes ($2n = 32$). A common example of a polyploid organism is the potato:

> "*Common cultivated potato varieties include tetraploid ($4n = 48$) with a basic chromosome number of 12, while there are cultivated species at the diploid ($2n = 24$) to pentaploid ($5n = 60$) levels. The triploid and pentaploid cultivated species are grown only on highland plateaus and slopes of the Andes, but diploid cultivated species are grown more widely and also used for breeding tetraploid varieties.*" (Watanabe, 2015, page 53).

To measure genetic diversity, we can look at the number of genes. However, we must be careful because genes can be divided into several categories based on their functions. For example, we generally distinguish between protein-coding genes, which encode instructions for the synthesis of proteins; non-coding genes, which produce RNA molecules that do not encode proteins but play an essential role in regulating gene expression and cellular processes; and pseudogenes, which are inactive copies of protein-coding genes. A more complex measure is genome size, also called C-value. The C-value is the amount of DNA contained in a haploid set of chromosomes. It is typically measured in picograms (pg) or base pairs (bp). A base pair is the basic unit of DNA sequence and corresponds to two nucleotides that combine to form the DNA double helix. The conversion between C-value and base pairs uses the following correspondence: 1 picogram is equal to 978 Mbp (million base pairs). For example, Gaston (2010, page 28) reports that the genome size of eukaryotic organisms (animals, plants, fungi, and many unicellular organisms) varies enormously, with C-values ranging from 0.0023 pg (or 2.25 million base pairs) for the parasitic microsporidium *Encephalitozoon intestinalis* to 1 400 pg (or 1.369 trillion base pairs) for the free-living amoeba *Chaos chaos*.

For a given organism, the number of genes and the C-value may vary from one measurement to another. They depend on the sample, the measurement instrument, the data size, etc. Therefore, most numbers are revised over time as data collection becomes more complete. Consider the human

genome. Twenty years ago, Taft and Mattick (2003) wrote: "*Until recently, the estimated number of protein-coding genes in the human genome was predicted to range from as low as 40 000 to as high as 120 000. However, it is now apparent that humans have no more than 30 000 protein-coding genes, similar to other vertebrates such as the mouse and pufferfish*". An important step in the sequencing of the human genome was taken in 2001 with the publication *The Sequence of the Human Genome* by Venter *et al.* (2001) in Science. They estimated 2.91 billion base pairs and 26 588 protein-coding genes. Since 2001, we have made great progress in sequencing the human genome, and the most recent published papers converge on some common numbers. Nurk *et al.* (2022) performed a new sequencing of the human genome and compared it to the previous reference studies performed by Schneider *et al.* (2017). Here are the results:

Statistics	GRCH38	T2T-CHM13
Base pairs (Gbp)	2.92	3.05
Number of genes	60 090	63 494
Number of protein-coding genes	19 890	19 969
% of repeats	51.89	53.94

where GRCH38 is the genomic database used by Schneider *et al.* (2017) and T2T-CHM13 is the genomic database used by Nurk *et al.* (2022). We can conclude that the human genome has 3 billion base pairs and the number of genes is 20 000. For many other organisms, the uncertainty in the number of base pairs and genes is more important because there are not enough resources (human and capital) to sequence their genomes with sophisticated instruments. Therefore, we may prefer to use the third metric of genetic diversity, the number of chromosomes, which is a more stable measure. For example, humans have exactly 46 chromosomes[10], while a mouse has exactly 40 chromosomes.

Table 2: Genetic diversity of some organisms

Organism	C-value (in pg)	Base pairs (in Mbp)	Genes ($\times 10^3$)	Chromosomes ($2n$ or kn)
Mycoplasma (bacterium)		0.580	$0.45 - 0.70$	1*
Haemophilus influenzae (bacterium)		1.8	1.750	1*
Escherichia coli (bacterium)		4.6	$4 - 5$	1*
Drosophila melanogaster (fruit fly)	0.17	180	$13 - 17$	8
Arabidopsis thaliana (mustard plant)	0.14	135	27	10
Caenorhabditis elegans (nematode)	0.10	100	21	12
Saccharomyces cerevisiae (yeast)	0.02	12	6	16
Zea mays (corn)	2.30	2 300	$32 - 40$	20
Oryza sativa (rice)	0.40	430	$32 - 50$	24
Musmusculus (mouse)	2.60	2 700	$20 - 25$	40
Rattus norvegicus (brown rat)	2.75	2 700	$20 - 25$	42
Homo sapiens (human)	3.20	3 050	20	46
Solanum tuberosum (tetraploid potato)	3.50	3 400	$39 - 45$	48*
Fragaria ananassa (octoploid strawberry)	2.50	2 500	$35 - 45$	56*
Canis lupus familiaris (dog)	2.80	2 800	20	78
Agrodiaetus shahrami (butterfly)	0.75	750	$12 - 14$	$100 - 268$*
Ophioglossum reticulatum (polyploid fern)	6.25	6 200	$30 - 50$	1 440*

Source: Author's research.

[10]This is not always true. Some humans have 47 chromosomes (trisomy), while others have 45 chromosomes (monosomy).

Table 2 shows the genetic diversity of some organisms. The first column gives the scientific name of the organism and indicates the family. Then we have the C-value calculated in pg, the genome size expressed in million base pairs, and the number of (protein-coding) genes. The last column is the number of chromosomes. The symbol * indicates that the cells are not diploid. The fern *Ophioglossum reticulatum* is the organism with the highest number of chromosomes. Interestingly, the number of chromosomes in butterflies can vary greatly from species to species. Most butterfly species have between 28 and 100 chromosomes. For example, common butterflies such as the Monarch (*Danaus plexippus*) have 30 chromosomes. Some species may have as few as 20 chromosomes or as many as 268 chromosomes, such as some *Agrodiaetus* butterflies.

Figure 2: Blue Morpho butterfly

Source: www.color-meanings.com/colorful-butterflies.

1.1.2 Species diversity

Organismal diversity can be assessed at different levels, but the most common is species diversity. Individuals represent the first level. They are grouped into populations, which form the second level of organismal diversity. Individuals and populations are also the two last levels of genetic diversity. Finally, populations are grouped into species. Defining a species is not straightforward (De Queiroz, 2007). In common language, species refer to a group of organisms that share certain physical or morphological characteristics. For example, we might say that butterflies form a species. However, this is not true from a biological standpoint. According to *Nature*[11], "*a biological species is a group of organisms that can reproduce with one another in nature and produce fertile offspring. Species are defined by the fact that they are reproductively isolated from other groups, meaning that organisms within one species cannot successfully reproduce with those of another species.*" For example, butterflies belong to families, not species. Some well-known butterfly species include the Monarch (*Danaus plexippus*) and the Blue Morpho (*Morpho menelaus*). Phylogenetics is another widely used approach to classifying organisms into species. A phylogenetic species is defined as the smallest group of organisms that share a common ancestor and can be distinguished by unique genetic or physical characteristics. Species are then grouped into genera (singular: genus), genera are assembled into families, families into phyla, and so on, progressing through higher taxonomic levels. The principal ranks in modern biological taxonomies are domain, kingdom, phylum (or division), class, order, family, genus, and species. For example, humans are classified as *Homo sapiens*, a

---

[11]Source: https://www.nature.com/scitable/definition/species-312.

species within the genus *Homo*. The *Homo* genus includes *Homo sapiens* (the only surviving species today) and several extinct species, such as *Homo neanderthalensis*, *Homo erectus*, and *Homo habilis*. Homo belongs to the *Hominidae* family, also known as the great apes. This family also includes chimpanzees, bonobos, and gorillas. Humans are further classified into the *Primates* order, the *Mammalia* class, the *Chordata* phylum, the *Animalia* kingdom, and the *Eukarya* domain. Readers can explore the species taxonomic tree on specialized websites[12].

In 1988, Robert May published a landmark article in Science: *How Many Species are There on Earth?* This article does not answer the question in the title. Why not? Because he didn't have enough information at the time to make a confident estimate. May (1988) preferred to review the different kinds of information scientists need to produce an answer that isn't just a guess. Thirty-five years later, can we give an accurate answer? In fact, not as many scientific articles suggest:

> "In 2010, Robert May pointed out an embarrassing truth about modern science[13]. Even as we invest huge amounts of time, money, and effort to find life on other planets, we still do not know how much life (i.e., how many species) is on our own. Although 'do not know' might sound like hyperbole, estimates have ranged wildly, from 2 million to 3 trillion." (Wiens, 2023, page 1).

The current reference paper on this topic is Mora *et al.* (2011), who estimated 8.7 million ($\pm$1.3 million standard error) eukaryotic species worldwide, of which 2.2 million ($\pm$0.18 million SE) are marine. The decomposition of their estimates is shown in Table 3. This result contrasts with the 1.5 or 2 million of species catalogued in current databases, suggesting that many species remain to be discovered. However, these figures continue to be challenged by new research, most of which puts the number of species on Earth at around 11 million, not excluding the possibility that there are at least one billion species on Earth (Larsen *et al.*, 2017).

Table 3: Currently catalogued and predicted total number of species on Earth and in the ocean

Species	Earth			Ocean		
	Catalogued	Predicted	$\pm$ SE	Catalogued	Predicted	$\pm$ SE
Eukaryotes	1 233 500	8 740 000	1 300 000	193 756	2 210 000	182 000
Animalia	953 434	7 770 000	958 000	171 082	2 150 000	145 000
Chromista	13 033	27 500	30 500	4 859	7 400	9 640
Fungi	43 271	611 000	297 000	1 097	5 320	11 100
Plantae	215 644	298 000	8 200	8 600	16 600	9 130
Protozoa	8 118	36 400	6 690	8 118	36 400	6 690
Prokaryotes	10 860	10 100	3 630	653	1 320	436
Archaea	502	455	160	1	1	0
Bacteria	10 358	9 680	3 470	652	1 320	436
Total	1 244 360	8 750 000	1 300 000	194 409	2 210 000	182 000

Source: Mora *et al.* (2011, Table 2, page 5).

---

[12]The two most popular are `www.ncbi.nlm.nih.gov/taxonomy`, developed by the NCBI (National Center for Biotechnology Information), and `www.fws.gov/explore-taxonomic-tree`, provided by the FWS (US Fish & Wildlife Service).

[13]Here is the abstract of Robert May's paper:

> "If some alien version of the Starship Enterprise visited Earth, what might be the visitors' first question? I think it would be: How many distinct life forms — species — does your planet have? Embarrassingly, our best-guess answer would be in the range of 5 to 10 million eukaryotes (never mind the viruses and bacteria), but we could defend numbers exceeding 100 million, or as low as 3 million." (May, 2010, page 41).

Table 4: Exploring the taxonomy classification tree

| Kingdom	Phylum	Class	Order	Family	Genus	Species	Vernacular name
Animalia	34	109	704	10 119	164 366	1 551 595	Animals
	Arthropoda	Insecta	43	1 738	89 273	994 767	Insects
	Arthropoda	Insecta	Lepidoptera	Nymphalidae	Morpho	Morpho menelaus	Blue morphos
	Chordata	Mammalia	Carnivora	Phocidae	14	19	True seals
	Chordata	Mammalia	Carnivora	Phocidae	Phoca	Phoca largha	Large seals
	Chordata	Mammalia	Carnivora	Phocidae	Phoca	Phoca vitulina	Common seals
	Chordata	Mammalia	Primates	16	83	528	Primates
	Chordata	Mammalia	Primates	Hominidae	Homo	Homo sapiens	Humans
	Mollusca	Gastropoda	Stylommatophora	Helicidae	Helix	Helix pomatia	Escargots
Archaea	2	13	16	27	112	377	
	Crenarchaeota	Thermoprotei	Thermoproteales	Thermoproteaceae	Caldivirga	Caldivirga maquilingensis	
Bacteria/Monera	29	51	115	297	1 996	9 980	Bacteria
	Firmicutes	Bacilli	Bacillales	Bacillaceae	Bacillus	Bacillus anthracis	B. anthracis
	Pseudomonadota	Gammaproteobacteria	Enterobacterales	Enterobacteriaceae	Escherichia	Escherichia coli	E. coli
Chromista	13	58	200	1 101	7 248	61 900	
	Foraminifera	5	22	435	4 016	49 654	
Fungi	12	61	274	1 086	12 778	155 869	
	Basidiomycota	Agaricomycetes	23	148	1 875	40 825	
	Basidiomycota	Agaricomycetes	Agaricales	Amanitaceae	Amanita	Amanita phalloides	Death caps
	Basidiomycota	Agaricomycetes	Boletales	Boletaceae	Boletus	Boletus edulis	Ceps
Plantae	9	44	256	1 079	21 463	385 774	Plants
	Tracheophyta	Liliopsida	Liliales	Liliaceae	Tulipa L.	96	Tulips
	Tracheophyta	Magnoliopsida	Fabales	Fabaceae	Phaseolus	Phaseolus vulgaris	Common bean
	Tracheophyta	Magnoliopsida	Rosales	Rosaceae	110	8 147	Roses
	Tracheophyta	Magnoliopsida	Solanales	Solanaceae	102	2 808	
	Tracheophyta	Magnoliopsida	Solanales	Solanaceae	Capsicum	Capsicum annuum	Pimientos
	Tracheophyta	Magnoliopsida	Solanales	Solanaceae	Solanum	Solanum lycopersicum	Tomatos
	Tracheophyta	Magnoliopsida	Solanales	Solanaceae	Solanum	Solanum tuberosum	Potatos
Protozoa	10	41	74	227	1 090	2 659	Protozoans
	Choanozoa	Ichthyosporea	Eccrinida	Amoebidiidae	Amoebidium	Amoebidium parasiticum	

For each taxon, we indicate the parent nodes of the tree on the left and the number of taxa on the right. For example, *Insecta* belongs to the phylum *Arthropoda* in the kingdom *Animalia* and includes 43 orders, 1 738 families, 89 273 genera, and 994 767 species.

Source: Catalogue of Life, www.catalogueoflife.org.

1.1.3   Ecological diversity

The third element of biodiversity is ecosystems. Again, there are several levels of ecological diversity. Populations, which are also part of genetic and organismal diversity, are the first level. Populations are grouped into habitats. The other three levels are ecosystems, ecoregions, and provinces. Then we find the biomes, which are large-scale ecosystems characterized by similar climatic conditions, vegetation, and wildlife. We generally distinguish between terrestrial and aquatic biomes. Terrestrial biomes include boreal forests (taiga), chaparral (Mediterranean climate), deserts, savannas, temperate forests, temperate grasslands, tropical rainforests, and tundra. Aquatic biomes include freshwater biomes such as wetlands and marine biomes such as oceans, coral reefs and mangroves. The highest level of ecological diversity corresponds to biogeographic realms, which are the broadest divisions of the Earth's land surface delineated by natural barriers such as oceans, deserts, and mountain ranges. Olson et al. (2001) defined eight realms: Australasia, Antarctic, Afrotropic, Indo-Malaya, Nearctic, Neotropic, Oceania and Palearctic.

Figure 3: The 867 terrestrial ecoregions of Olson et al. (2001)
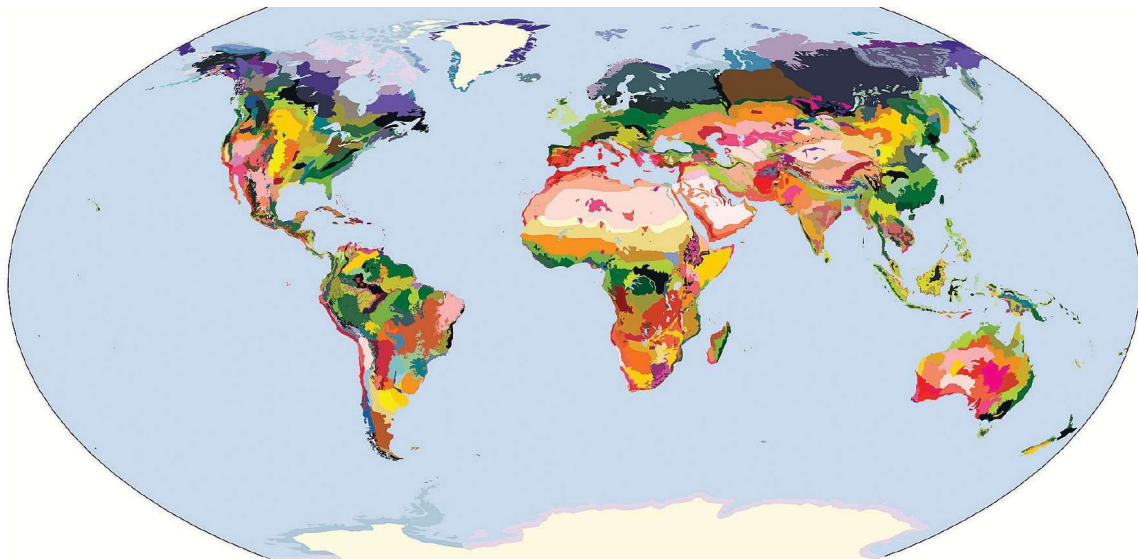
Source: Olson et al. (2001, Figure 2, page 935).

In general, ecoregions are the most common level at which ecological diversity is assessed. The World Wide Fund for Nature (WWF) describes them as biogeographic units, which are "*defined as relatively large units of land or water containing a distinct assemblage of natural communities sharing a large majority of species, dynamics, and environmental conditions.*" Most current world ecoregion maps[14] are based on the seminal work of Olson et al. (2001), who defined 867 distinct ecoregions (Figure 3). Among these ecosystems, Olson and Dinerstein (2002) identified 238 priority ecoregions for protection (142 terrestrial, 53 freshwater, and 43 marine). This research has been used extensively by the WWF and the International Union for Conservation of Nature (IUCN) to define protected areas[15]. The 2001 study was recently updated by Dinerstein et al. (2017), which

---

[14]See, for example, the maps available at https://ecoregions.appspot.com and https://www.oneearth.org/bioregions.

[15]IUCN has developed a system of protected area management categories to define, record and classify the wide variety of specific goals and concerns in categorizing protected areas and their objectives. The six categories are: strict nature reserve and wilderness area (Cat. I), national park (Cat. II), natural monument or feature (Cat. III),

now has a list of 846 terresterial ecoregions. A more recent study used a different mapping approach and identified 431 global ecosystems (Sayre *et al.*, 2020). By conducting a global gap analysis of the representation of these ecosystems in protected areas, the authors showed that most natural and semi-natural ecosystems are inadequately protected, with protection rates of less than 20%.

1.2 Biodiversity loss (and gain)

Regardless of the element of biodiversity (genetic, organismal or ecological), most figures show that the loss of biodiversity is significant and has accelerated over the past 50 years. However, such a message is not really clear. Indeed, we can first ask ourselves what biodiversity loss is, how it is measured, and is the current figure really significant? For example, the second chapter of Gaston and Spicer (2004) is devoted to the temporal dynamics of biodiversity and illustrates that biodiversity has fluctuated over geological time scales, such as millions of years. This long-term perspective shows that changes in biodiversity are a natural part of Earth's history and makes it difficult to understand whether current trends represent an exceptional crisis or a continuation of these natural cycles.

Figure 4: Genus diversity during the Phanerozoic era
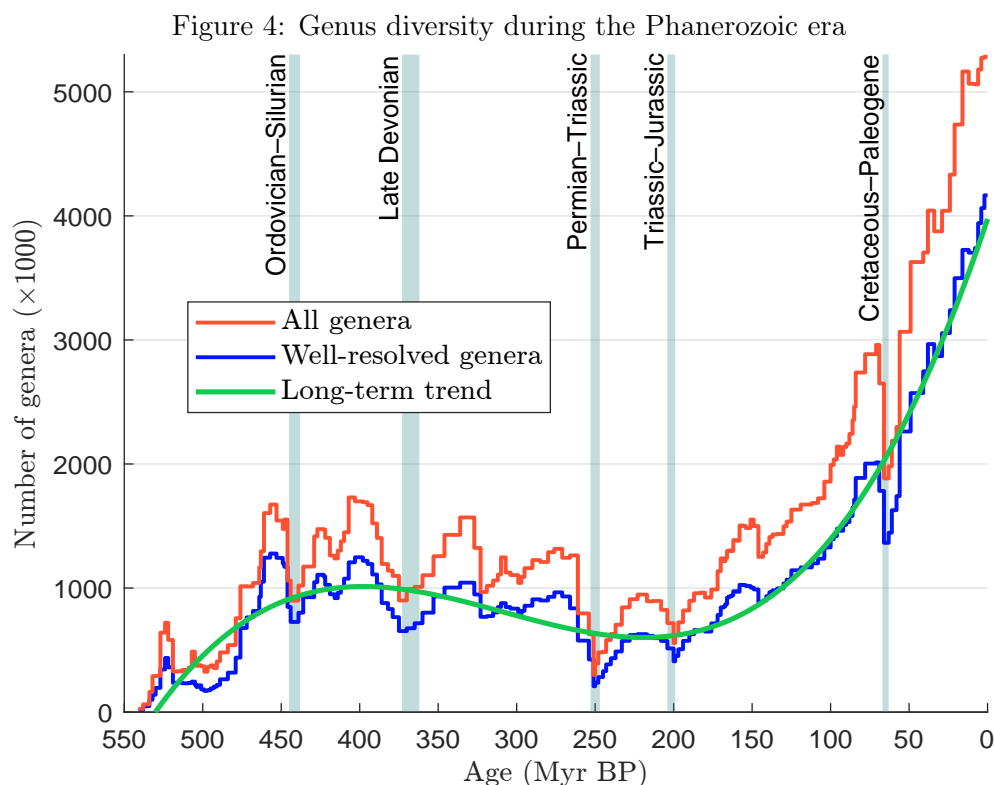
Source: Rohde and Muller (2005, Figure 1, page 208) & Supplementary Tables (www.nature.com/articles/nature03339).

The evolution of biodiversity over time is typically represented by a Sepkoski curve, which plots the number of genera over time. Although this is a simple metric, it is difficult to calculate due to

habitat or species management area (Cat. IV), protected landscape or seascape (Cat. V), and protected area with sustainable use of natural resources (Cat. VI). For example, in France, Les Landes de Gascogne is managed under IUCN category VI of protected areas, while Le Parc du Mercantour is managed under IUCN category II. Readers can explore protected areas and other effective area-based conservation measures (OECMs) at www.protectedplanet.net.

the complexity of data collection. Joseph John Sepkoski devoted much of his career to building a database of marine animal families and genera. This dataset, used extensively in numerous publications, was released in 2002 after Sepkoski's death (Sepkoski, 2002). Figure 4 shows the Sepkoski curve generated by Rohde and Muller (2005). The three series shown are: the total number of known genera of marine animals from Sepkoski's catalog[16], the total number of well-defined genera (*i.e.*, known genera excluding those with single occurrences or poorly dated records), and the long-term trend estimated using a third-order polynomial fitted to the data. First, we observe that the number of genera has fluctuated continuously throughout the Phanerozoic. About 500 million years ago, the number of genera was estimated at 370 000, while today it exceeds 5 million. Second, the increase in the number of genera was not linear. Genus diversity increased about 400 million years ago, then declined until about 200 million years ago, after which it increased dramatically. In the present era, genus diversity is higher than at any time in Earth's history. Finally, while the long-term trend is clear, there are numerous discontinuities with a frequency of about one million years. In particular, we observe several sharp declines known as extinction events or mass extinctions.

1.2.1   Speciation, extinction and the birth-death model

The number of species on Earth results from a balance between two evolutionary processes: speciation (the formation of new species) and extinction[17]. When speciation rates exceed extinction rates, the number of species increases. Conversely, when extinction rates exceed speciation rates, the number of species decreases. Both processes can occur naturally or be influenced by external factors. In fact, the processes of birth and death apply not only to individuals and populations, but also to higher levels of biological classification, such as species. For example, *Homo sapiens* appeared about 300 000 years ago, while *Australopithecus* disappeared about 1.9 million years ago. Similarly, dinosaurs became extinct about 65 million years ago, illustrating that species extinction is a natural process that can occur without human intervention. Thus, we generally recognize that each species and subspecies has a finite lifespan:

> "*Like all species, plants, mammals, and birds have been subject to extinction as a fundamental part of evolution. Indeed, only about 2–4% of all the species that have ever lived during the 600 million years of the fossil record still survive today. Looking at the fossil record, it can be said that invertebrate species and mammals have had an average life span of 5–10 and 1–2 million years, respectively.*" (Mace, 1998).

Even as some species disappear, new species continue to appear. This process of species formation is called speciation or diversification (Gaston and Spicer, 2004, Section 2.3.2, page 31). Speciation most often occurs when populations of the same species become geographically isolated. Over time, these populations evolve independently, accumulating genetic changes that can eventually lead to the emergence of distinct species. As these genetic differences increase, individuals from the two populations may no longer be able to interbreed or produce fertile offspring. A classic example of this phenomenon is donkeys and horses. Both belong to the same family (*Equidae*) and genus (*Equus*), but are classified as separate species. Donkeys (*Equus africanus asinus*) are a subspecies of the African wild ass (*Equus africanus*), while domestic horses (*Equus ferus caballus*) are a subspecies of the wild horse (*Equus ferus*). Although donkeys and horses can interbreed, their offspring are usually sterile[18], meaning they cannot reproduce. This sterility occurs because donkeys have 62

---

[16]The Sepkoski database can be found at https://strata.geology.wisc.edu/jack.

[17]Extinction refers to the complete disappearance of a species from the Earth, while extirpation refers to the disappearance of a species from a particular region, but the species continues to exist in other regions.

[18]The offspring of a female horse and a male donkey is a mule, while the offspring of a male horse and a female donkey is a hinny.

Figure 5: Rates of origination and extinction during the Phanerozoic era
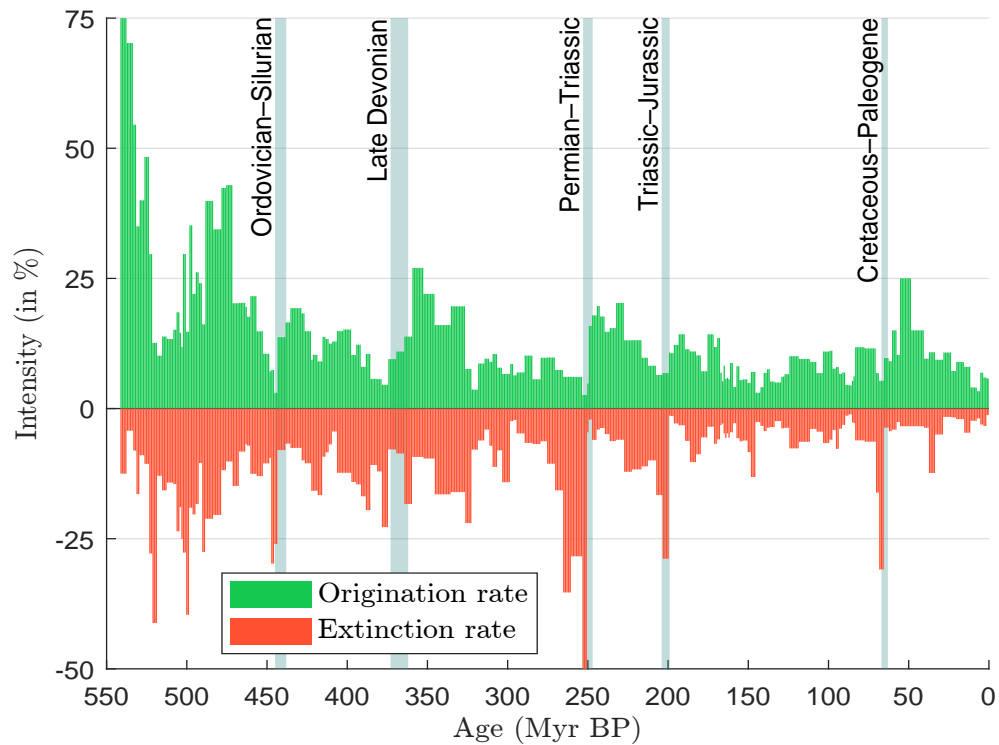
Source: Rohde and Muller (2005) & Author's calculations.

Figure 6: Net diversification rate during the Phanerozoic era

Source: Rohde and Muller (2005) & Author's calculations.

chromosomes while horses have 64, resulting in offspring with 63 chromosomes. In fact, donkeys, horses and zebras share a common ancestor, but diverged for various reasons. According to Carbone et al. (2006), zebras and donkeys split about 0.9 million years ago, while their common ancestor diverged from the horse about 2 million years ago.

The number of species $N(t)$ at time $t+1$ can be expressed as:

$$N(t+1) = N(t) + \Delta N^+(t+1) - \Delta N^-(t+1)$$
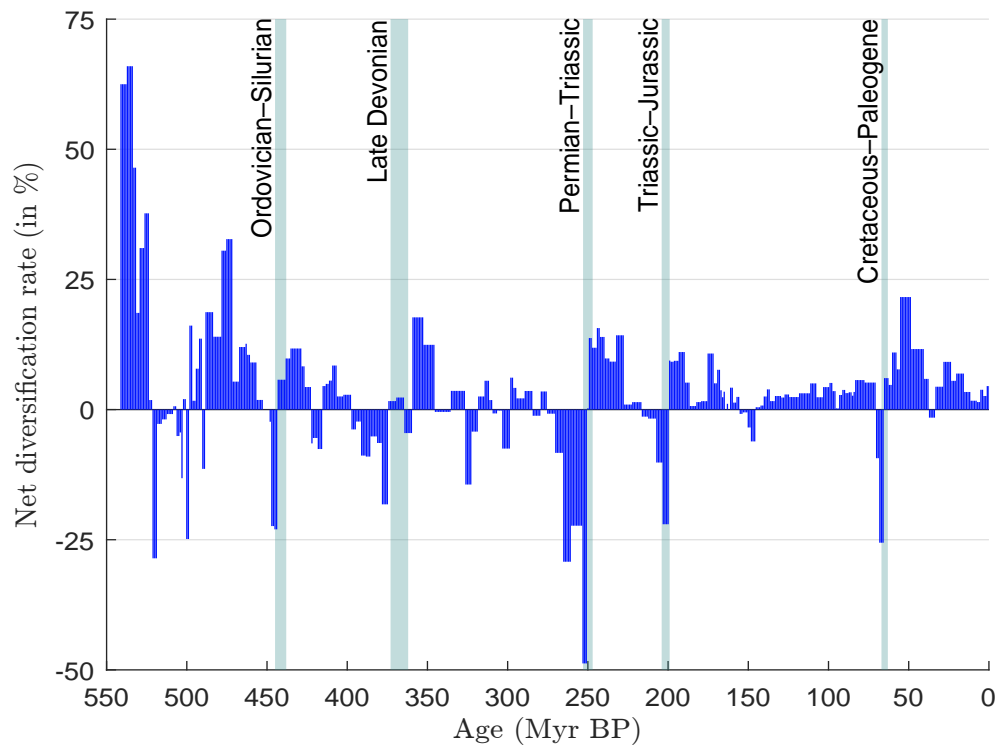
where $\Delta N^+(t+1)$ and $\Delta N^-(t+1)$ are the number of new species and extinct species between t and $t+1$. In continuous time, this equation becomes:

$$\frac{\mathrm{d}N(t)}{\mathrm{d}t} = \frac{\mathrm{d}N^+(t)}{\mathrm{d}t} - \frac{\mathrm{d}N^-(t)}{\mathrm{d}t}$$

Dividing both sides by $N(t)$ gives:

$$\underbrace{\frac{\mathrm{d}N(t)}{N(t)\,\mathrm{d}t}}_{\delta(t)} = \underbrace{\frac{\mathrm{d}N^+(t)}{N(t)\,\mathrm{d}t}}_{\lambda(t)} - \underbrace{\frac{\mathrm{d}N^-(t)}{N(t)\,\mathrm{d}t}}_{\mu(t)}$$

The growth rate $\delta(t)$ is the difference between the origination (or speciation) rate $\lambda(t)$ and the extinction rate $\mu(t)$:

$$\delta(t) = \lambda(t) - \mu(t) \tag{1}$$

$\delta(t)$ is also called the net diversification rate. Here, $\lambda(t)$, $\mu(t)$ and $\delta(t)$ are assumed to be instantaneous rates. Given two dates t_1 and t_2, we can compute the cumulative rates $\lambda(t_1, t_2) = \int_{t_1}^{t_2} \lambda(t)\,\mathrm{d}t$, $\mu(t_1, t_2) = \int_{t_1}^{t_2} \mu(t)\,\mathrm{d}t$, and $\delta(t_1, t_2) = \int_{t_1}^{t_2} \delta(t)\,\mathrm{d}t$. We derive the average rate by dividing the cumulative rate by the time interval. For example, the average net diversification rate is equal to:

$$\bar{\delta}(t_1, t_2) = \frac{\delta(t_1, t_2)}{t_2 - t_1} = \frac{1}{t_2 - t_1} \int_{t_1}^{t_2} \delta(t)\,\mathrm{d}t$$

In Figures 5 and 6, we report the origination, extinction, and net diversification rates calculated by Rohde and Muller (2005) from the Sepkoski database. For example, the range of the net diversification rate $\delta(t_1, t_2)$ is between -49% and $+66\%$. However, these numbers are difficult to compare because they represent time periods ranging from one million years to seven million years.

The previous remark indicates that we need to normalize the extinction (and other) rates. These rates can be expressed as a percentage per decade, century, or millennium. For long-term trends based on fossil records, we typically express them as a percentage per million years. For example, if the extinction rate μ is constant and equals 1% per century, this is equivalent to an extinction rate of:

$$\mu = \frac{1\%}{1 \text{ century}} = \frac{1\%}{100 \text{ years}} = 0.01\% \text{ per year}$$

If we assume that the speciation rate is zero, then the number of surviving species follows an exponential survival function:

$$S(t) = \frac{N(t)}{N_0} = e^{-\mu t} \tag{2}$$

We deduce that the lifespan (or average lifetime) of species is the inverse of the extinction rate:

$$\tau = \frac{1}{\mu}$$

For example, if the extinction rate of a genus is 0.1% per millennium, we obtain:

$$\tau = \frac{1000 \text{ years}}{0.1\%} = 10^6 \text{ years (or 1 million years)}$$

The lifespan of this genus is then one million years. Pimm *et al.* (1995) introduced a new metric η for assessing extinction rates. They use the number of extinctions (E) per million species per year (MSY) or E/MSY. The relationship between η, μ and τ is then:

$$\eta = 10^6 \mu = \frac{10^6}{\tau}$$

For example, if μ is 0.1% per millennium, we get:

$$\eta = \frac{0.1\%}{10^3 \text{ years}} \times 10^6 = \frac{10^{-3}}{10^3 \text{ years}} \times 10^6 = 1 \, \text{E/MSY}$$

If there are 1 million species, the number of extinctions per year would be one. Because scientists use these three metrics η, μ, and τ interchangeably to assess extinction rates, it is crucial to understand their definitions and how to convert one metric to another.

Remark 2 *We consider the previous example where the extinction rate of a genus equals 1% per century or 0.01% per year. We get:*

$$\mu = \frac{1\%}{1 \text{ century}} = \frac{1\%}{10^2 \text{ years}} \times \frac{10^6}{10^6} = 10\,000\% \text{ per million years}$$

This example shows that we must be careful with conversion formulas because they ignore the compound effect. Using Equation 2, we deduce that[19]:

$$\mu^\star = -\frac{1}{t} \ln\left(\frac{N(t)}{N_0}\right) = -\frac{1}{t} \ln\left(1 - \frac{N_0 - N(t)}{N_0}\right) = -\frac{1}{t} \ln\left(1 - \frac{N^+(t)}{N_0}\right)$$

where $N^+(t)$ is the number of extinctions between 0 and t. This formula was proposed by Spalding and Hull (2021) to calculate the extinction rate for long timescales.

Example 1 *We consider three datasets with different species:*

Species	N_0	ΔN^+	ΔN^-	Δt
Birds	5 000	7	5	10 years
Insects	75 000	25	50	3 centuries
Plants	10^6	30×10^3	15×10^3	1 millennium

where N_0 is the number of species at the beginning of the period, and ΔN^+ and ΔN^- are the number of new and dead species during the period Δt.

The calculated values of λ, μ, and δ are shown in the table below. For example, the net diversification rate for the bird species is 0.004% per year, or 4% per millennium. In this example, it is better to use a longer time unit (millennium instead of year) because of the magnitude of the rates.

Species	λ	μ	δ	λ	μ	δ
	(in % per year)			(in % per millenium)		
Birds	0.01400	0.01000	0.00400	14.00	10.00	4.00
Insects	0.00011	0.00022	−0.00011	0.11	0.22	−0.11
Plants	0.00300	0.00150	0.00150	3.00	1.50	1.50

---

[19]To distinguish the logarithmic approach from the arithmetic approach, we use the symbol $\mu^\star$ instead of μ. We also define $\tau^\star = 1/\mu^\star$ and $\eta^\star = 10^6 \mu^\star = 10^6/\tau^\star$.

We now focus on the extinction rate and calculate this metric with different units. $\mu(0, \Delta t)$ is the cumulative extinction rate. For the bird and plant species, it is equal to:

$$\mu_{\text{bird}}(0, \Delta t) = \frac{5}{5\,000} = 0.1\%$$

and:

$$\mu_{\text{plant}}(0, \Delta t) = \frac{15 \times 10^3}{10^6} = 1.5\%$$

These two rates cannot be directly compared because the time periods over which the extinction rate is assessed are very different (10 years versus 1 millennium). Therefore, it is important to normalize. The extinction rate μ is then expressed in % per year. We can also calculate the extinction rate $\mu^\star$ using the previous logarithmic formula. These two extinction rates can then be converted in lifetime (expressed in years) and E/MSY. Numerical results are given below:

Species	$\mu(0, \Delta t)$ (in %)	μ (in % per year)	$\mu^\star$	τ (in years)	$\tau^\star$	η (in E/MSY)	$\eta^\star$
Birds	0.10000	0.01000	0.01401	10 000	7 138	100.0	140.1
Insects	0.06667	0.00022	0.00011	450 000	899 850	2.2	1.1
Plants	1.50000	0.00150	0.00305	66 667	32 831	15.0	30.5

Several observations can be made. First, the figures for $\mu(0, \Delta t)$ cannot be compared directly due to their lack of normalization. We observe extinction rates of 0.1%, 0.07% and 1.5% for birds, insects, and plants, respectively, but these values correspond to different time periods: ten years, three centuries, and one millennium. Second, the results obtained using the arithmetic approach differ from those using the logarithmic approach. Finally, the lifetime and E/MSY figures are probably the easiest to interpret. For example, among one million species, we observe 100, 2.2, and 15 extinctions per year for birds, insects, and plants.

1.2.2 Background extension rate

The background extension rate is the normal or typical extension rate that has occurred over the past 500 million years. By normal, we mean the long-term rate at which species would go extinct in the absence of human presence. Thus, most estimates use data up to 1 500 AD. In a brief communication, Simpson (1952) estimated the average duration of a species to be between 0.5 and 5 million years. This was one of the first publications on the subject. For marine invertebrates, Valentine (1970) estimated the average lifetime to be between 5 and 10 million years. The publication of Van Valen (1973) marked a turning point and generated considerable controversy. In this influential paper, the author introduced the concept of Van Valen's Law, which states that extinction rates within a given taxonomic group remain constant over time. To explain this pattern, he proposed the Red Queen hypothesis, which suggests that species must constantly evolve to keep up with competitors and predators. This ongoing evolutionary *arms race* results in a constant extinction rate. Van Valen (1973, Table 1) calculated the background extinction rate for 20 families, 38 genera, and 3 species. His results satisfy the following coherent inequalities:

$$\tau_{\text{family}} \geq \tau_{\text{genus}} \geq \tau_{\text{species}}$$

We report some of his estimates[20] in Table 5. The work of Pimm *et al.* (1995) was a major milestone in the study of background extinction rates. Based on an analysis of 11 studies, they estimated the

---

[20]Van Valen (1973) used the macarthur (ma) measure to define the lifespan of species. One macarthur is the rate of extinction given a half-life of 500 years. Since the figures reported by Van Valen are expressed in micromacarthurs (μma), we estimate the lifespan in million years using the following formula: $\tau = 500/(\mu \ln 2)$ where μ is the extinction rate in μma.

Table 5: Estimates of the background extension rate $\bar{\eta}$

Taxonomy	τ (in myr)	η (in E/MSY)	Source
All species	$1 - 10$	$0.10 - 1.00$	Pimm *et al.* (1995)
All species	1.0	0.10	De Vos *et al.* (2015)
All fossil groups	$0.5 - 5$	$0.20 - 2.00$	Simpson (1952)
Marine fossil groups	$7.4 - 20$	$0.05 - 0.13$	Raup and Sepkoski (1982)
Marine invertebrates	$5 - 10$	$0.10 - 0.20$	Valentine (1970)
Cetacea (genus)	3.61	0.277	Van Valen (1973)
Devonian & Cenozoic bivalves	$6.5 - 9.7$	$0.10 - 0.15$	Valentine (1970)
Silurian graptolites	$2.0 - 3.0$	$0.33 - 0.50$	Rickards (1977)
Diatoms	8.02	0.125	Van Valen (1973)
Dinoflagellata	13.12	0.076	Van Valen (1973)
Foraminifera (planktonic)	7.21	0.139	Van Valen (1973)
Foraminifera (genus)	24.04	0.042	Van Valen (1973)
Foraminifera (family)	72.13	0.014	Van Valen (1973)
Arthropods	$1.07 - 11.11$	$0.090 - 0.934$	De Vos *et al.* (2015)
Chordates	$1.71 - 15.63$	$0.064 - 0.586$	De Vos *et al.* (2015)
Mammals	0.56	1.800	Barnosky *et al.* (2011)
Mammals & birds	$0.55 - 4.80$	$0.208 - 1.818$	Loehle and Eschenbach (2012)
Mammals	$9.80 - 43.48$	$0.023 - 0.102$	De Vos *et al.* (2015)
Mammals	0.50	2.000	Ceballos *et al.* (2015)
Mollusca	$0.60 - 7.41$	$0.135 - 1.672$	De Vos *et al.* (2015)
Primates (genus)	3.28	0.305	Van Valen (1973)
Reptilia (family)	24.05	0.042	Van Valen (1973)
Plants	$2.84 - 18.87$	$0.053 - 0.352$	De Vos *et al.* (2015)
Plants	$7.69 - 20.00$	$0.050 - 0.130$	Gray (2019)

background rate $\bar{\eta}$ to be between 0.1 and $1\,\mathrm{E/MSY}$. Since then, the $1\,\mathrm{E/MSY}$ benchmark has been widely adopted in many mass extinction studies. However, it's important to note that this benchmark can vary depending on the specific species or taxonomic group being considered. For example, Barnosky *et al.* (2011) proposed a benchmark of $1.8\,\mathrm{E/MSY}$ for mammals. De Vos *et al.* (2015) conducted a comprehensive study across different taxa (arthropods, chordates, mammals, mollusca, and plants) and suggested that the lower bound of the Pimm *et al.* (1995) estimate is a more appropriate benchmark, namely $\bar{\eta} = 0.1\,\mathrm{E/MSY}$.

1.2.3 Mass extinction

A mass extinction is a widespread and rapid decline in Earth's biodiversity (genetic or species diversity), during which a substantial proportion of the planet's species disappear over a relatively short period of time — typically thousands to millions of years, which is short on the geologic time scale. The characterization of an extinction event is then determined using calculated extinction rates. Mathematically, we have:

$$[t_1, t_2] \text{ is an extinction event period} \Leftrightarrow \mu(t_1, t_2) \geq \mu^\star \text{ and } \bar{\eta}(t_1, t_2) \gg \bar{\eta} \qquad (3)$$

where $\mu(t_1, t_2)$ is the (total) extinction rate expressed in % during the period $[t_1, t_2]$, $\bar{\eta}(t_1, t_2)$ is the mean extinction rate expressed in E/MSY, $\mu^\star$ is a threshold value and $\bar{\eta}$ is the background rate. For

example, $\mu^\star = 30\%$ means that 30% of species must disappear between times t_1 and t_2 for the period $[t_1, t_2]$ to be characterized as an extension event. Although there is no consensus on the threshold, scientists generally use a minimum of 30% for species and 15% for families to characterize a mass extinction.

Using fossil data records, Raup and Sepkoski (1982) demonstrated that four mass extinctions in the marine realm — occurring in the late Ordovician, Permian, Triassic, and Cretaceous periods — had extinction rates that were statistically significantly higher than background rate levels. However, this was not the case for a fifth extinction event in the Devonian. Benton (1995) used a new database that included both marine and continental fossil records and examined 22 extinction events. His results showed that extinction rates can be very different for marine and continental organisms. The study of Bambach (2006) identifies eighteen extinctions and comes to the same conclusion:

> "*A review of different methods of tabulating data from the Sepkoski database reveals 18 intervals during the Phanerozoic have peaks of both magnitude and rate of extinction that appear in each tabulating scheme. These intervals all fit Sepkoski's definition of mass extinction. However, they vary widely in timing and effect of extinction, demonstrating that mass extinctions are not a homogeneous group of events.*" (Bambach, 2006, page 127).

For this reason, paleontologists often use a scale to categorize mass extinction events, distinguishing between[21]:

- Small extinction events: Relatively minor events that do not drastically alter biodiversity;

- Pulse events: More pronounced extinctions that can significantly impact certain taxonomic groups;

- The '*Big Five*' extinctions: The five major mass extinctions in Earth's history that resulted in a significant loss of biodiversity.

The Big Five extinctions are those identified by Raup and Sepkoski (1982). For each event, we report below some figures[22] on the total extinction rate[23] and the possible causes:

1. Ordovician-Silurian mass extinction — LOME (445–443 Myr BP)
   About 27% of all families, 57% of all genera and 85% of all species became extinct. It is generally assumed that the cause is climate change (global cooling) and volcanic activity, which affect the chemistry of the atmosphere and oceans and CO_2 sequestration.

---

[21]For more informations and illustrations, the reader can consult Chapter 7 of Primack (2014) for detailed information on extinction with a lot of numbers and examples.

[22]Following the terminology of Algeo and Shen (2024), we use the following abbreviations for the five major mass extinctions: LOME for Late Ordovician, LDME for Late Devonian, EPME for end-Permian, ETME for end-Triassic and ECME for end-Cretaceous mass extinctions. Other commonly used abbreviations include: O-S for Ordovician-Silurian, L-D for Late Devonian, P-T for Permian-Triassic, T-J for Triassic-Jurassic, K-Pg for Cretaceous-Paleogene (previously called K-T for Cretaceous-Tertiary) extinctions. It's important to note that a mass extinction period can be characterized by multiple extinction events. According to Benton (1995), the Big Five extinctions can be further broken down as follows: 1 event for LOME (Ashgillian), 2 events for LDME (Givetian-Frasnian & Famennian), 3 events for EMPE (Ufimian, Kazanian-Tatarian & Tatarian), 3 events for ETME (Carnian, Norian-Rhaetian & Rhaetain) and 2 events for ECME (Cenomanian & Maastrichtian).

[23]These figures come from the Wikipedia page (https://en.wikipedia.org/wiki/Extinction_event) and are based on the book of Benton (2015). These estimates should be treated with caution, as they may vary from study to study. For example, Barnosky *et al.* (2011) estimated extinction rates for genera and species to be 57% and 86% for LOME, 35% and 75% for LDME, 56% and 96% for EPME, 47% and 80% for ETME, and 40% and 76% for ECME, respectively. However, we observe that the order of magnitude is the same in most studies.

2. Late Devonian mass extinction — LDME (372–359 Myr BP)
   About 19% of all families, 35-50% of all genera and 75% of all species became extinct. The cause is generally thought to be climate change (global cooling followed by global warming) and the removal of global CO_2.

3. Permian-Triassic extinction or '*The Great Dying*' — EPME (252–251 Myr BP)
   About 57% of marine families, 84% of marine genera, 81% of all marine species and 90% of terrestrial vertebrate species became extinct. The cause is generally thought to be climate change (global warming) and volcanic activity (massive volcanic eruptions in Siberia).

4. Triassic-Jurassic extinction — ETME (200–201 Myr BP)
   About 23% of all families, 48% of all genera (20% of marine families and 55% of marine genera) and 70-75% of all species became extinct. It is generally thought to be caused by volcanic activity (massive volcanic eruptions in the Central Atlantic Magmatic Province) and sea level changes.

5. Cretaceous-Paleogene extinction — ECME (66 Myr BP)
   About 17% of all families, 47% of all genera and 75% of all species became extinct. The Cretaceous extinction is marked by the disappearance of the Dinausores. It is generally assumed that the cause is an asteroid impact followed by widespread environmental disruption, including tsunamis, forest fires, and climate change.

We find that the causes, while diverse, are related to a small number of natural phenomena:

> "*Every mass extinction has both an ultimate cause, i.e., the trigger that leads to various climato-environmental changes, and one or more proximate cause(s), i.e., the specific climato-environmental changes that result in elevated biotic mortality. With regard to ultimate causes, strong cases can be made that bolide (i.e., meteor) impacts, large igneous province eruptions and bioevolutionary events have each triggered one or more of the Phanerozoic Big Five mass extinctions, and that tectono-oceanic changes have triggered some second-order extinction events. [...] With regard to proximate mechanisms, most extinctions are related to either carbon-release or carbon-burial processes, the former being associated with climatic warming, ocean acidification, reduced marine productivity and lower carbonate $\delta^{13}C$ values, and the latter with climatic cooling, increased marine productivity and higher carbonate $\delta^{13}C$ values.*" (Algeo and Shen, 2024, page 1).

The leading hypothesis for the fifth mass extinction is the impact of a large asteroid that struck the Earth near the Yucatán Peninsula in Mexico, forming the Chicxulub crater (Schulte *et al.*, 2010). The asteroid, estimated to be 10 to 15 kilometers in diameter, released an immense amount of energy, equivalent to billions of nuclear bombs. This catastrophic impact caused massive earthquakes, tsunamis, and forest fires. In addition, the impact likely caused a '*nuclear winter*' as a massive plume of debris and vaporized rock was ejected into the atmosphere and spread globally. This debris blocked sunlight, leading to a drastic cooling of the planet, reduced photosynthesis, and a collapse of food chains. While the asteroid impact hypothesis is widely accepted, other factors such as climate change and volcanic activity may also have contributed to the Cretaceous-Paleogene mass extinction. Interestingly, this extinction paved the way for the rise of mammals, including humans, as it wiped out the dinosaurs that had previously dominated the planet. As shown in Figure 5 on page 19, biodiversity tends to rebound significantly after each mass extinction. Although biodiversity loss is generally followed by strong gains, this recovery occurs on the paleontological timescale of millions of years.

Box 3: IUCN Red List of Threatened Species

Founded in 1964, the International Union for Conservation of Nature (IUCN) is responsible for maintaining and updating the IUCN Red List of Threatened Species. It is now considered the world's most comprehensive source of information on the global extinction status of animals, fungi and plants. They correspond to three kingdoms in organismal diversity or modern biological taxonomy, the other two being protista (single-celled eukaryota) and monera (single-celled prokaryota). IUCN (2012) assesses the risk status of a species according to the following A-E criteria: (A) population size reduction (population decline measured over the longer of 10 years or 3 generations, trend), (B) geographic range (extent of occurrence, area of occupancy), (C) small population size and decline (number of mature individuals, trend), (D) very small or restricted population (number of mature individuals, number of locations), and (E) quantitative analysis (probability of extinction). The Red List divides then species into nine categories:

- Not Evaluated (NE) & Data Deficient (DD)
  A taxon is NE if it has not yet been evaluated against the criteria. NE species are not published in the IUCN Red List. A taxon is DD if there is insufficient information to make a direct or indirect assessment of its risk of extinction based on its distribution and/or population status. A taxon in this category may be well studied and its biology well understood, but adequate data on abundance and/or distribution are lacking.

- Least Concern (LC) & Near Threatened (NT)
  A taxon is LC if it has been assessed against the Red List criteria and is not considered CR, EN, VU or NT. A taxon is NT if it has been evaluated against the criteria, but does not currently qualify as CR, EN, or VU, but is close to or is likely to qualify for a threatened category in the near future.

- Vulnerable (VU), Endangered (EN) & Critically Endangered (CR)
  A taxon is VU (EN or CR, respectively) if the best available evidence indicates that it meets any of the criteria A to E for VU and is therefore considered to be at high (very high or extremely high, respectively) risk of extinction in the wild.

- Extinct in the Wild (EW)
  A taxon is EW if it is known to survive only in cultivation, captivity, or as a naturalized population (or populations) far outside its historical range. A taxon is presumed to be EW if exhaustive surveys in known and/or expected habitats at appropriate times (diurnal, seasonal, annual) throughout its historical range have failed to record an individual. Surveys should be conducted over a period of time appropriate to the life cycle and life form of the taxon.

- Extinct (EX)
  A taxon is EX when there is no reasonable doubt that the last individual has died. A taxon is presumed EX when exhaustive surveys in known and/or expected habitat at appropriate times (diurnal, seasonal, annual) throughout its historical range have failed to record an individual. Surveys should be conducted over a period of time appropriate to the life cycle and life form of the taxon.

1.2.4 The Holocene extinction, the Anthropocene extinction or the sixth mass extinction?

At the October 1991 symposium *The Visions of a Sustainable World* at Caltech, Edward O. Wilson warned that "*we are now in the midst of a sixth extinction spasm, the greatest since the one that closed the age of the dinosaurs 66 million years ago.*" In 1995, Richard Leakey published the book *The Sixth Extinction*, which popularized the term in the scientific community (Leakey and Lewin, 1995). Since then, numerous research papers have been published (Pimm and Brooks, 2000; Wake and Vredenburg, 2008; Barnosky *et al.*, 2011; Dirzo *et al.*, 2014; Ceballos *et al.*, 2015; Cowie *et al.*, 2022). However, it was Elizabeth Kolbert's book *The Sixth Extinction: An Unnatural History*, which won the Pulitzer Prize in 2015, that introduced the term to the general public (Kolbert, 2014).

There is no doubt that the extinction rate observed since 1500 AD is largely higher than the background rate, as demonstrated by Pimm *et al.* (1995, page 347) ("*recent extinction rates are 100 to 1 000 times their pre-human levels in well-known, but taxonomically diverse groups from widely different environments*"), and De Vos *et al.* (2015, page 452) ("*current extinction rates are 1 000 times higher than natural background rates of extinction and future rates are likely to be 10 000 times higher*"). This is true for both terrestrial and marine extinctions (Ceballos *et al.*, 2017; Del Monte-Luna *et al.*, 2023). This is why we can speak of a Holocene extinction. There is also no doubt that this extinction event is due to humans, leading to the concept of Anthropocene extinction or defaunation (Dirzo *et al.*, 2014). However, it is still difficult to definitively classify our current epoch as the sixth mass extinction. While we meet the criterion for the elevated background extinction rate based on relation (3), we have yet to confirm the condition $\mu\left(t_1, t_2\right) \geq \mu^\star$. Therefore, there is no scientific research that claims that more than 75% of all marine and terrestrial vertebrate species have become extinct in the last five centuries or in the last 10 000 years. We do not really know. Moreover, a mass extinction is usually followed by a period of intense species origination. Therefore, it is difficult to say that the sixth mass extinction has already occurred (Barnosky *et al.*, 2011). The majority of scientists prefer to argue that "*we are either entering or in the midst of the sixth great mass extinction*" (Wake and Vredenburg, 2008).

Why are we talking about the sixth mass extinction? Because the number of species that have become extinct in the last few centuries is so large, these extinctions are due to human activities, and we do not expect these extinctions to stop in the next few years with population growth and deforestation. The trends are dramatic and we are clearly facing a biodiversity crisis. These facts are extensively documented in the research cited above, as well as in the monumental 1148-page report by the Intergovernmental Science-Policy Platform on Biodiversity and Ecosystem Services (IPBES, 2019).

The stylized facts about current extinction rates are based on the IUCN Red List of Threatened Species (Box 3). As of September 2024, the current Red List database contains 163 040 species whose extinction risk has been assessed. For each species, we can obtain the assessment report by using the search query https://www.iucnredlist.org/search. For example, the figures for the snow leopard are available at www.iucnredlist.org/species/22732/50664030. We learned that the snow leopard species (*Panthera uncia*) was assessed in November 2016. Panthera uncia is currently listed as VU (Vulnerable), whereas in 2008 it was listed as EN (Endangered). Much more information can be found in its assessment card[24].

---

[24]The snow leopard belongs to the following taxonomic classification tree: Animalia (kingdom), Chordata (phylum), Mammalia (class), Carnivora (order), Felidae (family), Panthera (genus), and Panthera uncia (species). The number of mature individuals is estimated to be between 2 710 and 3 386, with a decreasing population trend. It is found in Asia, including Afghanistan, Bhutan, China, India, Kazakhstan, Kyrgyzstan, Mongolia, Nepal, Pakistan, the Russian Federation, Tajikistan, and Uzbekistan. The Panthera uncia inhabits altitudes between 500 and 5 800 meters. Its home

Figure 7: Number of extinct species since 1500 AD
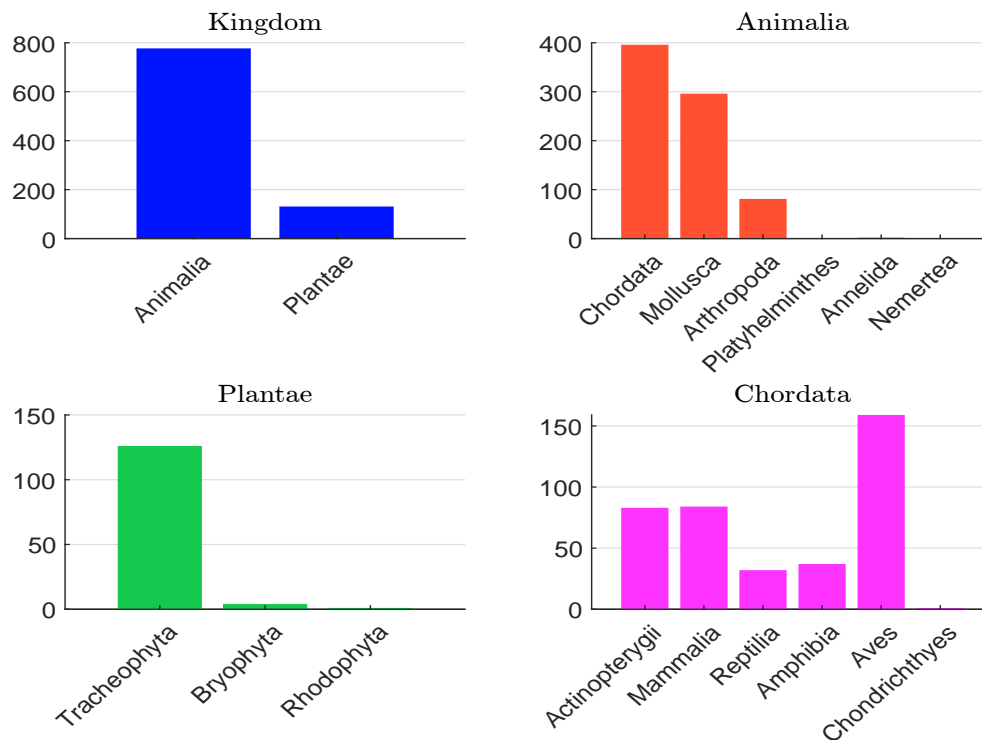
Among the 163 040 species evaluated, 908 are extinct, with the following distribution: 85.6% from Animalia and 14.4% from Plantae (Table 6). This corresponds to an extinction rate of 0.56%. Most of these extinct species belong to four phyla: Chordata, Mollusca, Arthropoda, and Tracheophyta (Figure 7). Within the Chordata phylum, the class Aves (birds) is the most represented, followed by Mammalia, Actinopterygii (ray-finned fishes), Amphibia, and Reptilia. In the Mollusca phylum, most extinct species are in the class Gastropoda, with the remainder in Bivalvia. In the Tracheophyta phylum, the class Magnoliopsida is the most dominant. Some examples of extinct species are the Dodo, the Splendid Poisson Frog, the Floreana Giant Tortoise, the St Helena Olive, the Stringwood and the Galapagos Amaranth.

Table 6 shows the breakdown of the 163 040 evaluated species according to the IUCN Red List categories. There are 81 species classified as Extinct in the Wild (EW), with a balanced distribution between Animalia and Plantae. Examples of EW species include the Spix's Macaw, the Polynesian Tree Snail, the Golden Skiffia, the Yellow Fatu, the Superb Cyanea, and Wood's Cycad. A similar distribution between Animalia and Plantae is observed for Critically Endangered (CE) species, but their number is much larger, totaling 10 031 species. Examples include the Hainan Gibbon, the Golden Line Fish, the Gomera Stick Grasshopper, the Didymous Chamomile, the French Grass, and the Hawaiian Gardenia.

According to IUCN (2024b), the number of threatened species (TH) is defined as follows:

$$TH = EW + CR + EN + VU$$

---

range is estimated to be about 2.8 million km^2 and its generation length is approximately 7.54 years. Additionally, a list of threats and conservation actions has been documented.

Table 6: Statistics of the IUCN Red List database

Kingdom	Animalia	Chromistra	Fungi	Plantae	Total
Extinct	777			131	908
Extinct in the Wild	36			45	81
Critically Endangered	4 067	4	45	5 915	10 031
Endangered	6 426	1	105	11 477	18 009
Vulnerable	7 165	1	178	9 937	17 281
Conservation Dependent	18			114	132
Near Threatened	5 149		66	4 203	9 418
Least Concern	51 689		240	33 373	85 302
Data Deficient	15 895	12	160	5 811	21 878
Total	91 222	18	794	71 006	163 040

Source: IUCN (2024a), www.iucnredlist.org & Author's calculations.

Table 7: Number of species assessed and number of threatened species by major group of organisms

Taxon	Clade	Number of species	Evaluated species #	Evaluated species %	Threatened species #	Threatened species %
Vertebrates	Mammals	6 701	5 983	89.3%	1 338	22.4%
	Birds	11 195	11 195	100.0%	1 354	12.1%
	Reptiles	12 162	10 309	84.8%	1 844	17.9%
	Amphibians	8 744	8 011	91.6%	2 873	35.9%
	Fishes	36 863	27 972	75.9%	3 927	14.0%
	Subtotal	75 665	63 470	83.9%	11 336	17.9%
Invertebrates	Insects	1 053 578	12 718	1.2%	2 415	19.0%
	Molluscs	86 859	9 111	10.5%	2 451	26.9%
	Crustaceans	90 531	3 213	3.5%	747	23.2%
	Corals	5 623	831	14.8%	252	30.3%
	Arachnids	95 894	774	0.8%	272	35.1%
	Velvet Worms	222	11	5.0%	9	81.8%
	Horseshoe Crabs	4	4	100.0%	2	50.0%
	Others	157 543	1 090	0.7%	174	16.0%
	Subtotal	1 490 254	27 752	1.9%	6 322	22.8%
Plants	Mosses	21 925	327	1.5%	181	55.4%
	Ferns and Allies	11 800	821	7.0%	321	39.1%
	Gymnosperms	1 113	1 059	95.1%	451	42.6%
	Flowering Plants	369 000	68 704	18.6%	26 367	38.4%
	Green Algae	13 960	17	0.1%	0	0.0%
	Red Algae	7 523	78	1.0%	9	11.5%
	Subtotal	425 321	71 006	16.7%	27 329	38.5%
Fungi	Mushrooms, etc.	156 313	794	0.5%	328	41.3%
	Brown Algae	4 683	18	0.4%	6	33.3%
	Subtotal	160 996	812	0.5%	334	41.1%
	Total	2 152 236	163 040	7.6%	45 321	27.8%

Source: IUCN (2024b, Table 1a), www.iucnredlist.org & Author's calculations.

It is usually expressed in %:

$$\text{TH} (\%) = \frac{\text{TH}}{\text{TOT} - \text{EX} - \text{DD}} = \frac{\text{EW} + \text{CR} + \text{EN} + \text{VU}}{\text{TOT} - \text{EX} - \text{DD}}$$

where TOT is the total number of species assessed[25]. We deduce that:

$$\text{TH} = 81 + 10\,031 + 18\,009 + 17\,281 = 45\,402$$

In Table 7 we reproduce the calculations that can be found in IUCN (2024b, Table 1a). In this case, the number of threatened species does not include the EW category, which means that:

$$\text{TH}^{\star} = 10\,031 + 18\,009 + 17\,281 = 45\,321$$

The percentage of threatened species is 27.8%. Excluding the clades with low population numbers, we conclude that two categories are particularly threatened: Amphibians and flowering plants with a threat rate of 35.9% and 38.4% respectively. Figure 8 shows the evolution of the number of threatened species over time. Over the past 24 years, the number of threatened species has increased by 310%, which corresponds to an annual growth rate of 6.1%. This graph is widely cited and can be found in numerous publications on the current biodiversity crisis. However, caution is needed. A significant part of this trend is due to the fact that the database has become more comprehensive over time. For instance, the IUCN Red List aims to assess 260 000 species and reassess 142 000 of those already assessed by 2030. Naturally, the number of threatened species will rise as the database's coverage increases. For this reason, we have included the proportion of threatened species in Figure 9. Since 2010, this proportion has remained stable at around 30%.

However, the previous observation could not hide the fact that the current biodiversity crisis is real and serious, and that we may be in a sixth mass extinction period. There are so many facts that demonstrate this critical situation (Barnosky *et al.*, 2011; Ceballos *et al.*, 2015; Cowie *et al.*, 2022). A major challenge in addressing the current biodiversity crisis is the concept of '*extinction debt*' (Kuussaari *et al.*, 2009; Figueiredo *et al.*, 2019). This refers to the delayed extinction of species following environmental changes such as habitat loss, fragmentation or degradation. Despite these threats, species may persist for years, decades, or even centuries before succumbing to extinction. This lag creates a debt, where species are essentially doomed, but survive temporarily in their environment. Therefore, extension debt is related to habitat loss and relaxation time:

> "*The idea that species can initially survive habitat change but later become extinct without any further habitat modification has a long history. It was first conceptualized in island biogeography (MacArthur and Wilson, 1967) and further elaborated by Jared Diamond, who introduced the term relaxation time as the delay of expected extinctions after habitat loss. According to theoretical predictions and supporting empirical data, the relaxation time increases with increasing patch area and with decreasing isolation. A second root stems from metapopulation modeling. Tilman et al. (1994) introduced the term extinction debt and considered the order of extinctions in relation to competitive dominance [...] The concept of extinction debt is related to relaxation time but specifies the number or proportion of extant species predicted to become extinct as the species community reaches a new equilibrium after an environmental perturbation.*" (Kuussaari et al., 2009, page 565).

---

[25]Sometimes the IUCN gives a lower and an upper bound for the estimated percentage of threatened species: $\text{LB} (\%) \leq \text{TH} (\%) \leq \text{UB} (\%)$ where $\text{LB} (\%) = \frac{\text{TH}}{\text{TOT} - \text{EX}} = \frac{\text{EW} + \text{CR} + \text{EN} + \text{VU}}{\text{TOT} - \text{EX}}$ and $\text{UB} (\%) = \frac{\text{TH}}{\text{TOT} - \text{EX}} = \frac{\text{EW} + \text{CR} + \text{EN} + \text{VU} + \text{DD}}{\text{TOT} - \text{EX}}$.

Figure 8: Number of species in the threatened categories (CR, EN, and VU)
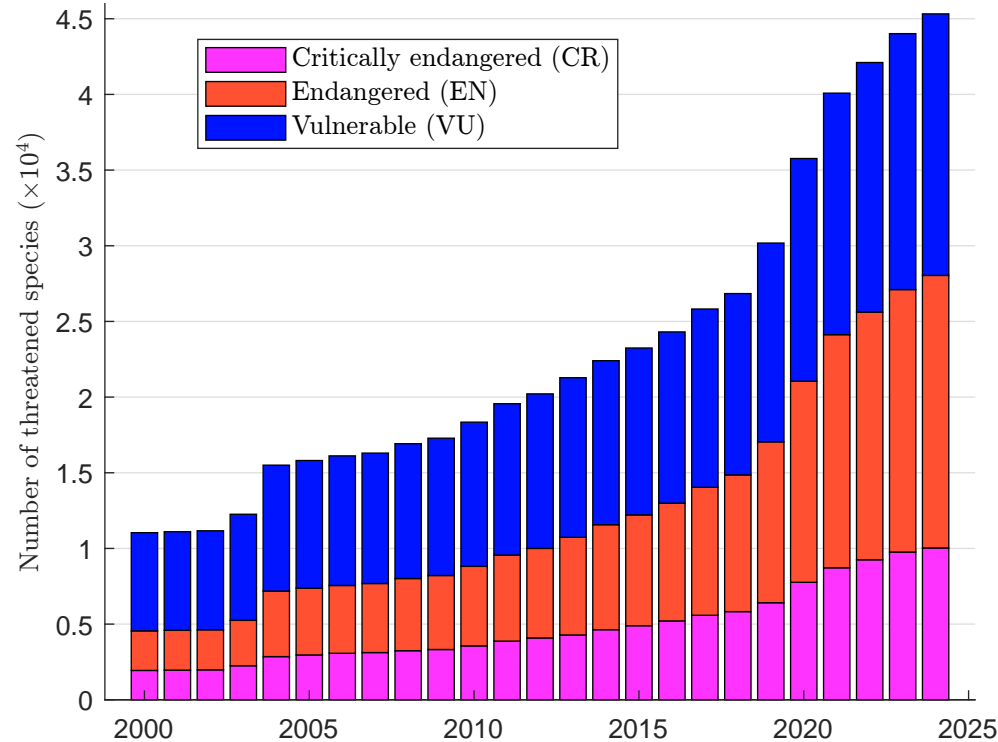
Figure 9: Percentage of species in the threatened categories (CR, EN, and VU)
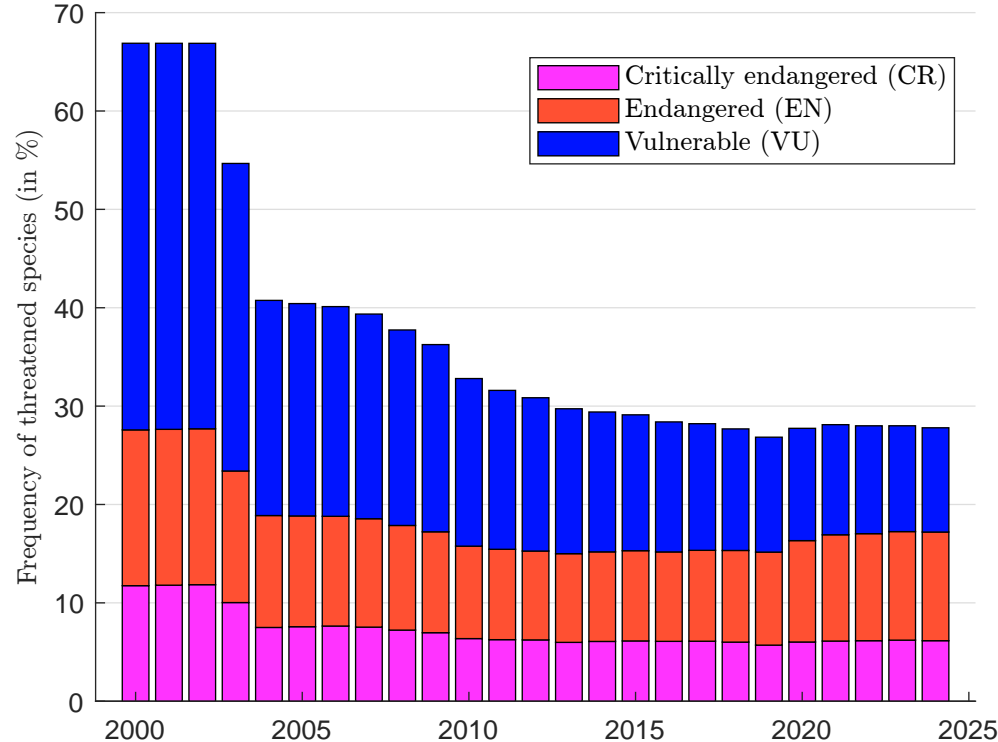
The issue of habitat loss is explored on page 75, while the issue of relaxation time[26] can be described as follows. Kuussaari et al. (2009, Glossary, page 564) defined the equilibrium (or stable) state in an ecological community when the number of species does not change because the local extinction rate is equal to the local origination rate. The relaxation time scale is then the time to reach a new equilibrium. Assessing the extinction debt for a given species involves estimating whether the species will eventually go extinct and, if so, determining the likely time of extinction. Kuussaari et al. (2009, Box 1, page 567) outline five main approaches for evaluating extinction debt:

- Detection of extinction debt using past and present habitat characteristics;

- Estimating extinction debt by comparing present-day stable and unstable landscapes;

- Estimating extinction debt based on past and present species richness and habitat characteristics;

- Tracking extinction debt based on time series data;

- Evaluating extinction debt for single species using empirical population data and spatially explicit modeling.

The survey of empirical studies on extinction debt by Kuussaari et al. (2009, Table 1, page 568) found inconsistencies across these approaches. For instance, studies using the first approach typically conclude that amphibians are subject to extinction debts, while studies using the second approach often suggest that amphibians are not subject to extinction debts. However, empirical evidence consistently suggests that forest birds, primates, wood-living fungi, and forest beetles are likely to have extinction debts.

In Halley et al. (2016b), it is assumed that the remaining habitat area is reduced from A_0 to A, leading to a corresponding decline in species richness to a new value $S(t)$ at time t. The equation governing species loss is given by:

$$\frac{\mathrm{d}S(t)}{\mathrm{d}t} = \lambda(t) - \mu(t)S(t) \tag{4}$$

where $\lambda(t)$ is the origination rate and $\mu(t)$ is the extinction date. The remaining habitat contains a (constant) number $N(t)$ of individuals, which is proportional to the area A and the density ρ of individuals per unit area: $N(t) = \rho A$. Let $n(t) = N(t)/S(t)$ be the average population size per species. At time $t = 0$, we have $n = N_0/S_0 = \rho A/S_0$ where $S(0) = S_0$ is the initial species richness. The authors further assumed that the extinction rate is described by:

$$\mu(t) = kn(t)^{-\alpha} = k\left(\frac{S(t)}{N(t)}\right)^\alpha$$

Therefore, Equation (4) becomes:

$$\frac{\mathrm{d}S(t)}{\mathrm{d}t} = \lambda(t) - k\left(\frac{S(t)}{\rho A}\right)^\alpha S(t) = \lambda(t) - \frac{k}{n^\alpha S_0^\alpha}S(t)^{\alpha+1} \tag{5}$$

The numerical solution can be easily found when the origination rate $\lambda(t)$ is specified. In the case of extinction debt, we can assume that $\lambda(t) = 0$ and the solution is[27]:

$$S(t) = S_0\left(1 + \frac{k\alpha}{n^\alpha}t\right)^{-1/\alpha} \tag{6}$$

---

[26]The concept of relaxation time is used extensively in equilibrium temperature modeling (see Roncalli (2025, pages 671 and 683)) and bifurcation theory (see Roncalli (2025, page 692).

[27]This is derived from the known solution of the differential equation $x'(t) = -bx(t)^{\alpha+1}$ with initial condition $x(0) = x_0$, which is $x(t) = \left(\alpha bt + x_0^{-\alpha}\right)^{-1/\alpha}$.

Figure 10 shows the evolution of the relative species richness for various values of α with fixed parameters $A = 500$, $k = 0.20$, $\rho = 0.90$ and $S_0 = 100$. As the value of α approaches 0, the solution converges to the exponential model, which assumes species richness is independent of population size. In this case we have $S(t) = S_0 e^{-kt}$. When α approaches 1, we obtain the neutral model, where species richness remains constant over time: $S(t) = S_0$. In the other cases $\alpha \in (0, 1)$, the extinction curve follows a hyperbolic trajectory. To understand the effect of time, Halley *et al.* (2016b) examine the case $\alpha = 0.5$ and show that the extinction debt is inversely proportional to the square of time:
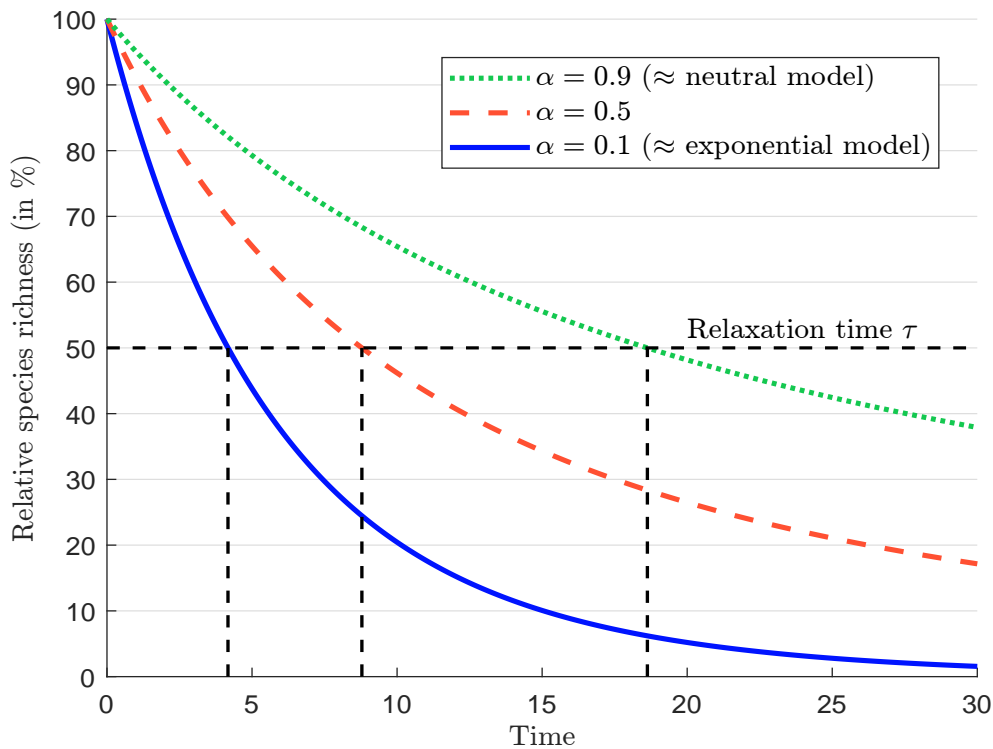
$$S(t) = \frac{S_0}{\left(1 + \dfrac{k}{2\sqrt{n}}t\right)^2} \sim \frac{2S_0}{k^2}t^{-2}$$

Extinction debt is typically quantified by the relaxation time τ, which represents the time required for species richness to decrease by half. Solving the equation $S(t) = S_0/2$ gives the following solution:

$$S_0 \left(1 + \frac{k\alpha}{n^\alpha}\tau\right)^{-1/\alpha} = \frac{S_0}{2} \Leftrightarrow \tau = (2^\alpha - 1)\frac{n^\alpha}{k\alpha} \propto n^\alpha$$

In the previous example, τ is equal to 4.2, 8.8 and 18.6, respectively.

Figure 10: Relative species richness and relaxation time

The previous analysis assumes no speciation, which means that the equilibrium species richness $\bar{S} = \lim_{t \to \infty} S(t)$ ultimately approaches zero. To get a more realistic model, we now introduce a constant origination rate: $\lambda(t) = \lambda$. The equilibrium state $\bar{S}$ is reached when the rate of change in species richness becomes zero:

$$\frac{\mathrm{d}S(t)}{\mathrm{d}t} = 0 \Leftrightarrow \lambda - \frac{k}{n^\alpha S_0^\alpha}\bar{S}^{\alpha+1} = 0 \Leftrightarrow \bar{S} = \left(\frac{\lambda n^\alpha S_0^\alpha}{k}\right)^{1/(\alpha+1)}$$

This is the value of the steady state after the reduction of the area to A. Before reducing the area, the steady state $\bar{S}_0$ satisfies the following equation:

$$\lambda - \frac{k}{n_0^\alpha \bar{S}_0^\alpha} \bar{S}_0^{\alpha+1} = 0 \Leftrightarrow \bar{S}_0 = \left(\frac{\lambda (\rho A_0)^\alpha}{k} \right)^{1/(\alpha+1)}$$

because the original habitat area was A_0 and $n_0 = \rho A_0 / \bar{S}_0$. In Figure 11 we illustrate the transition from one steady state to another. We use the following parameters: $A_0 = 1000$, $A = 500$, $k = 0.10$, $\alpha = 0.5$, $\rho = 10$ and $\lambda = 5\%$. Initially, at time $t = -1000$ years, we consider two starting values for species richness: $S(-1000) = 15$ and $S(-1000) = 12$. Both trajectories converge to the steady state value $\bar{S}_0 = 13.572$. At time $t = 0$, we reduce the available habitat by 50%, causing the species richness to shift to a new steady state $\bar{S}_0 = 10.772$. However, it takes time, and the transition between the two equilibria is not instantaneous. It is gradual, resulting in what is known as an extinction debt. The key challenge is to determine whether we are in the early or late stages of this extinction debt process.

Figure 11: Extinction debt and steady state
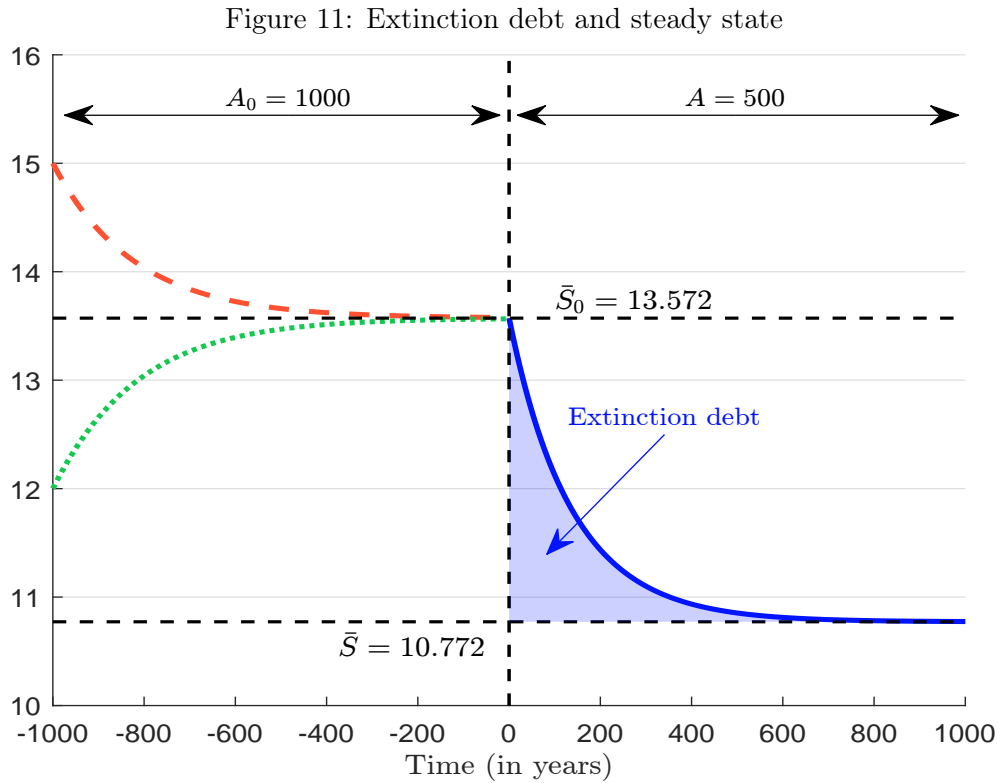
Remark 3 *The modeling of extinction debt, particularly in relation to the current biodiversity crisis, has generated extensive research. Notable contributions include the work of Tilman et al. (1994), Hanski and Ovaskainen (2002, 2003), and more recently, Spalding and Hull (2021) with the pulse event model (Box 4).*

Box 4: The Spalding-Hull pulse model

Spalding and Hull (2021) extended the constant birth-death model by introducing extinction pulses:

$$\mu^{(\text{pulse})}(t) = \mu_0 - \sum_{k=1}^{n^{(\text{pulse})}} \omega_k^{(\text{pulse})} \ln\left(1 - A_k^{(\text{pulse})}\right) f_k\left(t - t_k^{(\text{pulse})}\right)$$
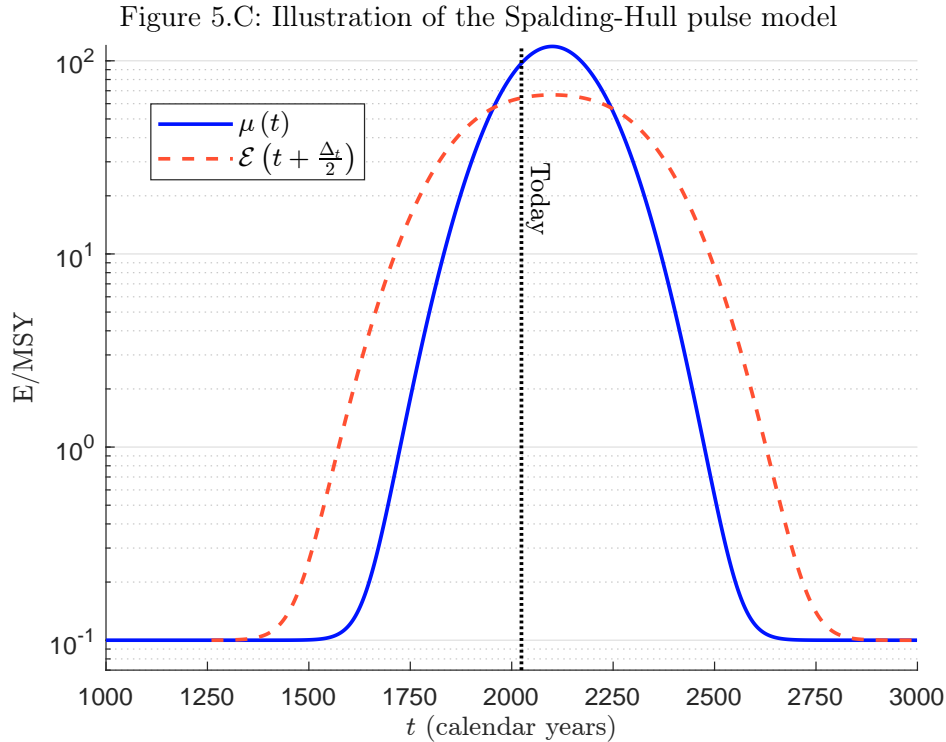
where μ_0 is the background rate, $n^{(\text{pulse})}$ is the number of pulses, $\omega_k^{(\text{pulse})}$, $A_k^{(\text{pulse})}$ and $t_k^{(\text{pulse})}$ are the scaling factor, the fraction of species removed and the date of the kth extinction pulse event, and $f_k(x)$ is the probability density function. For example, Spalding and Hull (2021) used the Gaussian single pulse model:

$$\mu^{(\text{pulse})}(t) = \mu_0 - \omega^{(\text{pulse})} \frac{\ln\left(1 - A^{(\text{pulse})}\right)}{\sigma\sqrt{2\pi}} \exp\left(-\frac{1}{2}\left(\frac{t - t^{(\text{pulse})}}{\sigma}\right)^2\right)$$

where σ is the standard deviation controlling the pulse duration. We deduce that:

$$
\begin{aligned}
\mathcal{E}(t) &= \frac{1}{\Delta t} \int_t^{t+\Delta t} \mu^{(\text{pulse})}(s)\ \mathrm{d}s \\
&= \mu_0(s) - \frac{\omega^{(\text{pulse})} \ln\left(1 - A^{(\text{pulse})}\right)}{\Delta t}\left(\Phi\left(\frac{t + \Delta t - t^{(\text{pulse})}}{\sigma}\right) - \Phi\left(\frac{t - t^{(\text{pulse})}}{\sigma}\right)\right)
\end{aligned}
$$

Using the following parameters: $\mu_0 = 0.1\,\text{E/MSY}$, $\omega = 10^5$, $A^{(\text{pulse})} = 30\%$, $\sigma = 120$ years, and $t^{(\text{pulse})} = 2100$ years AD, we obtain the results given in Figure 5.C.

Figure 5.C: Illustration of the Spalding-Hull pulse model


Lecture Notes on Biodiversity

1.3 Biodiversity hotspot

A biodiversity hotspot is a region of the world that is both rich in plant and animal species and highly threatened by human activities. Specifically, it is characterized by the following two criteria:

- Exceptional levels of endemism: The region must have at least 1 500 species of vascular plants that are endemic, meaning that they are found nowhere else on Earth;

- High levels of habitat loss: The region must have lost at least 70% of its original natural vegetation, typically due to human activities such as deforestation, agriculture, or urbanization.

The term biodiversity hotspot was coined by Norman Myers, who identified 10 geographic regions as conservation priorities (Myers, 1988). This list has been updated twice by Norman Myers: 18 hotspots in 1990 and 25 hotspots in 2000 (Myers, 1990; Myers et al., 2000). New publications have updated this list several times (Mittermeier et al., 2011). The last update is done by Noss et al. (2015), who included the North American Coastal Plain. Today we recognize 36 biodiversity hotspots (Figure 12).

Figure 12: The 36 biodiversity hotspots
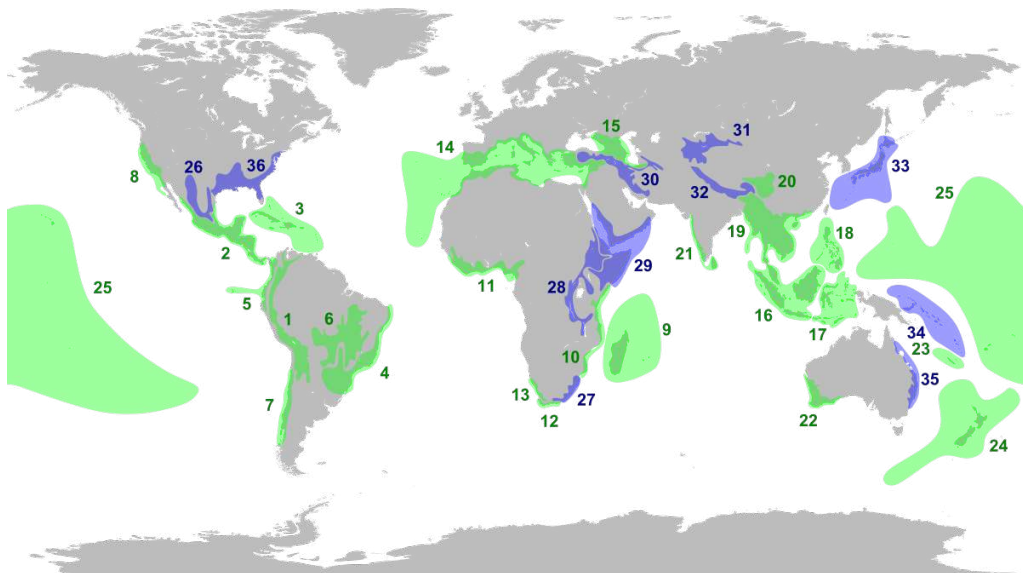
The 25 original biodiversity hotspots identified by Myers et al. (2000) are in green, while the added eleven regions are in blue. The 36 regions are (1) Tropical Andes, (2) Mesoamerica, (3) Caribbean Islands, (4) Atlantic Forest, (5) Tumbes-Chocó-Magdalena, (6) Cerrado, (7) Chilean Winter Rainfall-Valdivian Forests, (8) California Floristic Province, (9) Madagascar and the Indian Ocean Islands, (10) Coastal Forests of Eastern Africa, (11) Guinean Forests of West Africa, (12) Cape Floristic Region, (13) Succulent Karoo, (14) Mediterranean Basin, (15) Caucasus, (16) Sundaland, Indonesia and Nicobar islands of India, (17) Wallacea of Indonesia, (18) Philippines, (19) Indo-Burma, Bangladesh, India and Myanmar, (20) Mountains of Southwest China, (21) Western Ghats and Sri Lanka, (22) Southwest Australia, (23) New Caledonia, (24) New Zealand, (25) Polynesia-Micronesia, (26) Madrean pine-oak woodlands, (27) Maputaland-Pondoland-Albany, (28) Eastern Afromontane, (29) Horn of Africa, (30) Irano-Anatolian, (31) Mountains of Central Asia, (32) Eastern Himalaya, (33) Japan, (34) East Melanesian Islands, (35) Eastern Australian temperate forests, and (36) North American Coastal Plain.

Source: upload.wikimedia.org/wikipedia/commons/9/93/Biodiversity_Hotspots.svg.

These biodiversity hotspots cover only 2.5% of the Earth's land surface, but support more than half of the world's endemic plant species. As shown in Figure 12, many of these hotspots are concentrated around the tropics. Biodiversity is unevenly distributed across the Earth's surface, a pattern known as the biodiversity gradient. This concept refers to the variation in species diversity across geographic regions, often along specific environmental gradients. The most common example is the latitudinal biodiversity gradient, which describes how species richness generally increases as one moves from the poles toward the equator (Willig *et al.*, 2003). As noted by Gaston and Spicer (2004, Section 3.4, pages 71-85), it is hard to explain this phenomenon[28], understand the causes and draw general conclusions.

In fact, biodiversity hotspots are often characterized by a high extinction debt because they frequently host species that are on a delayed extinction pathway due to past habitat destruction. These regions are at high risk of losing species in the future, even if no additional habitat loss occurs. The existence of an extinction debt makes conservation efforts in hotspots particularly urgent, as many species may already be committed to extinction. Fragmentation and isolation in these areas exacerbate the problem by weakening the long-term survival chances of species. Therefore, unless immediate action is taken, biodiversity hotspots may face significant hidden biodiversity loss and a substantial extinction debt.

2 Ecosystem functions and services

2.1 Definition

Ecosystem functions are natural processes, such as nutrient cycling, while ecosystem services are the benefits humans derive from these processes, such as food:

> "*In our increasingly technological society, people give little thought to how dependent they are on the proper functioning of ecosystems and the crucial services for humanity that flow from them. Ecosystem services are* "the conditions and processes through which natural ecosystems, and the species that make them up, sustain and fulfill human life" *(Daily, 1997, page 3); in other words,* "the set of ecosystem functions that are useful to humans" *(Kremen, 2005, page 468). Although people have been long aware that natural ecosystems help support human societies, the explicit recognition of* "ecosystem services" *is relatively recent (Mooney and Ehrlich, 1997).*" (Sekercioglu, 2010, page 45).

Sekercioglu (2010) classified ecosystem services into 6 categories: (1) climate and biogeochemical cycles (climate stability, air purification, UV protection), (2) regulation of the hydrological cycle (drought mitigation, flood mitigation, water purification), (3) soils and erosion (detoxification and decomposition of wastes, soil formation and soil fertility), (4) biodiversity and ecosystem function (ecosystem goods), (5) mobile linkages (pollination, seed dispersal), and (7) nature's remedies for emerging diseases (medicine, pest control). For his part, Gaston and Spicer (2004, Chapter 4) made

---

[28]Gaston and Spicer (2004, pages 72 and 73) highlights four key features of the latitudinal biodiversity gradient:

- Persistence: The latitudinal gradient has been a consistent feature throughout much of Earth's history;

- Equatorial Peak: The peak of biodiversity often occurs slightly off-center from the equator;

- Asymmetry: The gradient often shows an asymmetric pattern, with a steeper increase from northern regions toward the equator and a more gradual decrease from the equator to southern regions;

- Steepness variation: The steepness of the gradient can vary considerably among taxonomic groups. For example, butterflies are more tropical than birds.

the distinction between direct-use and indirect-use values of ecosystem services. The direct-use value describes the role of biological resources in consumption or production and mainly concerns commodities such as food, medicine and industrial materials. This category also includes biological control, recreational use (*e.g.*, hunting and fishing), and ecotourism. Indirect-use values are more related to ecosystem functions such as atmospheric regulation, climate regulation, hydrological regulation, nutrient cycling, pest control, pollination, and soil formation and maintenance.

One of the first classifications of ecosystem services was developed by Millennium Ecosystem Assessment (2005, Table 1, page 7 & Box 3.1, page 50). They distinguished 4 families: supporting, provisioning, regulating and cultural services. However, they emphasized the main role of supporting ecosystem services (nutrient cycling, soil formation, primary production), which is essential for the other three ecosystem services[29]. In other words, without supporting ecosystem services, there is no life. The major report of IPBES (2019, Glossary, page 1031) adopted a different classification based on three categories: material (corresponding to provisioning services), regulating (corresponding to the merger of supporting and regulating services), non material (corresponding to cultural services). This three-category system has also been adopted by ENCORE (2024) and TNFD (2023, page 28), which distinguish between (1) provisioning, (2) regulation and maintenance, and (3) cultural services. However, the categorization between the last three systems changes relatively when we consider the Level 2 system[30]. Below is a list of the different ecosystem services described in the 4 classification systems:

1. Aesthetic and cultural services

   - Aesthetic, symbolic and spiritual values (nature inspires creativity, provides spiritual connections, and contributes to cultural identity)
   - Cultural and spiritual significance (many ecosystems have deep cultural, historical or spiritual significance for local communities and indigenous peoples)
   - Educational, scientific and research services (biodiversity provides opportunities for scientific study and learning)
   - Recreational opportunities and tourism (forests, parks and other natural areas provide opportunities for recreation and tourism)
   - Visual amenity services (non-material benefits that contribute to well-being, emotional satisfaction, and cultural enrichment)

2. Provisioning services

   - Energy (natural processes by which ecosystems produce energy such as biomass, solar energy capture, and fossil fuels)
   - Food and feed (agriculture, biomass supply, fisheries, plants, animals, seafood, and livestock)
   - Genetic resources (biodiversity provides genetic material essential for breeding crops and livestock, and developing new technologies)

---

[29]Provisioning services include food, freshwater, timber, wood, fiber, fuel, and genetic resources; regulating services include the regulation of climate, floods, disease, water quality, and waste management; and cultural services include recreation, aesthetic enjoyment, education, and spiritual fulfillment.

[30]In the case of ENCORE, the classification system is described in the two CSV files of the 2024 zipped database: `ENCORE knowledge base/Encore files/02. Ecosystem services definition.csv` and `ENCORE knowledge base/Encore files/08. Ecosystem services and ecosystem components.csv`. A comparison of the three systems (IPBES, ENCORE and TNFD) can be found in NGFS (2024, Table 1, page 45).

- Medicinal and biochemical resources (many medicines and pharmaceutical products are derived from natural compounds found in biodiversity)
- Raw materials (timber, fuel wood, minerals, fibers, and other natural resources)
- Water supply (clean water for drinking, irrigation, and industrial use)

3. Regulating services

- Air quality regulation (ecosystems filter pollutants from the air, improving air quality)
- Climate regulation (forests absorb carbon dioxide and help regulate global temperatures)
- Waste detoxification and decomposition (natural decomposition of organic matter, natural ability to detoxify harmful chemicals and pollutants)
- Erosion control (vegetation helps stabilize soils, reducing erosion and preventing landslides)
- Hazard and extreme event regulation (flood, storm, rainfall)
- Pest and disease control (natural predators and parasites help regulate populations of harmful organisms)
- Pollination and seed dispersal (bees, birds, insects, and other pollinators allow many plants to reproduce)
- Water purification (freshwater, wetlands, and forests filter pollutants from water)

4. Supporting services

- Habitat creation and maintenance (habitats are the natural environments in which organisms live, grow, and reproduce; they form the basis of ecosystems by providing the resources necessary for species to thrive)
- Nutrient cycling (the movement of nutrients through ecosystems, essential for plant growth and productivity)
- Photosynthesis (plants convert solar energy into chemical energy, producing oxygen and forming the base of the food chain)
- Primary production (the production of organic material by plants and algae forms the foundation of ecosystems)
- Soil formation and fertility (the breakdown of rocks and organic matter to create soil)
- Water cycle regulation (ecosystems play an important role in regulating the water cycle, from evaporation to precipitation)

Rather than examining all of these ecosystem services, we focus on two of them (pollination and food) to illustrate the importance of ecosystem functions. We also develop the concept of natural capital, which is essential for valuing these ecosystem services.

2.2 Natural capital

Ecosystem services are derived from natural capital, which can be defined as the world's stock of natural assets, including geology, soil, air, water, and all living things. The concept of natural capital in biodiversity is generally attributed to David Pearce, an environmental economist, with his work on the economics of sustainable development (Pearce, 1988). However, the concept itself draws on earlier ideas in ecological economics[31]. For example, the underlying idea of natural capital can be

---

[31]For a historical perspective on natural capital in economics, the reader can refer to Åkerman (2003) and Missemer (2018).

found in the extension of input-output models[32] proposed by Daly (1968), who argued that biology and economics are not two separate sciences but need to be integrated:

> "*The purpose of this essay is to bring together some of the more salient similarities between biology and economics and to argue that, far from being superficial, these analogies are profoundly rooted in the fact that the ultimate subject matter of biology and economics is one, viz., the life process.*" (Daly, 1968, page 392).

However, the concept was really popularized by Robert Costanza in 1997 and his seminal paper on the valuation of ecosystem services and natural capital (Costanza *et al.*, 1997). The definition of natural capital has remained largely consistent since Pearce (1988), for whom natural capital is "*the set of all environmental assets*". Costanza and Daly (1992) used the stock-flow model to define capital as a stock that provides a flow of valuable goods or services into the future. In this context, natural capital and natural income are simply the stock and flow components, respectively, of natural resources. Today, natural capital is broadly recognized as the stock of environmental assets and ecosystem services that provide goods and services to humans and life. The challenge, once this definition is accepted, is to determine the full extent of these assets and services and to value them accurately.

Table 8: Total value of annual ecosystem services in 1997 (1995 price levels)

Biome	Area (in ha $\times 10^6$)	Value (in \$/ha/yr)	Total value (in \$ bn/yr)	Breakdown (in %)
Marine	36 302	577	20 949	63.0
Open ocean	33 200	252	8 381	25.2
Coastal	3 102	4 052	12 568	37.8
Terrestrial	15 323	804	12 319	37.0
Forest	4 855	969	4 706	14.1
Grassland & meadow	3 898	232	906	2.7
Wetland	330	14 785	4 879	14.7
Lake & river	200	8 498	1 700	5.1
Desert	1 925			
Tundra	743			
Ice & rock	1 640			
Cropland	1 400	92	128	0.4
Urban	332			
Total	51 625		33 268	100.0

Source: Costanza *et al.* (1997, Table 2, page 256) & Author's calculations.

The publication of Costanza *et al.* (1997) marked a milestone in the valuation of natural capital. They estimated that the value of ecosystem services was in the range of \$16–\$54 trillion per year, with an average of \$33 tn/yr in 1995. Given that world GDP was \$28 trillion per year, ecosystems would represent 1.2 times the economic value created by humans (Pearce, 1998). The positive reception of the paper published in *Nature* was largely supported by the scientific community, although we can find some criticism of the methodology, the total figure of \$33 tn/yr and the applicability to environmental policy. However, the impact of the paper has been profound, leading to further research on ecosystem service valuation.

---

[32]See Roncalli (2025, Section 8.4.2).

The natural capital $\mathcal{K}$ is the sum of the natural capital $\mathcal{K}_{i,j}$ for n biomes and m ecosystem services:

$$\mathcal{K} = \sum_{i=1}^{n} \sum_{j=1}^{m} \mathcal{K}_{i,j} \tag{7}$$

We can assume that the value of a biome's ecosystem service is proportional to its area:

$$\mathcal{K}_{i,j} = A_i V_{i,j} \tag{8}$$

where A_i is the area of biome i (in hectares) and $V_{i,j}$ is the monetary value of ecosystem service j (in dollars per hectare per year). Therefore, $\mathcal{K}_{i,j}$ and $\mathcal{K}$ are expressed in dollars per year. From Equation (7), we deduce that:

$$\mathcal{K} = \sum_{i=1}^{n} \mathcal{K}_i^{(\text{biome})} = \sum_{j=1}^{m} \mathcal{K}_j^{(\text{service})} \tag{9}$$

where $\mathcal{K}_i^{(\text{biome})} = \sum_{j=1}^{m} A_i V_{i,j} = A_i \sum_{j=1}^{m} V_{i,j}$ and $\mathcal{K}_j^{(\text{service})} = \sum_{i=1}^{n} A_i V_{i,j}$. To calculate $\mathcal{K}_{i,j}$ or $V_{i,j}$, Costanza et al. (1997) estimated the willingness-to-pay of individuals for ecosystem services. For example, if a 10-hectare forest provides $500 per year in market benefits for raw materials and $250 per year in non-market benefits for aesthetic services, the total value of ecosystem services for that forest would be $750 per year or $75\,\text{ha}^{-1}\text{yr}^{-1}$. In Table 8, we report the values of annual ecosystem services for the different biomes estimated by Costanza et al. (1997). Of the $33 tn, 63% comes from marine biomes and 37% from terrestrial biomes. In the case of marine biomes, both open ocean and coastal areas make a significant contribution, the former because of its large area ($33\,200$ ha), the latter because of its high unit value ($4\,052\,\text{ha}^{-1}\text{yr}^{-1}$). In the case of terrestrial biomes, forest and wetland are the two main contributors, the former because of its large area ($4\,855$ ha), the latter because of its high unit value ($14\,785\,\text{ha}^{-1}\text{yr}^{-1}$). Table 9 shows the breakdown of the $33 tn in terms of the 17 ecosystem services examined by the authors. 51.3% comes from nutrient cycling, followed by cultural services at 9.1%, waste treatment at 6.8%, and disturbance regulation at 5.3%.

The previous study has been updated in 2014 using the same methodology, but with a more comprehensive approach to estimate the unit value $V_{i,j}$. In fact, the unit values in Costanza et al. (2014) are based on the TEEB valuation database developed by Van der Ploeg and de Groot (2010), which collected $1\,310$ value estimates from 320 publications. An analysis of this database can be found in De Groot et al. (2012), who selected 665 unit values. For example, using 2007 price levels, they estimate that the mean value of coral reefs is $352\,249\,\text{ha}^{-1}\text{yr}^{-1}$, while the mean value of open oceans is only $491\,\text{ha}^{-1}\text{yr}^{-1}$. Other interesting figures are: $193\,845\,\text{ha}^{-1}\text{yr}^{-1}$ for coastal wetlands, $25\,682\,\text{ha}^{-1}\text{yr}^{-1}$ for coastal wetlands, $5\,264\,\text{ha}^{-1}\text{yr}^{-1}$ for tropical forests, $4\,267\,\text{ha}^{-1}\text{yr}^{-1}$ for lakes and rivers, etc. We report the calculations made by Costanza et al. (2014) for the year 2011 in Table 10. The authors estimated 4 total values of natural capital by considering both 1997 and 2011 figures. Using 2007 price levels[33], they obtained $45.9 tn/yr when considering 2011 biome areas and unit values, $41.6 tn/yr when considering 2011 biome areas and 1997 unit values, $145 tn/yr when considering 1997 biome areas and 2011 unit values, and $124.8 tn/yr when considering 2011 biome areas and unit values. These different figures can be used to assess changes in biome areas and the effect of updated unit values. They concluded that changes in global land use have resulted in a loss of ecosystem services ranging from $4.3 to $20.2 tn/yr.

---

[33]The 1997 study used 1995 prices to calculate unit values. To convert them to 2007 prices, we need to multiply them by a factor of 1.38.

Table 9: Average global value of annual ecosystem services in 1997 (1995 price levels)

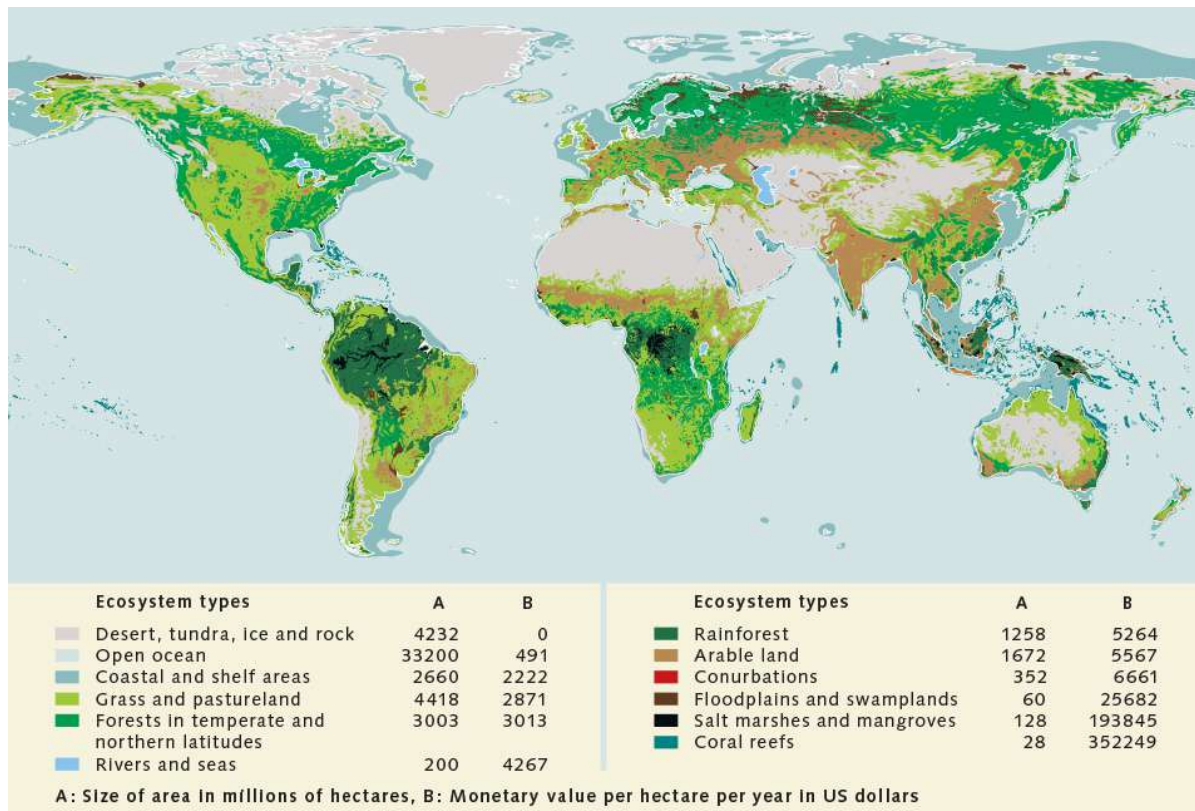| #	Ecosystem service	Ecosystem functions	Value (in $ bn/yr)	Breakdown (in %)
1	Gas regulation	Regulation of atmospheric chemical composition	1341	4.0
2	Climate regulation	Regulation of global temperature, precipitation, and other biologically mediated climatic processes at global or local levels	684	2.1
3	Disturbance regulation	Capacitance, damping, and integrity of ecosystem response to environmental fluctuations	1779	5.3
4	Water regulation	Regulation of hydrological flows	1115	3.4
5	Water supply	Storage and retention of water	1692	5.1
6	Erosion control and sediment retention	Retention of soil within an ecosystem	576	1.7
7	Soil formation	Soil formation processes	53	0.2
8	Nutrient cycling	Storage, internal cycling, processing, and acquisition of nutrients	17075	51.3
9	Waste treatment	Recovery of mobile nutrients and removal or breakdown of excess or xenic nutrients and compounds	2277	6.8
10	Pollination	Movement of floral gametes	117	0.4
11	Biological control	Trophic-dynamic regulations of populations	417	1.3
12	Refugia	Habitat for resident and transient populations	124	0.4
13	Food production	That portion of gross primary production extractable as food	1386	4.2
14	Raw materials	That portion of gross primary production extractable as raw materials	721	2.2
15	Genetic resources	Sources of unique biological materials and products	79	0.2
16	Recreation	Providing opportunities for recreational activities	815	2.4
17	Cultural	Providing opportunities for non-commercial uses	3015	9.1
	Total		33 268	100.0

Source: Costanza et al. (1997, Table 2, page 256) & Author's calculations.

Table 10: Changes in annual ecosystem services between 1997 and 2011

	Area (in hectare)		Unit values (in \$/ha/yr)		Total value (in \$/yr)				
Price levels			2007	2007	1995	2007	2007	2007	2007
Area	1997	2011			1997	1997	2011	1997	2011
Unit values			1997	2011	1997	1997	1997	2011	2011
Marine	36 302	36 302	796	1 368	20.9	28.9	29.5	60.5	49.7
Open Ocean	33 200	33 200	348	660	8.4	11.6	11.6	21.9	21.9
Coastal	3 102	3 102	5 592	8 944	12.6	17.3	18.0	38.6	27.7
Terrestrial	15 323	15 323	1 109	4 901	12.3	17.0	12.1	84.5	75.1
Forest	4 855	4 261	1 338	3 800	4.7	6.5	4.7	19.5	16.2
Grassland	3 898	4 418	321	4 166	0.9	1.2	1.4	16.2	18.4
Wetland	330	188	20 404	140 174	4.9	6.7	3.4	36.2	26.4
Lake & river	200	200	11 727	12 512	1.7	2.3	2.3	2.5	2.5
Cropland	1 400	1 672	126	5 567	0.1	0.2	0.2	7.8	9.3
Urban	332	352		6 661				2.2	2.3
Total	51 625	51 625			33.3	45.9	41.6	145.0	124.8
Difference							−4.3		−20.2

Source: Costanza *et al.* (2014, Table 3, page 156) & Author's calculations.

Figure 13: World map with the different ecosystem types and the calculated values of their ecosystem services (in US dollars per hectare per year)

Ecosystem types	A	B
Desert, tundra, ice and rock	4232	0
Open ocean	33200	491
Coastal and shelf areas	2660	2222
Grass and pastureland	4418	2871
Forests in temperate and northern latitudes	3003	3013
Rivers and seas	200	4267

Ecosystem types	A	B
Rainforest	1258	5264
Arable land	1672	5567
Conurbations	352	6661
Floodplains and swamplands	60	25682
Salt marshes and mangroves	128	193845
Coral reefs	28	352249

A: Size of area in millions of hectares, B: Monetary value per hectare per year in US dollars

Source: World Ocean Review (2015, Figure 1.12, page 27).

Remark 4 *Since 1997, the valuation of ecosystem services has been widely adopted by scientists, organizations and policy makers[34] (Hein et al., 2020; Legesse et al, 2022). The following are some of the frameworks, projects and initiatives for the valuation of ecosystem services[35]: System of Environmental-Economic Accounting (SEEA), Common International Classification of Ecosystem Services (CICES), The Economics of Ecosystems and Biodiversity (TEEB), Natural Capital Accounting and Valuation of Ecosystem Services (NCAVES).*

Box 5: The System of Environmental-Economic Accounting (SEEA)

The System of Environmental-Economic Accounting (SEEA), endorsed by the United Nations, is a framework that integrates economic and environmental data to provide a comprehensive view of the interactions between the economy and the environment, and the stocks and flows of environmental assets. It establishes common concepts, definitions, classifications, and accounting rules, to enable the production of internationally comparable statistics and accounts. The SEEA framework follows an accounting structure similar to the System of National Accounts (SNA), ensuring coherence with traditional economic accounting practices. The SEEA is modular, with each module addressing a specific topic. The SEEA central framework develops the rules and guidelines for measuring the relationship between the environment and the economy, focusing on three key areas: environmental flows (changes in natural assets), stocks of environmental assets (measurement of natural assets) and economic activity related to the environment (monetary economic flows related to natural assets). The four main modules are:

- Ecosystem accounting (SEEA EA) with 4 types of accounts: ecosystem extent accounts, ecosystem condition accounts, ecosystem services flow accounts (physical and monetary), and monetary ecosystem asset accounts;

- Agriculture, forestry and fisheries with two types of accounts: flow accounts and asset accounts (both physical and monetary);

- SEEA-Energy with two types of accounts: flow accounts and asset accounts (both physical and monetary);

- SEEA-Water with three types of accounts: physical flow accounts, physical asset accounts and economic accounts.

In addition, four other modules have been developed on air emissions, environmental activities, land and material flow accounts. Examples of SEEA accounts can be found at seea.un.org/content/projects.

In January 2020, the World Economic Forum published a series of reports aimed at "*providing pathways for business to be part of the transition to a nature-positive economy*". In particular, World Economic Forum (2020a) estimated that \$44 trillion of economic value creation — more than half of global GDP — is moderately or highly dependent on nature[36]. Among the 163 economic

---

[34] World maps of ecosystem valuation, such as Figure 13, are very common in academic and policy publications.

[35] The corresponding websites are seea.un.org, www.cices.eu, www.teebweb.org, and seea.un.org/home/natural-capital-accounting-project.

[36] The exact figures are \$31 tn or 37% of the world GDP for moderately dependent industries and \$13 tn or 15% of the world GDP for highly dependent industries.

sectors considered in the study, construction (\$4 tn), agriculture (\$2.5 tn), and food and beverages (\$1.4 tn) are the three largest industries most dependent on nature. The impact on secondary and tertiary sectors can also be significant through their supply chains. This publication was followed by several public studies in 2021 showing how GDP creation is strongly linked to biodiversity[37]. These reports consistently highlight that the link between GDP and biodiversity is currently poorly understood, while the economic and financial risks posed by biodiversity loss are enormous.

2.3   Pollination service

Pollination is the process by which pollen is transferred from the male part of a flower (the anther) to the female part (the stigma) of the same or another flower. This is a crucial step in the reproductive cycle of many plants, as it leads to the production of seeds and fruits. There are two main types of pollination:

1. Self-pollination, in which pollen from one flower is transferred to the stigma of the same flower. For example, many crops and fruit trees are self-pollinating, including aubergines, barley, beans, cauliflower, lentils, lettuce, olives, onions, peppers, potatoes, soybeans, tomatoes, rice, and wheat;

2. Cross-pollination, when pollen is transferred from the anther of one flower to the stigma of a flower on another plant of the same species. Examples include apples, blackberries, black-currants, broccoli, carrots, cacao, daffodils, lavender, pears, plums, pumpkins, raspberries, strawberries, and tulips.

We also distinguish three methods of cross-pollination:

1. Abiotic pollination involves natural transport phenomena such as wind, water, and rain. Examples of wind-pollinated plants include conifers, grasses, and many trees.

2. Biotic pollination requires living pollinators to move pollen from one flower to another. Most pollinators are insects (ants, beetles, bees, butterflies, flies, wasps and moths), but some are vertebrates (bats, birds, *e.g.*, honeyeaters and hummingbirds).

3. Hand pollination (also known as mechanical or human pollination) is a technique in which humans manually transfer pollen from the male to the female plant. Examples of plants that are commonly hand pollinated include corn, cucumbers, melons, vanilla, and zucchini.

These classifications are only theoretical. Most plants are pollinated in more than one way. For example, a self-pollinating species may also be pollinated by animals or by hand. Similarly, 100% of apples are not 100% animal pollinated. Olhnuud *et al.* (2022) showed that the animal-dependent pollination rate varies from species to species (*e.g.*, Gala vs. Golden apple) and from region to region (*e.g.*, Asia vs. Europe).

By analyzing data of 137 single crops and 115 commodity[38] crops provided by FAO, Klein *et al.* (2007) identified 124 major crops (57 single crops and 67 commodity crops) used for human food with significant annual production, representing 99% of total world food production. They

---

[37]We can cite Dasgupta (2021), OECD (2021) and Svartzman *et al.* (2021) among others.

[38]A single crop refers to a specific plant species. A commodity, on the other hand, represents a group of different crop species. For instance, the fresh vegetables category as defined by the FAO includes 21 distinct crops, such as celery and rhubarb. Similarly, other commodity categories include fresh fruits (15 crops, including litchi and pawpaw), fresh tropical fruits (17 crops, including guava and passion fruit), roots and tubers (8 crops, such as yam bean and topinambur), and pulses (6 crops, including guar bean and velvet bean).

Box 6: The story of the original vanilla bean

The Chinantla Forest is considered the birthplace of vanilla, and the vanilla plant, or vine, is native to Mexico. There, the vines grew and flourished without the help of humans. Wild vanilla is naturally pollinated by melipona bees and small hummingbirds found only in Mexico. Before 1850, all vanilla beans came from the forests of Mexico, and France was the number one importer of the '*black flower*'. The Aztecs, and the Mayans before them, believed that the scent of vanilla could help them communicate with the gods and had long mastered the fermentation techniques needed to cure the beans. They cultivated '*tlilxotchitl*' or black flowers so that the flavors could be combined with cocoa and coffee. In 1521, Cortés was the first European to bring the dark pods or beans back to Charles Quint. Vanilla beans first arrived in France in 1664. Later, Louis XIV fell in love with the taste of vanilla and wanted vanilla beans to be grown on the island of Réunion, then known as Bourbon Island. But until the mid-19th century, vanilla beans were still only made in Mexico. Although the technique of curing the beans was known, pollination of the flower was not. In 1836 and 1841, Charles Morren, a Belgian botanist, and Edmond Albius, a slave on Réunion Island discovered how to bypass bee pollination by manually pollinating vanilla flowers. Soon after, vanilla plants were exported by the French to plantations in Tahiti, Madagascar, Mauritius, Réunion Island, and the Comoros.

Text reproduced from www.epices-roellinger.com.

estimated that 70% of these major crops depend on animal pollination (87 crops), 23% do not rely on animal pollination (28 crops), while 7% have not been evaluated (9 crops). Despite this, in terms of global production in 2004, these three categories contributed 35%, 60%, and 5%, respectively. This is because the four largest crops (sugar cane, corn, wheat, and rice) do not require animal pollination, but represented more than 50% of global crop production in 2004. Klein *et al.* (2007) also created a classification of the pollination dependence of different crops. They considered a crop to be pollinator dependent if animal pollination is required to increase the quantity and/or quality of fruits or seeds directly consumed by humans. Alternatively, a crop is considered non-dependent if it is pollinated either abiotically (wind) or autogamously (self-fertilizing). They created five categories:

1. Essential
   Animal pollinators are essential for most varieties, otherwise we observe a reduction in production of more than 90%, comparing experiments with and without animal pollinators;

2. High
   Animal pollinators are strongly needed (40 to less than 90% reduction);

3. Modest
   Animal pollinators are clearly beneficial (10 to less than 40% reduction);

4. Little
   Some evidence suggests that animal pollinators are beneficial (greater than 0 to less than 10% reduction);

5. No increase
   No increase in production with animal pollination.

Table 11 shows the classification found by Klein *et al.* (2007, Supplemental Material 2) (103 crops) and updated by Aizen *et al.* (2019, Appendix S1) (11 additional crops).

Table 11: How dependent are foods on pollinator insects?

No dependency	Yields are not affected by pollinators
	Cereals: barley, maize, millet, oats, rice, rye, sorghum, wheat
	Roots and tubers: carrots, cassava, potatoes, sweet potatoes
	Legumes including chickpeas, lentils, peas
	Fruit and veg including bananas, grapes, lettuce, pepper, pineapples
	Sugar crops: sugar beet, sugar cane
	Also includes areca nuts, asparagus, broccoli, cabbages, castor oil seed, cauliflower, chicory roots, dates, garlic, hazelnuts, jojoba seeds, leeks, olives, onions, pistachios, quinoa, spinach, taro, triticale, walnuts, yams
Little dependency	**Yield reduction of 0% to 10% without pollinators**
	Fruits and veg including lemons, limes, oranges, papayas, tomatoes
	Oilcrops including linseed, palm oil, poppy seed, safflower seed
	Legumes including beans (dry & green), cow peas, pigeon peas
	Groundnuts
	Also includes bambara beans, chillies, clementines, grapefruit, mandarins, persimmons, string beans, tangerines
Modest dependency	**Yield reduction of 10% to 40% without pollinators**
	Oilcrops including mustard seed, rapeseed, sesame, sunflower seed
	Soybeans
	Fruits including currants, egglant, figs, gooseberries, strawberries
	Coconuts and okra
	Coffee beans
	Also includes broad beans, chestnut, karite nuts, seed cotton
High dependency	**Yield reduction of 40% to 90% without pollinators**
	Fruits including apples, apricots, blueberries, cherries, cranberries, guavas, mangoes, nectarines, peaches, plums, pears, raspberries
	Nuts including almonds, cashew nuts, kola nuts
	Avocados
	Also includes anise, badian, buckwheat, coriander, cucumber, fennel, nutmeg
Essential	**Yield reduction greater than 90% without pollinators**
	Fruits including kiwi, melons, pumpkins, watermelons
	Cocoa beans
	Brazil nuts
	Also includes quinces, vanilla

Box 7: Who are animal pollinators?

Bees are the most important group of animal pollinators. There are an estimated 20 000 species of bees (family *Apidae*), but only nine species of honey bees are recognized and form the genus *Apis* (*Apidae; Apinae; Apini; Apis*). The Western honey bee (*Apis mellifera*) is the most common honey bee and the one most often domesticated for honey production. The other species are *Apis andreniformis*, *Apis cerana* (Asiatic honey bee), *Apis dorsata* (Giant honey bee), *Apis florea* (Little honey bee), *Apis koschevnikovi*, *Apis laboriosa* (Himalayan honey bee), *Apis nigrocincta* and *Apis nuluensis*. We generally distinguish between honey bees that are managed by humans and wild bees. There are many species in the latter category, but the most important are Bumble bees (*Apidae; Apinae; Bombini*), Carpenter bees (*Apidae; Xylocopinae*), Stingless bees (*Apidae; Apinae; Meliponini*), and solitary bees such as sand bees (family *Andrenidae; Andreninae; Andrena*) or nomad bees (*Apidae; Nomadinae; Nomadini; Nomada*). Bees are generally attracted to yellow (and blue) flowers.

Non-bee insects also play a significant role in global crop pollination. For instance, Rader *et al.* (2016) found that approximately 40% of visits to crop flowers are made by non-bee insects. In fact, butterflies and moths (order *Lepidoptera*) are the second most important group of animal pollinators. Other insects that contribute to pollination include ants (family *Formicidae*), beetles (order *Coleoptera*), and flies (order *Diptera*). In the case of ants, pollination typically occurs in low-growing flowers positioned close to the stem. Examples of ant-pollinated plants include small's stonecrop (*Diamorpha smallii*), alpine nailwort (*Paronychia pulvinata*), and cascade knotweed (*Polygonum cascadense*). Butterflies have excellent color vision, which explains why they are attracted to red, orange, yellow, blue and purple flowers. Moths, on the other hand, prefer pale or white flowers because they tend to come out at night.

The primary pollinators of cacao are tiny flies from the families of biting midges (*Ceratopogonidae*, including the genus *Forcipomyia*) and, to a lesser extent, gall midges (*Cecidomyiidae*). These small flies, sometimes only a few millimeters long, are uniquely suited to pollinate cacao because the reproductive parts of cacao flowers are very small (less than 2 mm) and complex, with structures that make them difficult for larger insects to access.

In addition to insect pollinators, vertebrate pollinators also participate in the reproductive success of plants, especially tropical plants (Ratto *et al.*, 2018). Bird pollinators include hummingbirds (*Trochilidae*), sunbirds (*Nectariniidae*), honeycreepers (*Meliphagidae*), and some parrots. Birds are generally attracted to red, orange, and yellow flowers. Some known bird-pollinated plants include hibiscus, eucalyptus, and some orchids. Bats, like moths, prefer pale or white flowers. They are involved in the pollination of mango, banana, durian, guava, and agave (used to make tequila). While rodents and reptiles are less common vertebrate pollinators, they can still contribute to the reproduction of certain plants.

It is very difficult to estimate the contribution of each species to pollination. However, it is generally accepted that managed honey bees provide 50–75% of agricultural pollination, while wild bees and other pollinators account for the remaining 25–50% (Garibaldi *et al.*, 2013; IPBES, 2016).

Source: www.fs.usda.gov/managing-land/wildflowers/pollinators/who-are-the-pollinators & www.cacaopollination.com/cacao-pollinators.

Using the previous classification, Aizen et al. (2009) estimated that the direct reduction in total agricultural production in the absence of animal pollination would be 5% for developed regions and 8% for developing regions. These figures are based on the production deficit in volume, calculated as:

$$D_t^{(\text{volume})} = \frac{\sum_{i=1}^n P_{i,t} - \sum_{i=1}^n P_{i,t}\left(1 - \delta_i\right)}{\sum_{i=1}^n P_{i,t}} = \frac{\sum_{i=1}^n P_{i,t}\delta_i}{\sum_{i=1}^n P_{i,t}} = \sum_{i=1}^n w_{i,t}\delta_i \tag{10}$$

where n is the number of crops, $P_{i,t}$ is the volume production in metric tonnes of crop i in year t, $w_{i,t}$ is the weight of crop i in the total agricultural production, δ_i is the dependency rate, which is equal to 0% for crops that are not dependent on animal pollinators and 100% for crops that are completely dependent on animal pollinators[39]. Aizen et al. (2009) also calculated the percentage increase in area needed to compensate for the production deficit:

$$A_t^{(\text{compensation})} = \frac{\sum_{i=1}^n \frac{A_{i,t}}{1 - \delta_i} - \sum_{i=1}^n A_{i,t}}{\sum_{i=1}^n A_{i,t}} = \frac{\sum_{i=1}^n A_{i,t}\frac{\delta_i}{1 - \delta_i}}{\sum_{i=1}^n A_{i,t}} = \sum_{i=1}^n w_{i,t}\frac{\delta_i}{1 - \delta_i} \tag{11}$$

where $A_{i,t}$ is the cultivated area (in hectares) of crop i in year t and $(1 - \delta_i)^{-1} A_{i,t}$ is the area needed to produce $P_{i,t}$ in the absence of pollination[40]. They found that area compensation is 15% in developed regions and 42% in developing regions. Another interesting finding is that production deficit and area compensation have generally increased over time. These different results are mainly explained by the fact that human diets have changed over time and that human diets today are more diversified than fifty years ago, with more vegetables and fruits being consumed. In addition, the low figures for production deficit are mainly due to the importance of cereals in the human diet, while the high figures for area compensation are mainly due to the greater area needed to cultivate crops that depend on animal pollination, e.g., apples, avocados, cocoa, mangoes, peaches. In terms of volume and metric tonnes, the production yield of the first category is higher than that of the second. However, it's worth considering whether a volume-based analysis is the most appropriate approach to assess the importance of pollinators. For example, 1 kg of wheat and 1 kg of tomatoes provide different nutritional values, suggesting that volume alone may not accurately reflect their contribution to human well-being. Eilers et al. (2011) conducted a similar analysis using the same data and methodology but focused on the nutritional value of crops instead of volume. Let $V_{j,t}^{(\text{nutritional})}$ be the total amount of nutrient j in year t. We have:

$$V_{j,t}^{(\text{nutritional})} = \sum_{i=1}^n V_{i,j}^{(\text{nutritional})} P_{i,t}\left(1 - R_i\right) \tag{12}$$

where $V_{i,j}^{(\text{nutritional})}$ is the amount of nutrient j in a metric tonne of crop i, $P_{i,t}$ is the volume production in tonnes of crop i in year t, and R_i is the proportion of crop i that is not consumed by humans due to inedible parts, such as pits, stems, or shells. We can decompose $V_{j,t}^{(\text{nutritional})}$ into three components: $V_{j,t}^{(1)} = \sum_{i=1}^n \mathbb{1}\left\{\delta_i = 0\right\} \cdot V_{i,j}^{(\text{nutritional})} P_{i,t}\left(1 - R_i\right)$ is the nutritional value of pollinator-independent crops; $V_{j,t}^{(2)} = \sum_{i=1}^n \mathbb{1}\left\{\delta_i > 0\right\} \cdot \left(1 - \delta_i\right) V_{i,j}^{(\text{nutritional})} P_{i,t}\left(1 - R_i\right)$ is the nutritional value of pollinator-dependent crops due to abiotic and self-pollination; $V_{j,t}^{(3)} = \sum_{i=1}^n \mathbb{1}\left\{\delta_i > 0\right\} \cdot \delta_i V_{i,j}^{(\text{nutritional})} P_{i,t}\left(1 - R_i\right)$ is the nutritional value of pollinator-dependent crops attributed to animal pollination alone. Results are shown in Table 12, where the key metric to consider

---

[39] Aizen et al. (2009) used the following values for δ_i: 0%, 5%, 25%, 65% and 95% for no, little, modest, high and essential dependency classes.

[40] We assume that production is proportional to area: $P_{i,t} \propto A_{i,t}$.

is $V_{j,t}^{(3)}$ (last column). In terms of energy (calories) and protein, about 80% of the human diet comes from pollinator-independent crop production. The proportion attributed to crop production dependent on animal pollination is low, at less than 3%. Similar figures are observed for minerals, except for fluoride and calcium, where the proportions attributed to animal pollination are 19.83% and 9.11%, respectively. The most significant effects of animal pollination are observed for vitamins[41], especially vitamin A (41.03%), carotene (about 40%), certain forms of vitamin E (about 20%) and vitamin C (19.64%). We conclude that animal pollination has a significant impact on human diets by contributing to nutritional diversification, particularly at the vitamin level.

Table 12: Proportion in % of nutrients derived from pollinator-independent and pollinator-dependent crops

Nutrient		$V_{j,t}^{(1)}$	$V_{j,t}^{(2)}$	$V_{j,t}^{(3)}$
Macro-nutrients	Energy	78.83	18.59	2.58
	Protein	83.43	13.57	3.00
	Fat	26.02	66.98	7.00
Vitamins	A	28.71	30.26	41.03
	β-carotene	27.44	34.19	38.37
	α-carotene	32.25	29.83	37.92
	β-cryptoxanthin (carotene)	0.77	56.99	42.24
	Lycopene (carotene)	0.00	56.67	43.33
	Lutein & Zeaxanthin (carotene)	94.05	3.92	2.03
	E (α-tocopherol)	63.73	28.94	7.33
	E (β-tocopherol)	0.63	72.50	26.87
	E (γ-tocopherol)	32.92	52.66	14.42
	E (δ-tocopherol)	14.87	62.50	22.63
	K	71.55	19.28	9.17
	C	6.99	73.37	19.64
	B1 (Thiamin)	95.29	4.00	0.71
	B2 (Riboflavin)	97.66	1.92	0.42
	B3 (Niacin)	89.46	8.93	1.61
	B5 (Pantothenic acid)	87.57	9.34	3.09
	B6	97.93	1.58	0.49
	B9 (Folate)	55.49	37.19	7.32
Minerals	Calcium	42.40	48.49	9.11
	Iron	70.66	23.14	6.20
	Magnesium	88.50	9.06	2.44
	Phosphorus	89.06	8.72	2.22
	Potassium	72.74	20.93	6.33
	Sodium	87.18	8.63	4.19
	Zinc	91.80	6.54	1.66
	Copper	80.92	15.21	3.87
	Mangan	93.87	4.94	1.19
	Selenium	97.46	1.97	0.57
	Fluoride	45.57	34.60	19.83

Source: Eilers et al. (2011, Table 1, page 2011).

---

[41]Vitamin A is essential for vision, vitamin C is a powerful antioxidant and vital for collagen production, vitamin E plays a role in immune function, and carotenes act as precursors to vitamin A.

Another interesting figure is that 308 000 out of a total of 352 000 flowering plants are partially or totally pollinated by animals, which represents a proportion of 87.5% (Ollerton *et al.*, 2011). These species, known as angiosperms (*Angiospermae*), include many fruit trees and flowers such as roses and tulips. While the primary benefits of these species are food and medicine, they also provide secondary benefits such as reducing pest populations and improving soil and water quality. Another important service is the enhancement of rural aesthetics and the provision of cultural and visual amenities (Wratten *et al.*, 2012; Dicks *et al.*, 2021). Without bees and butterflies, the world would not be the same, and many blue, orange, pink, purple, red, violet and yellow flowers would disappear, as these pollinators are essential for their reproduction. The loss of these vibrant flowers would have a significant impact on the beauty of natural landscapes.

Figure 14: Trend in the number of bee colonies (1961–2022)
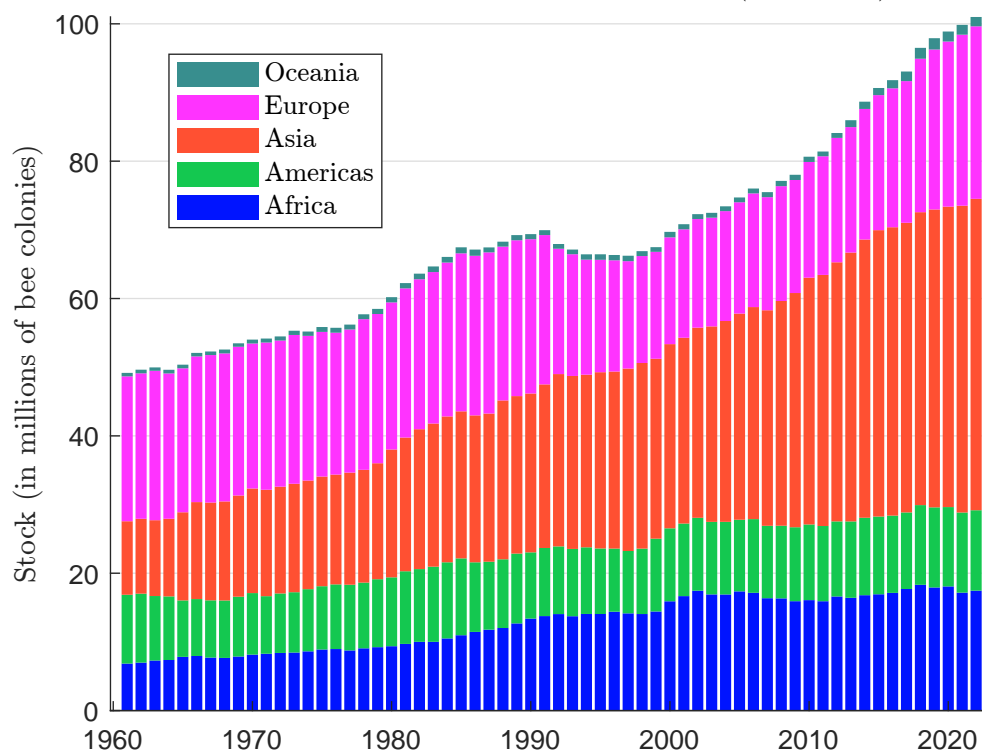
Source: www.fao.org/faostat/en/#data/QCL & Author's calculations.

Potts *et al.* (2010) alerted the scientific community and policy makers to the global decline of pollinators and its potential impact on human well-being:

> "*Pollinators are a key component of global biodiversity, providing vital ecosystem services to crops and wild plants. There is clear evidence of recent declines in both wild and domesticated pollinators, and parallel declines in the plants that rely upon them.*" (Potts *et al.*, 2010, page 345).

It is challenging to accurately define pollinator decline, as data can sometimes initially be contradictory. For example, Potts *et al.* (2010) reported declines in honey bee populations in the United States (59% loss of colonies between 1947 and 2005) and Central Europe (25% loss of colonies between 1985 and 2005). Globally, however, the number of managed honey bee colonies has increased over the past six decades. From 1965 to 2015, production of pollinator-dependent crops has increased by 300% (IPBES, 2016, page XXI). This increase is mainly due to the growing presence

Table 13: Regional distribution of managed honey bee colonies (in millions)

Region	Stock (in million colonies)				Growth (in %)	
	1961	1980	2000	2022	1961–2022	2000–2022
Europe	21.10	21.42	15.55	25.12	19.1	61.6
Western Europe	3.76	3.35	2.45	3.55	−5.5	45.3
Northern Europe	0.44	0.40	0.27	0.64	45.6	138.3
Eastern Europe	14.02	13.71	7.36	10.66	−24.0	44.8
Southern Europe	2.87	3.95	5.47	10.27	257.3	87.6
Americas	10.02	10.03	10.62	11.71	16.9	10.2
Northern America	5.85	4.75	3.22	3.40	−41.9	5.5
Central America	2.26	2.80	2.19	2.68	18.5	22.3
Caribbean	0.23	0.32	0.28	0.40	72.5	45.8
South America	1.67	2.16	4.94	5.23	212.4	6.0
Africa	6.85	9.37	15.92	17.46	155.1	9.7
Asia	10.70	18.61	26.82	45.34	323.6	69.1
Oceania	0.51	0.76	0.80	1.36	168.7	70.9
World	49.17	60.20	69.71	101.00	105.4	44.9

Source: www.fao.org/faostat/en/#data/QCL & Author's calculations.

of fruits in human diets (such as tropical and seasonal fruits). However, many pollinator species are listed as vulnerable, endangered or critically endangered on the IUCN Red List. In fact, we need to distinguish between managed honey bees and other animal pollinators. According to FAO statistics[42], the number of managed bee colonies has doubled between 1961 and 2022 (Figure 14). In 1961, there were 49.2 million colonies, while today there are more than 100 million (Table 13). Most of this growth has occurred in Asia (+324%), Africa (+155%), Southern Europe (+257%) and South America (+212%). Below is a regional breakdown of colony numbers:

Year	Europe	America	Africa	Asia	Oceania
1961	42.9%	20.4%	13.9%	21.8%	1.0%
2022	24.9%	11.6%	17.3%	44.9%	1.3%

Asia now accounts for 45% of the global market, followed by Europe with 25%. Three regions have experienced a decline in honey bee populations over the last sixty years: North America (−41.9%), Eastern Europe (−24.0%), and Western Europe (−5.5%). However, in the past 20 years, they have reversed this trend, showing positive growth. The current problem is not the decline of honey bee colonies, but the dramatic decline of insects worldwide. For example, Hallmann et al. (2017) measured a decline in total flying insect biomass of more than 75 percent over 27 years in 63 German protected areas. Sánchez-Bayo and Wyckhuys (2019) estimate that 40% of the world's insect species could become extinct in the next few decades. The case of butterflies, for example, is dramatic, as shown by Warren et al. (2021), who studied the status of butterflies in the United Kingdom, the Netherlands, and Belgium:

> "[...] In the United Kingdom, 8% of resident species have become extinct, and since 1976 overall numbers declined by around 50%. In the Netherlands, 20% of species have become extinct, and since 1990 overall numbers in the country declined by 50%. Distribution

---

[42]The data can be obtained from the FAO website: www.fao.org/faostat/en/#data/QCL. Select the domain *Crops and livestock products*, then the item *Live Animals/Bees* and the element *Stocks*.

trends showed that butterfly distributions began decreasing long ago, and between 1890 and 1940, distributions declined by 80%. In Flanders (Belgium), 20 butterflies have become extinct (29%), and between 1992 and 2007 overall numbers declined by around 30%. A European Grassland Butterfly Indicator from 16 European countries shows there has been a 39% decline of grassland butterflies since 1990. The 2010 Red List of European butterflies listed 38 of the 482 European species (8%) as threatened and 44 species (10%) as near threatened [...]." (Warren *et al.*, 2021, page 1).

According to Butterfly Conservation[43], 80% of butterfly species have declined in abundance or distribution since the 1970s. In the United States, the situation is even worse than in Europe, where some butterfly species have experienced declines of up to 2% per year in the recent period (Thogmartin *et al.*, 2017; Wepprich *et al.*, 2019). In fact, the decline of wild bees and other pollinators cannot be compensated by an increase in honeybees because they play different roles in crop pollination and do not visit plants in the same way or at the same time (Rader *et al.*, 2016). Therefore, crop yield and quality depend on pollinator biodiversity.

The drivers and risks associated with pollinator decline have been extensively reviewed in the 2016 report of the Intergovernmental Science-Policy Platform on Biodiversity and Ecosystem Services (IPBES). A summary can be found in Potts *et al.* (2016). According to IPBES (2016, Chapter 2, pages 30–149), there are five main drivers of change in pollination networks:

1. Land use and its change ("*It is well established that habitat loss and degradation [...] affect pollinator diversity, abundance and richness. These changes can negatively affect community stability, pollination networks and the survival and evolutionary potential of pollinator and plant species.*")

2. Pesticides, GMOs, veterinary medicines and pollutants ("*It is clear that pollinators may be exposed to a wide range of pesticides in both agricultural and urban environments. The risk posed by pesticides is driven by a combination of the toxicity (hazard) and the level of exposure; [...] Insecticides are toxic to insect pollinators and their exposure, and thus the risk posed, is increased if, for example, labels do not provide use information to minimise pollinator exposure or the label is not complied with by the pesticide applicator.*")

3. Pollinator diseases and pollinator management ("*Bee management is a global and complex driver of pollinator loss. Spreading of diseases by managed honey bees and bumble bees into wild bee species has been shown to present a threat to some wild species and populations.*")

4. Invasive alien species ("*Invasive predators can directly kill pollinators or disrupt pollinator communities and associated pollination systems, whilst invasive pollinators can outcompete or transmit diseases to native pollinator species or simply be accommodated in the existing pollinator assemblage.*")

5. Climate change ("*Many plant and pollinator species have moved their ranges, altered their abundance, and shifted their seasonal activities in response to observed climate change over recent decades.*")

Using this classification, Dicks *et al.* (2021) conducted a formal expert elicitation process to assess the regional and global importance of these drivers. Results are presented in Table 14. Globally, land cover and management are the most important drivers of pollinator decline, followed by pesticide

---

[43]See the latest report *The State of the UK's Butterflies 2022*, available at www.butterfly-conservation.org/state-of-uk-butterflies-2022.

Table 14: Assessment of the importance of the top eight drivers of pollinator decline

Drivers	Africa	Asia Pacific	Australasia	Europe	Latin America	North America	Global
Land cover	○ (large)	● (large)	◐ grey (large)	● (large)	● (large)	◐ grey (large)	● (large)
Land management	◐ grey (small)	● (large)	◐ grey (large)	● (largest)	● (large)	● (large)	● (large)
Pesticide use	◐ grey (large)	● (large)	◐ grey (med)	◐ grey (large)	● (large)	◐ grey (large)	◐ grey (large)
Climate change	◐ grey	◐ grey	◐ grey	◐ grey	◐ grey	◐ grey	◐ grey
Pests and pathogens	◐ grey (small)	◐ grey	◐ grey (small)	●	◐ grey	◐ grey	◐ grey
Pollinator management	◐ grey (small)	◐ grey	◐ grey	◐ grey	◐ grey	○	◐ grey
Invasive alien species	◐ grey (small)	◐ grey	○ (large)	◐ grey (small)	◐ grey	○	◐ grey
Genetically modified crops	◐ grey (tiny)	◐ grey	◐ grey	◐ grey	◐ grey (large)	○	◐ grey

The circle size is proportional to the importance score between 1 (not important) and 4 (the most important). The circle color corresponds to the confidence score: ● = well established, ◐ grey = established but incomplete, and ○ = inconclusive.

Source: Dicks *et al.* (2021, Figure 2, page 1457 & Supplementary Table 2).

use. Climate change, pests and pathogens, pollinator management and invasive alien species are also important, but to a lesser extent, and contribute equally. GMOs are the least important driver. However, there are some strong differences between regions. Pesticide use is very important in Asia Pacific and Latin America. In Europe and North America, land management is the most important issue. The impact of these changes can be divided into two main categories:

- Impact on food production (pollination deficits, yield instability, honey production, food security, wild fruit availability, managed pollinators)

- Impact on biocultural diversity (wild pollinator and plant diversity, aesthetic and cultural values)

Although we have some estimates of these risks, it is currently difficult to predict the future trajectory of pollination ecosystem services and the consequences for human quality of life. The conclusion of Dicks *et al.* (2021) summarized perfectly what science can say about this issue: "*Despite extensive research on pollinator decline, our analysis reveals considerable scientific uncertainty about what this means for human society.*" Regarding the impact on food production, the future is not entirely bleak, especially with the potential for hand pollination and advancements in robotic pollination. The impact on biocultural diversity is more complex and harder to address.

2.4 Food and feed service

There are several ways to look at food and feed in the context of biodiversity. Food biodiversity refers to the diversity of plants, animals and other organisms used for human consumption. It can be analyzed from two main perspectives. From a production perspective, food biodiversity describes the supply of food in terms of volume (*e.g.*, tonnes produced). From a consumption perspective, it describes the demand for food in terms of nutrient intake, such as calories, proteins, vitamins and minerals. Additional approaches can be explored, such as comparing farmed foods to wild foods, examining the diversity of local versus global food systems, or exploring sustainable versus conventional agricultural practices.

The main source of food is agriculture, which involves food production managed by humans. Historically, wild foods were the sole component of human diets. Today, the proportion of food production attributed to wild foods is relatively small compared to agricultural sources, although it continues to play an important role in certain communities, particularly for indigenous peoples, in certain regions, and in some rural areas[44]. Therefore, we will only consider non-wild foods for which data have been collected by the FAO since 1961 and are freely available for more than 245 countries.

2.4.1 Food production

World production of primary crops reached 9.61 billion tonnes in 2022 (Table 15). Since 1961, this figure has been multiplied by a factor of 3.78, representing an annual growth rate of 2.2% over the past sixty years. Cereals and sugar crops account for 31.8% and 22.7% of global production, respectively, while fruits, roots and tubers, and vegetables each contribute approximately 10%. In Table 15 we have also reported the top 20 crops by production. We see that sugar cane has the largest share, accounting for 20% of global primary crop production. In second place is maize with 12.11%. This is followed by wheat (8.41%), rice (8.08%), and oil palm (4.42%). The top five crops account for more than 50% of total production, the top 10 for about 70%, and the top 20 for more than 80%. This indicates a high concentration of production in a small number of crops. In Figure 15, we present the Lorenz curve for the 162 crops in the FAO database. The graph confirms the previous findings and highlights the high concentration, as 10% of the crops account for 80% of the total production volume. Moreover, this lack of diversity is the same in 2022 as it was in 1961, but this does not mean that the structure of crop production has not changed. In fact, we observe that the market shares are very different between 1961 and 2022. For example, potatoes represented 10.7% of total production in 1961, but only 3.9% today. The shares of corn, oil palm fruits, soybeans, onions, cucumbers, yams, and rapeseed have increased significantly, while the shares of sugar beets, barley, and sweet potatoes have experienced notable declines. Figure 16 illustrates the evolution of harvested area over the past sixty years. Between 1961 and 2022, cropland expanded by 51.6%, though this growth was uneven. The period before 2000 saw an annual growth rate of 0.5%, while after 2000, this rate accelerated to 1% per year. As a result, the overall 278% increase in crop production during this period was largely due to productivity gains and shifts in production structure. In Table 15, we report crop yield, which is defined as the ratio between production (expressed in tonnes) and harvested area (expressed in hectares). Yield has increased for all crops, on average by a factor of 2.49. We notice that fruits have a better yield than staples. All these factors explain the dynamics of world crop production.

---

[44]In the early 1990s, it was estimated to be less than 10% worldwide. However, reliable data are lacking. In the European Union, according to Schulp *et al.* (2014), the amount of wild foods collected is very small compared to total food, and the economic and nutritional value of wild foods is a few thousandths of the total consumption. However, wild foods provide an important cultural ecosystem service, as a wide variety of game (38 species), mushrooms (27 species), and vascular plants (81 species) are collected and consumed by more than 100 million EU citizens.

Table 15: World production of primary crops

Crop	Production (in billion tonnes)					1961 breakdown		2022 breakdown		Yield (in t/ha)	
	1961	1980	2000	2020	2022	(in %)	(% cum.)	(in %)	(% cum.)	1961	2022
Primary crops	2.54	4.02	6.14	9.38	9.61	100.00		100.00		2.61	6.49
Cereals	0.88	1.55	2.06	3.00	3.06	34.58		31.84		1.35	4.18
Fruit	0.22	0.40	0.68	1.07	1.10	8.87		11.44		7.62	14.09
Oil crops	0.07	0.15	0.32	0.66	0.68	2.90		7.06		0.33	1.01
Pulses, Roots and Tubers	0.50	0.56	0.75	0.96	1.00	19.56		10.44		4.45	6.02
Sugar crops	0.61	1.00	1.50	2.13	2.18	24.02		22.73		38.16	71.61
Vegetables	0.20	0.29	0.69	1.15	1.17	7.79		12.21		9.34	20.13
Other	0.06	0.06	0.15	0.41	0.41	2.28		4.29			
Sugar cane	0.45	0.73	1.25	1.88	1.92	17.66	17.66	20.00	20.00	50.27	73.67
Maize (corn)	0.21	0.40	0.59	1.16	1.16	8.09	25.75	12.11	32.11	1.94	5.72
Wheat	0.22	0.44	0.59	0.76	0.81	8.77	34.52	8.41	40.52	1.09	3.69
Rice	0.22	0.40	0.60	0.77	0.78	8.50	43.02	8.08	48.60	1.87	4.70
Oil palm fruit	0.01	0.03	0.12	0.42	0.42	0.54	43.56	4.42	53.02	3.77	14.15
Potatoes	0.27	0.24	0.32	0.37	0.37	10.67	54.23	3.90	56.92	12.22	21.07
Soya beans	0.03	0.08	0.16	0.36	0.35	1.06	55.29	3.63	60.55	1.13	2.61
Cassava, fresh	0.07	0.12	0.18	0.31	0.33	2.81	58.10	3.44	63.99	7.40	10.31
Other vegetables, fresh n.e.c.	0.06	0.09	0.21	0.29	0.30	2.46	60.55	3.10	67.09	8.42	14.53
Sugar beet	0.16	0.27	0.25	0.25	0.26	6.33	66.88	2.72	69.81	23.17	60.77
Tomatoes	0.03	0.05	0.11	0.19	0.19	1.09	67.97	1.94	71.74	16.43	37.84
Barley	0.07	0.16	0.13	0.16	0.15	2.86	70.83	1.61	73.36	1.33	3.29
Bananas	0.02	0.04	0.07	0.13	0.14	0.88	71.71	1.41	74.76	10.65	22.75
Onions and shallots	0.01	0.02	0.05	0.11	0.11	0.55	72.26	1.15	75.91	11.68	18.54
Watermelons	0.02	0.03	0.08	0.10	0.10	0.70	72.96	1.04	76.95	9.13	34.27
Apples	0.02	0.03	0.06	0.09	0.10	0.67	73.64	1.00	77.95	9.91	19.86
Cucumbers and gherkins	0.01	0.01	0.04	0.09	0.09	0.38	74.01	0.99	78.94	9.43	43.56
Yams	0.01	0.01	0.04	0.08	0.09	0.33	74.34	0.92	79.85	7.23	8.49
Rape or colza seed	0.00	0.01	0.04	0.07	0.09	0.14	74.48	0.91	80.76	0.57	2.18
Sweet potatoes	0.10	0.14	0.14	0.09	0.09	3.87	78.36	0.90	81.66	7.35	11.92

Source: www.fao.org/faostat/en/#data/QCL & Author's calculations.

Figure 15: Lorenz curve of world crop production
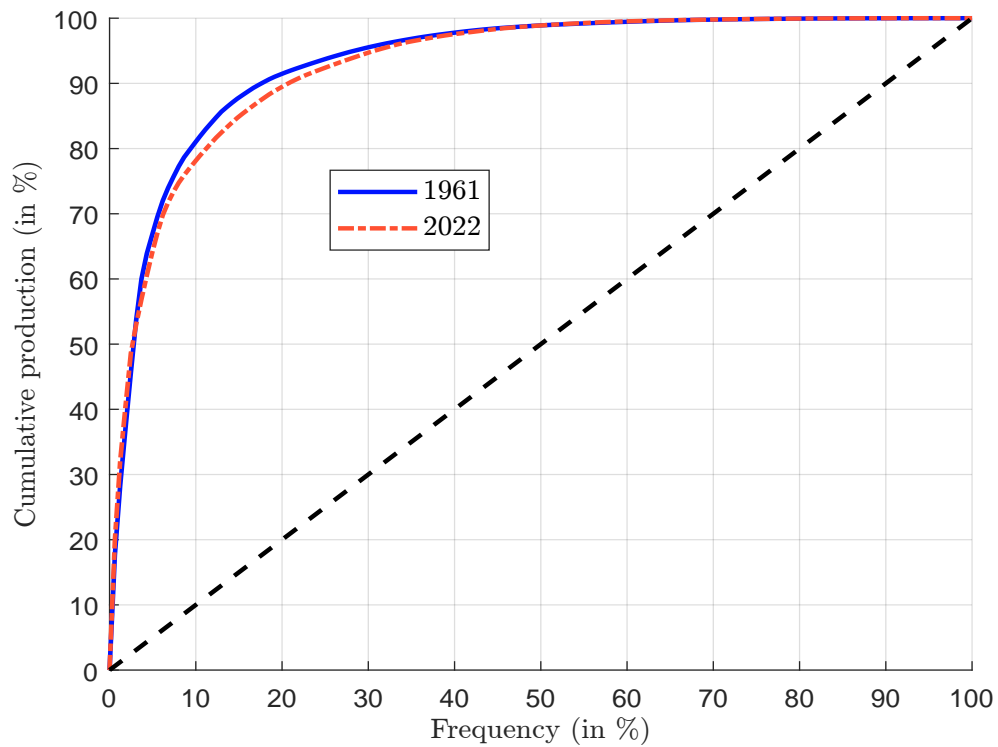
Figure 16: Harvested area for crop production
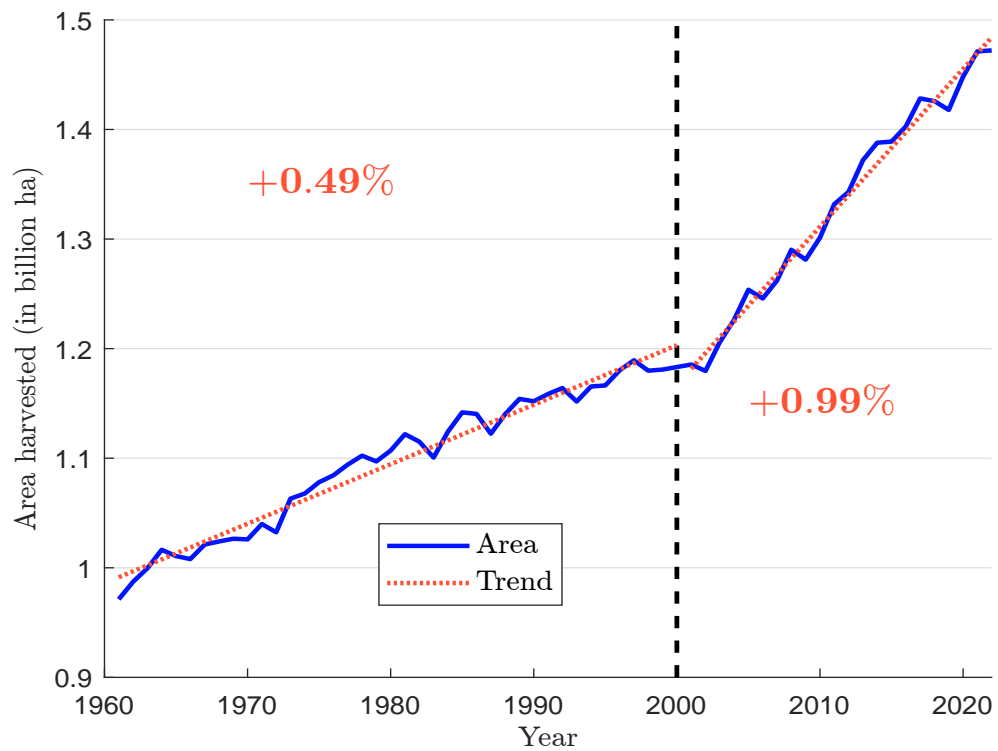
We now look at livestock production (Table 16). Like crops, livestock has experienced remarkable growth: $+1\,456\%$ for poultry meat, $+517\%$ for eggs, $+395\%$ for pork meat, etc. However, the magnitude of the production volume is not the same. In fact, we get a total of less than 1.4 billion tonnes, smaller compared to the 9.6 billion tonnes of crop production.

Table 16: World production of primary livestock (in million tonnes)

Livestock	1961	1970	1980	1990	2000	2010	2020	2021	2022	Growth
Eggs	15	20	27	37	55	69	93	93	93	517%
Milk	344	392	466	542	579	725	921	941	930	170%
Meat	71	101	137	180	232	294	339	355	361	405%
Beef & Buffalo	29	40	47	55	58	67	74	75	76	165%
Pork	25	36	53	70	89	108	108	121	123	395%
Poultry	9	15	26	41	69	99	135	136	139	1 456%
Sheep & Goat	6	7	7	10	11	14	16	16	17	176%
Other	3	3	4	4	4	6	6	6	6	106%

Source: www.fao.org/faostat/en/#data/QCL & Author's calculations.

The remarkable growth in primary crops and livestock can be attributed to three key factors: expansion of cultivated area (although we have seen that only one-third of this growth is due to this factor), the adoption of intensive agricultural practices, and the increased use of inputs such as fertilizers and pesticides. Fertilizer use has increased sixfold in the last sixty years, while pesticide use has doubled between 1990 and 2022 (Table 17).

Table 17: Agricultural use of inputs (fertilizers and pesticides)

Input	1961	1980	2000	2020	2022	1961	1980	2000	2020	2022
	Agricultural use (in million tonnes)					Use par area of cropland (in kg/ha)				
Fertilizer	31.0	116.6	135.2	201.7	185.4	20.8	76.8	85.9	123.5	113.1
Nitrogen	11.5	60.6	81.0	114.7	108.1	7.6	39.6	51.3	69.6	65.4
Phosphate	10.9	31.8	32.5	47.8	41.9	7.5	21.4	21.0	29.8	26.0
Potash	8.6	24.2	21.7	39.3	35.5	5.7	15.8	13.7	24.1	21.7
Pesticide			2.2	3.4	3.7			1.5	2.2	2.4

Source: www.fao.org/faostat/en/#data/RFN, www.fao.org/faostat/en/#data/RP & Author's calculations.

Remark 5 *The figures presented in this paragraph can be analyzed at the country or regional level. In this case, we observe large differences between regions of the world, for example between the Americas and Africa, or between developed and developing countries (FAO, 2023b).*

2.4.2 Food consumption

Table 18 shows the food supply[45] per capital and per day for the different regions of the world. In general, food supply is assessed along three primary dimensions: energy intake, protein intake, and fat intake. In 2022, the global average daily per capita intake was 2 985 kilocalories of energy[46], 92 grams of protein, and 87 grams of fat. Over the past sixty years, these figures have increased by 36%, 51%, and 81%, respectively. However, these averages mask significant differences between regions. For example, fat intake is currently only 41 g/capita/day in Middle Africa, while it reaches 177 g/capita/day in North America. These differences are even more pronounced when we look

---

[45]Food supply measures the amount available for consumption at the end of the supply chain and does not include consumption waste.

[46]In the context of nutrition, 1 Calorie (with a capital C) is used as a shorthand for 1 kilocalorie (kcal).

Table 18: Food supply per capital per day (energy, protein & fat)

Region	Energy (in Cal/capita/day)			Protein (in g/capita/day)			Fat (in g/capita/day)		
	1961	1990	2022	1961	1990	2022	1961	1990	2022
Africa	1 993	2 291	2 567	53	59	66	40	47	56
Eastern Africa	1 989	1 925	2 263	56	50	59	29	32	47
Middle Africa	2 018	1 847	2 312	49	45	46	36	44	41
Northern Africa	1 920	2 851	3 142	53	78	91	38	60	74
Southern Africa	2 603	2 755	2 713	70	73	79	58	64	91
Western Africa	1 909	2 199	2 644	46	52	65	46	49	57
Americas	2 559	2 953	3 392	77	82	104	78	97	135
Northern America	2 873	3 447	3 881	95	107	122	110	138	177
Central America	2 180	2 796	3 173	59	73	94	48	69	101
Caribbean	1 992	2 390	2 828	47	57	75	42	65	78
South America	2 329	2 599	3 111	63	65	95	49	73	118
Asia	1 805	2 414	2 944	47	61	93	25	49	78
Central Asia			3 169			103			104
Eastern Asia	1 594	2 564	3 361	44	69	124	18	56	95
Southern Asia	2 014	2 242	2 584	52	54	72	30	40	62
South-eastern Asia	1 836	2 178	2 880	40	48	80	27	41	69
Western Asia	2 501	3 273	3 128	76	93	93	57	84	101
Europe	3 041	3 367	3 471	90	104	112	89	125	140
Eastern Europe	3 100	3 360	3 375	95	105	109	73	108	121
Northern Europe	3 176	3 214	3 402	91	96	113	131	134	141
Southern Europe	2 838	3 469	3 519	82	107	116	72	136	149
Western Europe	3 016	3 374	3 615	89	103	113	113	149	162
Oceania	3 021	3 139	3 101	100	105	101	108	126	128
Australasia	3 060	3 188	3 417	103	109	115	111	129	152
Melanesia	2 534	2 547	2 314	54	65	66	60	86	66
Micronesia	2 424	2 622	2 937	51	64	86	116	94	126
Polynesia	2 239	2 683	2 959	55	77	107	73	107	117
World	2 196	2 621	2 985	61	70	92	48	67	87

Source: www.fao.org/faostat/en/#data/FBS, www.fao.org/faostat/en/#data/FBSH & Author's calculations.

at countries. Figure 17 shows the dispersion of food supply for the 200 countries included in the FAO database. We can see that the dispersion has not decreased since 1961, in fact it has increased! Countries with the lowest average energy intake include Burundi, Lesotho, Somalia, Haiti, and Madagascar, while those with the highest energy intake are Israel, the United States, Ireland, Belgium, and Turkey. For protein intake, the lowest levels are found in the Democratic Republic of the Congo, Madagascar, Burundi, Somalia, and Mozambique, while Iceland, Israel, Ireland, Mongolia, and Montenegro have the highest. In terms of fat intake, Burundi, DR Congo, Madagascar, Rwanda, and Cambodia rank the lowest, while Belgium, Austria, the United States, Israel, and Germany rank the highest. This reflects economic disparities, but also some of the dietary habits of the countries with the highest levels. The vegetal/animal structure of the human diet also has an impact (Table 19). In fact, protein intake from animal sources has increased over the past sixty years, while the contribution of animal products to fat intake has decreased.

Figure 17: Country dispersion of food supply

Table 19: Split of food supply between vegetal and animal products

Food	1961			2022		
Origin	Energy	Protein	Fat	Energy	Protein	Fat
Vegetal	1 858	41.80	22.80	2 460	53.45	51.33
Animal	338	19.66	24.72	525	38.08	35.98
Total	2 196	61.46	47.52	2 945	91.52	87.31

2.4.3 Food security

Biodiversity is closely linked to food security, as it provides the foundation for resilient and sustainable food systems. This interconnectedness has several dimensions. Moreover, the concept of double materiality is highly relevant, as biodiversity impacts food production, while food and agricultural production also has a significant impact on biodiversity. In this context, it is challenging to classify and list all the dimensions. Therefore, we will focus on a few key dimensions that are essential for food security. The first dimension is the genetic diversity of crops and livestock. Below is an excerpt from the press release of the FAO 2019 biodiversity assessment publication (FAO, 2019):

"*Less biodiversity means that plants and animals are more vulnerable to pests and diseases. Compounded by our reliance on fewer and fewer species to feed ourselves, the increasing loss of biodiversity for food and agriculture puts food security and nutrition at risk.*" (José Graziano da Silva, FAO Director-General, 22 February 2019, Rome).

Many crop species are no longer cultivated because production is concentrated on the most profitable crops. Over time, this has led to an industrial selection of species, resulting in the homogenization and globalization of the human diet. In this context, we are more vulnerable when a species faces problems such as disease. Here are some examples:

- Irish potato famine (1845–1852)
  The main cause was the infection of potato crops by the potato blight (caused by the fungus-like microorganism *Phytophthora infestans*). This blight led to one million deaths and caused the mass emigration of another million people. The severity of the disease was largely due to Ireland's dependence on a single crop, the potato.

- Coffee leaf rust outbreak in Sri Lanka (1860–1890)
  Coffee leaf rust (CLR) is a disease of the coffee plant caused by the fungus *Hemileia vastatrix*. In the 1860s, coffee production was an important resource for Sri Lanka, but the outbreak of coffee leaf rust destroyed the coffee industry in the region and led to a shift to tea cultivation.

- Panama disease in bananas (1950s)
  Panama disease, caused by the fungus *Fusarium oxysporum*, infects banana plants and nearly eradicated the Gros Michel variety in the 1950s. This led to its replacement with the Cavendish variety, which now faces a similar threat from a new strain of the disease.

- Southern corn leaf blight in the United States (1970)
  Southern corn leaf blight is a disease of corn caused by the plant pathogen *Bipolaris maydis* (Race O, Race C, and Race T). The 1970 epidemic in the USA was triggered by the widespread use of Texas male sterile cytoplasm corn, which made 90% of hybrid crops susceptible to the newly emerged Race T pathogen. This outbreak, which began in the southern U.S. and spread rapidly in the north, destroyed approximately 15% of corn production.

- Wheat stem rust Ug99 in Africa (1998–present)
  Ug99 is a strain of wheat stem rust caused by the fungus *Puccinia graminis*. It was first identified in 1998 and has spread to several countries in Africa and the Middle East. It poses a significant threat to global wheat production due to the high susceptibility of many wheat varieties.

- Citrus greening disease in Florida (2005–present)
  Citrus greening disease, caused by *Liberibacter bacteria*, affects citrus plants and exists in three forms: a heat-tolerant Asian type and heat-sensitive African and American types. First identified in 1929 and reported in southern China in 1943, the disease has severely impacted citrus production in the United States, particularly in Florida, where orange production has declined by more than 50% since 2005.

These diseases highlight the risks of focusing on one or a few crop species. In fact, reliance on a limited number of crop species increases the vulnerability of agriculture to disease. When a single pathogen targets a widely grown crop, such as Panama disease in bananas or Southern corn leaf blight in maize, the impact can be catastrophic, causing widespread losses. Biodiversity is then essential for building resilience to future outbreaks. Coffee is a typical example. According to Davis et al. (2019), coffee production is concentrated in a small number of coffee species. In particular, Arabica (*Coffea arabica*) and Robusta (*Coffea canephora*) account for 60% and 40% of traded coffee, respectively, leaving little room for other species. Arabica coffee has been cultivated for at least several hundred years, which is not the case with Robusta, which was first cultivated in the mid-1800s. Robusta coffee went from being a minor African crop to a major global commodity in only

about 150 years, and Davis *et al.* (2019) concluded that "*Robusta coffee provides a good example of how a (relatively) newly discovered wild species has transformed a globally important crop.*" One of the main reasons for its success is its resistance to coffee leaf rust. Of the 124 known coffee species worldwide, their conservation status according to the IUCN extinction risk classification is as follows: 13 are Critically Endangered (CR); 40 are Endangered (EN); 22 are Vulnerable (VU); 9 are Near Threatened (NT); 26 are Least Concern (LC); 14 are Not Evaluated (NE) or Data Deficient (DD). This means that 75% of coffee species are threatened with extinction (Davis *et al.*, 2019, Figure 1, page 2). Therefore, coffee production is at significant risk if existing diseases[47] become more severe or if new diseases emerge, as the number of alternative species that could potentially replace today's Arabica or Robusta varieties has declined over the past century.

The previous example deals with intraspecific diversity (for example, the different types of coffee in the genus *Coffea*), but biodiversity loss is also related to interspecific diversity (for example, the different crops in the clade *Mesangiospermae*). While intraspecific diversity of the food supply has declined in recent times, interspecific diversity has increased with the diversification of diets and trade in commodities, especially in developed countries. Many people now eat exotic fruits, fish and vegetables that would not have been available less than a century ago. Agricultural specialization and the diversity of human diets explain the growth of agricultural trade. Table 20 shows that the export share of most crops and commodities has increased. For example, avocado exports represented less than 1% of production in 1961, compared to more than 35% of production in 2021. FAO statistics show that the largest increases (more than 30% between 1961 and 2021) are for cherries, coconut oil, cranberries, kiwi, lentils, mustard seeds, natural honey, olive oil, peas, quinoa, and soybeans. Looking at OECD statistics, the largest increases (+20% between 1990 and 2023) are for edible fish meals, skim milk powder, soybeans, and sugar. Agricultural trade is a resilient factor in food security, but it also reveals the vulnerability of some countries that have specialized in the most profitable crops.

<center>Box 8: Founder crops</center>

The concept of "*founder crops*" was introduced by Zohary and Hopf (1988). The authors proposed that eight plant species were first domesticated by early farming communities, laying the foundation of early Neolithic agriculture in Southwest Asia (the Fertile Crescent region of the Near East) around 10 500 years BP. These crops are thought to form the basis of modern agriculture in Europe, Southwest Asia, South Asia, and North Africa. The original founder crops included three cereals (emmer wheat, einkorn wheat, and barley), four pulses (lentil, pea, chickpea, and bitter vetch), and flax.

Subsequent research has suggested that many other species could also be considered as founder crops. This list has been extended for various regions and may include rice and foxtail millet in the Yangtze and Yellow River valleys (about 9 500 years BP), maize, squash, and common bean in southwest Mexico (5 300 years BP), potato, quinoa, and common bean in the Central Andes (5 100 years BP), as well as goosefoot, sunflower, and squash in the Eastern United States (5 100 years BP).

---

[47]There are many coffee diseases that can be classified into four main categories: bacterial diseases, fungal diseases, root diseases, and viral diseases. Here are some examples: anthracnose (*Colletotrichum*), bacterial blight of coffee (*Pseudomonas syringae*), black rot (*Koleroga noxia*), brown eye spot (*Cercospora coffeicola*), cercospora leaf spot (*Cercospora coffeicola*), coffee leaf rust (*Hemileia vastatrix*), coffee berry disease (*Colletotrichum kahawae*), coffee ringspot virus (*Brevipalpus phoenicis*), coffee wilt disease (*Fusarium xylarioides*), root-knot nematode disease (*Meloidogyne*).

Table 20: Share of world crop production exported (in %)

	Crop	1961	2021	Crop	1961	2021
FAO statistics	Apples	9.4	8.8	Olive oil	14.9	66.2
	Apricots	5.0	8.6	Onions and shallots	2.0	9.1
	Avocados	0.2	36.3	Oranges	16.3	10.0
	Bananas	16.6	19.3	Peaches and nectarines	6.0	7.0
	Barley	9.9	30.0	Peas	4.0	48.7
	Blueberries	36.9	39.7	Persimmons	0.4	14.0
	Cauliflowers	6.4	6.1	Pineapples	2.8	12.7
	Cherries	2.9	35.2	Pomelos	10.3	11.0
	Coconut oil	21.1	80.6	Potatoes	1.0	3.8
	Cranberries	0.0	50.9	Quinoa	0.0	68.8
	Cucumbers	1.5	3.5	Sesame seeds	11.0	32.2
	Dates	14.0	19.1	Soybeans	15.5	43.2
	Eggplants	0.2	1.1	Spinach	0.3	1.1
	Kiwi fruit	0.0	36.4	Strawberries	5.4	11.1
	Lentils	6.5	67.5	Tomatoes	3.9	4.4
	Maize	6.8	16.2	Vanilla	73.8	91.6
	Mustard seeds	19.3	53.8	Watermelons	0.9	4.7
	Natural honey	11.0	42.3	Wheat	17.8	25.9
	Commodity	1990	2023	Commodity	1990	2023
OECD statistics	Beef meat	9.2	18.2	Pork meat	1.9	8.7
	Butter	10.0	7.8	Poultry meat	8.5	11.2
	Cheese	4.0	13.6	Pulses	10.5	19.8
	Cotton	24.2	36.5	Rice	3.4	10.1
	Edible fish meals	44.7	67.6	Roots and tubers	7.3	7.8
	Eggs	2.6	1.6	Sheep meat	12.2	9.0
	Fish	15.4	23.0	Skim milk powder	26.4	57.9
	Fresh dairy products	0.0	0.1	Soybeans	26.6	45.1
	Maize	12.8	15.3	Sugar	9.8	36.8
	Oilseed meals	24.2	24.5	Vegetable oils	24.3	37.2
	Other coarse grains	7.7	14.0	Wheat	19.4	24.1
	Other oilseeds	15.2	13.6	Whole milk powder	45.9	49.9

Source: www.fao.org/faostat/en/#data/QCL, www.fao.org/faostat/en/#data/TCL,
https://data-explorer.oecd.org & Author's calculations.

A typical example of crop expansion is maize (Pollan, 2007; Hartigan, 2017). In 2022, maize (*Zea mays*) was the world's most widely produced grain crop (1.16 billion tonnes, covering the second-largest cultivated area (203.5 million hectares) and achieving the highest grain yield (5.72 tonnes per hectare). Today, maize appears in a wide range of foods, including candy corn, corn dogs, corn flakes, corn soup, cornstarch, corn tortillas, cornbread, polenta, popcorn, tamales, and more. This proliferation is especially noticeable in the Americas. For instance, Maize is the focus of the documentary film *King Corn*, which was released in October 2007. The film explores the trend of increased corn production and its impact on American society. However, maize has not always been the dominant crop that "*has conquered the world.*" Native to Central America, maize was introduced to Europe in the early 16th century following Christopher Columbus's voyages to the Americas. Initially brought to Spain by explorers returning from the New World, maize gradually spread

across southern Europe, the Mediterranean, and eventually to Africa and Asia. Its global spread was largely due to its adaptability to different climates and soil conditions. Figure 18 illustrates the expansion of maize in world agriculture. The first panel shows the area harvested. In 1961, this was 105.6 million hectares — less than the area cultivated for rice (115.4 million hectares) and wheat (204.2 million hectares). By 2022, the area cultivated for maize is nearly equal to that of wheat and surpasses that of rice. Maize production has accelerated since 2000, driven by a significant expansion of harvested area and the introduction of genetically modified (GMO) maize varieties. One of the key issues with maize production is its substitution effect on the supply of other crops. In particular, the primary use of maize is not for direct human consumption but as animal feed. Using FAO statistics, we report below the breakdown of maize use[48]:

Year	Animal feed	Human food	Losses	Seed	Processing	Other uses
2010	55.3%	13.6%	3.5%	0.7%	5.7%	21.2%
2022	60.4%	11.4%	5.2%	0.7%	5.8%	16.5%

60% of maize is used as animal feed, mainly for poultry and cattle. Direct human consumption accounts for only 11% of total production, which is less than the *other uses* category. In fact, a significant portion of maize (between 10% and 20%) is processed to produce ethanol, a biofuel used primarily in gasoline blends.

Figure 18: Area harvested, production and yield of cereal crops
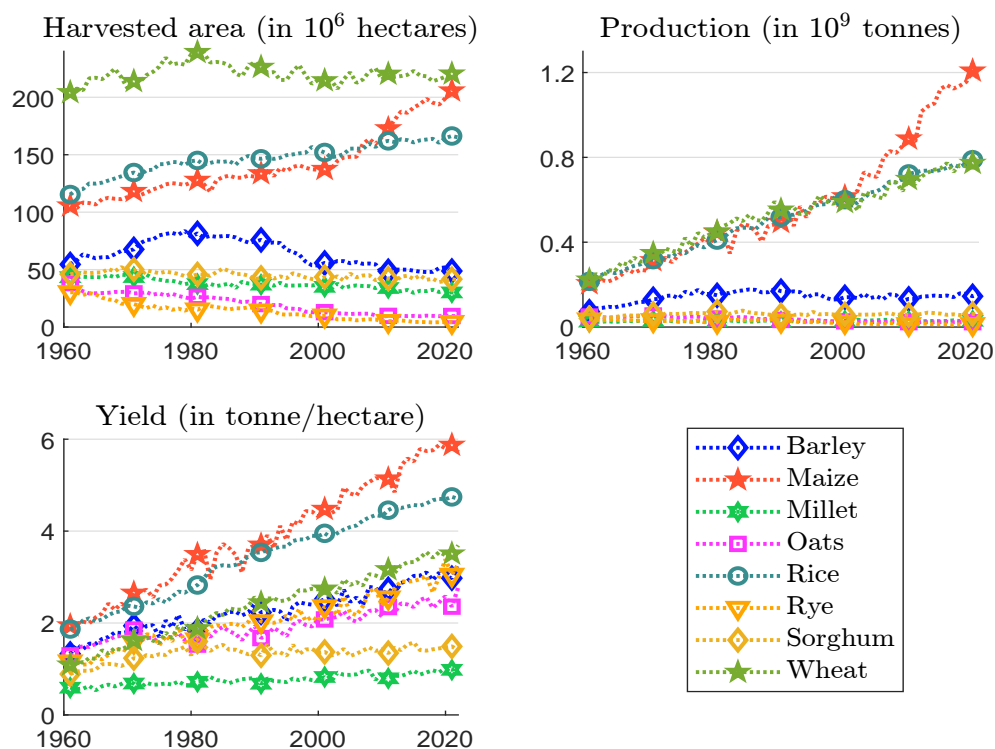
Source: www.fao.org/faostat/en/#data/QCL & Author's calculations.

The previous issue relates to the Earth's capacity to provide all necessary ecosystem functions without compromising others. Here, the *Do No Significant Harm* (DNSH) concept plays a crucial

---

[48]We first calculate the net supply quantity with the following equations: Supply quantity = Production + Imports − Exports − Stock variation. Then, we use the following decomposition: Supply quantity = Feed + Seed + Losses + Processing + Other uses (non-food) + Tourist consumption + Residuals + Food.

role. But it's not just a matter of choosing one ecosystem service over another. Instead, we see a global deterioration of ecosystem services when examining the ecological footprint and the Earth's biocapacity. The ecological footprint, introduced by Wackernagel and Rees (1996), measures the rate at which we consume resources and produce waste compared to the rate at which nature can regenerate those resources and absorb waste. This metric balances the demand for ecosystem services against their supply. On the demand side, the ecological footprint assesses the use of productive land areas, and quantifies the ecological assets required by a population or product to produce the resources it consumes and to absorb its wastes. On the supply side, biocapacity measures the productivity of ecological assets (such as cropland, grazing land, forests, fisheries, and built-up areas). Both metrics are expressed in global hectares, either for a region or per capita, allowing for meaningful comparisons across regions.

Figure 19: Global ecological footprint and biocapacity (in global hectares per capita)
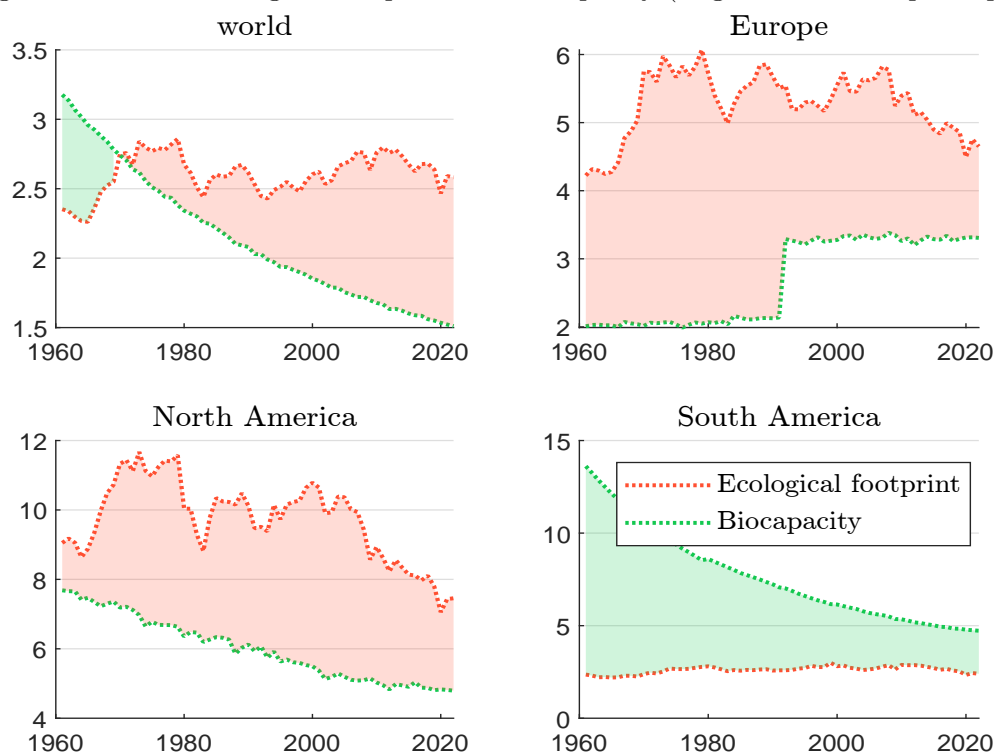
Source: https://data.footprintnetwork.org & Author's calculations.

Figure 19 shows the global ecological footprint when considering the various ecological assets. If the ecological footprint exceeds biocapacity, the region has a biocapacity deficit (red area); otherwise, it has a biocapacity reserve (green area). Before 1970, global biocapacity was greater than the ecological footprint, but since then, a biocapacity deficit has emerged. This shift has occurred because, while the per capita ecological footprint has remained relatively constant, the per capita biocapacity has declined, as the Earth's resources are finite. There are significant regional differences. South America's biocapacity balance has declined over time but remains positive, while Europe has experienced a biocapacity deficit for many years. If we focus specifically on the ecosystem service of cropland (Figure 20), we see different regional trends. In Asia, Europe, and South America, both demand and supply per capita have increased. However, the biocapacity balance remains positive in South America, is negative but significantly reduced in Europe, and is negative and increasing in Asia. In North America, the biocapacity reserve has remained roughly constant since 2000.

Figure 20: Cropland ecological footprint and biocapacity (in global hectares per capita)
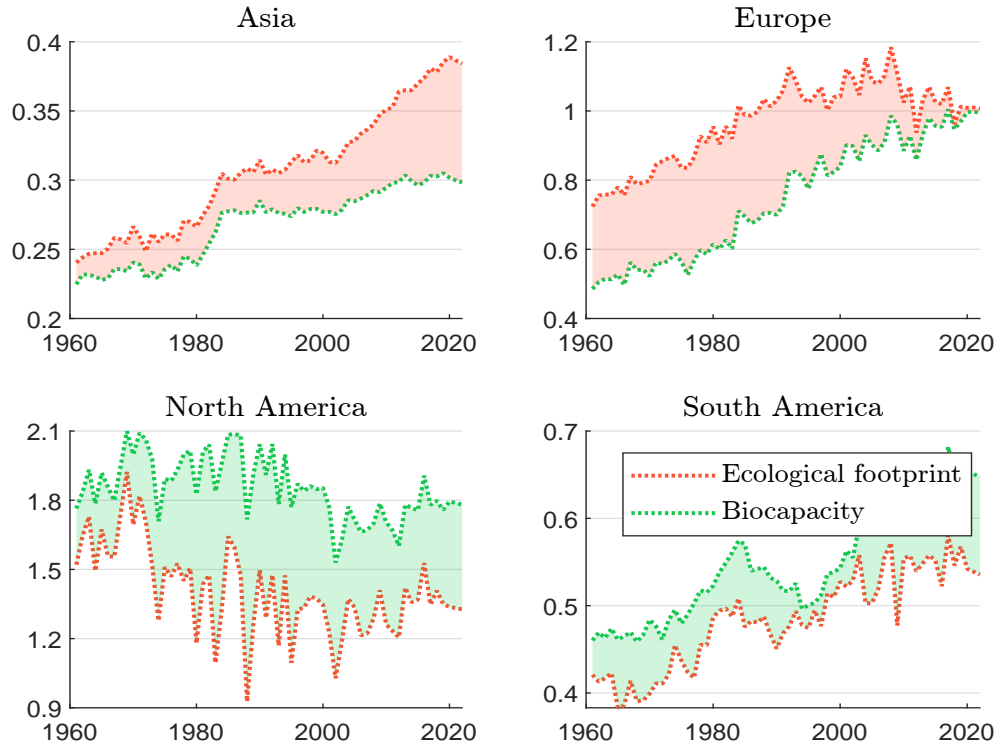
In addition to food diversity, a second important dimension of food security is the Earth's capacity to feed the planet, or 8.2 billion people. The FAO uses several measures to assess food insecurity. One of the main metrics is the prevalence of (severe/moderate) food insecurity. Let X and R be the random variables for energy intake and energy requirement, respectively, with a joint probability distribution $\mathbf{F}(x, r)$. Sukhatme (1961, Equation 1, page 466) defines the prevalence of undernourishment as the probability that intake is less than requirement:

$$\text{PoU} = \Pr\{X < R\} = \iint \mathbb{1}\{x < r\} \cdot \mathrm{d}\mathbf{F}(x, r) = \iint_{x<r} f(x, r) \, \mathrm{d}x \, \mathrm{d}r \tag{13}$$

where $f(x, r)$ is the bivariate density function of (X, R). The non-parametric estimator of PoU is the empirical frequency:

$$\text{PoU} = \frac{1}{n} \sum_{i=1}^{n} \mathbb{1}\{x_i < r_i\}$$

where n denotes the population size and (x_i, r_i) are the observed intake and requirement values for individual i. Another approach assumes a parametric density function $f(x, r; \theta)$, estimates the vector of parameters θ, and calculates $\text{PoU} = \iint_{x<r} f(x, r; \hat{\theta}) \, \mathrm{d}x \, \mathrm{d}r$. Both statistical methods require a sample (x_i, r_i) of energy intake and requirement values. However, in practice, determining an individual's exact energy requirement is challenging. Therefore, the FAO approximates the prevalence of undernourishment as follows:

$$\text{PoU} = \Pr\{X < r_L\} = \int_{x<r_L} f_x(x) \, \mathrm{d}x = \mathbf{F}_x(r_L) \tag{14}$$

where $\mathbf{F}_x(x)$ is the cumulative distribution function of energy intake, often called dietary energy consumption (DEC), and r_L is a cut-off point representing the minimum requirement, also known as the minimum dietary energy requirement (MDER)[49]. The univariate approach is valid when applied to a homogenous group such that $\sigma(R) \approx 0$. Therefore PoU is calculated at the group level (*e.g.*, sex × age) and then aggregated across the different groups in a population. It is commonly accepted that $X \sim \mathcal{LN}\left(\mu_x, \sigma_x^2\right)$. The calibration of the parameters μ_x and σ_x is done by matching the first two statistical moments of X. Let $\mu(X)$ and $\mathrm{CV}(X) = \sigma(X)/\mu(X)$ be the empirical mean[50] and the coefficient of variation of X, respectively. Since we have $\mu(X) = \exp\left(\mu_x + \frac{1}{2}\sigma_x^2\right)$ and $\mathrm{CV}^2(X) = \exp\left(\sigma_x^2\right) - 1$, we deduce that:

$$\begin{cases} \mu_x = \ln \mu(X) - \dfrac{1}{2}\ln\left(\mathrm{CV}^2(X) + 1\right) \\ \sigma_x = \sqrt{\ln\left(\mathrm{CV}^2(X) + 1\right)} \end{cases}$$

According to FAO (2024a), the minimum energy requirement m_i by sex and age group is calculated by estimating the basal metabolic rate (BMR) and multiplying it by the ideal weight for a healthy person in that sex/age group. These ideal weights are derived from the body mass index (BMI) reference tables published by the World Health Organization (WHO). The minimum energy requirement is then adjusted using a physical activity level (PAL) coefficient. Finally, the cut-off point is obtained as the weighted average of the minimum energy requirements: $r_L = \sum_{i=1}^{n} f_i m_i$ where f_i is the frequency of individuals in sex/age group i within the population.

Remark 6 *While the estimation of $\mu(X)$ is simply the empirical mean, the estimation of $\mathrm{CV}(X)$ is more complex. According to Naiken (2002), the coefficient of variation is assumed to have two components:*

$$\mathrm{CV}^2(X) = \mathrm{CV}^2(X \mid Y) + \mathrm{CV}^2(X \mid R)$$

where $\mathrm{CV}(X \mid Y)$ is the coefficient of variation of X due to income dispersion and $\mathrm{CV}(X \mid R)$ is the coefficient of variation of X due to energy requirement. In general, $\mathrm{CV}(X \mid R)$ is assumed to be constant and equal to 20%.

Example 2 *We assume[51] that the average dietary energy consumption (ADEC) $\mu(X)$ is 2 589 kcal/capita/day, the coefficient of variation $CV(X)$ is 0.27, the minimum dietary energy requirement (MDER) r_L is 1 803 kcal/capita/day and the average dietary energy requirement (ADER) is 2 333 kcal/capita/day.*

We first calibrate the log-normal distribution of the dietary energy consumption. The estimated values of the parameters are:

$$\sigma_x = \sqrt{\ln\left(0.27^2 + 1\right)} = 0.2653$$

---

[49]This approximation is suggested in Sukhatme (1961, Equation 4, page 473). See also Exercise A.1 on page 230 for a comparison between the bivariate and univariate distribution approaches.

[50]The mean dietary energy consumption is given by:

$$\mu(X) = \frac{1}{365}\left(\frac{1}{N}\sum_{i=1}^{m} Q_i C_i\right)$$

where Q_i is the amount (in kg) of food product i consumed annually by the population, C_i is the energy density (in Calories/kg) of food product i, and N is the population size. The term $\sum_{i=1}^{m} Q_i C_i$ represents the total calories consumed by the population in one year, while $\mu(X)$ is the average number of calories per capita per day. We recall that food available for human consumption is equal to the total food supply (production + imports − exports − changes in stocks) minus animal feed minus seeds minus other non-human uses minus waste.

[51]These figures are those obtained from the FAO in the case of India in 2022.

and:

$$\mu_x = \ln(2\,589) - \frac{0.2653^2}{2} = 7.8238$$

We can then deduce that the prevalence of undernourishment is 10.91%:

$$\text{PoU} = \Pr\{X < 1803\} = \Phi\left(\frac{\ln(1\,803) - 7.8238}{0.2653}\right) = 0.1091$$

Figure 21 shows the probability distribution of the dietary energy consumption X, the MDER and the prevalence of undernourishment. We also report the values of ADER and ADEC, which measure the average dietary energy requirement and consumption. In this case, we observe that ADER < ADEC, which is the normal situation.

Figure 21: Dietary energy consumption and prevalence of undernourishment (India, 2022)
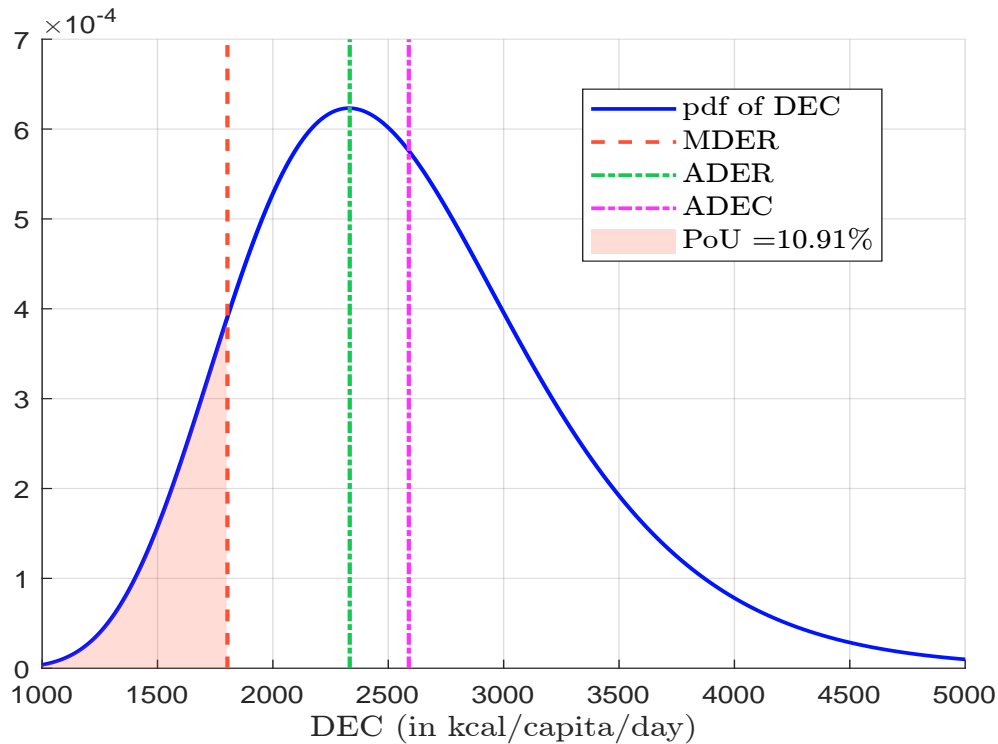
Source: www.fao.org/faostat/en/#data/FS & Author's calculations.

Figure 22 shows the evolution of several statistics from 2000 to 2022. The first panel compares ADEC, ADER and MDER. As expected, the average and minimum dietary energy requirements are relatively stable. On average, ADER is equal to 2 360 kcal/capita/year, while MDER is equal to 1 820 kcal/capita/year. On the contrary, the average dietary energy consumption is increasing over time at the global level. It is now close to 3 000 kcal/capita /year. However, these global figures hide some large differences between countries, as some countries have experienced large declines in recent years. In fact, we observe that the prevalence of undernourishment has decreased from 2000 to 2019, but it is increasing since 2020. As a result, the number of undernourished people is currently around 730 million. Figure 23 highlights this wide variability across countries. Average dietary energy consumption ranges from 1 834 Calories per capita per day in Somalia to 3 912 Calories in the USA. Somalia also has the highest prevalence of undernourishment, at 51% in 2022. The suite of

Figure 22: Prevalence of undernourishment and number of undernourished people (World)
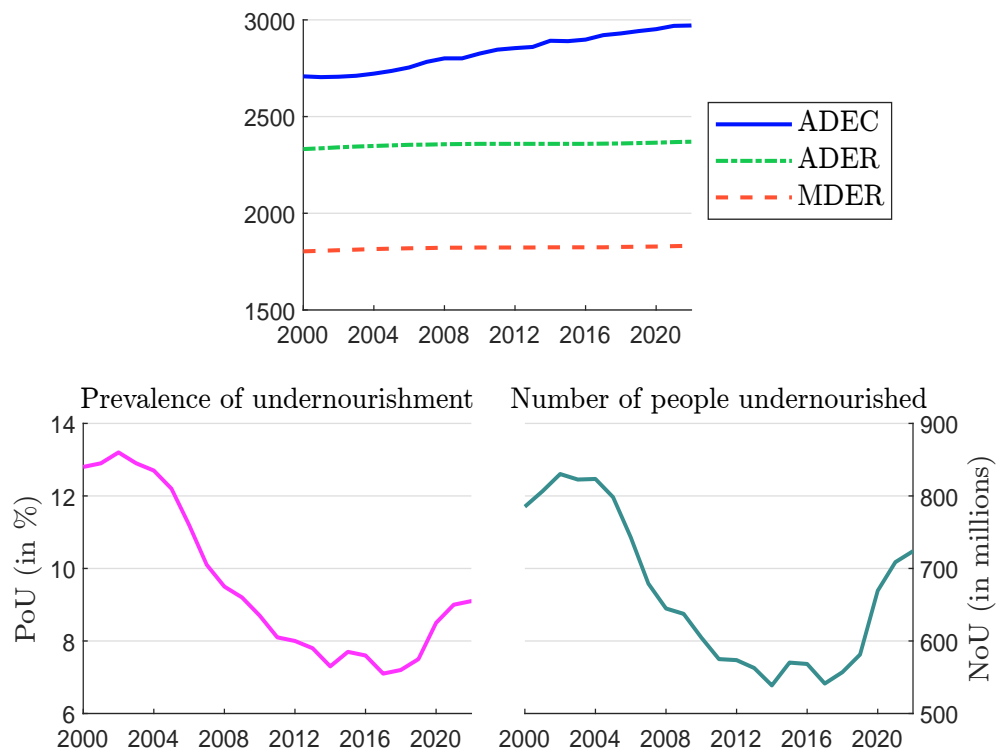
Source: www.fao.org/faostat/en/#data/FS & Author's calculations.

Figure 23: Histogram of food insecurity indicators (country level, 2022)
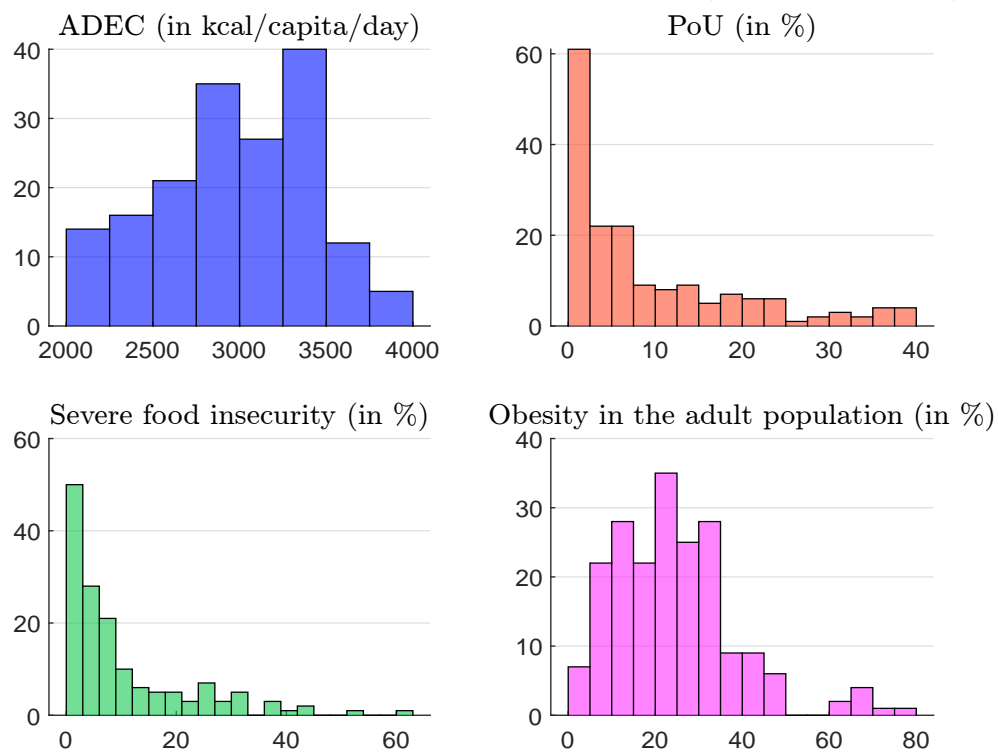
Source: www.fao.org/faostat/en/#data/FS & Author's calculations.

food security indicators on the FAOSTAT website includes many other statistics on food insecurity. For example, the bottom panels of Figure 23 show the prevalence of severe food insecurity in the total population and the prevalence of obesity in adults (18 years and older). Other indicators are presented in table 21 for the different regions of the world.

Table 21: Food security indicators by region (2022)

Indicator	Africa	Asia	Europe	North America	Oceania	South America	World
MDER (kcal/capita/day)	1 736	1 831.0	1 931	1 962	1 871	1 856	1 832
ADER (kcal/capita/day)	2 237	2 369.0	2 505	2 554	2 424	2 403	2 370
ADEC (kcal/capita/day)	2 578	2 917.0	3 467	3 882	3 104	3 104	2 971
Prevalence of undernourishment	19.9	8.2			7.1	6.6	9.1
People undernourished (million)	284.1	386.5			3.2	43.9	723.8
Severe food insecurity							
Total population	21.7	9.7	1.8	0.9	9.3	11.0	10.8
Rural adult population	23.5	10.4	1.7	0.8	2.8	13.5	12.2
Town adult population	22.2	10.9	1.9	0.7	4.0	12.9	11.5
Urban adult population	19.8	8.3	1.8	1.2	3.0	9.6	9.3
Male adult population	20.8	8.6	1.7	0.7	8.5	9.6	9.1
Female adult population	21.3	9.9	1.9	1.2	8.3	12.0	10.2
Total population (million)	309.0	459.2	13.3	3.5	4.2	72.5	861.7
Male adults (million)	87.9	157.2	6.4	1.0	1.5	23.7	277.7
Female adults (million)	92.0	177.6	7.8	1.9	1.4	31.2	311.9
Water services							
Safely managed drinking water	33.0	76.0	93.0	97.0		75.0	73.0
Basic drinking water	66.0	95.0	98.0	100.0		98.0	91.0
Sanitation services							
Safely managed sanitation	26.0	59.0	79.0	96.0	73.0	49.0	57.0
Basic sanitation	36.0	86.0	97.0	100.0	80.0	90.0	81.0
Children under 5 years							
Affected by wasting	5.8	9.3		0.2		1.4	6.8
Who are stunted	30.0	22.3	4.0	3.6	22.0	11.5	22.3
Who are overweight	4.9	5.1	7.3	8.2	16.8	8.6	5.6
Affected by wasting (million)	12.2	31.6				0.7	45.0
Who are stunted (million)	63.1	76.6	1.4	0.7	0.8	5.7	148.1
Who are overweight (million)	10.2	17.7	2.6	1.7	0.6	4.2	37.0
Obesity							
Adult population	16.2	10.4	21.4	40.3	29.5	29.9	15.8
Adult population (million)	123.9	353.9	129.0	119.2	9.6	141.4	880.7

All statistics are expressed in %, except those whose units are indicated.

Source: www.fao.org/faostat/en/#data/FS & Author's calculations.

Remark 7 *As discussed in Roncalli (2025, Section 2.1.1), food security encompasses many dimensions and issues. Here, we focus on two critical aspects: genetic diversity and the capacity to feed the global population. In a fragmented world, a third important dimension is each country's dependence on external sources for its food supply.*

3 Biodiversity threats and risks

Primack (2014) categorizes different threats to biodiversity into three main clusters: (1) extinction, (2) habitat destruction, fragmentation, degradation, and global climate change, and (3) overexploitation, invasive species, and disease. Sodhi and Ehrlich (2010) consider a similar list of biodiversity risks but groups them differently: (1) extinction, (2) habitat loss and fragmentation, (3) overexploitation, (4) invasive species, (5) climate change, and (6) fire. In reality, these factors often interact with each other, amplifying their combined effects. Moreover, it is important to distinguish between biodiversity threats and biodiversity risks:

- Biodiversity threats are the specific drivers or causes of biodiversity loss. They are external factors that contribute directly or indirectly to biodiversity loss by impacting species, habitats, and ecosystems. For example, invasive species can severely disrupt an ecosystem and therefore constitute a threat to biodiversity.

- Biodiversity risks refer to the potential consequences of biodiversity loss due to these threats. Specifically, biodiversity risks encompass the likelihood and severity of negative impacts on human life and ecosystem functions. For example, the emergence of new diseases as a result of ecosystem disturbances is a biodiversity risk.

The distinction between biodiversity threats and biodiversity risks is not always clear. For example, habitat loss is a threat because it directly reduces biodiversity and disrupts ecosystems. But it is also a risk because activities such as agriculture and land-use change contribute to further habitat loss. Similarly, pollution can be both a threat and a risk to biodiversity. It is a direct factor in biodiversity loss, but it can also result from that loss. In this context, the boundary between threats and risks to biodiversity can be somewhat artificial. Furthermore, these different threats are often interrelated, and the same is true of risks. In addition, feedback loops can complicate the distinction between the two concepts. For instance, habitat fragmentation may reduce biodiversity, but the resulting loss of biodiversity may in turn exacerbate further habitat fragmentation. According to Wilson (1989), the central cause of biodiversity risk is the destruction of natural ecosystems by human beings. He identified five major threats: habitat destruction, overexploitation, pollution, global climate change and invasion by introduced species. He argued that these five causes are driven by underlying social conditions, in particular increased per capita consumption, rapid population growth and unsound economic policies. Since this seminal paper on biodiversity loss, these key elements have been extensively studied and documented by scientists, showing that the Earth's ecosystems are dominated by humans (Vitousek et al., 1997), and that humans are ultimately the cause of the current biodiversity crisis. Land-use change is undoubtedly the greatest threat (Sala et al., 2000), while the decline in species richness is the most visible risk.

The possibility of a sixth mass extinction (Late Quaternary Mass Extinction or LQME), has been raised before[52]. According to Algeo and Shen (2024), the LQME differs from previous extinctions because it is driven by technological advances, particularly those that have allowed humans to exert widespread influence over the Earth's climate and ecosystems. The extinction process occurred in phases. In the first phase (50 Kyr BP–1750 AD), overhunting and the loss of top predators led to the extinction of many large animal species, especially after human expansion into new regions such as Australasia and the Americas. The first phase is characterized by limited global impacts (less than 1% of species loss) but significant ecosystem impacts. The current phase (1750 AD to present) is driven by habitat loss as humans convert land for agriculture and urbanization, with invasive species and climate change also contributing to species loss. The current phase is characterized by current

---

[52]See the section on page 27 dedicated to the LQME.

Figure 24: Stages of the Late Quaternary mass extinction
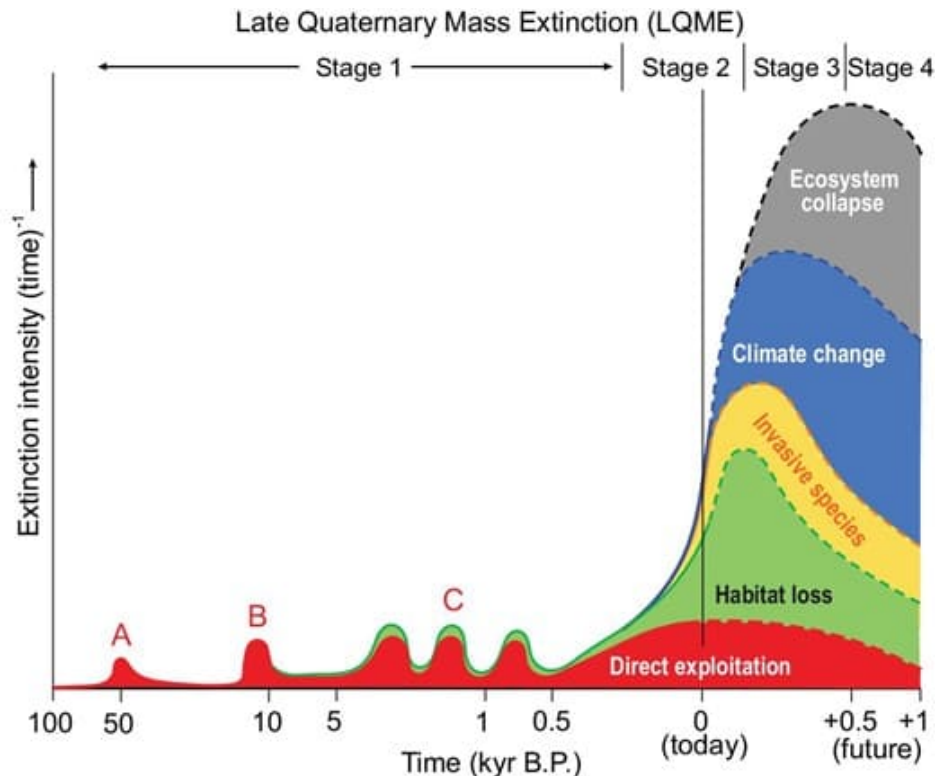
Stage 1 (from ~ 50 to 0.25 ka), characterized by direct exploitation of species, comprised megafaunal extinctions in (A) Australasia, (B) the Americas and (C) the Indo-Pacific region. Stage 2 (from ~ 0.25 ka to the near future) is dominated by extinctions due to habitat loss. Stages 3 and 4 (future, timeline speculative) will be marked by climate change and ecosystem collapse, respectively, as the dominant proximate causes of extinction, while invasive species will play a supporting role during Stages 2 to 4.

Source: Algeo and Shen (2024, Figure 5, page 11).

losses of 1–2% of total biodiversity, but the extinction rate is about 1 000 times the background extinction rate. Algeo and Shen (2024) suggest that the near future phase will be dominated by climate change, which will become the primary driver of biodiversity loss, while they estimate that the final phase could lead to widespread ecosystem collapse. In this case, the final phase could be characterized by a rapid and extensive loss of biodiversity, comparable to Earth's largest historical extinction events. Figure 24 illustrates this worst-case scenario of the sixth mass extinction.

Remark 8 *World Economic Forum (2020b) published the New Nature Economy Report to address the growing threats posed by biodiversity loss and the current biodiversity crisis to economies and businesses worldwide. The report emphasizes that biodiversity decline is not only an environmental issue but also a significant economic risk. The report outlines 15 major threats to biodiversity and identifies 15 critical transitions across three socio-economic systems. These threats are linked to issues such as habitat loss, overexploitation, and pollution, which pose not only risks to human welfare but also substantial risks to our economic systems. The proposed transitions aim to reduce nature-related risks while unlocking economic opportunities, potentially generating $10 trillion in economic value and creating 395 million jobs by 2030.*

Box 9: New Nature Economy Report II (World Economic Forum, 2020)

In 2000, the World Economic Forum issued an alarming report on the impact of business on biodiversity and biodiversity on business (double materiality). This report highlights three key socio-economic systems: (1) food, land and ocean use, (2) infrastructure and the built environment, and (3) energy and extractives. These systems contribute 12%, 40% and 23% of global GDP, respectively, and employ 40%, 18% and 16% of the world's workforce. They also exert the greatest pressure on biodiversity, with 80% of threatened and near-threatened species at risk from activities in these sectors, and 72% affected by the food, land and ocean use sector alone. The WEF estimates that over half of the global GDP (around $44 trillion in economic value) relies heavily or moderately on natural resources. It also identifies 15 major pressing business-related threats to nature:

- Food, land and ocean use: (1) annual and perennial non-timber crops, (2) logging and wood harvesting, (3) livestock farming and ranching, (4) invasive non-native/alien species/diseases, (5) fire and fire suppression, (6) agricultural and forestry effluents, (7a) water management/use*, (8) fishing and aquatic resources;

- Infrastructure and the built environment: (9) housing and urban areas, (10) tourism and recreational areas, (11) domestic and urban wastewater, (12) roads and railroads, (13) commercial and industrial areas, (14) industrial and military effluents;

- Energy and extractives: (15) mining and quarrying, (7b) dams*.

In a similar way, the WEF identifies 15 key socio-economic transitions needed to tackle the nature crisis:

- Food, land and ocean use: (1) ecosystem restoration and avoided expansion, (2) productive and regenerative agriculture, (3) healthy and productive ocean, (4) sustainable management of forests, (5) planet-compatible consumption, (6) transparent and sustainable supply chains;

- Infrastructure and the built environment: (7) densification of the urban environment, (8) nature-positive built environment design, (9) planet-compatible urban utilities, (10) nature as infrastructure, (11) nature-positive connecting infrastructure;

- Energy and extractives: (12) circular and resource efficient models, (13) nature-positive metals and minerals extraction, (14) sustainable materials supply chains, (15) nature-positive energy transition.
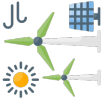
*Dams and water management/use are treated as separate threats because they involve different economic activities.

Box 9: New Nature Economy Report II (continued)

The capital investment required to implement these fifteen transitions accross the three systems is approximately \$2.7 trillion per year, which the following breakdown: 16% for the six transitions related to food, land and ocean use, 64% for the five transitions related to infrastructure and the built environment, and 31% for the four transitions related to energy and extractives. However, implementing these transitions could generate \$10 trillion in business opportunities and create approximately 400 million jobs by 2030. Among these, the food, land, and ocean use system is expected to yield the greatest socio-economic benefits.

Table 5.C: Key figures of the New Nature Economy Report II

System	Description	Share of threatened species impacted	Threats	Total business opportunities by 2030	Total jobs by 2030	Annualized investment costs (2020–2030)
	Food, land and ocean use	72%	8	\$3 565 bn	191 mm	\$440 bn
	Infrastructure and the built environment	29%	6	\$3 015 bn	117 mm	\$1 430 bn
	Energy and extractives	18%	2	\$3 530 bn	87 mm	\$840 bn
	Total[†] of the three socio-economic systems	79%	15	\$10 110 bn	395 mm	2 710 bn

[†]Because some species are affected by more than one of the three systems, the percentage of species impacted by all systems is less than the sum of the percentages impacted by each individual system. The total number of threats is also 15 because water management/use and dams are considered as a single threat.

Source: World Economic Forum (2020b, pages 8-16).

Figure 25: Habitat loss vs. fragmentation vs. degradation
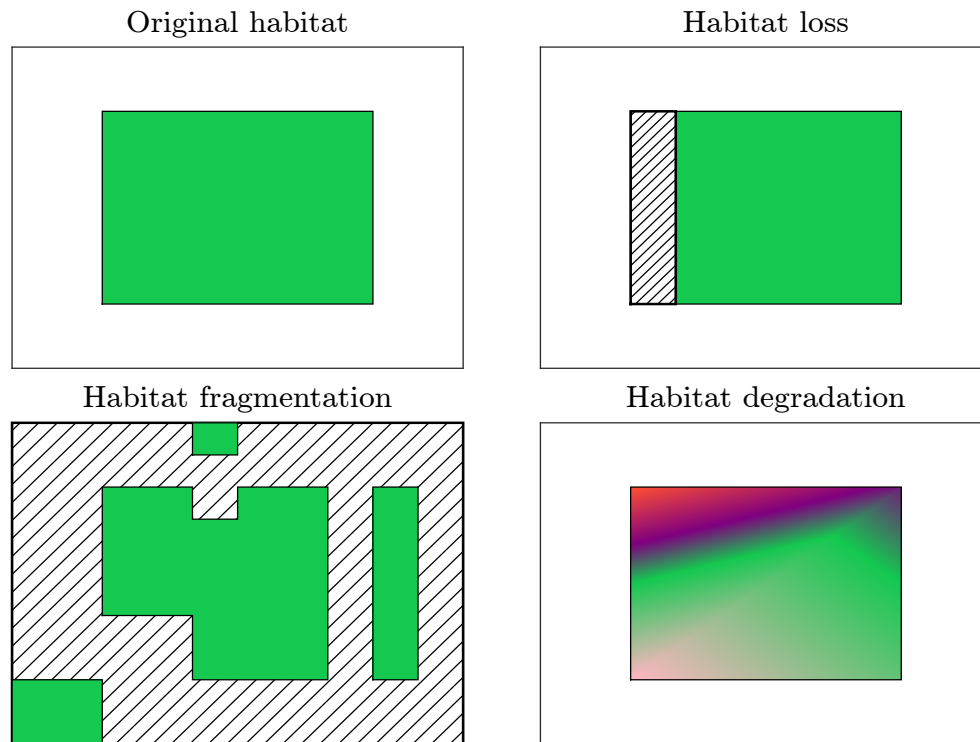
3.1 Habitat loss, fragmentation and degradation

Habitat loss, fragmentation, and degradation is the largest cause of biodiversity loss and the primary threat leading to species extinction. Written in the singular form, this sentence suggests that these three processes are interconnected or form a single, overarching factor. However, it's important to distinguish between them:

- Habitat loss occurs when a natural habitat is completely removed, destroyed, or converted to another use, resulting in the disappearance of species that previously lived there. For example, deforestation — transforming a forest into cropland or an urban area — is a typical case of habitat loss. This process is the most severe form of habitat disruption, because it eliminates the existing living space and is often irreversible.

- Habitat fragmentation occurs when a large, continuous habitat is divided into smaller, isolated patches by human-made structures. Building highways through a forest, for instance, is a typical example of habitat fragmentation. Fragmentation creates habitat islands that may be too small to support the original populations, increasing the risk of species decline or extinction.

- Habitat degradation is the process by which the quality of a habitat is damaged or reduced, making it less suitable for the species that live there. Factors such as pollution, water contamination, water stress, climate change or invasive species often contribute to degradation. In such cases, species may become endangered as their populations decline or suffer from poor health.

In summary, loss is the total elimination of a habitat, fragmentation is the breaking up of a habitat into smaller habitats, and degradation is the decline in habitat quality (Figure 25). The distinction

between these three concepts and the definition of habitat fragmentation were popularized by Fahrig (2003). In her research, Lenore Fahrig challenges common perceptions of habitat fragmentation. She argues that while habitat loss typically has detrimental effects on biodiversity, the effects of fragmentation itself[53] are more nuanced. In particular, fragmentation can sometimes have neutral or even potentially beneficial consequences for some species by creating more diverse landscape configurations that increase habitat heterogeneity and enhance dispersal opportunities (Fahrig, 2017):

> "*I found 118 studies reporting 381 significant responses to habitat fragmentation independent of habitat amount. Of these responses, 76% were positive. Most significant fragmentation effects were positive, irrespective of how the authors controlled for habitat amount, the measure of fragmentation, the taxonomic group, the type of response variable, or the degree of specialization or conservation status of the species or species group. [...] Thus, although 24% of significant responses to habitat fragmentation were negative, I found no conditions in which most responses were negative. Authors suggest a wide range of possible explanations for significant positive responses to habitat fragmentation: increased functional connectivity, habitat diversity, positive edge effects, stability of predator-prey/host-parasitoid systems, reduced competition, spreading of risk, and landscape complementation.*" (Fahrig, 2017, page 1).

This conclusion contrasts sharply with the findings of Haddad *et al.* (2015), who reported very negative impacts:

> "*We conducted an analysis of global forest cover to reveal that 70% of remaining forest is within 1 km of the forest's edge, subject to the degrading effects of fragmentation. A synthesis of fragmentation experiments spanning multiple biomes and scales, five continents, and 35 years demonstrates that habitat fragmentation reduces biodiversity by 13 to 75% and impairs key ecosystem functions by decreasing biomass and altering nutrient cycles.*" (Haddad *et al.*, 2015, page 1).

These conflicting results have fueled a lively debate in the journal *Biological Conservation*, reflected in two contrasting publications: *Is Habitat Fragmentation Good for Biodiversity?* (Fletcher *et al.*, 2018) and *Is Habitat Fragmentation Bad for Biodiversity?* (Fahrig *et al.*, 2019). To this day, the debate remains open, especially when we consider human pressures and matrix conditions[54] (Ramírez-Delgado *et al.*, 2022).

3.1.1 Theory of island biogeography

This theory (known as TIB) was proposed by MacArthur and Wilson (1967) to explain the factors that influence biodiversity on islands. They emphasised the importance of studying islands because they are less complex and more common than larger ecosystems, meaning that research can be easily replicated. Their theory describes how the size of an island and its distance from the mainland affect the balance between immigration and extinction rates of species. This balance ultimately determines an equilibrium, or the number and types of species an island can support. An illustration is provided in Figure 26. Two key elements characterize the theory of island biogeography. First, the distance from the mainland measures the isolation of the island. Indeed, islands closer to the mainland have more species because they are easier for species to reach, receive colonizers more frequently, and so

---

[53]We generally speak of fragmentation '*per se*', *i.e.*, fragmentation independent of habitat loss.

[54]In the context of biodiversity, the matrix condition refers to the quality and characteristics of the landscape that surrounds habitat patches or fragements. It's essentially the non-habitat environment that separates discrete areas of suitable habitat.

on. Second, the size of the island determines species richness. Larger islands support greater species diversity because they offer more diverse habitats, contain more resources, and so forth. Specifically, MacArthur and Wilson (1967) proposed that the immigration rate[55] $\lambda(t)$ decreases with the number of species present and the isolation of the island (first panel in Figure 26), while the extinction rate $\mu(t)$ increases with the number of species present but decreases with the size of the island (second panel in Figure 26). Equilibrium occurs when immigration and extinction rates are equal, implying that the net diversification rate is zero: $\delta(t) = \lambda(t) - \mu(t) = 0$ (third panel in Figure 26).

Figure 26: Theory of island biogeography
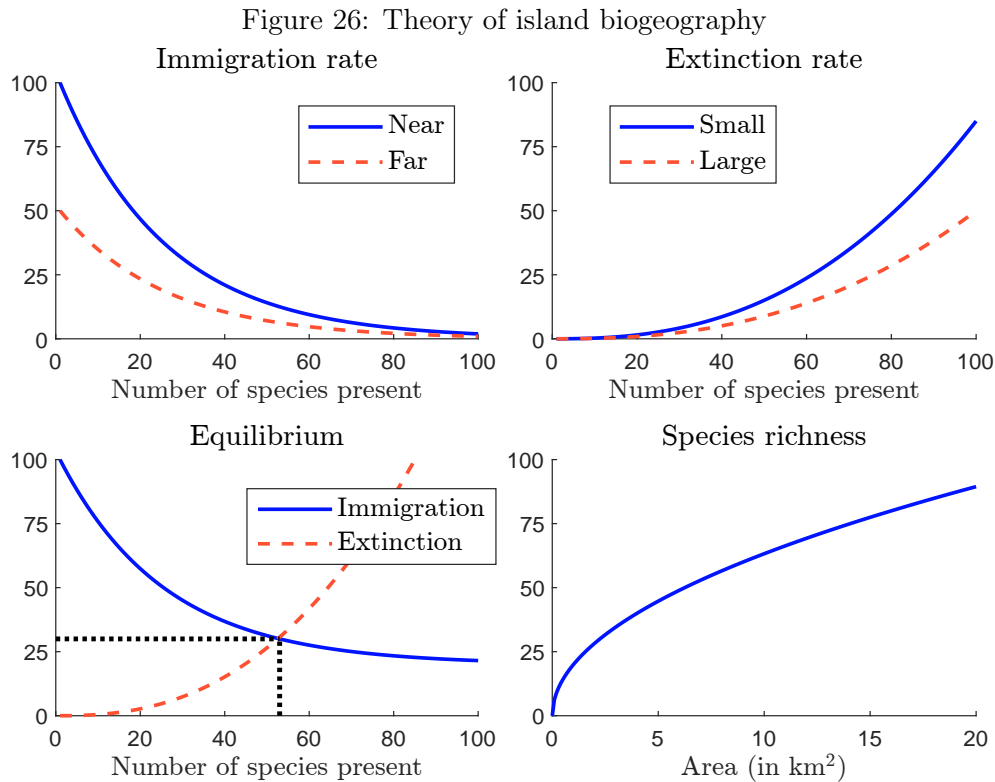
3.1.2 Species-area relationship

The previous equilibrium model is often associated with the species-area relationship (SAR). Since extinction dynamics are influenced by the size of an island, an increase in island size shifts the equilibrium point to the right on the immigration-extinction diagram, indicating higher species richness. However, the rate of increase in species richness is generally slower than the rate of increase in area[56] (fourth panel in Figure 26). This reflects "*an ecological version of the law of diminishing returns*" (Lomolino, 2001): as area increases, each additional unit of area contributes proportionally less to species diversity. Certainly, the most famous species-area relationship is the power model originally formulated by Arrhenius (1921):

$$S = cA^z \tag{15}$$

where S is species richness, c is a constant, A is the area of the island and z is the slope of the log-log A–S curve. Typical values of z are between 0.15 and 0.35. If the areas of the original and

---

[55]In the theory of island biogeography, the immigration rate corresponds to the origination rate in the birth-death model.

[56]See Exercise A.2 on page 232 for a mathematical derivation of the species-area relationship from the theory of island biogeography.

current habitats are A_0 and A, respectively, we obtain the following survival function:

$$\frac{S}{S_0} = \left(\frac{A}{A_0}\right)^z$$

This equation is used by Pimm *et al.* (1995) to calibrate species loss due to habitat loss:

$$\mathcal{L}oss_{species} = 1 - (1 - \mathcal{L}oss_{habitat})^z \tag{16}$$

Assuming $z = 0.25$, Pimm *et al.* (1995, page 349) found that 50% of habitat loss should reduce the number of species by 15.91%, while 90% of habitat loss leads to 43.77% of species loss (Table 22).

Table 22: Species loss $\mathcal{L}oss_{species}$

z	$\mathcal{L}oss_{habitat}$					
	0.00%	25.00%	50.00%	75.00%	90.00%	100.00%
0.05	0.00%	1.43%	3.41%	6.70%	10.87%	100.00
0.10	0.00%	2.84%	6.70%	12.94%	20.57%	100.00%
0.25	0.00%	6.94%	15.91%	29.29%	43.77%	100.00%
0.35	0.00%	9.58%	21.54%	38.44%	55.33%	100.00%

While ecologists are nearly unanimous in accepting the principles of the species-area relationship[57], they do not always agree on the specific form it should take. An alternative to Equation (15) is the exponential model proposed by Gleason (1922):

$$S = c + z \ln(A) \tag{17}$$

These two models (power and exponential) were extensively studied in the seminal review by Connor and McCoy (1979). The authors provided a comprehensive and critical analysis of the species-area curve, arguing that many estimated SAR curves could be explained by statistical sampling effects rather than underlying biological mechanisms. Therefore, they emphasized the importance of distinguishing between ecological drivers (*e.g.*, habitat diversity, island biogeography) and statistical drivers (*e.g.*, sampling bias, incomplete sampling, inappropriate statistical methods) of SAR. By examining 100 datasets, they showed that the value of z varies across scales and contexts (*e.g.*, small versus large areas) and concluded that the species-area relationship is not a fixed law but rather a complex, context-dependent pattern. This variation depends on specific ecological settings, taxonomic groups, and geographic regions. In particular, they noted that the parameters c and z estimated for one island or archipelago cannot be reliably applied to another island or archipelago. Furthermore, reducing the species-area relationship to a function of a single variable with two parameters fails to account for several second-order factors, such as elevation, latitude, and the density of small- and large-bodied species. Nevertheless, the search for the best species-area relationship model has continued to fascinate researchers since the publication of Connor and McCoy's paper in 1979. While it is impossible to cite all of the subsequent studies, some have significantly shaped this field. For instance, the default value of $z = 0.25$ for the power model is largely due to the influential

---

[57]The relationship between species and area is considered to be a fundamental ecological principle:

"*It is common, perhaps axiomatic, to refer to the species-area relationship as one of ecology's few laws [...]. According to a very broad consensus of ecologists, the pattern has two principal features: 1) species richness of a given taxon increases with the area sampled, and 2) the rate of increase slows for the larger islands or patches of habitat.*" (Lomolino, 2001, page 1).

book by Rosenzweig (1995). Similarly, Tjørve (2003) made an important contribution by organizing a comparison of 14 statistical models to identify the best-fitting SAR model. More recently, Dengler (2009) and Triantis *et al.* (2012) reviewed 23 and 20 functions, respectively, and concluded that no single function universally outperforms all others. However, they emphasized that the power model often provides the best fit and remains a robust choice when it does not. Triantis *et al.* (2012) also identified three other simple models that can rival the power model for certain datasets: the linear model ($S = c + zA$), the exponential model ($S = c + z\ln(A)$), and the Kobayashi model ($S = c\ln(1 + zA)$).

Figure 27: Analyzing the species-area relationship in Mediterranean islands

(a) Tyrrhenian islands

(b) Aegean islands
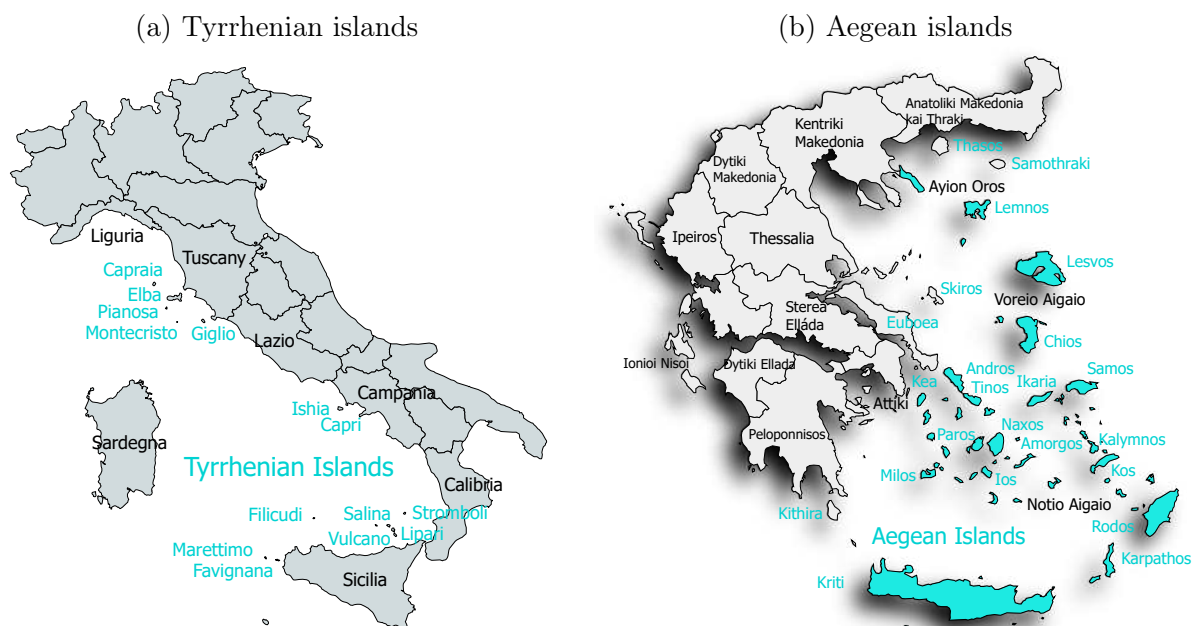
Source: Fattorini *et al.* (2017, Figure 1), created with `www.paintmaps.com`.

Let us now examine an empirical application to understand how the species-area relationship is estimated. For this purpose, we consider the study[58] by Fattorini *et al.* (2017). The authors estimated the SAR curves for two groups of Mediterranean islands: the Tyrrhenian Islands, located in Italy, and the Aegean Islands, located between Greece and Turkey. In Figure 27, we present the Tyrrhenian islands with areas larger than $10\,\mathrm{km}^2$ and the Aegean islands with areas exceeding $100^{,}\mathrm{km}^2$. The Tyrrhenian islands are mainly located off the western coast of Italy, near regions such as Tuscany, Lazio, Campania, Calabria, and Sicily. The dataset includes 47 islands, with the largest being Elba ($223\,\mathrm{km}^2$) and the smallest being Scoglietto di Portoferraio ($24.9\,\mathrm{m}^2$). The Aegean Sea is known for its multitude of islands, the total number of which is estimated to be around $6\,000$. However, the dataset contains only 127 islands, with the largest being Rodos ($1\,401\,\mathrm{km}^2$) and the smallest being Petallidi ($6\,000\,\mathrm{m}^2$). The results for various taxonomic groups (centipedes, isopods, land snails, reptiles and tenebrionid beetles) are given in Table 23 and Figure 28. Fattorini *et al.* (2017) found that z varies between 0.141 and 0.308, while c varies between 2.716 and 12.274 species per km^2. According to the authors, these results "*demonstrate the importance of comparing SARs either of different groups within the same area, or of the same group in different areas.*"

---

[58]The advantage of this study is that the dataset is relatively small, and the results are easily reproducible since the data are freely available on the paper's webpage: `onlinelibrary.wiley.com/doi/abs/10.1111/jbi.12874`.

Table 23: Estimated values of c, z, and S for different area values A

Islands	Species	c	z	Area A (in km^2)					
				0.01	0.10	1	10	100	1 000
Tyrrhenian	Centipedes	6.281	0.308	1.52	3.09	6.28	12.77	25.94	52.73
	Isopods	9.226	0.262	2.76	5.05	9.23	16.87	30.83	56.36
	Land snails	12.274	0.225	4.35	7.31	12.27	20.61	34.59	58.08
	Reptiles	3.357	0.141	1.75	2.43	3.36	4.64	6.43	8.89
	Tenebrionids	8.610	0.270	2.48	4.62	8.61	16.03	29.85	55.59
Aegean	Centipedes	3.864	0.243	1.26	2.21	3.86	6.76	11.83	20.70
	Isopods	9.354	0.203	3.67	5.86	9.35	14.93	23.82	38.02
	Land snails	9.572	0.184	4.10	6.27	9.57	14.62	22.34	34.12
	Reptiles	2.716	0.278	0.75	1.43	2.72	5.15	9.77	18.53
	Tenebrionids	4.055	0.268	1.18	2.19	4.05	7.52	13.93	25.82

Source: Fattorini *et al.* (2017, Table 1).

Figure 28: SAR curves in Tyrrhenian and Aegean islands
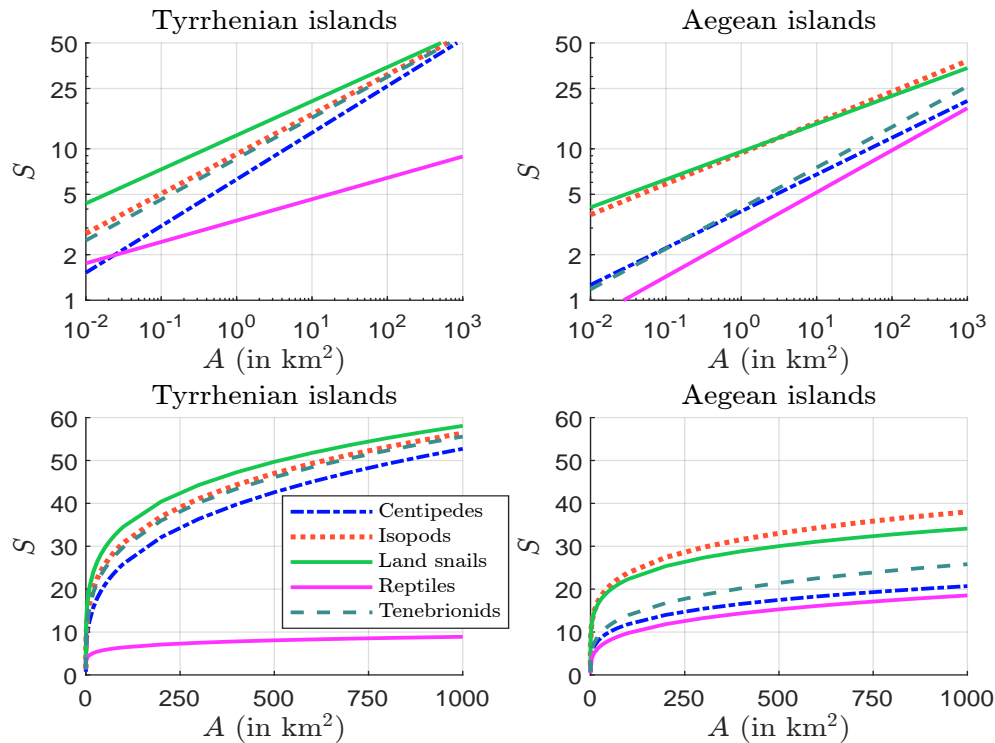
Source: Fattorini *et al.* (2017) & Author's calculations.

Example 3 *Table 24 shows the data used by Fattorini et al. (2017, Appendix S1) to estimate the SAR curve of land snail species in the Tyrrhenian Islands. The area A is expressed in km^2.*

Table 24: Number of species of land snails in the Tyrrhenian islands

Island	A	S	Island	A	S	Island	A	S
Alicudi	5.000	11	Filicudi	9.000	20	Montecristo	10.430	18
Argentarola	0.012	4	Formica di Grosseto	0.145	5	Panarea	3.380	22
Basiluzzo	0.270	11	Giannutri	2.390	19	Pianosa	10.410	28
Capraia	19.000	18	Giglio	21.000	35	Salina	26.000	25
Cerboli	0.051	8	Gorgona	2.270	24	Stromboli	12.000	18
Elba	223.000	50	Lipari	37.000	28	Vulcano	21.000	13

Source: Fattorini *et al.* (2017, Appendix S1).

Since the equation $S = cA^z$ is equivalent to $\ln(S) = \ln(c) + z\ln(A)$, the species-area relationship is generally estimated using the log-log regression model:

$$Y_i = \beta^\top X_i + \varepsilon_i$$

where $i = 1, \ldots, n$, n is the number of observations, S_i and A_i are the number of species and the area of the ith observation, $Y_i = \ln(S_i)$, $X_i = \begin{pmatrix} 1 & \ln(A_i) \end{pmatrix}$, $\beta = \begin{pmatrix} \ln(c) \\ z \end{pmatrix}$ and $\varepsilon_i \sim N\left(0, \sigma_\varepsilon^2\right)$ is the noise process. We have:

$$
\begin{aligned}
\hat{\beta} &= \left(X^\top X\right)^{-1} X^\top Y \\
&= \begin{pmatrix} n & \sum_{i=1}^n \ln(A_i) \\ \sum_{i=1}^n \ln(A_i) & \sum_{i=1}^n \ln^2(A_i) \end{pmatrix}^{-1} \begin{pmatrix} \sum_{i=1}^n \ln(S_i) \\ \sum_{i=1}^n \ln(A_i)\ln(S_i) \end{pmatrix} \\
&= \begin{pmatrix} 18 & 24.5506 \\ 24.5506 & 141.5006 \end{pmatrix}^{-1} \begin{pmatrix} 50.6670 \\ 93.3758 \end{pmatrix} \\
&= \begin{pmatrix} 2.5084 \\ 0.2247 \end{pmatrix}
\end{aligned}
$$

We deduce that $\hat{c} = \exp\left(\hat{\beta}_1\right) = 12.285$ and $\hat{z} = \hat{\beta}_2 = 0.225$. In Table 25, we compare the figures presented in the research paper (columns c and z) and our estimates (columns $\hat{\beta}_1$, $\exp\left(\hat{\beta}_1\right)$ and $\hat{\beta}_2$). We get the same values for z and very close values for c, the difference being due to rounding.

Table 25: Comparison of SAR values: research paper results vs. our estimates

Species	Tyrrhenian islands						Aegean islands					
	n	c	z	$\hat{\beta}_1$	$e^{\hat{\beta}_1}$	$\hat{\beta}_2$	n	c	z	$\hat{\beta}_1$	$e^{\hat{\beta}_1}$	$\hat{\beta}_2$
Centipedes	32	6.281	0.308	1.837	6.275	0.308	43	3.864	0.243	1.352	3.865	0.243
Isopods	28	9.226	0.262	2.221	9.216	0.262	43	9.354	0.203	2.236	9.360	0.203
Land snails	18	12.274	0.225	2.508	12.285	0.225	65	9.572	0.184	2.258	9.567	0.184
Reptiles	28	3.357	0.141	1.212	3.360	0.141	56	2.716	0.278	1.001	2.720	0.277
Tenebrionids	46	8.610	0.270	2.153	8.607	0.270	32	4.055	0.268	1.417	4.125	0.265

Source: Fattorini *et al.* (2017, Table 1) & Author's calculations.

We have seen how the species-area relationship can be used to measure the effect of habitat loss, *i.e.*, when area A is reduced. Hanski *et al.* (2013) suggested reformulating Equation (15) to account for habitat fragmentation. Let φ be the degree of fragmentation. The authors introduce the function $P(\varphi)$, which measures the fraction of the species that are expected to persist when the degree of fragmentation of A is given by φ and assume that $P(\varphi) = e^{-b\varphi}$ where b is a parameter. We have $P(0) = 1$ and $P(\infty) = 0$. We deduce that the species-area relationship becomes:

$$S = cA^z P(\varphi) = cA^z e^{-b\varphi} \tag{18}$$

If the initial area A_0 is reduced to A, we have:

$$\frac{S}{S_0} = \left(\frac{A}{A_0}\right)^z e^{-b(\varphi - \varphi_0)}$$

where φ_0 is the degree of fragmentation of A_0. We deduce that:

$$\mathcal{Loss}_{\text{species}} = 1 - (1 - \mathcal{Loss}_{\text{habitat}})^z e^{-b\Delta_{\text{frag}}} \tag{19}$$

where $\Delta_{\text{frag}} = \varphi - \varphi_0$ is the variation in the fragmentation. When $\varphi = \varphi_0$, we retrieve Equation (17).

Example 4 *We assume that $c = 10$, $z = 0.25$ and $b = 0.10$. We consider two initial landscapes, each with an initial area A_0 equal to $100\,\text{km}^2$. The first landscape is unfragmented ($\varphi_0 = 0$), while the second landscape is fragmented ($\varphi_0 = 0.50$). Both landscapes experience a habitat loss of 50%. In the first landscape, this habitat reduction is accompanied by habitat fragmentation ($\varphi = 0.50$), while in the second landscape we observe an improvement in habitat quality ($\varphi = 0.25$).*

We obtain the following results:

Landscape	#1	#2
S_0	31.6228	30.0805
S	25.2946	25.9349
$\mathcal{Loss}_{\text{species}}$	20.01%	13.78%

Normally, the impact of habitat loss alone on the species loss is $0.50^{0.25}$, or 15.91%. However, the species loss is higher in the first landscape because habitat fragmentation has increased. In contrast, the species loss is lower in the second landscape because the fragmentation has increased.

3.1.3 Species distribution, sampling and endemics-area curve

The species-area relationship describes the impact of area size on the number of species. It is a simple two-parameter model and may be limited in its ability to capture the effects of habitat loss on species richness and biodiversity. In particular, it overlooks important aspects of biodiversity such as species evenness and abundance[59]. It also ignores the spatial distribution of species and sampling effects. In this section, we explain these two effects, show how sampling affects the species-area relationship, and define species loss more precisely by introducing the endemics-area relationship.

---

[59]Abundance refers to the total number of individuals per species or in an ecosystem, while evenness is the degree to which individuals are evenly distributed across species.

Species abundance models We consider a region or community[60] with S species. For each species i, the number of individuals is denoted by n_i. The species abundance can be described by a traditional frequency distribution table[61]:

Species	1	2	$\cdots$	i	$\cdots$	S
Frequency	n_1	n_2		n_i		n_S

Another approach is to calculate the species abundance distribution (SAD), which summarizes the number of species by their abundance (McGill *et al.*, 2007):

Number of individuals	1	2	$\cdots$	j	$\cdots$	n^+
Number of species	$s(1)$	$s(2)$		$s(j)$		$s(n^+)$

where $s(j)$ is the number of species with j individuals, and $n^+ = \max n_i$ is the maximum number of individuals found in any single species in the community. Mathematically, we have:

$$s(j) = \sum_{i=1}^{S} \mathbb{1}\{n_i = j\}$$

The two representations — the frequency table and the species abundance distribution — then convey the same information about the structure of the community. However, it is not possible to retrieve the exact value of n_i from the SAD. This is because individual species are not identified in the SAD, unlike in the frequency table, where species are explicitly listed.

Example 5 *We consider a community consisting of* 25 *species and* 407 *individuals, distributed across a region of* $2\,\mathrm{km}^2$. *The abundances of the* 25 *species are as follows:* 2, 10, 13, 2, 1, 5, 25, 17, 1, 4, 28, 117, 23, 10, 13, 1, 4, 3, 10, 5, 7, 70, 10, 25, 1.

There are four species with only one individual, so $s(1) = 4$. Similarly, $s(2) = 2$ because there are two species with two individuals each. For $s(3)$, we have $s(3) = 1$, as only one species has three individuals, and so on. Finally, we get the resulting species abundance distribution:

j	1	2	3	4	5	7	10	13	17	23	25	28	70	117
$s(j)$	4	2	1	2	2	1	4	2	1	1	2	1	1	1

We confirm that the total abundance is exactly 407 individuals[62]. In practice, the label j is omitted when $s(j) = 0$ (McGill *et al.*, 2007). However, when the number of species is large, the species abundance distribution can become highly atomic or fragmented, with many values of $s(j) = 1$. To address this, it is important to group the number of individuals into classes. We have $s(\mathcal{C}_c) = \sum_{j \in (\mathcal{C}_c)} s(j)$ where $\mathcal{C}_c$ represents the cth grouping class. Here is an example where we group species whose number of individuals is greater than 5:

$\mathcal{C}_c$	1	2	3	4	5	6–10	11–25	26–50	51–100	100–117
$s(\mathcal{C}_c)$	4	2	1	2	2	5	6	1	1	1

---

[60]A community is the total set of species in an ecosystem.

[61]It is called the rank-abundance distribution when n_i are sorted (in ascending or descending order).

[62]We have the following property:

$$\sum_{j=1}^{\infty} s(j) \cdot j = \sum_{i=1}^{S} n_i = n$$

There are five species with an abundance of 6 to 10 individuals, six species with an abundance of 11 to 25 individuals, and so on. According to McGill *et al.* (2007, page 996), another way to illustrate the relative abundance and diversity of species within a community is to use a rank-abundance diagram (RAD), which is a graphical representation used in ecology to provide insights into species richness and species evenness. On the x-axis, species are ranked according to their abundance, from most abundant (rank 1) to least abundant (rank S), while on the y-axis, we plot relative abundance, that is the proportion of individuals belonging to each species. Mathematically, we calculate the order statistics of the set $\{n_1, \ldots, n_S\}$:

$$\underset{\mathcal{R}_S}{n_{1:S}} \leq \underset{\mathcal{R}_{S-1}}{n_{2:S}} \leq \cdots \leq \underset{\mathcal{R}_k}{n_{S-k+1:S}} \leq \cdots \leq \underset{\mathcal{R}_1}{n_{S:S}}$$

We then assign the rank $\mathcal{R}_k$ to the order statistic $n_{S-k+1:S}$. The relative abundance f_k associated with $\mathcal{R}_k$ is defined as $f_k = \dfrac{n_{S-k+1:S}}{n} = \dfrac{n_i}{n}$ where index i is the solution to the equation $n_i = n_{S-k+1:S}$. By construction we have $f_1 = \dfrac{\max n_i}{n}$ and $f_S = \dfrac{\min n_i}{n}$. Looking at the previous example, we get the following rank-abundance distribution:

k	1	2	3	4, 5	6	7	8, 9	$\cdots$	19	20, 21	22–25
i	12	22	11	7, 24	13	8	3, 15		18	1,4	5, 9, 16, 25
n_i	117	70	28	25	23	17	13	$\cdots$	3	2	1
f_k (in %)	28.75	17.20	6.88	6.14	5.65	4.18	3.19		0.74	0.49	0.25

Species 12 ranks first and represents 28.75% of the total abundance of the community. It is followed by species 22 and 11, whose relative abundance is 17.20% and 6.88%, respectively.

In 1949–1951, Robert H. Whittaker studied plant community composition in the Siskiyou Mountains to understand variation across environmental gradients. He developed the concept of diversity partitioning. His work, published in 1960, led to extensive data analyses and contributed significantly to the study of community structure (Whittaker, 1960). Since 2022, the data are freely available at https://doi.org/10.6084/m9.figshare.19661094.v3 (Whittaker *et al.*, 2022). We use the tree data CSV file, which contains 2 078 observations with the following information:

- The first column represents the sample number, corresponding to one of the 359 sampling locations;

- The second column lists the species name;

- The third column gives the number of individuals of each species in the sample;

- The fourth column indicates the number of large individuals with a diameter at breast height[63] (DBH) greater than 30 inches (76.2 cm).

For each species, we pooled the data from the 359 sampling sites. We obtain the abundance of 59 tree species. The five most represented trees are *Lithocarpus densiflorus*, *Quercus chrysolepis*, *Abies concolor*, *Pseudotsuga menziesii* and *Chrysolepis chrysophylla*. Their abundance is 8 439, 4 207, 4 172, 3 725 and 1 886, respectively. The species abundance distribution is shown in Figures 29 and 30. The species abundance curve is constructed with classes of length 50. Most of these classes have one or two species, except for the first three classes: 22 species for the first class (between 1 and 50 individuals), 7 species for the second class (between 51 and 100 individuals), and 3 species for the third class (between 101 and 150 individuals).

---

[63]In the United States, DBH refers to the diameter of the tree measured 4.5 feet above the ground.

Figure 29: Species abundance curve (Preston plot)
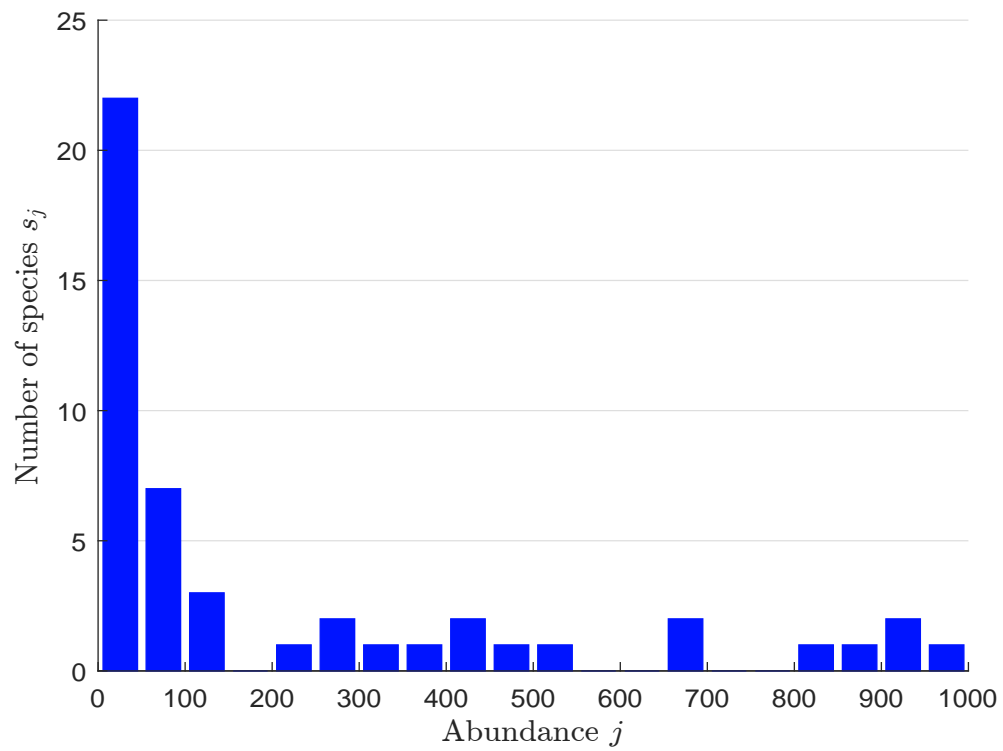
Figure 30: Rank-abundance curve (Whittaker plot)
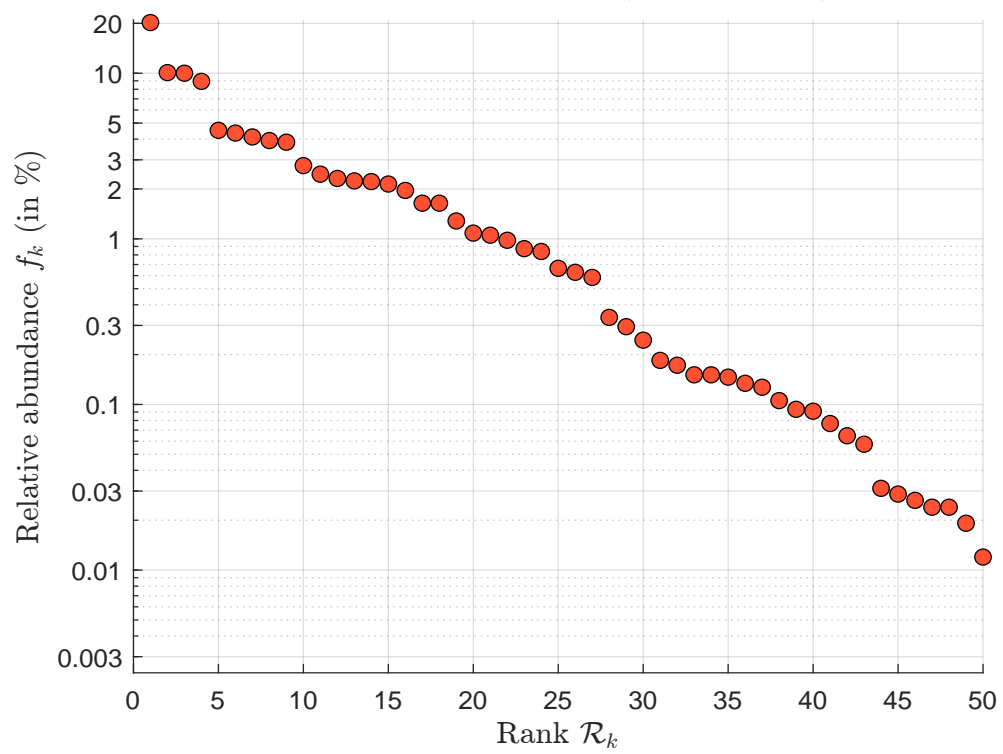
Figure 31: Barro Colorado Island (Panama)

There are many ways to plot a species abundance distribution. The species abundance curve (also called a frequency histogram) and the rank-abundance curve (Whittaker, 1965) are just a few examples. Other methods include the species rarefaction curve, the empirical cumulative distribution function (ECDF), the k-dominance plot, and the Robbins curve, among others (Matthews and Whittaker, 2015). Moreover, the axes of these graphs can be linear, but they are often transformed using $\log_2$ or $\log_{10}$ functions to better display the variability in the shape of the species abundance distribution. One particularly famous plot was proposed by Preston (1948), who popularized the use of a frequency histogram with $\log_2$-based classes along the x-axis. In this approach, the number of species is grouped into intervals of 2^k (*e.g.*, 1, 2, 4, 8, 16, 32, 64, etc.), called octaves. Using Example 5, we obtain the following results[64]:

Octave k	1	2	3	4	5	6	7
$\mathcal{C}_k$	1	2–3	4–7	8–15	16–31	32–63	64–127
$s(k)$	4	3	5	6	5	0	2

We now consider another community ecology dataset, the Barro Colorado Island (BCI) data, which was established by the Smithsonian Tropical Research Institute (STRI) and studied to understand the dynamics of tropical forest vegetation. The data contain 50 contiguous 1-ha plots and record tree species identity, spatial coordinates, size measurements, and environmental variables. Periodic censuses have been conducted every five years since 1980 until 2015. Such analysis and data collection has been done in many other regions of the world, especially in South America. In Figure 32 we show the species abundance distribution of the tropical forest tree dataset[65] compiled by Condit *et al.* (2002). This dataset includes 100 plots from Barro Colorado Island in Panama, the Yasuni National Park in Ecuador and the Manu Biosphere Reserve in Peru. The histogram shows that many species are found in the first octaves. Preston (1948) proposed that species abundances in

---

[64]The general formula for the range of each octave k is 2^{k-1} to $2^k - 1$. The first octave contains the species with one individual, the second octave contains the species with two and three individuals, the third octave contains the species with four to seven individuals, and so on.

[65]The `conditwebtable.xls` file is available at www.science.org/doi/abs/10.1126/science.1066854.

natural communities follow a log-normal distribution. When the logarithm of species abundances forms a bell-shaped curve, this pattern suggests that most species are moderately abundant, with fewer species being either extremely rare or extremely common. In some cases, when the positive skew of the log-normal distribution is very pronounced, the number of species decreases logarithmically with abundance, indicating that most species have only a few individuals. Preston (1948) further concluded that because many species in an ecological community are rare, they are often not observed in traditional ecological surveys[66]. This means that traditional sampling methods tend to underestimate total species richness, because rare species are likely to be missed in small samples.

Figure 32: Species abundance distribution of tropical forest trees
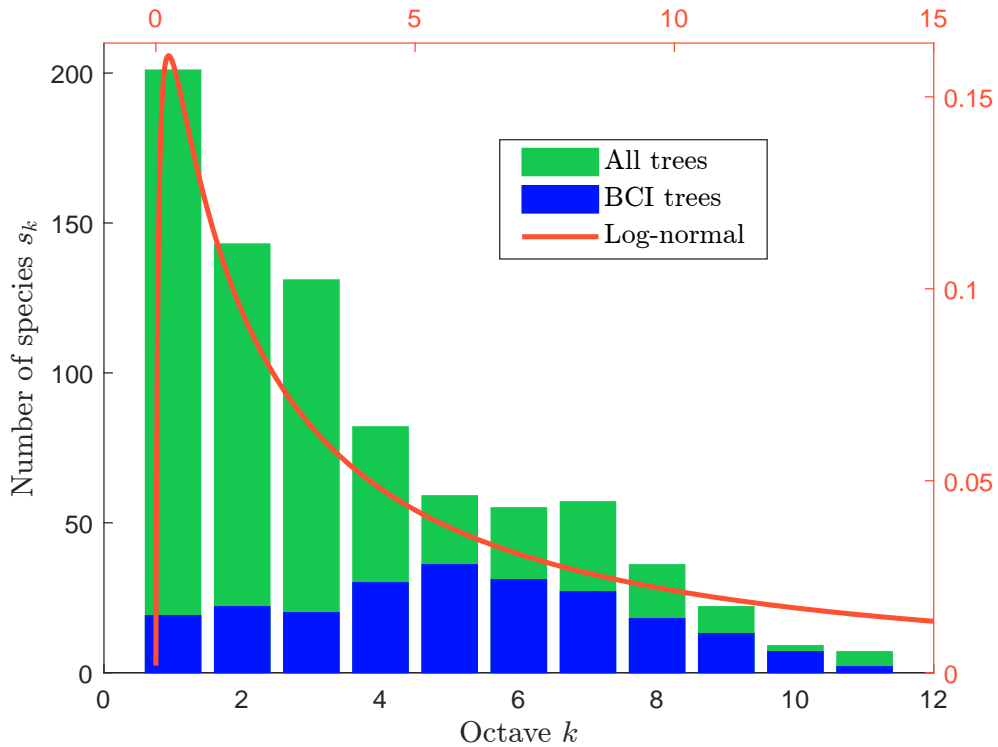
Empirical analysis of the number of species has led to the formulation of several probability models of species abundance. In 1932, Isao Motomura developed the resource (or niche) preemption model, which assumes that one species preempts a fraction $\kappa \in (0, 1)$ of the resource, a second species the same fraction κ of the remaining resource $(1 - \kappa)$, and so on. Assuming that the abundance of species i is proportional to its share of the resource, i.e., $(1 - \kappa)^{i-1} \kappa$, we obtain the geometric rank-abundance model[67]:

$$n_i = \frac{n\kappa (1 - \kappa)^{i-1}}{1 - (1 - \kappa)^S} \tag{20}$$

where S is the number of species and n is the total number of individuals. Another approach was proposed by Fisher et al. (1943), who developed a model where the number of species is derived

---

[66]This concept is often called the 'invisible fraction' in ecology.

[67]The scaling factor ensures that the sum of the individuals equals the total abundance:

$$\sum_{i=1}^{S} n_i = \frac{n\kappa}{1 - (1 - \kappa)^S} \sum_{i=1}^{S} (1 - \kappa)^{i-1} = \frac{n\kappa}{1 - (1 - \kappa)^S} \cdot \frac{1 - (1 - \kappa)^S}{1 - (1 - \kappa)} = n$$

from the limiting form of the negative binomial distribution $\mathcal{NB}(r, p)$, excluding zero observations. They demonstrated that the expected number of species with exactly j individuals is given by:

$$s(j) = \alpha \frac{x^j}{j} \tag{21}$$

where $x = (1-p)^{-1} p \in (0, 1)$, p is the success probability of the negative binomial distribution, and α is a scaling factor that depends on the parameters r and p. Since the total expected number of species is $S = \sum_{j=1}^{\infty} s(j) = -\alpha \ln(1-x)$ and the total expected number of individuals is $n = \sum_{j=1}^{\infty} s(j) \cdot j = \sum_{j=1}^{\infty} \alpha x^j = \alpha x / (1-x)$), the parameters of the log-series distribution $\mathcal{LS}(\alpha, x)$ can be determined by solving the following system of equations[68]:

$$\begin{cases} S = \alpha \ln\left(1 + \dfrac{n}{\alpha}\right) \\ x = \dfrac{n}{\alpha + n} \end{cases} \tag{22}$$

In chronological order, the third and fourth important SAD models are the log-normal model of Preston (1948), seen earlier on page 86, and the broken-stick model formulated by MacArthur (1957). In the log-normal model, the probability that a species has j individuals is given by $\Pr\{X = j\}$ where $X \sim \mathcal{LN}(\mu, \sigma^2)$. In practice, j is discrete rather than continuous. Considering the disjoint intervals $\left[j - \frac{1}{2}, j + \frac{1}{2}\right]$, we get[69]:

$$s_j = S \frac{\Phi\left(\sigma^{-1}\left(\ln\left(j + \frac{1}{2}\right) - \mu\right)\right) - \Phi\left(\sigma^{-1}\left(\ln\left(j - \frac{1}{2}\right) - \mu\right)\right)}{1 - \Phi\left(\sigma^{-1}\left(\ln\left(\frac{1}{2}\right) - \mu\right)\right)} \tag{23}$$

By construction we have $\sum_{j=1}^{\infty} s_j = S$. To calibrate μ and σ, we can fit the first moment — $\frac{n}{S} = e^{\mu + \frac{1}{2}\sigma^2}$ (or use the discrete version $\sum_{j=1}^{\infty} s_j \cdot j = n$ — or we can estimate μ and σ using the method of maximum likelihood. The broken-stick model assumes that the total resources (or individuals) available in a community are divided randomly among species, leading to a characteristic pattern of abundances. The community is represented as a stick of fixed length, the stick is broken into S segments at $S-1$ randomly chosen points, and the lengths of the resulting segments are proportional to the abundances of the S species — they follow a uniform distribution. The ith largest segment corresponds to a specific harmonic expectation based on the number of breaks. The abundance of the ith species is then given by $n_i = \frac{n}{S} \sum_{k=i}^{S} \frac{1}{k}$. May (1975) demonstrated that the corresponding species abundance distribution is:

$$s(j) = \frac{S}{n}(S-1)\left(1 - \frac{j}{n}\right)^{S-2} \tag{24}$$

---

[68]However, this approach ignores the distribution of the number of individuals $(n_1, n_2, \ldots, n_S)$. This means that two communities with the same number of species, the same total abundance, but different distributions of individuals among species will have the same species abundance distribution. To overcome this limitation, it is preferable to estimate the parameters x using the maximum likelihood method with the following probability mass function: $\Pr\{N = j\} = -\frac{x^j}{j \ln(1-x)}$ where N is the random variable representing the abundance of a species. Once the parameter x is estimated, the parameter α can be calculated as it serves as a scaling factor to fit the total number of species S.

[69]The normalization factor is needed because the support of the log-normal distribution is $(0, +\infty)$, while in this case we use the support $\left(\frac{1}{2}, +\infty\right)$.

where $j \in [0, S]$. We verify that the total number of species is exactly equal to S[70]. Figure 22 illustrates the four distributions when the number of species is $S = 15$ and the total abundance is $n = 80$. For the geometric model, the parameter κ is set to 0.50. The parameters of the log-series model are determined by solving Equation (22), yielding $\alpha = 5.450$ and $x = 0.936$. In the case of the log-normal model, we set $\sigma = 1$, which implies $\mu = \ln\left(\dfrac{80}{15}\right) - 0.5 \times 1^2 = 1.174$. The broken-stick model is already parameterized using n and S. The calibration of the parameters can be improved if the rank-abundance distribution $(n_1, \ldots, n_S)$ or the species abundance distribution $(s(1), \ldots, s(n^+))$ is known, by using the method of maximum likelihood. However, this approach is applicable only for the first three models.

Figure 33: Species abundance models
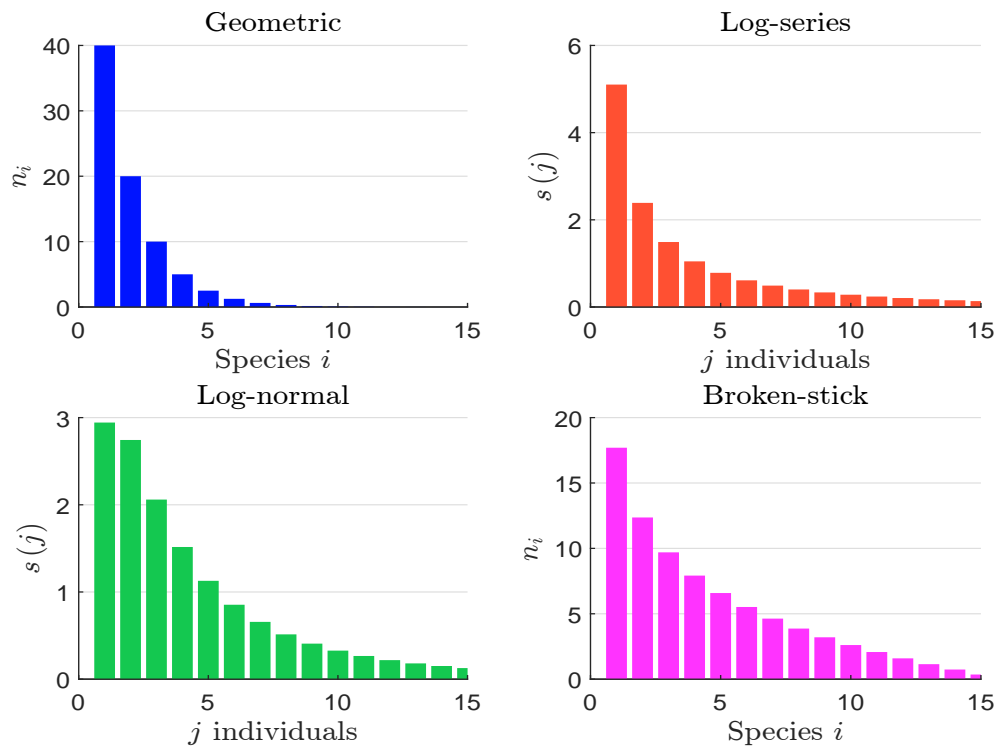
Sampling The species accumulation curve (SAC) is a graphical representation that illustrates how the number of observed species in a particular environment increases with additional sampling effort. It is also referred to as the species discovery curve or the collector's curve. The x-axis represents the sampling effort, such as the number of samples, individuals, cells, or plots surveyed, while the y-axis represents the cumulative number of species recorded. Let $n_i(s)$ be the number of individuals

---

[70]Specifically, we have:

$$\int_0^n s(j) \, \mathrm{d}j = S(S-1) \int_0^n \left(1 - \frac{j}{n}\right)^{S-2} \frac{\mathrm{d}j}{n}$$

Using the change of variable $u = \dfrac{j}{n}$, we obtain the desired result:

$$\int_0^n s(j) \, \mathrm{d}j = S(S-1) \int_0^1 (1-u)^{S-2} \, \mathrm{d}u = S(S-1) \left[-\frac{(1-u)^{S-1}}{S-1}\right]_0^1 = S$$

of species i recorded in the sth sample. The SAC function is defined as:

$$\text{SAC}(m) = \sum_{i=1}^{S} \mathbb{1}\left\{\sum_{s=1}^{m} n_i(s) \geq 1\right\}$$

where $m \leq m_s$ is the number of samples, and m_s is the total number of samples available. $\text{SAC}(m)$ counts the number of species present in the m samples. When a sample represents an individual, $\text{SAC}(m)$ is the expected number of species among m individuals selected at random. Hurlbert (1971, Equation (13), page 581) shows that[71]:

$$\text{SAC}(m) = \sum_{i=1}^{S}\left(1 - \frac{\dbinom{n-n_i}{m}}{\dbinom{n}{m}}\right)$$

where n_i is the abundance (number of individuals) of the ith species and n is the total abundance of the community. In this case, the species accumulation curve is often referred to as the species rarefaction curve. In the Barro Colorado Island census, the database contains 21 457 trees and 225 species, located in 50 1-ha plots. For each plot, the species and the number of individuals per species are recorded. Figure 34 shows the distribution of individual trees across the 50 plots. The species rarefaction curve is given in Figure 35. In addition to the theoretically expected number of species, the 95% confidence interval is also reported.

Figure 34: Number of individuals per plot (BCI trees)
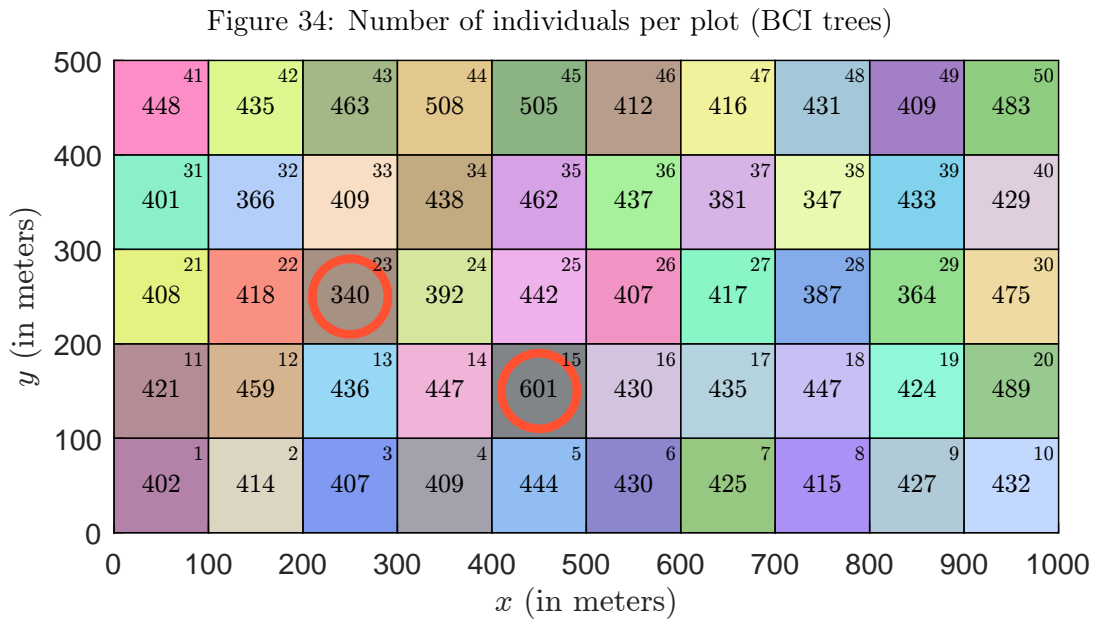
More generally, the species accumulation curve is represented as the parametric curve $(\text{SAC}(1), \ldots, \text{SAC}(m_s))$, where the sample set at iteration m is constructed by adding one sample to the set used in the previous iteration $m-1$, selected from the $m_s - m + 1$ remaining samples. Thus, the species accumulation curve is sensitive to the order in which the m_s samples are arranged.

---

[71]The binomial coefficient $\dbinom{n-n_i}{m}$ is zero when $m > n - n_i$.

Figure 35: Species accumulation curve (BCI trees)
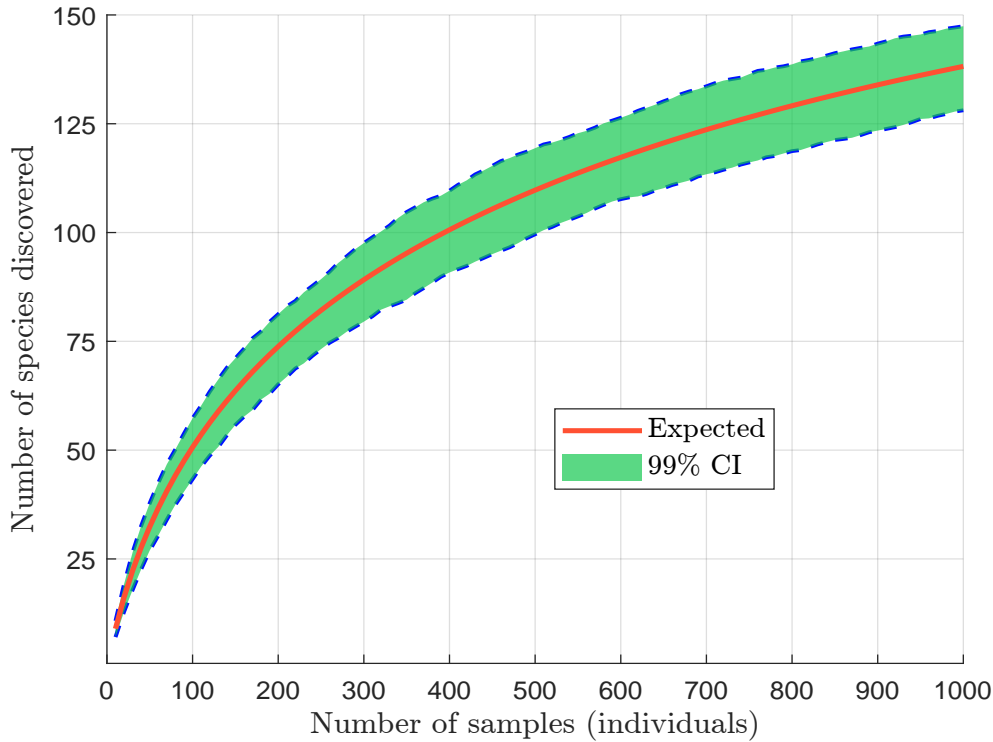
For instance, samples may be ordered by size, either from smallest to largest or vice versa. Alternatively, the historical order of sampling, from first to last, may be considered. Considering the BCI dataset, we discover 77 tree species if we start by sampling the 11th plot, and 109 tree species if the first sample is the 39th plot (Figure 36). To eliminate the sensitivity of the results to the ordering of the samples, we can use a third approach, which consists of generating random permutations of the entire sample set $(1, \ldots, m_s)$, computing the SAC function for each permutation, and performing a Monte Carlo simulation. By repeating this process r times and averaging the resulting curves, a more robust estimate of the species accumulation curve can be obtained. Figure 37 shows the species accumulation curve for trees in the Barro Colorado Island census. The mean curve (in red) is estimated using the Monte Carlo method with $1\,000$ replications. The 99% confidence interval is also shown in green.

The previous estimator of the species accumulation curve has some bias because it does not account for the underestimation of rare species. To address this problem, more sophisticated approaches are often used, in particular the estimators developed by Anne Chao. The *Chao1* estimator is a non-parametric method for estimating species richness from abundance data (Chao, 1984). It uses the frequency of rare species (singletons and doubletons) in the dataset to estimate the likely number of undetected species. The *Chao2* estimator is a variant of *Chao1* designed for use with presence-absence data across multiple samples (Chao, 1987). Instead of focusing on individual counts, it examines how often species are detected in different samples. The formula for this estimator is as follows:

$$S_{\mathrm{Chao2}}(m_s) = S_{\mathrm{obs}}(m_s) + \frac{(m_s - 1)}{m_s} \left(\frac{q_1(q_1 - 1)}{2(q_2 + 1)} \right)$$

where $S_{\mathrm{obs}}(m_s) = \mathrm{SAC}(m_s)$ is the total number of species observed in the set of m_s samples, q_m is the number of species present in exactly m samples — q_1 and q_2 are then the number of singleton and

Figure 36: Number of species per plot (BCI trees)
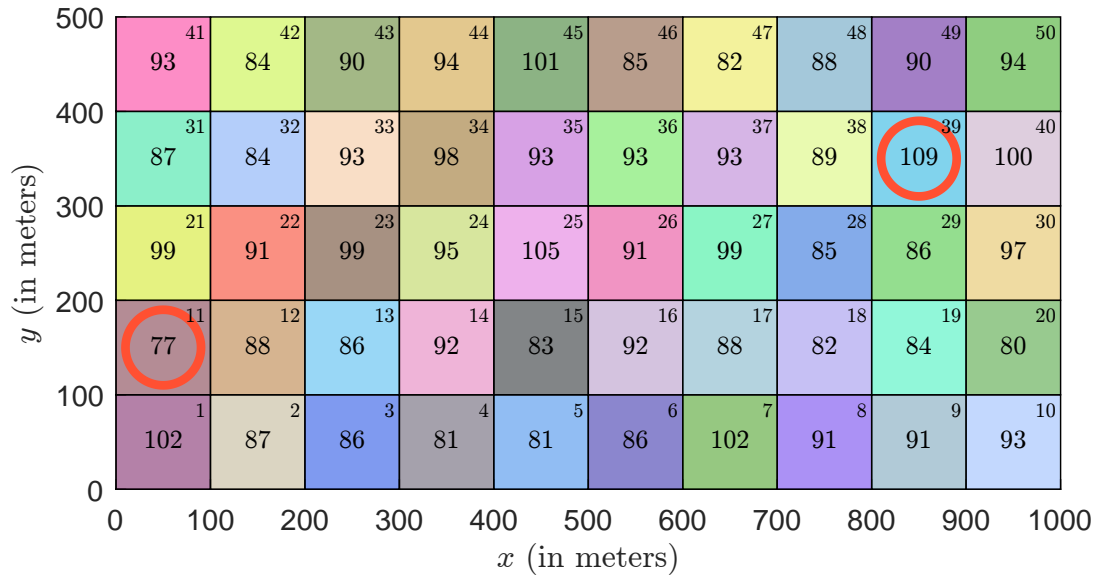
Figure 37: Species accumulation curve (BCI trees)
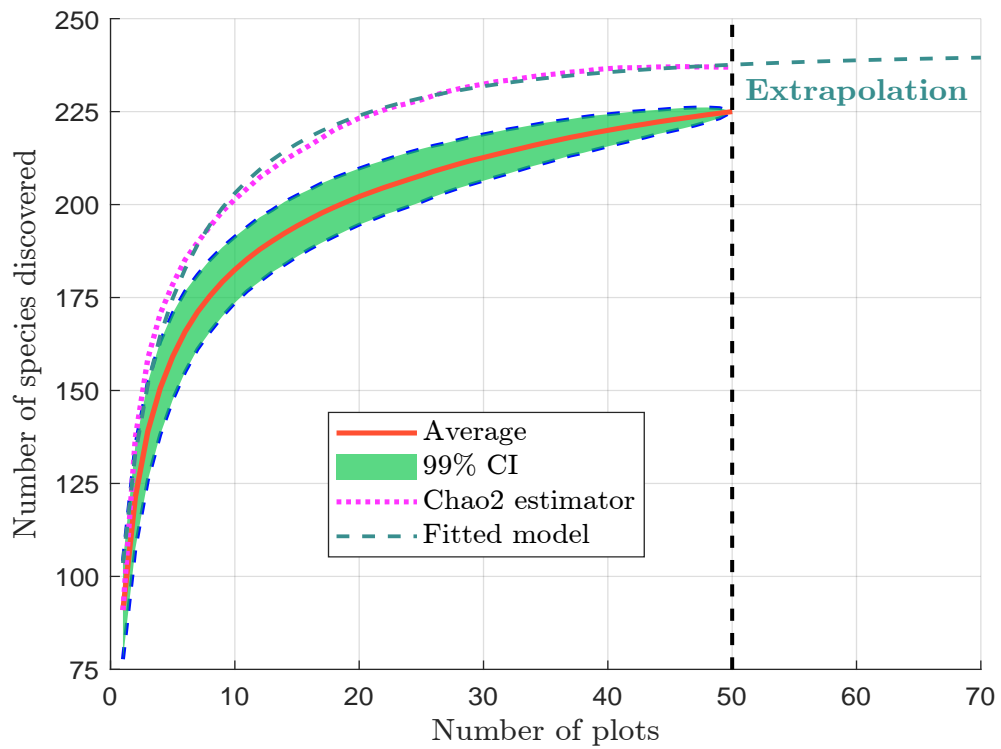
doubleton species. In Figure 37 we have added the *Chaos2* estimator to compare with the traditional empirical estimator. In this case, the number of tree species for the 50 ha patch is estimated to be 237 instead of 225.

The species accumulation curve is widely used to estimate the number of species in a region larger than the sampled area. This approach, known as extrapolation, was popularized by Robert K. Colwell in numerous published research papers (Colwell and Coddington, 1994; Gotelli and Colwell, 2001; Colwell *et al.*, 2004) . For example, Cazzolla Gatti *et al.* (2022) used this method to estimate the number of tree species on Earth. They first fitted a log-series model, then estimated the species accumulation curve, corrected it with the *Chao2* estimator, and finally extrapolated it by considering the lower 95% confidence bound. Their results indicate that there are 73 271 tree species globally, with the following distribution: 11 874 in Africa, 16 262 in Eurasia, 11 129 in North America, 31 110 in South America, and 8 232 in Oceania. Returning to the BCI tree database, we assume that the number of species follows the exponential model: $\text{SAC}(m) = \theta_1\left(1 - \exp\left(-\theta_2 m^{\theta_3}\right)\right)$. Using the species accumulation curve, we fit the parameters $(\theta_1, \theta_2, \theta_3)$ using the method of non-linear least squares. We find $\hat{\theta}_1 = 241.064$, $\hat{\theta}_2 = 0.562$ and $\hat{\theta}_3 = 0.517$. Since the 50 plots corresponds to 50 hectares, we would need to sample $15.6 \times 100 = 1\,560$ plots to cover the entire area of Barro Colorado Island, which spans $15.6\,\text{km}^2$. We estimate that there are about 241 different tree species[72], suggesting that 16 species remain to be discovered in the island (Figure 37).

Species-area relationship vs. endemics-area relationship   We consider a region (or area) A where the total number of species and the number of individuals per species are known exactly to be S and n_i. The species-area relationship can be expressed as the equality: $\text{SAR}(A) = S$. Our goal is to determine the expected number of species S_a of a subregion (or subarea) a contained within the larger region A. Assuming random placement of individuals within the area, we can show that the species-area relationship becomes[73]:

$$\text{SAR}(a) = S_a = S - \sum_{i=1}^{S}\left(1 - \frac{a}{A}\right)^{n_i}$$

where n_i is the number of individuals of species i in region A. We define two types of endemism as follows:

- Global endemism: A species is globally endemic to A if it is found exclusively in region A and nowhere else.

- Local endemism: A species is locally endemic to a if it occurs exclusively in subarea a and not in the complementary area $A - a$.

Under the assumption of random placement, the endemics-area relationship (EAR) is[74]:

$$\text{EAR}(a) = E_a = \sum_{i=1}^{S}\left(\frac{a}{A}\right)^{n_i}$$

where E_a is the expected number of species endemic to the subregion a. In Table 26, we report the expressions for $\text{SAR}(a)$ and $\text{EAR}(a)$ under different models (He and Legendre, 2002; Green and

---

[72]We have:
$$\text{SAC}(1\,560) = \hat{\theta}_1\left(1 - \exp\left(-\hat{\theta}_2 \times 1\,560^{\hat{\theta}_3}\right)\right) \approx 241$$

[73]The proof is given in Question 1 of Exercise A.3 on page 234.
[74]The proof is given in Question 2 of Exercise A.3 on page 234.

Table 26: Species-area and endemics-area relationships for various species abundance models

Model	Specification	SAR(a)	EAR(a)
Random placement	n_i is known	$S_a = S - \sum_{i=1}^{S}\left(1 - \frac{a}{A}\right)^{n_i}$	$E_a = \sum_{i=1}^{S}\left(\frac{a}{A}\right)^{n_i}$
Most even	$n_i = \frac{n}{S}$	$S_a = S\left(1 - \left(1 - \frac{a}{A}\right)^{\frac{n}{S}}\right)$	$E_a = S\left(\frac{a}{A}\right)^{\frac{n}{S}}$
Most uneven	$n_{i<S} = 1, n_S = n - S + 1$	$S_a = 1 + (S-1)\frac{a}{A} - \left(1 - \frac{a}{A}\right)^{n-S+1}$	$E_a = (S-1)\frac{a}{A} + \left(\frac{a}{A}\right)^{n-S+1}$
Geometric	$n_i = \frac{n\kappa(1-\kappa)^{i-1}}{1-(1-\kappa)^S}$		
Mixed even-uneven	$n_{i\le s} = 1,\ n_{i>s} = \frac{n-s}{S-s}$	$S_a = s\frac{a}{A} + (S-s)\cdot\left(1 - \left(1 - \frac{a}{A}\right)^{\frac{n-s}{S-s}}\right)$	$E_a = S - s\left(1 - \frac{a}{A}\right) - (S-s)\left(1 - \left(\frac{a}{A}\right)^{\frac{n-s}{S-s}}\right)$
Random placement	$s(j)$ is known	$S_a = S - \sum_j s_j\left(1 - \frac{a}{A}\right)^j$	$E_a = \sum_j s_j\left(\frac{a}{A}\right)^j$
Log-series	$s(j) = \alpha\frac{x^j}{j}$	$S_a = \alpha\ln\left(1 + \frac{x\frac{a}{A}}{1 - x\frac{a}{A}}\right)$	$E_a = -\alpha\ln\left(1 - x\frac{a}{A}\right)$
Broken-stick	$s(j) = \frac{S}{n}(S-1)\left(1 - \frac{j}{n}\right)^{S-2}$	$S_a = \frac{S\ln\left(1 - \frac{a}{A}\right)}{\ln\left(1 - \frac{a}{A}\right) - \frac{n}{S}}$	$E_a = -\frac{S^2}{n\ln\left(\frac{a}{A}\right) - S}$
Truncated negative binomial distribution	$s(j) = \frac{\Gamma(\gamma+j)}{\Gamma(j+1)\Gamma(\gamma)}\cdot\frac{\phi^j}{(1+\phi)^{\gamma+j} - (1+\phi)}$	$S_a = S\frac{1 - \left(1 + \phi\frac{a}{A}\right)^{-\gamma}}{1 - (1+\phi)^{-\gamma}}$	$E_a = S\frac{\left(1 + \phi\left(1 - \frac{a}{A}\right)\right)^{-\gamma} - (1+\phi)^{-\gamma}}{1 - (1+\phi)^{-\gamma}}$

n_i is the number of individuals of species i, s_j is the number of species with j individuals, α and x are the parameters of the log-series model, κ is the resource preemption parameter, and γ and ϕ are the shape and scale parameters of the TNBD model.

Source: He and Legendre (2002, Table 1, page 1187), Green and Ostling (2003, Table 1, page 3091) & Author's calculations.

Ostling, 2003). According to He and Hubbell (2011), the expected number of species lost due to the loss of area a can be calculated as:

$$\mathcal{L}oss\left(a \mid A\right) = S_A - S_{A-a} = S - \left(S - \sum_{i=1}^{S}\left(1 - \frac{A-a}{A}\right)^{n_i}\right) = \sum_{i=1}^{S}\left(\frac{a}{A}\right)^{n_i} = E_a$$

Thus, E_a can be interpreted as the number of species lost if habitat area a is destroyed. This gives the following identity:

$$\text{SAR}\left(A\right) = \text{SAR}\left(A - a\right) + \text{EAR}\left(a\right)$$

which states that the number of species in region A is equal to the sum of the species found in subregion $A - a$ and the species locally endemic in subregion a.

He and Legendre (2002) used the tree dataset from the Pasoh Forest Reserve in Malaysia. The research area consists of a 50-ha plot (500×1000 m), established in 1986 and resurveyed several times between 1990 and 2016. The 1987 survey recorded 335 356 individual stems and 814 tree species. He and Legendre (2002) calibrated several species abundance models[75]. Figure 38 shows the estimated species-area relationship for each model compared to the empirical species-area relationship derived from the recorded data. We observe that the empirical curve lies between the broken-stick and geometric models. The endemics-area relationship is plotted in Figure 39. We restrict the analysis to surface areas larger than 1 ha because $\text{EAR}\left(a\right) \approx 0$ when $a \approx 0$. This is not the case for the function $\text{SAR}\left(a\right)$. As noted by He and Hubbell (2011), there is an asymmetry between the two curves. In fact, it is easier to discover a species quickly when exploring a patch, whereas the extinction of a species requires the destruction of a large proportion of the patch. He and Hubbell (2011) concluded that species-area relationships always overestimate extinction rates due to habitat loss:

> "*Here we show that extinction rates estimated from the SAR are all overestimates. [...] These overestimates are due to the false assumption that the sampling problem for extinction is simply the reverse of the sampling problem for the SAR. The area that must be added to find the first individual of a species is in general much smaller than the area that must be removed to eliminate the last individual of a species. Therefore, on average, it takes a much greater loss of area to cause the extinction of a species than it takes to add the species on first encounter, except in the degenerate case of a species having a single individual. [...] Only in a very special and biologically unrealistic case, when all species are randomly and independently distributed in space, is it possible to derive the EAR from the SAR.*" (He and Hubbell, 2011, page 368).

In this context, the choice of the power-law model can create some bias. Recall that $S_A = cA^z$. We can deduce that $S_{A-a} = c\left(A - a\right)^z$ and $E_a = S_A - S_{A-a} = cA^z - c\left(A - a\right)^z$. It follows that:

$$\mathcal{L}oss_{species} = \frac{E_a}{S_A} = 1 - \frac{\left(A - a\right)^z}{A^z} = 1 - \left(1 - \mathcal{L}oss_{habitat}\right)^z \tag{25}$$

We retrieve Equation (16) on page 78. At first glance, it seems that the approach based on the endemics-area relationship is coherent with the species-area relationship. In fact, the issue lies in the calibration of the endemics-area curve, which generally produces a value of z smaller than

---

[75]The estimated parameters are $\kappa = 0.009927$ for the geometric model, and $\alpha = 100.3014$ and $x = 0.999701$ for the log-series model. The other models are completely determined by the number of individuals ($n = 335\,356$) and the number of species ($S = 814$).

Figure 38: Species-area relationship (Pasoh Forest Reserve)
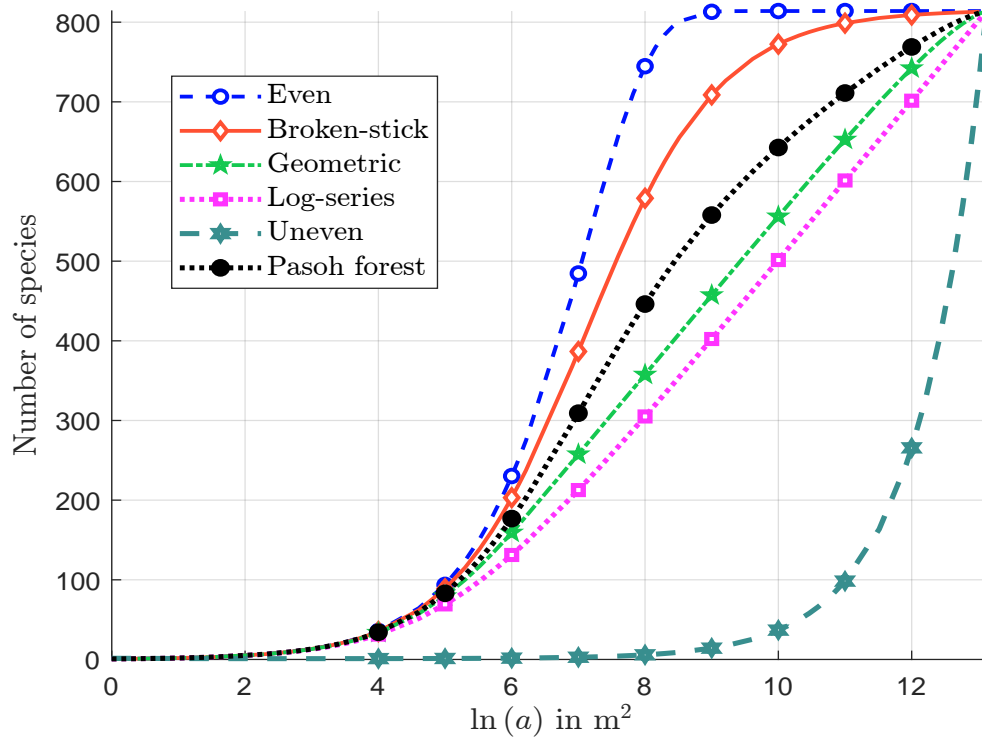
Source: He and Legendre (2002, Figure 2a, page 1191) & Author's calculations.

Figure 39: Endemics-area relationship (Pasoh Forest Reserve)
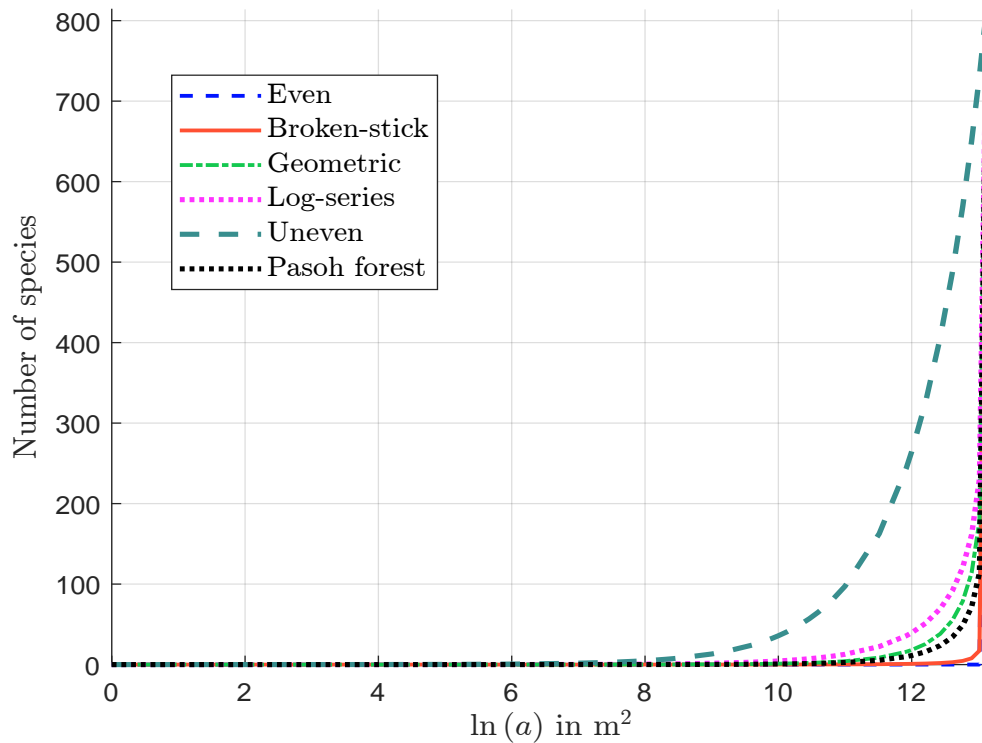
Source: Green and Ostling (2003, Figure 1a, page 3093) & Author's calculations.

Figure 40: Comparison of species-area and endemics-area curves (Barro Colorado Island)
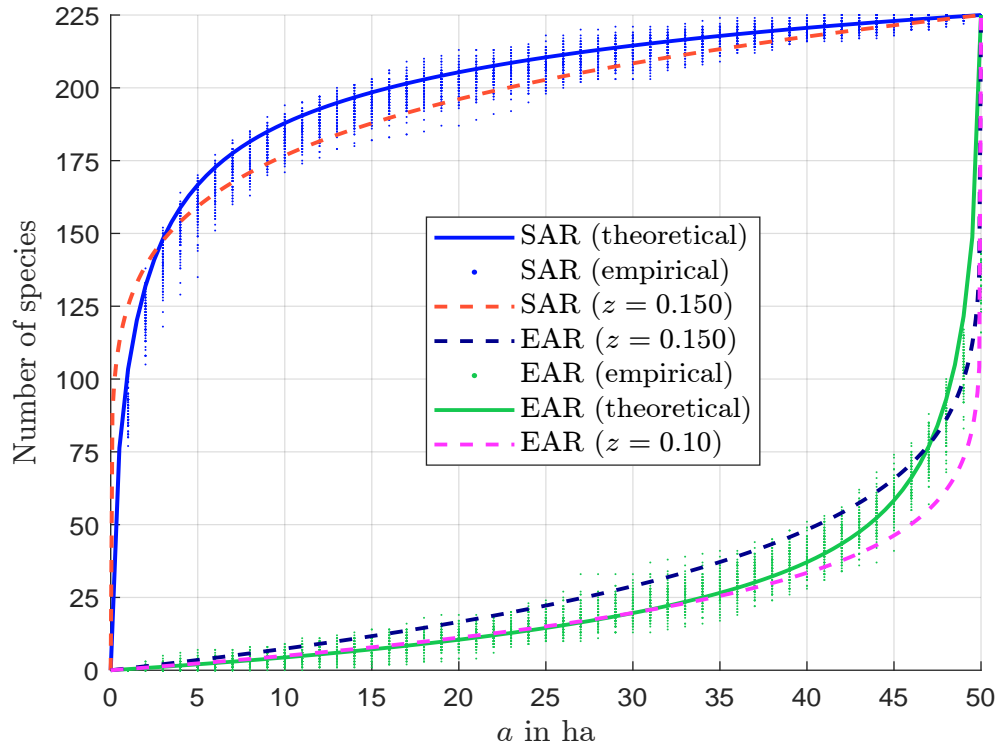
the value obtained with the species-area curve. As a result, we deduce that the extinction rate is overestimated:

$$\mathcal{L}oss_{species} = 1 - (1 - \mathcal{L}oss_{habitat})^{z_{\text{EAR}}} \leq 1 - (1 - \mathcal{L}oss_{habitat})^{z_{\text{SAR}}}$$

To illustrate this bias, He and Hubbell (2011) considered nine datasets, including those from the Barro Colorado Island and the Pasoh Forest, and found that $z_{\text{EAR}} \leq z_{\text{SAR}}$ in all cases. For example, for the Pasoh Forest Reserve, they found $z_{\text{EAR}} = 0.0536$ and $z_{\text{SAR}} = 0.124$. Figure 40 shows the empirical and theoretical SAR and EAR curves, along with the calibrated power-law models. We verify that $\mathcal{L}oss_{species}$ is overestimated when z_{SAR} is used instead of z_{EAR}. On page 78 we estimate that 50% of habitat loss should reduce the number of species by 15.91%, while 90% of habitat loss leads to 43.77% of species loss because we use the value $z_{\text{SAR}} = 0.25$ suggested by Pimm *et al.* (1995). If we consider a value of $z_{\text{EAR}} = 0.10$, which is the median value obtained by He and Hubbell (2011), 50% of habitat loss should reduce the number of species by 6.70%, while 90% of habitat loss leads to 20.57% of species loss (Table 22, page 78). The numbers are quite different.

Remark 9 *Censuses of tree data are abundant and valuable for studying relationships between habitat and species richness. Many of these datasets (including those from Barro Colorado Island and the Pasoh Forest Reserve) are available at* http://ctfs.si.edu/datarequest, *the data portal of ForestGEO (Forest Global Earth Observatory). ForestGEO is a global network dedicated to the study of forests and their ecosystems. Hosted by the Smithsonian Institution, it is one of the most comprehensive forest monitoring programs in the world. The network includes 78 forest research sites in the Americas, Africa, Asia, Europe, and Oceania, that monitor the growth and survival of approximately 7 million trees representing nearly 13 000 species.*

Box 10: Forest definitions adopted by major international environmental and forestry organizations

- United Nations Food and Agriculture Organization (2000)
  Land with tree crown cover (or equivalent stocking level) of more than 10% and an area of more than 0.5 ha. Trees should be able to reach a minimum height of 5 m at maturity *in situ.*

- United Nations Framework Convention on Climate Change (2002)
  Minimum area of 0.05–1.0 ha of land with tree crown cover (or equivalent stocking level) of more than 10–30% with trees that have the potential to reach a minimum height of 2–5 m at maturity *in situ.*

- United Nations Convention on Biological Diversity
  Land area of more than 0.5 ha, with a tree canopy cover of more than 10%, which is not primarily under agriculture or other specific non-forest land use.

- United Nations Convention to Combat Desertification (2000)
  Dense canopy with multi-layered structure including large trees in the upper story.

- International Union of Forest Research Organizations (2002)
  Land area with a minimum 10% tree crown coverage (or equivalent stocking level), or formerly having such tree cover and that is being naturally or artificially regenerated or that is being afforested.

Source: Chazdon *et al.* (2016, Box 1, page 542).

3.1.4 Forest loss

Among the various types of habitat loss, forests are particularly important because they are biodiversity hotspots, home to numerous endemic species. These ecosystems provide essential services, including climate regulation, water cycle maintenance, and soil stabilization. In addition, forests are complex, interconnected networks where species are highly interdependent. Loss of forest habitat can trigger trophic cascades, destabilizing entire ecological systems by disrupting some fundamental biological relationships. However, the concept of forest loss is somewhat vague and requires a clear definition of what constitutes a forest and what does not. According to the Oxford English Dictionary, a forest is defined as "*a large area of land that is thickly covered with trees*", while the Cambridge Dictionary defined it as "*a large area of land covered with trees and plants, usually larger than a wood*". However, despite its common usage, there is no universally agreed-upon definition of the word forest. The concept of a forest extends far beyond a simple description of tree coverage and must encompass various dimensions of biodiversity, particularly when aiming to measure ecosystem functions or address key aspects of forest conservation biology (Zalles *et al.*, 2024). For instance, these aspects include forest loss, degradation, afforestation, reforestation, and other related processes. In Box 10, we report the forest definitions of five international organizations collected by Chazdon *et al.* (2016). While the definition depends on the purpose and the organization, the FAO definition is the most widely used globally. The FAO definition is practical because it uses measurable parameters such as tree height, canopy cover, and area. Here is the latest version used for the 2025 FRA[76]:

---

[76]A forest is defined by the presence of trees and the absence of dominant non-forest land uses. It includes young or regenerating areas that are expected to reach a height of 5 meters and a canopy cover of 10%. Forests also include

"*Land spanning more than 0.5 hectares with trees higher than 5 meters and a canopy cover of more than 10 percent, or trees able to reach these thresholds in situ. It does not include land that is predominantly under agricultural or urban land use.*" (FAO, 2023a, Section 1a, page 7).

Another success factor is that data on forest status and trends are easily available thanks to the Global Forest Resources Assessment (FRA), which is collected and published by the FAO every five years[77].

Figure 41: Proportion and distribution of global forest area by climatic domain in 2020

Tropical
45%

Boreal
27%

Temperate
16%
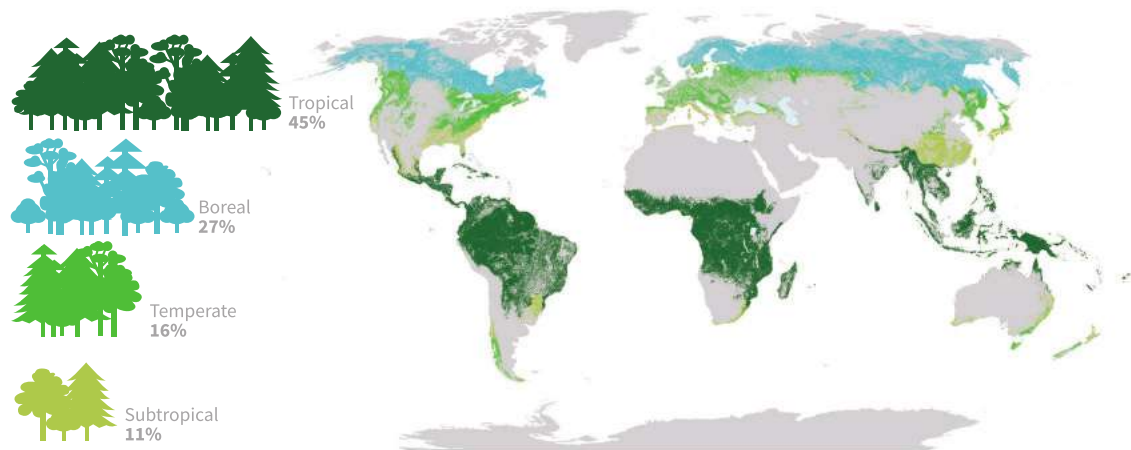
Subtropical
11%

Source: FAO (2020, page 1).

According to FAO (2020), the world has a total forest area of 4.06 billion hectares, which represents 31% of the total land area. This area corresponds to 0.52 ha per person. Tropical forests[78] account for 45% of the world's forests, followed by boreal forests (27%), temperate forests (16%) and subtropical forests (11%), while polar forests account for less than 1% (Figure 41). More than 50% of the world's forests are located in just five countries: Russia, Brazil, Canada, the United States and China. In Table 27, we present the forest area of the top 20 countries, changes by decade, the distribution of the world's forest area in 2020, and the proportion of primary forest[79] in 2020. For instance, Brazil had 589 million hectares of forest in 1990, which decreased to 497 million hectares in 2020. The country experienced forest area losses of 6.42%, 7.17%, and 2.92% between 1990–2000, 2000–2010, and 2010–2020, respectively. In 2020, Brazil accounted for 12.24% of the world's forest area, and 43.53% of its forests were classified as primary forests. Figure 42 shows the percentage of land area covered by forests. Globally, forests cover 31.1% of the total land area, but there are significant differences between countries. Seven countries have more than 90% of their land area covered by forest: Suriname (97.41%), French Guiana (97.36%), Guyana (93.55%), Micronesia

---

mangroves, shelterbelts, bamboo, palms, and specialty plantations such as rubber and cork oak. Protected areas, forest infrastructure and abandoned shifting cultivation areas with tree regeneration are included. Agricultural tree systems such as orchards, fruit plantations and agroforestry with crops are excluded.

[77]The FRA website is www.fao.org/forest-resources-assessment while the FRA data are available at https://fra-data.fao.org/assessments/fra/2020.

[78]The climatic groups are defined as follows: tropical (all months without frost; in marine areas above $18°C$), subtropical (eight months or more above $10°C$), temperate (four to eight months above $10°C$), boreal (up to three months above $10°C$) and polar (all months below $10°C$).

[79]Primary forests are old-growth natural forests that have been largely undisturbed by human activity and have retained their original biodiversity and ecological processes.

Table 27: Forest area (top 20 countries and six world regions)

Country/region	Value (in million ha)				Variation by decade (in %)			Geographical distribution		Primary forest in %
	1990	2000	2010	2020	2000	2010	2020	in %	Cumulated	
Russia	809	809	815	815	0.04	0.72	0.02	20.09	20.09	31.30
Brazil	589	551	512	497	−6.42	−7.17	−2.92	12.24	32.32	43.53
Canada	348	348	347	347	−0.14	−0.14	−0.11	8.55	40.87	59.13
United States of America	302	304	309	310	0.36	1.71	0.35	7.63	48.50	24.31
China	157	177	201	220	12.64	13.34	9.65	5.42	53.92	5.21
Australia	134	132	130	134	−1.54	−1.72	3.44	3.30	57.22	
Congo (DRC)	151	144	137	126	−4.47	−4.68	−8.03	3.11	60.33	65.59
Indonesia	119	101	100	92	−14.56	−1.60	−7.55	2.27	62.60	48.56
Peru	76	75	74	72	−1.51	−1.66	−2.32	1.78	64.38	
India	64	68	69	72	5.71	2.82	3.83	1.78	66.16	21.76
Angola	79	78	72	67	−1.96	−7.14	−7.69	1.64	67.80	40.15
Mexico	71	68	67	66	−3.13	−2.10	−1.87	1.62	69.42	48.77
Colombia	65	63	61	59	−3.42	−3.07	−2.74	1.46	70.88	
Bolivia	58	55	53	51	−4.68	−3.66	−4.24	1.25	72.13	
Venezuela	52	49	48	46	−5.53	−3.35	−2.68	1.14	73.27	97.06
Tanzania	57	54	50	46	−6.48	−6.93	−8.42	1.13	74.40	62.32
Zambia	47	47	47	45	−0.76	−0.76	−4.03	1.10	75.50	
Mozambique	43	41	39	37	−5.05	−5.38	−5.72	0.91	76.40	
Papua New Guinea	36	36	36	36	−0.33	−0.27	−0.89	0.88	77.29	
Argentina	35	33	30	29	−5.19	−9.48	−5.43	0.70	77.99	
Africa	743	710	676	637	−4.41	−4.79	−5.82	15.68	15.68	19.30
Asia	585	587	611	623	0.34	4.01	1.92	15.34	31.03	13.79
Europe	994	1 002	1 014	1 017	0.80	1.17	0.34	25.07	56.09	25.22
North and Central America	755	752	754	753	−0.39	0.24	−0.20	18.54	74.64	41.62
Oceania	185	183	181	185	−0.89	−1.26	2.34	4.56	79.20	1.41
South America	974	923	870	844	−5.24	−5.69	−2.98	20.80	100.00	35.38
World	4 236	4 158	4 106	4 059	−1.85	−1.24	−1.15	100.00	200.00	26.61

Figure 42: Percentage of land area covered by forest, by country (2020)

Share of land covered by forest, 2020

Forest area includes land with natural or planted groups of trees at least five meters tall, excluding those in agricultural systems.

No data   0%   10%   20%   30%   40%   50%   60%   70%   80%   90%   100%

Data source: Food and Agriculture Organization of the United Nations and historical sources
OurWorldinData.org/forests-and-deforestation | CC BY

Source: Our World in Data, https://ourworldindata.org/forest-area.

Figure 43: Distribution of global forest area (2020)

Share of global forest area, 2020

No data   0%   0.25%   0.5%   0.75%   1%   2.5%   5%   10%

Data source: UN Food and Agriculture Organization (FAO). Forest Resources Assessment.   OurWorldinData.org/forest-area | CC BY
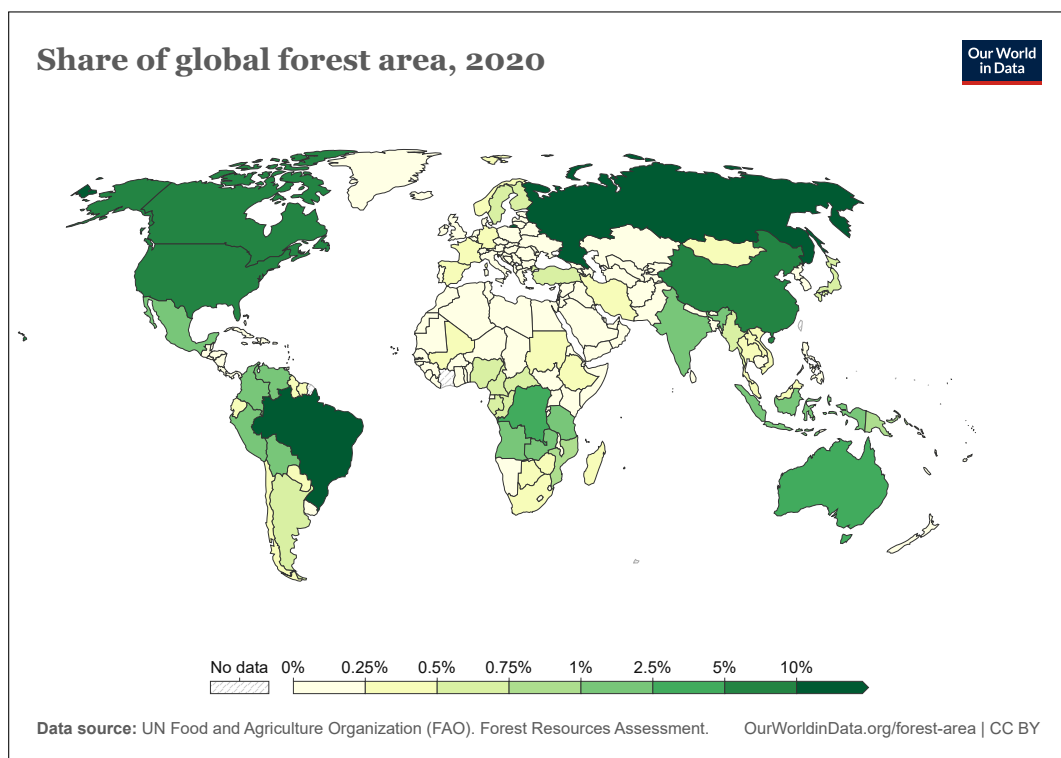
Source: Our World in Data, https://ourworldindata.org/forest-area.

(92.03%), Gabon (91.32%), Solomon Islands (90.14%), and Palau (90.02%). Some of the world's largest countries also have a significant proportion of their land area covered by forest. For example, Russia (49.78%), China (23.34%), the United States (33.87%), Canada (38.15%), and Brazil (59.42%) all have significant forest cover. Conversely, other large countries have relatively low forest cover, such as Argentina (10.44%), Kazakhstan (1.28%), and Algeria (0.82%). Among the largest European countries (those with a land area of more than 20 million hectares), forest cover also varies widely. Most of these countries have at least 30% forest cover, including Belarus (43.19%), Germany (32.73%), Spain (37.17%), Finland (73.74%), France (31.51%), Italy (32.52%), Norway (40.05%), Poland (30.97%), Romania (30.12%) and Sweden (68.69%). However, some countries fall below this threshold, such as Ukraine (16.73%) and the United Kingdom (13.19%).

Table 28 presents some key forest characteristics. Globally, 17% of forests are located in protected areas, representing more than 700 million hectares. Among the six world regions, South America has the highest proportion of forests in protected areas (30.5%), followed by Africa (24.8%). Natural (regenerative) forests account for 92.4% of the global forest area, while 7.2% consists of planted forests. In addition, the majority of the world's forests are publicly owned (71.5%), compared to 21.7% under private ownership, with the remainder classified as unknown. Public ownership predominates in all regions, especially in Europe (88.2%), largely due to Russia, where 100% of forests are publicly owned.

We have seen that the world lost 177 million hectares of forest between 1990 and 2020. Focusing on the period 2015–2020, the annual forest loss was about 5 million hectares. This figure, representing the net change, is the difference between the forest expansion rate and the deforestation rate. In Table 28, we present these two statistics together with the reforestation rate, all expressed in 1 000 hectares per year. For some countries, data on forest expansion, deforestation, and reforestation[80] are missing (*e.g.*, the United States, Australia, Congo, Angola), which introduces bias into the global rates. However, estimates from FAO (2020, page 4) indicate that the annual net loss of 5 million hectares is the result of a deforestation rate of 10 million hectares per year offset by a forest expansion rate of 5 million hectares per year. Although there is a declining trend in forest loss in the short term, the average rate of forest loss has accelerated in the long term. In fact, between the invention of agriculture and the beginning of the Industrial Revolution, we lost 2% of forest area every 5 000 years. Since 1700, as shown in Table 29, this rate has accelerated, especially since 1950.

The GFA dataset is not dedicated to the study of forest loss, although it contains a lot of information on this topic. To obtain information at a higher resolution than regional and country levels, and at a higher frequency than the 5-year period (for example, to obtain statistics on the Amazon rainforest on quarterly basis), other sources of information are available:

- The Global Forest Review (GFR) is an initiative of the World Resources Institute (WRI) that provides data, analysis and insight on the world's forests (https://research.wri.org/gfr/global-forest-review). It serves as a resource for tracking the state of the world's forests, understanding deforestation trends, and evaluating forest conservation efforts. GFR uses many datasets derived from geospatial data and maps.

- Global Forest Watch (GFW) is an online platform, available at www.globalforestwatch.org and developed by the World Resources Institute (WRI), that provides near real-time

---

[80]Forest expansion refers to the growth of forest on land previously used for other purposes, involving a change of land use from non-forest to forest. It includes both afforestation (planting of trees on land that was not previously forested) and natural expansion of forests. Deforestation is the conversion of forested land to other land uses, whether this change is caused by human activities or by natural processes. Reforestation is the reestablishment of forest on land that is still classified as forest, typically through planting or deliberate seeding. Unlike forest expansion, it does not involve a change in land use.

Table 28: Forest characteristics, ownership and annual change (top 20 countries and six world regions)

Country/region	Forest area (10^6 ha)	Protected (%)	Regenerative (%)	Planted (%)	Private ownership (%)	Public ownership (%)	Expansion (10^3 ha/year)	Deforestation (10^3 ha/year)	Reforestation (10^3 ha/year)	Coverage (%)	Net change (10^3 ha/year)
Russia	815	2.3	97.7	2.3	0.0	100.0	76	0	945	100.0	76
Brazil	497	30.1	97.7	2.3	44.2	55.8	243	1 696	257	100.0	−1 453
Canada	347	8.5	94.8	5.2	8.2	91.4	0	38	427	100.0	−38
United States of America	310	10.2	91.1	8.9	58.1	41.9			691	0.0	−60
China	220	13.8	61.5	38.5	41.3	58.7	2 070	133	273	100.0	1 937
Australia	134	18.0	98.2	1.8	32.3	67.0				0.0	182
Congo (DRC)	126	19.3	100.0	0.0	0.0	100.0				0.0	−1 101
Indonesia	92	56.2	95.1	4.9	1.1	91.2	71	650	7	100.0	−579
Peru	72	31.6	98.5	1.5	16.0	84.0	6	179		100.0	−173
India	72	19.4	81.6	18.4	18.5	81.5	935	668		100.0	266
Angola	67	2.8	98.8	1.2	0.0	100.0			0	0.0	−555
Mexico	66		99.8	0.2	79.3	3.6	38	166	159	100.0	−128
Colombia	59	21.0	99.3	0.7	30.4	66.0	1	199	497	100.0	−199
Bolivia	51	24.5	99.9	0.1	0.1	99.9	4	243	3	100.0	−239
Venezuela	46	98.6	97.1	2.9	2.3	97.7	18	108	4	100.0	−90
Tanzania	46	62.3	98.8	1.2	7.3	4.1	5	474	27	100.0	−469
Zambia	45	71.0	99.9	0.1	6.4	26.2	2	190	4	100.0	−188
Mozambique	37	41.4	99.8	0.2	0.2	99.8	28	267	2	100.0	−239
Papua New Guinea	36	3.8	99.8	0.2	99.9	0.1	0	34	0	99.4	−34
Argentina	29	6.7	95.0	5.0	4.4	0.0	30	135	17	100.0	−105
Africa	637	24.8	98.2	1.8	5.5	71.4	404	2 149	353	44.0	−3 969
Asia	623	21.9	78.2	21.7	21.6	76.8	3 477	1 922	1 221	118.2	1 316
Europe	1 017	4.9	91.3	7.4	9.1	88.2	255	69	1 593	56.0	331
North and Central America	753	9.5	93.7	6.2	35.2	60.5	79	372	1 322	84.2	−348
Oceania	185	15.7	97.1	2.6	47.2	52.2	16	40	56	−15.0	163
South America	844	30.5	97.6	2.4	31.9	61.6	460	2 962	947	100.9	−2 481
World	4 059	17.3	92.4	7.2	21.7	71.5	4 691	7 514	5 492	56.6	−4 987

Source: FAO (2020), https://fra-data.fao.org/assessments/fra/2020 & Author's calculations.

Table 29: Distribution of habitable land on Earth (excluding glaciers and deserts)

Time	Forests	Cropland	Grazing land	Wild grassland and shrubs	Urban and built-up land
10 000 years ago	57%			42%	
5 000 years ago	55%		1%	44%	
1700	52%	3%	6%	38%	
1900	48%	8%	16%	27%	
1950	44%	12%	31%	12%	1%
2020	37%	16%	31%	14%	2%

Source: Our World in Data, https://ourworldindata.org/forest-area & Author's calculations

monitoring of global forest change. It uses advanced satellite technology, big data, and open access to empower users to monitor forests and take action against deforestation.

- Academic studies are extensively documented on specific regions and provide high-level analysis of data provided by GFA, GFR, GFW and other datasets. They may include a new way of observing forests, for example using satellite imagery[81], an in-depth analysis of forms of forest degradation[82], etc.

According to the Global Forest Review, the top 10 countries with the highest global tree cover loss between 2001 and 2023 are Russia (83.7 Million hectares or Mha), Brazil (68.9 Mha), Canada (57.5 Mha), the United States (47.9 Mha), Indonesia (30.8 Mha), the Democratic Republic of Congo (19.7 Mha), China (12.1 Mha), Malaysia (9.2 Mha), Australia (9 Mha), and Bolivia (8 Mha). However, tree cover loss does not always equate to deforestation. In some cases, such as commercial forestry, tree cover loss is temporary because forests are allowed to regrow after harvesting. This is particularly true in countries such as Russia and Canada, which have a permanent tree cover loss rate of 0%. Similarly, the United States, China and Australia have permanent loss rates of less than 5%. In contrast, countries such as Indonesia, Malaysia and Bolivia have permanent tree cover loss rates of more than 80%, indicating significant deforestation. Brazil and the Democratic Republic of the Congo fall between these two extremes, with permanent forest loss rates of 71% and 35%, respectively. Together, these 10 countries are responsible for 71% of the global tree cover loss of 488 Mha between 2001 and 2023. Curtis et al. (2018) propose a classification of forest loss into five main drivers (Box 11). Forestry accounts for 32% of global forest loss between 2001 and 2023, followed by shifting agriculture and wildfires, each contributing 23%. Commodity-driven deforestation accounts for 21%, while urbanization is responsible for less than 1%. According to the Global Forest Review, the drivers of forest loss vary significantly from one region to another (Figure 44). While commodity-driven deforestation is the leading cause of forest loss in Latin America and Southeast Asia, its impact is minimal in other regions, which are dominated by wildfires and forestry, with the exception of Africa, where 95% of forest loss is attributed to shifting agriculture.

The Global Forest Review also provides many interesting figures for understanding deforestation. For example, we learn that seven commodities account for 57% of all agricultural-related tree cover

---

[81]Three notable examples are the studies by Hansen et al. (2013b) and Potapov et al. (2022), which use a dataset of land cover at a 30-meter spatial resolution derived from NASA's Landsat program, and the study by Lesiv et al. (2022), which is based on a dataset of forest management practices at a 100-meter resolution for the year 2015, derived from the European Space Agency's PROBA-V satellite imagery program.

[82]See for example Lapola et al. (2023), who studied four primary disturbances contributing to Amazon forest degradation: timber extraction, fire (sometimes used for land clearing, which can escape control and damage surrounding forests), edge effects (resulting from deforestation and habitat fragmentation), and extreme drought.

Box 11: Drivers of forest loss

- Forestry
  Large-scale forestry operations in managed forests or tree plantations where future regrowth is likely. Regrowth may occur through natural regeneration or tree planting.

- Commodity-driven deforestation
  Long-term permanent conversion of forest and shrubland to non-forest land for commodity production, including agriculture, mining, or oil and gas production.

- Wildfire
  Burning of vegetation without visible human conversion or agricultural activity afterward. Some of these fires occur naturally, but others are set by humans. In humid tropical forests, fires are not natural to the ecosystem and are almost always set by humans, usually to clear land for agriculture.

- Shifting agriculture
  Agricultural practices in which forests are cleared, used for agricultural production for a few years, and then temporarily abandoned to allow trees to regrow. Shifting agriculture involves many different types of smallholder farming practices.

- Urbanization
  Permanent conversion of forests to human settlements for the expansion and intensification of existing urban centers.

Source: Curtis *et al.* (2018, pages 1108-1109).

Figure 44: Drivers of tree cover loss by region (2001–2023)

Source: https://research.wri.org/gfr/global-forest-review.

Lecture Notes on Biodiversity
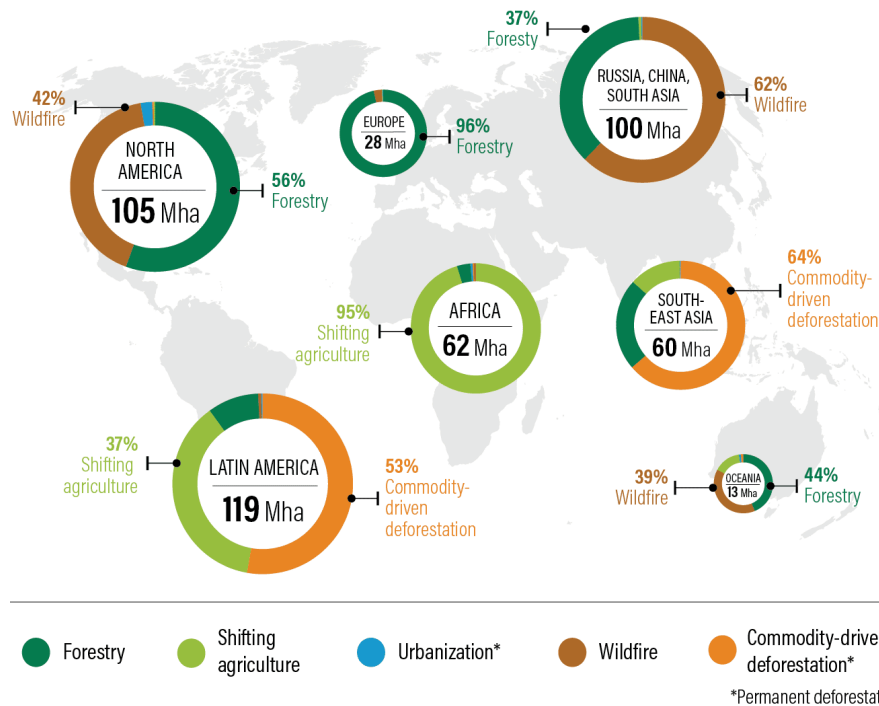
loss between 2001 and 2015, with cattle (pasture use) alone accounting for 36%, followed by oil palm (8%), soy (6.5%) and cocoa (2%). As mentioned earlier, forest loss and deforestation are major drivers of biodiversity loss[83], but forest degradation also plays a significant role in this process. In particular, the detrimental consequences of forest degradation have been highlighted by Barlow *et al.* (2016) and Watson *et al.* (2018), who showed that the impact of degradation can equal that of deforestation in some regions. However, the concept of forest degradation is not easy to define and requires a multi-dimensional analysis:

> "*Forest degradation is broadly defined as a reduction in the capacity of a forest to produce ecosystem services such as carbon storage and wood products as a result of anthropogenic and environmental changes. [...] There is, however, no generally recognized way to identify a degraded forest because perceptions of forest degradation vary depending on the cause, the particular goods or services of interest, and the temporal and spatial scales considered. [...] the types of degradation can be represented using five criteria that relate to the drivers of degradation, loss of ecosystem services and sustainable management, including: productivity, biodiversity, unusual disturbances, protective functions, and carbon storage.*" (Thompson *et al.*, 2013, page 1).

Among the 11 indicators proposed by Thompson *et al.* (2013, Table 1, page 3), the Global Forest Review has selected three approaches to measure forest degradation and forest disturbance:

1. Forest area experiencing a partial (more than 20% and less than 90%) loss of tree canopy cover;

2. Tree cover extent experiencing tree cover loss due to fire;

3. Intact forest landscapes that can no longer be considered intact due to evidence of human disturbance.

Their results are as follows[84]. Between 2001 and 2012, 185 Mha of forest experienced a partial reduction in tree canopy cover, representing 5% of the global forest area, with 85% of this occurring in tropical forests. Additionally, 113 Mha of tree cover loss was associated with fire between 2001 and 2023, accounting for 2.8% of the global forest area. Lastly, 155 Mha of forest area classified as intact in 2000 could no longer be considered intact by 2020, representing 4% of the global forest area.

3.2 Invasive species

An invasive species is a non-native (or alien) species (plants, animals, or microorganisms) that is intentionally or accidentally introduced into a new environment and poses a threat to native species and biodiversity. The main characteristics of invasive species are:

- Non-native
  Invasive species are plants and animals that live in areas where they do not naturally exist. However, not all non-native species are invasive. For instance, corn is not native to Europe but is not considered an invasive species.

---

[83]For example, Betts *et al.* (2017) examined how deforestation affects biodiversity in different landscapes. They found that deforestation significantly increased the likelihood of species being listed as threatened, upgraded to higher threat categories, or experiencing population declines. Crucially, "*these risks were disproportionately high in relatively intact landscapes; even minimal deforestation had severe consequences for vertebrate biodiversity loss.*" In contrast, in already fragmented landscapes, the effects of forest loss were less pronounced.

[84]Source: https://research.wri.org/gfr/forest-condition-indicators/forest-degradation.

- Rapid spread
  Invasive species tend to reproduce and grow very quickly because they lack natural predators in the new environment.

- Harmful effects
  Invasive species often outcompete native species for resources, take over habitats, and disrupt native ecosystems.

These three characteristics are typically assessed to determine whether a species is invasive[85]. In addition, invasive species are usually introduced with (intentional or accidental) human assistance (Simberloff *et al.*, 2013). One of the greatest challenges is managing alien invasions because eradication of established invaders is rare and post-invasion control is difficult (Mack *et al.*, 2000).

Many countries have developed their own taxonomy of invasive alien species (IAS). For example, the National Invasive Species Information Center (NISIC), established in 2005 under the US Department of Agriculture (USDA), manages the website www.invasivespeciesinfo.gov, which lists invasive species in the United States. As of December 2024, 194 species are reported to be invasive in the United States. In alphabetical order, the first invasive species listed[86] is the African clawed frog (*Xenopus laevis*), which is native to Africa. It was introduced to California in 1968 and imported for laboratory research and the pet trade. This species negatively impacts native amphibian and fish populations. The $107^m athrmth$ invasive species on the list is kudzu (*Pueraria montana*), which is native to Asia. It was introduced to the USA in the late 1800s as an ornamental plant and for erosion control. Kudzu vine outcompetes native species and disrupts ecosystems. In the European Union, invasive alien species are controlled by EU Regulation 1143/2014, which contains a set of measures to be taken throughout the EU in relation to invasive alien species. In addition, the European Union has established a list of 88 regulated invasive alien species[87] (47 animal species and 41 plant species). Here are some examples of invasive species: Egyptian goose (*Alopochen aegyptiaca*), western mosquitofish (*Gambusia affinis*), fox squirrel (*Sciurus niger*), tropical fire ant (*Solenopsis geminata*), African clawed frog (*Xenopus laevis*), Senegal tea plant (*Gymnocoronis spilanthoides*), floating pennywort (*Hydrocotyle ranunculoides*), water primrose (*Ludwigia grandiflora*), kudzu vine (*Pueraria montana*). At the global level, the Global Invasive Species Database (GISD) is a free, online, searchable source of information on alien and invasive species that negatively impact biodiversity. However, this database was developed in 2000 and is no longer maintained in the 2020s.

The previous examples focus on invasive animal and plant species. However, invasive species can also include infectious diseases and microorganisms. For example, Berger *et al.* (1998) studied the devastating effects of the amphibian chytrid fungus (*Batrachochytrium dendrobatidis*) and its impact on amphibian mortality and population decline. While these authors suggested that environmental factors such as climate change and habitat modification were responsible for the spread of the fungus, Weldon *et al.* (2004) found that "*Africa was the origin of amphibian chytrid and that the international trade in Xenopus laevis frogs, which began in the mid-1930s, was the means of dissemination.*" Although the chytrid fungus is not a traditional invasive species in the sense of an animal or plant, it is an example of an invasive pathogen that has had a devastating impact on native amphibian populations. Another example is the *Pseudogymnoascus destructans* fungus that causes white-nose syndrome, a fatal disease that has killed millions of bats in North America (Blehert *et al.*, 2009). This fungus is thought to have originated in Europe, where local bats evolved resistance. It

---

[85]For instance, IPBES (2023, page 76) estimates that 37 000 species are established aliens, but only 5 250 are invasive alien species.

[86]The list is available at www.invasivespeciesinfo.gov/species-profiles-list.

[87]They are listed in the 187-page report *An Introduction to the Invasive Alien Species of Union Concern*, published by the European Commission in 2022.

was introduced to North America by humans and has since become an invasive pathogen for native bats in North America.

Primack (2014, pages 226-237) and Simberloff (2010, pages 131-142) report numerous striking cases of invasive species. For example, the introduction of predatory snakes has led to a decline in bird populations on several small islands. Simberloff (2010, page 136) notes that predators have often been intentionally introduced as biological control agents for specific target species, but in some cases these predators have also attacked non-target species and driven them to extinction:

> "*One of the worst such disasters was the introduction of the rosy wolf snail (Euglandina rosea), native to Central America and Florida, to many Pacific islands to control the previously introduced giant African snail (Achatina fulica). The predator not only failed to control the targeted prey (which grows to be too large for the rosy wolf snail to attack it) but caused the extinction of over 50 species of native land snails [...] The small Indian mongoose, implicated as the sole cause or a contributing cause in the extinction of several island species of birds, mammals, and frogs, was deliberately introduced to all these islands as a biological control agent for introduced rats [...] The mosquitofish (Gambusia affinis) from Mexico and Central America has been introduced to Europe, Asia, Africa, Australia, and many islands for mosquito control. Its record on this score is mixed [...] However, it preys on native invertebrates and small fishes and in Australia is implicated in extinction of several fish species.*" (Simberloff, 2010, page 137).

Biological control is one of the reasons for the introduction of alien species, the other three being European colonization (birds, mammals, and fish for food), agriculture (including horticulture and aquaculture), and accidental transport (especially rats, snakes, and insects) (Primack, 2014, page 226). Among the regions most affected by invasive species, New Zealand is a special case. Non-native predators kill over 25 million native birds annually, and many native land species have already been lost, including sixty bird species, three frog species, seven vascular plants, and numerous invertebrates. Currently, more than 3 000 native land species are either threatened or endangered. In July 2016, the New Zealand government launched the *Predator Free 2050* initiative[88], which aims to completely eradicate certain introduced predators by the year 2050. The goals of Predator Free 2050 are ambitious, seeking to restore New Zealand's ecosystems to a state where native species can thrive without the constant threat of introduced predators. The initiative targets three primary groups of invasive species:

1. Mustelids: stoats (*Mustela erminea*), ferrets (*Mustela furo*), and weasels (*Mustela nivalis*).

2. Rats: ship rats (*Rattus rattus*), Norway rats (*Rattus norvegicus*), and kiore (*Rattus exulans*).

3. Possums: brushtail possums (*Trichosurus vulpecula*).

In 2024, New Zealand's Department of Conservation published the biennial progress report (2021–2023) to evaluate progress toward the seven interim targets. One target was achieved[89], four are on track to be achieved by 2025, and two will not be met[90]. New Zealand's situation is far from unique. In fact, many islands — especially those in the Pacific — face similar challenges (Simberloff, 2010).

---

[88]Documents on the strategy, implementation plan, and progress report are available at www.doc.govt.nz/nature/pests-and-threats/predator-free-2050.

[89]This relates to Goal 1 ("*By 2025, we will increase by 1 million hectares (compared with 2016) the area of New Zealand mainland where predators are suppressed, through Predator Free 2050 project*").

[90]This relates to Goal 3 ("*By 2025, we will have eradicated all mammalian predators from New Zealand's uninhabited offshore islands*") and Goal 4 ("*By 2025, we will have developed a breakthrough science solution that would be capable of eradicating at least one small mammal predator from the New Zealand mainland*").

The isolation of island habitats favors the evolution of endemic species, but this same isolation also makes these species exceptionally vulnerable to the threats posed by invasive species:

> "*Because they evolved in the absence of selective pressures from mammalian grazers and predators, many endemic island plants and animals have evolutionarily lost or never developed defenses against these enemies and often lack a fear of them. Many island plants do not produce the bad-tasting, tough vegetative tissue that discourages herbivores, nor do they have the ability to resprout rapidly following damage. Some birds have lost the power of flight and simply build their nests on the ground.*" (Primack, 2014, pages 228-229).

This vulnerability of endemic species helps explain why invasive alien species have contributed to 60% of recent species extinctions, of which 90% occurred on islands[91] (IPBES, 2023).

Figure 45: Average annual cost of invasive species (in 2017 $ mn)
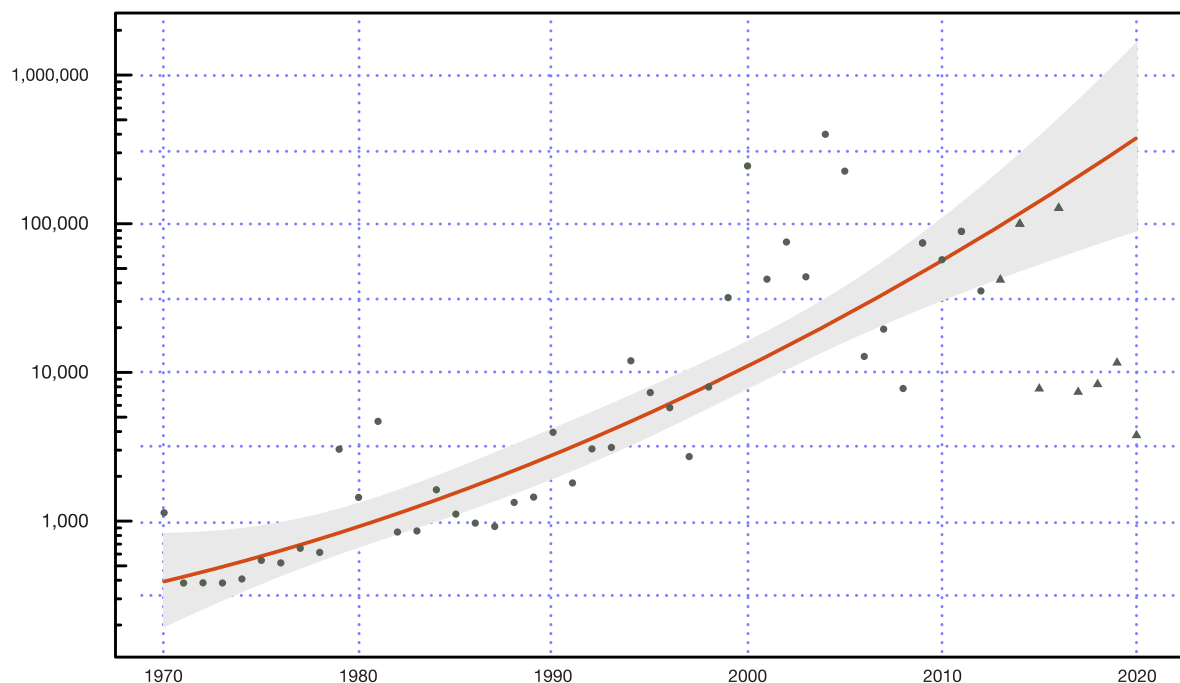
Using the methodology and database developed by Diagne *et al.* (2021), IPBES (2023) estimated that the global annual economic cost of biological invasions amounted to $423 billion in 2019. Of these costs, 92% are due to the negative impacts of invasive alien species on nature's contribution to people or quality of life, while only 8% are related to the management of biological invasions. A significant proportion of these costs are attributed to reductions in food supply (66%), followed by impacts on human health, livelihoods, and water security. Notably, these costs have been observed to quadruple every decade (Figure 45). Over the past 50 years (1970–2019), the cumulative economic costs of biological invasions amount to $1.738 trillion when considering only the most reliable data (observed and high reliability). When potential and low-reliability costs are included, the total rises to $11.633 trillion (IPBES, 2023, Box 4.13, page 456).

---

[91] According to IPBES (2023, Figure SPM 3), 218 invasive alien species have caused 1 215 local extinctions of native species.

3.3 Pollution

According to the IPBES glossary, "*pollution is the introduction of contaminants into the natural environment that cause adverse change*". This is a general definition that can lead to different interpretations. If we refer to the UN Data glossary, pollution is the "*presence of substances and heat in environmental media (air, water, land) whose nature, location, or quantity produces undesirable environmental effects*" and is the "*activity that generates pollutants*". A pollutant or contaminant is a substance present in concentrations that can harm organisms (humans, plants, and animals) or exceed an environmental quality standard. In this context, concentration is a critical factor, as pollution is typically associated with quantities that excess thresholds, leading to a reduction in quality of life. We generally distinguish between point source and non-point source pollution:

- Point source pollution comes from a single, identifiable source, such as a pipe, drain, or specific location. It is easier to monitor and control because the source is clearly identified.

- Non-point source pollution comes from multiple diffuse sources rather than a single point of origin. It is often carried into water bodies by rainfall, snowmelt, or runoff.

It's impossible to give an exact number of pollutants in the world because many pollutants can undergo chemical reactions to form different compounds in the environment, creating secondary pollutants, and new chemical compounds are constantly being created by industrial processes. Nevertheless, we can categorize pollutants in three main ways:

- By source:
  - Natural pollutants occur without human intervention, such as volcanic eruptions, forest fires, and natural decomposition processes;
  - Anthropogenic pollutants result from human activities, including industrial emissions, vehicle exhaust, and agricultural practices;

- By chemical composition:
  - Organic pollutants contain carbon-based compounds, such as pesticides, petroleum products, and plastic waste;
  - Inorganic pollutants lack carbon in their structure, including heavy metals (such as mercury and lead), mineral acids, and inorganic salts;

- Through environmental persistence:
  - Persistent pollutants remain in the environment for long periods of time without breaking down, such as certain pesticides, heavy metals, and some industrial chemicals;
  - Non-persistent pollutants break down relatively quickly through natural processes, such as many biological wastes and some air pollutants.

3.3.1 Types of biodiversity pollution

Because there is a wide range of contaminants[92], pollution can also be divided into different categories. The eight major types of pollution are listed below:

---

[92]For example, the European Chemicals Agency has registered 26 865 unique chemical substances that can be placed on the European Economic Area market by companies with a valid registration as of November 2024 (https://echa.europa.eu/information-on-chemicals). In the United States, the non-confidential portion of EPA's Toxic Substances Control Act (TSCA) Inventory contains 86 770 chemicals, of which 42 377 are active as of May 2024 (www.epa.gov/tsca-inventory).

1. Air pollution
   According to the WHO glossary, "*air pollution is contamination of the indoor[93] or outdoor[94] environment by any chemical, physical or biological agent that modifies the natural characteristics of the atmosphere*". It can harm living organisms, damage the natural environment, or degrade air quality. Pollutants can be in the form of solid particles, liquid droplets, or gases, and can be either natural (such as volcanic ash) or man-made (such as industrial emissions). Air pollutants can be classified as particulate matter (such as $PM_{2.5}$, PM_{10}, ultrafine particles, and dust), primary pollutants (those emitted directly into the atmosphere, such as carbon monoxide CO, nitrogen oxides NO_x, and sulfur dioxide SO_2), and secondary pollutants (those formed in the air through chemical reactions, such as acid rain, aerosols and ozone O_3). Air pollution measurement is the assessment of air quality, or the concentration of pollutants in the air. This is done using ground-based stations or satellite-based monitoring (remote sensing). Measurements are typically expressed in terms of concentration (*e.g.*, milligrams per cubic meter) or parts per million/billion by volume (ppmv/ppbv).

2. Biological pollution
   Biological pollution refers to the introduction of harmful or invasive living organisms into an ecosystem where they do not occur naturally. It includes invasive species, the spread of pathogens, and biologically active agents (such as some genetically modified organisms (GMOs) or antibiotic-resistant microbes). Biological pollution often intersects with air, chemical, and water pollution. For example, nutrient runoff from fertilizers (chemical pollution) creates conditions for harmful algal blooms (biological pollution). Similarly, cholera is an example of biological pollution, because it involves the contamination of water with a pathogenic microorganism, the bacterium *Vibrio cholerae*.

3. Chemical pollution
   Chemical pollution refers to the release of harmful chemical substances into the environment — air, water, soil, or living organisms — causing adverse effects on ecosystems. Consequently, chemical pollution is often a component of other pollution categories: air pollution, plastic pollution, soil pollution, and water pollution. Given its significant impact and the serious challenges it poses to humanity, governments and the UN Environment Assembly (UNEA) are planning to establish a global intergovernmental science-policy panel on chemicals, waste, and pollution prevention. The number of chemical pollutants is unknown because there is no comprehensive inventory of chemical substances. However, Wang *et al.* (2020) estimated that more than 350 000 chemicals and chemical mixtures have been produced and synthesized by humans. Moreover, the global use of chemicals is expected to increase by 70% between 2020 and 2030 (Naidu *et al.*, 2021, page 2), with the largest growth anticipated in China, which is projected to account for nearly 50% of the global chemical market by 2030. Of course, not all chemicals are harmful and dangerous, but a large proportion are. For example, the European Environment Agency (EEA) estimates that about 60% of the total volume consumed in Europe is hazardous to health, and that 8% of deaths can be attributed to hazardous chemicals[95]. It is not easy to find a universally accepted classification of hazardous chemicals in the context of biodiversity. However, in the context of industrial activities, the Globally Harmonized System

---

[93]Contamination of the air inside a home or building, often caused by cooking, smoking, or poor ventilation. According to González-Martín *et al.* (2021), more than 5 million people die each year from diseases caused by indoor air pollution. The problem of exposure to indoor air pollution is growing as people spend more time indoors. In Europe, for example, people spend 90% of their time indoors.

[94]Pollution in the open air, often from industrial or vehicular sources.

[95]Source: www.eea.europa.eu/en/topics/in-depth/chemicals.

Box 12: Silent Spring by Rachel Carson (1962)

Silent Spring[a] is a landmark environmental book published in 1962 by Rachel Carson. It's considered one of the most influential environmental books ever written and is widely credited with launching the modern environmental movement. The book documents the harmful effects of pesticides on the environment and wildlife. Carson focused particularly on DDT, which was widely used after World War II. She showed how these chemicals not only harmed pests, but also accumulated in ecosystems, harming wildlife and humans. The book faced fierce opposition from the chemical industry, but captured widespread public attention and sparked debates about environmental health and the unregulated use of chemicals. It led to the eventual ban of DDT in the United States in 1972 and inspired stricter pesticide regulations worldwide.
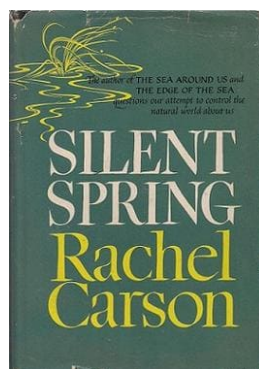
[a]The title refers specifically to the absence of birdsong in spring, traditionally a time when birds sing and nature comes back to life after winter.

of Classification and Labelling of Chemicals (GHS) is an internationally recognized system for classifying and communicating the hazards of chemical substances and mixtures. The GHS defines a set of nine hazard classes, such as flammables, oxidizers, corrosives, and acute toxins, and divides each class into categories based on the severity of the hazard (Table 30). Another approach to classifying hazardous chemicals is by the source of contamination. This classification helps to understand the origin of these chemicals and their potential impact on the environment:

- Industrial emissions
  These are chemicals released into the environment during industrial processes such as manufacturing, chemical production, and power generation. Common pollutants from industrial emissions include volatile organic compounds (VOCs), heavy metals (mercury, lead), persistent organic pollutants (POPs), and solvents, which can contaminate air, water, and soil.

- Agricultural runoff
  Agricultural activities contribute significantly to chemical pollution, especially through runoff of pesticides, herbicides, fertilizers (containing nitrates and phosphates), and animal waste. These chemicals are often washed into rivers and lakes when it rains, contaminating the water and harming aquatic life.

Table 30: Globally harmonized system of classification and labelling of chemicals (GHS) pictogram for hazardous substances

GHS01: Explosive	GHS02: Flammable	GHS03: Oxidizing
GHS04: Compressed gas	GHS05: Corrosive	GHS06: Fatal or toxic
GHS07: Low level toxicity	GHS08: Serious health hazard	GHS09: Hazardous to the environment

Source: https://unece.org/transport/dangerous-goods/ghs-pictograms.
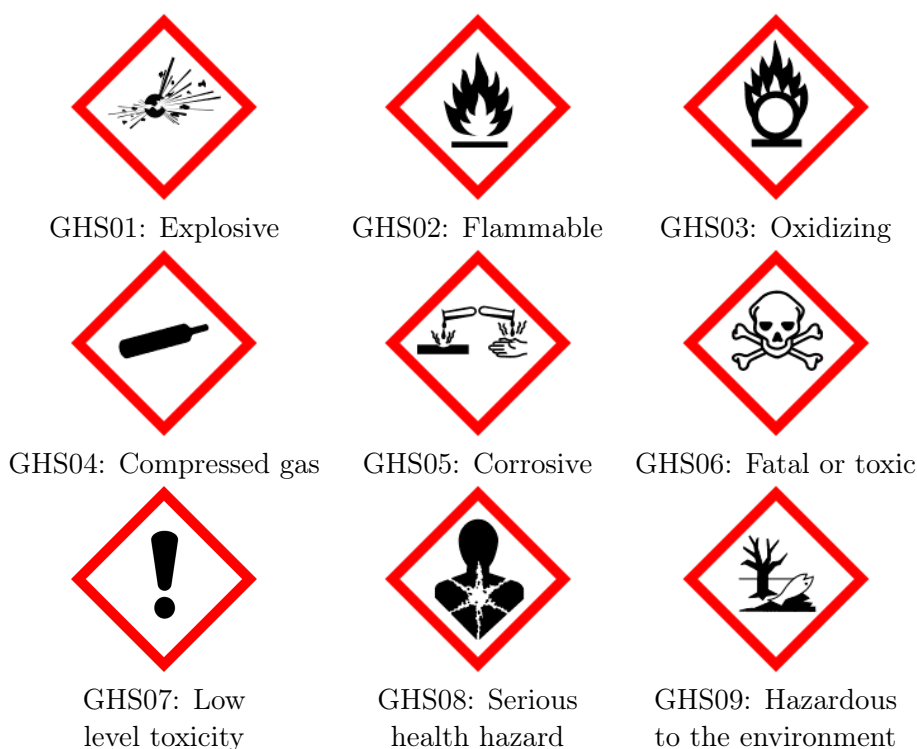
- Household and municipal waste
  Household products, including cleaning products (containing solvents and disinfectants), pharmaceuticals, personal care products, paints, batteries, and plastics, contribute to pollution when disposed of improperly. Wastewater from homes and businesses can carry contaminants such as detergents, synthetic chemicals, and pharmaceuticals into sewage systems, which are not always fully treated before being released into the environment.

- Petroleum products
  Oil spills and runoff from petroleum-related activities are also sources of chemical pollutants. Petroleum products such as gasoline, diesel, and oils, can have a devastating effect on aquatic ecosystems, because they are toxic to marine life and persist in the environment for long periods of time.

- Transportation emissions
  Road vehicles, aircraft, and ships, especially those powered by fossil fuels, emit harmful pollutants such as nitrogen oxides (NO_x), sulfur dioxide (SO_2), carbon monoxide (CO), and particulate matter (PM) into the air. These pollutants contribute to air quality problems, acid rain, and human respiratory illnesses. Additionally, the particulate matter can affect soil and water quality.

An alternative to the previous classification is to divide hazardous chemicals into four categories[96]: conventional pollutants, heavy metals, persistent organic pollutants, and emerging

---

[96]In both classifications, a chemical may belong to more than one category.

contaminants. Conventional pollutants typically refer to pollutants that have been recognized and regulated for many years (*e.g.*, CO, NO_x, SO_2, PM). Heavy metals are a group of metallic elements that have a relatively high density and are toxic to humans and wildlife even at low concentrations. In biodiversity, a density greater than $5\,g/cm^3$ is used to define them. Examples of heavy metals hazardous to human health[97] include arsenic (As), cadmium (Cd), chromium (Cr), lead (Pb), and mercury (Hg). According to the Stockholm Convention on Persistent Organic Pollutants, POPs "*are organic chemical substances, that is, they are carbon-based. They possess a particular combination of physical and chemical properties such that, once released into the environment, they remain intact for exceptionally long periods of time (many years); they become widely distributed throughout the environment as a result of natural processes involving soil, water and, most notably, air; they accumulate in the living organisms including humans, and are found at higher concentrations at higher levels in the food chain; and they are toxic to both humans and wildlife.*" When this international environmental treaty was signed in 2001, 12 POPs were recognized and classified into 3 categories: pesticides (aldrin, chlordane, DDT, dieldrin, endrin, heptachlor, hexachlorobenzene HCB, mirex, toxaphene), industrial chemicals (hexachlorobenzene HCB, polychlorinated biphenyls PCB), and by-products (hexachlorobenzene HCB, polychlorinated dibenzo-p-dioxins PCDD and polychlorinated dibenzofurans PCDF, polychlorinated biphenyls PCB). The Stockholm Convention has been revised several times. As of December 2024, there are 32 POPs. The last category concerns emerging contaminants, which are chemical substances that are not commonly monitored or regulated, pose potential risks, and may be persistent. Examples of emerging contaminants include pharmaceuticals and personal care products (PPCP), endocrine-disrupting chemicals (EDC), micro and nanoplastics, antibiotic-resistant genes (ARG), among others (Wang *et al.*, 2024, Table 1, page 4). The challenge with emerging contaminants is tracking these substances and assessing the potential risks posed by novel chemical mixtures. For example, Escher *et al.* (2020) reported that "*the number of new chemicals is rising, with the Chemical Abstract Service Registry growing from 20 million to 156 million chemicals between 2002 and 2019*", which equates to approximately $20\,000$ new chemical products being synthesized every day.

4. Light pollution
   Light pollution is the presence of unwanted, excessive, misdirected, or obtrusive artificial light that interferes with the natural environment. It occurs when artificial lighting disrupts the natural darkness of the night[98], affecting processes such as wildlife migration, reproduction, and feeding. It is often the result of poor lighting design, over-illumination, or the scattering of light in the atmosphere. Only recently has light pollution been widely recognized as a significant threat to biodiversity and a growing environmental concern (Hölker *et al.*, 2010). Although the full effects of light pollution are not yet known, we now have a better understanding of how it affects ecosystems, species, and human health[99]. Some well-known examples include disorientation of sea turtles, bird migration, insect disruption, human sleep disturbance, metabolic

---

[97]Note that some metals are essential to human health in trace amounts, meaning that they are necessary for proper biological functions and play critical roles in enzymes, metabolism, immune functions, protein synthesis, etc. Typical examples include calcium (Ca), copper (Cu), iron (Fe), potassium (K), magnesium (Mg), and zinc (Zn). However, even essential metals can be toxic in excess.

[98]Longcore and Rich (2004) distinguished between '*astronomical light pollution*', which obscures the view of the night sky, and '*ecological light pollution*', which alters the natural light regime in terrestrial and aquatic ecosystems.

[99]See the special issue *Light Pollution* (Volume 380, Issue 6650) published by *Science* on June 16, 2023. Below is the introduction to this special issue:

"*For most of history, the only lights made by humans were naked flames. Daily life was governed by the times of sunrise and sunset, outdoor nighttime activities depended on the phase of the Moon, and viewing the stars was a common and culturally important activity. Today, the widespread deployment of outdoor*

Box 13: Persistent organic pollutants

According to the Stockholm Convention on Persistent Organic Pollutants (Annex D, pages 74-75, 2023 version), the assessment of POPs focuses on four key properties[a]:

- Persistence
  The chemical must resist degradation by environmental processes and persist in the environment for long periods of time. In particular, its half-life must be greater than 2 months (60 days) in water or 6 months (180 days) in soil/sediment.

- Bioaccumulation
  The chemical must accumulate in the tissues of living organisms, and increases in concentration as it moves up the food chain (biomagnification). In particular, its bio-concentration factor (BCF) is greater than 5 000 or its log K_{ow} (n-octanol-water partition coefficient) is greater than 5.

- Potential for long-range environmental transportation
  The chemical can travel long distances through air and water, affecting ecosystems far from its original source. In particular, its half-life in air must be greater than 2 days, which is equivalent to a distance of 690 km, assuming an average wind speed of 4 m/s (Scheringer et al., 2012, page 384).

- Adverse effects
  The chemical has a significant level of toxicity or ecotoxicity.

Below we report figures of different chemicals, which has been collected by Scheringer et al. (2012, Supporting material):

CAS	Chemical	Half-life	log K_{ow}	Transportation	Toxicity
50-29-3	DDT	289	6.85	3.11	Yes
53-19-0	Mitotane	130	5.87	2.46	Yes
57-74-9	Chlordane	1 440	6.24	2.12	Yes
95-94-3	Tetrachlorobenzene	86	4.61	130	Yes
118-74-1	Hexachlorobenzene	229	5.79	158	Yes
307-43-7	Perflubrodec	5 670	7.91	10^6	Yes
307-45-9	Perfluorodecane	7 960	7.51	10^6	No
2172-49-8	Propionyl chloride	192	6.45	2.13	Yes
3182-02-3	Dichlorophenyl	344	6.08	2.35	Yes
13947-96-1	Trichloromethyl	213	4.86	198	Yes
25267-15-6	Polychloropinene	4 410	8.09	10.80	No
27753-52-2	Nonabrombiphenyl	2 060	11.77	439	Yes

By applying the screening criteria of persistence, bioaccumulation, long-range transport potential and toxicity to a set of 93 144 organic chemicals, they identified 510 chemicals that exceed all four criteria and can be considered potential POPs. They also estimated that the number of potential POPs ranges from 190 (lower bound) to 1 200 (upper bound) chemicals.

---

[a]Source: www.pops.int.

disorders, and increased risk of some cancers (Walker *et al.*, 2020). Recently, Anderson *et al.* (2024) estimated that the annual loss of ecosystem service value due to light pollution is \$3.4 trillion, which is about 3% of the total global value of ecosystem services and 3% of global GDP.

5. Noise pollution

   Noise pollution refers to unwanted, disturbing, or excessive[100] sounds that negatively affect the health and well-being of humans, animals, and the environment. It typically results from human activities and disrupts natural auditory environments. The emergence of noise pollution as a biodiversity threat precedes that of light pollution, with research studies dating back to the 1990s. However, as with light pollution, much remains to be learned about its full extent and long-term consequences. To date, the impacts of noise pollution are evident in both human health — such as hearing loss, sleep disturbance, mental health issues, and cognitive impairments — and wildlife — where it disrupts communication, leads to habitat abandonment, and interferes with pollination processes. Among these effects, marine noise pollution is a well-documented issue (Di Franco *et al.*, 2020; Solé *et al.*, 2023) because fish rely on sound for essential activities such as mating calls, territorial defense, predator alerts, and navigation during migration. Underwater communication is vital to their survival, but can be severely disrupted by shipping traffic, sonar noise and other anthropogenic sounds.

6. Plastic pollution

   Plastic pollution is the accumulation of plastic materials and particles in the environment. Plastics are a wide range of synthetic or semi-synthetic materials made from polymers derived from fossil fuels such as natural gas or petroleum. In general, plastic pollutants are categorized by size as nano-, micro-, or macro-debris. Plastics pose a critical environmental threat to wildlife through multiple mechanisms: direct physical harm through suffocation and entanglement, and chemical toxicity through leaching. A particularly insidious threat comes from micro-plastics — fragments smaller than 5 mm — which are readily ingested by both marine and terrestrial organisms. These particles not only accumulate throughout the food chain, but also act as vectors for concentrated toxins and pollutants. When ingested, they can trigger cascading health effects, compromising animals' immune systems, disrupting endocrine function and impairing reproductive capabilities, ultimately threatening species survival rates. Plastic pollution is pervasive and highly persistent in the environment due to slow natural degradation processes. This explains its widespread presence in diverse ecosystems around the world, including deserts, farms, mountaintops, oceans, and even Arctic snow (MacLeod *et al.*, 2021). Furthermore, plastic emissions are increasing and are projected to continue rising, even under optimistic waste reduction scenarios. Figure 46 shows the evolution of global thermoplastic production[101] since 1950 and its projections to 2050. In 1950 the production was less

---

electric lighting means that the night is no longer dark for most people — few can see the Milky Way from their homes. Outdoor lighting has many legitimate uses that have benefited society. However, it often leads to illumination at times and locations that are unnecessary, excessive, intrusive, or harmful: light pollution." (Smith *et al.*, 2023).

[100]Unwanted sound refers to any unpleasant or disruptive noise. Disturbing sounds interfere with daily activities like sleeping, working, or communicating. Excessive sounds are those that are too loud or too frequent.

[101]It is difficult to obtain reliable figures on global plastics production because the definition of plastics is not standardized and because of double counting in production statistics. Thermoplastics are a type of plastic that becomes soft and malleable when heated and hardens when cooled. They account for about 85% of all plastics produced worldwide. The other major category of plastics is thermosets, which, unlike thermoplastics, cannot be remelted once formed.

Figure 46: Global production of thermoplastics with projections, 1950–2050 (in Mt)
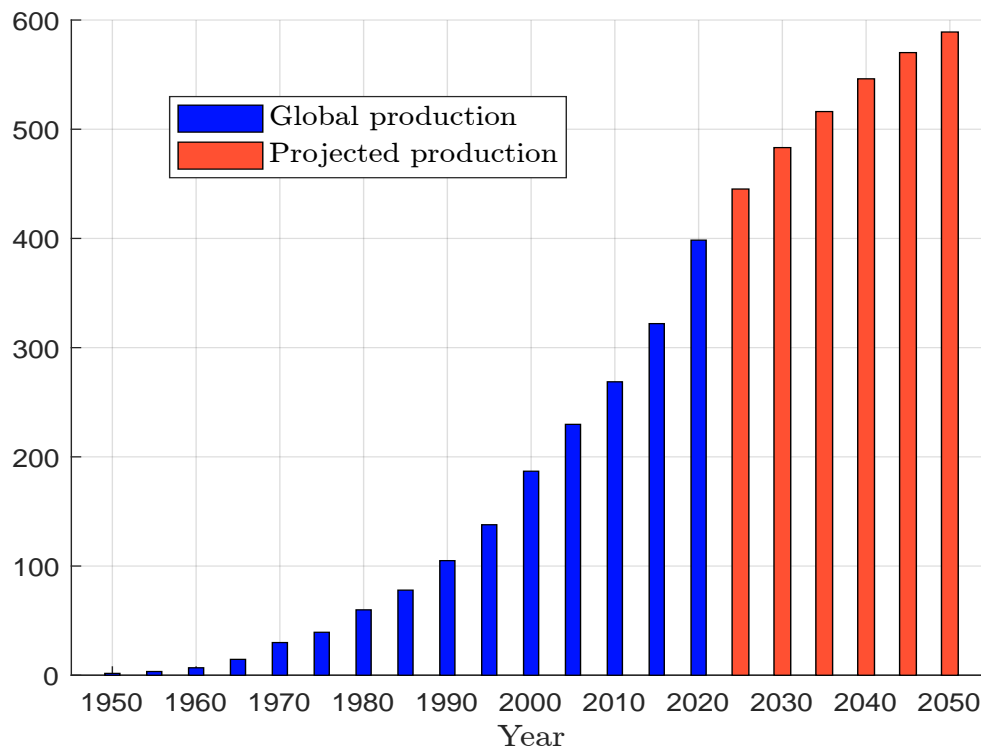
than 2 million tonnes, in 2023 it was 414 million tonnes, and we expect a production of 590 million tonnes in 2050. The expected annual growth rate over the next 30 years is 1.3% — lower than the 4.6% annual growth observed over the past three decades, but still significant. This indicates that plastics production will continue to grow, making the search for solutions to establish a circular economy an ongoing and critical discussion. According to OECD (2022), approximately 25% of plastic waste is mismanaged, with a small fraction (less than 1%) eventually being transported into the oceans. This has led to the formation of garbage patches[102]. One of the best-known plastic accumulation zones is the Great Pacific Garbage Patch (GPGP), located in the subtropical waters between California and Hawaii. This patch covers an area of approximately 1.6 million square kilometers — comparable to the size of Mongolia or Iran. A study by Lebreton et al. (2018) estimated that at least 79 000 tonnes (ranging between 45 000 and 129 000 tonnes) of marine plastics are currently floating within the GPGP. Notably, over 75% of the mass of the GPGP consists of debris larger than 5 centimeters, with discarded fishing nets accounting for at least 46% of the total. While microplastics make up only 8% of the total mass, they account for a staggering 94% of the estimated 1.8 trillion (ranging from 1.1 to 3.6 trillion) pieces of plastic floating in the region. About 1 600 rivers are responsible for 80% of marine plastic pollution, which is estimated to be between 0.8 and 2.7 million tonnes of plastic waste discharged into the oceans annually (Meijer et al., 2021). The top 10 plastic-emitting rivers are Pasig (Philippines), Tullahan (Philippines), Ulhas (India), Klang (Malaysia), Meycauayan (Philippines), Pampanga (Philippines), Libmanan (Philippines), Ganges (India), Rio

---

[102]Vast gyres of marine debris created by ocean currents and the increasing influx of plastic pollution from human activities

Grande de Mindanao (Philippines), and Agno (Philippines) (Meijer *et al.*, 2021, Table S5). As a result[103], Asia accounts for 81% of marine plastic pollution, followed by Africa (8%), South America (5.5%) and North America (4.5%).

7. Soil pollution
   Soil pollution (or soil contamination) is the presence or accumulation of toxic substances, harmful chemicals, salts, pathogens, or other contaminants in soil that adversely affect soil quality, reduce soil fertility, and pose risks to human health and ecosystems. The most common sources of soil pollution are industrial activities (*e.g.*, chemical pollutants, heavy metals, radioactive contaminants), agricultural practices (*e.g.*, soil degradation and the use of fertilizers, pesticides and herbicides), waste disposal and mining (*e.g.*, petroleum hydrocarbons, solvents). The impacts of soil pollution are many, but the most important are health risks, food security[104], ecosystem degradation and habitat loss. A typical example of soil pollution is the use of nitrogen-based products (*e.g.*, ammonium nitrate, ammonium sulfate) commonly found in fertilizers and pesticides. Stevens *et al.* (2004) and Clark and Tilman (2008) conducted extensive studies on the long-term effects of chronic, low-level nitrogen deposition in prairie grasslands. Their research showed that even modest nitrogen inputs significantly reduced plant species diversity over time by favoring nitrogen-tolerant species, ultimately disrupting ecological balance. These findings were further supported by Bobbink *et al.* (2010), whose comprehensive synthesis of the effects of nitrogen deposition on terrestrial plant diversity showed that excessive nitrogen inputs fundamentally alter soil chemistry. Their work showed that this change creates conditions that favor fast-growing species while reducing overall biodiversity in different ecosystems.

8. Water pollution
   Water pollution is the contamination of water bodies (*e.g.*, rivers, lakes, oceans, groundwater, and streams) by harmful substances that degrade water quality and make water unsafe for drinking, swimming, agriculture, and other uses. It occurs when pollutants such as chemicals, waste, or microorganisms are discharged into water systems without adequate treatment to remove harmful compounds. Water pollution also includes thermal (or heat) pollution, which occurs when hot water is discharged from industrial processes, raising water temperatures. This increase in temperature depletes oxygen levels and disrupts species adapted to cooler environments. This example shows that water pollution is not a single phenomenon, but comes in many forms. The same is true for other types of pollution. This diversity presents a challenge in accurately measuring pollution. For water pollution in particular, there are several ways to measure it. The five most common are: (1) pH level, which measures the acidity or alkalinity of water (normal readings range from 6.5 to 8.5); (2) biological oxygen demand (BOD), which measures the amount of oxygen required by microorganisms to break down organic matter (high BOD indicates high levels of organic pollution because microorganisms require more oxygen); (3) turbidity, which measures the presence of suspended solids such as silt, clay, or organic matter (high turbidity can harm aquatic organisms and block sunlight needed for photosynthesis); (4) dissolved oxygen (DO), which measures the amount of dissolved oxygen in the water (low levels indicate organic pollution or high nutrient loading, which leads to oxygen

---

[103]The top 15 countries contributing to marine plastic pollution are the Philippines, India, Malaysia, China, Indonesia, Brazil, Vietnam, Bangladesh, Thailand, Nigeria, Turkey, Cameroon, Sri Lanka and Guatemala.

[104]For example, Zhang *et al.* (2015) emphasized that soil contamination by heavy metals is a major concern in China, posing a significant risk to food safety and public health. They found that 10.18% of farmland soils in China are polluted with heavy metals, primarily cadmium (Cd), mercury (Hg), copper (Cu), and Nickel (Ni). Furthermore, approximately 13.86% of grain production in China is potentially contaminated with heavy metals.

depletion); and (5) nitrate and phosphate levels (excessive nutrients lead to eutrophication, which causes algal blooms and oxygen depletion). However, this list is far from exhaustive. For example, Syeed *et al.* (2023) list a total of 69 water quality parameters (6 biological indicators, 10 physical indicators, and 53 chemical indicators[105]) as represented in Figure 47.

Figure 47: Taxonomy of the 69 water quality parameters along their natural factors (biological, physical, chemical)
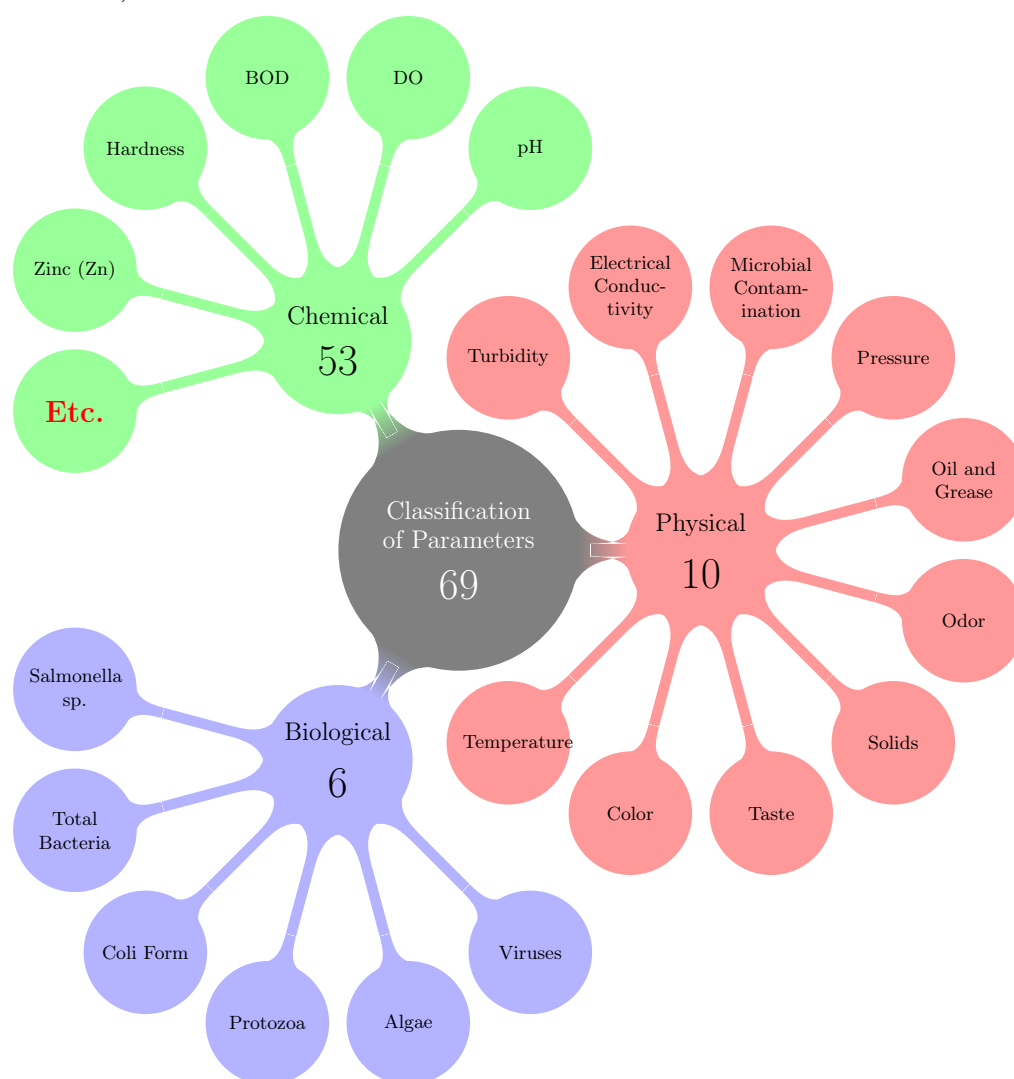
Source: Syeed *et al.* (2023, Figure 5, page 7).

---

[105]The 53 chemical measures are pH, total dissolved solid (TDS), oxidation-reduction potential (ORP), dissolved oxygen (DO), ammonia (NH_3), colored dissolved organic matter, Sulphide (S^{2-}), chemical oxygen demand (COD), biochemical oxygen demand (BOD), chloride (Cl^-), nitrate (NO_3^-), salinity, tryptophan ($C_{11}H_{12}N_2O_2$), bicarbonate ($NaHCO_3$), alkalinity (HCO_3^-), total hardness as $CaCO_3$, arsenic (As), zinc (Zn), phosphate (PO_4^{3-}), chlorine (Cl), fluoride (F^-), aluminum (Al), chromium (Cr), copper (Cu), iron (Fe), nitrogen (N) total, potassium (K), organic matter by $KMnO_4$, barium (Ba), carbonate (HCO_3^-), chromium hexavalent (Cr(VI)), hydrocarbons (C_nH_{2n+2}), sulfate (SO_4^{2-}), hydrogen sulphide as H_2S, beryllium (Be), dissolved organic carbon (DOC), silver (Ag), phosphorus (P), carbon tetrachloride (CCl_4), iodine (I), tin (Sn), Boron (B), manganese (Mn), mercury (Hg), nickel (Ni), selenium (Se), lead (Pb), cyanide (CN^-), pesticides, nitrogen (N), cadmium (Cd), calcium (Ca) and sodium (Na).

Box 14: Environmental toxicology and ecotoxicology

The study and assessment of pollution impacts fall under the disciplines of environmental toxicology and ecotoxicology. Environmental toxicology primarily focuses on how toxic substances — such as pollutants, chemicals, heavy metals, and pesticides — affect humans, animals, plants, and other living organisms. It also investigates the mechanisms by which these contaminants enter the environment, their distribution, and how they are metabolized or eliminated by organisms. Ecotoxicology, while closely related, is more concerned with studying pollution at the ecosystem level rather than focusing on individual organisms. It examines how contaminants affect populations, communities, and ecological processes. Despite this distinction, there is considerable overlap between the two fields. For instance, two foundational textbooks *Environmental Toxicology* (Wright and Welbourn, 2002) and *Fundamentals of Ecotoxicology* (Newman, 2019) cover substantially similar content and concepts.

3.3.2 Dose-response relationship

The dose-response model[106] describes how the amount of a contaminant (dose) affects health or environmental outcomes (response). Toxicologists use this model to understand how different doses of pollutants cause different levels of harm.

Figure 48: Sigmoidal dose-response curve
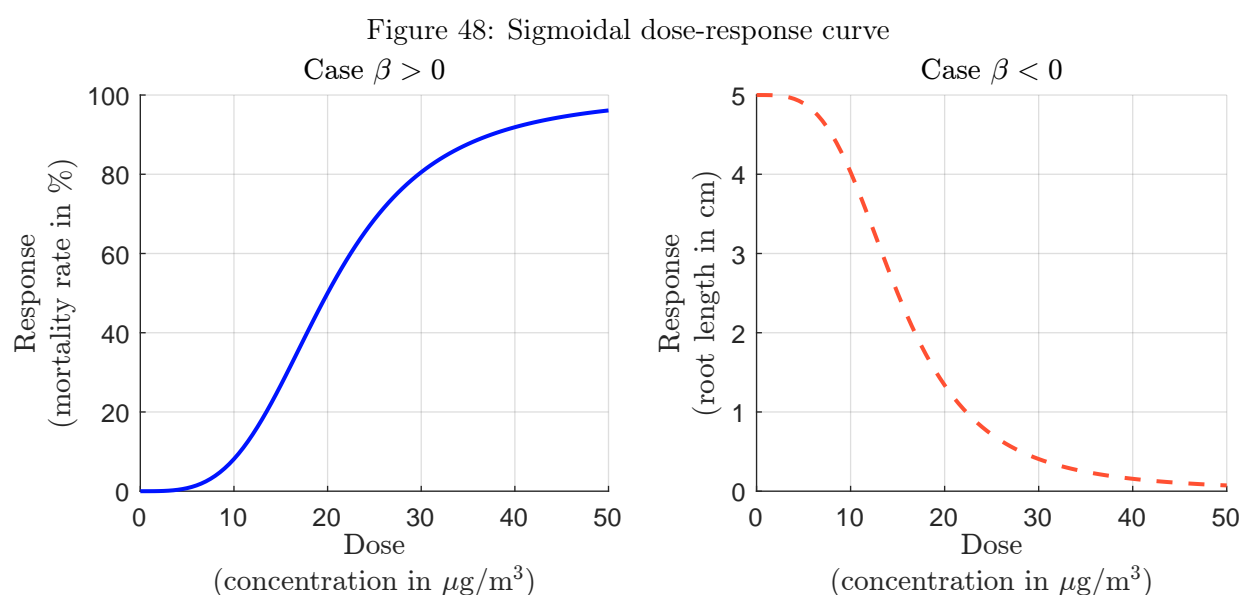
Figure 48 shows a typical dose-response curve, with the applied dose plotted on the x-axis and the observed response plotted on the y-axis. The curve is generally sigmoidal in shape and can be classified into two distinct forms depending on the nature of the response:

- Increasing response
  In this form, the response increases with the concentration of the substance. For example, mortality rates may increase with increasing levels of air, soil, or water pollution.

---

[106]In the scientific literature, this relationship is also known as the concentration-response relationship or exposure-response relationship. The World Health Organization (WHO) and the European Environment Agency (EEA) use the term concentration-response function (CRF).

- Decreasing response
  In this form, the response decreases with increasing concentration. For example, physical characteristics such as production levels, weight, or height may decrease in response to increasing levels of air, soil, or water pollution.

According to Ritz *et al.* (2015), the (generalized) log-logistic function is the most commonly dose-response model[107]:

$$y = f\left(x; \alpha, \beta, y_{\min}, y_{\max}\right) = y_{\min} + \frac{y_{\max} - y_{\min}}{1 + \exp\left(-\beta\left(\ln\left(x\right) - \ln\left(\alpha\right)\right)\right)} = y_{\min} + \frac{y_{\max} - y_{\min}}{1 + \left(\frac{x}{\alpha}\right)^{-\beta}} \quad (26)$$

where $x \geq 0$ is the concentration rate of the dose, $y \in (y_{\min}, y_{\max})$ is the response, $\alpha > 0$ is the scale parameter, and $\beta \in \mathbb{R}$ is the shape parameter. If $\beta > 0$, the dose-response curve is increasing, otherwise it is decreasing[108]. The second popular function is the log-normal model:

$$y = y_{\min} + (y_{\max} - y_{\min}) \Phi\left(\beta \ln\left(\frac{x}{\alpha}\right)\right) \quad (27)$$

Ritz (2010, Table 1, page 226) listed another class of dose-response model based on the Weibull distribution[109]:

$$y = y_{\min} + (y_{\max} - y_{\min}) \exp\left(-\left(\frac{x}{\alpha}\right)^{\beta}\right) \quad (29)$$

The three previous classes of models ignore the hormesis phenomenon, where a substance or environmental factor produces opposite effects at low and high doses. Specifically, the substance may have a stimulatory effect at low doses, while the same substance becomes toxic at high doses. To account for hormesis, a popular approach is to include a bump term in the log-logistic model:

$$y = y_{\min} + \frac{y_{\max} - y_{\min} + \gamma g\left(x\right)}{1 + \left(\frac{x}{\alpha}\right)^{-\beta}} \quad (30)$$

where $\gamma \geq 0$ and $g\left(x\right)$ is the bump function. In the Brain-Cousens model, $g\left(x\right) = x$, whereas in the Cedergreen-Ritz-Streibig model, $g\left(x\right) = \exp\left(-x^{-\eta}\right)$ (Cedergreen *et al.*, 2005). Figure 49 shows the different dose-response models and the biological phenomenon of hormesis. The parameters are $\alpha = 20$, $\beta = -3.5$, $y_{\min} = 0$, $y_{\max} = 5$. The Brain-Cousens model uses $\gamma = 0.2$, while the parameters of the Cedergreen-Ritz-Streibig model are $\gamma = 3$ and $\eta = 0.4$. An example of hormesis in biodiversity toxicology is provided by Eze *et al.* (2021), who analyzed 15 plant species to assess their tolerance to diesel fuel toxicity. The dose-response analysis showed that increasing diesel fuel concentrations in soil generally resulted in a consistent decrease in biomass for 13 species. However, the study found that hydrocarbons had a statistically significant hormetic effect on alfalfa (*Medicago sativa*), where low concentrations of diesel fuel stimulated growth, but higher concentrations resulted in a decrease in biomass. Carbon monoxide and oxygen are other examples of hormesis. Similarly, radiation hormesis refers to the hypothesis that low doses of ionizing radiation may induce beneficial biological effects, such as enhanced DNA repair mechanisms or improved immune system function. However, while the concept of radiation hormesis is intriguing and has supporting data, it remains controversial, particularly in public health and regulatory contexts (Calabrese and Mattson, 2017).

---

[107]The log-logistic probability distribution corresponds to $y_{\min} = 0$, $y_{\max} = 1$ and $\beta > 0$.

[108]The increasing dose-response curve in Figure 48 was generated using the following set of parameters: $\alpha = 20$, $\beta = 3.5$, $y_{\min} = 0$ and $y_{\max} = 100$. The decreasing dose-response curve uses $\alpha = 15$, $\beta = -3.5$, $y_{\min} = 0$ and $y_{\max} = 5$.

[109]This model is called Weibull-1 and generates an increasing response. To model a decreasing response, we consider the Weibull-2 function:

$$y = y_{\min} + (y_{\max} - y_{\min}) \left(1 - \exp\left(-\left(\frac{x}{\alpha}\right)^{\beta}\right)\right) \quad (28)$$

Figure 49: Hormesis biological phenomenon
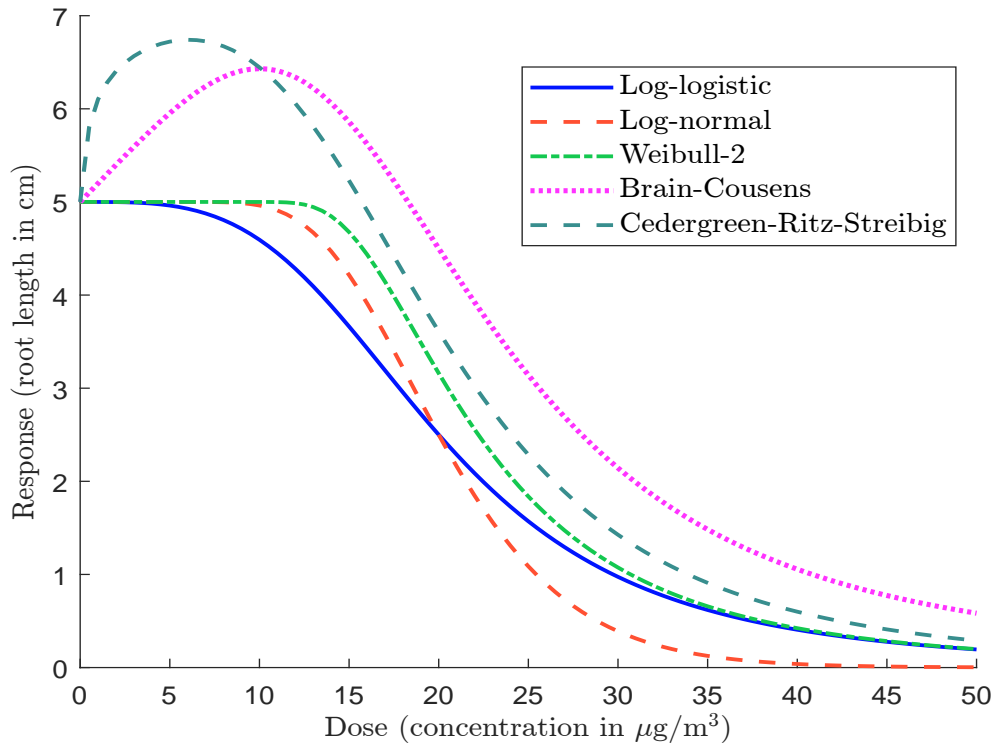
It is clear that a dose-response model can be thought of as a nonlinear regression model, where the dependent variable y represents the response or effect, and the independent variable x is the dose or concentration. In general, different types of response are distinguished: (1) continuous response (measures a continuous variable, such as biomass); (2) binary response (measures the presence or absence of a specific event, such as dead/alive); (3) time-to-response (measures the time it takes for a response to occur after exposure to a dose, such as the time to onset of toxicity after exposure to a chemical); (4) discrete or categorical response (the response falls into one of several ordered categories, such as none, mild, moderate, or severe effects). From a dose-response model where the response is the percentage of individuals who respond to a given dose of a drug, we can calculate the statistic ED_p, which is the dose required to achieve the desired therapeutic effect in $p\%$ of the population. When $p = 50\%$, we obtain the median effective dose, ED_{50}, which is the dose of the drug that produces the therapeutic response in 50% of the population. ED_{50} is a standard statistic in pharmacology. By analogy, we can define the median toxic dose TD_{50} and the median lethal dose LD_{50}, which represent the dose at which 50% of the population will experience a specific toxic effect or die, respectively. When the dose refers to the concentration of a pollutant or chemical, we use the terms half-maximal effective concentration EC_{50} or half-lethal concentration LC_{50} instead. In the log-logistic and log-normal models, the median effective concentration corresponds to the parameter α of the function[110]:

$$y = \frac{y_{\max} + y_{\min}}{2} \Leftrightarrow x = EC_{50} = \alpha$$

---

[110]Notice that $\dfrac{y_{\max} + y_{\min}}{2} = y_{\min} + \dfrac{y_{\max} - y_{\min}}{2}$. This implies that $\left(\dfrac{x}{\alpha}\right)^{-\beta} = 1$ in the case of the log-logistic model and $\Phi\left(\beta \ln\left(\dfrac{x}{\alpha}\right)\right) = \dfrac{1}{2}$ in the case of the log-normal model.

This result is not surprising because dose-response curves are related to the famous Hill equation[111] (Goutelle *et al.*, 2008):

$$E = E_0 + (E_{\max} - E_0) \frac{[C]^n}{\text{EC}_{50}^n + [C]^n}$$

where E is the effect produced by the drug/agonist at concentration $[C]$, E_0 is the baseline response, $E_{\max}$ is the maximum effect, EC_{50} is the concentration that produces half the maximum effect, and n is the Hill coefficient (or the slope of the curve).

Figure 50: Threshold concentration
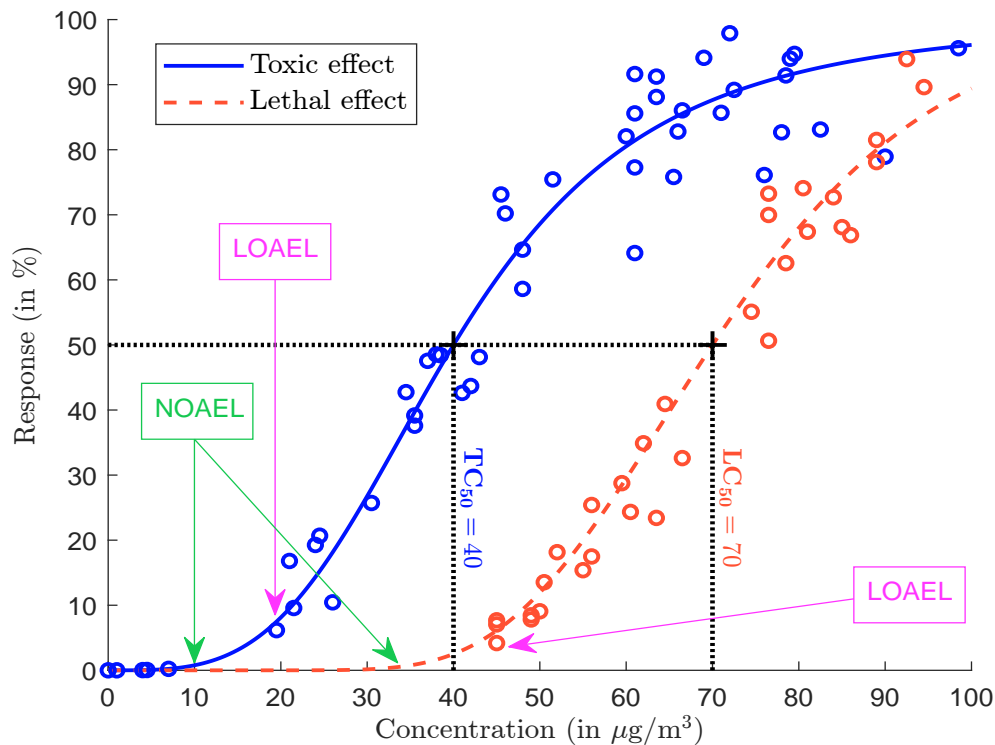
Because dose-response curves help identify relationships between exposure levels and effects, they are widely used to set safe exposure limits (threshold concentrations) to prevent adverse health outcomes in humans and adverse effects on the environment. For instance, the World Health Organization has developed a dose-response framework to measure the risk of chemicals on health (World Health Organization, 2009). Similarly, in 2021, the US Environmental Protection Agency (EPA) published tabulated dose-response assessments for both chronic and acute exposures to air pollutants[112]. The European Union has long used dose-response curves linking traffic noise to annoyance and sleep disturbance to inform and shape public policy on noise pollution mitigation. To understand how thresholds and safe exposure limits are set, let's examine the dose-response curves

---

[111]We have:

$$\frac{E - E_0}{E_{\max} - E_0} = \frac{1}{1 + \left(\dfrac{[C]}{\text{EC}_{50}}\right)^{-n}}$$

and we identify the parameters of the log-logistic dose-response model: $\alpha = \text{EC}_{50}$, $\beta = n$, $y_{\min} = E_0$, and $y_{\max} = E_{\max}$.

[112]Tables with values for long-term (chronic) inhalation and oral exposure and values for short-term (acute) inhalation exposure are available at www.epa.gov/fera/dose-response-assessment-assessing-health-risks-associated-exposure-hazardous-air-pollutants.

in Figure 50. The figure shows two functions: one that measures toxicity and another that measures mortality. From these curves, we can determine critical values including TC_{50} and LC_{50}, as well as two key regulatory statistics:

- NOAEL (no observed adverse effect level) represents the highest dose or concentration at which no adverse effects are observed. This metric is fundamental to establishing maximum safe exposure levels for humans and ecosystems, as it indicates the threshold below which a substance demonstrates no harmful effects.

- LOAEL (lowest observed adverse effect level) is the lowest dose or concentration at which adverse effects are first observed. This measure helps policymakers identify the point at which a substance begins to pose a risk.

Figure 50 illustrates NOAEL and LOAEL values for both toxic and lethal effects. For toxicity, the data shows a NOAEL of $10\,\mu g/m^3$ and a LOAEL of $20\,\mu g/m^3$, suggesting a potential threshold concentration of $10\,\mu g/m^3$. In contrast, if mortality alone is considered, the threshold concentration could be set as high as $40\,\mu g/m^3$. In practice, the setting of threshold concentrations involves several considerations. While theoretical best practice suggests using the NOAEL as the threshold, regulatory agencies often default to the LOAEL. To ensure adequate protection for vulnerable populations — including children, elderly individuals, and those with pre-existing health conditions — authorities often apply safety factors to these baseline values. The final threshold concentration is then calculated by dividing either the NOAEL or LOAEL by the appropriate safety factor.

Remark 10 *In the case of pollution, safe exposure limits are set primarily in terms of toxic effects. In the case of medicine and pharmacology, agencies use both therapeutic effects, toxic effects, and lethal effects, i.e., there is a trade-off between benefits and risks.*

3.3.3 Application to air quality standards

The previous framework has been extensively used to set air quality standards. In 2000, the World Health Organization published a report entitled "*Guidelines for Air Quality*". This report has been updated twice, in 2006 and 2021 (World Health Organization, 2006, 2021). The purpose of these reports is to provide recommended limits for key air pollutants to protect public health. The methodology is based on the concentration-response function (CRF), which is another term for the dose-response relationship. In Table 31, we present the WHO air quality guidelines (AQG), which represent the concentration levels of pollutants below which adverse health effects are expected to be minimal (World Health Organization, 2021). For example, the AQG level for particulate matter[113] $PM_{2.5}$ is $5\,\mu g/m^3$ on an annual basis. We have also included air quality standards for several regions and countries (Brazil, China, EU, India, US, and Switzerland), which generally correspond to the limit values established to protect human health. For a long time, air quality standards in Europe were governed by Directive 2008/50/EC. Since October 2024, the EU has introduced a new directive (2024/2881) that sets limit values for the year 2030. It is important to note that the limit values depend on the time period, but they can also vary depending on the objective. For example, there are different limits for the protection of human health, vegetation, and ecosystems. In the United States, limits are set under the Clean Air Act, which was last amended in 1990. For some pollutants, two separate standards are set: primary standards (which focus on protecting the health of sensitive

---

[113]Particulate matter consists of microscopic particles of solid or liquid substances suspended in the air. They are generally divided into three categories. Inhalable coarse particles, designated PM_{10}, are particles with a diameter of $10\,\mu m$ or less. Fine particles, designated $PM_{2.5}$, are particles with a diameter of $2.5\,\mu m$ or less. Finally, ultrafine particles (UFP) are particles with a diameter of $100\,nm$ or less.

Table 31: Air quality standards (limit values for the protection of human health)

Pollutant	Symbol	Unit	Period	WHO 2021	EU 2008	EU 2030	US 1990	China 2012	India 2009	Brazil 1990	Switzerland 2024
Particulate matter	$PM_{2.5}$	µg/m³	Annual	5	25	10	9/15	15/35	40		10
			24-hour	15		25	35	35/75	60		20
	PM_{10}		Annual	15	40	20		40/70	60		20
			24-hour	45	50	45	150	50/150	100		50
Ozone	O_3	µg/m³	Peak-season	60							
			8-hour	100	120	120	137	100/160	100	100	
Nitrogen dioxide	NO_2	µg/m³	Annual	10	40	20	100	40	30/40		30
			24-hour	25		50		80	80		80
			1-hour	200	200	200	188	200		190/320	
Sulfur dioxide	SO_2	µg/m³	Annual			20	26	20/60	20/50	40/80	30
			24-hour	40	125	50		50/150	80	100/365	100
			1 hour		350	350	196	150/500			
			10-minute	500							
Carbon monoxide	CO	mg/m³	24-hour	4		4		4			8
			8-hour	10	10	10	10		2	10	
			1-hour	35			40	10	4	40	
			15-minute	100							
Lead	Pb	µg/m³	Annual	0.5	0.5	0.5		0.5	0.5		
			3-month				0.15				
Amonia	NH_3	µg/m³	Annual						100		
Arsenic	As	ng/m³	Annual	6.6	6	6			6		
Benzene	C_6H_6	µg/m³	Annual	1.7	5	3.4			5		
Benzo[a]pyrene	BaP	ng/m³	Annual	0.12		1		1	1		
Cadmium	Cd	ng/m³	Annual	5	5	5					
Nickel	Ni	ng/m³	Annual	25	20	20			20		
Total suspended particles	TSP	µg/m³	Annual					80/200		60/80	

populations, such as asthmatics, children, and the elderly) and secondary standards (which focus on protecting the welfare of the public, including animals, crops, vegetation, and buildings). In China, India, and Brazil, air quality standards may also include two separate limits. The first generally applies to special regions, such as national parks and protected areas, while the second applies to all other areas.

Remark 11 *Similar figures are established for other quality standards (e.g., noise pollution, soil pollution, water pollution), but they are less comprehensive than those for air quality*[114].

3.3.4 Air quality index

An air quality index (AQI) is a standardized system used to communicate air quality to the public in an understandable way. It provides a single number that indicates the level of air pollution and its potential impact on health. The concept of air quality indices was first developed by academics in the 1950s and later adopted by environmental agencies, typically at the federal, provincial, or municipal level, in the 1960s and 1970s (Ott and Thorn, 1976; Ott, 1978). The first country-wide AQI systems were introduced in Canada (1970) and the United States (1976), followed by several European countries in the 1980s. Today, most countries have established their own air quality index systems. While these systems share some common features and have become more consistent over time, they are still not uniform. They often differ in the pollutants measured, the critical thresholds used, and, most importantly, the scales on which their indices are reported, making cross-country comparisons difficult. For example, Canada's AQI scale ranges from 1 to 10+, while China's ranges from 0 to 500. In Europe, the index typically ranges from 0 to 100+, and in Australia from 0 to 200+. These variations highlight the difficulties of harmonizing AQI systems across regions, despite their common goal of informing and protecting public health. The World Health Organization has published numerous guidelines to harmonize standards and reduce disparities between countries. However, we are still far from a single global AQI system. Nevertheless, several initiatives are helping to compare air quality indices across countries. One of the most prominent is the World Air Quality Index project (`aqicn.org` and `waqi.info`), which collects data from government monitoring stations in over 100 countries.

Although there is no globally harmonized AQI system, the one developed by the US EPA is undoubtedly one of the most widely used and has served as a model for many other countries' AQI frameworks. For example, the US AQI system is also used by the World Air Quality Index project. The US AQI is calculated based on five key pollutants: carbon monoxide (CO), nitrogen dioxide (NO_2), ground-level ozone (O_3), particulate matter (PM_{10} and $PM_{2.5}$), and sulfur dioxide (SO_2). For each pollutant, a sub-index is calculated based on its concentration:

$$I_j = I_{j,\text{low}} + \left(\frac{[C_j] - [C_j]_{\text{low}}}{[C_j]_{\text{high}} - [C_j]_{\text{low}}} \right) (I_{j,\text{high}} - I_{j,\text{low}}) \tag{31}$$

where j represents the pollutant, $[C_j]$ is the concentration of the pollutant in the air, $[C_j]_{\text{low}}$ and $[C_j]_{\text{high}}$ are the breakpoints for the concentration range, and $I_{j,\text{low}}$ and $I_{j,\text{high}}$ are the sub-index values corresponding to the low and high breakpoints, respectively. The overall Air Quality Index (AQI) is then calculated as the maximum of the sub-indices for all pollutants:

$$\text{AQI} = \max_j I_j$$

---

[114]In Canada, these figures are available on the CCME website (`https://ccme.ca/en/summary-table`), where users can select a chemical and obtain the following limits: Water Quality Guidelines for the Protection of Agriculture; Sediment Quality Guidelines for the Protection of Aquatic Life; Soil Quality Guidelines for the Protection of Environmental and Human Health; etc.

Table 32: US AQI categories

Category	AQI band	Levels of concern	Daily AQI color	
1	0 to 50	Good	Green	🟩
2	51 to 100	Moderate	Yellow	🟨
3	101 to 150	Unhealthy for sensitive groups	Orange	🟧
4	151 to 200	Unhealthy	Red	🟥
5	201 to 300	Very unhealthy	Purple	🟪
6	301 and higher	Hazardous	Maroon	🟫

Source: US EPA (2024, Tables 1 and 5, paged 3–12).

Since the highest breakpoint is typically 500, each sub-index is mapped to a score between 0 and 500. Once calculated, the sub-index is assigned to one of six categories, each represented by a specific color that indicates the health risk posed by the level of air pollution (Table 32). For instance, if the sub-index is less than 50, the category is good and the color is green, meaning that air quality is satisfactory, air pollution poses little or no risk, and it's great to be active outside. If the sub-index is between 101 and 150, members of sensitive groups may experience health effects and need to limit outdoor activity, while the general public is less likely to be affected.

To understand how the air quality index is calculated, we consider an example with particulate matter $PM_{2.5}$. Below we report the breakpoints $[C_j]_{\text{low}}$ and $[C_j]_{\text{high}}$ for the concentration range, and the values $I_{j,\text{low}}$ and $I_{j,\text{high}}$ of the corresponding AQI band[115]:

AQI category	1	2	3	4	5	6
$[C_j]_{\text{low}}$ (in µg/m^3)	0.0	9.1	35.5	55.5	125.5	225.5
$[C_j]_{\text{high}}$ (in µg/m^3)	9.0	35.4	55.4	125.4	225.4	500.4
$I_{j,\text{low}}$	0	51	101	151	201	301
$I_{j,\text{high}}$	50	100	150	200	300	500

Suppose we have a 24-hour $PM_{2.5}$ value of $27.4\,\text{µg/m}^3$. This value falls into the second AQI category, those concentration values that are above 9.1 and below 35.4. Applying Equation (31) gives:

$$I_{\text{PM}_{2.5}} = 51 + \left(\frac{27.4 - 9.1}{35.4 - 9.1} \right) (100 - 51) = 85.0951$$

A 24-hour $PM_{2.5}$ value of $27.4\,\text{µg/m}^3$ then corresponds to an air quality index of 85. Figure 51 shows the piecewise function (31) applied to particulate matter $PM_{2.5}$ and the corresponding AQI colors.

Figure 52 illustrates the AQI levels for particulate matter $PM_{2.5}$ in 2024 across four cities: New Delhi, Beijing, Paris, and Montreal. The data show significant disparities in air quality between these cities. In particular, New Delhi experienced 175 days with an AQI above 150, compared to 41 days in Beijing. In contrast, the maximum AQI value observed in Paris and Montreal was 113 and 104, respectively. In 2024, the average AQI values for these cities were 164 (New Delhi), 91 (Beijing), 49 (Paris), and 31 (Montreal). This indicates that Paris was more polluted than Montreal, as Paris had 136 days with an AQI above 50, while Montreal reported only 44 such days.

---

[115]Source: US EPA (2024, Table 6, page 14).

Figure 51: US air quality index for particulate matter PM$_{2.5}$
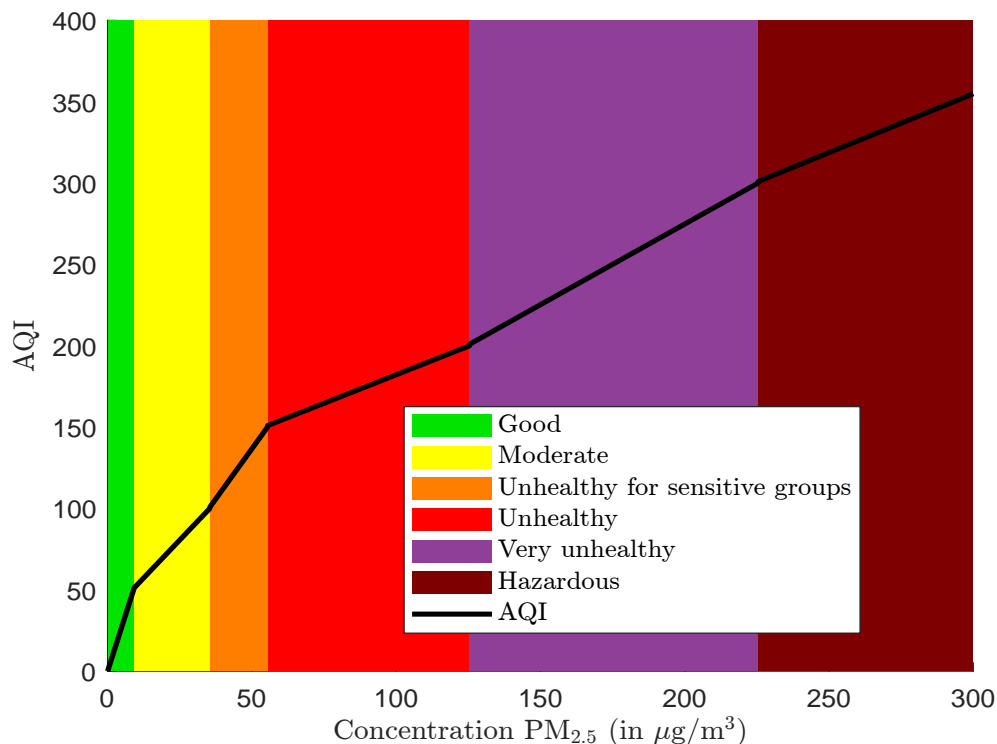
Figure 52: 2024 AQI PM$_{2.5}$ values in New Delhi, Beijing, Paris, and Montreal

Lecture Notes on Biodiversity
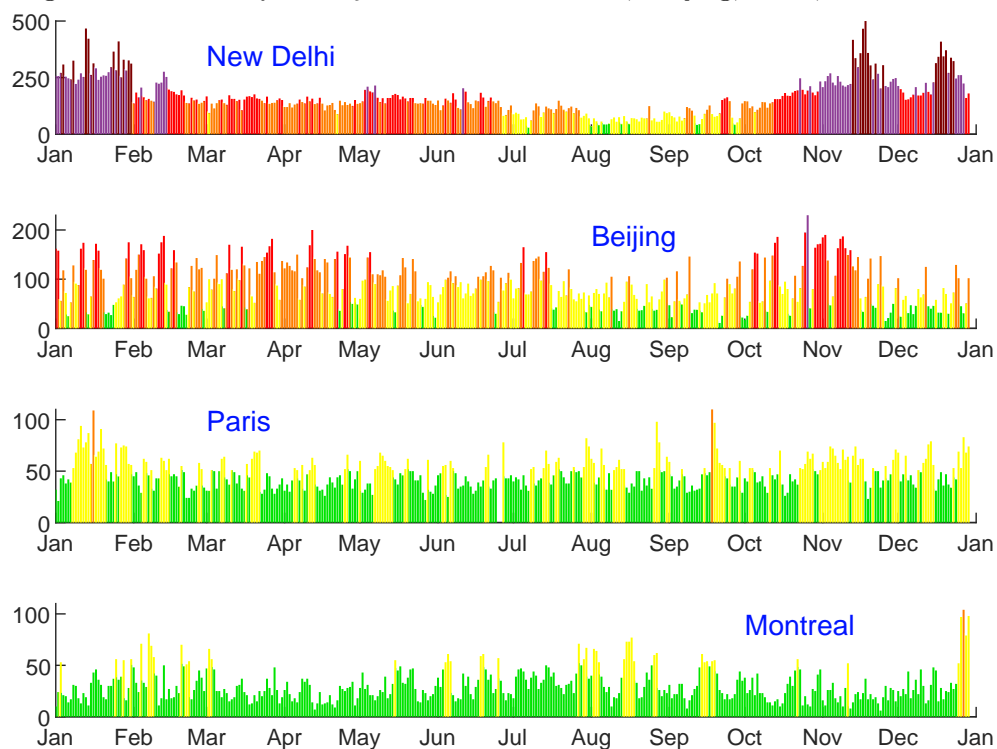
3.3.5 The cost of pollution

Measuring the costs of pollution is a complex challenge for several reasons. The first difficulty lies in defining what is meant by the term '*cost*'. Pollution does not result in a single type of cost, but rather a wide range of impacts, including health-related costs, lost productivity, damage to infrastructure and property, ecosystem degradation, reduced crop yields, resource depletion, and cleanup efforts. Identifying and categorizing these diverse costs is a fundamental step that adds to the complexity of the task. The second challenge is how to estimate these costs. Measuring the economic impact of pollution requires making assumptions and building statistical models. Results can vary widely depending on the methods and assumptions used, underscoring the importance of careful model selection in producing reliable estimates. A third major obstacle is the availability and relevance of data. Pollution measurements are often incomplete or inconsistent across countries because some countries lack the infrastructure to monitor certain pollutants. In addition, global coverage of pollutants is far from comprehensive. For example, particulate matter $PM_{2.5}$ is the most widely measured pollutant in the world, but reliable data on other types of pollution, such as soil, water, noise, and light pollution, remain scarce. This lack of comprehensive data makes it particularly difficult to assess the global impacts of these less-studied forms of pollution. Given these complexities, our discussion will focus primarily on two key issues: the health impacts and the economic costs associated with air pollution.

Health impacts The health effects of pollution are well documented in the scientific literature. However, air pollution is the most extensively studied topic, followed by water and plastic pollution. We estimate that 70% to 85% of health impact studies focus on air pollution. Research on water and plastic pollution each accounts for approximately 7% to 13%, while studies on soil and noise pollution make up about 2% to 4% each. Chemical pollution[116] represents around 1%, and light and biological pollution each account for less than 1%.

Table 33: Human health effects of pollution

Health impact	Air	Biological	Chemical	Light	Noise	Plastic	Soil	Water
Cancer	✓		✓			✓	✓	✓
Cardiovascular problems	✓		✓		✓			
Cognitive development	✓	✓	✓					
Endocrine disruption			✓			✓	✓	✓
Food contamination		✓				✓	✓	✓
Hearing loss					✓			
Infectious diseases		✓					✓	✓
Mental health	✓		✓	✓	✓			
Neurological effects	✓		✓					
Physical development	✓		✓					✓
Poisoning	✓	✓	✓			✓	✓	✓
Respiratory problems	✓	✓	✓			✓		
Skin problems	✓	✓						✓
Sleep disruption	✓			✓	✓			

Source: Author's research.

In Table 33 we summarize the different effects of the eight pollution categories on human health. Most scientific studies typically look at only a subset of pollution types and health categories. For example, consider the famous study by the *Lancet* Commission on Pollution and Health (Landrigan

---

[116]The underrepresentation of chemical pollution stems from its overlap with air, soil, and water pollution.

Table 34: Global estimated pollution-attributable deaths (in millions) in 2019

Pollution type	Female	Male	Total	in %
Total air pollution	2.92	3.75	6.67	74.0
Household air	1.13	1.18	2.31	25.6
Ambient particulate	1.70	2.44	4.14	45.9
Ambient ozone	0.16	0.21	0.37	4.1
Total water pollution	0.73	0.63	1.36	15.1
Unsafe sanitation	0.40	0.36	0.76	8.4
Unsafe source	0.66	0.57	1.23	13.7
Total occupational pollution	0.22	0.65	0.87	9.7
Carcinogens	0.07	0.28	0.35	3.9
Particulates	0.15	0.37	0.52	5.8
Lead pollution	0.35	0.56	0.90	10.0
Total pollution	3.92	5.09	9.01	100.0

Source: Fuller *et al.* (2022).

et al., 2018). The *Lancet* Commission has divided the pollutome (*i.e.*, the totality of all forms of pollution that have the potential to harm human health) into three zones:

- "*Zone 1 includes well established pollution-disease pairs, for which there are robust estimates of their contributions to the global burden of disease. The associations between ambient air pollution and noncommunicable disease are the prime example.*

- *Zone 2 includes the emerging effects of known pollutants, where evidence of causation is building, but associations between exposures and disease are not yet fully characterised and the burden of disease has not yet been quantified. Examples include associations between $PM_{2.5}$ air pollution and diabetes, pre-term birth, and diseases of the central nervous system, including autism in children, and dementia in the elderly. [...]*

- *Zone 3 includes new and emerging pollutants, most of them chemical pollutants whose effects on human health are only beginning to be recognised and are not yet quantified. [...] This zone includes developmental neurotoxicants; endocrine disruptors; new classes of pesticides such as the neonicotinoids; chemical herbicides such as glyphosate and nano-particles; and pharmaceutical wastes.*" (Landrigan *et al.*, 2018, page 11).

Focusing on Zone 1, the *Lancet* Commission estimated[117] that pollution is the leading environmental cause of disease and premature death, responsible for 9 million deaths in 2015 — 15.6% of the global 54.75 million deaths — disproportionately affecting the poor, vulnerable, and children in low- and middle-income countries (more than 90% of pollution-related deaths). These figures have been updated for 2019 using the same set of pollution types[118]. Fuller *et al.* (2022) found that the global

---

[117]The data used by the *Lancet* Commission (and many other international bodies studying pollution) come from the Global Burden of Disease (GBD) study, which is both a comprehensive research program and a database designed to quantify the impact of diseases, injuries, and risk factors on the health of populations worldwide. Initiated by the World Health Organization in 1990, it is now managed by the Institute for Health Metrics and Evaluation at the University of Washington. Data and results can be downloaded from `https://vizhub.healthdata.org/gbd-results`.

[118]The study covers the pollution related to the contamination of air by fine particulate matter ($PM_{2.5}$); ozone; sulfur and nitrogen oxides; freshwater pollution; contamination of the ocean by mercury, nitrogen, phosphorus, plastic, and petroleum waste; and poisoning of the land by lead, mercury, pesticides, industrial chemicals, electronic waste, and radioactive waste.

figure of 9 million deaths remains unchanged, accounting for one in six global deaths (Table 34). While deaths from poverty-related pollution (household air and water) have decreased, deaths from modern pollution sources (ambient air and chemicals such as lead) have increased by 7% since 2015 and 66% since 2000. Pollution — especially air pollution, which accounts for about 75% of pollution-related deaths each year — is now the leading risk factor for morbidity and mortality. It is on a par with smoking and far ahead of malnutrition, drug and alcohol use, HIV, and road traffic injuries (Fuller *et al.*, 2022, Figure 1, page 536).

The differences in air pollution-related deaths between regions and countries are significant. Figure 53 shows the proportion of deaths attributable to air pollution in 2021. The top five countries are North Korea (30.7%), Solomon Islands (27.3%), Vanuatu (23.4%), Bangladesh (22.2%), and Myanmar (21.2%), while the bottom five countries are Finland (0.8%), Sweden and Iceland (1%), and Canada, Estonia, and Norway (1.2%). The figures for China and India are 20.1% and 18.5% respectively. In South Asia, more than 18% of deaths are due to air pollution, compared with less than 2% in North America. There is also a significant difference between low-income countries (13.6%) and high-income countries (3.3%).

Figure 53: Share of deaths attributed to air pollution (2021)

Source: Our World in Data, https://ourworldindata.org/air-pollution.
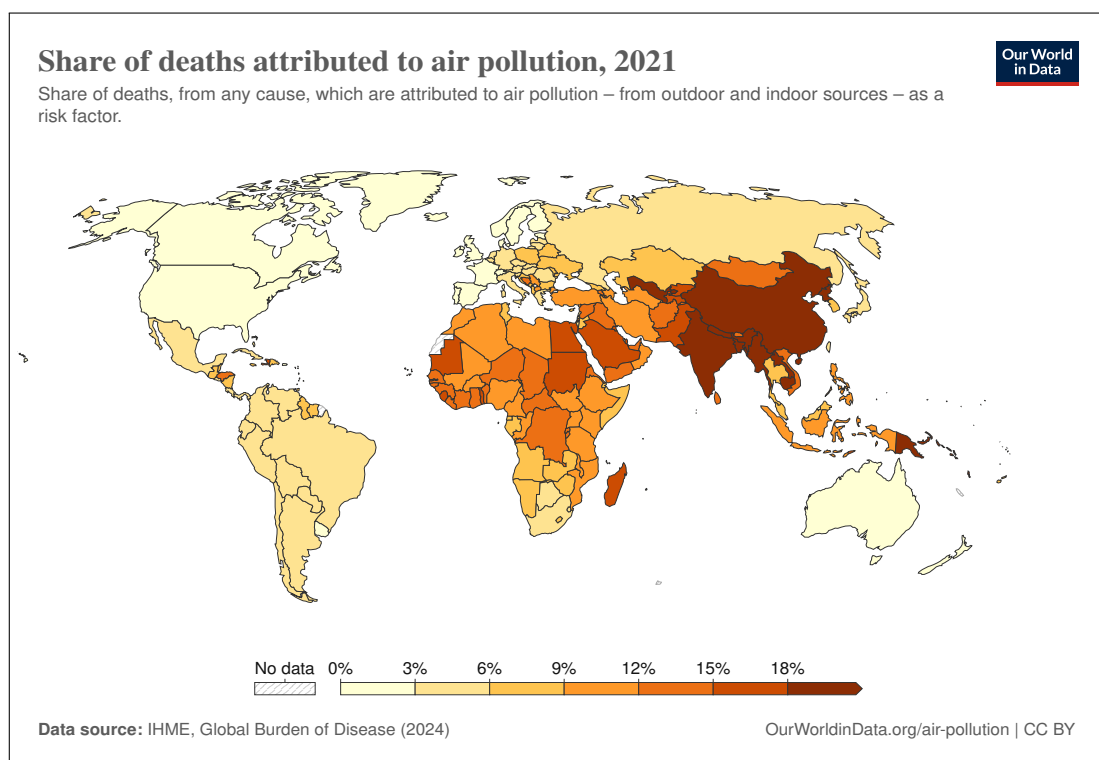
A significant number of deaths attributed to pollution from unsafe water sources are concentrated in Africa, India, and Southeast Asia[119]. The top five countries with the highest proportion of such deaths are Chad (7.0%), South Sudan (6.6%), Niger (5.3%), Somalia (4.1%), and Kiribati (4.0%). In sub-Saharan Africa, 2.5% of deaths are related to unsafe water sources, compared with 0% in North America and Europe. Again, the difference between low-income countries (2.3%) and high-income countries (0%) is large.

---

[119]Source: Our World in Data, https://ourworldindata.org/grapher/share-deaths-unsafe-water.

Box 15: Non-monetary value of health impacts

The Global Burden of Disease (GBD) defines three non-monetary values of health effects:

- Years of life lost (YLL)
  The YLL measures the burden of premature mortality. For an individual, it is calculated by comparing the age at which a person dies and the standard life expectancy. For example, if a person in a population dies at the age of 50 and the standard life expectancy is 75, the years of life lost are 25. For a homogeneous population we have:
  $$\text{YLL} = \sum_{i=1}^{n} \text{YLL}_i = \sum_{i=1}^{n} (L_i - L^\star)$$
  where L_i is the age of the deceased, $L^\star$ is the standard life expectancy of the polution and n is the number of deaths.

- Years lost/lived with disability (YLD)
  The YLD measures the burden of living with a health condition that causes disability or reduced quality of life but does not result in death. For an individual, it is calculated as the product of the disability weight (DW) and the average duration of the condition. The disability weight is a value between 0 (for perfect health) and 1 (equivalent to death) that reflects the severity of the health condition. For a population and a given disease, the YLD is calculated as the sum of individual YLD values, which is the number of cases of the disease multiplied by the disability weight of the disease and the average duration of the disease.

- Disability-adjusted life years (DALY)
  The DALY is the sum of YLL and YLD. It provides a single, comprehensive measure of health loss because it is a combined measure of both premature mortality and non-fatal health loss.

Another interesting study is the World Bank report, which uses data from the Global Burden of Disease[120] 2019, but focuses only on particulate matter $PM_{2.5}$, both outdoor (ambient air pollution) and indoor (household air pollution, *i.e.*, the use of fuels for cooking and heating). Global pollution exposure to ambient $PM_{2.5}$ was $43\,\mu g/m^3$ in 2019 compared to the WHO recommended level of $5\,\mu g/m^3$. World Bank (2022, page xiii) distinguishes two types of costs:

1. Death and premature mortality;

2. Morbidity due to illness and disability.

For premature deaths, World Bank (2022) reported that 6.45 million premature deaths in 2019 were attributed to exposure to $PM_{2.5}$ pollution. $PM_{2.5}$ was responsible for about 8.1% of global mortality. Globally, 64.2% of all $PM_{2.5}$ deaths were due to ambient air pollution (outdoor pollution), while 35.8% were due to household air pollution from the use of solid fuels (indoor pollution). About 95% of these deaths occurred in low- and middle-income countries, with 27.7% in China, 24.6% in India, 3.6% in Pakistan, 3.1% in Nigeria, and 2.9% in Indonesia. In terms of morbidity, World Bank (2022) estimated that air pollution has caused 21 million years lived with disability (YLD) and 93 billion days lived with illness (DLI) in 2019. The YLD figures are calculated by the Global Burden

---

[120]This is the same data used by Fuller *et al.* (2022) (see Footnote 117 on page 130).

of Disease (GBD) using the methodology described in Box 15, while the DLI figures are estimated by the World Bank using this formula:

$$\text{DLI} = \frac{365 \times \text{YLD}}{\text{DW}}$$

where DW is the disability weight. The breakdown of the morbidity impact is shown in Table 35. Type 2 diabetes accounts for 33% of days lived with illness, COPD (chronic obstructive pulmonary disease) for 24%, stroke for 11%, cataracts for 12%, ischaemic heart disease (IHD) for 18%, and low respiratory infections (LRI) for 1%.

Table 35: Global burden of morbidity from $PM_{2.5}$ exposure in 2019

Disease	YLD (in mn)	YLD (in %)	DLI (in bn)	DLI (in %)	DW (in %)
Type 2 diabetes	6.653	31.34	30.252	32.52	8.03
COPD	5.831	27.47	22.780	24.49	9.34
Stroke	5.028	23.68	10.497	11.29	17.48
Cataracts	2.143	10.10	11.370	12.22	6.88
IHD	1.248	5.88	16.654	17.90	2.74
LRI	0.198	0.93	1.214	1.31	5.95
Lung cancer	0.099	0.47	0.214	0.23	16.92
Neonatal disorders	0.019	0.09	0.035	0.04	20.32
Other	0.008	0.04	0.000	0.00	
Total	21.229	100.00	93.016	100.00	8.33

Source: World Bank (2022, Table 3.6, page 22) & Author's calculations.

Understanding the health effects of pollution remains a complex and multifaceted challenge for researchers and policy makers. While significant progress has been made in certain areas, such as the study of the effects of particulate matter, many other forms of pollution remain poorly understood. $PM_{2.5}$ has been the subject of extensive scientific investigation due to its well-documented and profound effects on human health. A substantial body of literature, including the seminal work of Pope and Dockery (2006), has elucidated the biological mechanisms by which $PM_{2.5}$ contributes to a range of adverse health outcomes, such as cardiovascular and respiratory disease. Subsequent studies, such as those by Lelieveld *et al* (2015) and Thangavel *et al.* (2022), have expanded our understanding, highlighting the risk factors associated with long-term exposure to this pollutant and its contribution to global mortality. Despite this progress, our knowledge of the health effects of other forms of pollution is less comprehensive, leaving significant gaps in our understanding. Research conducted by the *Lancet* Commission has highlighted areas known as Zone 2 and Zone 3, which include emerging and less studied pollutants. These zones represent critical frontiers in pollution research that require further exploration and scientific investigation. For example, soil contamination by heavy metals such as lead and mercury has long been recognized as a public health concern, but its broader impacts on ecosystems and human health need to be better understood. Similarly, the effects of black carbon, a component of soot produced by incomplete combustion of fossil fuels and biomass, are increasingly understood to have both direct and indirect health effects. Another prominent example is glyphosate, a widely used herbicide that has generated considerable public and scientific debate. While some studies suggest potential health risks (Van Bruggen *et al.*, 2018), such as links to cancer or endocrine disruption, others argue that these findings remain inconclusive due to methodological limitations and conflicting evidence. This controversy underscores the broader challenge of assessing the health effects of complex chemical exposures,

particularly in the absence of robust long-term studies. Moreover, the health effects of pollution are not limited to morbidity and mortality. Impacts on other dimensions of health must also be considered, such as cognitive and physical development, mental health, skin conditions, and more. Addressing these broader dimensions is critical to developing a comprehensive understanding of how pollution affects human well-being.

Global economic costs Estimating the economic costs of pollution poses significant challenges due to complex methodological issues and considerable data uncertainty. The time horizon is particularly important, as the inclusion of long-term costs yields very different results than the analysis of short-term impacts. Consequently, the following results should be interpreted with considerable caution. When examining such estimates, orders of magnitude and relative rankings tend to be more reliable indicators than absolute figures. This explains the considerable variation in results among the scientific research publications on this topic. In the following, we focus mainly on two reports: *Quantifying the Economic Costs of Air Pollution from Fossil Fuels* (Myllyvirta, 2020) and *The Global Health Cost of PM$_{2.5}$ Air Pollution: A Case for Action Beyond 2021* (World Bank, 2022). But there are other reports that can be used. For example, the *Lancet* Commission estimated that welfare losses due to pollution are more than \$4.6 trillion per year, or 6.2% of global economic output, and that 81.5% of these economic losses are due to ambient air pollution and household air pollution, with the remainder explained by lead exposure (9.8%) and water pollution (8.7%) (Landrigan *et al.*, 2018, Table 5, page 487). These figures already give an idea of the global economic cost of pollution.

Myllyvirta (2020) proposes a simple method for estimating the economic cost of pollution. He divides the impacts of pollution into various health and economic outcomes. A common health outcome of air pollution is premature death, but pollution also causes other health issues such as childhood asthma, preterm births, illnesses, or disabilities, as well as economic outcomes like work absences or productivity losses. The total cost is calculated as the sum of the economic costs of these different health and economic outcomes:

$$\mathcal{C} = \sum_{j=1}^{m} \mathcal{C}_j = \sum_{j=1}^{m} n_j c_j$$

where m is the number of health or economic outcomes, n_j is the number of cases of the jth outcome, and c_j is the average unit cost of the jth outcome. Consider the example of a hypothetical country. If the average unit cost of a lost workday is \$150 and pollution is responsible for 2.5 million lost workdays, the pollution-related cost of lost workdays is $2.5 \times 10^6 \times 150 = \$375$ mn. If the average unit cost of a preterm birth (including initial hospitalization and long-term health effects) is \$30 000 and pollution is responsible for 2 000 preterm births, the pollution-related cost of preterm birth is $30 \times 10^3 \times 2\,000 = \$60$ mn. The total cost of these two health and economic outcomes is then \$435 million. Using published concentration-response functions (to estimate n_j) and unit costs by country (to assess n_j), and considering six health and economic outcomes, Myllyvirta (2020) estimated that air pollution from fossil fuels resulted in a global economic cost equivalent to 3.3% of GDP in 2018:

> "The economic costs of air pollution from fossil fuels are estimated at \$2.9 trillion in 2018, or 3.3% of global GDP [...] An estimated 4.5 million people died in 2018 due to exposure to air pollution from fossil fuels. On average, each death was associated with a loss of 19 years of life. [...] Fossil fuel PM$_{2.5}$ pollution was responsible for 1.8 billion days of work absence, 4 million new cases of child asthma and 2 million preterm births, among other health impacts that affect healthcare costs, economic productivity and welfare." (Myllyvirta, 2020, page 2).

The distribution of this total cost is as follows: 84% is attributed to adult deaths, followed by disability due to chronic diseases (7%), sick leave (3.5%), preterm births (3.15%), child deaths (1.75%), and asthma (0.6%). The global figure of 3.3% masks disparities between countries, as shown in Table 36. China has the highest costs (6.6% of GDP), followed by Bulgaria and Hungary (6.0% of GDP). On the contrary, Brazil and Spain have low costs, less than 2% of their GDP. However, these figures do not reflect the full reality. In fact, by measuring costs by GDP, the analysis favors high-income countries because of their high GDP. Myllyvirta (2020) provided the economic cost of air pollution per capita. In this case, the country with the highest costs is Luxembourg ($2 600 per capita), followed by the US ($1 900 per capita), Switzerland ($1 900 per capita), Austria ($1 700 per capita) and Germany ($1 700 per capita). Interestingly, the cost in France is $800 per capita.

Table 36: Economic costs of air pollution from fossil fuels (% of GDP, 2018)

	Country	Cost		Country	Cost
	China	6.6%		Bulgaria	6.0%
	Hungary	6.0%		Ukraine	5.8%
	Serbia	5.8%		Belarus	5.4%
	India	5.4%		Romania	5.3%
	Bangladesh	5.1%		Moldova	5.0%
	Poland	4.9%		Russia	4.1%
	Germany	3.5%		South Korea	3.4%
	USA	3.0%		Japan	2.5%
	UK	2.3%		France	2.0%
	Spain	1.7%		Brazil	0.8%

Source: Myllyvirta (2020, page 6) & Centre for Research on Energy and Clean Air (CREA).

The report of the World Bank focuses only on the particulate matter $PM_{2.5}$, and distinguishes two types of cost: (1) death and premature mortality and (2) morbidity due to illness and disability. The economic cost of premature deaths is estimated using the approach based on the value of statistical life (VSL), while the economic cost of morbidity is estimated by the years lost with disability (YLD) (see Box 16). The global economic cost of mortality and morbidity was estimated at $8.1 trillion, or 6.1% of global GDP in 2019, with the following breakdown: 85% from premature mortality and 15% from morbidity. Low- and middle-income countries bear a disproportionate share of these costs, accounting for more than 90% of the global health burden of $PM_{2.5}$ pollution. The most affected regions are South Asia, and East Asia and Pacific, with costs equivalent to 10.3% and 9.3% of GDP, respectively (Table 37). Table 38 lists the top three countries in each region ranked by percentage of GDP. For example, China ranks first in East Asia & Pacific (EAP) with an economic cost equivalent to 12.9% of GDP. In Europe, Serbia is the leading country with a cost of 18.9% of GDP. Table 39 provides the top 15 countries in terms of absolute cost in billions of dollars. For each country, we also indicate the breakdown between outdoor and indoor pollution, and the proportion attributed to mortality and morbidity. For instance, China has a total cost of $3 029 billion, of which 79% arises from outdoor pollution, and 12% is attributed to morbidity.

Table 37: Annual cost of health damages from PM$_{2.5}$ by region (% of GDP, 2019)

Region	Outdoor	Indoor	Mortality	Morbidity	Total
East Asia and Pacific (EAP)	7.3%	2.0%	8.1%	1.2%	9.3%
Europe and Central Asia (ECA)	4.4%	0.2%	4.0%	0.6%	4.6%
Latin America and Carribean (LAC)	2.7%	0.7%	2.9%	0.5%	3.4%
Middle Easth and North Africa (MNA)	5.5%	0.0%	4.7%	0.8%	5.5%
North America (NA)	1.7%	0.0%	1.3%	0.4%	1.7%
South Asia (SA)	5.9%	4.3%	8.3%	2.0%	10.3%
Sub-Saharan Africa (SSA)	3.6%	2.4%	5.2%	0.8%	6.0%
Low-income countries	1.3%	4.6%	5.0%	0.9%	5.9%
Lower-middle-income countries	5.4%	3.6%	7.5%	1.5%	9.0%
Upper-middle-income countries	7.1%	1.8%	7.8%	1.1%	8.9%
High-income non OECD countries	4.3%	0.2%	4.0%	0.5%	4.5%
High-income OECD	2.8%	0.0%	2.3%	0.5%	2.8%

Source: World Bank (2022, Figures 3.13 & 3.14, pages 20 & 21) & Author's calculations.

Table 38: Annual cost of health damages from PM$_{2.5}$ by country (% of GDP, 2019)

Region	Top 1 country		Top 2 country		Top 3 country	
EAP	China	12.9%	Papua New Guinea	12.0%	Myanmar	11.4%
ECA	Serbia	18.9%	Bulgaria	16.3%	North Macedonia	15.9%
LAC	Barbados	8.8%	Haiti	8.1%	Trinidad/Tobago	7.8%
MNA	Egypt	8.6%	Morocco	7.3%	Tunisia	6.5%
NA	USA	1.7%	Canada	1.2%		
SA	India	10.6%	Nepal	10.2%	Pakistan	8.9%
SSA	Burkina Faso	9.1%	Mali	9.1%	Central African Republic	8.7%

Source: World Bank (2022, Table 3.5, page 21).

Table 39: Annual cost of health damages from PM$_{2.5}$ by country in 2019 (Top 15)

Country	Total (in $ bn)	Total (in % of GDP)	Outdoor (in %)	Indoor (in %)	Mortality (in %)	Morbidity (in %)
China	3 029	12.9	79	21	88	12
India	1 022	10.6	60	40	81	19
United States	373	1.7	100	0	78	22
Russia	241	5.7	97	3	91	9
Indonesia	220	6.6	56	44	85	15
Japan	210	3.8	100	0	82	18
Germany	178	3.8	100	0	81	19
Turkey	134	5.8	99	1	85	15
Italy	132	5.0	99	1	83	17
Poland	127	9.8	91	9	86	14
South Korea	114	5.1	100	0	83	17
Egypt	105	8.6	100	0	87	13
Mexico	104	4.0	78	22	84	16
Saudi Arabia	96	5.7	100	0	89	11
Pakistan	94	8.9	48	52	82	18

Source: World Bank (2022, Table A.3, page 40) & Author's calculations.

<div align="center">Box 16: A basic economic model of pollution costs</div>

Dechezleprêtre *et al.* (2019) consider a classical output function that uses capital and labor as factors of production, but also incorporates pollution as an additional variable: $Y = F(K, L, P)$, where Y is economic output, K is capital, L is labor, and P is pollution. The labor input L can be expressed as $L = N \cdot A_L \cdot T_L$ where N is the workforce size (or the population), A_L is labor productivity, $T_L = \tau - \varsigma$ is the time individuals spend working, which is the difference between the total endowment of labor time τ and sick time ς. It is assumed that all three variables (N, A_L, and ς) depend on the pollution P. Consequently, the output function can be rewritten as:

$$Y = F\left(K, N\left(P\right) A_L(P)\left(\tau - \varsigma\left(P\right)\right), P\right)$$

From this, we deduce the derivative of the logarithm of output with respect to pollution:

$$\frac{d \ln Y}{dP} = \frac{\partial \ln Y}{\partial \ln L} \frac{\partial \ln L}{\partial P} + \frac{\partial \ln Y}{\partial P} = \epsilon_L \frac{\partial \ln L}{\partial P} + \frac{\partial \ln Y}{\partial P}$$

where $\varepsilon_L \geq 0$ is the elasticity of output with respect to labor. Breaking this down further:

$$\frac{d \ln Y}{dP} = \epsilon_L \left(\frac{\partial \ln N}{\partial P} + \frac{\partial \ln A_L}{\partial P} + \frac{\partial \ln\left(\tau - \varsigma\left(P\right)\right)}{\partial P} \right) + \frac{\partial \ln Y}{\partial P}$$

Expanding the third term:

$$\frac{\partial \ln\left(\tau - \varsigma\left(P\right)\right)}{\partial P} = -\frac{1}{\tau - \varsigma\left(P\right)} \frac{\partial \varsigma\left(P\right)}{\partial P} = -\frac{\varsigma\left(P\right)}{\tau - \varsigma\left(P\right)} \frac{\partial \ln \varsigma\left(P\right)}{\partial P}$$

Substituting this into the equation and introducing the notation $\theta = \dfrac{\varsigma}{\tau - \varsigma}$, which represents the ratio of sick time to effective labor time, we get:

$$\frac{d \ln Y}{dP} = \epsilon_L \underbrace{\left(\frac{\partial \ln N}{\partial P} + \frac{\partial \ln A_L}{\partial P} - \theta \frac{\partial \ln \varsigma\left(P\right)}{\partial P} \right)}_{\text{Pollution-related labor impact}} + \frac{\partial \ln Y}{\partial P}$$

This equation can be expressed in the following compact form:

$$\beta_P = \epsilon_L \beta_{L,P} + \beta_{L,P}$$

Therefore, pollution has an indirect impact on output through the labor factor, which operates through three dimensions:

1. Pollution increases mortality, reducing the size of labor force: $\dfrac{\partial \ln N}{\partial P} < 0$.

2. Pollution increases morbidity, decreasing labor productivity: $\dfrac{\partial \ln A_L}{\partial P} < 0$.

3. Pollution increases morbidity, leading to more work absences: $\frac{\partial \ln \varsigma(P)}{\partial P} > 0$.

Box 16: A basic economic model of pollution costs (Continued from previous page)

> The labor-related impact of pollution also depends on the labor-output elasticity. A higher value of ϵ results in a higher cost of pollution, especially in labor-intensive industries (Graff Zivin and Neidell, 2013). Consequently, the labor-related impact of pollution is always negative: $\epsilon_L \beta_{L,P} \leq 0$. In contrast, the direct impact of pollution on output can be either positive or negative: $\beta_{L,P} = \dfrac{\partial \ln Y}{\partial P} \lessgtr 0$. When pollution levels are low, increasing pollution can have a positive impact because GDP is boosted by an increase in energy supply. However, when pollution levels are very high, increasing pollution has a negative impact due to the negative externalities (*e.g.*, infrastructure damage, reduced agricultural yields, water stress) that affect the production system. Therefore, the direct relationship follows a bell curve: $\beta_{L,P}$ is initially positive, but becomes negative as pollution increases. The aggregation of these two effects is not straightforward. While β_P may be positive when pollution levels are low, it is certain to become negative when pollution levels are high.

Economic costs in Europe   Studying the economic costs of air pollution in Europe is particularly valuable because of the availability of more reliable and comprehensive data. This allows researchers to consider additional pollutants beyond $PM_2.5$, such as heavy metals (*e.g.*, arsenic) and organic pollutants (*e.g.*, benzene). They can also examine trends in economic costs over time and assess the impact of policy regulations on air quality and associated costs. For instance, Dechezleprêtre *et al.* (2019) estimated that a $1\,\mu g/m^3$ increase in $PM_2.5$ concentration leads to a 0.8% reduction in real GDP within the same year. Notably, 95% of this impact is attributed to a decline in output per worker, which can result from higher absenteeism or reduced labor productivity. Since $PM_2.5$ pollution in Europe has decreased by $0.2\mu g/m^3$ per year since 2000, reducing air pollution could increase real GDP by 1.6% per decade. Thus, this study shows that reducing air pollution generates economic growth through improved labor productivity.

More recently, Mejino-López and Oliu-Barton (2024) studied the allocation of EU funds among member states and the cost-effectiveness of European air pollution policies. Using the results of Dechezleprêtre *et al.* (2019), they estimated the costs of particulate matter $PM_2.5$ as follows[121]:

$$\mathcal{C} = \beta_P \cdot ([C] - \text{AQG})^+ \cdot \text{GDP} = 0.8\% \cdot \max\left([C]_{\text{PM}_{2.5}} - 5\,\mu g/m^3, 0\right) \cdot \text{GDP}$$

On a global basis, they found that costs have declined since 2014, but remain at high levels:

> "*Despite significant progress, air pollution still causes €600 billion in losses each year in the European Union — equal to 4% of its annual GDP. These costs stem from productivity losses such as increased absenteeism, the reduction of in-job productivity and harm to ecosystems. Air pollution costs are disproportionately high in eastern Europe and Italy, where losses are projected to remain above 6% of GDP until 2030. The EU's 10% most-polluted regions suffer 25% of the burden of mortality attributable to air pollution.*" (Mejino-López and Oliu-Barton, 2024, page 1).

The large differences between countries are shown in Figure 54. For each country, Mejino-López and Oliu-Barton (2024) calculated the cost of air pollution for three seven-year periods[122]: 2014–2020,

---

[121]Since we have $\beta_P = \Delta \ln Y / \Delta P$, we deduce that $\Delta Y = \beta_P \cdot \Delta P \cdot Y$.

[122]For the 2024–2030 period, they used World Bank projections of GDP and extrapolated $PM_2.5$ concentrations based on linear regressions.

Figure 54: Estimated cost of air pollution by country (in % of GDP)
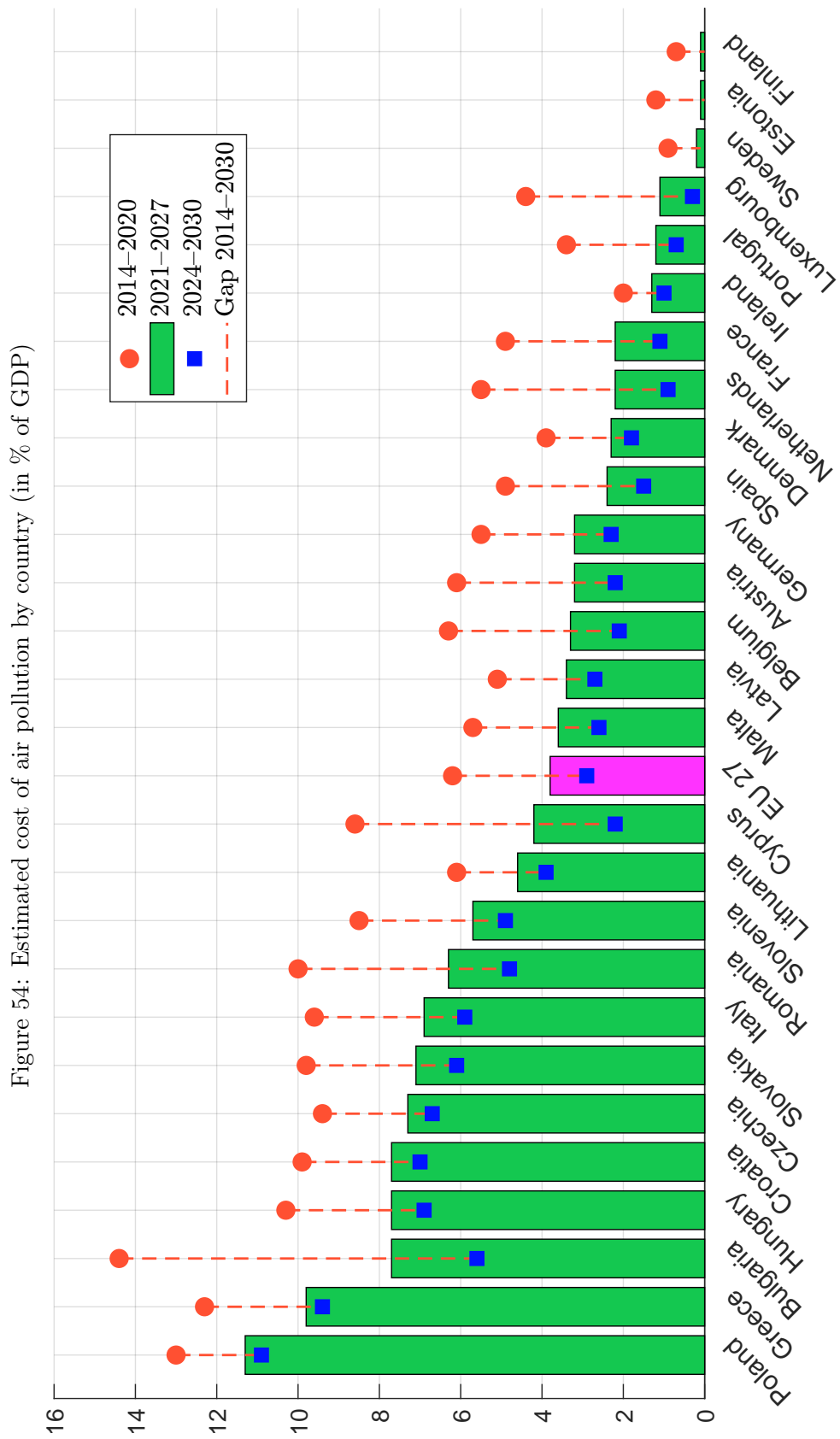
2021–2027, and 2024–2030. Some countries, such as Bulgaria, Romania, Cyprus, Belgium, and the Netherlands have dramatically reduced air pollution when considering the gap 2014–2030. However, there are still some air pollution hotspots in Europe. Considering the 234 EU regions, Mejino-López and Oliu-Barton (2024) identified 16 hotspots: 5 in Bulgaria, 4 in Poland, 2 in Romania, and 1 each in Czechia, Croatia, and Hungary. These hotspots represent 7% of the EU population, but concentrate 14% of air pollution mortality.

EEA (2024a) uses a different methodology to estimate the economic costs of pollution. The analysis focuses on industrial facilities in Europe[123] and considers the following groups of pollutants:

- Main air pollutants: particulate matter ($PM_{2.5}$, PM_{10}), sulfur dioxide (SO_2), ammonia (NH_3), nitrogen oxides (NO_x), and non-methane volatile organic compounds (NM VOC);

- Greenhouse gases (GHG): carbon dioxide (CO_2), methane (CH_4) and nitrous oxide (N_2O);

- Heavy metals: arsenic (As), cadmium (Cd), chromium VI (Cr), lead (Pb), mercury (Hg), and nickel (Ni);

- Organic pollutants: 1,3 butadiene, benzene, formaldehyde, polycyclic aromatic hydrocarbons, dioxins and furans.

The study examines only air pollution and estimates the external costs of these facilities, taking into account both health effects (mortality and morbidity) and non-health effects (damage to buildings, crops, and forests). Health effects for the main pollutants are quantified using concentration-response functions and unit costs based on the value of a statistical life (VSL) and the value of life year (VOLY). For greenhouse gases, negative externalities are assessed by calculating the marginal abatement cost of carbon emissions required to meet the Paris Agreement targets. The results, broken down by country, are presented in Table 40. EEA (2024a) estimates that the economic costs associated with the value of a statistical life and the value of a life year are 2.23% and 1.39% of GDP, respectively, for the EU-27. The most affected countries are Bulgaria, Poland, Greece, Romania and Estonia, while the top five Member States with facilities contributing the highest external costs are Germany, Poland, Italy, France and Spain. Table 41 shows the amount of negative externalities in millions of euro. In 2012, the costs for the EU-27 were 326.5 and 536.7 billion euros, depending on the approach (VOLY vs. VSL). In 2021, these figures become 219.4 and 352.7 billion euros, representing a decrease of 32.8% and 34.3% of total external costs, respectively. During the period 2012-2021, the cumulative externalities were 2.7 and 4.3 trillion euros, respectively.

We see that heavy metals and organic pollutants are responsible for less than 5% of the economic costs, and these costs are mainly concentrated on lead, followed by cadmium and mercury. For the group of major air pollutants, sulfur dioxide and nitrogen oxides are the main contributors. EEA (2024a) also finds that 129 facilities (out of about 9 400 facilities) are responsible for about 50% of the total damage caused by air emissions:

> "It is worth noting that half (25) of the 50 most polluting facilities in 2021 were thermal power stations, with most of them located in Germany (nine) and Poland (six). Twenty-three of these 25 plants burn lignite or hard coal as their main fuel." (EEA, 2024a, page 10).

---

[123]The study is based on the European Pollutant Release and Transfer Register (E-PRTR) dataset, a comprehensive database established under European Union Regulation 166/2006 to provide public access to environmental data from large industrial facilities across Europe. E-PRTR contains data reported annually by more than 30 000 industrial facilities in the EU, Iceland, Liechtenstein, Norway, Serbia, Switzerland and the United Kingdom from 65 economic activities and covers 91 pollutants, including emissions to air, water and land as well as waste transfers.

Table 40: External costs of air pollution (2021)

	Country	Relative cost		Breakdown of external costs	
		VOLY/GDP	VSL/GDP	VOLY	VSL
	Austria	0.71%	1.07%	1.43%	1.34%
	Belgium	1.59%	2.68%	3.96%	4.16%
	Bulgaria	7.87%	16.11%	2.77%	3.53%
	Croatia	1.72%	2.89%	0.50%	0.52%
	Cyprus	2.89%	3.02%	0.34%	0.22%
	Denmark	0.47%	0.64%	0.78%	0.66%
	Estonia	3.35%	3.75%	0.52%	0.36%
	Finland	2.12%	2.36%	2.63%	1.82%
	France	0.68%	1.07%	8.39%	8.25%
	Germany	1.54%	2.63%	27.41%	29.19%
	Greece	2.93%	4.76%	2.63%	2.67%
	Hungary	2.21%	4.27%	1.69%	2.03%
	Ireland	0.50%	0.62%	1.06%	0.82%
	Italy	1.06%	1.79%	9.35%	9.87%
	Latvia	0.69%	1.05%	0.11%	0.11%
	Luxembourg	0.35%	0.65%	0.13%	0.15%
	Netherlands	1.37%	1.91%	5.81%	5.03%
	Poland	5.63%	8.68%	16.06%	15.43%
	Portugal	1.67%	2.18%	1.77%	1.45%
	Romania	2.47%	4.55%	2.96%	3.38%
	Slovenia	1.76%	2.99%	0.46%	0.48%
	Spain	1.07%	1.77%	6.40%	6.58%
	Sweden	1.07%	1.18%	2.86%	1.95%
	EU-27	1.39%	2.23%		

Source: EEA (2024b, Figure 4.2, Tables 4.2 & 4.3, pages 31–34), Author's calculations & icons taken from https://icons8.com/icons.

Table 41: External costs of air pollution in € mn (2021)

Pollutants	2012	2021	Cumulative	2021 Breakdown
Main air (VOLY)	119 042	59 728	834 066	SO_2: 45.3%, NO_x: 41.1%, NH_3: 7.5%, PM_{10}: 5.0%, NM VOC: 1.2%
Main air (VSL)	329 152	193 056	2 426 585	SO_2: 45.7%, NO_x: 40.5%, NH_3: 7.7%, PM_{10}: 5.0%, NM VOC: 1.0%
GHG	193 641	150 657	1 728 224	CO_2: 94.5%, CH_4: 4.9%, N_2O: 0.6%
Heavy metals	13 803	8 924	120 622	Pb: 79.6%, Cd: 15.9%, Hg: 3.2%, As: 1.3%, Cr(VI): 0.1%, Ni: 0.0%
Organic	66	69	1 071	Dioxins: 82.6%, B(a)P: 15.9%, Benzene: 1.4%
Total (VOLY)	326 553	219 378	2 683 984	GHG: 68.7%, Main air: 27.2%, Heavy metals: 4.1%, Organic: 0.0%
Total (VSL)	536 663	352 707	4 276 503	Main air: 54.7%, GHG: 42.7%, Heavy metals: 2.5%, Organic: 0.0%

Source: EEA (2024b, Table 4.1, Figures 4.4–4.7, pages 28 & 35–37) & Author's calculations.

The technical report contains an interesting analysis of marginal damage costs (MDC) for different pollutants and countries. The MDC represents the monetary value of the damage caused by emitting one additional tonne of a specific pollutant into the environment. For the main air pollutants, the average marginal costs for 2019, expressed in 2021 thousand euros per kg of pollutant emitted into the air, are as follows[124]:

Pollutant	NO_x	SO_2	PM_{10}	$PM_{2.5}$	NM VOC	NH_3
MDC (VOLY)	15.4	16.2	51.5	86.5	1.8	19.0
MDC (VSL)	43.0	38.3	141.1	237.1	4.5	52.3

while for heavy metals and organic compounds they find these values:

Pollutant	Arsenic	Cadmium	Chromium VI	Lead	Mercury
MDC	10.3	253.1	0.7	45.2	16.8
Pollutant	Nickel	1,3 Butadiene	Benzene	B(a)P	Dioxins
MDC	0.02	0.00	0.00	1.4	132 600

We read these numbers as follows. One additional tonne of NO_x emitted to the air induces an additional cost of 15 400 euros in the VOLY method, while one additional tonne of $PM_{2.5}$ emitted to the air induces an additional cost of 237 100 euros in the VSL method. The pollutant with the highest marginal damage cost is dioxins with an MDC of 132.6 million euro per kg.

Remark 12 *Although the EEA report is certainly one of the most comprehensive, well-documented and data-driven studies of the economic costs of air pollution, it also shows that this is a complex task and that there are many uncertainties about these costs. Key assumptions include the specification of concentration-response functions and the modelling of $PM_{2.5}$ impacts. In addition, this report is far from exhaustive as it does not include some important activities that do not correspond to industrial installations. For example, the industrial facilities reported in the E-PRTR database cover*

---

[124]Source: EEA (2024a, Tables 3.1 & 3.4, pages 26 & 27).

49% of SO$_\mathrm{x}$ and 48% of mercury, but only 3% of PM$_{10}$ and 10% of lead. Furthermore, the study only analyses outdoor pollution and does not consider indoor pollution, in particular the impact of emissions on workers inside the facilities.

Box 17: Monetary economic value of health impacts

In Box 16 on page 137, we have defined three non-monetary measures of health impact: years of life lost (YLL), years lived with disability (YLD) and disability-adjusted life years (DALY). To assess economic costs, we need to convert these physical measures into monetary ones. Some standard approaches are described below.

- The quality-adjusted life year (QALY) is a unit of measurement that combines both the quantity and quality of life lived into a single index. One QALY represents one year of perfect health, and zero QALYs represent one year of death. It can be used to evaluate the benefits of a policy[a]:

$$\mathrm{QALY} = \text{Years of Life Gained} \times \text{Average Quality of Life Weight}$$

  This approach is called linear because it is equivalent to directly summing the annual quality of life weights:

$$\mathrm{QALY} = \sum_{u=t}^{T} Q(u)$$

  where T is the maximum time horizon and $Q(t) \in [0, 1]$ is the quality life of weight at time t. According to Hammitt (2023, Equation 2.5), a non-linear approach is to calculate the quality-adjusted life expectancy (QALE)[b]:

$$\mathrm{QALE} = \frac{1}{S(t)} \int_{t}^{T} e^{-\varrho(u-t)} \mathbf{S}(u) \, \mathbb{E}[Q(u)] \, \mathrm{d}u$$

  where $\mathbf{S}(t)$ is the survival function at time t, ϱ is the discount rate and $\mathbb{E}[Q(t)]$ is the expected quality weight.

- The value of a statistical life (VSL) is the economic value placed on the benefit of avoiding a death. It is not the value of an individual's life *per se*, but rather a measure of society's collective willingness to pay for small reductions in mortality risk. As such, the VSL is closely related to the concept of willingness-to-pay. The VSL is based on the amount of money that individuals are willing to pay for a given reduction in the risk of premature death. Several approaches are used to estimate VSL, including revealed preferences (*e.g.*, wage premiums for risky jobs) and stated preferences (*e.g.*, surveys asking about risk reduction choices). Hammitt (2023) mathematically defines the VSL as follows:

$$\mathrm{VSL} = \frac{v}{\Delta L}$$

  where v is the monetary value of the risk reduction and ΔL is the expected number

---

[a]When we want to evaluate the cost of a disease, we replace Years of Life Gained by Years of Life Lost.
[b]T can be set to ∞, since $S(\infty) = 0$.

Box 17: Monetary economic value of health impacts (Continued from previous page)

of lives saved. For example, if workers in an industry are paid an additional \$1 000 per year to face a 1 in 10 000 increased risk of death, the VSL can be calculated as $\text{VSL} = \dfrac{1\,000}{1/10\,000} = \$10\,\text{mn}$. In this example, the VSL is \$10 million, reflecting the monetary value associated with risk reductions that collectively save one statistical life. In the case of the economic costs of air pollution, EEA (2024b, page 19) used a VSL of €4.2 million — for infant mortality, it is set to €6.5 million.

- The value per statistical life year (VSLY) — or the value of a life year (VOLY) — is equal to the value of a statistical life divided by the remaining expected life years Hammitt (2023, Equation 2.10):

$$
\text{VSLY} = \frac{\text{VSL}}{\dfrac{1}{\mathbf{S}\,(t)} \displaystyle\int_t^T e^{-\varrho(u-t)} \mathbf{S}\,(u)\ \mathrm{d}u}
$$

It represents the economic value of extending the life of a population by one additional year. Using the previous example, if the average remaining expected life in the industry is 40 years, $\text{VSLY} = \dfrac{\$10\,\text{mn}}{40} = \$250\,000$. In the case of air pollution, EEA (2024b, page 19) used a VOLY of €111 470, which means that the remaining expected life years used for this study is 37.68 years.

- VSL, VSLY, and VOLY are not available for all countries, as their computation requires extensive data and statistical resources. These metrics are generally well documented for OECD countries, the United States, and Europe, where data availability and research capacity are higher. For other countries, country-specific figures can be estimated by adjusting a baseline statistic using a transfer function, as described by Hammitt and Robinson (2011) and Viscusi and Masterman (2017):

$$
\text{VSL}_c = \text{VSL}_b \left(\frac{(Y/N)_c}{(Y/N)_b} \right)^{\epsilon}
$$

where VSL_c is the country-specific VSL, VSL_b is the baseline VSL, (Y/N) is the GDP per capita and ϵ is the income elasticity of VSL, which captures how VSL scales with income. For high-income countries, ϵ is typically less than 1, reflecting the diminishing marginal utility of income. For low-income countries, $\epsilon \geq 1$ because the value of risk reduction increase more sharply as income rises[a].

Other approaches are available, but most are less popular than QALY and VSL, with the exception of willingness-to-pay[b] and cost of illness (COI). COI includes direct medical costs (medical care, hospitalization), direct non-medical costs (transportation to medical care, home modification), and indirect costs (loss of productivity and income).

---

[a]In very poor countries, each additional dollar has extremely high utility for basic consumption. This makes people relatively less willing to trade income for risk reduction.

[b]Willingness-to-pay is defined in Roncalli (2025, Box 5.2).

3.4 Overexploitation and resource extraction

Overexploitation is the practice of harvesting renewable resources faster than they can be replenished. This unsustainable practice often leads to significant declines in species populations, ecosystem degradation, evolutionary consequences, and in some cases, extinction. It commonly occurs through activities such as overfishing, in which fish stocks are harvested at a rate that exceeds their ability to reproduce; deforestation, in which timber is harvested at a rate that exceeds forest regeneration; hunting and poaching, characterized by the excessive killing of animals for food, sport, or trade; and illegal wildlife trade, including the poaching of animals for their body parts or the pet trade, such as the ivory and rhino horn markets. The concept of overexploitation can also be applied to natural resources such as minerals (*e.g.*, phosphorus and rare earth elements) and fossil fuels (*e.g.*, oil and natural gas). Even if they are not expected to become extinct by 2100, many natural resources will face problems as high-grade deposits are rapidly depleted and easily accessible deposits become increasingly scarce. Cobalt and zinc are typical examples.

Overexploitation is neither a new nor a recent phenomenon. It has existed throughout history, with varying degrees of severity in different contexts:

> "*Although there is considerable variation in detail, there is remarkable consistency in the history of resource exploitation: resources are inevitably overexploited, often to the point of collapse or extinction.*" (Ludwig *et al.*, 1993, page 17).

Peres (2010) highlights numerous examples of overexploitation that underscore the profound impact of human activities on wildlife. One notable pattern is the extinction of large-bodied vertebrates, which has been largely attributed to human overhunting and overkilling in the post-Pleistocene. Evidence suggests that humans historically shifted their hunting practices from larger to smaller animals after depleting populations of larger species. Large animals are particularly attractive targets because their size provides a greater yield of meat, hides, and bones, making them economically valuable. However, these species often have slower reproductive rates, characterized by longer gestation periods and fewer offspring per birth. This makes it difficult for their populations to recover from significant declines caused by hunting or habitat destruction. As large species declined or went extinct, humans increasingly relied on hunting smaller animals to meet their needs. This pattern — overhunting of large animals followed by a shift to smaller species — has been documented across regions and historical periods. Svenning *et al.* (2021, Figure 1, page 3) found that among terrestrial mammals, only 11 of 57 species of megaherbivores (mean adult body mass greater than 1 000 kg) survived to 1 000 AD:

Status	Cetartiodactyla	Cingulata	Diprotodontia	Litopterna	Notoungulata	Rhinocerotidae	Pilosa	Elephantidae	Proboscidea	Total
Survivor	4					4		3		11
Extinct	4	4	1	2	3	4	16	7	5	46

Survivors include three species of elephant, four species of rhinoceros, the common hippopotamus, the giraffe, and two species of cattle. The extinct species include seven species of elephant, four species of rhinoceros, one species of hippopotamus, the mastodon, etc. Ripple *et al.* (2019) studied the threats to megafauna, which are large vertebrate species. They considered all species weighing more than 100 kg for mammals, ray-finned fish, and cartilaginous fish, and all species weighing more than 40 kg for amphibians, birds, and reptiles. They found that the proportion of threatened

species was significantly higher among megafauna than among all vertebrates (58.6% vs. 21.3%). Furthermore, 70% of megafauna species have declining populations, with birds and amphibians being particularly affected (100% of species in these groups have declining populations), followed by cartilaginous fish (89.7%) and ray-finned fish (83.8%). Focusing on specific species, Ripple *et al.* (2019) identified various threats to megafauna. They concluded that harvesting of megafauna for human consumption[125] is the single most important threat across all classes studied (Table 42), far outweighing other factors. Harvesting is a threat in more than 95% of cases, while invasive species and habitat development are threats in less than 40% of cases. Interestingly, climate change was found to be a threat in less than 20% of cases.

Table 42: Current threats to megafauna

	Megafauna	n	Animal husbandry	Climate	Cropping	Development	Harvesting	Invasives	Pollution	Transportation
	Cartilaginous fish	38	3%	11%		13%	100%		13%	8%
	Mammals	73	53%		61%	56%	98%	54%		51%
	Ray-finned fish	29				14%	100%	31%	40%	28%
	Reptiles	20		40%	25%	40%	90%	65%		25%

Source: Ripple *et al.* (2019, Figure 2, page 5).

As explained by Peres (2010), overexploitation can lead to the rapid collapse of species. In some cases, just a few years or decades are sufficient, and it does not necessarily take centuries or millennia for a species to become nearly extinct. One of the best known examples is the North American buffalo (*Bison bison*), which experienced a dramatic collapse in less than 40 years:

> "*Prior to European exploration and settlement of North America, the buffalo or American bison inhabited vast stretches of the continent. [...] At its greatest moment, the total numbers for the continent may have been as high as 25 to 30 million before white settlement. On the Great Plains, where the bison were most suited and most plentiful, its population is estimated to have been 20 million as late as 1800. Even by 1850, substantially more than 10 million bison roamed the plains. Yet, by 1890, these plains held just 1 000 bison.*" (Lueck, 2002, page 609).

After 1890, the story of the American bison took a more hopeful turn, thanks to conservation efforts. A few individuals established small herds on private ranches to preserve the species. The US government protected a small population of wild bison in Yellowstone, providing an important sanctuary. Laws were also passed prohibiting the hunting of bison. Over time, through the combined efforts of individuals, conservation groups, and the government, the bison population began to recover. Today, bison are no longer endangered. There are approximately 400 000 bison in North America, but most are managed as livestock on private ranches. In fact, only about 30 000 are wild bison[126].

---

[125]The unsustainable hunting of wild animals for food is called the bushmeat crisis.
[126]Source: https://bisoncentral.com/bison-by-the-numbers.

Box 18: The Tragedy of the Commons

Published in Science in 1968, *The Tragedy of the Commons* by Garrett Hardin is a seminal essay that explores the conflict between individual interests and the common good in the context of shared resources. The article focuses on how individuals, acting in their own self-interest, can deplete or degrade shared resources (referred to as '*commons*'), even when it is not in the collective best interest to do so. Hardin (1968) illustrates this dilemma with a hypothetical example of a shared pasture (the commons) where each herder individually benefits by adding more cattle to the pasture. Each herder reasons that adding one more animal will bring him personal gain, while the negative consequences (overgrazing) are shared by all users of the commons. Therefore, from an individual perspective, it's rational to add more animals. However, if every herder follows this logic, the collective overuse of the pasture leads to its destruction, as the resources become insufficient to sustain the community. This illustrates the dilemma of individual gain versus collective ruin.

The essay applies this principle to various domains, including national parks, pollution, and environmental issues. It had a profound and far-reaching impact across multiple fields, influencing academic thought, public policy, and environmental management. However, the article has also faced significant criticism. For instance, Nobel laureate Elinor Ostrom provided empirical evidence demonstrating that communities can often self-organize to manage commons effectively, challenging the assumption that the tragedy is inevitable. More recently, the concept of the tragedy of the commons has resonated with contemporary challenges such as climate change. It has been extensively revisited, notably inspiring the idea of the '*tragedy of the horizon*' (Carney, 2015), which highlights the short-term focus of financial markets and policy-making in addressing long-term environmental risks.

Beyond species extinction, overexploitation occurs in other areas and can take different forms. One important form is the depletion and impoverishment of natural resources. We often think of excessive logging for timber, overgrazing by livestock, and unsustainable harvesting of medicinal plants, all of which involve the depletion of plants that reduce soil fertility and lead to erosion. However, natural resource depletion also includes other essential resources such as water, minerals, and energy resources. In this context, IPBES provides a highly critical assessment of resource extraction:

> "*Extraction of living biomass and nonliving materials is increasing as both populations and per capita consumption increased sixfold from 1970 to 2010, while the demand for materials used in construction and industry quadrupled during that time. [...] Materials for construction and industry increased 4-fold, with the most dramatic increases for lower-middle (7-fold) and upper-middle income countries (11-fold) and the Asia and the Pacific region (10-fold for whole region) and, generally, the growing economies. The use of biomass, fossil fuels, metal ores and non-metallic minerals doubled from 2005 (26.3 billion tons) to 2015 (46.4 billion tons), growing an annual rate of 6.1%.*" (IPBES, 2019, page 121).

The root causes of overexploitation lie in the expanding size and growth of the human population, coupled with rising standards of living. These driving forces are described by various terms, such as '*the scale of the human enterprise*' (Ehrlich, 1995; Gaston and Spicer, 2004), '*the great acceleration*' (Steffen *et al.*, 2015a), and others. Collectively, they underscore the profound impact of human activities on the planet's natural systems.

3.4.1 An example with freshwater

Overexploitation of water resources includes both the overdrawing of groundwater from aquifers for irrigation or consumption, and the unsustainable use of surface water, such as river diversions and lake exploitation. Figure 55 shows the annual freshwater withdrawals measured in trillion m^3. We observe four main periods. From 1900 to 1950, the trend is relatively slow. Then there is a sharp acceleration in freshwater withdrawals until 1980, followed by a first slowdown from 1980 to 2010 and a second slowdown since 2010. This graph illustrates '*The Great Acceleration*' described by Steffen *et al.* (2015a), which refers to the dramatic, rapid increase in human activity and its profound impact on Earth's systems that began after World War II.

Figure 55: Global freshwater withdrawals (in trillion m^3 per year)
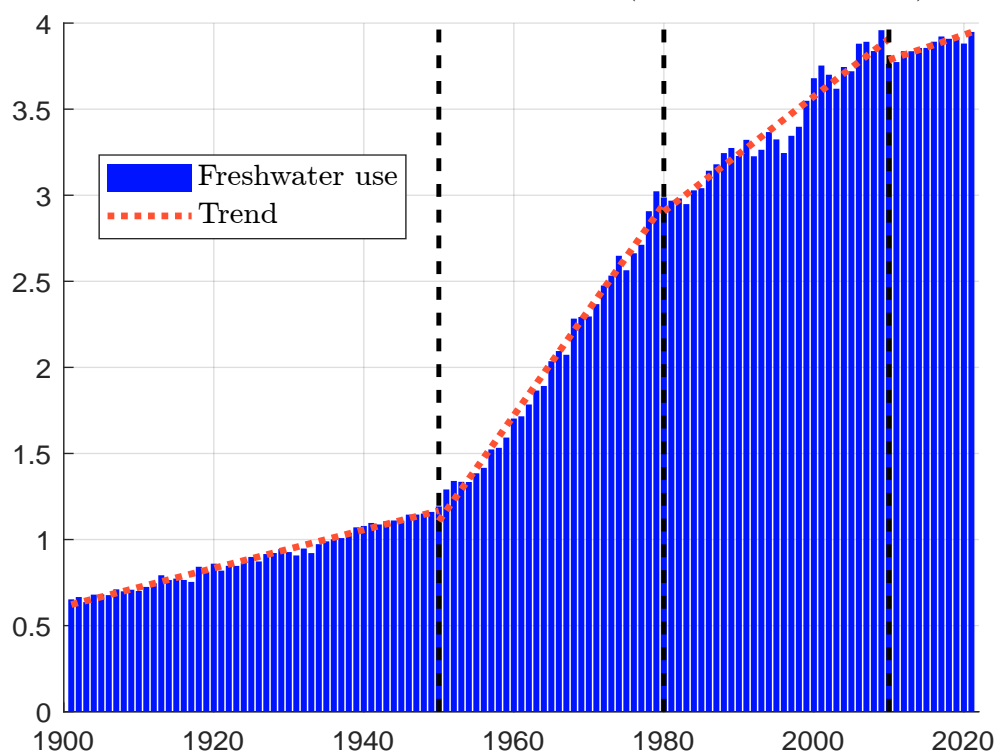
Source: Flörke *et al.* (2013), Steffen *et al.* (2015a), World Bank & Author's calculations.

Freshwater resources and withdrawals are unevenly distributed. In Table 43, we report several statistics for different countries: (1) the total annual freshwater withdrawals in billion cubic meters in 2000, (2) the total annual freshwater withdrawals in billion cubic meters in 2021, (3, 4, 5) the distribution among agriculture, industry, and domestic use, (6) the renewable internal freshwater resources[127] in billion cubic meters in 2021, (7) the renewable internal freshwater resources per capita, and (8) the water stress. The total volume of renewable freshwater resources worldwide is approximately 42.8 trillion cubic meters, with more than 50% concentrated in just seven countries: Brazil, Canada, China, India, Indonesia, Russia, and the United States. Some countries have very limited renewable freshwater resources. For instance, Egypt, Libya, and Saudi Arabia each have less than 2 billion cubic meters of freshwater resources, despite their large land areas. These disparities

---

[127]Renewable internal freshwater resource flows measure the total volume of freshwater generated by natural processes within a country's borders. This includes water from precipitation (rain, snow) that contributes to rivers, lakes, and groundwater but excludes any water that flows in from other countries.

Table 43: Freshwater withdrawals by country

Country	Total		Agriculture	Industry	Domestic	Renewable resources	Renewable per capita	Water stress
	2000	2021		2021			2021	
	(in bn m^3)			(in %)		(in bn m^3)	(in m^3)	(in %)
Algeria	5.6	9.8	63.8	1.8	34.4	11	251	137.9
Argentina	30.4	37.7	73.9	10.6	15.5	292	6 444	10.5
Australia	21.7	11.4	67.8	18.1	14.0	492	19 155	4.6
Bangladesh		35.9	87.8	2.1	10.0	105	626	5.7
Brazil	56.1	67.3	61.3	14.5	24.2	5 661	27 015	1.5
Canada	41.9	36.3	11.4	74.2	14.4	2 850	74 530	3.7
China	550.9	568.5	62.1	17.7	20.1	2 813	1 992	41.5
Congo (DRC)	0.6	0.7	10.5	21.5	68.0	900	9 077	0.2
Egypt	57.0	77.5	79.2	7.0	13.9	1	9	141.2
France	32.7	24.7	13.9	64.3	21.7	200	2 948	21.6
Gabon	0.1	0.1	29.0	10.1	60.9	164	69 003	0.5
Germany	44.9	25.8	4.2	54.3	41.5	107	1 286	35.4
Iceland	0.2	0.3	0.1	71.1	28.7	170	456 351	0.4
India	610.4	647.5	90.4	2.2	7.4	1 446	1 022	66.5
Indonesia	113.3	222.6	85.2	4.1	10.7	2 019	7 294	29.7
Iran	88.5	93.0	92.2	1.2	6.6	128	1 453	81.3
Italy	45.1	33.6	50.2	22.7	27.1	182	3 086	29.6
Kazakhstan	21.0	24.6	62.7	18.5	18.8	64	3 259	34.1
Korea, Rep.	27.7	29.2	58.9	16.4	24.6	65	1 253	85.2
Libya	4.3	5.7	83.2	4.8	12.0	1	98	817.1
Madagascar	13.4	13.5	95.9	1.2	2.9	337	11 350	11.3
Malaysia	5.6	6.7	45.6	29.9	24.5	580	16 918	3.4
Mexico	68.2	89.9	75.7	9.5	14.8	409	3 204	45.0
Netherlands	8.4	7.9	1.0	73.5	25.5	11	627	16.1
Nigeria	10.3	12.5	44.2	15.8	40.1	221	1 011	9.7
Pakistan	172.6	264.2	94.0	0.8	5.3	55	230	162.1
Philippines		89.0	76.2	13.4	10.3	479	4 235	27.2
Qatar	0.2	0.2	33.3	4.3	62.4	0	22	431.0
Russia	75.9	64.8	28.8	44.8	26.5	4 312	29 790	4.1
Saudi Arabia	19.7	23.4	81.6	5.4	13.1	2	78	974.2
South Africa	12.7	20.9	61.3	21.2	17.4	45	728	66.9
Spain	36.1	29.0	65.3	19.0	15.7	111	2 345	43.3
Sudan		26.9	96.2	0.3	3.5	4	83	118.7
Ukraine	18.3	9.5	31.0	40.9	28.1	55	1 244	12.3
United Kingdom	12.5	8.4	14.0	12.0	74.0	145	2 163	14.4
United States	473.5	444.4	39.7	47.2	13.1	2 818	8 487	28.2
Viet Nam	71.8	81.9	94.8	3.7	1.5	359	3 633	18.1
World	3 679.8	3 948.7	71.6	15.1	13.1	42 809	5 429	

Source: https://databank.worldbank.org/source/world-development-indicators.

are even more pronounced when considering renewable internal freshwater resources per capita. For example, Canada has more than $70\,000\,\text{m}^3$ of freshwater per capita, while Egypt has less than $10\,\text{m}^3$. In addition, a worrying downward trend in available freshwater resources has been observed (Figure 56). Over the past 60 years, the global volume of renewable internal freshwater resources has declined by about 60%. In India, this decline is even more severe, approaching 70%. This downward trend is primarily driven by high withdrawal rates. Globally, about 4 trillion cubic meters of freshwater are withdrawn each year. Agriculture is the largest contributor, accounting for 71% of total withdrawals, followed by industry at 15%. Domestic use accounts for 13% of total withdrawals worldwide. However, domestic water use has grown much faster than agricultural and industrial use, increasing sevenfold over the past 50 years. In some countries, domestic freshwater use accounts for more than 40% of total withdrawals, such as in many African countries, as well as in Germany and the United Kingdom. In Table 43, we also report the ratio of total freshwater withdrawals to total renewable freshwater resources, referring specifically to internal freshwater resources. This ratio is commonly known as water stress. Water stress is considered high when the ratio exceeds 75% and critical when it exceeds[128] 100%. We observe that some countries are experiencing critical water stress, including Algeria, Egypt, Libya, Pakistan, Qatar, Saudi Arabia, and Sudan. In fact, as of 2021, there are 25 countries with water stress levels exceeding 75%.

Figure 56: Renewable internal freshwater resources per capita (base 100 in 1961)
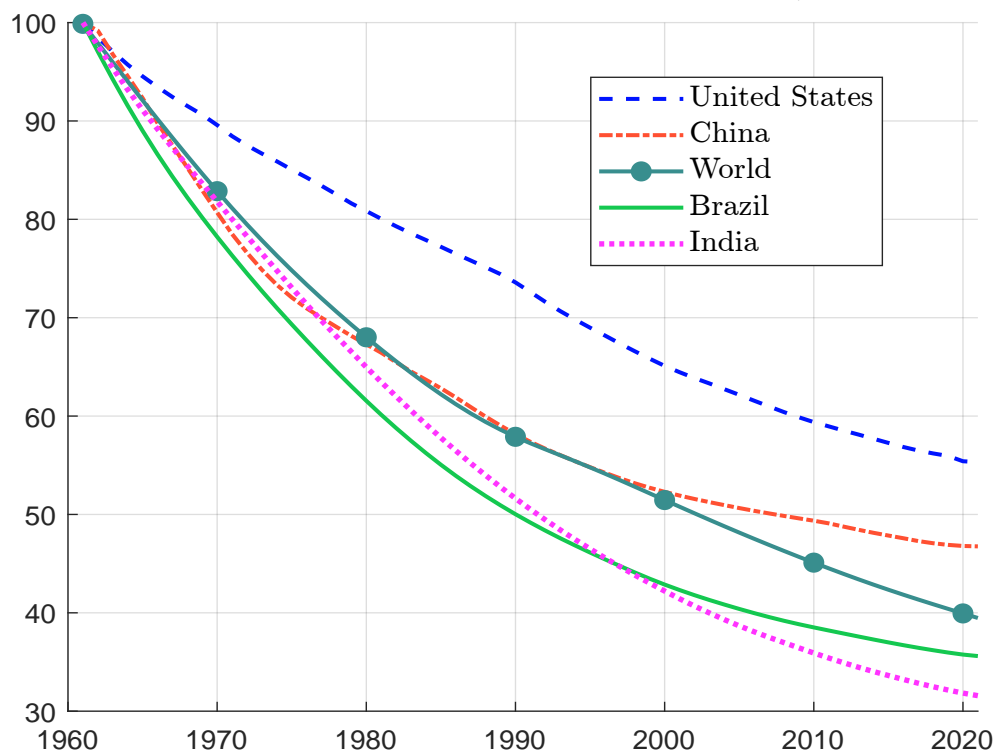
Source: https://databank.worldbank.org/source/world-development-indicators & Author's calculations.

---

[128] A water stress level greater than 100% means that a country is withdrawing more freshwater annually than the total amount of renewable internal freshwater resources. This indicates overexploitation of additional water sources beyond what is naturally replenished within the country. For example, a country may rely on non-renewable groundwater, external freshwater resources that originate outside its borders and flow in through rivers and lakes (*e.g.*, the Nile and the Danube), or desalination, which involves the conversion of seawater into freshwater (*e.g.*, in Qatar and Saudi Arabia).

3.4.2   Mathematical models of population and resource ecology with harvesting

Historically, the Malthusian growth model is considered the first mathematical population model. In this case, the population growth rate is constant:

$$\frac{\mathrm{d}N\left(t\right)}{\mathrm{d}t} = \delta N\left(t\right)$$

where $N\left(t\right)$ is the number of individuals, $N\left(t_0\right) = N_0$ is the initial population size and $\delta = \lambda - \mu$ is the difference between the birth rate and the death/mortality rate. Malthus (1798) believed that the population tends to grow exponentially[129], whereas he believed that food production and other resources increase at a linear rate due to the finite nature of land and labor. Therefore, Malthus predicted that the world would eventually face a crisis where resources would not be sufficient to support the growing population. However, his conclusions were later criticized by Verhulst (1838), who highlighted the role of the law of diminishing returns. Verhulst provided numerous examples demonstrating that population growth is inherently limited and cannot continue indefinitely. To model this, he proposed that population size follows the nonlinear differential equation:

$$\frac{\mathrm{d}N\left(t\right)}{\mathrm{d}t} = \delta N\left(t\right) - \varphi\left(N\left(t\right)\right)$$

By considering the specific case where $\varphi\left(x\right) = \eta x^2$, Verhulst derived the well-known logistic population model:

$$N\left(t\right) = \frac{\delta N_0 e^{\delta(t-t_0)}}{\delta + \eta N_0\left(e^{\delta(t-t_0)} - 1\right)}$$

This model illustrates how population growth slows as it approaches a finite carrying capacity, offering a more realistic depiction of population dynamics compared to Malthus' original exponential growth predictions. In the 1920s, mathematician Vito Volterra introduced a class of population dynamics models describing multiple species competing for the same food or resources, or interacting as predators and prey (Volterra, 1928). During the same period, biophysicist Alfred Lotka independently developed similar equations to analyze predator-prey interactions (Lotka, 1925). These equations are now known as the Lotka-Volterra equations and form a pair of first-order nonlinear differential equations:

$$\begin{cases} \dfrac{\mathrm{d}x\left(t\right)}{\mathrm{d}t} = ax\left(t\right) - bx\left(t\right)y\left(t\right) \\ \dfrac{\mathrm{d}y\left(t\right)}{\mathrm{d}t} = cx\left(t\right)y\left(t\right) - dy\left(t\right) \end{cases} \tag{32}$$

where $x\left(t\right)$ is the prey population, $y\left(t\right)$ is the predator population, a is the intrinsic growth rate of the prey (in the absence of predators), b is the predation rate coefficient, c is the reproduction rate of predators per prey consumed, and d is the natural mortality rate of predators. These three models (Malthus, Verhulst, and Lotka-Volterra) form the basis for modeling population and resource dynamics with harvesting.

In the following, $x\left(t\right)$ represents the size of a population, the amount of a resource or the biomass stock of a species in a finite environment. When the stock $x\left(t\right)$ is small, the size of the environment has no impact, and $x\left(t\right)$ can grow at an exponential rate δ, also known as the intrinsic growth rate. However, beyond a certain threshold, the density of the stock or population becomes too high to sustain the growth rate, and the regenerative rate of the stock decreases. This suggests the existence of a threshold κ at which $x\left(t\right)$ remains constant. Therefore, we assume that the stock

---

[129]The solution of the differential equation is an exponential curve: $N\left(t\right) = N_0 e^{\delta(t-t_0)}$.

variation is determined by the product of three factors: the constant intrinsic growth rate δ (or biotic potential), the regenerative rate[130] $\xi(t) = \dfrac{\kappa - x(t)}{\kappa}$ (or biotic resistance), which depends on the distance between the current stock $x(t)$ and the threshold κ which is called the carrying capacity, and the current stock $x(t)$. This results in the following differential equation:

$$\frac{\mathrm{d}x(t)}{\mathrm{d}t} = \delta\left(\frac{\kappa - x(t)}{\kappa}\right)x(t)$$

This model corresponds to the logistic model formulated by Verhulst (1838), where $\eta = \delta/\kappa$. We deduce that the solution is:

$$x(t) = \frac{\kappa N_0 e^{\delta(t-t_0)}}{\kappa + N_0\left(e^{\delta(t-t_0)} - 1\right)}$$

We verify that $x(t)$ tends asymptotically to κ as $t \to \infty$. This model can be easily modified by considering exploitation:

$$\frac{\mathrm{d}x(t)}{\mathrm{d}t} = \delta x(t)\left(1 - \frac{x(t)}{\kappa}\right) - h(x(t))$$

where $h(x(t))$ is the harvest, catch or removal rate. This model has been considered by Gordon (1954) and Schaefer (1954) in the case of fisheries management. The maximum sustainable yield (MSY) is the largest harvest rate of a renewable resource that can be sustained indefinitely without causing the population to decline. The sustainable harvest rate is given by:

$$h(x(t)) = \delta x(t)\left(1 - \frac{x(t)}{\kappa}\right)$$

The maximum value of $h(x)$ is reached when $h'(x) = 0$ or $\delta\left(1 - \dfrac{x}{\kappa}\right) - \delta\dfrac{x}{\kappa} = 0$. We deduce that the maximum sustainable yield is achieved when the stock is at half the carrying capacity: $x(t) = \dfrac{\kappa}{2}$. We deduce that:

$$\mathrm{MSY} := \max h(x(t)) = h\left(\frac{\kappa}{2}\right) = \frac{\delta}{4}\kappa$$

Figure 57 shows the function $g(x) = \delta x\left(1 - \dfrac{x}{\kappa}\right) - h$ when $\delta = 30\%$, $\kappa = 200$ and $h = \epsilon \cdot \mathrm{MSY}$. The stability analysis demonstrates that the number of stable equilibria depends on the harvest rate[131]. If $h = 0$, we have a stable equilibrium at $x^\star = \kappa$ and an unstable equilibrium at $x^\star = 0$. If $0 < h < \dfrac{\delta}{4}\kappa$, the two equilibria lie between 0 and κ. Among them, only the equilibrium $x^\star = \dfrac{\delta\kappa + \sqrt{\delta\kappa(\delta\kappa - 4h)}}{2\delta}$

---

[130]The regenerative rate $\xi(t)$ is positive if $x(t) < \kappa$, zero at $x(t) = \kappa$, and negative if $x(t) < \kappa$. In the latter case, the stock is declining because the population density is too high to sustain it.

[131]We obtain a second order polynomial:

$$\frac{\mathrm{d}x(t)}{\mathrm{d}t} = g(x) = 0 \Leftrightarrow -\delta x^2 + \delta\kappa x - h\kappa = 0$$

We have $\Delta = \delta\kappa(\delta\kappa - 4h)$. If $h > \mathrm{MSY}$, then there is no root and $\dfrac{\mathrm{d}x(t)}{\mathrm{d}t} < 0$. It follows that $x(t)$ converges to the stable equilibrium $x_1^\star = 0$. If $h = \mathrm{MSY}$, there is a root: $x' = \kappa/2$. Therefore, we have two stable equilibria: $x_1^\star = 0$ and $x_2^\star = \kappa/2$. If $h < \mathrm{MSY}$, we have $\sqrt{\Delta} < \delta\kappa$ and there are two roots: $x' = \left(\delta\kappa - \sqrt{\Delta}\right)/(2\delta)$ and $x'' = \left(\delta\kappa + \sqrt{\Delta}\right)/(2\delta)$. Therefore, we have two stable equilibria $x_1^\star = 0$ and $x_3^\star = \left(\delta\kappa + \sqrt{\Delta}\right)/(2\delta)$ and one unstable equilibrium $x_2^\star = \left(\delta\kappa - \sqrt{\Delta}\right)/(2\delta)$.

Figure 57: Stability analysis of the logistic model with harvesting
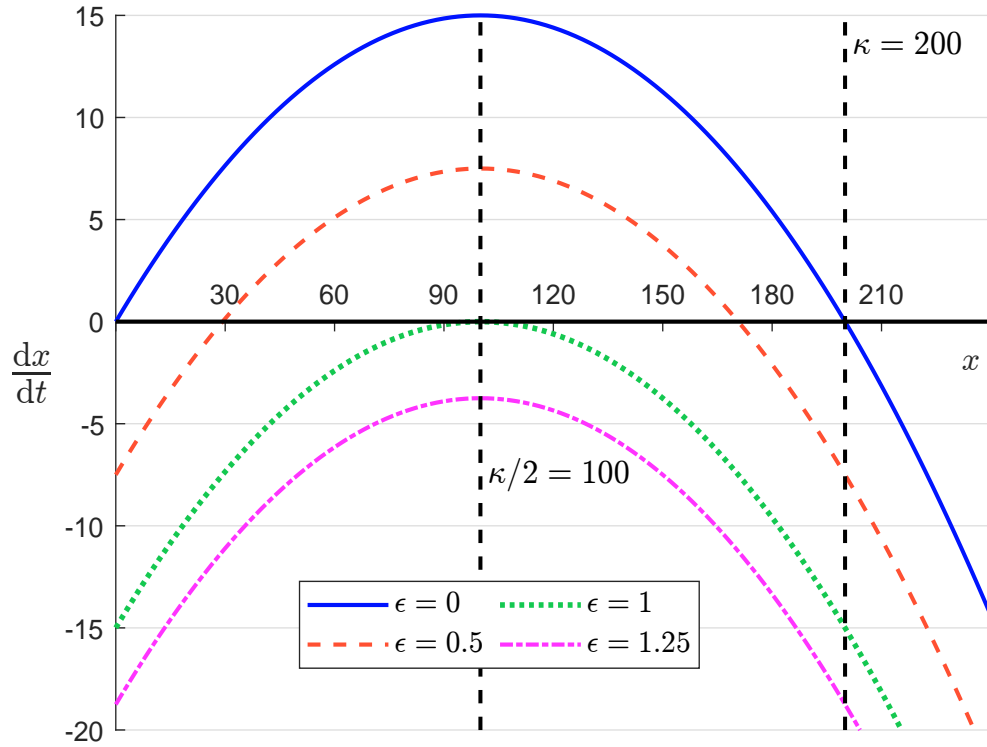
is stable. If $h = \text{MSY} = \dfrac{\delta}{4}\kappa$, the equilibrium at $x^\star = \dfrac{\kappa}{2}$ is unstable. Indeed, if $x(t) > x^\star$, $\dfrac{dx(t)}{dt} < 0$ and $x(t)$ tends toward $x^\star$, but if $x(t) < x^\star$, $\dfrac{dx(t)}{dt} < 0$ and $x(t)$ tends to 0. Finally, if $h > \text{MSY}$, $x(t)$ tends asymptotically to 0. These results are summarized in Table 44. In Figure 58, we have simulated the model with three different starting values x_0 and four values of the parameter ϵ. This shows the stability of each equilibrium. In particular, when $h = \text{MSY}$, we obtain an equilibrium at $x^\star = \kappa/2$ only when the initial stock is already larger than the equilibrium.

Table 44: Sign table of $\dfrac{dx(t)}{dt}$

x	0		$\dfrac{\delta\kappa - \sqrt{\delta\kappa(\delta\kappa-4h)}}{2\delta}$		$\dfrac{\kappa}{2}$		$\dfrac{\delta\kappa - \sqrt{\delta\kappa(\delta\kappa-4h)}}{2\delta}$		κ		∞
$h = 0$	0	$+$	$+$	$+$	$+$	$+$	$+$	$+$	0	$-$	$-$
$0 < h < \dfrac{\delta}{4}\kappa$	$-$	$-$	0	$+$	$+$	$+$	0	$-$	$-$	$-$	$-$
$h = \dfrac{\delta}{4}\kappa$	$-$	$-$	$-$	$-$	0	$-$	$-$	$-$	$-$	$-$	$-$
$h > \dfrac{\delta}{4}\kappa$	$-$	$-$	$-$	$-$	$-$	$-$	$-$	$-$	$-$	$-$	$-$

Figure 58: Simulation of the logistic model with harvesting
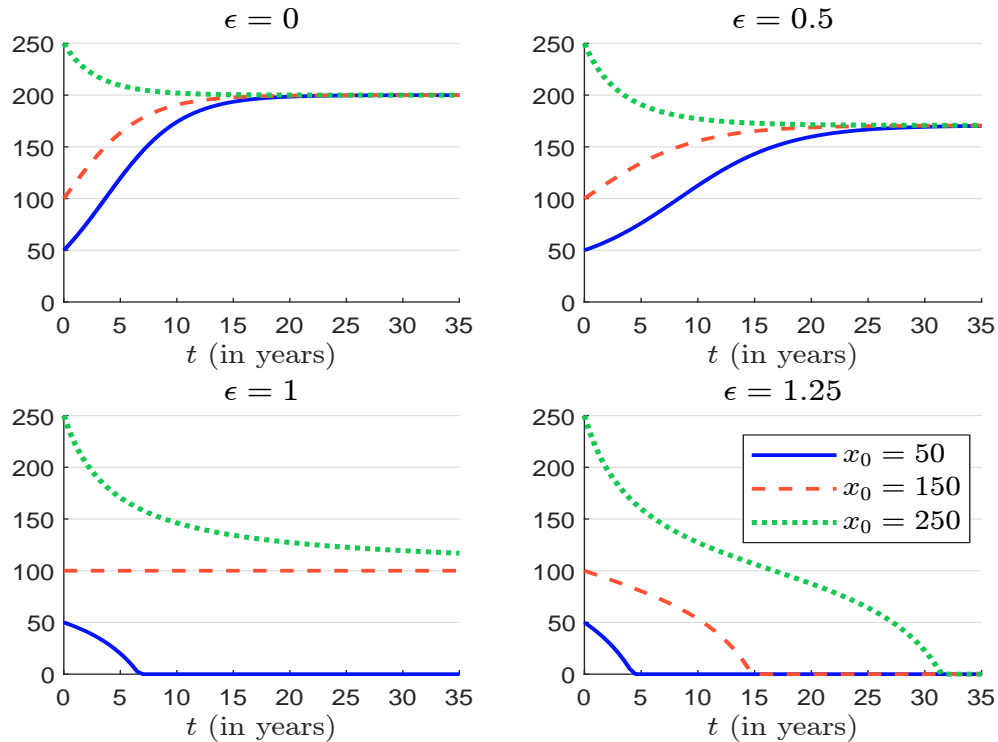
Figure 59 illustrates the equilibrium $x^\star$ and the harvest rate h as a function of the coefficient ϵ. By construction, $x^\star$ decreases with respect to ϵ. When $\epsilon = 1$ or $h = \text{MSY}$, we verify that the equilibrium is unstable, indicating that $h = \text{MSY}$ is indeed a critical and undesirable harvest rate. To prevent overexploitation, it is essential that the absolute harvest rate remains below the maximum sustainable yield. Consequently, the relative harvest rate, defined as the ratio of the absolute harvest rate to the carrying capacity, must be less than one quarter of the intrinsic growth rate:

$$\eta = \frac{h}{\kappa} < \eta^\star = \frac{\delta}{4}$$

For example, if $\delta = 30\%$ per year, then $\eta^\star = 7.5\%$, meaning that the relative harvest rate must be less than 7.5% per year. Conversely, if $\delta = 2\%$, the relative harvest rate must be much lower, less than 0.5% per year ($\eta^\star = 0.5\%$). Here are some typical values of intrinsic growth rates for various species:

- Fish species
  In general, small and fast growing fish species such as sardines and anchovies can have rates of 100% or higher, while large and slow growing fish species such as sharks and tuna often have rates below 10%. Many commercial fish species, such as cod and haddock, have intrinsic growth rates between 10% and 50% per year.

- Mammals
  Large mammals such as whales and elephants typically have low rates (5%–20% per year) because they reproduce slowly and have long gestation periods, while small mammals such as rodents and rabbits can have higher rates (50%–200% per year), reflecting their ability to reproduce rapidly.

Figure 59: Equilibrium $x^\star$ and harvest rate h
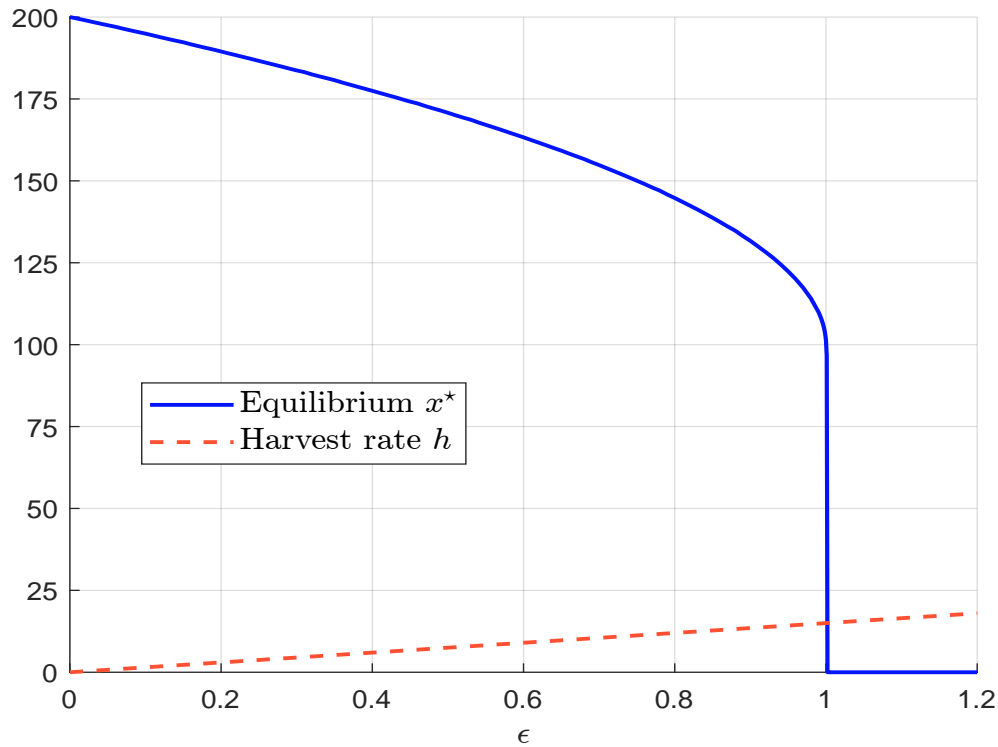
- Bacteria
  Bacteria can have very high intrinsic growth rates, sometimes doubling several times a day. For example, Escherichia coli (E. coli) can have rates of 20+ per day under optimal conditions.

Because large, slow-growing animals (such as many large fish species and mammals) have low intrinsic growth rates, they are highly vulnerable to overharvesting.

Table 45: Proportion in % of remaining buffalo under different harvest rate assumptions

	η (in %)	1.00	2.00	3.00	4.00	4.10	4.20	4.30	4.40
	10 years	93.55	86.81	79.77	72.40	71.65	70.89	70.12	69.36
t	20 years	90.88	80.64	68.95	55.35	53.85	52.34	50.79	49.22
	30 years	89.71	77.32	61.63	40.10	37.45	34.68	31.78	28.74
	40 years	89.18	75.41	55.85	21.32	16.04	10.18	3.62	0.00

Consider the dramatic collapse of the American buffalo. Suppose the intrinsic growth rate is 10% per year (Lueck, 2002; Jolles, 2007), and the initial buffalo population is at its carrying capacity $(x_0 = \kappa)$. Table 45 shows the proportion of the remaining buffalo population under different relative harvest rate assumptions after 10, 20, 30, and 40 years.

- If the relative harvest rate η is 1%, the remaining buffalo population after 10, 20, 30, and 40 years is 93.6%, 90.9%, 89.7%, and 89.2%, respectively.

- If the relative harvest rate is 4%, these figures decrease to 72.4%, 55.4%, 40.1%, and 21.3%.

- At a relative harvest rate of 4.4%, the buffalo population is completely wiped out (0% remaining) after 40 years.

The previous model can be extended in several directions (Quinn and Deriso, 1999). Gilpin *et al.* (1976) introduced a parameter $\theta \geq 0$ to control the asymmetry of the growth curve:

$$\frac{\mathrm{d}x(t)}{\mathrm{d}t} = \delta x(t) \left(1 - \left(\frac{x(t)}{\kappa} \right)^{\theta} \right) - h(x(t))$$

In this formulation, θ allows the inflection point of the growth curve to vary between 0 and κ. When $\theta < 1$ (resp. $\theta > 1$), the maximum growth occurs for $x(t) < \kappa/2$ (resp. $x(t) < \kappa/2$). The case $\theta < 1$ is generally observed when resources are limited. Another extension is to consider different parameterizations of the harvest function. According to Begon and Townsend (2021), the three most popular functions $h(x)$ are:

1. Fixed quota (or constant catch) management
   This specifies a predetermined, fixed number of animals that can be harvested. In this case, $h(x) = q$ is a constant, corresponding to the case we have already studied.

2. Fixed proportion harvesting
   This specifies a proportion e of animals that can be harvested, rather than a specific number:

   $$h(x) = ex$$

   where e is the exploitation rate expressed as a percentage.

3. Fixed escapement (or constant escapement rule)
   This specifies not the number of animals to be harvested, but rather the number of animals to remain unharvested. In this approach, harvest occurs only when the population exceeds a threshold $x_{\min}$, ensuring a minimum escapement:

   $$h(x) = e(x - x_{\min})^{+}$$

Figure 60 shows the impact of the parameter θ and different harvesting management strategies on population size[132]. We note that the parameter θ has a significant impact when a fixed quota is used, whereas its effect is less pronounced under fixed proportion harvesting. In the latter case, the population dynamics follow the equation:

$$\frac{\mathrm{d}x(t)}{\mathrm{d}t} = (\delta - e)x(t) - \delta \frac{x(t)^2}{\kappa} \left(\frac{x(t)}{\kappa} \right)^{\theta - 1}$$

Here, the term $x(t)^2/\kappa$ has a greater magnitude than $(x(t)/\kappa)^{\theta-1}$, particularly when $\theta \geq 1$. We also observe that fixed escapement is the safest exploitation approach, as it ensures that $x^{\star} > x_{\min}$ — the limit case is obtained as $e \to \infty$.

Overexploitation can also be studied using a second class of multi-species models based on the Lotka-Volterra formulation. In the two-dimensional case, the system is given by:

$$\begin{cases} \dfrac{\mathrm{d}x(t)}{\mathrm{d}t} = ax(t) - bx(t)y(t) - h_x(x(t), y(t)) \\ \dfrac{\mathrm{d}y(t)}{\mathrm{d}t} = cx(t)y(t) - dy(t) - h_y(x(t), y(t)) \end{cases}$$

---

[132]The intrinsic growth rate δ is set to 30%, while x_0 and κ are both equal to 100.

Figure 60: Impact of the harvest function and the inflection point
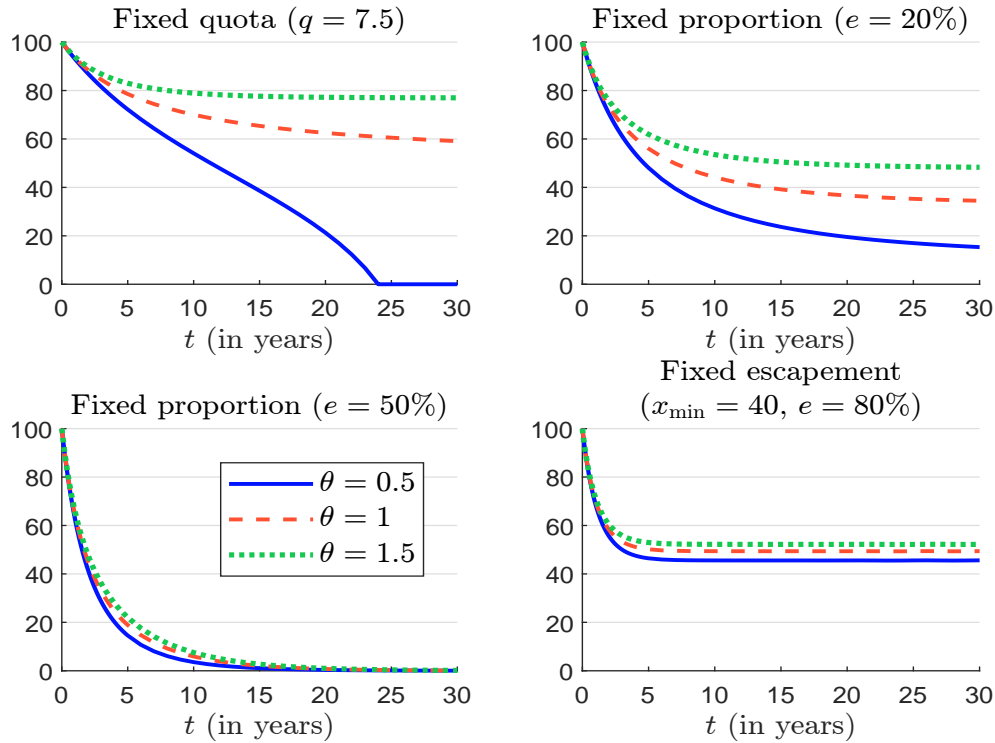
where $h_x(x, y)$ and $h_{x,y}(y)$ are the harvest functions of the prey and predator species, respectively. The classical Lotka-Volterra model is obtained by setting $h_x(x) = h_y(y) = 0$. This model has been extensively studied in both population dynamics modeling and the mathematical field of nonlinear systems, because it can be linked to the theory of deterministic chaos (characterized by sensitive dependence on initial conditions, strange attractors, and bifurcations). We can show that the classical Lotka-Volterra model has an unstable equilibrium at $(0,0)$ and a stable equilibrium at $\left(\dfrac{d}{c}, \dfrac{a}{b}\right)$. Let us assume that $a = 2$, $b = 3$, $c = 2$ and $d = 4$. Figure 61 shows the solutions $x(t)$ and $y(t)$ when the initial biomass values are $x_0 = 0.5$ and $y_0 = 1.5$ tonnes. Since there are initially too many predators and not enough prey, the predator population declines in the first phase. This allows the prey population to recover and reproduce, leading to an increase in prey biomass. In the second phase, as the prey population grows, the predators have more food available and begin to increase in number. Ultimately, this predator-prey system generates cyclical dynamics, as illustrated by the vector field analysis of the dynamical system (Figure 62). In this example, the cycle lasts 2.70 years. Figure 63 shows the phase portrait of the Lotka-Volterra model[133], depicting the orbits or limit cycles generated by the system of differential equations.

---

[133]We have:

$$\frac{\mathrm{d}y}{\mathrm{d}x} = \frac{cxy - dy}{ax - bxy}$$

It follows that $(ax - bxy)\,\mathrm{d}y = (cxy - dy)\,\mathrm{d}x$. Dividing by xy, we get $c\,\mathrm{d}x - d\dfrac{\mathrm{d}x}{x} + b\,\mathrm{d}y - a\dfrac{\mathrm{d}y}{y} = 0$. We deduce that the solution is:

$$cx - d\ln x + by - a\ln y = C \tag{33}$$

where C is a constant. The phase portrait is the set of solutions (x, y) that satisfy Equation (33) for a given value of C.

Figure 61: Simulation of the Lotka-Volterra model ($a = 2$, $b = 3$, $c = 2$, $d = 4$)
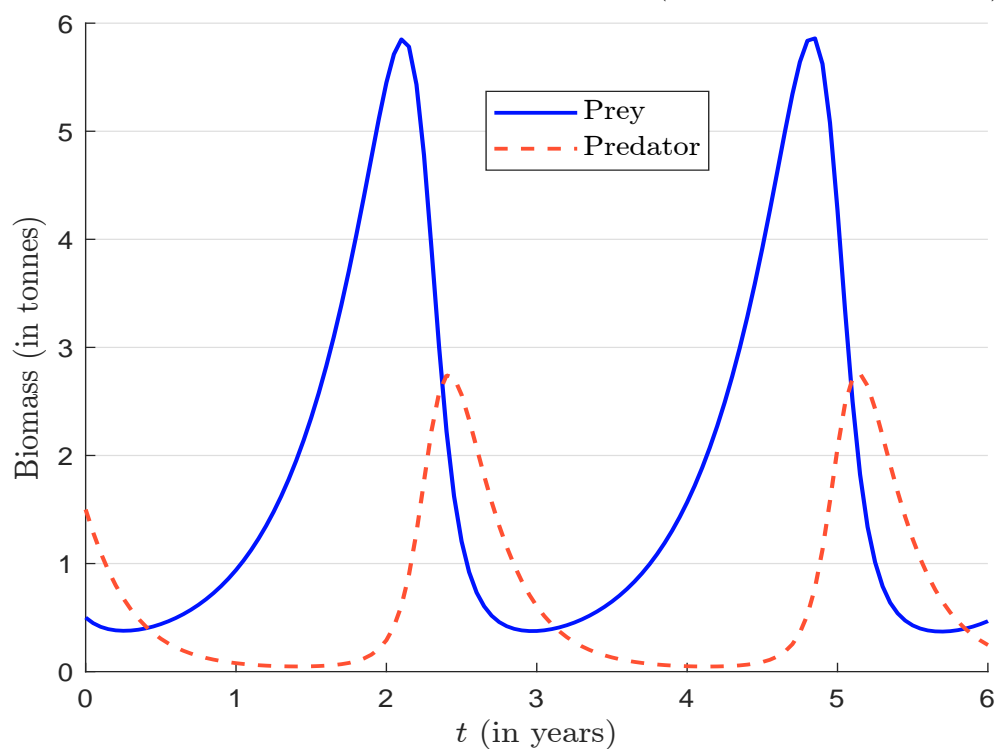
Figure 62: Vector field representation of the Lotka-Volterra model ($a = 2$, $b = 3$, $c = 2$, $d = 4$)
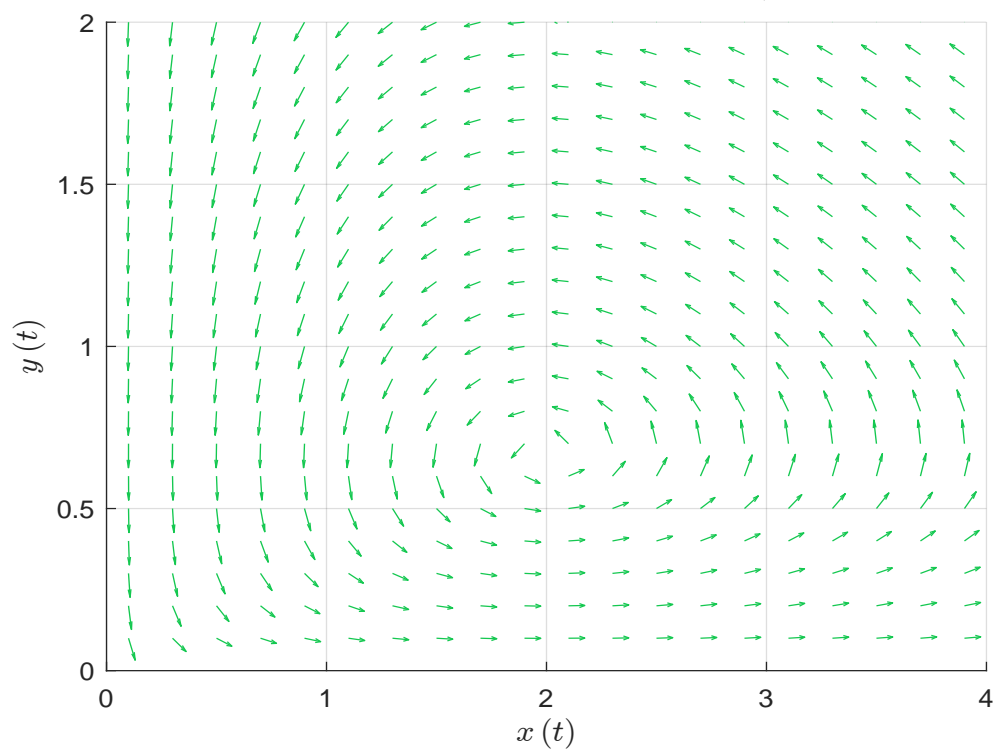
Figure 63: Phase portrait of the Lotka-Volterra model ($a = 2$, $b = 3$, $c = 2$, $d = 4$)
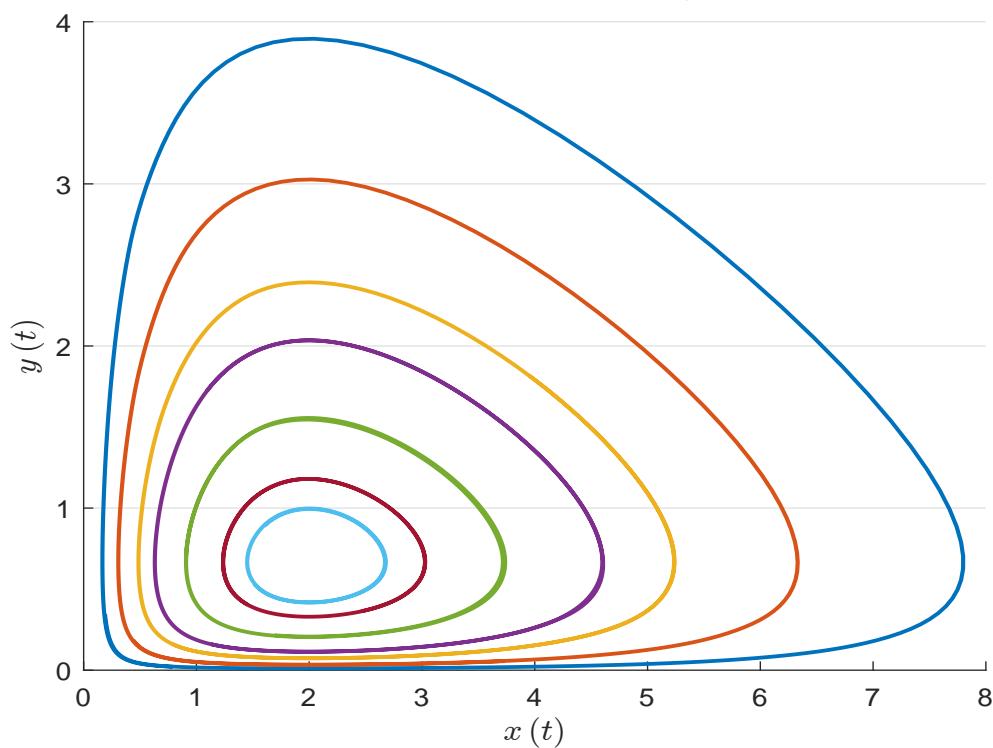
Figure 64: Simulation of the Lotka-Volterra model with harvesting ($a = 2$, $b = 3$, $c = 2$, $d = 4$, $e_y = 5$, $y_{\min} = 1$)
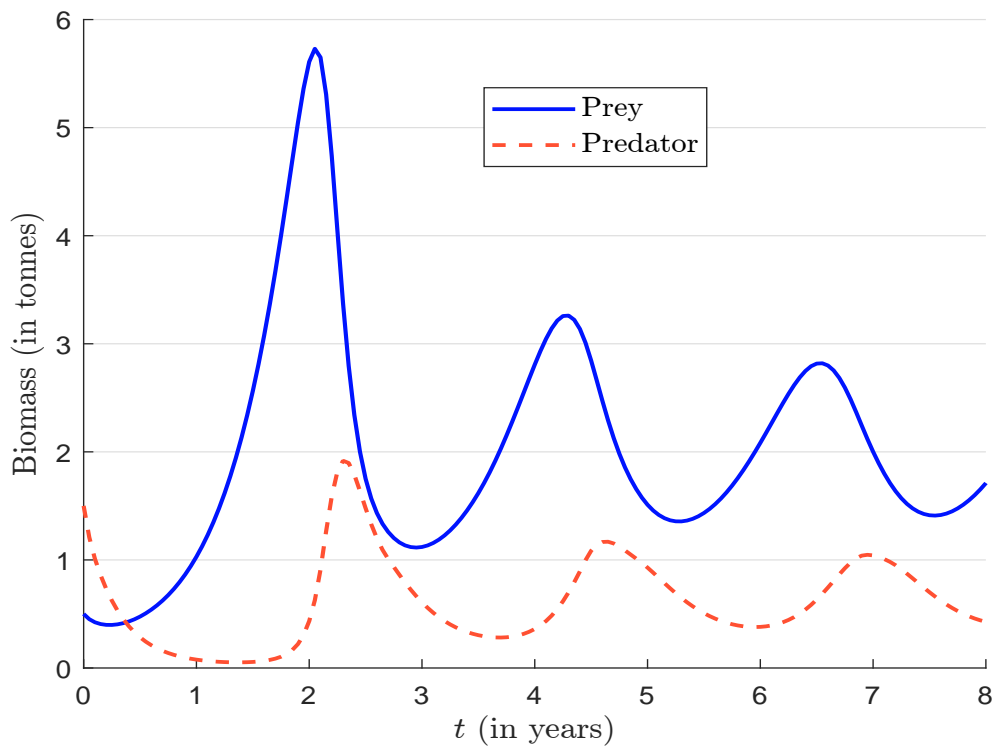
Now let us consider exploitation. There are many ways to specify the harvest functions $h_x(x,y)$ and $h_y(x,y)$. If we aim to protect the prey species, we can set $h_x(x,y) = 0$ and $h_y(x,y) = e_y(y - y_{\min})^+$, where e_y is the exploitation rate of the predator species above the threshold $y_{\min}$. This leads to a dynamic in which the biomass of both prey and predator species becomes more stable (Figure 64). Another approach is to protect the prey species when its population falls below a threshold $x_{\min}$. In this case, for example, we can define the harvest function as $h_y(x,y) = e_y y(x_{\min} - x)^+$.

Remark 13 *The Lotka-Volterra model can also be used to study the impact of invasive species, which can be considered as another form of overexploitation. In this context, x represents the native species, while y represents the invasive species (Roques et al., 2015).*

After its publication, the Lotka-Volterra model was rapidly extended in many directions. In reviewing these developments, Solomon (1949) introduced the concepts of functional and numerical responses:

1. The '*functional response*' describes how the predation rate (*i.e.*, the number of prey consumed per predator) varies with prey density. It quantifies the efficiency of individual predators in capturing and consuming prey.

2. The '*numerical response*' describes how predator population density changes in response to prey density. It reflects the total population-level effect of prey availability on predator numbers, including factors such as predator consumption, reproduction and migration, but excluding natural mortality.

From a mathematical point of view, we can write:

$$\begin{cases} \dfrac{\mathrm{d}x(t)}{\mathrm{d}t} = \delta(t)\,x(t) - f(x(t),y(t))\,y(t) \\ \dfrac{\mathrm{d}y(t)}{\mathrm{d}t} = g(x(t),y(t))\,y(t) - \mu(t)\,y(t) \end{cases}$$

where $\delta(t)$ is the growth rate of the prey species, $f(x,y)$ is the functional response, $g(x,y)$ is the numerical response, and $\mu(t)$ is the mortality rate of the predator species. The classical Lotka-Volterra model is obtained by setting $\delta(t) = a$, $f(x,y) = bx$, $g(x,y) = cx$ and $\mu(t) = d$. In the late 1950s, Holling (1959a,b) conducted a comprehensive review of predation theory and proposed a classification of predation models based on the form of their functional responses. These types describe how predation rate varies with prey density:

- Type I (linear)
  Predation rate increases linearly with prey density until a maximum is reached. This simple, though somewhat unrealistic, model assumes that predators can process prey immediately upon encounter. It's often used in simplified models.

- Type II (decelerating)
  Predation rate still increases with prey density, but the rate of increase slows as prey becomes more abundant. This reflects factors such as predator handling time (the time it takes to consume each prey item) or satiation (when the predator becomes full).

- Type III (sigmoidal)
  Predation rate follows a sigmoidal curve, *i.e.*, a slow initial increase at low prey densities, followed by an accelerated increase at moderate densities, and finally saturation at high densities.

This pattern often results from more complex predator behavior, such as learning, improved search efficiency, or the presence of prey refugia. It suggests that predators initially struggle to find or handle prey, but become more efficient over time.

Since Holling's publication, a fourth type has been added. Type IV responses are not monotonic. They increase to a maximum rate and decrease for higher values of x. The decrease can be explained by resource toxicity or predator confusion (Gentleman *et al.*, 2003). These responses can be found for some bacterial processes. Below, we give some examples of functional responses:

Type	I	II	III	IV
$f(x,y)$	cx	$\dfrac{\alpha x}{\beta + x}$	$\dfrac{\alpha x^2}{\beta + x^2}$	$\dfrac{\alpha x}{\beta + x + \gamma x^2}$

These responses are illustrated[134] in Figure 65. Type II responses are the most well-known, as they are associated with the Michaelis-Menten-Monod equation.

Figure 65: Holling functional responses
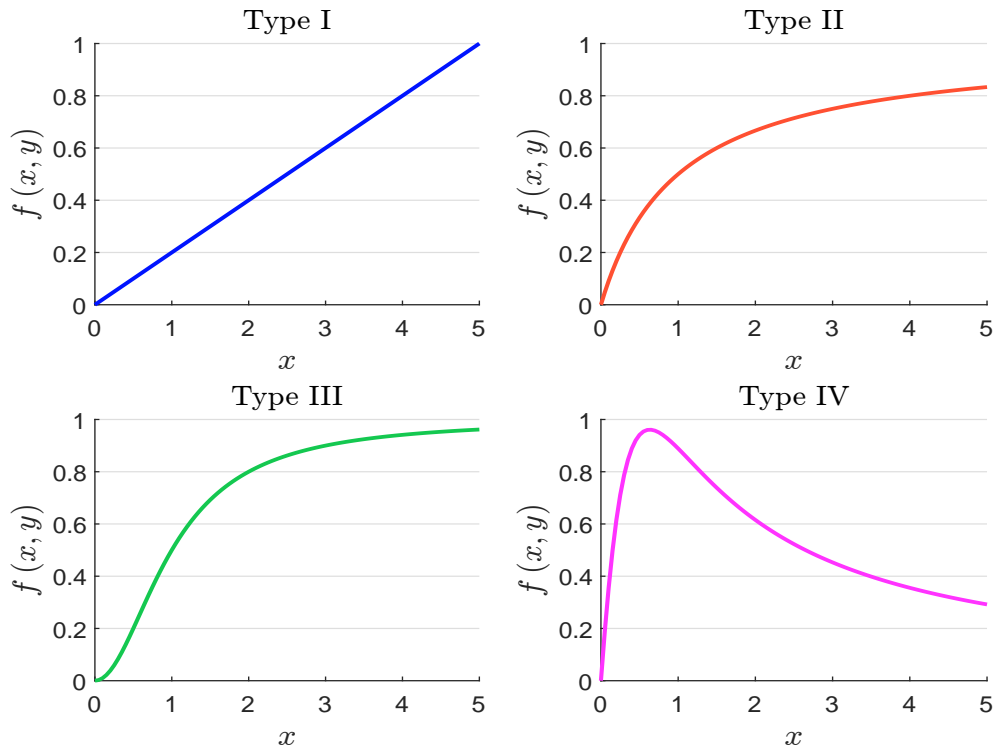
Tanner (1975) used the Holling Type II functional response and assumed that both prey and predator populations follow a logistic growth model. This leads to the Holling-Tanner predator-prey model:

$$\begin{cases} \dfrac{\mathrm{d}x(t)}{\mathrm{d}t} = \delta x(t)\left(1 - \dfrac{x(t)}{\kappa}\right) - \dfrac{\alpha x(t)}{\beta + x(t)} y(t) \\ \dfrac{\mathrm{d}y(t)}{\mathrm{d}t} = \sigma y(t)\left(1 - \dfrac{y(t)}{\gamma x(t)}\right) \end{cases}$$

---

[134]We have used the following parameters: $c = 0.2$ (type I), $\alpha = \beta = 1$ (types II and III), $\alpha = 4$, $\beta = 1$ and $\gamma = 2.5$ (type IV).

where $x(t)$ is the prey population and $y(t)$ is the predator population. Here, the carrying capacity of the predator population is related to the size of the prey population: $\kappa_y = \gamma x(t)$. The interpretation of the parameters is the following: δ is the intrinsic growth rate of the prey, κ is the carrying capacity of the prey, α is the maximum predation rate, β is the half-saturation constant that determines how prey abundance affects predation, σ is the intrinsic growth rate of the predators, and γ is the maximum predator-prey ratio. This model is more complex than the single logistic growth model because it can have four critical points[135]. Figure 66 shows the simulation[136] of the Holling-Tanner predator-prey model when the initial values are $x_0 = 8$ and $y_0 = 5.5$, and the parameters are $\delta = 10\%$, $\kappa = 100$, $\alpha = 4$, $\beta = 20$, $\sigma = 20\%$, and $\gamma = 10\%$.

Figure 66: Simulation of the Holling-Tanner predator-prey model
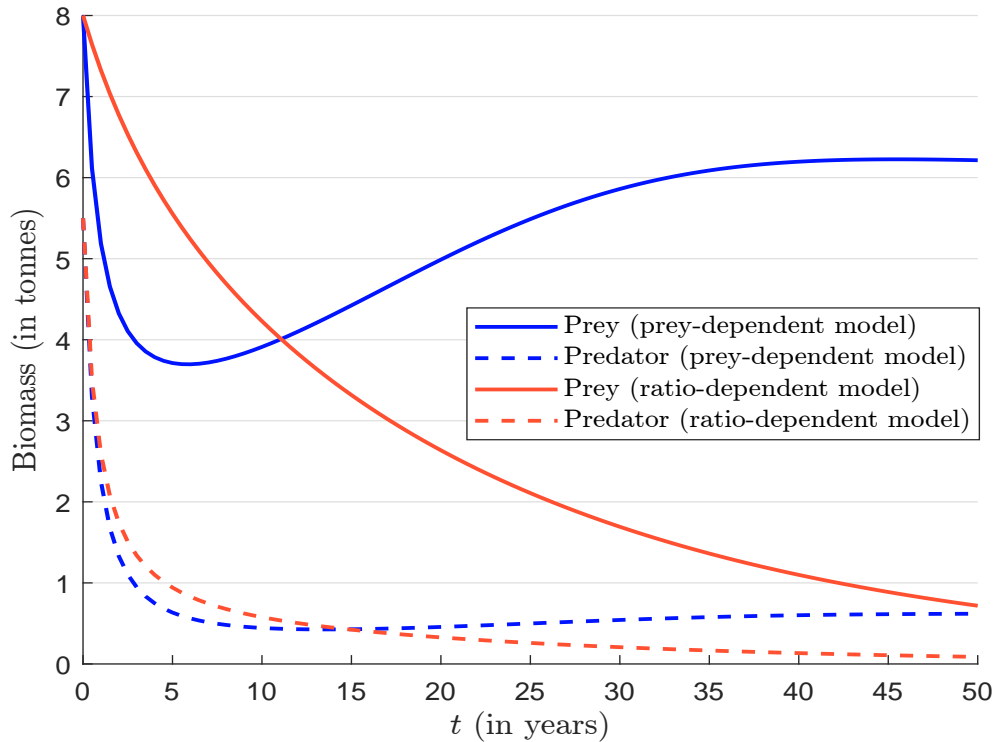
Previous functional responses depend only on the prey population. In a seminal paper, Arditi and Ginzburg (1989) challenge the traditional view of predator-prey interactions in which the predator's consumption rate depends solely on prey density. They propose an alternative approach in which

---

[135]The stability analysis implies that:

$$\frac{\mathrm{d}y(t)}{\mathrm{d}t} = 0 \Leftrightarrow y(t) = 0 \wedge y(t) = \gamma x(t)$$

and:

$$\frac{\mathrm{d}x(t)}{\mathrm{d}t} = 0 \Leftrightarrow \delta x(\kappa - x)(\beta + x) - \alpha\gamma\kappa x^2 = 0$$

We can show that there can be four equilibria: $(0,0)$, $(\kappa, 0)$, $(x_-, \gamma x_-)$ and $(x_+, \gamma x_+)$ where:

$$x_\pm = \frac{(\delta\kappa - \delta\beta - \alpha\gamma\kappa) \pm \sqrt{(\delta\kappa - \delta\beta - \alpha\gamma\kappa)^2 + 4\beta\delta^2\kappa}}{2\delta}$$

[136]It corresponds to the blue curve.

the predator's consumption rate depends on the ratio of prey to predator densities, introducing the concept of ratio-dependent predation $r = x/y$:

$$f(x, y) = \frac{\alpha r}{\beta + r} = \frac{\alpha x}{\beta y + x}$$

In prey-dependent models (Holling type II), when prey is rare, predation is still significant. In ratio-dependent models, when prey is rare relative to predators, predation decreases dramatically, which is more realistic in nature. Figure 66 shows the effect of using a ratio-dependent model instead of a prey-dependent model[137].

Remark 14 *The introduction of harvesting in the Holling-Tanner predator-prey model is the same as in the Lotka-Volterra model. We can then derive the equilibria (Diz-Pita and Otero-Espinar, 2021), analyze the effects of harvesting policy and define the maximum sustainable yield (Ghosh and Kar, 2013; Kar and Ghosh, 2013).*

While predator-prey models describe interactions in which one species benefits at the expense of another, competition models describe interactions in which both species suffer from their coexistence due to competition for shared resources such as food, space, or other ecological resources (Polis *et al.*, 1989). The most well-known competition model is the Lotka-Volterra multi-species competition model, which is mathematically similar to the predator-prey model but with negative interactions for both species (Case and Gilpin, 1974):

$$\frac{\mathrm{d}x_i(t)}{\mathrm{d}t} = \delta_i x_i(t) \left(1 - \frac{\sum_{j=1}^{n} \omega_{i,j} x_j(t)}{\kappa_i} \right) \tag{34}$$

where $i = 1, \ldots, n$ is the species index, n is the number of species, δ_i and κ_i are the intrinsic growth rate and the carrying capacity of species i, and $\omega_{i,j} \geq 0$ is the competition coefficient (how much species j affects species i). Another interference competition model consists in considering that each species is a prey for the other species. In this case, we consider a multi-species logistic growth model and include Lotka-Volterra penalties:

$$\frac{\mathrm{d}x_i(t)}{\mathrm{d}t} = \delta_i x_i(t) \left(1 - \frac{x_i(t)}{\kappa_i} \right) - \sum_{j \neq i} \alpha_{i,j} x_i(t) x_j(t) \tag{35}$$

where $\alpha_{i,j} \geq 0$ is the coefficient of interaction between species i and j. More generally, interference competition models combine the logistic growth model and Holling functional responses:

$$\frac{\mathrm{d}x_i(t)}{\mathrm{d}t} = \delta_i x_i(t) \left(1 - \frac{x_i(t)}{\kappa_i} \right) - \sum_{j \neq i} f_{i,j}(x_1(t), \ldots, x_n(t)) x_j(t) \tag{36}$$

Model (35) is a special case of model (36) when we use a Holling type I linear response: $f_{i,j}(x_1, \ldots, x_n) = \alpha_{i,j} x_i$. For Holling type II responses, we can write:

$$f_{i,j}(x_1, \ldots, x_n) = \frac{\alpha_{i,j} x_i}{\beta_{i,j} + x_i}$$

These different models can exhibit chaotic behavior, even in low dimension. For instance, Vano *et al.*

---

[137]We use exactly the same parameters and initial values as in the classical Holling-Tanner prey-dependent model. The blue curves correspond to the prey-dependent model, while the red curves correspond to the ratio-dependent model.

Box 19: Symbiosis and interspecific interactions

The term symbiosis, derived from Greek roots meaning '*together*'and '*living*', describes a close and long-term biological interaction between two different organisms. An ecological community includes all the populations of different species that coexist in a given area. The interactions between these species are called interspecific interactions. They can be categorized as positive (+), negative (−), or neutral (0) based on their effects on the species involved (Polis *et al.*, 1989). There are seven broad types of symbiosis:

1. Amensalism (−/0)
   One species is harmed and the other is unaffected, often through the release of a chemical compound.

2. Commensalism (+/0)
   One species benefits while the other remains unaffected. A classic example is barnacles that attach themselves to whales for transportation, gaining a mobile habitat while the whale remains indifferent.

3. Competition (−/−)
   Both species are negatively affected by the limited availability of shared resources such as food, water, or nesting sites. For example, the swift fox (*Vulpes velox*) and coyotes (*Canis latrans*) competing for the same resources may both experience reduced reproductive success (Kitchen *et al.*, 1999).

4. Mutualism (+/+)
   Both species benefit from the interaction. A common example is the relationship between bees and flowers, where bees receive food (nectar) and flowers receive pollination assistance.

5. Neutralism (0/0)
   Neither species is affected by the interaction. Although theoretically possible, true neutralism is difficult to prove definitively in complex ecosystems. For example, a butterfly and a snake living in the same habitat may appear neutral.

6. Parasitism (+/−)
   One species (the parasite) benefits at the expense of the other (the host). Ticks that feed on the blood of a mammal are an example of this relationship, where the tick gains nourishment while the host experiences potential harm and irritation.

7. Predation (+/−)
   One species (the predator) benefits by killing and consuming the other (the prey). A lion hunting a zebra is a clear example of predation.

(2006) studied model (34) with four species and the following parameters: $\delta = (1.00, 0.72, 1.53, 1.27)$, $\kappa = (10, 10, 10, 10)$ and:

$$\Omega = (\omega_{i,j}) = \begin{pmatrix} 1 & 1.09 & 1.52 & 0 \\ 0 & 1 & 0.44 & 1.36 \\ 2.33 & 0 & 1 & 0.47 \\ 1.21 & 0.51 & 0.35 & 1 \end{pmatrix}$$

They showed that the chaotic attractor of this dynamical system corresponds to homoclinic orbits (Figure 67).

Figure 67: Phase portrait of the Lotka-Volterra four-species competition model
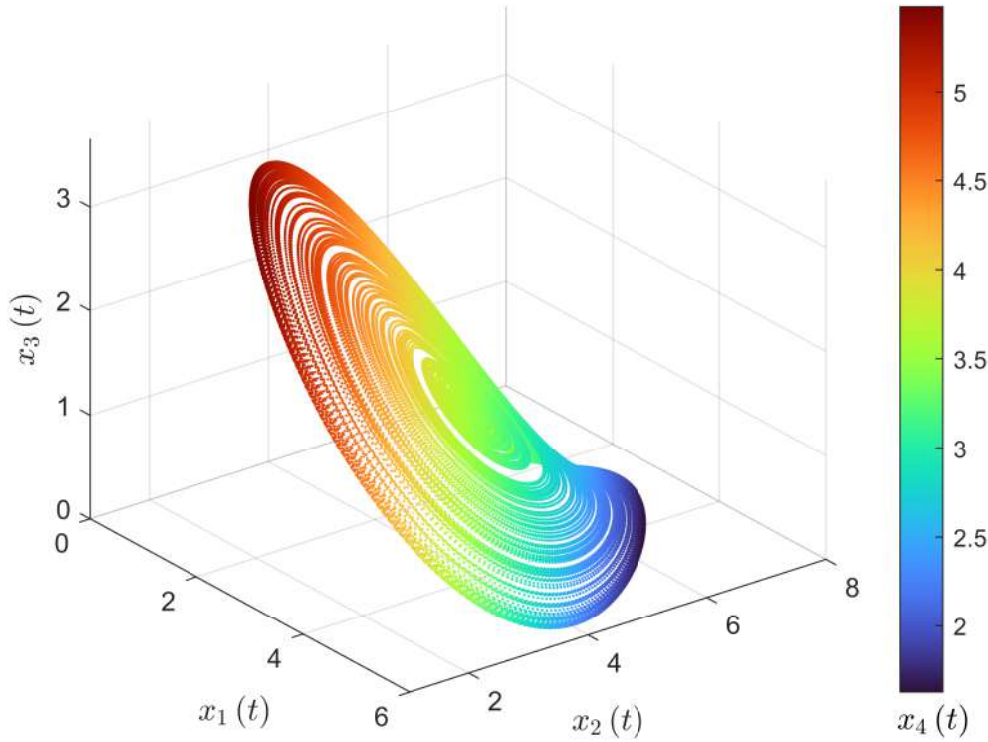
A second family of competition models explicitly introduces a set of resources. One of the first explicit resource competition models was proposed by MacArthur and Levins (1964). This model has been extensively used and extended by Robert MacArthur in several research papers and is now known as MacArthur consumer-resource model (Chesson, 1990). In MacArthur (1970), the model is formulated as follows:

$$
\begin{cases}
\dfrac{\mathrm{d}x_i(t)}{\mathrm{d}t} = \beta_i x_i(t) \left(\sum_{j=1}^{m} \alpha_{i,j} \omega_j y_j(t) \right) - \mu_i x_i(t) \\
\dfrac{\mathrm{d}y_j(t)}{\mathrm{d}t} = \delta_j y_j(t) \left(1 - \dfrac{y_j(t)}{\kappa_j} \right) - \sum_{i=1}^{n} \alpha_{i,j} x_i(t)
\end{cases}
$$

where $x_i(t)$ represents the population density of species i, $y_j(t)$ represents the population density of resource j (e.g., food resources), β_i is a conversion factor that translates resource consumption into per capita growth rate, $\alpha_{i,j}$ is the rate at which species i captures resource j, ω_j is the value of a unit of resource j to the consumer (e.g., caloric energy), μ_i is the mortality rate of species i, and δ_j is the intrinsic growth rate of resource j. A variant of the MacArthur model assumes that resource availability depends on three factors: supply, depletion and consumption. In this case, we

Box 20: Robert H. MacArthur

Despite his tragically short life (1930–1972), Robert MacArthur was one of the most influential ecologists of the 20th century (Fretwell, 1975; Brown, 1999). He received his Ph.D. from Yale University in 1957 under the direction of G. E. Hutchinson and was a professor at the University of Pennsylvania and Princeton University. He is known for developing the theory of island biogeography, the study of limiting similarity (niche theory), consumer-resource theory, and his contributions to the complexity-stability debate. According to Brown (1999), "*MacArthur's influence stems not only from his substantial and frequently cited published works but also from his direct personal interactions and collaborations with contemporary scientists, especially young people*". He had a significant influence on his co-authors, all of whom went on to brilliant careers: Martin L. Cody, Joseph Hurd Connell, Jared Mason Diamond, Henry Stainken Horn, George Evelyn Hutchinson, James R. Karr, Peter Hubert Klopfer, Richard Levins, Robert McCredie May, Harry Frederick Recher, Eric Rodger Pianka, Michael L. Rosenzweig, and Edward Osborne Wilson.

obtain the following Lotka-Volterra competition model with externally supplied resources (Cui *et al.*, 2024):

$$\begin{cases} \dfrac{\mathrm{d}x_i(t)}{\mathrm{d}t} = \beta_i x_i(t) \left(\sum_{j=1}^{m} \alpha_{i,j} \omega_j y_j(t) \right) - \mu_i x_i(t) \\ \dfrac{\mathrm{d}y_j(t)}{\mathrm{d}t} = \kappa_j - \varrho_j y_j(t) - \left(\sum_{i=1}^{n} \alpha_{i,j} x_i(t) \right) y_j(t) \end{cases}$$

where κ_j is the supply of resource j, ϱ_j is the natural depletion or decay rate of resource j, and $\alpha_{i,j}$ is the rate at which species i consumes resource j. Along with Robert MacArthur, David Tilman is another prolific researcher on competition models and their impact on community structure. In his book, Tilman (1982) used the following general formulation:

$$\begin{cases} \dfrac{\mathrm{d}x_i(t)}{\mathrm{d}t} = f_i(y_1(t), \ldots, y_m(t)) x_i(t) - \mu_i(t) x_i(t) \\ \dfrac{\mathrm{d}y_j(t)}{\mathrm{d}t} = g_j(y_j(t)) - \sum_{i=1}^{n} \alpha_{i,j}(y_1(t), \ldots, y_m(t)) f_i(y_1(t), \ldots, y_m(t)) x_i(t) \end{cases}$$

where $f_i(y_1, \ldots, y_m)$ is the growth function of consumer i, $\mu_i(t)$ is the mortality rate function of consumer i, $g_j(y_j)$ is the growth function of resource j, and $\alpha_{i,j}(y_1, \ldots, y_m)$ is the conversion factor function from resource j to consumer i. The MacArthur consumer-resource model and the Lotka-Volterra competition model with externally supplied resources are both special cases of Tilman's general model[138].

---

[138]The MacArthur consumer-resource model is obtained by setting $f_i(y_1, \ldots, y_m) = \beta_i \sum_{j=1}^{m} \alpha_{i,j} \omega_j y_j$, $\mu_i(t) = \mu_i$,

The competitive exclusion principle (or Gause's law) states that two species competing for exactly the same resource cannot stably coexist indefinitely. One will outcompete the other. For coexistence to occur, the species must occupy slightly different niches or use resources differently (niche theory). This traditional interpretation of competitive exclusion and niche theory has been challenged by much research. In fact, although there are many examples where the traditional interpretation is valid[139], there are also many examples where multiple competitive species can coexist[140]. Moreover, Armstrong and McGehee (1980) demonstrated that under certain conditions, multiple species can coexist with fewer resources in a Lotka-Volterra model of multi-species competition. In fact, the relationship between biodiversity and competition is more complex, as demonstrated by Chesson (1990), who examined the processes that allow multiple species to coexist within the same ecological community and addressed the apparent paradox of high biodiversity despite competitive interactions. He categorized mechanisms that promote species coexistence into two primary types: equalizing mechanisms (which reduce average fitness differences between species, minimizing competitive inequalities) and stabilizing mechanisms (which increase negative intraspecific interactions relative to interspecific interactions, promoting coexistence by ensuring that species limit their own population growth more than they limit that of others). He also emphasized that environmental variability, both spatial and temporal, can facilitate coexistence. It follows that competition and harvesting are not equivalent. It is not obvious that competition dramatically reduces biodiversity, which is not the case with harvesting. However, the effects of harvesting strategies in multi-species consumer-resource metapopulations are not well known. For example, Strevens and Bonsall (2011) found that certain harvesting strategies, particularly fixed proportion harvesting, resulted in larger regional population sizes, fewer local extinctions, and higher yields compared to unharvested metapopulations. This counterintuitive result suggests that increasing local mortality through specific harvesting methods can increase overall population sizes — a phenomenon referred to as the '*hydra effect*'. However, as Abrams (2009) points out, there is little empirical evidence for hydra effects in nature. Thus, there is a gap between previous theoretical and empirical results.

3.4.3 Overexploitation in aquatic systems

In the early 2000s, several important research papers alerted the scientific community to the threat of overfishing and the potential collapse of marine ecosystems. Jackson *et al.* (2001) examined how historical overfishing had led to the degradation and collapse of coastal ecosystems over time. Using a variety of historical data — including archaeological records, historical documents, and paleoecological studies — the authors described how the removal of top predators and key species (*e.g.*, sharks, sea otters, cod, oysters) through overfishing could trigger cascading effects throughout the food web, leading to shifts in the abundance and distribution of other species. For example,

---

$g_j(y_j) = \delta_j y_j \left(1 - \kappa_j^{-1} y_j\right)$, and $\alpha_{i,j}(y_1, \ldots, y_m) = \left(\beta_i \sum_{j=1}^{m} \alpha_{i,j} \omega_j y_j\right)^{-1} \alpha_{i,j}$. For the Lotka-Volterra competition model with externally supplied resources, the generic functions for the resources are $g_j(y_j) = \kappa_j - \varrho_j y_j$, and $\alpha_{i,j}(y_1, \ldots, y_m) = \left(\beta_i \sum_{j=1}^{m} \alpha_{i,j} \omega_j y_j\right)^{-1} \alpha_{i,j} y_j$.

[139]A famous example is the competition between the flour beetles *Tribolium castaneum* and *Tribolium confusum* (Park, 1962; Pointer *et al.*, 2021).

[140]A well-known example that challenges the competitive exclusion principle is the plankton paradox, first described by Hutchinson (1961). In aquatic ecosystems, numerous species of phytoplankton coexist despite competing for a limited number of resources such as light, nitrogen, and phosphorus. According to the principle of competitive exclusion, only a few dominant species should survive because they would outcompete the others. In natural environments, however, dozens of phytoplankton species coexist in the same habitat. A second well-known example was described by MacArthur (1958), who studied five species of warblers (small songbirds) coexisting in the same forest areas and apparently feeding on the same insects. This apparent contradiction of competitive exclusion led to the development of the theory of niche differentiation.

the loss of large predators led to an increase in prey species, which in turn overgrazed habitats. In addition, the destruction of habitat-forming species (*e.g.*, oyster reefs, seagrass beds, corals) led to a decline in biodiversity and ecosystem functions. Pauly *et al.* (2002) introduced the concept of '*fishing down marine food webs*', where fisheries increasingly target smaller, lower trophic level species as larger predatory fish become scarce. The authors emphasized that without significant intervention, global fisheries would continue to decline, putting marine biodiversity at risk. Pauly *et al.* (2005) built on these themes and expanded the discussion of the consequences of overfishing for marine ecosystems and global food security:

> "*With the development of industrial fishing, and the resulting invasion of the refuges previously provided by distance and depth, our interactions with fisheries resources have come to resemble the wars of extermination that newly arrived hunters conducted 40 000– 50 000 years ago in Australia, and 12 000–13 000 years ago against large terrestrial mammals in North America.*" (Pauly *et al.*, 2005, page 5).

Another milestone was reached with the publication of empirical research by Myers and Worm (2003) and Worm *et al.* (2006) in *Nature* and *Science*. Myers and Worm (2003) defined the following biomass time-trend model:

$$N_i\left(t\right) = N_i\left(0\right)\left(\left(1 - \varphi_i\right)e^{-r_i(t-t_0)} + \varphi_i\right)$$

where $N_i\left(t\right)$ is the biomass at time t, $N_i\left(0\right)$ is the initial biomass before industrialized exploitation, r_i is the rate of decline and φ_i is the fraction of the community that remains at equilibrium as $t \to \infty$. Using large predator biomass data from nine oceanic ecosystems (tropical/subtropical/temperate $\times$ Atlantic/Indian/Pacific) and four shelf ecosystems (Gulf of Thailand, South Georgia, Southern Grand Banks, and Saint Pierre Banks), they estimated the coefficients $\hat{r}_i$ and $\hat{\varphi}_i$ by using the method of maximum likelihood, and the parameters of the nonlinear mixed-effects models assuming that $r_i \sim \mathcal{N}\left(\mu_r, \sigma_r^2\right)$ and $\varphi_i \sim \mathcal{N}\left(\mu_\varphi, \sigma_\varphi^2\right)$. Figure 68 shows the results for the global region and three specific regions[141]. The authors concluded that industrialized fisheries typically reduce community biomass by 80% within 15 years of exploitation, and that the biomass of large predatory fishes is now only about 10% of pre-industrial levels. Worm *et al.* (2006) "*analyzed local experiments, long-term regional time series, and global fisheries data to test how biodiversity loss affects marine ecosystem services across temporal and spatial scales.*" They found that "*rates of resource collapse increased and recovery potential, stability, and water quality decreased exponentially with declining diversity.*" They emphasized that their findings highlight the societal consequences of the ongoing erosion of

---

[141]Below, we report the estimated values found by Myers and Worm (2003, Table 1, page 281):

Region	$\hat{r}_i$	$\hat{\mu}_r$	$\hat{\varphi}_i$	$\hat{\mu}_\varphi$
Tropical Atlantic	16.6	16.7	12.1	11.9
Subtropical Atlantic	12.9	13.0	8.1	8.3
Temperate Atlantic	21.4	20.3	4.7	5.3
Tropical Indian	9.2	9.5	17.6	16.8
Subtropical Indian	6.5	6.8	8.2	9.2
Temperate Indian	30.7	27.7	5.5	6.3
Tropical Pacific	12.1	12.4	15.5	14.9
Subtropical Pacific	12.8	13.5	23.5	21.5
Temperate Pacific	20.8	20.4	8.2	8.5
Gulf of Thailand	25.6	22.2	9.3	9.8
South Georgia	166.6	30.8	20.9	16.0
Southern Grand Banks	4.0	5.7	0.0	10.0
Saint Pierre Banks	5.1	6.3	2.7	7.9
Global		16.0		10.3

biodiversity, which appears to be accelerating globally. Moreover, they expressed serious concern about this trend, as their regression model predicted the global collapse of all commercially fished taxa by the mid-21st century (specifically, by 2048). Some newspapers and journalists have focused on this figure, interpreting it as a prediction that "*the oceans will be empty by 2048*". For example, this claim was mentioned in the controversial documentary *Seaspiracy*, which premiered on Netflix in 2021.

Figure 68: Time trends of community biomass in oceanic and shelf ecosystems
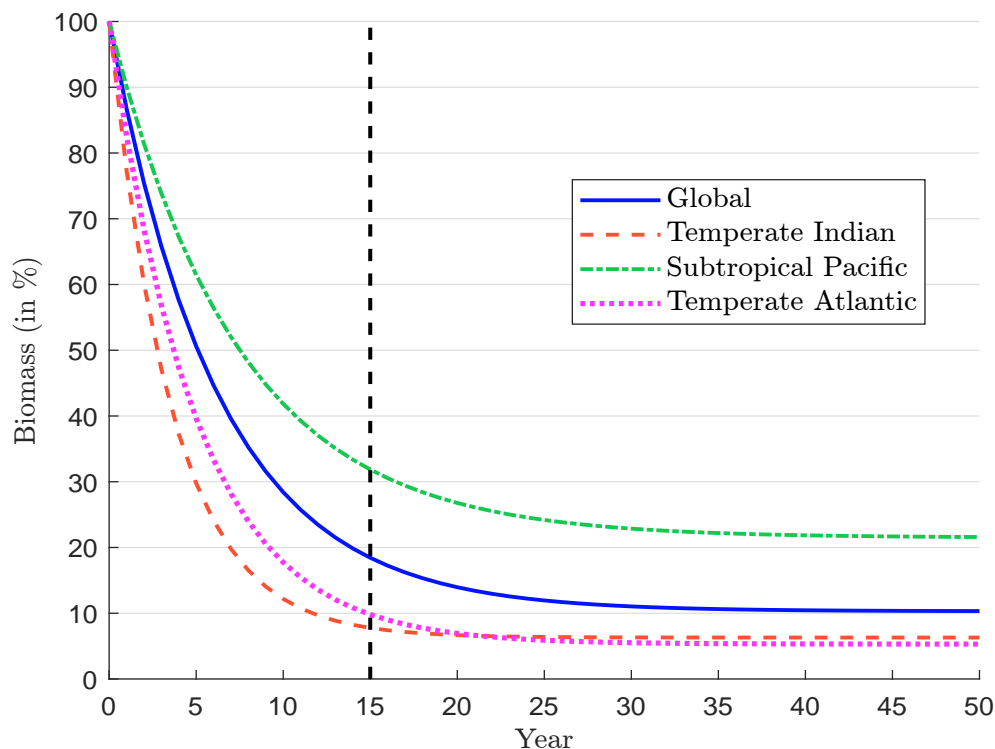
Source: Myers and Worm (2003, Figure 1, page 280) & Author's calculations.

As Boris Worm later explained, this period marked the peak of pessimism. Indeed, Worm's study was not the only one with a gloomy outlook — many studies in the 2000s warned that the collapse of global fisheries could become a reality. Thurstan *et al.* (2010) analyzed annual demersal fish landings from bottom trawls in the United Kingdom from 1889 to 2007 (Figure 69). Their results showed a dramatic decline in the commercial productivity of fisheries, with landings per unit of fishing power falling by 94% over the past 118 years. Another well-known example is the collapse of the Atlantic cod fishery in eastern Canada (Myers *et al.*, 1997). According to Schijns *et al.* (2021), "*the fishery for Northern Atlantic cod (Gadus morhua) off Newfoundland and Labrador, Eastern Canada, presents the most spectacular case of an exploited stock crashed in a few decades by an industrial bottom trawl fishery under a seemingly sophisticated management regime after half a millennium of sustainable fishing. The fishery, which had generated annual catches of 100 000 to 200 000 tonnes from the beginning of the 16th century to the 1950s, peaked in 1968 at 810 000 tonnes, followed by a devastating collapse and closure 24 years later.*" Figure 70 illustrates the evolution of cod harvests in eastern Canada. We observe a continuous increase throughout the 18th and 19th centuries, with a sharp acceleration in the 20th century, especially after 1960. Schijns *et al.* (2021) estimated the maximum sustainable yield at 380 000 tonnes, a level well below the harvest volumes

Figure 69: Fish catch in the United Kingdom
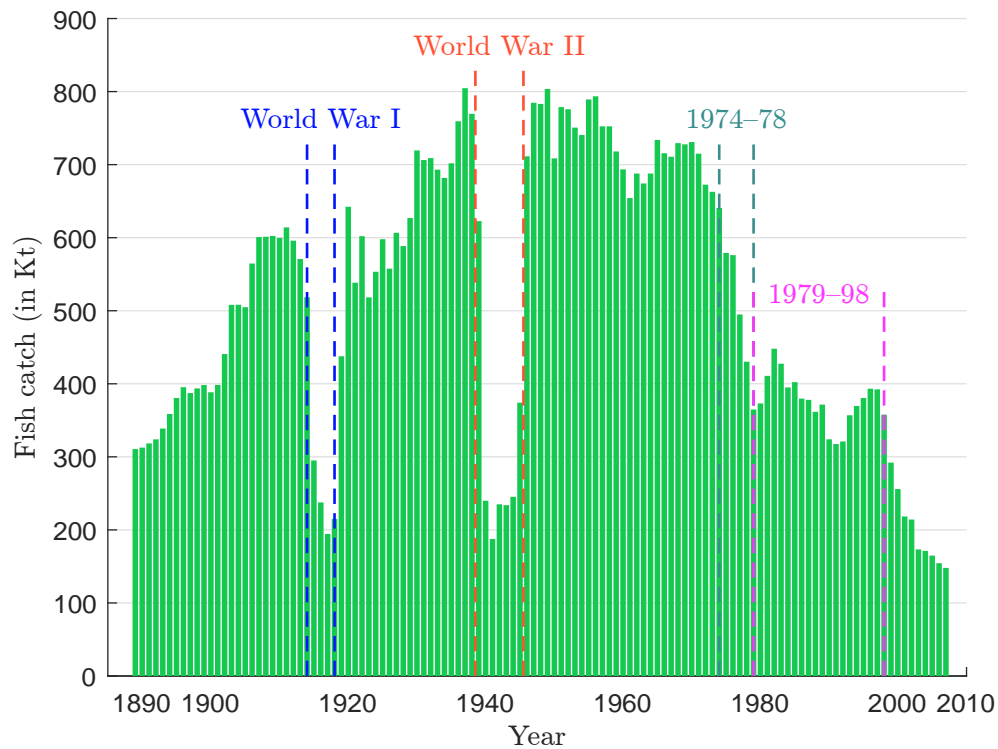
Source: Thurstan *et al.* (2010, Figure 1a, page 2) & www.ourworldindata.org/fish-and-overfishing.

Figure 70: Northern cod catch in eastern Canada
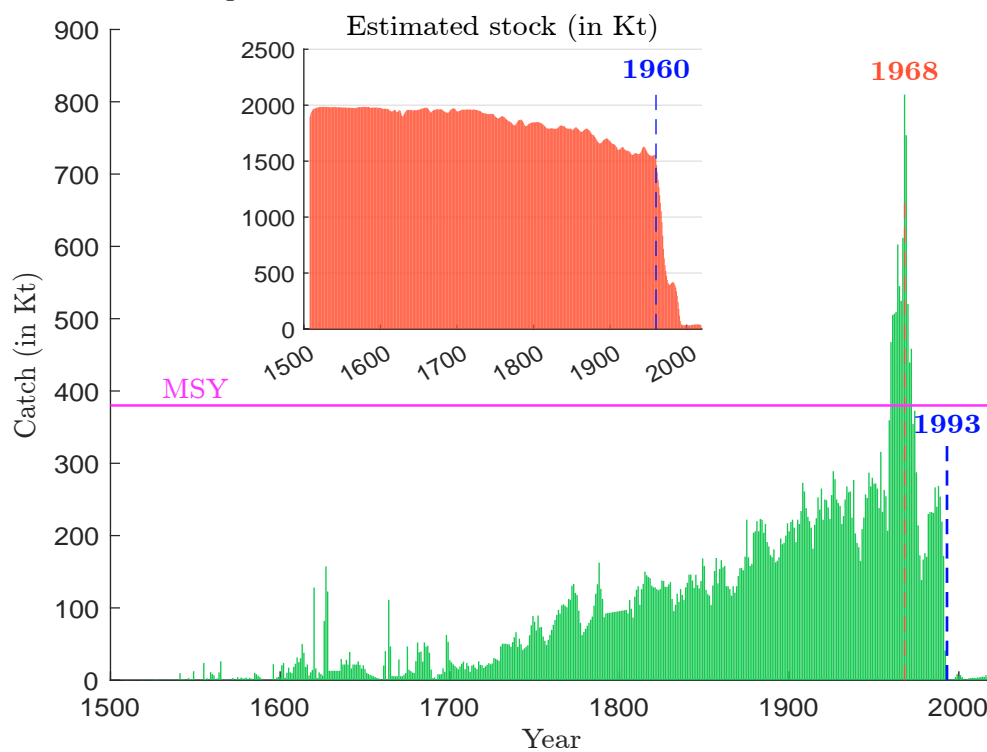
Source: Schijns *et al.* (2021, Figure 1, page 2679) & Author's calculations.

recorded between 1960 and 1990. We have also reported the estimated stock levels in Figure 70, which clearly shows the abrupt collapse in just thirty years[142]. On July 2, 1992, the Canadian government announced a moratorium on cod fishing. Originally intended to be a temporary two-year ban to allow the northern cod population to recover, the moratorium has effectively become permanent, as cod stocks have shown very limited signs of recovery even after more than 30 years. This decision had a devastating impact on coastal communities that depended on the fishery, resulting in the loss of approximately 30 000 jobs — one of the largest mass layoffs in Canadian history. Other notable examples of fishery collapses and management challenges include the Californian Pacific sardine collapse (which reached its lowest point in the mid-1950s), the Peruvian anchoveta crisis (1972-1973, triggered by an El Niño event combined with overfishing), the overexploitation of orange roughy (beginning in the 1980s, particularly severe in New Zealand and Australia), the significant decline of Pacific bluefin tuna (throughout the 20th century), and the Namibian sardine collapse (late 1960s to early 1970s). In some cases, however, these species have shown signs of recovery.

Figure 71: Global seafood production in Mt (1960–2022)
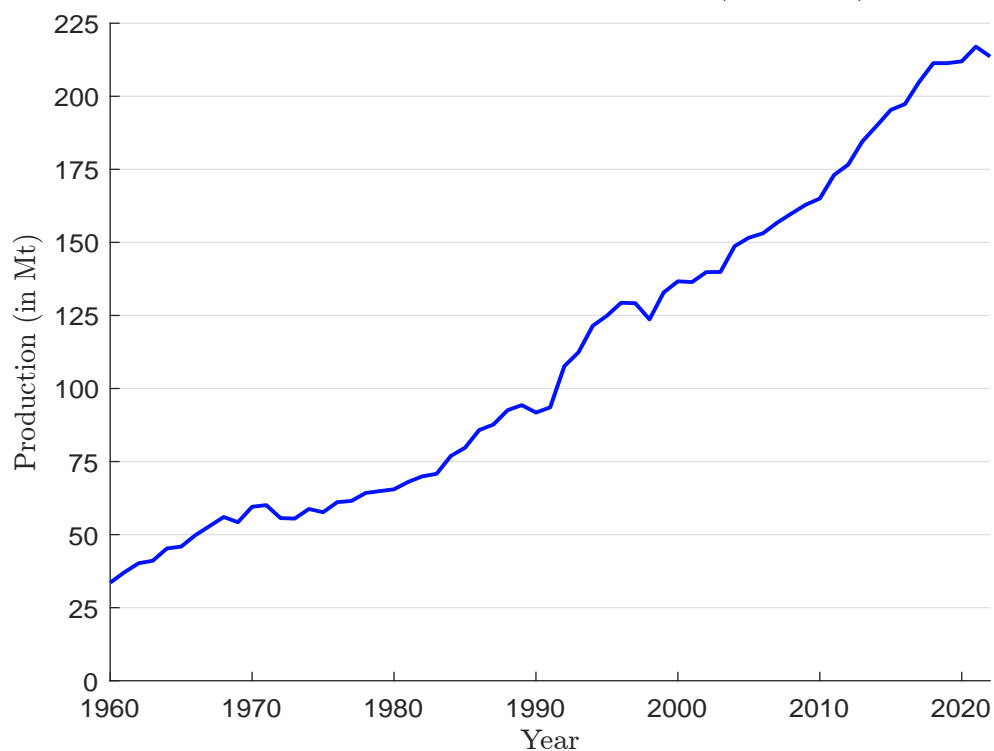
Source: https://databank.worldbank.org/source/world-development-indicators & Author's calculations.

To better understand the current sustainability of fisheries in the world, we refer to the FAO report on world fisheries and aquaculture. According to FAO (2024b), fish production (including algae production) reached a new record high, with a total production[143] of 223.2 million tonnes

---

[142]The biomass stock is estimated using the discrete version of the logistic growth population model with harvest:

$$x(t+1) = x(t) + \delta x(t)\left(1 - \frac{x(t)}{\kappa}\right) - h(t)$$

where $x(t)$ is the biomass stock in year t, δ is the intrinsic growth rate, κ is the carrying capacity and $h(t)$ is the fish harvest in year t.

[143]63% of this production is finfish, 17% algae, 11% molluscs and 8% crustaceans.

(Figure 71). Of this production, 89% is used for human consumption, equivalent to an estimated 20.7 kg per capita, while the remainder is mainly used for fishmeal and fish oil. The FAO estimates that 61.8 million people are employed in the primary production sector. In sixty years, fish production has increased by a factor of more than 5, while the growth rate between 1960 and 2022 is 2.98%. These figures can be explained by two factors: an increase in the world's population and an increase in the share of seafood in the human diet.

Figure 72: Global capture fisheries and aquaculture in Mt (1960–2022)
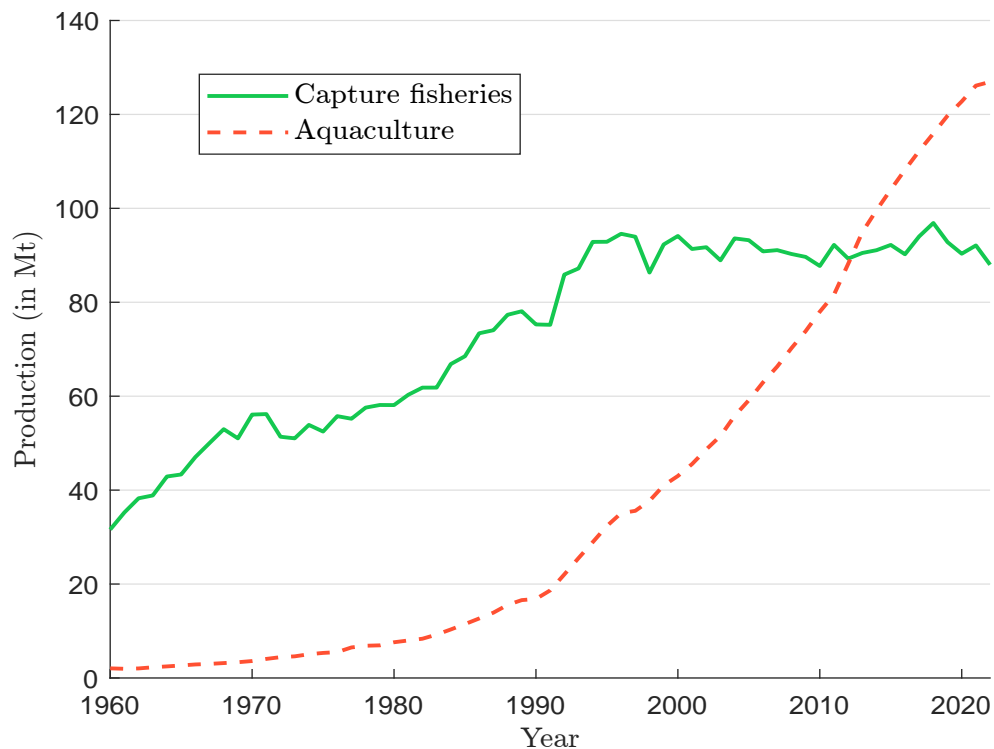
Source: https://databank.worldbank.org/source/world-development-indicators & Author's calculations.

An annual growth rate of 3% means a multiplication factor of 19 over one century and 369 over two centuries! In this context, it is understandable that some people predict that sooner or later the oceans will be empty. However, if we examine the components of the production, namely capture fisheries and aquaculture[144], we observe two distinct phases (Figure 72):

- From 1960 to 1990, production growth was driven primarily by capture fisheries.

- Since 1990, capture fisheries have remained constant, while aquaculture has experienced impressive growth.

In 1960, capture fisheries accounted for 95% of seafood production, while today aquaculture contributes about 60% of total seafood production. As a result, fish production has shifted from an

---

[144]Here are the definitions used by the FAO. Capture fisheries production measures the volume of fish catches landed by a country for all commercial, industrial, recreational and subsistence purposes. Aquaculture is understood to mean the farming of aquatic organisms including fish, molluscs, crustaceans and aquatic plants. Aquaculture production specifically refers to output from aquaculture activities, which are designated for final harvest for consumption. Total fisheries production measures the volume of aquatic species caught by a country for all commercial, industrial, recreational and subsistence purposes. The harvest from mariculture, aquaculture and other kinds of fish farming is also included.

industry based on the capture of wild fish to one based on aquaculture. Table 46 shows seafood

Table 46: Fisheries production by country (1960–2022)

Country		1960	1980	2000	2010	2020	2022
		Capture fisheries production					
World (in Mt)		31.6	58.1	94.1	87.7	90.3	88.0
Top 10 (in %)	China	7.0	5.4	15.8	17.2	14.9	15.0
	Indonesia	2.2	2.8	4.4	6.1	7.7	8.4
	India	3.5	3.6	4.0	5.4	5.2	6.3
	Peru	11.1	4.7	11.3	4.9	6.3	6.1
	Russia	0.0	0.0	4.3	4.6	5.6	5.7
	United States	8.6	6.4	5.1	5.0	4.7	4.8
	Vietnam	1.4	0.8	1.7	2.6	3.9	4.1
	Japan	18.7	17.3	5.5	4.8	3.6	3.4
	Chile	1.1	5.0	4.8	3.5	2.4	3.1
	Norway	4.4	4.4	3.1	3.2	2.9	3.0
		Aquaculture production					
World (in Mt)		2.0	7.6	43.0	78.0	122.8	126.9
Top 10 (in %)	China	46.8	40.8	69.2	61.3	57.4	59.4
	Indonesia	3.9	3.0	2.3	8.0	12.1	11.5
	India	2.2	4.8	4.5	4.9	7.0	8.1
	Vietnam	1.8	1.3	1.2	3.5	3.8	4.1
	Bangladesh	2.4	1.2	1.5	1.7	2.1	2.2
	Philippines	3.0	4.4	2.6	3.3	1.9	1.9
	Norway	0.1	0.1	1.1	1.3	1.2	1.3
	Egypt	0.2	0.2	0.8	1.2	1.3	1.2
	Chile	0.0	0.0	1.0	0.9	1.2	1.2
	Myanmar	0.0	0.0	0.2	1.1	0.9	0.9
		Total production					
World (in Mt)		33.6	65.5	136.7	165.0	211.9	213.6

Source: https://databank.worldbank.org/source/world-development-indicators & Author's calculations.

production by country across different decades[145]. In 1960, fish production was led by Japan, Peru, China, and the United States, with production shares of 18.6%, 10.4%, 9.5%, and 8.4%, respectively. These countries were followed by Norway (4.1%), India (3.5%), the United Kingdom (3.0%), Canada (2.8%), Spain (2.7%), South Africa (2.6%), Germany (2.3%), France (2.3%), Indonesia (2.3%), and Iceland (1.9%). In 2022, seafood production had become dominated by China with a production share of 41.5%, followed by Indonesia (10.3%), India (7.4%), Vietnam (4.1%), Peru (2.6%), Russia (2.5%), Bangladesh (2.2%), the United States (2.2%), Norway (2.0%), and Chile (2.0%). This represents a complete transformation of global seafood production over sixty years. For example, in 2022, former major producers had dropped significantly in rank: Japan (13th, 1.83%), Spain (23rd, 0.51%), Canada (25th, 0.41%), France (30th, 0.34%), and Germany (54th, 0.10%). Today, 70% of production is located in Asia, while South America, Europe, Africa and North America represent 9%, 9%, 7% and 3%, respectively. We also observe a long-term upward trend in per capita consumption of aquatic food products. Between 1961 and 2021, consumption rises from 9.1 kg to 20.6

---

[145]These figures differ from previous ones because they exclude some forms of algae production.

kg per person, an average annual increase of about 1.4%. The growth in fish production can then be attributed equally to demographic expansion and changes in dietary preferences.

FAO (2024b) assesses the sustainability of fisheries by comparing the biomass stock $x\,(t)$ with the maximum sustainable yield (MSY) and defines three categories:

Category	Overfished	Maximally sustainably fished	Underfished
$\dfrac{x\,(t)}{\text{MSY}}$	$[0, 0.8[$	$[0.8, 1.2]$	$]1.2, +\infty)$
Unsustainable	✓		
Sustainable		✓	✓

The FAO analysis shows that the proportion of fishery stocks within biologically sustainable levels declined from 94% in 1974 to 62% in 2021[146]. This means that 38% of fishery stocks are not sustainable. This figure masks a large discrepancy between the 15 major FAO fishing regions[147]. Indeed, four areas have more than 50% of their fish stocks at unsustainable levels: the eastern central Atlantic (51.3%), the northwest Pacific (56%), the Mediterranean and Black Sea (62.5%), and the southeast Pacific (66.7%). In contrast, four areas have more than 75% of fisheries stocks that are sustainable: the eastern central Pacific (84.2%), the northeast Atlantic (79.4%), the northeast Pacific (76.5%), and the southwest Pacific (75.9%). According to FAO (2024b, Figure 20, page 45), three distinct patterns emerge:

1. Areas with a continuously increasing trend in landings since 1950
   This group includes four areas: the eastern central Atlantic, the eastern and western Indian Ocean, and the western central Pacific.

2. Areas with landings oscillating around a globally stable value since 1990, associated with the dominance of pelagic, short-lived species
   This group includes three areas: the northwest, northeast and eastern central Pacific.

3. Areas with an overall declining landing trend following historical peaks
   This group includes the remaining eight regions.

With fisheries production expected to increase by 10% over the next decade, FAO has proposed a process to achieve this goal and improve sustainability: the *FAO Blue Transformation Roadmap 2022–2030*. This roadmap focuses on three main pillars: expanding sustainable aquaculture, improving fisheries management, and strengthening value chains and market access (FAO, 2022). Since we have reached a limit in terms of harvesting wild fish, the growth of fisheries production would be mainly through aquaculture. It is also important to improve fisheries management. For example, there is an urgent need to reduce discards or bycatch:

> "*Discards, or discarded catch is that portion of the total organic material of animal origin in the catch, which is thrown away, or dumped at sea for whatever reason. It does not include plant materials and post-harvest waste such as offal. The discards may be dead, or alive.*" (Pérez Roda *et al.*, 2019, page 1).

---

[146]Each fishery stock is weighted equally in this assessment. When the stocks are weighted by the volume of landings, the 62% figure increases to 77%.

[147]These are the Atlantic (eastern central, northeast, northwest, southeast, southwest, western central), the Indian Ocean (eastern, western), the Mediterranean and Black Sea, and the Pacific (eastern central, northeast, northwest, southeast, southwest, western central).

Figure 73: Estimated fish discards in Mt (1950–2018)
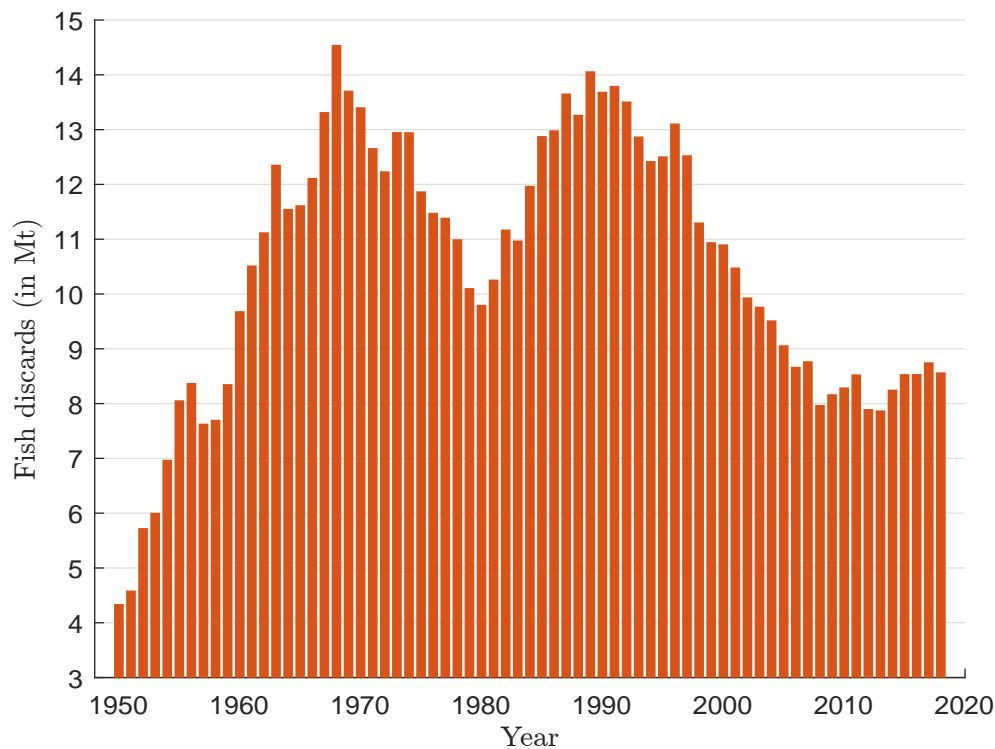
This happens for various reasons, such as the fish are too small or young, they're not the target species, the fish have low commercial value, the catch exceeds the storage capacity of the vessel, the fish are damaged, etc. Precise estimates of global fish discards are difficult to obtain, but approximate values are available. Zeller et al. (2018) estimated that discards increased from 5 million tonnes per year in the early 1950s to a peak of 18.8 million tonnes in 1989, before declining to less than 10 million tonnes per year in recent years. This represented 10–20% of the total fish catch until 2000 and now represents less than 10% of the total annual catch. Similarly, Pérez Roda et al. (2019) estimated that annual discards averaged 9.1 million tonnes between 2010 and 2014, representing 10.8% of the total annual catch during this period. From a regional perspective, the northwest Pacific and northeast Atlantic together accounted for 39% of global discards. Among fisheries, those targeting crustaceans had the highest discard rates. In fact, the problem is not just bycatch, but fish waste in general. For example, Coppola et al. (2021) report that about two thirds of the total amount of fish is discarded. This explains why fish and seafood products provide about 1% of the total calories in the human diet at the global level. However, fish remains an important source of essential nutrients, providing omega-3 fatty acids, vitamins (A, B12 and D) and minerals such as iron (Fe), iodine (I), zinc (Zn) and calcium (Ca), which are essential for human health. Moreover, many local communities rely heavily on fisheries for their livelihoods. In this global context, the call of Worm et al. (2009) to rebuild global fisheries remains highly relevant (Duarte et al., 2020).

Remark 15 *To go further, the most prominent fisheries databases[148] include the FAO FishStat database, now called FishStatJ (data on fish production, trade and consumption), the RAM Legacy*

---

[148]The websites are www.fao.org/fishery/en/statistics/software/fishstatj, www.ramlegacy.org and www.seaaroundus.org.

3.4.4 Overexploitation in tropical forests

By definition, overexploitation in tropical forest ecosystems is related to deforestation and habitat degradation. However, we need to distinguish between the two concepts: deforestation and over-exploitation (Wilkie *et al.*, 2011). According to Peres (2010), overexploitation of tropical forests involves three main issues:

- Timber extraction refers to the process of harvesting trees for commercial purposes, such as logging for wood, paper, and construction materials;

- Tropical forest vertebrates have been hunting in tropical forests for over $100\,000$ years, but their consumption increased during the 20th century;

- Non-timber forest products are biological resources such as plants and raw materials.

Rice *et al.* (1997) questioned the feasibility and effectiveness of sustainable forest management in tropical regions. They argued that sustainable logging in tropical forests is often ineffective because it yields less timber than conventional logging. Empirical studies support this (Pearce *et al.*, 2003). Another important challenge is the lack of financial incentives for loggers to harvest at sustainable levels and invest in forest regeneration, as economic principles suggest that trees should be harvested when their volume growth rate falls below the prevailing interest rate (Peres, 2010). Delaying harvesting beyond this point entails an opportunity cost, as profits from immediate harvesting could be reinvested elsewhere for higher returns. Reynolds and Peres (2006) used a study of Bolivian mahogany by Raymond Gullison to illustrate this problem. Despite legal restrictions, trees as small as 40 cm in diameter were harvested — well below the legal limit — because at this size, mahogany trees grow in volume at a rate of 4% per year, and their market value increases at about 1% per year due to rising timber prices, while Bolivia's real interest rates averaged 17% in the mid-1990s. This significant gap between tree growth rates and high interest rates creates strong economic pressure to harvest trees as soon as they have market value, rather than waiting for them to mature.

Let us formalize the opportunity cost problem. If we denote by Δp and Δv the annual changes in timber prices and tree volume relative to a reference age t_0, the market value $W(t)$ of the trees is given by:

$$W(t) = p(t)\,v(t) = p_0 v_0 \left(1 + \Delta p\right)^{t-t_0} \left(1 + \Delta v\right)^{t-t_0}$$

where p_0 and v_0 are the price level and the volume of trees at age t_0. Now assume that trees are harvested at age $\tau \leq t$ and the proceeds are invested at the risk-free rate r. The resulting wealth conditional on this harvest is equal to:

$$W\left(t \mid \tau \leq t\right) = p\left(\tau\right) v\left(\tau\right) \left(1 + r\right)^{t-\tau}$$

The economic objective is to maximize the conditional wealth $W\left(t \mid \tau \leq t\right)$ or to find the optimal harvest age τ that maximizes the return. Figure 74 illustrates the economic problem with the following assumptions: $t_0 = 20$ years, $p_0 = \$500/\mathrm{m}^3$, $v_0 = 2\,\mathrm{m}^3$, $\Delta p = 1\%$ and $\Delta v = 4\%$. If the tree is harvested at age 20, the income is $W(20) = 500 \times 2 = \$1\,000$. If the harvest is delayed by 30 years, the income increases to $W(50) = \left(500 \times 1.01^{30}\right) \times \left(2 \times 1.04^{30}\right) = \$4\,371.6$. Now suppose the

Figure 74: Opportunity cost of logging in tropical forests
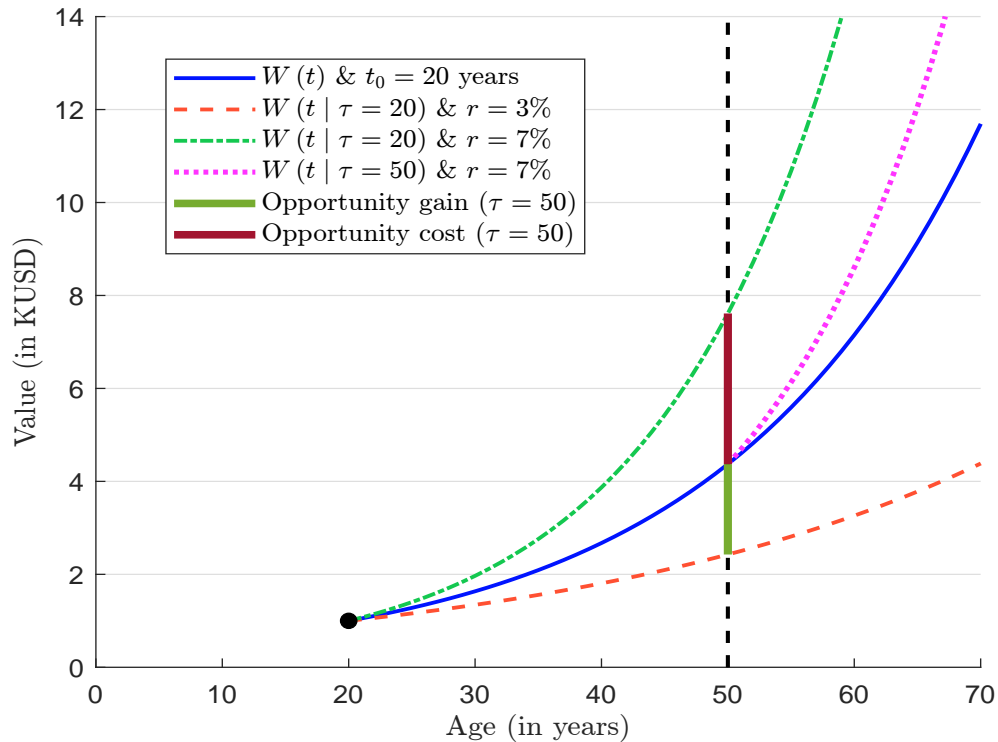
interest rate is 3%, the income from logging at age 20 and reinvesting would be $W(50 \mid \tau = 20) = 1\,000 \times 1.03^{30} = \$2\,427.3$. Since $W(50 \mid \tau = 20) < W(50)$, there is a financial gain from waiting another 30 years before harvesting. However, if the interest rate is 7%, we have $W(50 \mid \tau = 20) = 1\,000 \times 1.07^{30} = \$7\,612.3$. This implies a significant opportunity cost for delaying the harvest[149]. In general, there is an opportunity cost when the interest rate is relatively high, especially when $r \geq \Delta p + \Delta v$. According to Rice *et al.* (1997), there is no economic solution to this problem, and they suggest that protected areas are the only viable way to manage tropical forests sustainably. Twenty-five years later, the debate about selective logging and its impact on biodiversity remains open (Bicknell *et al.*, 2015; Burivalova *et al.*, 2021).

Hunting wild animals is a practice with deep historical roots, initially driven by the basic need for food. Today, food security in developed countries rarely depends on hunting. Conversely, it remains a vital source of food in many developing countries. In addition to providing food for personal consumption, hunting can be an important source of income for hunters and their families. In these cases, harvested animals are sold not only for food but also for other purposes, such as the production of leather goods and medicinal products. There is much evidence of overexploitation over the last fifty years, especially as the trade of wild animals has increased. This has two major consequences. First, hunting of wild animals causes biodiversity loss. For example, Peres and Palacios (2007) provided a meta-analysis of changes in population density for 30 species of mammals, birds, and

---

[149]This opportunity cost is underestimated because two harvests could occur within 50 years. Therefore, the opportunity cost is given by:

$$\mathcal{C} = \underbrace{W(50 \mid \tau = 20)}_{\text{Income from 1st harvest}} + \underbrace{W(30 \mid \tau = 20)}_{\text{Income from 2nd harvest}} + \underbrace{W(10)}_{\text{3rd tree at age 10}} - \underbrace{W(50)}_{\text{Tree at age 50}}$$

Box 21: The bushmeat crisis

Bushmeat is the meat of wild animals that are hunted for food (Nasi *et al.*, 2008; Fa *et al.*, 2002). The meat is either eaten by the hunter or sold to make money. In the media, the term bushmeat is generally used to refer to the illegal hunting of protected animals in Africa. This includes various species such as antelopes, monkeys, rodents and other wild animals. Bushmeat has historically been a vital protein source in parts of Africa, Latin America and South Asia. In remote rural areas of West and Central Africa, it constitutes 80–90% of animal protein intake. While subsistence hunting by local communities isn't the main conservation issue, growing commercial demand is problematic. The market for bushmeat is now increasingly driven by urban consumers and diaspora communities, leading to unsustainable harvesting in several African regions.

Estimating the global impact of bushmeat harvesting is challenging. However, according to Nasi *et al.* (2011), "*the harvest of animals such as tapir, duikers, deer, pigs, peccaries, primates and larger rodents, birds and reptiles [...] represents around 6 million tonnes of animals extracted yearly [...] with an estimated yearly extraction rate in the Congo Basin of 4.5 million tonnes.*". While more than 1 000 animal species are affected by bushmeat hunting, Ripple *et al.* (2016) estimated that approximately 300 of these terrestrial mammal species are threatened with extinction. This also means that the majority of mammal species (70%) are not listed as threatened on the IUCN Red List.

The term '*bushmeat crisis*' refers to this paradox: the need for local people to hunt wild animals to improve their food security and well-being, while at the same time this practice has a significant negative impact on biodiversity. In this context, trade-offs and dilemmas are more difficult to resolve, as the study by Cawthorn and Hoffman (2015) shows.

reptiles in 101 forest sites. Populations declined by up to 75% in more intensively hunted areas compared to less intensively hunted areas. Of the 30 species studied, 22 declined significantly at high levels of hunting. As expected, body size significantly influenced the magnitude of changes in abundance, with large-bodied species declining faster in overhunted areas. Considering the 12 most hunted species, mean total biomass decreased almost elevenfold from $980 \, \text{kg/km}^2$ in unhunted areas to only $89 \, \text{kg/km}^2$ in highly hunted areas (Peres, 2010, page 111). The second consequence is the threat to the food security of local populations that depend on wildlife hunting. Indeed, hunting has become more sophisticated, systematic, and industrialized. For example, several studies indicate that African bushmeat has become an organized luxury market in African urban centers and restaurants (Gluszek *et al.*, 2021), as well as in Europe (Gombeer *et al.*, 2021), with porcupines, pangolins, antelopes, and snakes being the most sought-after products. For instance, Chaber *et al.* (2023) estimate that an average of 3.9 tonnes of bushmeat is smuggled through Brussels Airport each month. While the wildlife trade provides short-term financial benefits to hunters and their families, most do not make significant profits. Moreover, the ongoing loss of biodiversity today means food insecurity for these families in the future (Nasi *et al.*, 2011).

Another way to understand the impact of overexploitation on biodiversity loss is the growth of trafficking in protected species of wild fauna and flora. According to Traffic (www.traffic.org), "*the illegal trade in wild species is one of the most profitable criminal activities in the world, estimated to be worth up to $23 billion each year.*" The UNODC (United Nations Office on Drugs and Crime) published the third edition of the World Wildlife Crime Report in 2024. This report shows that despite two decades of concerted action at the international and national levels and the entry into

Box 22: Operation Thunder 2024

On 4 February 2025, INTERPOL announced that nearly 20 000 live animals, all endangered or protected species, were seized in a global operation against wildlife and forestry trafficking networks jointly coordinated by INTERPOL and the World Customs Organization (WCO). *Operation Thunder 2024* took place in 138 countries between 11 November and 6 December 2024. Authorities arrested 365 suspects and identified six transnational criminal networks suspected of trafficking in animals and plants protected by the Convention on International Trade in Endangered Species of Wild Fauna and Flora (CITES). In addition to live animals, participating countries seized hundreds of thousands of protected animal parts and derivatives, trees, plants, marine life and arthropods. Timber cases represented the most significant seizures, occurring primarily in maritime container shipments, while most other seizures took place at airports and postal hubs. More than 100 companies involved in the trade of protected species were also identified. Significant seizures included:

- 134 tonnes of timber headed to Asia via ocean freight (Indonesia);

- 41 tonnes of exotic timber headed to Asia via ocean freight (Kenya);

- 4 472 kg of pangolin scales (Nigeria);

- 6 500 live songbirds discovered during a vehicle inspection at the Syrian border (Turkey);

- 5 193 live red-eared slider turtles concealed in passenger suitcases arriving from Malaysia at Chennai Airport (India);

- 3 700 protected plants intercepted en route from Ecuador (Peru);

- 8 rhino horns found in a suspect's luggage while transiting from Mozambique to Thailand (Qatar);

- One tonne of sea cucumbers, considered a seafood delicacy, smuggled from Nicaragua (United States);

- 973 kg of dried shark fins originating from Morocco seized at the airport (Hong Kong);

- 8 tigers, aged between two months and two years, discovered in a suspected illegal breeding facility (Czech Republic);

- 846 pieces of reticulated python skin, from the world's longest snake species, concealed onboard a ship (Indonesia).

Source: INTERPOL (2025), https://www.interpol.int/News-and-Events.

force in 1975 of CITES (the Convention on International Trade in Endangered Species of Wild Fauna and Flora), wildlife trafficking continues worldwide. Moreover, the report estimates that "*wildlife crime is interconnected with the activities of large and powerful organized crime groups operating in some of the most fragile and diverse ecosystems from the Amazon to the Golden Triangle[150].*" UNDOC (2024, page 46) reports that from 2015 to 2021, more than 140 000 seizures of wildlife products were made in 162 countries, involving 4 000 different species. Analysis of seizure records shows that coral pieces were the most common item found in the illegal wildlife trade, accounting for 16% of the total number of seizures. Other seizures included crocodiles (9%), elephants (6%), bivalves and carnivores (5% each), parrots and cockatoos (4%), orchids (4%), and many other species. Figure 75 illustrates the most affected species based on the standardized seizure index, which serves as a proxy for the market value of the seized goods. In this case, seizures of rhinos (29%) rank first, followed by pangolins (28%) and elephants (15%).

Figure 75: Percentage share by species group aggregated by standardized seizure index (2015–2021)
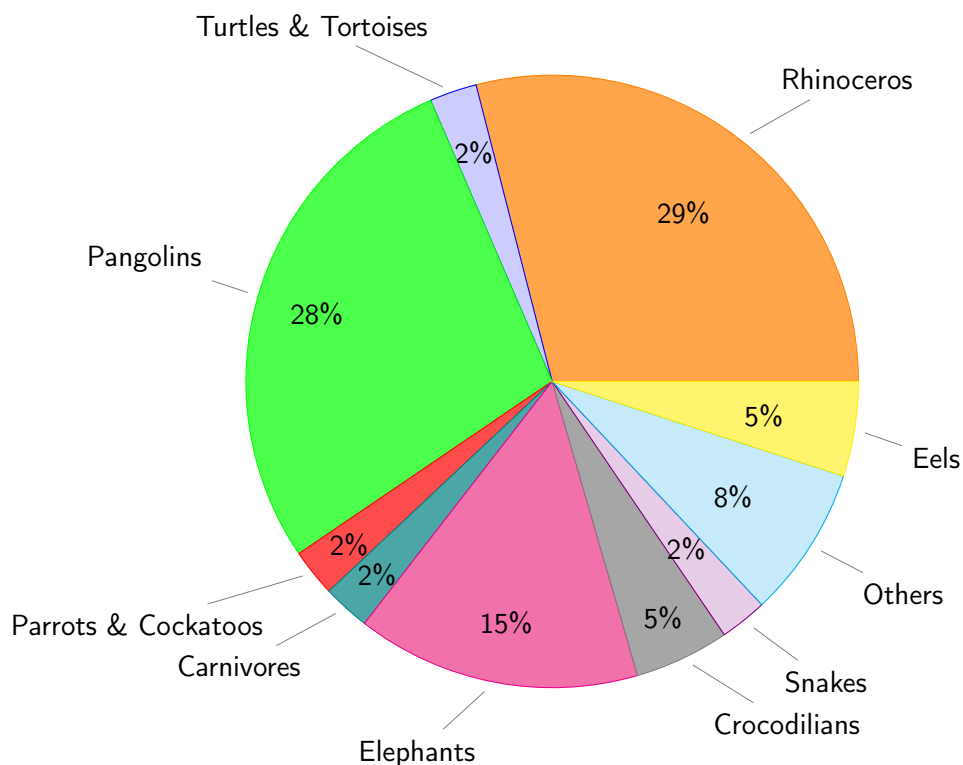
Source: UNDOC (2024, Figure 2.3, page 63).

The case of the rhinoceros is emblematic, as hunting has had a devastating impact on rhinoceros populations, pushing several species to the brink of extinction since 1900. The number of black rhinos declined by over 95% from around 100 000 in 1960 to fewer than 2 500 in the 1990s due to hunting and poaching. Although conservation efforts have helped, they remain critically endangered with only about 6 200 animals recorded in 2021. White rhinos were nearly extinct, with the southern population falling to fewer than 100 individuals in the early 20th century. They have been saved by rigorous conservation and breeding programs. As of 2021, there are approximately 16 000 individuals.

---

[150]The Golden Triangle refers to a mountainous region in Southeast Asia where the borders of Thailand, Laos and Myanmar meet.

In contrast, the northern white rhino has virtually disappeared, with only two females remaining in 2021. Indian rhinos were reduced to less than 100 individuals in 1900 due to hunting, but have since recovered thanks to conservation efforts and now number around 4 000. Javan and Sumatran rhinos were already rare in 1900, but continued to decline due to hunting and habitat loss, and both species now number fewer than 100 individuals. In Figure 76, we show the evolution of the number of rhinos in the world. We observe that only three of the six species are really significant, and that the recovery since 1990 is mainly due to the expansion of the white rhino in southern Africa[151].

Figure 76: Number of rhinoceros in the world (1960–2021)
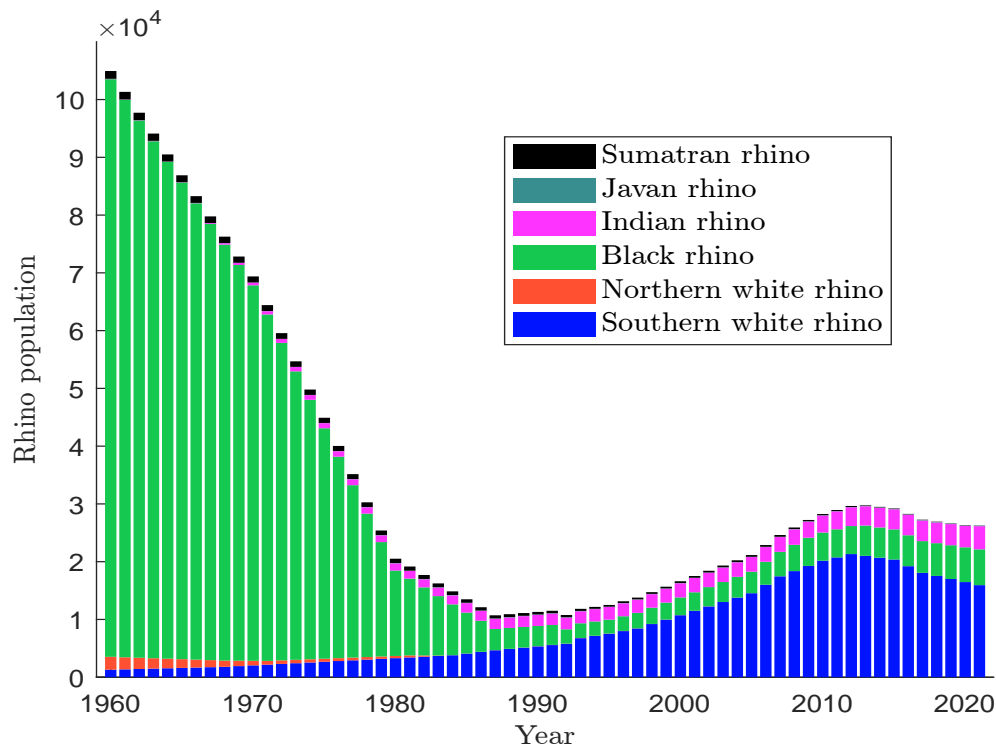
Two decades ago, Bengis et al. (2004) and Kruse et al. (2004) raised concerns about the growing risk of zoonotic pandemics and the role of biodiversity loss, particularly deforestation and habitat alteration. Zoonoses are diseases transmissible from animals to humans caused by pathogens — viruses, bacteria, fungi, or parasites — that circulate naturally in animal populations[152]. In a landmark study, Taylor et al. (2001) analyzed 1 415 human pathogenic species and found that 61% were zoonotic. Since then, the emergence of new diseases and pandemics, many of which are linked or suspected to be linked to the wildlife trade, has underscored these concerns. Examples include avian influenza (H5N1), COVID-19, Ebola, H1N1 influenza, MERS, SARS, and Zika. In addition, research has established or strongly suggested a zoonotic origin for diseases such as bubonic plague, chikungunya, dengue fever, HIV/AIDS, Lyme disease, the 1918 Spanish flu, salmonellosis, and rabies. It is also now widely accepted that hunting and the bushmeat trade have become important factors in the transmission of zoonotic diseases (Hilderink and De Winter, 2021). The case of SARS-CoV-2 (COVID-19) is emblematic. While many hypotheses were initially proposed, it is now widely

---

[151]As of 2021, the numbers of rhinoceros are as follows: 15 940 southern white rhinos, 2 northern white rhinos, 6 195 black rhinos, 4 014 Indian rhinos, 76 Javan rhinos, and 41 Sumatran rhinos.

[152]The list of major zoonotic diseases can be found in Rahman et al. (2020).

accepted that bats and pangolins likely played a role as reservoirs or intermediate hosts in the transmission of the virus (Zhang *et al.*, 2021). However, Bernstein *et al.* (2022) identified three key areas for pandemic prevention: regulation of wildlife trade and hunting, mitigation of agricultural intensification and expansion, and conservation of tropical forests. The study also estimated that the cost of primary pandemic prevention measures is significantly less than the economic and human losses caused each year by emerging viral zoonoses.

The overexploitation of tropical forests is not limited to timber and wild animals. According to Peres (2010), it also includes plant products such as fruits, nuts, oil seeds, latex, resins, gums, medicinal plants, spices, dyes, ornamental plants, and raw materials such as firewood, climbing palms, bamboo, and rattan. Palm oil is a prominent example, and wild orchids are another[153].

3.5   Climate change

The case of climate change is examined in detail in Part 2 of Roncalli (2025). For example, Chapter 8 explains the concept and economic implications of climate change, while Chapter 12 discusses the physical risk of climate change. Climate change and biodiversity are inextricably linked. A rise in temperature, more intense precipitation, and an increase in natural disasters will naturally affect biodiversity. Animals such as butterflies, insects and birds are typical examples. Similarly, climate change has significant impacts on many aspects of non-animal biodiversity, including agriculture, forests, freshwater ecosystems and soil health.

4   Biodiversity measurement

Measuring biodiversity is essential for governments, regions, municipalities, companies, financial institutions and investors for two primary reasons. First, they operate within regulatory frameworks that increasingly require biodiversity risk monitoring[154]. Second, they must make decisions that either affect or are affected by biodiversity, a concept known as double materiality. For example, a company's corporate social responsibility strategy must include a biodiversity dimension, project financing should consider the potential for biodiversity loss, and governments need biodiversity metrics to develop effective conservation strategies and policies. Similar to ESG and climate risk assessment, measuring biodiversity risk requires the collection of relevant data. This data is then used within standardized methodologies to calculate biodiversity metrics, such as mean species abundance. In addition, a variety of commercial and open source solutions are available to assess biodiversity risk at various scales, including geospatial points, regional, national, and company-specific levels.

4.1   Essential biodiversity variables

Measuring biodiversity is complex due to its multifaceted nature and numerous dimensions. Moreover, even when focusing on a single dimension, data availability is often limited. However, these data are critical for assessing progress towards biodiversity goals. Mace and Baillie (2007) emphasized the importance of developing effective biodiversity indicators that are relevant to policy objectives and simple enough to facilitate comparisons between regions and countries. They discussed the distinction between pressures, status and responses, and called for urgent action to define a set of biodiversity indicators that are truly relevant for measuring biodiversity risks. Nearly twenty years

---

[153]According to UNODC (2024), the five most trafficked plant species are cedar and other sapindales, rosewood, agarwood and other myrtales, golden chicken fern, and orchids. Palm oil is not listed in CITES.
[154]This is discussed further in the following section on biodiversity governance and regulation.

later, significant progress has been made, but biodiversity measurement remains a challenge due to the lack of consistent and clear indicators. The article by Mace and Baillie was written in the context of the 2010 Biodiversity Target adopted by the Convention on Biological Diversity (CBD), whose objective was to "*halt the loss of biological diversity at all levels by the year 2010.*" The monitoring of progress was defined with respect to 22 headline indicators[155]. In fact, a number of these indicators were vague, for example the indicators (8) Ecological footprint and related concepts, (10) Trends in invasive alien species and (15) Incidence of human-induced ecosystem failure.

Table 47: EBV classes and names

#	EBV class	EBV theme
1	Genetic composition	Genetic diversity (richness and heterozygosity), genetic differentiation (number of genetic units and genetic distance), effective population size, inbreeding
2	Species populations	Species distributions, species abundances
3	Species traits	Morphology, physiology, phenology, movement, reproduction
4	Community composition	Community abundance, taxonomic/phylogenetic diversity, trait diversity, interaction diversity
5	Ecosystem functioning	Primary productivity, ecosystem phenology, ecosystem disturbances
6	Ecosystem structure	Live cover fraction, ecosystem distribution, ecosystem vertical profile

Source: https://geobon.org/ebvs/what-are-ebvs.

The lack of clear indicators led Pereira *et al.* (2013) to introduce the concept of essential biodiversity variables (EBVs), with the aim of establishing a standardized framework for monitoring biodiversity change worldwide:

> "*Despite progress in digital mobilization of biodiversity records and data standards, there is insufficient consistent national or regional biodiversity monitoring and sharing of such information. Along with inadequate human and financial resources, a key obstacle is the lack of consensus about what to monitor. Many initiatives collect data that could be integrated into an EBV global observation network, though important gaps remain. Different organizations and projects adopt diverse measurements, with some important biodiversity dimensions, such as genetic diversity, often missing.*" (Pereira *et al.*, 2013, page 277).

The essential biodiversity variables are maintained by the Group on Earth Observations Biodiversity Observation Network[156] (GEO BON). Table 47 shows the 6 EBV classes and the associated EBV themes[157]. Schmeller *et al.* (2018) proposed to focus on the eight candidate EBVs given in Table 48. Many other indicators have been proposed by the scientific community, the latest and most promising indicators are certainly the remote sensing geospatial patterns measured by satellites (Skidmore *et al.*, 2021). All these indicators can be used to build a biodiversity scoring system. However, the lack of consensus and standardization remains an obstacle to biodiversity monitoring.

---

[155]For instance, the first three indicators were (1) Trends in extent of selected biomes, ecosystems, and habitats, (2) Trends in abundance and distribution of selected species and (3) Coverage of protected areas.

[156]The website is www.geobon.org, while the EBV datasets are available at https://portal.geobon.org/datasets.

[157]Here are some examples of EBV indicators promoted by GEO-BON: Biodiversity Habitat Index (BHI), Genetic Diversity Indicator (GDI), Global Ecosystem Restoration Index (GERI), Local Biodiversity Intactness Index (LBII),

Table 48: Eight essential biodiversity variables (Schmeller *et al.*, 2018)

Indicator	Definition
Abundance	Abundance is the number of individuals of a species within a local population.
Allelic diversity	Allelic diversity is the average number of alleles per locus in a population of a given species.
Body mass	Body mass scaled by body size, or the body mass index (BMI), indicates the condition and energy reserves of animals.
Ecosystem heterogeneity	Ecosystem heterogeneity describes the amount of variability in space and time of ecosystems.
Phenology	Phenology is defined as annually recurring life-cycle events, such as the timing of migration or flowering.
Range dynamics	Range dynamics are changes in species distributions through time, space and shape. This EBV is derived from the species distribution EBV for detecting critical ecological change early.
Size at first reproduction	Size at first reproduction is the individual body size (length) reached by an organism at the time when its first reproduction occurs.
Survival rates	Survival rate is the average probability that an organism will stay alive between two time points.

Source: Schmeller *et al.* (2018).

4.2 Biodiversity metrics

We have already mentioned the Living Planet Index and the Red List Index[158]. These indices focus on the extinction risk of species, and the better geographic resolution we have is the country. Below we present alternative simple measures of biodiversity that are available at higher resolutions.

4.2.1 Mean species abundance (MSA)

Mean species abundance is one of the most popular biodiversity indicators because it is easy to understand and has been widely popularized by GLOBIO (`www.globio.info`). Let n_i be the abundance of species i in an area A, $n_i^\star$ be the abundance of species i in a reference state, and S_A be the number of native species in the area. The MSA of area A is calculated as follows:

$$\text{MSA} = \frac{1}{S_A} \sum_{i=1}^{S_A} \min\left(\frac{n_i}{n_i^\star}, 1\right)$$

By construction we have $\text{MSA} \in [0, 1]$. An MSA of 1 corresponds to an undisturbed area, while a low MSA value indicates a highly disturbed area, where many native species have disappeared or experienced significant population declines. Consider the example illustrated in Figure 77. There are four native species in the reference area. In the disturbed area, the parrots have disappeared and have been replaced by rodents. The MSA is then calculated as follows:

$$\text{MSA} = \frac{1}{4}\left(\frac{0}{2} + \frac{2}{4} + \frac{3}{4} + \frac{1}{2}\right) = 43.75\%$$

Protected Area Representativeness & Connectedness indices (PARC), Invasive Alien Species Rate (IAS), Species Habitat Index (SHI), Species Protection Index (SPI), and Species Status Information Index (SSII).

[158]See Roncalli (2025, Chapter 2).

Figure 77: Computation of the MSA

Reference   Disturbed
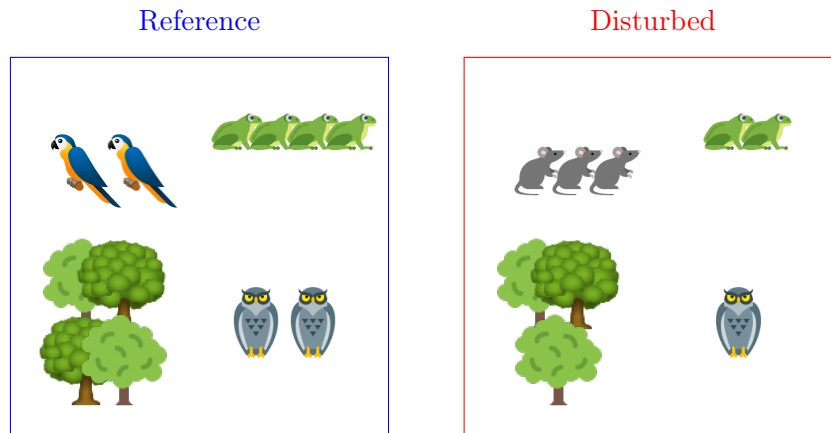
In GLOBIO, the MSA is calculated for different pressures: land use, climate change, roads, nitrogen deposition, hunting. An overall MSA is calculated by combining the MSA of the different pressures (Alkemade *et al.*, 2009):

$$\text{MSA} = \prod_{j=1}^{p} \text{MSA}_{(j)}$$

where $\text{MSA}_{(j)}$ is the MSA for pressure j and p is the number of pressures (between 1 and 5). According to Schipper *et al.* (2020), the contribution of pressure j to biodiversity loss is equal to:

$$C_{(j)} = \frac{\left(1 - \text{MSA}_{(j)}\right)}{\sum_{j=1}^{p} \left(1 - \text{MSA}_{(j)}\right)} \left(1 - \text{MSA}\right)$$

where $1 - \text{MSA}_{(j)}$ is the biodiversity loss for pressure j.

Figure 78 shows global MSA values for the year 2015. Notably, MSA values approach one in polar regions and deserts. This pattern requires careful interpretation because the MSA does not measure biodiversity richness, but rather the intactness of biodiversity relative to an undisturbed reference state (Schipper *et al.*, 2020). In naturally species-poor ecosystems such as deserts, tundra, and polar regions, where reference biodiversity is already low, even limited human disturbance results in high MSA values. This reflects minimal deviation from the natural state rather than high biodiversity. In essence, when the reference biodiversity of a region is naturally low, the potential for biodiversity loss is limited, resulting in MSA values close to one in these ecosystems despite their relatively low species richness. This illustrates an important characteristic of the MSA metric: it quantifies the relative preservation of native ecological communities rather than absolute biodiversity.

Remark 16 *Since the release of the first version of GLOBIO in 2000, the model has been improved and enriched over the years. Three extensions of GLOBIO have been developed to cover additional relevant aspects of nature. GLOBIO-ES models changes in global ecosystem services by assessing current conditions, trends and future scenarios of nature's benefits to humans, such as food, water, climate regulation, soil health and health support. GLOBIO-Aquatic models the health of freshwater ecosystems by quantifying biodiversity (MSA) and water quality (algal blooms) based on human pressures such as land use, flow alteration, eutrophication and temperature. GLOBIO-Species models how human pressures affect the distribution and population size of individual vertebrate species, enabling the calculation of biodiversity indicators such as the RLI and LPI metrics to track progress towards biodiversity goals.*

Figure 78: Mean species abundance values for 2015 (GLOBIO 4)
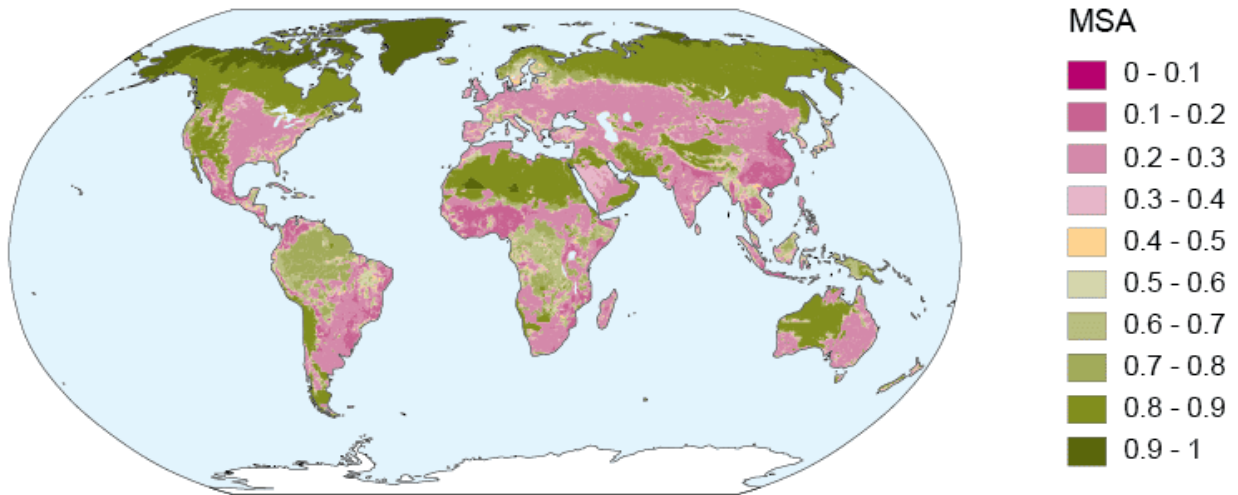
4.2.2 Potentially disappeared fraction (PDF)

The potentially disappeared fraction is a metric used to assess the biodiversity loss due to environmental change, particularly human activities such as pollution, habitat destruction, and climate change. Originally developed by Müller-Wenk (1998), it has been widely used in life cycle assessment (LCA) models to evaluate the environmental footprint of products and activities. PDF represents the fraction of species that have disappeared or are expected to disappear from a region due to environmental pressures such as land use, climate change, or pollution[159]. The PDF of area A is:

$$\text{PDF} = \frac{S_0 - S_A}{S_0} = \frac{1}{S_0} \sum_{j=1}^{S_0} \mathbb{1}\left\{j \notin A\right\}$$

where S_0 is the undisturbed species richness of A, S_A is the current species richness of A, and j is the species index. PDF equals zero if no species disappear (no biodiversity loss), while PDF equals one if all species in the considered ecosystem disappear (total biodiversity loss). PDF is equal to 25% for the area shown in Figure 77, because 25% of the species in this area have disappeared (parrot species have disappeared, while frogs, trees, and owls remain).

The PDF approach has been popularized by the ReCIPe LCA model (Goedkoop *et al.*, 2008), which provides characterization factors (CFs) that translate human interventions in the environment (emissions, resource use, land use) into potential impacts on biodiversity, often expressed as PDF values. More complex approaches have been developed to calculate PDFs and CFs, such as the model of Kuipers *et al.* (2021), which uses the species-area relationship and defines new characterization factors[160]. The unit PDF.m^2.yr is often used. It represents the potential area (in square meters) where all species are potentially lost per year. For instance, 10 PDF.m^2.yr means that $10\,\text{m}^2$ has lost all its species during a year.

---

[159]We have already encountered the PDF measure when studying the species-area relationship. The PDF measure is a generalization of the metric $\mathcal{L}oss_{species}$ when the pressures are not limited to habitat loss (see Equation (16) on page 78).

[160]CF and PDF values can be found in the Supplementary Data available online (Tables S2 and S3).

4.2.3 Biodiversity intactness index (BII)

A biodiversity intactness index is a metric that aims to measure how much of a region's natural biodiversity remains, despite human impacts. For instance, if we measure intactness at the species level, we can define the BII from the PDF: BII = 1 − PDF. Scholes *et al.* (2005) proposed the following empirical estimator of the biodiversity intactness index:

$$\text{BII} = \frac{\sum_i \sum_j \sum_k S_{i,j} A_{j,k} I_{i,j,k}}{\sum_i \sum_j \sum_k R_{i,j} A_{j,k}} \tag{37}$$

where i is the taxon index, j is the ecosystem index, k is the land use index, $S_{i,j}$ is the species richness of taxon i in ecosystem j, $A_{j,k}$ is the area of land use k in ecosystem j, and $I_{i,j,k}$ is the population impact or relative population of taxon i (compared to the reference state) under land use k in ecosystem j. We generally assume that $I_{i,j,k} \leq 1$, but there may be special situations where the population has increased, meaning that $I_{i,j,k}$ may be greater than 1. At first glance, Formula (37) seems complex, but it is simply a weighted average of the various population impacts:

$$\text{BII} = \sum_i \sum_j \sum_k w_{i,j,k} I_{i,j,k}$$

where $w_{i,j,k} = \dfrac{S_{i,j} A_{j,k}}{\sum_i \sum_j \sum_k R_{i,j} A_{j,k}}$ and the sum of weights is equal to one — $\sum_i \sum_j \sum_k w_{i,j,k} = 100\%$. If there is only one ecosystem and one land use, Formula (37) reduces to the weighted average of the population impacts where the weights are proportional to the species richness S_i of taxon i. For example, assuming there are three taxonomic groups (birds, mammals, and plants), the species richness is 100 bird species, 50 mammal species, 200 plant species, and the population impacts are 50%, 80%, and 90%, respectively, we get:

$$\text{BII} = \frac{100 \times 50\% + 50 \times 80\% + 200 \times 90\%}{100 + 50 + 200} = \frac{270}{350} = 77.14\%$$

Table 49: Biodiversity intactness index in % of tropical forests (2001–2012)

Region	Metric	ISO code							
		ARG	BOL	BRA	CHL	COL	CUB	PER	PRY
South America	2001 BII	48.3	72.8	82.7	14.6	81.2	18.0	88.2	58.2
	2012 BII	46.4	71.2	80.7	16.1	80.0	19.3	87.5	53.0
	Change (in %)	−3.8	−2.2	−2.4	10.2	−1.4	7.8	−0.8	−8.9
		CIV	CMR	COD	COG	GAB	LBR	SLE	TGO
Africa	2001 BII	57.0	79.7	84.2	89.7	87.9	72.6	60.2	58.7
	2012 BII	41.9	79.3	83.2	88.8	87.3	72.8	57.2	57.7
	Change (in %)	−26.4	−0.5	−1.2	−1.1	−0.7	0.3	−4.9	−1.8
		CHN	KHM	IDN	IND	LAO	MYS	THA	VNM
South Asia	2001 BII	38.6	41.2	75.8	13.3	64.5	79.6	31.0	39.5
	2012 BII	36.4	34.5	70.4	13.0	61.3	70.5	29.7	38.2
	Change (in %)	−5.5	−16.2	−7.1	−1.5	−4.9	−11.4	−4.2	−3.4

Source: De Palma *et al.* (2021), https://doi.org/10.5519/5wriutqz & Author's calculations.

The calculation of the biodiversity intactness index requires the collection of population impacts for different pressures and taxa. Data sets can be found on various websites such as www.nhm.ac.

uk/our-science/services/data/biodiversity-intactness-index.html. In Table 49 we report the values of the biodiversity intactness index in tropical forests calculated by De Palma *et al.* (2021) between 2001 and 2012. We find high heterogeneity even within the same region. For example, Peru had a BII of 88% in 2012, while it was only 19% in Argentina. Côte d'Ivoire experienced the largest decline (-26%), while the intactness of biodiversity in Chile improved by 10% between 2011 and 2012.

4.2.4 Species threat abatement and restoration (STAR)

The species threat abatement and restoration (STAR) metric is a global framework designed to quantify and guide efforts to reduce biodiversity loss. It measures the potential contribution of specific conservation actions (reducing pressure on species and restoring habitats) to improving the status of threatened species. According to Mair *et al.* (2021), for a given location i and a given threat j, the STAR threat-abatement score is calculated as a weighted average of the species IUCN Red List status:

$$T_{i,j} = \sum_{s=1}^{S} T_{i,j}^{(s)} = \sum_{s=1}^{S} \pi_{i,s} w_s c_{j,s}$$

where $\pi_{i,s} \in [0,1]$ is the current area of habitat (AOH) of species s within location i — expressed as a percentage of the current global AOH of the species, $w_s \in \{1,2,3,4\}$ is the IUCN Red List category weight[161] of species s, $c_{j,s}$ is the relative contribution of threat j to the extinction risk of species s, and S is the species richness at location i. The STAR restoration score for a given location i and a given threat j is calculated as:

$$R_{i,j} = \sum_{s=1}^{S} R_{i,j}^{(s)} = \sum_{s=1}^{S} \varphi_{i,s} w_s c_{j,s} m_{i,s}$$

where $\varphi_{i,s} \in [0,1]$ is the amount of restorable AOH for species s at location i — expressed as a percentage of the current global AOH of the species, and $m_{i,s} > 0$ is a multiplier appropriate for the habitat at location i to discount restoration results — the default value is 29%. The scores $T_{i,j}$ and $R_{i,j}$ can be decomposed to obtain the contribution $T_{i,j}^{(s)}$ and $R_{i,j}^{(s)}$ of each species. By construction, the contributions are between 0 and 1, while the scores are between 0 and the species richness S. Below, we provide an example to compute $T_{i,j}$ and $R_{i,j}$ and their species contribution $T_{i,j}^{(s)}$ and $R_{i,j}^{(s)}$:

Species	Red List	w_s	$\pi_{i,s}$	$c_{j,s}$	$\varphi_{i,s}$	$m_{i,s}$	$T_{i,j}^{(s)}$	$R_{i,j}^{(s)}$
Salmo salar (salmon)	NT	1	25%	90%	10%	29%	0.225	0.026
Phengaris teleius (butterfly)	VU	2	50%	90%	25%	29%	0.900	0.131
Conraua goliath (frog)	EN	3	80%	80%	25%	29%	1.920	0.174
Pericallis malvifolia (magnolia)	CR	4	75%	80%	20%	29%	2.400	0.186
Total							5.445	0.516

The site contains four species, each belonging to a different IUCN Red List category. Salmon occupy 25% of the habitat, indicating this is either a marine site or one with rivers. The threat contribution is high at 90%, meaning this threat is responsible for 90% of the extinction risk to salmon. Potential habitat restoration is 10%, suggesting we can reduce extinction risk by that amount. This yields an absolute contribution of 0.225 for salmon, representing 4.1% of the total threat-abatement score.

---

[161]w_s takes the values 1, 2, 3, and 4 for near threatened, vulnerable, endangered, and critically endangered, respectively.

In contrast, magnolias represent 44% of the threat-abatement score due to two main factors: they cover a larger habitat area, and the species *Pericallis malvifolia* is classified as critically endangered on the IUCN Red List.

Figure 79: Global STAR threat-abatement score for amphibians, birds and mammals (at a 50-km grid cell resolution)
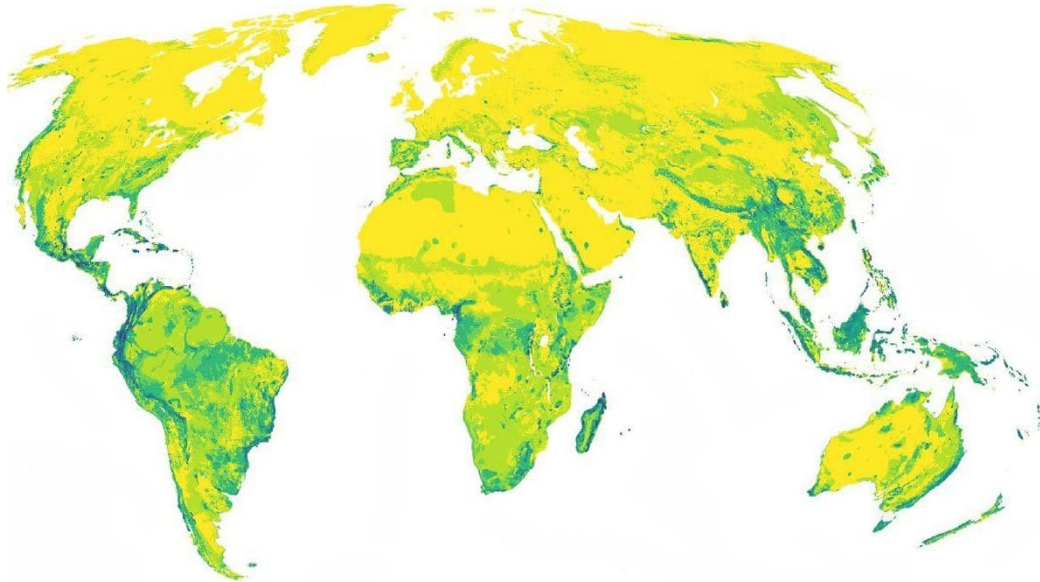
Source: Mair *et al.* (2021, Figure 2).

Figure 79 illustrates the global STAR threat-abatement scores for amphibians, birds, and mammals as calculated by Mair *et al.* (2021). The color gradient ranges from yellow (low scores) to green (high scores). The distribution shows that biodiversity conservation priorities are geographically concentrated in some regions, particularly South America, South Asia, and southern Africa, suggesting that effective biodiversity risk management requires targeted approaches in these hotspots:

> "*While every nation can contribute towards halting biodiversity loss, Indonesia, Colombia, Mexico, Madagascar and Brazil combined have stewardship over 31% of total STAR values for terrestrial amphibians, birds and mammals. Among actions, sustainable crop production and forestry dominate, contributing 41% of total STAR values for these taxonomic groups. Key Biodiversity Areas cover 9% of the terrestrial surface but capture 47% of STAR values.*" (Mair *et al.*, 2021, page 836).

4.2.5 Comparison of these methodologies

Which methodology is best? There is no definitive answer. First, in addition to the widely accepted approaches, there are numerous other valuable methodologies that receive less attention but provide important insights into biodiversity assessment. Second, these methodologies target different aspects of biodiversity — from species abundance and richness to density and ecosystem integrity — making direct comparisons problematic. Third, while all of these methodologies require substantial data inputs, they often present simplified perspectives by focusing on single dimensions of biodiversity. In particular, they focus primarily on species populations, which represent only one of the six essential biodiversity variables. This explains why these methods are so closely related (Rossberg,

2022; Rossberg *et al.*, 2023). Fourth, a major limitation of these approaches is their general failure to incorporate ecosystem services — a critical dimension for a comprehensive understanding of biodiversity and its relationship to human well-being.

4.3 Commercial solutions

In addition to the established biodiversity measurement practices seen previously, a wide range of commercial approaches has emerged, offering diverse tools such as datasets, analytical software, calculation methods and comprehensive assessment services. In their Update Report 5 for the EU Business & Biodiversity Platform, De Ryck *et al.* (2024) documented 37 different approaches, indicating a significant increase in demand for biodiversity advisory services. However, concerns remain about the robustness and long-term viability of these tools. This pattern mirrors the evolution of ESG measurement, which has experienced rapid expansion followed by a period of consolidation. Critically, despite widespread agreement on the need for standardization and alignment, neither regulatory nor voluntary disclosure frameworks mandate specific measurement approaches. This is a significant barrier.

Table 50 provides an overview of available biodiversity assessment solutions. De Ryck *et al.* (2024) proposes a framework for evaluating these tools based on eight key criteria: business context, biodiversity pressures, level of ambition, scope, metrics, data requirements, implementation effort, and sector applicability. This framework allows companies to select methodologies that meet their specific needs and capabilities[162]. The landscape of biodiversity assessment tools varies widely in specialization — some are tailored to specific industries such as finance, mining or agriculture, while others are broadly applicable. These solutions also vary in their measurement granularity, with capabilities ranging from localized assessments (site or project level) to broader assessments (product, company or entire supply chain analysis). They also address different dimensions of biodiversity, including species diversity, habitat integrity, and ecosystem services, while accounting for different environmental pressures, such as land-use change, climate impacts, pollution sources, and the spread of invasive species. A critical criterion for selecting an approach is the scope of the solution, which defines the boundaries of what is included when measuring impacts and dependencies. These scopes can be categorized as follows[163]:

1. Scope 1: Impacts generated within the entity's control and other impacts directly caused by the entity during the assessment period;

2. Scope 2: Impacts resulting from the generation of non-fuel energy (electricity, steam, heat and cooling) for use at the site level, including impacts from land use change, fragmentation and related factors;

3. Scope 3

    (a) Scope 3 Upstream: Impacts that are a consequence of the company's activities, but are caused by sources not owned or controlled by the company within its upstream supply chain;

    (b) Scope 3 Downstream: Impacts that are a consequence of the company's activities, but are caused by sources not owned or controlled by the company within its downstream consumption and waste processes.

---

[162]See also Bailon *et al.* (2024) for a comparison of the different solutions.

[163]These scope definitions are based on the GHG Protocol and are analogous to the scope definitions used to measure GHG emissions (see Roncalli (2025, Section 9.1.3)).

Table 50: List of commercial solutions for measuring biodiversity

Sigle	Name	Sponsors	OS[‡]
ABD Index	AgroBioDiversity Index	Alliance of Bioversity International, CIAT	
B-INTACT	Biodiversity Integrated Assessment Computation Tool	FAO	✓
BFFI	Biodiversity Footprint for Financial Institutions	ASN Bank, CREM, PRé Sustainability	✓
BFM	Biodiversity Footprint Methodology	Plansup	
BIA-GBS	Biodiversity Impact Analytics – Global Biodiversity Score	CDC Biodiversité, Carbon4 Finance	
BIAT	Biodiversity Impact Assessment Tool	ISS ESG	
BII	Biodiversity Intactness Index	Natural History Museum (UK)	
BIM	Biodiversity Impact Metric	Cambridge Institute for Sustainable Leadership	
BRF	Biodiversity Risk Filter	WWF	✓
CBF	Corporate Biodiversity Footprint	Iceberg Datalab	
ENCORE	Exploring Natural Capital Opportunities, Risks and Exposure	Global Canopy, UNEP FI, UNEP-WCMC	✓
GBS	Global Biodiversity Score	CDC Biodiversité	
GBSFI	Global Biodiversity Score for Financial Institutions	CDC Biodiversité	
GID	Global Impact Database	Impact Institute	
GIST NBS	Nature & Biodiversity Suite (BIGER/SLAM/DIRO 360)	GIST Impact	
IBAT	Integrated Biodiversity Assessment Tool	BirdLife International, Conservation International, IUCN, UNEP-WCMC	
InVEST	Integrated Valuation of Ecosystem Services and Trade-offs	Natural Capital Project	✓
MBFM	MSCI Biodiversity Footprint Metrics	MSCI	
NRP	Nature Risk Profile	S&P Global	
NVE	Nature Value Explorer	Flemish Institute for Technological Research	✓
PBF	Product Biodiversity Footprint	I Care	

[‡]OS stands for Open Source.

Comparison of biodiversity assessment solutions reveals a paradoxical landscape characterized by both significant uniformity and heterogeneity. On the one hand, there is considerable homogeneity in the basic approaches, with most methodologies primarily emphasizing metrics of species abundance and diversity. Many solutions are based on identical underlying data sets, which are simply presented through different interfaces or analytical frameworks. On the other hand, there is considerable heterogeneity in the maturity of these solutions. Established tools have been widely adopted by many institutions over long periods of time and have evolved into comprehensive, integrated platforms. Meanwhile, other solutions remain in earlier stages of development, functioning essentially as proofs of concept or experimental approaches with limited implementation history.

5 Biodiversity governance and regulation

Biodiversity risk, like climate risk, is subject to regulation, and its governance has evolved significantly in recent years. While the political agenda may lack clarity, its mere existence represents progress. In particular, the Conference of the Parties has recently received more media attention than in previous years.

5.1 Convention on Biodiversity (CBD)

The Convention on Biological Diversity was adopted at the 1992 Earth Summit in Rio de Janeiro and entered into force in 1993. The purpose of this international treaty is to address the global loss of biological diversity, with the following objectives:

1. The conservation of biological diversity;

2. The sustainable use of its components;

3. The fair and equitable sharing of the benefits arising out of the utilization of genetic resources.

Similar to the United Nations Framework Convention on Climate Change (UNFCCC), the Conference of the Parties (COP) serves as the governing body of the CBD, meeting every two years to make key decisions. Some of the major treaties and initiatives adopted under the CBD include:

- The International Coral Reef Initiative (1994, COP1, Bahamas), a partnership of nations and organizations to protect coral reefs;

- The Cartagena Protocol on Biosafety (2000), which regulates the international movement of living modified organisms to ensure biosafety;

- The Nagoya Protocol on Access and Benefit-Sharing (2010, COP10, Japan), which establishes a legal framework for the equitable sharing of benefits arising from the use of genetic resources, and adopts the Aichi Biodiversity Targets (2011–2020), which set 20 global targets for biodiversity conservation;

- The Pyeongchang Roadmap (2014, COP12, South Korea), which aims to accelerate global efforts to achieve the Aichi Biodiversity Targets;

- The Kunming-Montreal Global Biodiversity Framework, known as the GBF (2022, COP15), which includes the goal of protecting 30% of the Earth's land and marine areas by 2030 (the 30×30 target).

Table 51: Aichi Biodiversity Targets (2011–2020)

Strategic Goal A	Address the underlying causes of biodiversity loss by mainstreaming biodiversity across government and society (Target 1–4)
Strategic Goal B	Reduce the direct pressures on biodiversity and promote sustainable use (Target 5–10)
Strategic Goal C	To improve the status of biodiversity by safeguarding ecosystems, species and genetic diversity (Target 11–13)
Strategic Goal D	Enhance the benefits to all from biodiversity and ecosystem services (Target 14–16)
Strategic Goal E	Enhance implementation through participatory planning, knowledge management and capacity building (Target 17–20)
Target 5	By 2020, the rate of loss of all natural habitats, including forests, is at least halved and, where feasible, brought close to zero, and degradation and fragmentation are significantly reduced
Target 7	By 2020 areas under agriculture, aquaculture and forestry are managed sustainably, ensuring conservation of biodiversity
Target 8	By 2020, pollution, including from excess nutrients, has been brought to levels that are not detrimental to ecosystem function and biodiversity
Target 9	By 2020, invasive alien species are identified, priority species are controlled or eradicated, and measures are in place to manage pathways to prevent their introduction and establishment
Target 11	By 2020, at least 17% of terrestrial and inland water areas and 10% of coastal and marine areas are protected by well-connected systems of protected areas
Target 12	By 2020, the extinction of known threatened species has been prevented, and their conservation status has been improved and maintained, especially for those species most in decline
Target 15	By 2020, the resilience of ecosystems has been enhanced, including restoration of at least 15% of degraded ecosystems
Target 20	By 2020, the goal is to significantly increase financial resources for effective implementation of the Strategic Plan for Biodiversity 2011–2020

Source: https://www.cbd.int/sp/targets.

5.1.1 Aichi Biodiversity Targets

The Aichi targets are a set of 20 global biodiversity goals adopted at the 10th Conference of the Parties in Japan in 2010. These 20 targets are grouped into five strategic goals, as shown in Table 51. The overall objective is to reduce the rate of biodiversity loss, as reflected in some of the targets listed in Table 51. However, there is broad consensus that the world has failed to achieve any of the Aichi targets. Several factors have contributed to this failure. First, many of the targets are vague and lack clear, enforceable commitments, making it difficult to hold countries accountable. Enforcement mechanisms are limited, and the wording of many targets leaves room for interpretation. For example, Target 7 states that "*by 2020 areas under agriculture, aquaculture and forestry are managed sustainably, ensuring conservation of biodiversity.*" But what does that mean in practice? What specific actions should be taken? What metrics should be used to assess sustainability in these sectors? The lack of clear definitions and measurable indicators has weakened the impact of the targets. The second factor is inadequate funding, which creates a significant gap between what is needed and what is available for biodiversity conservation projects. For example, Target 20 states

that "*by 2020, at the latest, the mobilization of financial resources for effectively implementing the Strategic Plan for Biodiversity 2011–2020 from all sources, and in accordance with the consolidated and agreed process in the Strategy for Resource Mobilization, should increase substantially from the current levels.*" McCarthy *et al.* (2012) examined the financial costs of Targets 11 and 12, which relate to protected areas and extinction prevention. For Target 11, they estimated that protecting and effectively managing all terrestrial areas of global importance for bird conservation would cost $65.1 billion annually, and adding areas for other taxa would increase this to $76.1 billion annually. For Target 12, they estimated that reducing the risk of extinction of all globally threatened bird species by at least one IUCN Red List category would cost between $875 million and $1.23 billion, representing only 12% of current funding. In another study, by comparing actual expenditures with expected levels, Waldron *et al.* (2013) identified 40 severely underfunded countries, with the top five being Iraq, Djibouti, Angola, Kyrgyzstan, and Guyana. Most of the countries in this ranking are developing countries, with the exception of five developed countries: Finland, Iceland, France, Australia and Austria. More recently, the Paulson Institute, the Nature Conservancy, and the Cornell Atkinson Center for Sustainability conducted a comprehensive review of global biodiversity finance and concluded that there is a huge funding gap:

> "*This report determines that, in 2019, the total global annual flow of funds toward biodiversity protection amounted to approximately $124–143 billion per year against an estimated annual need of $722–967 billion to halt the decline in global biodiversity between now and 2030. Taken together, these figures reveal a biodiversity financing gap of $598–824 billion per year. [...] this report shows that annual governmental expenditures on activities harmful to biodiversity in the form of agricultural, forestry, and fisheries subsidies — $274–542 billion per year in 2019 — are two to four times higher than annual capital flows toward biodiversity conservation.*" (Deutz *et al*, 2020, page 12).

Finally, the third factor contributing to the failure of the Aichi targets was the lack of government commitment, inadequate monitoring and reporting by the CBD, and low public awareness. These factors combined to weaken stakeholder engagement, resulting in limited societal pressure for action.

5.1.2 Kunming-Montreal Global Biodiversity Framework

The failure of the Strategic Plan for Biodiversity 2011–2020 and its Aichi Biodiversity Targets created an urgent need for a more effective global approach. At CBD COP15 in December 2022, 192 countries responded by adopting the Kunming-Montreal Global Biodiversity Framework (GBF). This new framework aims to re-launch global biodiversity conservation efforts by addressing the gaps in national ambition and commitment, as well as previous initiatives. The GBF text is divided into several sections, the most important of which are Section F (2050 vision and 2030 mission), Section G (global goals for 2050) and Section H (global targets for 2030). According to Convention on Biological Diversity (2022), the vision of the Kunming-Montreal Global Biodiversity Framework is "*a world of living in harmony with nature where by 2050, biodiversity is valued, conserved, restored and wisely used, maintaining ecosystem services, sustaining a healthy planet and delivering benefits essential for all people.*" The four 2020 goals are to protect and restore (goal A), prosper with nature (goal B), share benefits fairly (goal C), and invest and collaborate (goal D). While the first three goals are easy to understand, the fourth goal is described as follows:

> "*Adequate means of implementation, including financial resources, capacity-building, technical and scientific cooperation, and access to and transfer of technology to fully implement the Kunming-Montreal Global Biodiversity Framework are secured and equitably accessible to all Parties, especially developing country Parties, in particular the*

Table 52: The 23 targets of the Kunming-Montreal Global Biodiversity Framework

Target	Purpose
1	Plan and manage all areas to reduce biodiversity loss
2	Restore 30% of all degraded ecosystems — terrestrial, inland water, and marine and coastal ecosystems
3	Conserve 30% of land, waters and seas — protected areas and other effective area-based conservation measures
4	Halt species extinction, protect genetic diversity, and manage human-wildlife conflicts
5	Ensure sustainable, safe and legal harvesting and trade of wild species (reducing the risk of pathogen spillover)
6	Reduce the introduction of invasive alien species by 50% and minimize their impact — eradicating or controlling invasive alien species, especially in priority sites, such as islands
7	Reduce pollution to levels that are not harmful to biodiversity — (a) reducing excess nutrients lost to the environment by at least half, (b) reducing the overall risk from pesticides and highly hazardous chemicals by at least half, (c) preventing, reducing, and working towards eliminating plastic pollution
8	Minimize the impacts of climate change on biodiversity and build resilience
9	Manage wild species sustainably to benefit people
10	Enhance biodiversity and sustainability in agriculture, aquaculture, fisheries, and forestry
11	Restore, maintain and enhance nature's contributions to people
12	Enhance green spaces and urban planning for human well-being and biodiversity
13	Increase the sharing of benefits from genetic resources, digital sequence information and traditional knowledge
14	Integrate biodiversity in decision-making at every level
15	Businesses assess, disclose and reduce biodiversity-related risks and negative impacts
16	Enable sustainable consumption choices to reduce waste and overconsumption
17	Strengthen biosafety and distribute the benefits of biotechnology
18	Reduce harmful incentives by at least $500 billion per year, and scale up positive incentives for biodiversity
19	Mobilize $200 billion per year for biodiversity from all sources, including $30 billion through international finance
20	Strengthen capacity-building, technology transfer, and scientific and technical cooperation for biodiversity
21	Ensure that knowledge is available and accessible to guide biodiversity action
22	Ensure participation in decision-making and access to justice and information related to biodiversity for all
23	Ensure gender equality and a gender-responsive approach for biodiversity action

Source: (Convention on Biological Diversity, 2022, pages 9–13).

least developed countries and small island developing States, as well as countries with economies in transition, progressively closing the biodiversity finance gap of $700 billion per year, and aligning financial flows with the Kunming-Montreal Global Biodiversity Framework and the 2050 Vision for biodiversity." (Convention on Biological Diversity, 2022, page 9).

Table 52 shows the 23 targets. At first glance, one might get the impression that the Kunming-Montreal targets are close to the Aichi targets. This is true, and we also note that some targets are always vague. However, if the official text is not technical, the CBD has done some work since its publication to be more precise. In fact, the guidelines for these targets, the indicators for monitoring progress and the national targets submitted to the CBD Secretariat are available on the website www.cbd.int/gbf/targets. For each target, we can find the following guidance notes prepared by the Secretariat:

A. Why is this target important?

B. Explanation of the target and its elements

C. Links to other elements of the Kunming-Montreal GBF, and other frameworks and processes

D. Guiding questions to national-setting

E. Indicators

F. Relevant resources that can assist implementation

Concerning indicators, they are split into three categories: headline indicators[164], component indicators and complementary indicators. For example, if we consider Target 6 on invasive alien species, there is one headline indicator (rate of invasive alien species establishment), three component indicators (rate of invasive alien species impact and rate of impact; rate of invasive alien species spread; number of invasive alien species introductions) and three complementary indicators (number of invasive alien species on national lists; trends in abundance, temporal occurrence and spatial distribution of non-indigenous species; Red List Index (impact of invasive alien species)).

A major challenge in implementing the Kunming-Montreal GBF is financing. Goal D of the GBF recognized a current biodiversity finance gap of $700 billion per year. To address this, Target 18 proposes to reduce incentives and subsidies that harm biodiversity by $500 billion per year by 2030, while

---

[164]Here are all the headline indicators identified by the CBD Secretariat as of March 2025: 1.A.1 Red List of ecosystems; 1.A.2 Extent of natural ecosystems; 1.1 Per cent of land and seas covered by biodiversity-inclusive spatial plans; 2.2 Area under restoration; 3.1 Coverage of protected areas and OECMs; 4.A.3 Red list Index; 4.A.4 The proportion of populations within species with an effective population size > 500; 5.1 Proportion of fish stocks within biologically sustainable levels; 6.1 Rate of invasive alien species establishment; 7.1 Index of coastal eutrophication potential; 7.2 Pesticide environment concentration; 9.1 Benefits from the sustainable use of wild species; 9.2 Percentage of the population in traditional occupations; 10.1 Proportion of agricultural area under productive and sustainable agriculture; 10.2 Progress towards sustainable forest management; 11.B.1 Services provided by ecosystems; 12.1 Average share of the built-up area of cities that is green/blue space for public use for all; 13.C.1 Indicator on monetary benefits received; 13.C.2 Indicator on non-monetary benefits; 15.1 Number of companies reporting on disclosures of risks, dependencies and impacts on biodiversity; 18.1 Positive incentives in place to promote biodiversity conservation and sustainable use; 19.D.1 International public funding, including official development assistance for conservation and sustainable use of biodiversity and ecosystems; 19.D.2 Domestic public funding of conservation and sustainable use of biodiversity and ecosystems; 19.D.3 Private funding (domestic and international) of conservation and sustainable use of biodiversity and ecosystems; 21.1 Indicator on biodiversity information for monitoring the global biodiversity framework. The first number is the GBF target number. Note that headline indicators have not yet been identified for some targets.

Target 19 specifies that at least \$200 billion per year needs to be mobilized by 2030 to implement national biodiversity strategies. The latter target includes increasing financial resources from developed countries, providing development assistance to developing countries, leveraging private finance, promoting blended finance, encouraging impact funds, and promoting innovative schemes such as payments for ecosystem services, green bonds, biodiversity offsets and credits, and benefit-sharing mechanisms. As previously noted, Deutz et al (2020) estimated biodiversity funding at \$124–143 billion per year in 2019, with the breakdown shown in Table 53. 57% and 20% are financed through domestic budgets and natural infrastructure, respectively. Green financial products, such as green bonds and nature-based solutions, account for less than 3%. Using the OECD's category of potential biodiversity subsidies, the authors estimated global harmful subsidies to be between \$274 and \$542 billion per year in 2019.

Table 53: Global biodiversity conservation financing in 2019 (in \$ bn)

Financial flows	Lower limit	Upper limit	Midpoint	Percentage
Domestic budgets and tax policy	74.6	77.7	76.2	57.1%
Natural infrastructure	26.9	26.9	26.9	20.2%
Biodiversity offsets	6.3	9.2	7.8	5.8%
Sustainable supply chains	5.5	8.2	6.8	5.1%
Official development assistance (ODA)	4.0	9.7	6.8	5.1%
Green financial products	3.8	6.3	5.0	3.8%
Philanthropy & conservation NGOs	1.7	3.5	2.6	2.0%
Nature-based solutions & carbon markets	0.8	1.4	1.1	0.8%
Total	123.6	142.9	133.3	100.0%

Source: Deutz et al (2020, Table 3.1, page 48).

Table 54: Global biodiversity conservation funding needs (in \$ bn)

Funding needs	Lower limit	Upper limit	Midpoint	Percentage
Croplands	315	420	367.5	43.5%
Protected areas	149	192	170.5	20.2%
Rangelands	81	81	81.0	9.6%
Urban environments	73	73	73.0	8.6%
Invasive alien species	36	84	60.0	7.1%
Coastal	27	37	32.0	3.8%
Fisheries	23	47	35.0	4.1%
Forests	19	32	25.5	3.0%
Total	722	967	844.5	100.0%

Source: Deutz et al (2020, Figure 4.1, page 55).

Estimated funding needs are reported in Table 54. Croplands and protected areas account for 64% of total funding, while fisheries and forest conservation accounts for only 7% of total funding (about \$60 billion per year). Deutz et al (2020) proposed nine financial and policy mechanisms to reduce the biodiversity financing gap. The optimistic estimate is a total positive financial flow of \$632.5 billion, which is insufficient to close the gap (Table 55). While significant progress has been made since 2022 (establishment of the Global Biodiversity Framework Fund (GBFF), launch of the Cali Fund), we are still not on track to meet the 23 goals of the Kunming-Montreal Global Biodiversity Framework.

Table 55: Estimated positive and negative flows to biodiversity conservation (in $ bn)

Financial flows	2019		2030	
	Lower limit	Upper limit	Lower limit	Upper limit
Harmful subsidy reform	−542.0	−273.9	−268.1	0.0
Domestic budgets and tax policy	74.6	77.7	102.9	155.4
Natural infrastructure	26.9	26.9	104.7	138.6
Biodiversity offsets	6.3	9.2	162.0	168.0
Sustainable supply chains	5.5	8.2	12.3	18.7
Official development assistance (ODA)	4.0	9.7	8.0	19.4
Green financial products	3.8	6.3	30.9	92.5
Philanthropy & conservation NGOs	1.7	3.5		
Nature-based solutions & carbon markets	0.8	1.4	24.9	39.9
Total	123.6	142.9	445.7	632.5

Source: Deutz *et al* (2020, Figure 5.1, page 64).

5.2 IPBES

Established in 2012, the Intergovernmental Science-Policy Platform on Biodiversity and Ecosystem Services (IPBES) is an international organization that assesses the state of the world's biodiversity and ecosystem services. It plays a similar role for biodiversity as the Intergovernmental Panel on Climate Change (IPCC) does for global warming. The current staff of the IPBES Secretariat is employed by UNEP and located in Bonn, Germany. In addition, about 2 900 experts participate or have participated in the work of IPBES. Its main functions are to provide comprehensive scientific assessments of the state of biodiversity and ecosystem services, to support policy development and implementation, and to identify key scientific information needed for policymakers. The organization has gained international recognition primarily through its influential assessment reports. As of March 2025, it has produced 13 assessment reports:

- Global reports

  - Global assessment report on biodiversity and ecosystem services (2019)

- Thematic reports

  - Pollinators, pollination and food production (2016)
  - Land degradation and restoration (2018)
  - Sustainable use of wild species (2022)
  - Invasive alien species and their control (2023)
  - Interlinkages among biodiversity, water, food and health (2024)

- Methodological reports

  - Scenarios and models of biodiversity and ecosystem services (2016)
  - The diverse values and valuation of nature (2022)
  - Underlying causes of biodiversity loss and the determinants of transformative change and options for achieving the 2050 Vision for Biodiversity (2024)

- Regional reports

  - Biodiversity and ecosystem services for Africa (2018)
  - Biodiversity and ecosystem services for the Americas (2018)
  - Biodiversity and ecosystem services for Asia and the Pacific (2018)
  - Biodiversity and ecosystem services for Europe and Central Asia (2018)

In addition, four new assessment reports will be published in the coming years: Impact and dependence of business on biodiversity and nature's contributions to people (2025); Monitoring biodiversity and nature's contributions to people (2026); Integrated biodiversity-inclusive spatial planning and ecological connectivity (2027); Second global assessment of biodiversity and ecosystem services (2028).

Figure 80: Some IPBES assessment reports
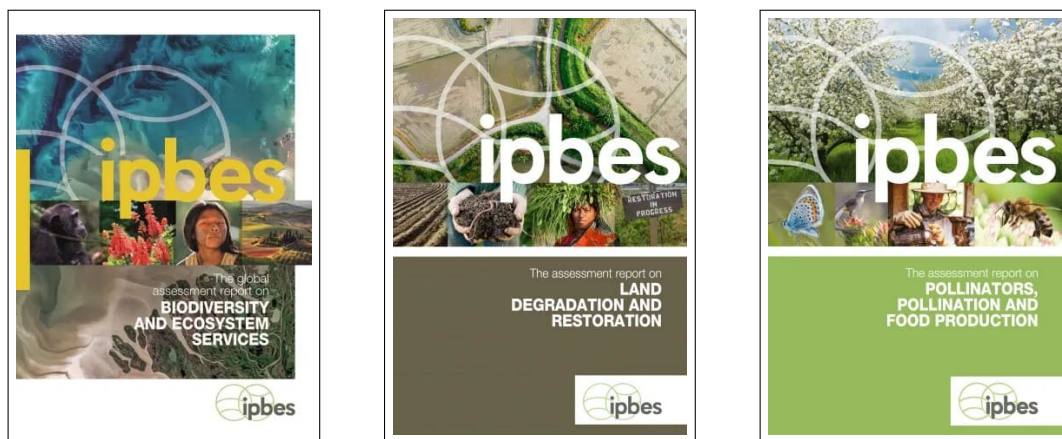
Source: IPBES & www.ipbes.net/assessing-knowledge.

5.3 TNFD

The Taskforce on Nature-related Financial Disclosures is a global initiative to develop a framework for companies and financial institutions to report and act on nature-related risks and opportunities. Officially launched in 2021 by four founding organizations (Global Canopy, UNDP, UNEP FI and WWF), the TNFD differs from the TCFD in that it is not supported by the Financial Stability Board (FSB) or any other international regulatory body. Instead, it is a market-driven initiative supported by national governments, corporations and financial institutions. The 40 members of the Taskforce are senior executives from financial institutions (17), corporations (17) and market service providers (6). In April 2024, the ISSB and TNFD announced joint research projects on risks and opportunities related to nature and human capital. However, there are currently no plans to integrate the TNFD framework into the ISSB's sustainability standards (IFRS S1 and IFRS S2).

TNFD uses the same structure as TCFD, organized into four pillars: Governance, Strategy, Risk & impact management, and Metrics & targets. The TNFD framework is based on 14 recommended disclosures, 11 of which are carried over from the TCFD framework (Table 56). The three additional recommended disclosures are (3) engagement with indigenous peoples, local communities (IPLC) and affected stakeholders, (7) disclosure of the location of assets and activities in direct operations and, where possible, in the upstream/downstream value chain, and (9) identification and assessment of

nature-related dependencies in the upstream/downstream value chain. According to TNFD (2023), the framework is consistent with ISSB and GRI standards, and is aligned with Target 15 of the Kunming-Montreal GBF. In addition, the TNFD has developed guidance for some specific sectors (*e.g.*, aquaculture, beverages, metals and mining, chemicals) and the following biomes: tropical and sub-tropical forests, savannas and grasslands, intensive land-use systems, urban and industrial ecosystems, rivers and streams, and marine shelf. Two types of indicators are included in TNFD:

- A small set of core indicators (global core indicators applicable to all sectors and sector core indicators for each sector)

- A large set of additional disclosure and assessment indicators (optional)

In TNFD (2023), there are 14 global core indicators, including 9 indicators for nature-related dependencies and impacts (Table 57) and 5 indicators for nature-related risks and opportunities (Table 58). In addition, TNFD (2023) introduces several additional global and sector-specific indicators[165].

Table 56: The 14 recommended disclosures (TNFD, 2023)

Pillar	#	Recommended Disclosure
Governance	1	Board oversight
	2	Management's role
	3	Human rights policies (IPLC)
Strategy	4	Risks and opportunities
	5	Impact on organization
	6	Resilience of strategy
	7	Locations of assets/activites/value chain
Risk management	8	Risk identification and assessment processes
	9	Dependencies in the value chain
	10	Risk management processes
	11	Integration into overall risk management
Metrics and targets	12	Nature-related metrics
	13	Metrics used to manage impacts and risks
	14	Nature-related targets

Source: TNFD (2023) & https://tnfd.global.

As of October 2024, there are 502 TNFD adopters, including 318 corporations and 129 financial institutions. The majority are located in Asia (236) and Europe (183). These adopters represent $17.7 trillion in assets under management and $6.5 trillion in market capitalization.

5.4   European biodiversity framework

The EU Biodiversity Strategy for 2030 was published in May 2020 and is part of the European Green Deal to tackle the ongoing biodiversity loss crisis. It replaces the Biodiversity strategy for 2020. The overall goal is to restore biodiversity and healthy ecosystems across the EU. Examples of quantitative targets include planting 3 billion trees by 2030, restoring 25 000 km of free-flowing rivers by removing barriers, increasing organic farming to 25% of agricultural land, and reducing pesticide use by 50%. In June 2022, the European Commission also adopted a proposal for a Nature Restoration Law. EU member states will have to develop their national restoration plans by 2026

---

[165]These can be found in TNFD (2023, Annex 2, pages 89–99) and Section 3 of the various sector guidance documents.

Table 57: TNFD core global disclosure indicators for nature-related dependencies and impacts

#	Indicator	Unit	GBF Targets
C1.0	Total spatial footprint	km^2	1, 2, 5, 11
C1.1	Extent of land/freshwater/ocean-use change	km^2	1, 2, 5, 11
C2.0	Pollutants released to soil split by type	tonne	7, 11
C2.1	Wastewater discharged	m^3	7, 11
C2.2	Waste generation and disposal	m^3	7, 11
C2.3	Plastic pollution	tonne	7, 11
C2.4	Non-GHG air pollutants	$PM_{2.5}$, etc.	7, 11
C3.0	Water withdrawal and consumption from areas of water scarcity	m^3	11
C3.1	Quantity of high-risk natural commodities sourced from land/ocean/freshwater	tonne	5, 9, 11
C4.0	Measures against unintentional introduction of invasive alien species		6, 11
C5.0	Ecosystem condition		1, 2, 3, 4, 11
C5.0	Species extinction risk		1, 2, 3, 4, 11

Table 58: TNFD core global disclosure indicators for nature-related risks and opportunities

#	Indicator
C7.0	Value of assets, liabilities, revenue and expenses that are assessed as vulnerable to nature-related transition risks (total and proportion of total)
C7.1	Value of assets, liabilities, revenue and expenses that are assessed as vulnerable to nature-related physical risks (total and proportion of total)
C7.2	Description and value of significant fines/penalties received/litigation action in the year due to negative nature-related impacts
C7.3	Amount of capital expenditure, financing or investment deployed towards nature-related opportunities, by type of opportunity, with reference to a government or regulator green investment taxonomy or third-party industry or NGO taxonomy, where relevant
C7.4	Increase and proportion of revenue from products and services producing demonstrable positive impacts on nature with a description of impacts

Table 59: Examples of TNFD additional global disclosure indicators

#	Indicator
A2.3	Light and noise pollution
A3.4	Area used for the production of natural commodities
A3.5	Use of wild species
A4.0	Number/extent of unintentionally introduced species, varieties or strains
A7.0	Value of write-offs and early retirements of assets due to nature-related risks
A8.4	Capital expenditure on adaption due to nature-related physical risks
A20.0	Proportion of sites that have active engagement with local stakeholders on nature-related issues

Source: TNFD (2023, Tables 6–10, pages 83–99).

with the following objectives: restore at least 30% of habitats in poor condition by 2030, 60% by 2040, and 90% by 2050. Since then, two guidelines on forest and soil monitoring have been published in 2023. In the coming years, we can expect new biodiversity laws and regulations in the European Union, following the establishment of the EU Biodiversity Platform (EUBP) in 2022. The platform currently consists of 10 working groups addressing various biodiversity issues[166].

6 Investment approaches

While ESG and climate investing are now two mainstream investment approaches in asset management, the concept of biodiversity investing is relatively new. In fact, the term '*biodiversity finance*' is generally more appropriate, as it encompasses a broader range of financial instruments beyond investment practices. Nevertheless, the field of biodiversity investing is developing rapidly. For example, with the exception of BIOFIN, which was launched by UNDP in 2012 following the CBD COP10 in Nagoya in 2010, most of the major biodiversity-focused financial initiatives and alliances have been created more recently, particularly following the One Planet Summit or the CBD COP15 in 2022 (Table 60). This also explains why biodiversity investing is a relatively new topic for academics[167], as most of the existing literature is in the gray area (Hutchinson and Lucey, 2024).

Table 60: Biodiversity finance initiatives

Acronym	Name	Website	Year
BCA	Biodiversity Credit Alliance	www.biodiversitycreditalliance.org	2022
BIOFIN	Biodiversity Finance Initiative	www.biofin.org	2012
BfN	Business for Nature	www.businessfornature.org	2019
FfB	Finance for Biodiversity Foundation	www.financeforbiodiversity.org	2021
NCIA	Natural Capital Investment Alliance	www.sustainable-markets.org	2021
NA 100	Nature Action 100	www.natureaction100.org	2023

Remark 17 *Biodiversity finance can include economic and financial instruments that are not related to the concepts of biodiversity investment. For example, most OECD research and publications on biodiversity finance focus on public finance, policy instruments such as taxes, subsidies or payments for ecosystem services.*

6.1 Financial instruments

The Global Biodiversity Framework considers that the private sector is essential to achieve the *2050 Vision for Biodiversity*, not just the public sector. For instance, the private sector is mentioned in several targets. Thus, Target 15 requires large companies and financial institutions to monitor, assess, and disclose biodiversity risks. Target 19 states that private resources must be mobilized by "*leveraging private finance, promoting blended finance, implementing strategies for raising new and additional resources, and encouraging the private sector to invest in biodiversity, including through impact funds and other instruments.*" To better understand biodiversity investing from the

---

[166]These are (1) Working group on forests and nature; (2) Invasive alien species expert group; (3) Sub-group on monitoring and assessment; (4) Working group on green infrastructure; (5) Working group on invasive alien species; (6) Commission expert group on the birds and habitats directives; (7) Marine issues; (8) Reporting under the nature directives; (9) Expert group on the nature restoration regulation; (10) Working group on pollinators.

[167]Recent academic research on biodiversity investing includes Giglio *et al* (2023b), Flammer *et al* (2025), Cherief *et al* (2025), and Coqueret *et al.* (2025).

perspective of private investors, one approach is to list the different instruments that fit into this category. Here is a classification of the main instruments:

- Fixed-income instruments

  - Blue bonds

    Definition Debt securities designed to raise capital for marine and ocean conservation projects (*e.g.*, protecting marine biodiversity, restoring coastal ecosystems, financing sustainable fisheries)

    Example Seychelles Blue Bond (2018), which raised $15 million to support sustainable marine areas and fisheries

  - Debt-for-nature swaps

    Definition Financial transactions in which a portion of a country's debt is forgiven in exchange for environmental commitments

    Example Gabon debt-for-nature swap (2023), which restructured $500 million of debt to protect 30% of marine and forest ecosystems

  - Green and sustainable bonds

    Definition Debt instruments that target environmental projects and sustainable land use

    Example Colombia Biodiversity Bond (BBVA/IFC), which raised $50 million to finance projects focused on reforestation and wildlife habitat restoration

  - Natural capital bonds, nature performance bonds and conservation performance bonds

    Definition Bonds that directly finance the protection and restoration of natural capital, with returns linked to specific ecological performance metrics and biodiversity outcomes, or that monetize the value of ecosystem services and biodiversity

    Example Voluntary carbon credit-linked bonds, such as the IFC Forest Bond

  - Sustainability-linked bonds and pay-for-success financial instruments

    Definition Bonds whose financial characteristics can change based on the achievement of sustainability targets

    Example Rhino Bond (2022), issued by the World Bank ($150 million), where returns are linked to the growth of the black rhino population in Africa

- Market-based instruments

  - Biodiversity credits/offsets

    Definition Tradable units representing positive biodiversity outcomes (market mechanisms to promote biodiversity conservation)

    Example UK Biodiversity Net Gain (BNG) policy (developers must ensure a 10% net gain in biodiversity by funding conservation projects or purchasing biodiversity credits)

  - Nature-based insurance products

    Definition Insurance mechanisms to protect natural capital and ecosystem services

    Example Parametric insurance for coral reef protection in the Caribbean and Central America (provides insurance coverage for coastal infrastructure and triggers payouts for reef restoration after hurricanes)

  - Payments for ecosystem services (PES)

Definition Schemes that provide financial incentives to landowners or communities to manage their land in a way that maintains or enhances ecosystem services

Example Vittel (Nestlé Waters) offers PES to farmers in the Vosges mountains in France to maintain water quality

- Investment funds

  - Biodiversity impact funds

    Definition Specialized investment vehicles focused on biodiversity conservation

    Example The African Forestry Impact Platform (AFIP) managed by Norfund, which invests in sustainable forestry and conservation projects

  - Blended finance

    Definition Combines public and private capital to attract more capital to biodiversity projects

    Example The Land Degradation Neutrality (LDN) Fund initiated by the United Nations Convention to Combat Desertification (UNCCD) and Mirova, which finances the rehabilitation of degraded land

  - Conservation trust funds

    Definition Long-term financing mechanisms for conservation and sustainable development

    Example Bhutan Trust Fund for Environmental Conservation (BTFEC)

  - Private equity and venture capital funds

    Definition Investment funds focused on companies and technologies that support biodiversity

    Example Regeneration VC Fund

6.2 The avoid-minimize-restore-offset approach

To effectively integrate biodiversity into investment processes, it is essential to understand the mitigation hierarchy, a fundamental principle of conservation biology (Arlidge *et al*, 2018). The mitigation hierarchy is a structured framework to guide decision-making in managing environmental impacts. It prioritizes actions to avoid, minimize, restore, and offset negative impacts on biodiversity (Figure 81). Avoid prevents negative impacts on biodiversity before they occur. This step emphasizes avoiding environmentally harmful activities and encourages decision-makers to choose alternative actions or project designs that have no or minimal adverse effects on biodiversity. For example, this might involve selecting a project site that is not located in a critical habitat or a biodiversity hotspot. Minimize aims to reduce the impact of unavoidable harm to biodiversity as much as possible by decreasing the magnitude, duration and/or intensity of potential impacts when they cannot be avoided completely. An example is implementing construction practices that reduce habitat destruction, such as minimizing land clearing or avoiding key wildlife breeding seasons. Restore focuses on rehabilitating ecosystems that have been damaged by development activities. This can include replanting trees in areas affected by deforestation, restoring native vegetation, or rebuilding habitat structures to support local ecological systems. Finally, if residual impacts remain after avoid, minimize, and restore measures, offsets are used to compensate for the remaining losses. This involves creating or enhancing biodiversity elsewhere to achieve no net loss or a net gain in ecological value.

Figure 81: Mitigation hierarchy for nature conservation
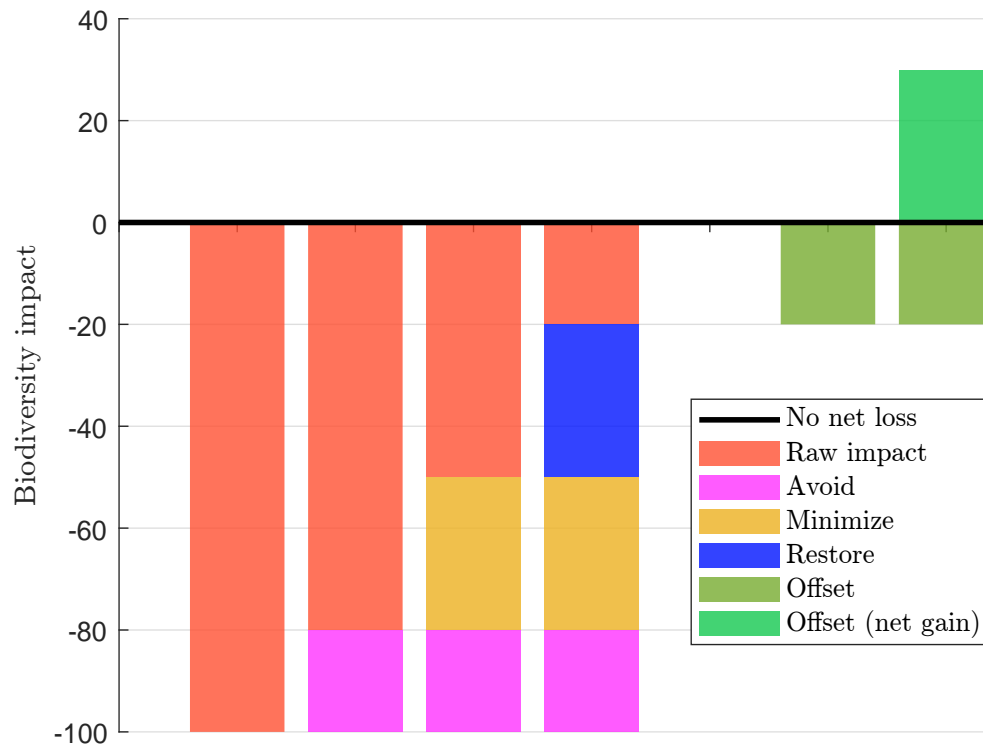
By construction, the mitigation hierarchy is an impact approach where we assess how companies and investments impact biodiversity. From a financial perspective, it is equally important to consider how companies and investments are affected by biodiversity loss. In this context, we can adopt a dependency approach based on four key risk dimensions: transition risk, physical risk, litigation risk and systemic risk. For instance, some sectors or companies are highly dependent on raw materials, soil productivity, or freshwater. As a result, loss of biodiversity can create physical risk directly or indirectly through the supply chain. Transitional risk can arise from new or emerging regulations and changes in consumer preferences. Litigation risk arises when companies face potential legal challenges related to environmental damage, failure to protect biodiversity, or non-compliance with environmental regulations. Such risks can result in significant financial penalties, reputational damage and lawsuits. The final category of risk is systemic risk, which affects companies indirectly. For example, they may be affected by severe pandemics that disrupt global ecosystems and economic systems. This dual perspective of biodiversity risk refers to the double materiality principle:

Double materiality principle		
Dependency	$\Longleftarrow$	How does biodiversity affect companies and investments?
Impact	$\Longrightarrow$	How do companies and investments affect biodiversity?
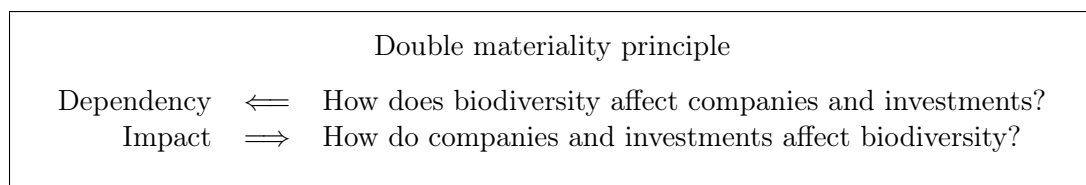
Applying the avoid dimension of the mitigation hierarchy to investments requires the adoption of negative screening and the establishment of exclusion criteria for issuers or projects that significantly harm biodiversity. The minimize dimension can be effectively implemented through best-in-class strategies or selective approaches that prioritize companies with stronger biodiversity practices. A key challenge in this dimension is the development and use of biodiversity metrics that appropriately

account for both sector-specific impacts and geographic contexts, as the importance of biodiversity varies widely across ecosystems. For the restore/offset dimension, the focus shifts to creating positive impacts. Traditional avoidance and minimization metrics prove inadequate here, as these final stages require the identification and selection of companies and projects that have a positive biodiversity footprint. This requires a different set of metrics that focus on restoration outcomes, additionality and measurable biodiversity gains. For example, an MSA metric is not relevant to this dimension. As a result, each progression through the hierarchy requires increasingly sophisticated measurement approaches, moving from harm reduction to positive contribution assessment.

Figure 82: Linking ESG investment strategies and biodiversity mitigation dimensions
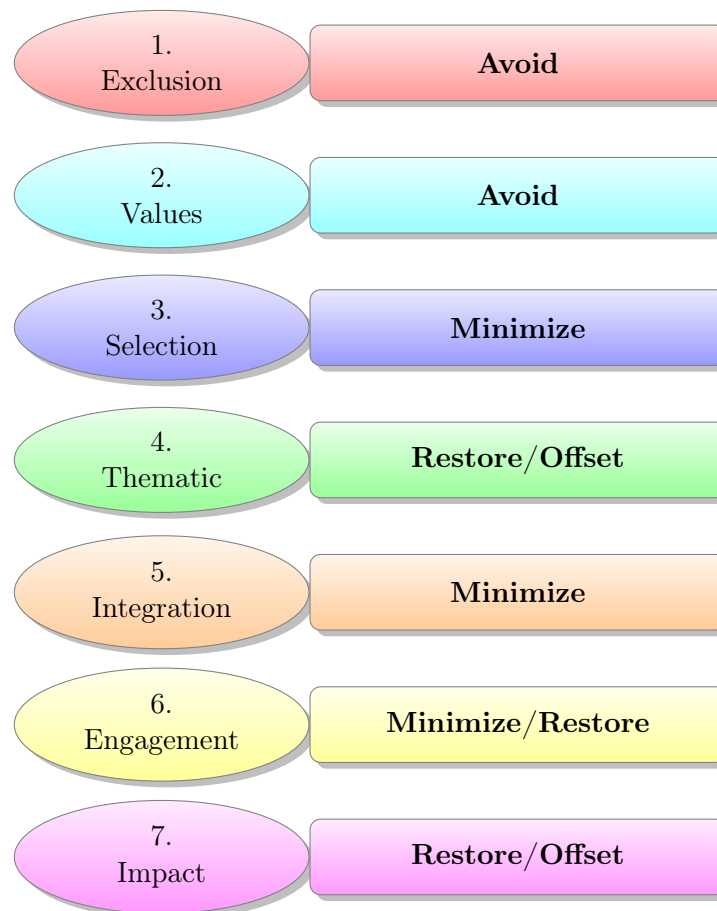
6.3 The impact investing approach

According to Phenix Capital (2024b), the biodiversity impact fund landscape appears robust at first glance, with 1 080 biodiversity-related funds and a market size of €129 billion in open-end investment funds. At first glance, these figures appear substantial, especially when compared to the investment required to meet the targets of the GBF. However, a deeper analysis reveals a more nuanced picture. A striking 69% of these funds primarily address food-related needs rather than direct biodiversity conservation. When focusing specifically on funds targeting SDG 14 (life below water) and SDG 15 (life on land), the numbers drop to 162 and 278 impact funds, respectively. Real assets and private equity dominate these specialized sectors, accounting for 33% and 30% of these biodiversity-focused funds, respectively. However, the geographic and thematic distribution

reveals significant gaps. Only 11 real asset impact funds focus on timber and forests in Asia, 12 in Africa, and 26 in South America — regions that contain much of the world's remaining primary biodiversity. This creates a paradox. While the aggregate numbers suggest impressive financial mobilization for biodiversity, an examination of specific critical issues, such as forest conservation, reveals low investment volumes.

References

ABRAMS, P. A. (2009). When Does Greater Mortality Increase Population Size? The Long History and Diverse Mechanisms underlying the Hydra Effect. *Ecology Letters*, 12(5), pp. 462-474.

AIZEN, M. A., AGUIAR, S., BIESMEIJER, J. C., ..., and SEYMOUR, C. L. (2019). Global Agricultural Productivity is Threatened by Increasing Pollinator Dependence without a Parallel Increase in Crop Diversification. *Global change biology*, 25(10), pp. 3516-3527.

AIZEN, M. A., GARIBALDI, L. A., CUNNINGHAM, S. A., and KLEIN, A. M. (2009). How Much Does Agriculture Depend on Pollinators? Lessons from Long-term Trends in Crop Production. *Annals of Botany*, 103(9), pp. 1579-1588.

ÅKERMAN, M. (2003). What Does 'Natural Capital' Do? The Role of Metaphor in Economic Understanding of the Environment. *Environmental Values*, 12(4), pp. 431-448.

ALGEO, T. J., and SHEN, J. (2024). Theory and Classification of Mass Extinction Causation. *National Science Review*, 11, nwad237, 21 pages.

ALKEMADE, R., VAN OORSCHOT, M., MILES, L., NELLEMANN, C., BAKKENES, M., and TEN BRINK, B. (2009). GLOBIO3: A Framework to Investigate Options for Reducing Global Terrestrial Biodiversity Loss. *Ecosystems*, 12, pp. 374-390.

ANDERSON, S. J., KUBISZEWSKI, I., and SUTTON, P. C. (2024). The Ecological Economics of Light Pollution: Impacts on Ecosystem Service Value. *Remote Sensing*, 16(14), 2591, 11 pages.

ARDITI, R., and GINZBURG, L. R. (1989). Coupling in Predator-prey Dynamics: Ratio-dependence. *Journal of Theoretical Biology*, 139(3), pp. 311-326.

ARLIDGE, W. N. S., BULL, J. W., ADDISON, P. F. E., ..., and MILNER-GULLAND, E. J. (2018). A Global Mitigation Hierarchy for Nature Conservation. *BioScience*, 68(5), pp. 336-347.

ARMSTRONG, R. A., and MCGEHEE, R. (1980). Competitive Exclusion. *American Naturalist*, 115(2), pp. 151-170.

ARRHENIUS, O. (1921). Species and Area. *Journal of Ecology*, 9(1), pp. 95-99.

BAILON, M., BOR, A. M., and REDÍN, J. G. (2024). *Biodiversity Measurement Approaches — A Practitioner's Guide for Financial Institutions*. November, 86 pages.

BAMBACH, R. K. (2006). Phanerozoic Biodiversity Mass Extinctions. *Annual Review of Earth Planetary Sciences*, 34(1), pp. 127-155.

BANDEIRA, B., JAMET, J.-L., JAMET, D., and GINOUX, J.-M. (2013). Mathematical Convergences of Biodiversity Indices. *Ecological Indicators*, 29, pp. 522-528.

BARLOW, J., LENNOX, G. D., FERREIRA, J., ..., and GARDNER, T. A. (2016). Anthropogenic Disturbance in Tropical Forests Can Double Biodiversity Loss from Deforestation. *Nature*, 535(7610), pp. 144-147.

BARNOSKY, A. D., MATZKE, N., TOMIYA, S., ..., and FERRER, E. A. (2011). Has the Earth's Sixth Mass Extinction Already Arrived?. *Nature*, 471, pp. 51-57.

BEAUGRAND, G., KLÉPARSKI, L., LUCZAK, C., GOBERVILLE, E., and KIRBY, R. R. (2024). A Niche-based Theory of Island Biogeography. *Ecology and Evolution*, 14(6), e11540, 14 pages.

BEGON, M., and TOWNSEND, C. R. (2021). *Ecology: From Individuals to Ecosystems*. Fifth edition, John Wiley & Sons, 864 pages.

BENGIS, R. G., LEIGHTON, F. A., FISCHER, J. R., ARTOIS, M., MÖRNER, T., and TATE, C. M. (2004). The Role of Wildlife in Emerging and Re-emerging Zoonoses. *Revue Scientifique et Technique (International Office of Epizootics)*, 23(2), pp. 497-512.

BENTON, M. J. (1995). Diversification and extinction in the history of life. *Science*, 268(5207), pp. 52-58.

BENTON, M. J. (2015). *When Life Nearly Died: The Greatest Mass Extinction of All Time*. Thames & Hudson, 336 pages.

BERGER, L., SPEARE, R., DASZAK, P., ..., and PARKES, H. (1998). Chytridiomycosis Causes Amphibian Mortality Associated with Population Declines in the Rain Forests of Australia and Central America. *Proceedings of the National Academy of Sciences*, 95(15), pp. 9031-9036.

BERNSTEIN, A. S., ANDO, A. W., LOCH-TEMZELIDES, T., ..., and DOBSON, A. P. (2022). The Costs and Benefits of Primary Prevention of Zoonotic Pandemics. *Science Advances*, 8(5), eabl4183, 13 pages.

BETTS, M. G., WOLF, C., RIPPLE, W. J., ..., and LEVI, T. (2017). Global Forest Loss Disproportionately Erodes Biodiversity in Intact Landscapes. *Nature*, 547(7664), pp. 441-444.

BICKNELL, J. E., STRUEBIG, M. J., and DAVIES, Z. G. (2015). Reconciling Timber Extraction with Biodiversity Conservation in Tropical Forests using Reduced-impact Logging. *Journal of Applied Ecology*, 52(2), pp. 379-388.

BLEHERT, D. S., HICKS, A. C., BEHR, M., ..., and STONE, W. B. (2009). Bat White-Nose Syndrome: An Emerging Fungal Pathogen?. *Science*, 323(5911), pp. 227.

BOBBINK, R., HICKS, K., GALLOWAY, J., ..., and DE VRIES, W. (2010). Global Assessment of Nitrogen Deposition Effects on Terrestrial Plant Diversity: A Synthesis. *Ecological Applications*, 20(1), pp. 30-59.

BROWN, J. H. (1999). The Legacy of Robert MacArthur: From Geographical Ecology to Macroecology. *Journal of Mammalogy*, 80(2), pp. 333-344.

BURIVALOVA, Z., PURNOMO, ORNDORFF, S., TRUSKINGER, A., ROE, P., and GAME, E. T. (2021). The Sound of Logging: Tropical Forest Soundscape Before, During, and After Selective Timber Extraction. *Biological Conservation*, 254, 108812, 6 pages.

BUTCHART, S. H. M., RESIT AKÇAKAYA, H., CHANSON, J., ..., and HILTON-TAYLOR, C. (2007). Improvements to the Red List Index. *PloS One*, 2(1), e140.

CALABRESE, E. J., and MATTSON, M. P. (2017). How Does Hormesis Impact Biology, Toxicology, and Medicine?. *npj Aging and Mechanisms of Disease*, 3(13), 8 pages.

CARBONE, L., NERGADZE, S. G., MAGNANI, E., ..., and GIULOTTO, E. (2006). Evolutionary Movement of Centromeres in Horse, Donkey, and Zebra. *Genomics*, 87(6), pp. 777-782.

CARNEY, M. (2015). Breaking the Tragedy of the Horizon — Climate Change and Financial Stability. *Speech given at Lloyd's of London*, 29 September 2015.

CARSON, R. (1962). *Silent Spring*. Houghton Mifflin Harcourt Publishing Company.

CASE, T. J., and GILPIN, M. E. (1974). Interference Competition and Niche Theory. *Proceedings of the National Academy of Sciences*, 71(8), pp. 3073-3077.

CAWTHORN, D. M., and HOFFMAN, L. C. (2015). The Bushmeat and Food Security Nexus: A Global Account of the Contributions, Conundrums and Ethical Collisions. *Food Research International*, 76, pp. 906-925.

CAZZOLLA GATTI, R., REICH, P. B., GAMARRA, J. G. P., ..., and LIANG, J. (2022). The Number of Tree Species on Earth. *Proceedings of the National Academy of Sciences*, 119(6), e2115329119, 11 pages.

CEBALLOS, G., EHRLICH, P. R., BARNOSKY, A. D., GARCÍA, A., PRINGLE, R. M., and PALMER, T. M. (2015). Accelerated Modern Human-induced Species Losses: Entering the Sixth Mass Extinction. *Science Advances*, 1(5), e1400253, 5 pages.

CEBALLOS, G., EHRLICH, P. R., and DIRZO, R. (2017). Biological Annihilation via the Ongoing Sixth Mass Extinction Signaled by Vertebrate Population Losses and Declines. *Proceedings of the National Academy of Sciences*, 114(30), pp. E6089-E6096.

CEDERGREEN, N., RITZ, C., and STREIBIG, J. C. (2005). Improved Empirical Models Describing Hormesis. *Environmental Toxicology and Chemistry: An International Journal*, 24(12), pp. 3166-3172.

CHABER, A. L., MOLONEY, G. K., RENAULT, V., ..., and GAUBERT, P. (2023). Examining the International Bushmeat Traffic in Belgium: A Threat to Conservation and Public Health. *One Health*, 17, 100605, 8 pages.

CHAO, A. (1984). Nonparametric Estimation of the Number of Classes in a Population. *Scandinavian Journal of Statistics*, 11(4), pp. 265-270.

CHAO, A. (1987). Estimating the Population Size for Capture-Recapture Data with Unequal Catchability. *Biometrics*, 43(4), pp. 783-791.

CHAZDON, R. L., BRANCALION, P. H. S., LAESTADIUS, L., ..., and WILSON, S. J. (2016). When is a Forest a Forest? Forest Concepts and Definitions in the Era of Forest and Landscape Restoration. *Ambio*, 45(5), pp. 538-550.

CHERIEF, A., SEKINE, T., and STAGNOL, L. (2025). A Novel Nature-based Risk Index: Application to Acute Risks and their Financial Materiality on Corporate Bonds. *Ecological Economics*, 228, 108427, 10 pages.

CHESSON, P. (1990). MacArthur's Consumer-Resource Model. *Theoretical Population Biology*, 37(1), pp. 26-38.

CHESSON, P. (2000). Mechanisms of Maintenance of Species Diversity. *Annual Review of Ecology and Systematics*, 31(1), pp. 343-366.

CLARK, C. M., and TILMAN, D. (2008). Loss of Plant Species After Chronic Low-level Nitrogen Deposition to Prairie Grasslands. *Nature*, 451(7179), pp. 712-715.

COLEMAN, B. D. (1981). On Random Placement and Species-Area Relations. *Mathematical Biosciences*, 54(3-4), pp. 191-215.

COLWELL, R. K., and CODDINGTON, J. A. (1994). Estimating Terrestrial Biodiversity Through Extrapolation. *Philosophical Transactions of the Royal Society of London Series B: Biological Sciences*, 345(1311), pp. 101-118.

COLWELL, R. K., MAO, C. X., and CHANG, J. (2004). Interpolating, Extrapolating, and Comparing Incidence-based Species Accumulation Curves. *Ecology*, 85(10), pp. 2717-2727.

CONDIT, R., PITMAN, N., LEIGH Jr, E. G., ..., and HUBBELL, S. P. (2002). Beta-Diversity in Tropical Forest Trees. *Science*, 295(5555), pp. 666-669.

CONNOR, E. F., and MCCOY, E. D. (1979). The Statistics and Biology of the Species-Area Relationship. *The American Naturalist*, 113(6), pp. 791-833.

Convention on Biological Diversity (2022). *15/4 Kunming-Montreal Global Biodiversity Framework*. Conference of the Parties, 16 pages.

COPPOLA, D., LAURITANO, C., PALMA ESPOSITO, F., RICCIO, G., RIZZO, C., and DE PASCALE, D. (2021). Fish Waste: From Problem to Valuable Resource. *Marine Drugs*, 19(2), 116, 39 pages.

COQUERET, G., GIROUX, T., and ZERBIB, O. D. (2025). The Biodiversity Premium. *Ecological Economics*, 228, 108435, 14 pages.

COSTANZA, R., D'ARGE, R., DE GROOT, R., ..., and VAN DEN BELT, M. (1997). The Value of the World's Ecosystem Services and Natural Capital. *Nature*, 387(6630), pp. 253-260.

COSTANZA, R., and DALY, H. E. (1992). Natural Capital and Sustainable Development. *Conservation Biology*, 6(1), pp. 37-46.

COSTANZA, R., DE GROOT, R., SUTTON, P., ..., and TURNER, R. K. (2014). Changes in the Global Value of Ecosystem Services. *Global Environmental Change*, 26, pp. 152-158.

COWIE, R. H., BOUCHET, P., and FONTAINE, B. (2022). The Sixth Mass Extinction: Fact, Fiction or Speculation?. *Biological Reviews*, 97(2), pp. 640-663.

CUI, W., MARSLAND III, R., and MEHTA, P. (2024). Les Houches Lectures on Community Ecology: From Niche Theory to Statistical Mechanics. *arXiv*, 2403.05497.

CURTIS, P. G., SLAY, C. M., HARRIS, N. L., TYUKAVINA, A., and HANSEN, M. C. (2018). Classifying Drivers of Global Forest Loss. *Science*, 361(6407), pp. 1108-1111.

DAILY, G. C. (1997). Introduction: What Are Ecosystem Services. In Daily, G. C. (Ed.), *Nature's Services: Societal Dependence On Natural Ecosystems*, Island Press, Chapter 1, pp. 1-10.

DALY, H. E. (1968). On Economics as a Life Science. *Journal of Political Economy*, 76(3), pp. 392-406.

DASGUPTA, P. (2021). *The Economics of Biodiversity: The Dasgupta Review*. London: HM Treasury, February, 610 pages.

DAVIS, A. P., CHADBURN, H., MOAT, J., O'SULLIVAN, R., HARGREAVES, S., and LUGHADHA, E. N. (2019). High Extinction Risk for Wild Coffee Species and Implications for Coffee Sector Sustainability. *Science Advances*, 5(1), eaav3473, 9 pages.

DE GROOT, R., BRANDER, L., VAN DER PLOEG, S., ..., and VAN BEUKERING, P. (2012). Global Estimates of the Value of Ecosystems and Their Services in Monetary Units. *Ecosystem Services*, 1(1), pp. 50-61.

DE PALMA, A., HOSKINS, A., GONZALEZ, R. E., ..., and PURVIS, A. (2021). Annual Changes in the Biodiversity Intactness Index in Tropical and Subtropical Forest Biomes, 2001–2012. *Scientific Reports*, 11(1), 20249, 13 pages.

DE QUEIROZ, K. (2007). Species Concepts and Species Delimitation. *Systematic biology*, 56(6), pp. 879-886.

DE RYCK, J., DRIESEN, K., VERHELST, J., and LAMMERANT, J. (2024). *Assessment of Biodiversity Measurement Approaches for Businesses and Financial Institutions.* Update Report 5 on behalf of the EU Business & Biodiversity Platform, October, 272 pages.

DE VOS, J. M., JOPPA, L. N., GITTLEMAN, J. L., STEPHENS, P. R., and PIMM, S. L. (2015). Estimating the Normal Background Rate of Species Extinction. *Conservation Biology*, 29(2), pp. 452-462.

DECHEZLEPRÊTRE, A., RIVERS, N., and STADLER, B. (2019). The Economic Cost of Air Pollution: Evidence from Europe. *OECD Economics Department Working Papers*, 1584, 62 pages.

DEL MONTE-LUNA, P., NAKAMURA, M., VICENTE, A., ..., and LLUCH-COTA, S. E. (2023). A Review of Recent and Future Marine Extinctions. *Cambridge Prisms: Extinction*, 1, e13, 9 pages.

DENGLER, J. (2009). Which Function Describes the Species-Area Relationship Best? A Review and Empirical Evaluation. *Journal of Biogeography*, 36(4), pp. 728-744.

DEUTZ, A., HEAL, G. M., NIU, R., ..., and TOBIN-DE LA PUENTE, J. (2020). *Financing Nature: Closing the Global Biodiversity Financing Gap.* The Paulson Institute, The Nature Conservancy, and the Cornell Atkinson Center for Sustainability, 262 pages.

DI FRANCO, E., PIERSON, P., DI IORIO, L., ..., and GUIDETTI, P. (2020). Effects of Marine Noise Pollution on Mediterranean Fishes and Invertebrates: A Review. *Marine Pollution Bulletin*, 159, 111450, 10 pages.

DIAGNE, C., LEROY, B., VAISSIÈRE, A. C., ..., and COURCHAMP, F. (2021). High and Rising Economic Costs of Biological Invasions Worldwide. *Nature*, 592(7855), pp. 571-576.

DICKS, L. V., BREEZE, T. D., NGO, H. T., ..., and POTTS, S. G. (2021). A Global-scale Expert Assessment of Drivers and Risks Associated With Pollinator Decline. *Nature Ecology & Evolution*, 5(10), pp. 1453-1461.

DINERSTEIN, E., OLSON, D. M., JOSHI, A., ..., and SALEEM, M. (2017). An Ecoregion-based Approach to Protecting Half the Terrestrial Realm. *BioScience*, 67(6), pp. 534-545.

DIRZO, R., YOUNG, H. S., GALETTI, M., CEBALLOS, G., ISAAC, N. J. B., and COLLEN, B. (2014). Defaunation in the Anthropocene. *Science*, 345(6195), pp. 401-406.

DIZ-PITA, E., and OTERO-ESPINAR, M. V. (2021). Predator-prey Models: A Review of Some Recent Advances. *Mathematics*, 9(15), 1783, 34 pages.

DUARTE, C. M., AGUSTI, S., BARBIER, E., ..., and WORM, B. (2020). Rebuilding Marine Life. *Nature*, 580(7801), pp. 39-51.

EILERS, E. J., KREMEN, C., SMITH GREENLEAF, S., GARBER, A. K., and KLEIN, A. M. (2011). Contribution of Pollinator-mediated Crops to Nutrients in the Human Food Supply. *PLoS One*, 6(6), e21363, 6 pages.

ENCORE (2024). *ENCORE: Exploring Natural Capital Opportunities, Risks and Exposure.* www.encorenature.org.

EHRLICH, P. R. (1995). The Scale of the Human Enterprise and Biodiversity Loss. In Lawton, J.H., and May, R. M. (Eds), *Extinction Rates*, Oxford University Press, Chapter 14, pp. 214-226.

ESCHER, B. I., STAPLETON, H. M., and SCHYMANSKI, E. L. (2020). Tracking Complex Mixtures of Chemicals in our Changing Environment. *Science*, 367(6476), pp. 388-392.

European Environment Agency (2024a). *The Costs to Health and the Environment from Industrial Air Pollution in Europe — 2024 Update.* Briefing 24/2023, January, 18 pages.

European Environment Agency (2024b). *Estimating the External Costs of Industrial Air Pollution — Trends 2012–2021.* Technical Note, January, 177 pages.

EZE, M. O., GEORGE, S. C., and HOSE, G. C. (2021). Dose-Response Analysis of Diesel Fuel Phytotoxicity on Selected Plant Species. *Chemosphere*, 263, 128382, 10 pages.

FA, J. E., PERES, C. A., and MEEUWIG, J. (2002). Bushmeat Exploitation in Tropical Forests: An Intercontinental Comparison. *Conservation Biology*, 16(1), pp. 232-237.

FAHRIG, L. (2003). Effects of Habitat Fragmentation on Biodiversity. *Annual Review of Ecology, Evolution, and Systematics*, 34(1), pp. 487-515.

FAHRIG, L. (2017). Ecological Responses to Habitat Fragmentation per se. *Annual Review of Ecology, Evolution, and Systematics*, 48(1), pp. 1-23.

FAHRIG, L., ARROYO-RODRÍGUEZ, V., BENNETT, J. R., ..., and WATLING, J. I. (2019). Is Habitat Fragmentation Bad for Biodiversity?. *Biological Conservation*, 230, pp. 179-186.

FATTORINI, S., BORGES, P. A., DAPPORTO, L., and STRONA, G. (2017). What Can the Parameters of the Species-Area Relationship (SAR) Tell Us? Insights from Mediterranean Islands. *Journal of Biogeography*, 44(5), pp. 1018-1028.

FIGUEIREDO, L., KRAUSS, J., STEFFAN-DEWENTER, I., and SARMENTO CABRAL, J. (2019). Understanding Extinction Debts: Spatio-temporal Scales, Mechanisms and A Roadmap for Future Research. *Ecography*, 42(12), pp. 1973-1990.

FISHER, R. A., CORBET, A. S., and WILLIAMS, C. B. (1943). The Relation between the Number of Species and the Number of Individuals in a Random Sample of an Animal Population. *Journal of Animal Ecology*, 12(1), pp. 42-58.

FLAMMER, C., GIROUX, T., and HEAL, G. M. (2025). Biodiversity Finance. *Journal of Financial Economics*, 164, 103987, 15 pages.

FLETCHER Jr, R. J., DIDHAM, R. K., BANKS-LEITE, C., ..., and HADDAD, N. M. (2018). Is Habitat Fragmentation Good for Biodiversity?. *Biological Conservation*, 226, pp. 9-15.

FLÖRKE, M., KYNAST, E., BÄRLUND, I., EISNER, S., WIMMER, F., and ALCAMO, J. (2013). Domestic and Industrial Water Uses of the Past 60 Years as a Mirror of Socio-economic Development: A Global Simulation Study. *Global Environmental Change*, 23(1), pp. 144-156.

Food and Agriculture Organization of the United Nations (2019). *The State of the World's Biodiversity for Food and Agriculture*. FAO Commission on Genetic Resources for Food and Agriculture, prepared by Bélanger J., and Pilling D. (Eds), February, 572 pages.

Food and Agriculture Organization of the United Nations (2020). *Global Forest Resources Assessment 2020 — Key Findings*. 16 pages.

Food and Agriculture Organization of the United Nations (2022). *Blue Transformation — Roadmap 2022–2030: A Vision for FAO's Work on Aquatic Food Systems*. 40 pages.

Food and Agriculture Organization of the United Nations (2023a). FRA 2025: Terms and Definitions. *Forest Resources Assessment Working Paper*, 194, 29 pages.

Food and Agriculture Organization of the United Nations (2023b). *World Food and Agriculture — Statistical Yearbook 2023*. November, 384 pages.

Food and Agriculture Organization of the United Nations (2024a). *The State of Food Security and Nutrition in the World 2024 – Financing to End Hunger, Food Insecurity and Malnutrition in all its Forms*. September, 316 pages.

Food and Agriculture Organization of the United Nations (2024b). *The State of World Fisheries and Aquaculture 2024 — Blue Transformation in action*. October, 264 pages.

FRETWELL, S. D. (1975). The Impact of Robert MacArthur on Ecology. *Annual Review of Ecology and Systematics*, 6, pp. 1-13.

FULLER, R., LANDRIGAN, P. J., BALAKRISHNAN, K., ..., and YAN, C. (2022). Pollution and Health: A Progress Update. *The Lancet Planetary Health*, 6(6), e535-e547.

GARIBALDI, L. A., STEFFAN-DEWENTER, I., WINFREE, R., ..., and KLEIN, A. M. (2013). Wild Pollinators Enhance Fruit Set of Crops Regardless of Honey Bee Abundance. *Science*, 339(6127), pp. 1608-1611.

GASTON, K. J. (2010). Biodiversity. In Sodhi, N. S., and Ehrlich, P. R. (Eds), *Conservation Biology for All*, Oxford University Press, Chapter 2, pp. 27-44.

GASTON, K. J., and SPICER, J. I. (2004). *Biodiversity: An Introduction*. Second Edition, Wiley-Blackwell, 208 pages.

GATTI, L. V., BASSO, L. S., MILLER, J. B., ..., and NEVES, R. A. (2021). Amazonia as a Carbon Source Linked to Deforestation and Climate Change. *Nature*, 595(7867), pp. 388-393.

GENTLEMAN, W., LEISING, A., FROST, B., STROM, S., and MURRAY, J. (2003). Functional Responses for Zooplankton Feeding on Multiple Resources: A Review of Assumptions and Biological Dynamics. *Deep Sea Research Part II: Topical Studies in Oceanography*, 50(22-26), pp. 2847-2875.

GHOSH, B., and KAR, T. K. (2013). Maximum Sustainable Yield and Species Extinction in a Prey-predator System: Some New Results. *Journal of Biological Physics*, 39, pp. 453-467.

GIGLIO, S., KUCHLER, T., STROEBEL, J., and ZENG, X. (2023b). Biodiversity Risk. *NBER*, 31137.

Gilpin, M. E., Case, T. J., and Ayala, F. J. (1976). θ-selection. *Mathematical Biosciences*, 32(1-2), pp. 131-139.

Gleason, H. A. (1922). On the Relation Between Species and Area. *Ecology*, 3(2), pp. 158-162.

Gluszek, S., Viollaz, J., Mwinyihali, R., Wieland, M., and Gore, M. L. (2021). Using Conservation Criminology to Understand the Role of Restaurants in the Urban Wild Meat Trade. *Conservation Science and Practice*, 3(5), e368, 13 pages.

Goedkoop, M., Heijungs, R., Huijbregts, M., De Schryver, A., Struijs, J., and Van Zelm, R. (2009). *ReCiPe 2008*. First edition, 132 pages.

Gombeer, S., Nebesse, C., Musaba, P., ..., and Verheyen, E. (2021). Exploring the Bushmeat Market in Brussels, Belgium: A Clandestine Luxury Business. *Biodiversity and Conservation*, 30, pp. 55-66.

González-Martín, J., Kraakman, N. J. R., Pérez, C., Lebrero, R., and Muõoz, R. (2021). A State-of-the-art Review on Indoor Air Pollution and Strategies for Indoor Air Pollution Control. *Chemosphere*, 262, 128376, 16 pages.

Gordon, H. S. (1954). The Economic Theory of a Common-Property Resource: The Fishery. *Journal of Political Economy*, 62(2), pp. 124-142.

Gotelli, N. J., and Colwell, R. K. (2001). Quantifying Biodiversity: Procedures and Pitfalls in the Measurement and Comparison of Species Richness. *Ecology Letters*, 4(4), pp. 379-391.

Goutelle, S., Maurin, M., Rougier, F., ..., and Maire, P. (2008). The Hill Equation: A Review of Its Capabilities in Pharmacological Modelling. *Fundamental & Clinical Pharmacology*, 22(6), pp. 633-648.

Graff Zivin, J., and Neidell, M. (2013). Environment, Health, and Human Capital. *Journal of Economic Literature*, 51(3), pp. 689-730.

Gray, A. (2019). The Ecology of Plant Extinction: Rates, Traits and Island Comparisons. *Oryx*, 53(3), pp. 424-428.

Green, J. L., and Ostling, A. (2003). Endemics-Area Relationships: The Influence of Species Dominance and Spatial Aggregation. *Ecology*, 84(11), pp. 3090-3097.

Haddad, N. M., Brudvig, L. A., Clobert, J., ..., and Townshend, J. R. (2015). Habitat Fragmentation and its Lasting Impact on Earth's Ecosystems. *Science Advances*, 1(2), e1500052, 9 pages.

Halley, J. M., Monokrousos, N., Mazaris, A. D., Newmark, W. D., and Vokou, D. (2016a). Dynamics of Extinction Debt Across Five Taxonomic Groups. *Nature Communications*, 7(1), 12283, 6 pages.

Halley, J. M., Monokrousos, N., Mazaris, A. D., Newmark, W. D., and Vokou, D. (2016b). Supplementary Information. *Nature Communications*, 7(1), 12283, 34 pages.

Hallmann, C. A., Sorg, M., Jongejans, E., ..., and De Kroon, H. (2017). More than 75 Percent Decline over 27 Years in Total Flying Insect Biomass in Protected Areas. *PloS One*, 12(10), e0185809, 21 pages.

HAMMITT, J. K. (2023). Consistent Valuation of a Reduction in Mortality Risk using Values per Life, Life Year, and Quality-Adjusted Life Year. *Health Economics*, 32(9), pp. 1964-1981.

HAMMITT, J. K., and ROBINSON, L. A. (2011). The Income Elasticity of the Value per Statistical Life: Transferring Estimates Between High and Low Income Populations. *Journal of Benefit-Cost Analysis*, 2(1), 28 pages.

HANSEN, M. C., POTAPOV, P. V., MOORE, R., ..., and TOWNSHEND, J. R. (2013b). High-Resolution Global Maps of 21st-century Forest Cover Change. *Science*, 342(6160), pp. 850-853.

HANSKI, I., and OVASKAINEN, O. (2002). Extinction Debt at Extinction Threshold. *Conservation Biology*, 16(3), pp. 666-673.

HANSKI, I., and OVASKAINEN, O. (2003). Metapopulation Theory for Fragmented Landscapes. *Theoretical Population Biology*, 64(1), pp. 119-127.

HANSKI, I., ZURITA, G. A., BELLOCQ, M. I., and RYBICKI, J. (2013). Species-fragmented Area Relationship. *Proceedings of the National Academy of Sciences*, 110(31), pp. 12715-12720.

HARDIN, G. (1968). The Tragedy of the Commons. *Science*, 162(3859), pp. 1243-1248.

HARTIGAN Jr, J. (2017). *Care of the Species: Races of Corn and the Science of Plant Biodiversity.* University of Minnesota Press, 376 pages.

HE, F., and HUBBELL, S. P. (2011). Species-Area Relationships Always Overestimate Extinction Rates from Habitat Loss. *Nature*, 473(7347), pp. 368-371.

HE, F., and LEGENDRE, P. (2002). Species Diversity Patterns Derived from Species-Area Models. *Ecology*, 83(5), pp. 1185-1198.

HEIN, L., BAGSTAD, K. J., OBST, C., ..., and CAPARRÓS, A. (2020). Progress in Natural Capital Accounting for Ecosystems. *Science*, 367(6477), pp. 514-515.

HEYWOOD, V. H. (1995). *The Global Biodiversity Assessment.* UNEP & Cambridge University Press, 1140 pages.

HILDERINK, M. H., and DE WINTER, I. I. (2021). No Need to Beat Around the Bushmeat — The Role of Wildlife Trade and Conservation Initiatives in the Emergence of Zoonotic Diseases. *Heliyon*, 7, e07692, 10 pages.

HÖLKER, F., WOLTER, C., PERKIN, E. K., and TOCKNER, K. (2010). Light Pollution as a Biodiversity Threat. *Trends in Ecology & Evolution*, 25(12), pp. 681-682.

HOLLING, C. S. (1959a). The Components of Predation as Revealed by a Study of Small-mammal Predation of the European Pine Sawfly. *Canadian Entomologist*, 91(5), pp. 293-320.

HOLLING, C. S. (1959b). Some Characteristics of Simple Types of Predation and Parasitism. *Canadian Entomologist*, 91(7), pp. 385-398.

HURLBERT, S. H. (1971). The Nonconcept of Species Diversity: A Critique and Alternative Parameters. *Ecology*, 52(4), pp. 577-586.

HUTCHINSON, G. E. (1961). The Paradox of the Plankton. *American Naturalist*, 95(882), pp. 137-145.

HUTCHINSON, M. C., and LUCEY, B. (2024). A Bibliometric and Systemic Literature Review of Biodiversity Finance. *Finance Research Letters*, 105377, 7 pages.

Intergovernmental Science-Policy Platform on Biodiversity and Ecosystem Services (2016). *The Assessment Report of the Intergovernmental Science-Policy Platform on Biodiversity and Ecosystem Services on Pollinators, Pollination and Food Production.* IPBES secretariat, prepared by Potts, S.G., Imperatriz-Fonseca, V. L., and Ngo H. T. (Eds), 552 pages.

Intergovernmental Science-Policy Platform on Biodiversity and Ecosystem Services (2019). *Global Assessment Report on Biodiversity and Ecosystem Services of the Intergovernmental Science-Policy Platform on Biodiversity and Ecosystem Services.* IPBES secretariat, prepared by Brondízio, E. S., Settele, J., Díaz, S., and Ngo, H. T. (Eds), 1144 pages.

Intergovernmental Science-Policy Platform on Biodiversity and Ecosystem Services (2019). *Thematic Assessment Report on Invasive Alien Species and their Control.* IPBES secretariat, prepared by Roy, H. E., Pauchard, A., Stoett, P., and Renard Truong, T. (Eds.), 952 pages.

IUCN (2012). *IUCN Red List Categories and Criteria.* Version 3.1, second edition, 32 pages.

IUCN (2022). *The IUCN Red List of Threatened Species.* Version 2022-1, www.iucnredlist.org.

IUCN (2024a). *The IUCN Red List of Threatened Species.* Version 2024-1, www.iucnredlist.org.

IUCN (2024b). *Summary Statistics.* Version 2024-1, www.iucnredlist.org.

JACKSON, J. B., KIRBY, M. X., BERGER, W. H., ..., and WARNER, R. R. (2001). Historical Overfishing and the Recent Collapse of Coastal Ecosystems. *Science*, 293(5530), pp. 629-637.

JOLLES, A. E. (2007). Population Biology of African Buffalo (*Syncerus caffer*) at Hluhluwe-iMfolozi Park, South Africa. *African Journal of Ecology*, 45(3), pp. 398-406.

KAR, T. K., and GHOSH, B. (2013). Impacts of Maximum Sustainable Yield Policy to Prey-predator Systems. *Ecological Modelling*, 250, pp. 134-142.

KITCHEN, A. M., GESE, E. M., and SCHAUSTER, E. R. (1999). Resource Partitioning Between Coyotes and Swift Foxes: Space, Time, and Diet. *Canadian Journal of Zoology*, 77(10), pp. 1645-1656.

KLEIN, A. M., VAISSIÈRE, B. E., CANE, J. H., ..., and TSCHARNTKE, T. (2007). Importance of Pollinators in Changing Landscapes for World Crops. *Proceedings of the Royal Society B: Biological Sciences*, 274(1608), pp. 303-313.

KOLBERT, E. (2014). *The Sixth Extinction: An Unnatural History.* Henry Holt and Company, 319 pages.

KREMEN, C. (2005). Managing Ecosystem Services: What Do We Need to Know about Their Ecology?. *Ecology letters*, 8(5), pp. 468-479.

KRUSE, H., KIRKEMO, A. M., and HANDELAND, K. (2004). Wildlife as Source of Zoonotic Infections. *Emerging Infectious Diseases*, 10(12), pp. 2067-2072.

KUIPERS, K. J. J., MAY, R., and VERONES, F. (2021). Considering Habitat Conversion and Fragmentation in Characterisation Factors for Land-use Impacts on Vertebrate Species Richness. *Science of the Total Environment*, 801, 149737, 10 pages.

Kuussaari, M., Bommarco, R., Heikkinen, R. K., ..., and Steffan-Dewenter, I. (2009). Extinction Debt: A Challenge for Biodiversity Conservation. *Trends in Ecology & Evolution*, 24(10), pp. 564-571.

Landrigan, P. J., Fuller, R., Acosta, N. J. R., ..., and Zhong, M. (2018). The *Lancet* Commission on Pollution and Health. *The Lancet*, 391(10119), pp. 462-512.

Lapola, D. M., Pinho, P., Barlow, J., ..., and Walker, W. S. (2023). The Drivers and Impacts of Amazon Forest Degradation. *Science*, 379(6630), eabp8622, 11 pages.

Larsen, B. B., Miller, E. C., Rhodes, M. K., and Wiens, J. J. (2017). Inordinate Fondness Multiplied and Redistributed: The Number of Species on Earth and the New Pie of Life. *Quarterly Review of Biology*, 92(3), pp. 229-265.

Leakey, R. E., and Lewin, R. (1995). *The Sixth Extinction: Patterns of Life and the Future of Humankind*. Doubleday, 271 pages.

Lebreton, L., Slat, B., Ferrari, F., ..., and Reisser, J. (2018). Evidence that the Great Pacific Garbage Patch is Rapidly Accumulating Plastic. *Scientific Reports*, 8(1), pp. 1-15.

Legesse, F., Degefa, S., and Soromessa, T. (2022). Valuation Methods in Ecosystem Services: A Meta-analysis. *World Journal of Forest Research*, 1(1), pp. 1-12.

Lelieveld, J., Evans, J. S., Fnais, M., Giannadaki, D., and Pozzer, A. (2015). The Contribution of Outdoor Air Pollution Sources to Premature Mortality on a Global Scale. *Nature*, 525(7569), pp. 367-371.

Lesiv, M., Schepaschenko, D., Buchhorn, M., ..., and Fritz, S. (2022). Global Forest Management Data for 2015 at a 100 m Resolution. *Scientific Data*, 9(1), 199, 14 pages.

Loehle, C., and Eschenbach, W. (2012). Historical Bird and Terrestrial Mammal Extinction Rates and Causes. *Diversity and Distributions*, 18(1), pp. 84-91.

Lomolino, M. V. (2001). The Species-Area Relationship: New Challenges for an Old Pattern. *Progress in Physical Geography*, 25(1), pp. 1-21.

Longcore, T., and Rich, C. (2004). Ecological Light Pollution. *Frontiers in Ecology and the Environment*, 2(4), pp. 191-198.

Lotka, A. J. (1925). *Elements of Physical Biology*. First edition, Williams and Wilkins Company, 495 pages.

Ludwig, D., Hilborn, R., and Walters, C. (1993). Uncertainty, Resource Exploitation, and Conservation: Lessons from History. *Science*, 260(5104), pp. 17-36.

Lueck, D. (2002). The Extermination and Conservation of the American Bison. *Journal of Legal Studies*, 31(S2), pp. 609-652.

MacArthur, R. H. (1957). On the Relative Abundance of Bird Species. *Proceedings of the National Academy of Sciences*, 43(3), pp. 293-295.

MacArthur, R. H. (1958). Population Ecology of Some Warblers of Northeastern Coniferous Forests. *Ecology*, 39(4), pp. 599-619.

MacArthur, R. (1970). Species Packing and Competitive Equilibrium for Many Species. *Theoretical Population Biology*, 1(1), pp. 1-11.

MacArthur, R. H., and Levins, R. (1964). Competition, Habitat Selection, and Character Displacement in a Patchy Environment. *Proceedings of the National Academy of Sciences*, 51(6), pp. 1207-1210.

MacArthur, R. H., and Wilson, E. O. (1967). *The Theory of Island Biogeography*. Princeton University Press, 203 pages.

Mace, G. M. (1998). Getting the Measure of Extinction. *People Planet*, 7(4):9, PMID: 12348876.

Mace, G. M., and Baillie, J. E. M. (2007). The 2010 Biodiversity Indicators: Challenges for Science and Policy. *Conservation Biology*, 21(6), pp. 1406-1413.

Mack, R. N., Simberloff, D., Lonsdale, W. M., Evans, H., Clout, M., and Bazzaz, F. A. (2000). Biotic Invasions: Causes, Epidemiology, Global Consequences, and Control. *Ecological Applications*, 10(3), pp. 689-710.

MacLeod, M., Arp, H. P. H., Tekman, M. B., and Jahnke, A. (2021). The Global Threat from Plastic Pollution. *Science*, 373(6550), pp. 61-65.

Mair, L., Bennun, L. A., Brooks, T. M., ..., and McGowan, P. J. (2021). A Metric for Spatially Explicit Contributions to Science-based Species Targets. *Nature Ecology & Evolution*, 5(6), pp. 836-844.

Malthus, T. R. (1798). *An Essay on the Principle of Population*. First edition, J. Johnson.

Matthews, T. J., and Whittaker, R. J. (2015). On the Species Abundance Distribution in Applied Ecology and Biodiversity Management. *Journal of Applied Ecology*, 52(2), pp. 443-454.

May, R. M. (1975). Patterns of Species Abundance and Distribution. In Cody, M., and Diamond, J. (Eds), *Ecology and Evolution of Communities*, Harvard University Press, pp. 81-120.

May, R. M. (1988). How Many Species are there on Earth?. *Science*, 241(4872), pp. 1441-1449.

May, R. M. (2010). Tropical Arthropod Species, More or Less?. *Science*, 329(5987), pp. 41-42.

McCarthy, D. P., Donald, P. F., Scharlemann, J. P. W., ..., and Butchart, S. H. (2012). Financial Costs of Meeting Global Biodiversity Conservation Targets: Current Spending and Unmet Needs. *Science*, 338(6109), pp. 946-949.

McGill, B. J., Etienne, R. S., Gray, J. S., ..., and White, E. P. (2007). Species Abundance Distributions: Moving Beyond Single Prediction Theories to Integration within an Ecological Framework. *Ecology Letters*, 10(10), pp. 995-1015.

Meijer, L. J. J., Van Emmerik, T., Van Der Ent, R., Schmidt, C., and Lebreton, L. (2021). More than 1000 Rivers Account for 80% of Global Riverine Plastic Emissions into the Ocean. *Science Advances*, 7(18), eaaz5803, 13 pages.

Mejino-López, J., and Oliu-Barton, M. (2024). How Much Does Europe Pay for Clean Air?. *Bruegel Working Paper*, 15/2024, June, 49 pages.

Millennium Ecosystem Assessment (2005). Ecosystems and Human Well-being: Synthesis. *Report*, 155 pages, www.millenniumassessment.org.

Missemer, A. (2018). Natural Capital as an Economic Concept, History and Contemporary Issues. *Ecological Economics*, 143, pp. 90-96.

Mittermeier, R. A., Turner, W. R., Larsen, F. W., Brooks, T. M., and Gascon, C. (2011). Global Biodiversity Conservation: The Critical Role of Hotspots. In Zachos, F. E., and Habel, J. C. (Eds), *Biodiversity Hotspots: Distribution and Protection of Conservation Priority Areas*, Springer, Chapter 1, pp. 3-22.

Mooney, H. A., and Ehrlich, P. R. (1997). Ecosystem Services: A Fragmentary History. In Daily, G. C. (Ed.), *Nature's Services: Societal Dependence On Natural Ecosystems*, Island Press, Chapter 2, pp. 11-19.

Mora, C., Tittensor, D. P., Adl, S., Simpson, A. G., and Worm, B. (2011). How Many Species are there on Earth and in the Ocean?. *PLoS biology*, 9(8), e1001127, 8 pages.

Müller-Wenk, R. (1998). Land Use — The Main Threat to Species: How to Include Land Use in LCA. Institut für Wirtschaft und Ökologie, Universität St. Gallen, *IWÖ Discussion Paper*, 64, 46 pages.

Myers, N. (1988). Threatened Biotas: "Hot Spots" in Tropical Forests. *Environmentalist*, 8, pp. 187-208.

Myers, N. (1990). The Biodiversity Challenge: Expanded Hot-spots Analysis. *Environmentalist*, 10(4), pp. 243-256.

Myers, N., Mittermeier, R., Mittermeier, C. G., Da Fonseca, G. A. B., and Kent, J. (2000). Biodiversity Hotspots for Conservation Priorities. *Nature*, 403, pp. 853-858.

Myers, R. A., Hutchings, J. A., and Barrowman, N. J. (1997). Why Do Fish Stocks Collapse? The Example of Cod in Atlantic Canada. *Ecological Applications*, 7(1), pp. 91-106.

Myers, R. A., and Worm, B. (2003). Rapid Worldwide Depletion of Predatory Fish Communities. *Nature*, 423(6937), pp. 280-283.

Myllyvirta, L. (2020). Quantifying the Economic Costs of Air Pollution from Fossil Fuels. *Centre for Research on Energy and Clean Air (CREA)*, *Working Paper*, February, 14 pages.

Naidu, R., Biswas, B., Willett, I. R., ..., and Aitken, R. J. (2021). Chemical Pollution: A Growing Peril and Potential Catastrophic Risk to Humanity. *Environment International*, 156, 106616, 12 pages.

Naiken, L. (2002). Keynote Paper: FAO Methodology for Estimating the Prevalence of Undernourishment. In *Measurement and Assessment of Food Deprivation and Undernutrition*, Proceedings of the International Scientific Symposium convened by the Agriculture and Economic Development Analysis Division, FAO, Rome, 26-28 June 2002.

Nasi, R., Brown, D., Wilkie, D., Bennett, E., Tutin, C., Van Tol, G., and Christophersen, T. (2008). *Conservation and Use of Wildlife-based Resources: The Bushmeat Crisis*. Secretariat of the Convention on Biological Diversity and Center for International Forestry Research, CBD Technical Series, 33, 50 pages.

Nasi, R., Taber, A., and Van Vliet, N. (2011). Empty Forests, Empty Stomachs? Bushmeat and Livelihoods in the Congo and Amazon Basins. *International Forestry Review*, 13(3), pp. 355-368.

Newman, M. C. (2019). *Fundamentals of Ecotoxicology — The Science of Pollution*. Fifth edition, CRC Press, 708 pages.

NGFS (2024). Nature-related Financial Risks: A Conceptual Framework to Guide Action by Central Banks and Supervisors. *Report*, July, 50 pages.

Noss, R. F., Platt, W. J., Sorrie, B. A., ..., and Peet, R. K. (2015). How Global Biodiversity Hotspots May Go Unrecognized: Lessons from the North American Coastal Plain. *Diversity and Distributions*, 21(2), pp. 236-244.

Nurk, S., Koren, S., Rhie, A., ..., and Phillippy, A. M. (2022). The Complete Sequence of a Human Genome. *Science*, 376(6588), pp. 44-53.

OECD (2021). Biodiversity, Natural Capital and the Economy: A Policy Guide for Finance, Economic and Environment Ministers. *OECD Environment Policy Papers*, 26, May, 83 pages.

OECD (2022). *Global Plastics Outlook: Policy Scenarios to 2060*. OECD Publishing, Paris.

Olhnuud, A., Liu, Y., Makowski, D., ..., and Van der Werf, W. (2022). Pollination Deficits and Contributions of Pollinators in Apple Production: A Global Meta-analysis. *Journal of Applied Ecology*, 59(12), pp. 2911-2921.

Ollerton, J., Winfree, R., and Tarrant, S. (2011). How Many Flowering Plants are Pollinated by Animals?. *Oikos*, 120(3), pp. 321-326.

Olson, D. M., Dinerstein, E., Wikramanayake, E. D., ..., and Kassem, K. R. (2001). Terrestrial Ecoregions of the World: A New Map of Life on Earth. *BioScience*, 51(11), pp. 933-938.

Olson, D. M., and Dinerstein, E. (2002). The Global 200: Priority Ecoregions for Global Conservation. *Annals of the Missouri Botanical Garden*, 89(2), pp. 199-224.

Ott, W. R. (1978). *Environmental Indices: Theory and Practice*. Ann Arbor Science, 371 pages.

Ott, W. R., and Thorn, G. C. (1976). Air Pollution Index Systems in the United States and Canada. *Journal of the Air Pollution Control Association*, 26(5), pp. 460-470.

Park, T. (1962). Beetles, Competition, and Populations. *Science*, 138(3548), pp. 1369-1375.

Pauly, D., Christensen, V., Guénette, S., ..., and Zeller, D. (2002). Towards Sustainability in World Fisheries. *Nature*, 418(6898), pp. 689-695.

Pauly, D., Watson, R., and Alder, J. (2005). Global Trends in World Fisheries: Impacts on Marine Ecosystems and Food Security. *Philosophical Transactions of the Royal Society B: Biological Sciences*, 360(1453), pp. 5-12.

Pearce, D. (1988). Economics, Equity and Sustainable Development. *Futures*, 20(6), pp. 598-605.

Pearce, D. (1998). Auditing the Earth: The Value of the World's Ecosystem Services and Natural Capital. *Environment: Science and Policy for Sustainable Development*, 40(2), pp. 23-28.

Pearce, D., Putz, F. E., and Vanclay, J. K. (2003). Sustainable Forestry in the Tropics: Panacea or Folly?. *Forest Ecology and Management*, 172(2-3), pp. 229-247.

PEREIRA, H. M., FERRIER, S., WALTERS, M., ..., and WEGMANN, M. (2013). Essential Biodiversity Variables. *Science*, 339(6117), pp. 277-278.

PERES, C. A. (2010). Overexploitation. In Sodhi, N. S., and Ehrlich, P. R. (Eds), *Conservation Biology for All*, Oxford University Press, Chapter 6, pp. 107-130.

PERES, C. A., and PALACIOS, E. (2007). Basin-wide Effects of Game Harvest on Vertebrate Population Densities in Amazonian Forests: Implications for Animal-mediated Seed Dispersal. *Biotropica*, 39(3), pp. 304-315.

PÉREZ RODA, M. A., GILMAN, E., HUNTINGTON, T., KENNELLY, S. J., SUURONEN, P., CHALOUPKA, M. and MEDLEY, P. A. H. (2019). A Third Assessment of Global Marine Fisheries Discards. *FAO Fisheries and Aquaculture Technical Paper*, 633, 78 pages.

Phenix Capital (2024b). Biodiversity Funds at a Glance. *Phenix Report*, April, 30 pages.

PIMM, S. L., and BROOKS, T. M. (2000). The Sixth Extinction: How Large, Where, and When. In Raven, P. H. (Ed.), *Nature and Human Society: The Quest for a Sustainable World — Proceedings of the 1997 Forum on Biodiversity*, National Academic Press, Chapter 4, pp. 46-62.

PIMM, S. L., RUSSELL, G. J., GITTLEMAN, J. L., and BROOKS, T. M. (1995). The Future of Biodiversity. *Science*, 269(5222), pp. 347-350.

POINTER, M. D., GAGE, M. J. G., and SPURGIN, L. G. (2021). Tribolium Beetles as a Model System in Evolution and Ecology. *Heredity*, 126(6), pp. 869-883.

POLIS, G. A., MYERS, C. A., and HOLT, R. D. (1989). The Ecology and Evolution of Intraguild Predation: Potential Competitors that Eat Each Other. *Annual Review of Ecology and Systematics*, 20, pp. 297-330.

POLLAN, M. (2007). *The Omnivore's Dilemma: A Natural History of Four Meals*. Penguin, 480 pages.

POPE III, C. A., and DOCKERY, D. W. (2006). Health Effects of Fine Particulate Air Pollution: Lines That Connect. *Journal of the Air & Waste Management Association*, 56(6), pp. 709-742.

POTAPOV, P. V., HANSEN, M. C., PICKENS, A., ..., and KOMMAREDDY, A. (2022). The Global 2000-2020 Land Cover and Land Use Change Dataset derived from the Landsat Archive: First Results. *Frontiers in Remote Sensing*, 3, 856903, 22 pages.

POTTS, S. G., BIESMEIJER, J. C., KREMEN, C., NEUMANN, P., SCHWEIGER, O., and KUNIN, W. E. (2010). Global Pollinator Declines: Trends, Impacts and Drivers. *Trends in Ecology & Evolution*, 25(6), pp. 345-353.

POTTS, S. G., IMPERATRIZ-FONSECA, V., NGO, H. T., ..., and VANBERGEN, A. J. (2016). Safeguarding Pollinators and Their Values to Human Well-being. *Nature*, 540(7632), pp. 220-229.

PRESTON, F. W. (1948). The Commonness and Rarity of Species. *Ecology*, 29(3), pp. 254-283.

PRESTON, F. W. (1960). Time and Space and the Variation of Species. *Ecology*, 41(4),pp. 612-627.

PRIMACK, R. B. (2014). *Essentials of Conservation Biology*. Sixth edition, Sinauer Associates & Oxford University Press, 603 pages.

Quinn, T. J., and Deriso, R. B. (1999). *Quantitative Fish Dynamics*. Oxford University Press, 560 pages.

Rader, R., Bartomeus, I., Garibaldi, L. A., ..., and Woyciechowski, M. (2016). Non-bee Insects are Important Contributors to Global Crop Pollination. *Proceedings of the National Academy of Sciences*, 113(1), pp. 146-151.

Rahman, M. T., Sobur, M. A., Islam, M. S., ..., and Ashour, H. M. (2020). Zoonotic Diseases: Etiology, Impact, and Control. *Microorganisms*, 8(9), 1405, 34 pages.

Ramírez-Delgado, J. P., Di Marco, M., Watson, J. E. M., ..., and Venter, O. (2022). Matrix Condition Mediates the Effects of Habitat Fragmentation on Species Extinction Risk. *Nature Communications*, 13(1), 595, 10 pages.

Ratto, F., Simmons, B. I., Spake, R., ..., and Dicks, L. V. (2018). Global Importance of Vertebrate Pollinators for Plant Reproductive Success: A Meta-analysis. *Frontiers in Ecology and the Environment*, 16(2), pp. 82-90.

Raup, D. M., and Sepkoski, J. J. (1982). Mass Extinctions in the Marine Fossil Record. *Science*, 215(4539), pp. 1501-1503.

Reynolds, J. D. and Peres, C. A. (2006). Overexploitation. In Groom, M. J., Meffe, G. K., and Carroll, C. R. (Eds), *Principles of Conservation Biology*, Third edition, Sinauer Associates, Chapter 8, pp 253-277.

Rice, R. E., Gullison, R. E., and Reid, J. W. (1997). Can Sustainable Management Save Tropical Forests?. *Scientific American*, 276(4), pp. 44-49.

Rickards, R. B. (1977). Patterns of Evolution in the Graptolites. In Halam, A. (Ed.), *Developments in Palaeontology and Stratigraphy — Patterns of Evolution as Illustrated by the Fossil Record*, 5, Elsevier, Chapter 10, pp. 333-358.

Ripple, W. J., Abernethy, K., Betts, M. G., ..., and Young, H. (2016). Bushmeat Hunting and Extinction Risk to the World's Mammals. *Royal Society Open Science*, 3(10), 160498, 16 pages.

Ripple, W. J., Wolf, C., Newsome, T. M., ..., and Worm, B. (2019). Are We Eating the World's Megafauna to Extinction?. *Conservation Letters*, 12(3), e12627.

Ritz, C. (2010). Toward a Unified Approach to Dose-Response Modeling in Ecotoxicology. *Environmental Toxicology and Chemistry*, 29(1), pp. 220-229.

Ritz, C., Baty, F., Streibig, J. C., and Gerhard, D. (2015). Dose-Response Analysis using R. *PloS One*, 10(12), e0146021, 13 pages.

Rohde, R. A., and Muller, R. A. (2005). Cycles in Fossil Diversity. *Nature*, 434(7030), pp. 208-210.

Roncalli, T. (2020a). *Handbook of Financial Risk Management*. Chapman and Hall/CRC Financial Mathematics Series.

Roncalli, T. (2025). *Handbook of Sustainable Finance*. SSRN, 4277875, 1272 pages.

Roques, L., Hosono, Y., Bonnefon, O., and Boivin, T. (2015). The Effect of Competition on the Neutral Intraspecific Diversity of Invasive Species. *Journal of Mathematical Biology*, 71, pp. 465-489.

ROSENZWEIG, M. L. (1995). *Species Diversity in Space and Time.* Cambridge University Press, 436 pages.

ROSSBERG, A. G. (2022). Quantifying Biodiversity Impact. *Technical Report*, Queen Mary University of London, 16 pages.

ROSSBERG, Axel G., O'SULLIVAN, J. D., MALYSHEVA, S., and SHNERB, N. M. (2023). A Metric for Tradable Biodiversity Credits Linked to the Living Planet Index and Global Species Conservation. *arXiv*, 2111.03867.

SALA, O. E., STUART CHAPIN III, F. , ARMESTO, J. J., ..., and WALL, D. H. (2000). Global Biodiversity Scenarios for the Year 2100. *Science*, 287(5459), pp. 1770-1774.

SÁNCHEZ-BAYO, F., and WYCKHUYS, K. A. G. (2019). Worldwide Decline of the Entomofauna: A Review of its Drivers. *Biological Conservation*, 232, pp. 8-27.

SAYRE, R., KARAGULLE, D., FRYE, C., ..., and POSSINGHAM, H. (2020). An Assessment of the Representation of Ecosystems in Global Protected Areas using New Maps of World Climate Regions and World Ecosystems. *Global Ecology and Conservation*, 21, e00860, 21 pages.

SCHAEFER, M. B. (1954). Some Aspects of the Dynamics of Populations Important to the Management of Commercial Marine Fisheries. *Bulletin of the Inter-American Tropical Tuna Commission*, 1(2), pp. 27-56.

SCHERINGER, M., STREMPEL, S., HUKARI, S., NG, C. A., BLEPP, M., and HUNGERBUHLER, K. (2012). How Many Persistent Organic Pollutants Should We Expect?. *Atmospheric Pollution Research*, 3(4), pp. 383-391.

SCHIJNS, R., FROESE, R., HUTCHINGS, J. A., and PAULY, D. (2021). Five Centuries of Cod Catches in Eastern Canada. *ICES Journal of Marine Science*, 78(8), pp. 2675-2683.

SCHIPPER, A. M., HILBERS, J. P., MEIJER, J. R., ..., and HUIJBREGTS, M. A. (2020). Projecting Terrestrial Biodiversity Intactness with GLOBIO 4. *Global Change Biology*, 26(2), pp. 760-771.

SCHMELLER, D. S., WEATHERDON, L. V., LOYAU, A., ..., and REGAN, E. C. (2018). A Suite of Essential Biodiversity Variables for Detecting Critical Biodiversity Change. *Biological Reviews*, 93(1), pp. 55-71.

SCHNEIDER, V. A., GRAVES-LINDSAY, T., HOWE, K., ..., and CHURCH, D. M. (2017). Evaluation of GRCh38 and de novo Haploid Genome Assemblies Demonstrates the Enduring Quality of the Reference Assembly. *Genome Research*, 27(5), pp. 849-864.

SCHOLES, R. J., and BIGGS, R. (2005). A Biodiversity Intactness Index. *Nature*, 434(7029), pp. 45-49.

SCHULP, C. J. E., THUILLER, W., and VERBURG, P. H. (2014). Wild Food in Europe: A Synthesis of Knowledge and Data of Terrestrial Wild Food as an Ecosystem Service. *Ecological Economics*, 105, pp. 292-305.

SCHULTE, P., ALEGRET, L., ARENILLAS, I., ..., and WILLUMSEN, P. S. (2010). The Chicxulub Asteroid Impact and Mass Extinction at the Cretaceous-Paleogene Boundary. *Science*, 327(5970), pp. 1214-1218.

SEPKOSKI, J. J. (2002). A Compendium of Fossil Marine Animal Genera. In Jablonski, D., and Foote, M. (Eds), *Bulletins of American paleontology*, 363, 560 pages.

SIMBERLOFF, D. (2010). Invasive Species. In Sodhi, N. S., and Ehrlich, P. R. (Eds), *Conservation Biology for All*, Oxford University Press, Chapter 7, pp. 131-152.

SIMBERLOFF, D., MARTIN, J. L., GENOVESI, P., ..., and VILÀ, M. (2013). Impacts of Biological Invasions: What's What and The Way Forward. *Trends in Ecology & Evolution*, 28(1), pp. 58-66.

SIMPSON, G. G. (1952). How Many Species. *Evolution*, 6(3), pp. 342

SEKERCIOGLU, C. H. (2010). Ecosystem Function and Services. In Sodhi, N. S., and Ehrlich, P. R. (Eds), *Conservation Biology for All*, Oxford University Press, Chapter 3, pp. 45-72.

SKIDMORE, A. K., COOPS, N. C., NEINAVAZ, E., ..., and WINGATE, V. (2021). Priority List of Biodiversity Metrics to Observe From Space. *Nature Ecology & Evolution*, 5(7), pp. 896-906.

SMITH, K. T., LOPEZ, B., VIGNIERI, S., and WIBLE, B. (2023). Losing the Darkness. *Science*, 380(6650), pp. 1116-1117.

SODHI, N. S. and EHRLICH, P. R. (2010). *Conservation Biology for All*. Oxford University Press, 351 pages.

SOLÉ, M., KAIFU, K., MOONEY, T. A., ..., and ANDRÉ, M. (2023). Marine Invertebrates and Noise. *Frontiers in Marine Science*, 10, 1129057, 34 pages.

SOLOMON, M. E. (1949). The Natural Control of Animal Populations. *Journal of Animal Ecology*, 18, pp. 1-35.

SPALDING, C., and HULL, P. M. (2021). Towards Quantifying the Mass Extinction Debt of the Anthropocene. *Proceedings of the Royal Society B (Biological Sciences)*, 288(1949), 20202332, 9 pages.

STEFFEN, W., BROADGATE, W., DEUTSCH, L., GAFFNEY, O., and LUDWIG, C. (2015). The Trajectory of the Anthropocene: The Great Acceleration. *Anthropocene Review*, 2(1), pp. 81-98.

STEVENS, C. J., DISE, N. B., MOUNTFORD, J. O., and GOWING, D. J. (2004). Impact of Nitrogen Deposition on the Species Richness of Grasslands. *Science*, 303(5665), pp. 1876-1879.

STREVENS, C. M. J., and BONSALL, M. B. (2011). The Impact of Alternative Harvesting Strategies in a Resource-Consumer Metapopulation. *Journal of Applied Ecology*, 48(1), pp. 102-111.

SUKHATME, P. V. (1961). The World's Hunger and Future Needs in Food Supplies. *Journal of the Royal Statistical Society: Series A*, 124(4), pp. 463-508.

SVARTZMAN, R., ESPAGNE, E., GAUTHEY, J., ..., and VALLIER, A. (2021). A "Silent Spring" for the Financial System? Exploring Biodiversity-Related Financial Risks in France. *Banque de France Working Paper*, 826, August, 95 pages.

SVENNING, J. C., LEMOINE, R. T., BERGMAN, J., ..., and PEDERSEN, R. Ø. (2024). The Late-Quaternary Megafauna Extinctions: Patterns, Causes, Ecological Consequences and Implications for Ecosystem Management in the Anthropocene. *Cambridge Prisms: Extinction*, 2, e5, 27 pages.

SYEED, M. M. M., HOSSAIN, M. S., KARIM, M. R., UDDIN, M. F., HASAN, M., and KHAN, R. H. (2023). Surface Water Quality Profiling Using the Water Quality Index, Pollution Index and Statistical Methods: A Critical Review. *Environmental and Sustainability Indicators*, 18, 100247, 23 pages.

TAFT, R. J., and MATTICK, J. S. (2003). Increasing Biological Complexity is Positively Correlated with the Relative Genome-wide Expansion of Non-protein-coding DNA Sequences. *Genome Biology*, 5(1), pp. 1-24.

TANNER, J. T. (1975). The Stability and the Intrinsic Growth Rates of Prey and Predator Populations. *Ecology*, 56(4), pp. 855-867.

Taskforce on Nature-related Financial Disclosures (2023). Recommendations of the Taskforce on Nature-related Financial Disclosures. *Final Report*, September, 154 pages.

TAYLOR, L. H., LATHAM, S. M., and WOOLHOUSE, M. E. J. (2001). Risk Factors for Human Disease Emergence. *Philosophical Transactions of the Royal Society B: Biological Sciences*, 356(1411), pp. 983-989.

THANGAVEL, P., PARK, D., and LEE, Y. C. (2022). Recent Insights into Particulate Matter ($PM_{2.5}$)-mediated Toxicity in Humans: An Overview. *International Journal of Environmental Research and Public Health*, 19(12), 7511, 22 pages.

THOGMARTIN, W. E., WIEDERHOLT, R., OBERHAUSER, K., ..., and LOPEZ-HOFFMAN, L. (2017). Monarch Butterfly Population Decline in North America: Identifying the Threatening Processes. *Royal Society Open Science*, 4(9), 170760, 16 pages.

THOMPSON, I. D., GUARIGUATA, M. R., OKABE, K., BAHAMONDEZ, C., NASI, R., HEYMELL, V., and SABOGAL, C. (2013). An Operational Framework for Defining and Monitoring Forest Degradation. *Ecology and Society*, 18(2), Art. 20, 23 pages.

THURSTAN, R. H., BROCKINGTON, S., and ROBERTS, C. M. (2010). The Effects of 118 Years of Industrial Fishing on UK Bottom Trawl Fisheries. *Nature Communications*, 1(15), 6 pages.

TILMAN, D (1982). *Resource Competition and Community Structure*. Monographs in Population Biology, 17, Princeton University Press.

TILMAN, D., MAY, R. M., LEHMAN, C. L., and NOWAK, M. A. (1994). Habitat Destruction and the Extinction Debt. *Nature*, 371(6492), pp. 65-66.

TJØRVE, E. (2003). Shapes and Functions of Species-Area Curves: A Review of Possible Models. *Journal of Biogeography*, 30(6), pp. 827-835.

TRIANTIS, K. A., GUILHAUMON, F., and WHITTAKER, R. J. (2012). The Island Species-Area Relationship: Biology and Statistics. *Journal of Biogeography*, 39(2), pp. 215-231.

United Nations Office on Drugs and Crimes (2024). *World Wildlife Crime Report 2024: Trafficking in Protected Species*. May, 242 pages.

US Environmental Protection Agency (2024). *Technical Assistance Document for the Reporting of Daily Air Quality — the Air Quality Index (AQI)*. EPA-454/B-24-002, May, 32 pages.

VALENTINE, J. W. (1970). How Many Marine Invertebrate Fossil Species? A New Approximation. *Journal of Paleontology*, 44(3), pp. 410-415.

VAN BRUGGEN, A. H., HE, M. M., SHIN, K., ..., and MORRIS Jr, J. G. (2018). Environmental and Health Effects of the Herbicide Glyphosate. *Science of the Total Environment*, 616, pp. 255-268.

VAN DER PLOEG, S., and DE GROOT, R. (2010). *The TEEB Valuation Database — A Searchable Database of 1310 Estimates of Monetary Values of Ecosystem Services.* Foundation for Sustainable Development, www.teebweb.org.

VAN VALEN, L. (1973). A New Evolutionary Law. *Evolutionary Theory*, 1, pp. 1-30.

VANO, J. A., WILDENBERG, J. C., ANDERSON, M. B., NOEL, J. K., and SPROTT, J. C. (2006). Chaos in Low-dimensional Lotka-Volterra Models of Competition. *Nonlinearity*, 19(10), pp. 2391âĂŞ2404.

VENTER, J. C., ADAMS, M. D., MYERS, E. W., ..., and KALUSH, F. (2001). The Sequence of the Human Genome. *Science*, 291(5507), pp. 1304-1351.

VERHULST, P. F. (1838). Notice sur la loi que la population poursuit dans son accroissement. *Correspondance Mathématique et Physique.* 10, pp. 113-121.

VISCUSI, W. K., and MASTERMAN, C. J. (2017). Income Elasticities and Global Values of a Statistical Life. *Journal of Benefit-Cost Analysis*, 8(2), pp. 226-250.

VITOUSEK, P. M., MOONEY, H. A., LUBCHENCO, J., and MELILLO, J. M. (1997). Human Domination of Earth's Ecosystems. *Science*, 277(5325), pp. 494-499.

VOLTERRA, V. (1928). Variations and Fluctuations of the Number of Individuals in Animal Species Living Together. *ICES Journal of Marine Science*, 3(1), pp. 3-51.

WACKERNAGEL, M., and REES, W. (1996). *Our Ecological Footprint: Reducing Human Impact on the Earth.* New Society Publishers.

WAKE, D. B., and VREDENBURG, V. T. (2008). Are We in the Midst of the Sixth Mass Extinction? A View from the World of Amphibians. *Proceedings of the National Academy of Sciences*, 105, pp. 11466-11473.

WALDRON, A., MOOERS, A. O., MILLER, D. C., ..., and GITTLEMAN, J. L. (2013). Targeting Global Conservation Funding to Limit Immediate Biodiversity Declines. *Proceedings of the National Academy of Sciences*, 110(29), pp. 12144-12148.

WALKER, W. H., BUMGARNER, J. R., WALTON, J. C., ..., and DEVRIES, A. C. (2020). Light Pollution and Cancer. *International Journal of Molecular Sciences*, 21(24), 9360, 18 pages.

WANG, F., XIANG, L., LEUNG, K. S. Y., .., and TIEDJE, J. M. (2024). Emerging Contaminants: A One Health Perspective. *The Innovation*, 5(4), 100612, 32 pages.

WANG, Z., WALKER, G. W., MUIR, D. C. G., and NAGATANI-YOSHIDA, K. (2020). Toward A Global Understanding of Chemical Pollution: A First Comprehensive Analysis of National and Regional Chemical Inventories. *Environmental Science & Technology*, 54(5), pp. 2575-2584.

WARREN, M. S., MAES, D., VAN SWAAY, C. A. M., ..., and ELLIS, S. (2021). The Decline of Butterflies in Europe: Problems, Significance, and Possible Solutions. *Proceedings of the National Academy of Sciences*, 118(2), e2002551117, 10 pages.

WATANABE, K. (2015). Potato Genetics, Genomics, and Applications. *Breeding Science*, 65(1), pp. 53-68.

WATSON, J. E. M., EVANS, T., VENTER, O., ..., and LINDENMAYER, D. (2018). The Exceptional Value of Intact Forest Ecosystems. *Nature Ecology & Evolution*, 2(4), pp. 599-610.

WELDON, C., DU PREEZ, L. H., HYATT, A. D., MULLER, R., and SPEARE, R. (2004). Origin of the Amphibian Chytrid Fungus. *Emerging Infectious Diseases*, 10(12), pp. 2100-2105.

WEPPRICH, T., ADRION, J. R., RIES, L., WIEDMANN, J., and HADDAD, N. M. (2019). Butterfly Abundance Declines over 20 Years of Systematic Monitoring in Ohio, USA. *PLoS One*, 14(7), e0216270, 21 pages.

WHITTAKER, R. H. (1960). Vegetation of the Siskiyou Mountains, Oregon and California. *Ecological Monographs*, 30(3), pp. 279-338.

WHITTAKER, R. H. (1965). Dominance and Diversity in Land Plant Communities: Numerical Relations of Species Express the Importance of Competition in Community Function and Evolution. *Science*, 147(3655), pp. 250-260.

WHITTAKER, R. H., HARRISON, S., and DAMSCHEN, E. (2022). Plant Community Data Collected by Robert H. Whittaker in the Siskiyou Mountains, Oregon and California, USA. *Ecology*, 103(9), e3764, https://doi.org/10.1002/ecy.3764.

WIENS, J. J. (2023). How Many Species are there on Earth? Progress and Problems. *PLoS biology*, 21(11), e3002388, 4 pages.

WILKIE, D. S., BENNETT, E. L., PERES, C. A., and CUNNINGHAM, A. A. (2011). The Empty Forest Revisited. *Annals of the New York Academy of Sciences*, 1223(1), pp. 120-128.

WILLIG, M. R., KAUFMAN, D. M., and STEVENS, R. D. (2003). Latitudinal Gradients of Biodiversity: Pattern, Process, Scale, and Synthesis. *Annual Review of Ecology, Evolution, and Systematics*, 34(1), pp. 273-309.

WILSON, E. O. (1989). Threats to Biodiversity. *Scientific American*, 261(3), pp. 108-117.

World Bank (2022). The Global Health Cost of $PM_{2.5}$ Air Pollution: A Case for Action Beyond 2021. *International Development in Focus*, January, 89 pages.

World Economic Forum (2020a). *Nature Risk Rising: Why the Crisis Engulfing Nature Matters for Business and the Economy.* January, 36 pages.

World Economic Forum (2020b). *New Nature Economy Report II: The Future of Nature and Business.* July, 111 pages.

World Health Organization (2009). *Principles for Modelling Dose-Response for the Risk Assessment of Chemicals.* Environmental Health Criteria, 239, 163 pages.

World Health Organization (2006). *Air Quality Guidelines — Global Update 2005.* August, 496 pages.

World Health Organization (2021). *WHO Global Air Quality Guidelines — Particulate Matter ($PM_{2.5}$ and PM_{10}), Ozone, Nitrogen Dioxide, Sulfur Dioxide and Carbon Monoxide.* Geneva, 300 pages.

World Ocean Review (2015). *Sustainable Use of Our Oceans — Making Ideas Work*. Volume 4, 78 pages, worldoceanreview.com.

WORM, B., BARBIER, E. B., BEAUMONT, N., ..., and WATSON, R. (2006). Impacts of Biodiversity Loss on Ocean Ecosystem Services. *Science*, 314(5800), pp. 787-790.

WORM, B., HILBORN, R., BAUM, J. K., ..., and ZELLER, D. (2009). Rebuilding Global Fisheries. *Science*, 325(5940), pp. 578-585.

WRATTEN, S. D., GILLESPIE, M., DECOURTYE, A., MADER, E., and DESNEUX, N. (2012). Pollinator Habitat Enhancement: Benefits to Other Ecosystem Services. *Agriculture, Ecosystems & Environment*, 159, pp. 112-122.

WRIGHT, D. A., and WELBOURN, P. (2002). *Environmental Toxicology*. Environmental Chemistry Series Book 11, Cambridge University Press, 656 pages.

YAARI, M. E. (1965). Uncertain Lifetime, Life Insurance, and The Theory of The Consumer. *Review of Economic Studies*, 32(2), pp. 137-150.

ZALLES, V., HARRIS, N., STOLLE, F., and HANSEN, M. C. (2024). Forest Definitions Require a Re-think. *Communications Earth & Environment*, 5(1), 620, 4 pages.

ZELLER, D., CASHION, T., PALOMARES, M., and PAULY, D. (2018). Global Marine Fisheries Discards: A Synthesis of Reconstructed Data. *Fish and Fisheries*, 19(1), pp. 30-39.

ZHANG, S., QIAO, S., YU, J., ..., and WANG, X. (2021). Bat and Pangolin Coronavirus Spike Glycoprotein Structures Provide Insights into SARS-CoV-2 Evolution. *Nature Communications*, 12(1), 1607, 12 pages.

ZHANG, X., ZHONG, T., LIU, L., and OUYANG, X. (2015). Impact of Soil Heavy Metal Pollution on Food Safety in China. *Plos One*, 10(8), e0135182, 14 pages.

ZOHARY, D., and HOPF, M. (1988). *Domestication of Plants in the Old World. The Origin and Spread of Cultivated Plants in West Asia, Europe, and the Nile Valley*. Clarendon Press, 249 pages. Fourth edition in 2012 with Weiss, E., Oxford University Press, 264 pages.

A Exercises

A.1 Calculating the prevalence of undernourishment

Let X and R be the random variables representing energy intake and energy requirement, respectively.

1. We assume that the random vector (X, R) follows a bivariate log-normal distribution: $(X, R) \sim \mathcal{LN}\left(\mu_x, \sigma_x^2, \mu_r, \sigma_r^2, \rho\right)$.

   (a) Find the probability distribution of $D = X/R$. Then, calculate the prevalence of undernourishment, denoted by $\text{PoU}^\star = \Pr\{X < R\}$.

   (b) Assume that $\mu_x = 7.50$, $\sigma_x = 0.20$, $\mu_r = 7.20$, and $\sigma_r = 0.05$. Plot the density functions of X and R.

   (c) Plot the function of $\text{PoU}^\star$ as ρ varies in the interval $[-1, 1]$. Comment on the results.

   (d) Compute the prevalence of undernourishment defined by $\text{PoU} = \Pr\{X < r_L\}$. Plot the relationship between r_L and PoU when $r_L \in [1000, 1600]$.

   (e) Find the value of $r_L^\star$ such as $\text{PoU} = \text{PoU}^\star$. Calibrate the parameter $r_L^\star$ for the prevalence of undernourishment calculated in Question 1.c.

2. We want to calibrate the probability distribution function of X. We assume that $X \sim \mathcal{LN}\left(\mu_x, \sigma_x^2\right)$.

   (a) Give the first two moments of X. We will denote them by $\mu(X)$ and $\sigma^2(X)$.

   (b) Deduce the coefficient of variation $\text{CV}(X)$.

   (c) Find the moment estimators of μ_x and σ_x from $\mu(X)$ and $\text{CV}(X)$.

   (d) We consider an hypothetical country with a population of 1 million and two food components (cereals and fruits/vegetables), whose the food balance sheet is as follows:

	Production	Imports	Exports	ΔStocks	Feed	Waste
#1	349 000	1 025	40 000	$-1\,000$	45 000	9 000
#2	50 000	9 010	1 000	6 000	500	500

   All the figures are expressed in tonnes. Calculate the food available for human consumption. Assuming that the average energy density is $3\,500$ and 500 Calories/kg for cereals and fruits/vegetables respectively, find the average dietary energy consumption $\mu(X)$ expressed in kcal/capita/day.

   (e) The average dietary energy consumption by household expenditure deciles are $1\,650$ (first decile), $1\,985$, $2\,150$, $2\,350$, $2\,530$, $2\,550$, $2\,650$, $2\,750$, $3\,100$ and $3\,630$ (last decile). Calculate the coefficient of variation $\text{CV}(X \mid Y)$. Check that $\mu(X \mid Y) = \mu(X)$. Assuming that $\text{CV}(X \mid R) = 0.20$, calculate $\text{CV}(X)$.

   (f) Calibrate the parameters μ_x and σ_x using the previous figures. What is the prevalence of undernourishment if we assume that $r_L = 1\,850$? Give an estimate of the number of undernourished people.

3. We seek to estimate the minimum dietary energy requirement.

(a) We recall that the body mass index (BMI) is expressed in kg/m^2 and is defined as the ratio of the weight (in kg) to the square of the height (in meter):

$$\text{BMI} = \frac{\text{weight}}{\text{height}^2}$$

The ideal value of BMI is 22. To define undernourished people, we assume that their weight is below a reference value:

$$\text{weight} \leq \text{weight}^\star$$

where:

$$\text{weight}^\star = \text{BMI}(p) \cdot \text{height}^2$$

where p is a percentile value that depends on age. If the age is less than ten years, p is set to 50%, while for individuals 10 years and older, it is set to 5%. Below, we give the values of $\text{BMI}(p)$ and the average height per age and sex:

	Age	−3	3–10	10–18	18–30	30–60	60+
BMI (p)	Female	15.5	15.5	17.0	17.5	17.5	17.5
	Male	15.5	15.5	17.0	18.5	18.5	18.5
Height	Female	0.80	1.20	1.55	1.60	1.60	1.60
	Male	0.88	1.24	1.58	1.72	1.72	1.72

Calculate the reference value weight* per age and sex to determine the undernourishment.

(b) We assume that the basal metabolic rate (BMR) is given by the Schofield equation:

$$\text{BMR} = \alpha + \beta \cdot \text{weight}^\star$$

where α_j and β_j are the estimates of the linear regression between weight and BMR:

	Age	−3	3–10	10–18	18–30	30–60	60+
α	Female	−31.1	485.9	692.6	486.6	845.6	658.5
	Male	−30.4	504.3	658.2	692.2	873.1	587.7
β	Female	58.317	20.315	13.384	14.818	8.126	9.082
	Male	59.512	22.706	17.686	15.057	11.472	11.711

Calculate the basal metabolic rate for each group.

(c) The minimum dietary energy requirement is equal to the physical activity level (PAL) times the basal metabolic rate:

$$\text{MDER} = \text{PAL} \cdot \text{BMR}$$

We assume that the population is on average lightly active, implying that PAL = 1.55. Calculate the minium dietary energy requirement for the different groups.

(d) We assume that the proportion of females and males is the same, while the distribution of the population by age is as follows:

Age	−3	3–10	10–18	18–30	30–60	60+
Frequency	9.9%	15%	16%	18%	29%	12.1%

Calculate the minium dietary energy requirement of the population.

4. We want to calculate the depth of the food deficit:

$$\text{FD} = \int_{x < r_L} (\bar{r} - x) f_x(x) \, \mathrm{d}x$$

where r_L is the minimum dietary energy requirement (MDER), $\bar{r}$ is the average dietary energy requirement (ADER), and $f_x(x)$ is the probability density function of the dietary energy consumption X.

(a) What is the interpretation of the indicator FD?

(b) Find the probabilistic expression of the indicator FD.

(c) Find the analytical value of FD when $X \sim \mathcal{LN}\left(\mu_x, \sigma_x^2\right)$.

(d) Calculate the depth of the food deficit in the case of Question 2 if we assume that the average dietary energy requirement is equal to $2\,500$ Calories per person per day.

A.2 Calculating the species-area relationship using the theory of island biogeography

1. We consider the model of island biogeography developed by Beaugrand *et al.* (2024). We denote species richness by $S(t)$. At the initial date t_0, we have $S(t_0) = S_0$ (we can assume that $S_0 = 0$). The authors assume the existence of a saturation date t_s, *i.e.*, the species richness cannot exceed a limit value:

$$0 \leq S(t) \leq S_s = S(t_s)$$

(a) Let $f(x) = a e^{b(x/c)^d}$ where $a > 0$, $c > 0$ and $d > 0$. The parameter b can take two values: -1 or $+1$. We also assume that $0 \leq x \leq c$. In which case do we get a decreasing, increasing, concave and convex function?

(b) Let $\lambda(t)$ represent the immigration rate. We assume that:

$$\lambda(t) = \lambda_0 \frac{e^{-\left(\frac{S(t)}{S_s}\right)^{\beta_1 \lambda_0}} - e^{-1}}{1 - e^{-1}} \qquad \text{for } \lambda_0 \geq \lambda(t) \geq \lambda_s = \lambda(t_s)$$

where $\lambda_0 \geq 0$ is the initial immigration rate, and $\beta_1 > 0$ is a parameter. Prove that $\lambda(t)$ is a decreasing function of $S(t)$, with $\lambda(t_0) = \lambda_0$ and $\lambda(t_s) = 0$. Determine whether $\lambda(t)$ is a convex or concave function. Plot the function $\lambda(t)$ for the following parameter sets $(\lambda_0, \beta_1, S_s)$: $(1.0, 0.2, 200)$, $(1.0, 0.5, 200)$, $(1.0, 1.0, 200)$, and $(0.9, 2.0, 150)$. Analyze and comment on these results.

(c) Let $\mu^{\text{long}}(t)$ be the long-term extinction rate. We assume that:

$$\mu^{\text{long}}(t) = \mu_s \frac{e^{\left(\frac{S(t)}{S_s}\right)^{\beta_2 \mu_s}} - 1}{e^1 - 1} \qquad \text{for } \mu_0^{\text{long}} \leq \mu^{\text{long}}(t) \leq \mu_s = \mu^{\text{long}}(t_s)$$

where $\mu_s \geq 0$ is the extinction rate at the saturation date, and $\beta_2 > 0$ is a parameter. Prove that $\mu^{\text{long}}(t)$ is an increasing function of $S(t)$, with $\mu^{\text{long}}(t_0) = 0$ and $\mu^{\text{long}}(t_s) = \mu_s$. Determine whether $\mu^{\text{long}}(t)$ is a convex or concave function. Plot the function $\mu^{\text{long}}(t)$ for the following parameter sets (μ_s, β_2, S_s): $(1.0, 0.2, 200)$, $(1.0, 0.5, 200)$, $(1.0, 1.0, 200)$, and $(0.5, 2.0, 150)$. Analyze and comment on these results.

(d) Let $\mu^{\text{short}}(t)$ be the short-term extinction rate. We assume that:

$$\mu^{\text{short}}(t) = \beta_3 \lambda(t) e^{-\beta_4 S(t)} \qquad \text{for } \mu_0^{\text{short}} \geq \mu^{\text{short}}(t) \geq \mu_s^{\text{short}} = \mu^{\text{short}}(t_s)$$

where β_3 and β_4 are two positive parameters. Prove that $\mu^{\text{short}}(t)$ is a decreasing function of $S(t)$, with $\mu^{\text{short}}(t_0) \leq \beta_3 \lambda_0$ and $\mu^{\text{short}}(t_s) = 0$. Plot the function[168] $\mu^{\text{short}}(t)$ for the following parameter sets (β_3, β_4, S_s): $(0.2, 0.02, 200)$, $(0.5, 0.02, 200)$, $(0.8, 0.02, 200)$, and $(1.0, 0.10, 150)$.

(e) Let $\mu(t) = \mu^{\text{short}}(t) + \mu^{\text{long}}(t)$ be the extinction rate. Show that $\mu(t_0) = \mu^{\text{short}}(t_0)$ and $\mu(t_s) = \mu_s$. Plot the function $\mu(t)$ for the following set of parameters: $\lambda_0 = 1$, $\beta_1 = 0.5$, $\mu_s = 1$, $\beta_2 = 2$, $\beta_3 = 0.70$, $\beta_4 = 0.01$, and $S_s = 200$. Comment on these results.

(f) The dynamics of species richness is governed by the following differential equation:

$$\frac{\mathrm{d}S(t)}{\mathrm{d}t} = \delta(t) = \lambda(t) - \mu(t)$$

What is the condition for $S(t)$ to reach an equilibrium? Illustrate and determine the equilibrium $S^\star$ using the set of parameters provided in Question 1.e.

(g) Under what conditions can two equilibria exist? Let $S_1^\star$ and $S_2^\star$ be the two equilibria, with $S_1^\star \leq S_2^\star$. Show that $S_1^\star$ is an unstable steady state, while $S_2^\star$ is a stable steady state. Deduce that there is a third equilibrium $S_0^\star$, with $S_0^\star \leq S_1^\star \leq S_2^\star$. Illustrate the three-equilibrium case with the following set of parameters: $\lambda_0 = 1$, $\beta_1 = 0.5$, $\mu_s = 1$, $\beta_2 = 2$, $\beta_3 = 1.70$, $\beta_4 = 0.02$, and $S_s = 200$.

(h) Using the two sets of parameters defined in Questions 1.e and 1.g, simulate the process $S(t)$ when the initial species richness S_0 is 0, 25, 30, 50 and 120, respectively. Comment on these results.

2. We aim to analyze the dynamics of the TIB steady state $S^\star$ under the assumption that there is no short-term extinction rate, meaning $\beta_3 = 0$ or $\mu^{\text{short}}(t) = 0$. The default parameter values are $\lambda_0 = 1$, $\beta_1 = 0.5$, $\mu_s = 1$, $\beta_2 = 1$, and $S_s = 200$.

(a) What is the impact of β_2 on the equilibrium $S^\star$? Compare the solutions for $\beta_2 = 0.2$, $\beta_2 = 1$, and $\beta_2 = 5$.

(b) Plot the relationship between β_2 and $S^\star$.

(c) What is the impact of μ_s on the equilibrium $S^\star$?

(d) Plot the relationship between μ_s and $S^\star$.

(e) What conclusion can we draw about the relationship between the area A and the equilibrium $S^\star$.

(f) We assume that the area A (expressed in km^2) is related to the parameter β_2 as follows: $A = \beta_2^{0.75}$. A sampling of β_2 is taken between 0.01 and 5.00 with a step size of 0.01. Use nonlinear least squares to estimate the power model $S = cA^z$, the exponential model $S = c + z \ln(A)$, and the Kobayashi model $S = c \ln(1 + zA)$. Compare the TIB equilibrium $S^\star$ with the forecasts of the fitted models. Comment on these results.

---

[168] We assume $\lambda_0 = 1.0$ and $\beta_1 = 0.5$ to define $\lambda(t)$.

A.3 Species abundance models

Remark: This exercise is inspired by the research articles of Coleman (1981), and He and Legendre (2002).

1. We consider an area (or an ecosystem) A containing S species. Let n_i denote the abundance of the ith species and let $n = \sum_{i=1}^{S} n_i$ represent the total abundance in the area. We focus on a subarea $a \subseteq A$ and denote by $\tilde{S}_a$ the random variable representing the number of species in this subarea. We introduce the notation $S_a = \mathbb{E}\left[\tilde{S}_a\right]$ to represent the expected number of species in the subarea.

   (a) Let p_i be the probability that species i is present in the subarea a, and $\tilde{S}_i \sim \mathcal{B}\left(p_i\right)$ the random variable indicating its presence ($\tilde{S}_i = 1$) or its absence ($\tilde{S}_i = 0$). What is the probability distribution of $\tilde{S}_a$? Deduce the value of S_a. Application: Given $p = (p_1, \ldots, p_5) = (20\%, 30\%, 10\%, 65\%, 10\%)$, calculate $\tilde{S}_a$ and S_a.

   (b) We assume a random placement of the species within the area A. What is the probability of observing k individuals of species i in the subarea a? Show that:
   $$\tilde{S}_i \sim \mathcal{PB}\left(p_i = 1 - \left(1 - \frac{a}{A}\right)^{n_i}\right)$$

   Find the value of S_a. Application: Given $(n_1, \ldots, n_5) = (10, 4, 25, 6, 8)$, $A = 10\,\text{km}^2$, and $a = 2\,\text{km}^2$, calculate $\tilde{S}_a$ and S_a.

   (c) Calculate S_a for the following models:

   i. Most even model:
   $$n_i = \frac{n}{S} \quad \text{for } i = 1, \ldots, S$$

   ii. Most uneven model:
   $$n_i = 1 \quad \text{for } i < S \quad \text{and} \quad n_S = n - S + 1$$

   Calculate $\tilde{S}_a$ and S_a.

   iii. Mixed even-uneven model:
   $$n_i = 1 \quad \text{for } i \leq s \quad \text{and} \quad n_i = \frac{n - s}{S - s} = n_{s+1} \text{ for } i > s$$

   iv. He-Gaston model:
   $$p_i = 1 - \left(1 - \frac{a}{A}\right)\left(1 + \frac{n_i a}{\kappa_i A}\right)^{-\kappa_i}$$

   where $\kappa_i \in (-\infty, m_i) \cup [0, \infty)$ is a parameter which describes the spatial pattern of species i and $m_i = n_i a / A$ is the mean density of species i in the subarea a.

   v. Broken-stick model[169]:
   $$n_i = \frac{n}{S} \sum_{k=i}^{S} \frac{1}{k}$$

---

[169]Hint: Approximate the harmonic sum by $\ln\left(\frac{S}{i}\right)$, and replace the sum $\sum_{i=1}^{S}\left(1 - \frac{a}{A}\right)^{n_i}$ with its integral form.

(d) The species abundance distribution is defined as the series $\{s(1), s(2), \ldots\}$ where $s(j)$ is the number of species with j individuals. Show that:

$$S_a = S - \sum_j s(j) \left(1 - \frac{a}{A}\right)^j$$

Application: Calculate S_a for the log-series distribution:

$$s(j) = \alpha \frac{x^j}{j}$$

where α is a parameter related to the total diversity and $x \in (0,1)$ is a parameter determining the relative abundance.

2. We say that the species is locally endemic to subarea $a \subseteq A$ if it is found exclusively in subarea a and not in the complementary area $A - a$.

(a) Calculate the probability $\breve{p}_i$ of endemism of species i.

(b) What is the expected number E_a of locally endemic species?

(c) Calculate S_{A-a} and E_{A-a} for the complementary area $A - a$. Deduce that:

$$S_{A-a} + E_a = S$$

(d) Show that:

$$0 \leq S_a + E_a \leq 2S$$

A.4   Valuation of risks to life and health

Remark: This exercise is inspired by the research article of Hammitt (2023).

Let τ be a survival time[170], whose survival function is $\mathbf{S}(t) = \Pr\{\tau > t\}$ and density function is $f(t) = -\partial \mathbf{S}(t)$. We have $\mathbf{S}(0) = 1$ and $\mathbf{S}(\infty) = 0$.

1. Assume that the individual is alive at time t. What is the conditional survival function $\mathbf{S}(u \mid t) = \Pr\{\tau > u \mid \tau > t\}$?

2. Show that the average length of life (or life expectancy) for an individual who is alive at time t is given by:

$$\mathrm{LE}(t) = \mathbb{E}[\tau \mid \tau > t] = \frac{1}{\mathbf{S}(t)} \int_t^\infty \mathbf{S}(u) \, \mathrm{d}u$$

3. Let ϱ be the discount rate and $X(t)$ a payoff function. Following the seminal paper of Yaari (1965), we define the expected present value of the payoff, taking into account the future lifetime, as:

$$\mathbb{E}[X; t, \varrho] = \int_t^\infty e^{-\varrho(u-t)} \mathbf{S}(u \mid t) X(u) \, \mathrm{d}u$$

What is the rationale behind this formula?

---

[170]In mortality analysis, this is referred to as time-to-event or time-to-death.

4. The discounted remaining life expectancy is defined as the expected present value of the future lifetime:
$$\text{LE}\left(t;\varrho\right) = \mathbb{E}\left[1;t,\varrho\right] = \frac{1}{\mathbf{S}\left(t\right)}\int_{t}^{\infty}e^{-\varrho(u-t)}\mathbf{S}\left(u\right)\,\mathrm{d}u$$

Shows that:
$$\text{LE}\left(t;\varrho\right) \geq \text{DLE}\left(t;\varrho\right) = \int_{t}^{\infty}e^{-\varrho(u-t)}\left(u-t\right)f\left(u\mid t\right)\,\mathrm{d}u$$

What is the interpretation of $\text{DLE}\left(t;\varrho\right)$? Under which condition do we have equality?

5. Assume that the survival time follows an exponential distribution: $\tau \sim \mathcal{E}\left(\lambda\right)$. Derive the formulas for $\text{LE}\left(t;\varrho\right)$ and $\text{DLE}\left(t;\varrho\right)$? Comment on these results.

6. We assume that life expectancy is 70 years ($\mathbb{E}\left[\tau\right] = 70$). We consider two survival functions: $\tau \sim \mathcal{E}\left(\lambda\right)$ and $\tau \sim \mathcal{W}_{\text{eibull}}\left(a,b\right)$, where the survival function is defined as $\mathbf{S}\left(t\right) = \exp\left(-\left(\frac{x}{a}\right)^{b}\right)$.

   (a) Calibrate the parameters λ and a so that $b = 5$. Plot the survival functions $\mathbf{S}\left(t\right)$ and $\mathbf{S}\left(u\mid t=50\right)$. Comment on these results.

   (b) We assume that $\varrho = 3\%$. Calculate $\text{LE}\left(0;\varrho\right)$ and $\text{DLE}\left(0;\varrho\right)$ if the survival time is exponential.

   (c) Assume that the survival time is Weibull distributed. Using numerical integration, plot the discounted life expectancy $\text{LE}\left(t;\varrho\right)$ for $t \in \left[0,100\right]$ and for different discount rates ϱ (0%, 1%, 2%, 3% and 10%). Comment on these results.

7. We assume that the quality life weight $\hat{Q}\left(t\right)$ is a random variable between 0 and 1, and we note $Q\left(t\right) = \mathbb{E}\left[\hat{Q}\left(t\right)\right]$ its expected value. The quality-adjusted life expectancy (QALE) is defined as $\text{QALE}\left(t;\varrho\right) = \mathbb{E}\left[Q\left(t\right);t,\varphi\right]$.

   (a) Give the formula of $\text{QALE}\left(t;\varrho\right)$ when the function $Q\left(t\right)$ is constant.

   (b) Show that:
   $$\text{QALE}\left(t;\varrho\right) \leq \text{LE}\left(t;\varrho\right)$$

   (c) Consider the previously calibrated Weibull distribution. We assume that:

   $$Q_{1}\left(t\right) = \begin{cases} 1 & \text{if } t \leq t_{1} \\ 1 - \kappa_{1}\dfrac{\left(t-t_{1}\right)}{t_{2}-t_{1}} & \text{if } t_{1} \leq t \leq t_{2} \\ 1 - \kappa_{1} - \kappa_{2}\dfrac{\left(t-t_{2}\right)}{t_{3}-t_{2}} & \text{if } t_{2} \leq t \leq t_{3} \\ 1 - \kappa_{1} - \kappa_{2} & \text{if } t \geq t_{3} \end{cases}$$

   What is the rationale for this specification? We consider a second HRQL function:

   $$Q_{2}\left(t\right) = \exp\left(-\kappa t\right)$$

   Compare $\text{QALE}\left(t;\varrho\right)$ and $\text{LE}\left(t;\varrho\right)$ for the following set of parameters: $t_{1} = 50$, $\kappa_{1} = 10\%$, $t_{2} = 70$, $\kappa_{2} = 20\%$, $t_{3} = 90$, and $\kappa = 2\%$.

8. Let $\mathcal{R}(t)$ be the impact on mortality risk. We use the convention that $\mathcal{R}(t)$ is positive if the impact is a risk reduction and negative if the impact is a risk increase. We define $\Delta L(t) = \mathcal{R}(t) \cdot \Delta t$ as the expected number of lives saved (or the decrease in the number of deaths) during the short time interval Δt. Hammitt (2023) also defines the increase in life expectancy as $\Delta \mathrm{LE}(t) = \Delta L(t) \cdot \mathrm{LE}(t; \varrho)$ and the increase in quality-adjusted life expectancy as $\Delta \mathrm{QALE}(t) = \Delta L(t) \cdot \mathrm{QALE}(t; \varrho)$. The monetary value v of the risk reduction $\mathcal{R}(t)$ is the product of the value of a statistical life (VSL) and the expected number of lives saved. Similarly, v can be expressed as the product of the value per statistical life year (VSLY) and the increase in life expectancy or as the product of the value per quality-adjusted life year (VQALY) and the increase in quality-adjusted life expectancy. Following Hammitt (2023), we have:

$$v = \mathrm{VSL}(t) \cdot \Delta L(t) = \mathrm{VSLY}(t) \cdot \Delta \mathrm{LE}(t) = \mathrm{VQALY}(t) \cdot \Delta \mathrm{QALE}(t)$$

(a) Find $\mathrm{VSL}(t)$ and express $\mathrm{VSLY}(t)$ and $\mathrm{VQALY}(t)$ as functions of $\mathrm{VSL}(t)$.

(b) Hammitt (2023) considers persistent risk impact $\mathcal{I}(t)$ and defines the economic gain from risk reduction as:

$$\mathcal{G}(t; \varrho) = \frac{1}{\mathbf{S}(t)} \int_t^\infty e^{-\varrho(u-t)} \mathbf{S}(u) \, \mathrm{VSL}(u) \, \mathcal{I}(u) \, \mathrm{d}u$$

What is the interpretation of $\mathcal{G}(t; \varrho)$? Assume that $\mathcal{I}(t) = \mathcal{R}(t)$. What is the associated payoff function. Give the expression for the payoff function using $\mathrm{VSLY}(t)$ or $\mathrm{VQALY}(t)$.

(c) What is the value of $\mathcal{G}(t; \varrho)$ if $\mathrm{VSL}(t)$ and $\mathcal{I}(t)$ are assumed to be constant?

(d) In the case of air pollution, the economic cost is sometimes estimated using the following formula:

$$\mathcal{C} = \mathrm{VSLY} \cdot \mathrm{YLL}$$

What is the rationale for this formula?

(e) Consider a numerical application using the previously calibrated Weibull distribution and the HRQL function $Q_1(t)$. Compute the values of $\mathrm{LE}(t; \varrho)$ and $\mathrm{QALE}(t; \varrho)$ for $t \in \{0, 40, 80\}$ and $\varrho \in \{0, 3\%\}$. Workers in an industry are paid an additional \$1 000 per year to face a 1 in 10 000 increased risk of death. Compute the value of a statistical life. Deduce the values of $\mathrm{VSLY}(t)$ and $\mathrm{VQALY}(t)$. What is the drawback of assuming a constant VSL regardless the worker's age. Therefore, we prefer to assume a constant $\mathrm{VSLY}(t)$, equal to \$150 000. Deduce the values of $\mathrm{VSL}(t)$ and $\mathrm{VQALY}(t)$. Calculate the economic gain $\mathcal{G}(t; \varrho)$ of a policy that avoids 5 deaths among 100 000 people. Comment on these results.

B   Solutions to the Tutorial Exercises

B.1   Calculating the prevalence of undernourishment

1. (a) We have:
$$\ln D = \ln X - \ln R \sim \mathcal{N}\left(\mu_d, \sigma_d^2\right)$$

where:
$$\mu_d = \mathbb{E}\left[\ln X - \ln R\right] = \mathbb{E}\left[\ln X\right] - \mathbb{E}\left[\ln R\right] = \mu_x - \mu_r$$

and:
$$
\begin{aligned}
\sigma_d^2 &= \operatorname{var}\left(\ln X - \ln R\right) \\
&= \operatorname{var}\left(\ln X\right) + \operatorname{var}\left(\ln R\right) - 2\operatorname{cov}\left(\ln X, \ln R\right) \\
&= \sigma_x^2 + \sigma_r^2 - 2\rho\sigma_x\sigma_r
\end{aligned}
$$

Thus, we deduce that $D = X/R$ is a log-normal random variable: $D \sim \mathcal{LN}\left(\mu_d, \sigma_d^2\right)$. It follows that:

$$
\begin{aligned}
\text{PoU}^\star &= \Pr\left\{X < R\right\} \\
&= \Pr\left\{D < 1\right\} \\
&= \Pr\left\{\ln D < 0\right\} \\
&= \Phi\left(-\frac{\mu_d}{\sigma_d}\right) \\
&= \Phi\left(-\frac{\mu_x - \mu_r}{\sqrt{\sigma_x^2 + \sigma_r^2 - 2\rho\sigma_x\sigma_r}}\right)
\end{aligned}
$$

(b) The probability density functions of X and R are given in Figure 83.

(c) Figure 84 illustrates the relationship between the correlation and the prevalence of undernourishment. We observe a decreasing function between ρ and $\text{PoU}^\star$, because the standard deviation of D is a decreasing function of the correlation between X and R and $\mu_x > \mu_r$. Conversely, if $\mu_x < \mu_r$, the relationship between ρ and $\text{PoU}^\star$ becomes increasing.

(d) We have:
$$\text{PoU} = \Pr\left\{X < r_L\right\} = \Pr\left\{\ln X < \ln r_L\right\} = \Phi\left(\frac{\ln r_L - \mu_x}{\sigma_x}\right)$$

The relationship between r_L and PoU is shown in Figure 85.

(e) We deduce that:
$$
\begin{aligned}
\text{PoU} = \text{PoU}^\star \quad &\Leftrightarrow \quad \Phi\left(\frac{\ln r_L^\star - \mu_x}{\sigma_x}\right) = \Phi\left(-\frac{\mu_x - \mu_r}{\sqrt{\sigma_x^2 + \sigma_r^2 - 2\rho_{x,r}\sigma_x\sigma_r}}\right) \\
&\Leftrightarrow \quad \frac{\ln r_L^\star - \mu_x}{\sigma_x} = -\frac{\mu_x - \mu_r}{\sqrt{\sigma_x^2 + \sigma_r^2 - 2\rho_{x,r}\sigma_x\sigma_r}}
\end{aligned}
$$

which implies:
$$r_L^\star = \exp\left(\mu_x - \frac{\left(\mu_x - \mu_r\right)\sigma_x}{\sqrt{\sigma_x^2 + \sigma_r^2 - 2\rho_{x,r}\sigma_x\sigma_r}}\right)$$

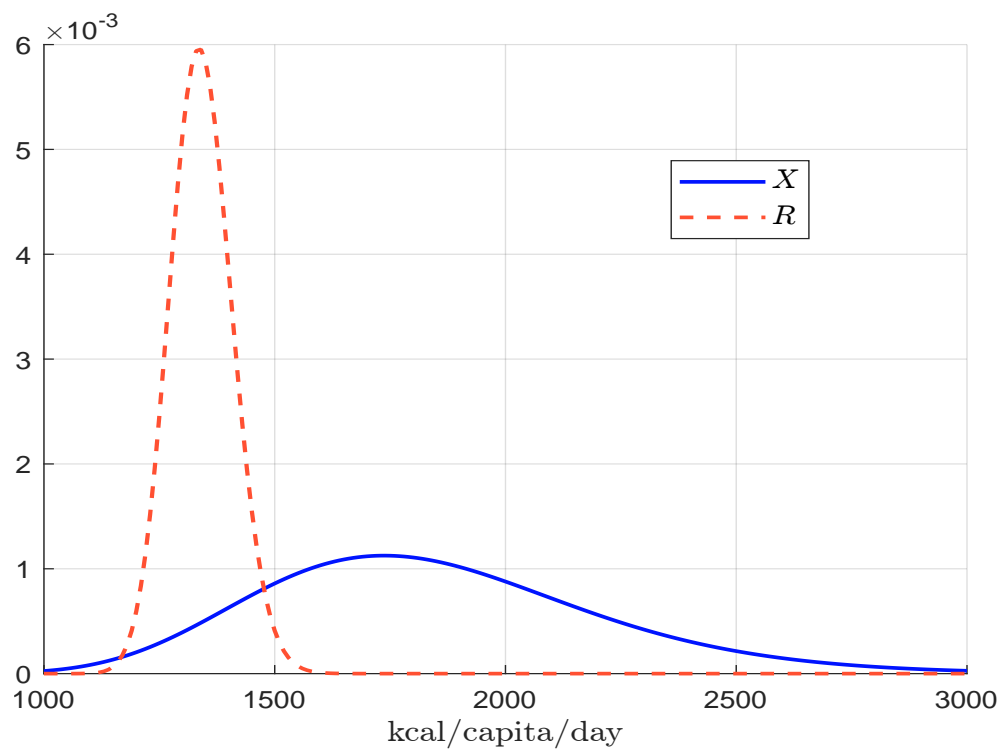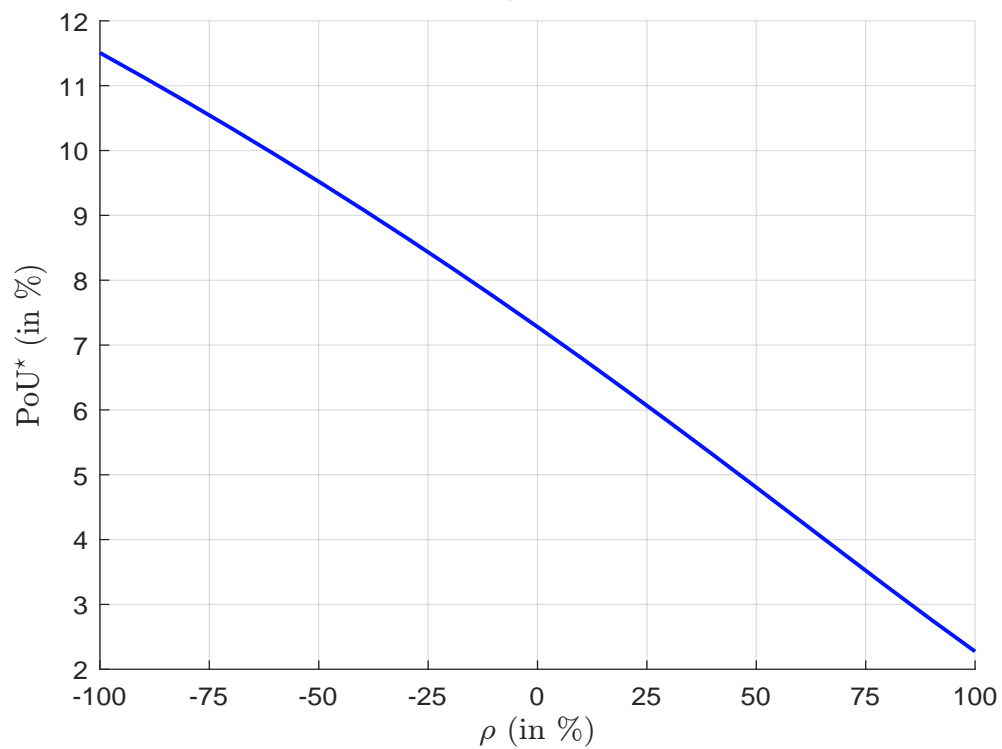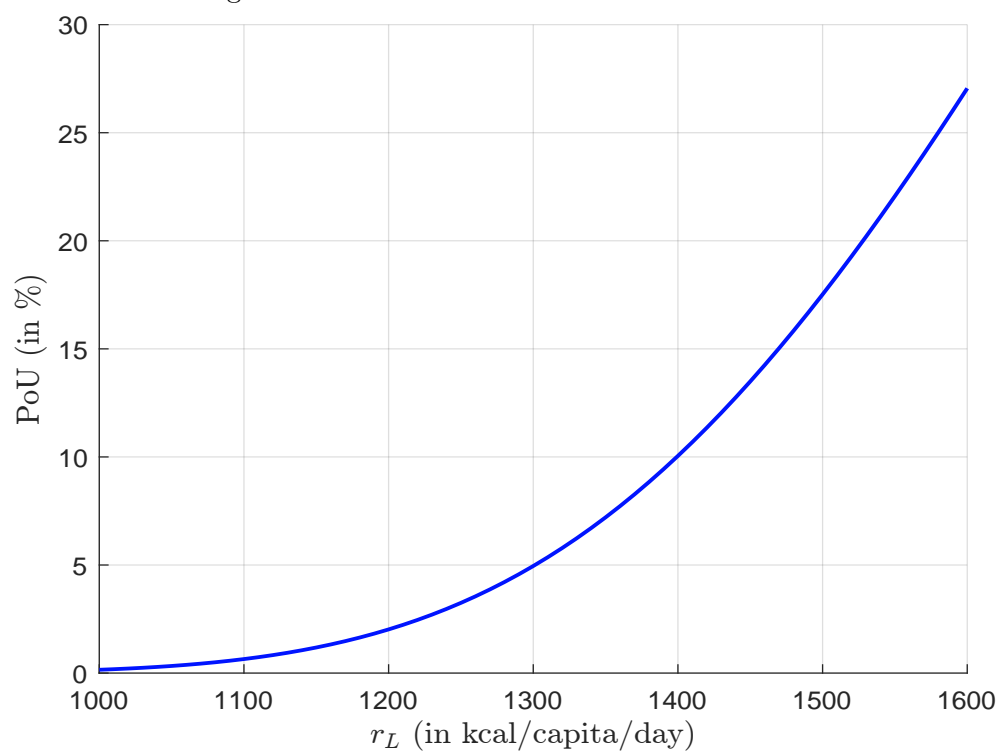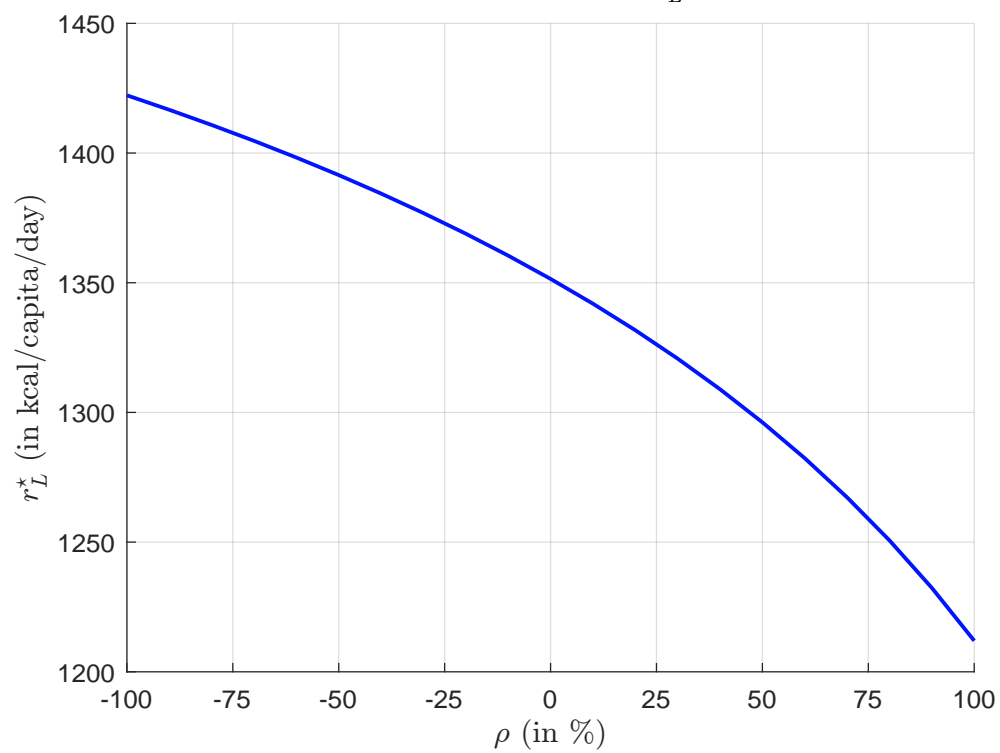The calibration of $r_L^\star$ is shown in Figure 86.

Figure 83: Probability density functions of X and R

Figure 84: Relationship between the correlation ρ and the prevalence of undernourishment PoU*

Figure 85: Prevalence of undernourishment PoU

Figure 86: Calibration of $r_L^\star$

2. (a) We have:
$$\mu(X) = e^{\mu_x + \frac{1}{2}\sigma_x^2}$$

and:
$$\sigma^2(X) = e^{2\mu_x + \sigma_x^2}\left(e^{\sigma_x^2} - 1\right) = \mu^2(X)\left(e^{\sigma_x^2} - 1\right)$$

(b) We deduce that:
$$\text{CV}(X) = \frac{\sigma(X)}{\mu(X)} = \sqrt{e^{\sigma_x^2} - 1}$$

(c) We have:
$$\text{CV}(X) = \sqrt{e^{\sigma_x^2} - 1} \quad \Leftrightarrow \quad e^{\sigma_x^2} = \text{CV}^2(X) + 1$$
$$\Leftrightarrow \quad \sigma_x = \sqrt{\ln\left(\text{CV}^2(X) + 1\right)}$$

and:
$$\mu(X) = e^{\mu_x + \frac{1}{2}\sigma_x^2} \quad \Leftrightarrow \quad \mu_x = \ln\mu(X) - \frac{1}{2}\sigma_x^2$$
$$\Leftrightarrow \quad \mu_x = \ln\mu(X) - \frac{1}{2}\ln\left(\text{CV}^2(X) + 1\right)$$
$$\Leftrightarrow \quad \mu_x = \ln\mu(X) - \ln\sqrt{\text{CV}^2(X) + 1}$$
$$\Leftrightarrow \quad \mu_x = \ln\frac{\mu(X)}{\sqrt{\text{CV}^2(X) + 1}}$$

(d) The food available for human consumption is equal to:
$$Q_1 = 349\,000 + 1\,025 - 40\,000 - (-1\,000) - 45\,000 - 9\,000 = 257\,025\,\text{tonnes}$$
$$Q_2 = 50\,000 + 9\,010 - 1\,000 - 6\,000 - 500 - 500 = 51\,010\,\text{tonnes}$$

We deduce that the ADEC value is:
$$\mu(X) = \frac{257\,025 \times 10^3 \times 3\,500 + 51\,010 \times 10^3 \times 500}{365 \times 10^6} = 2\,534.50\,\text{kcal/capita/day}$$

(e) Let x_j^y be the average dietary energy consumption for the jth household expenditure decile. We have:
$$\sigma(X \mid Y) = \sqrt{\sum_{j=1}^{10} f_j\left(x_i^y - \bar{x}^y\right)^2} = 533.4906$$

where $f_j = 10\%$ is the frequency of each decile group and $\bar{x}^y = \sum_{j=1}^{10} f_j x_i^y$ is the mean. We verify that $\bar{x}^y = 2\,534.50 = \mu(X)$. It follows that:
$$\text{CV}(X \mid Y) = \frac{\sigma(X \mid Y)}{\mu(X \mid Y)} = \frac{533.4906}{2\,534.50} = 0.2105$$

We deduce that:
$$\text{CV}(X) = \sqrt{\text{CV}^2(X \mid Y) + \text{CV}^2(X \mid R)} = \sqrt{0.2105^2 + 0.20^2} = 0.2904$$

(f) We have:
$$\sigma_x = \sqrt{\ln\left(0.2904^2 + 1\right)} = 0.2845$$

and:
$$\mu_x = \ln \frac{2\,534.50}{\sqrt{0.2904^2 + 1}} = 7.7973$$

The prevalence of undernourishment is equal to:

$$\text{PoU} = \Phi\left(\frac{1\,850 - 7.7973}{0.2845}\right) = 16.75\%$$

Finally, the number of undernourished people is around $167\,500$:

$$\text{NoU} = N \cdot \text{PoU} = 10^6 \times 16.75\% = 167\,451$$

3. (a) We have:
$$\text{weight}^\star_{age,sex} = \text{BMI}_{age,sex}\,(p) \cdot \text{height}^2_{age,sex}$$

For example, we have:

$$
\begin{aligned}
\text{weight}^\star_{-3yr,female} &= \text{BMI}_{-3yr,female}\,(5\%) \cdot \text{height}^2_{-3yr,female} \\
&= 15.5 \times 0.80^2 \\
&= 9.92\,\text{kg}
\end{aligned}
$$

We obtain the following results:

Age	−3	3–10	10–18	18–30	30–60	60+
Female	9.92	22.32	40.84	44.80	44.80	44.80
Male	12.00	23.83	42.44	54.73	54.73	54.73

This means that a 40-year-old woman is considered undernourished if she weighs less than 44.8 kg.

(b) The basal metabolic rate (BMR) is given by the Schofield equation:

$$\text{BMR}_{age,sex} = \alpha_{age,sex} + \beta_{age,sex} \cdot \text{weight}^\star_{age,sex}$$

For example, we have:

$$
\begin{aligned}
\text{BMR}_{-3yr,female} &= \alpha_{-3yr,female} + \beta_{-3yr,female} \cdot \text{weight}^\star_{-3yr,female} \\
&= -31.1 + 58.317 \times 9.92 \\
&= 547.40\,\text{kcal/capita/day}
\end{aligned}
$$

We obtain the following results:

Age	−3	3–10	10–18	18–30	30–60	60+
Female	547	939	1\,239	1\,150	1\,210	1\,065
Male	684	1\,045	1\,409	1\,516	1\,501	1\,229

(c) The minimum dietary energy requirement is equal to the physical activity level times the basal metabolic rate:

$$\text{MDER}_{age,sex} = \text{PAL}_{age,sex} \cdot \text{BMR}_{age,sex}$$

We obtain the following results:

Age	−3	3–10	10–18	18–30	30–60	60+
Female	848	1 456	1 921	1 783	1 875	1 651
Male	1 060	1 620	2 184	2 350	2 326	1 904

This means that a 40-year-old woman is considered undernourished if her dietary energy consumption is less than 1 875 Calories per day.

(d) The minimum dietary energy requirement of the population is the weighted average of the different MDER values:

$$\text{MDER} = \sum_{sex} \sum_{age} f_{age,sex} \cdot \text{MDER}_{age,sex}$$

where $f_{age,sex}$ is the frequency of the group in the population. Finally, we obtain:

$$\text{MDER} = 1\,849.90 \,\text{kcal/capita/day}$$

4. (a) FD indicates how many calories would be needed to ensure that undernourished would be eliminated if properly distributed.

(b) We have:

$$
\begin{aligned}
\text{FD} &= \int_{x<r_L} (\bar{r} - x) f_x(x) \, dx \\
&= \int_0^{r_L} \bar{r} f_x(x) \, dx - \int_0^{r_L} x f_x(x) \, dx \\
&= \bar{r} \int_0^{r_L} f_x(x) \, dx - \frac{\int_0^{r_L} x f_x(x) \, dx}{\int_0^{r_L} f_x(x) \, dx} \int_0^{r_L} f_x(x) \, dx \\
&= (\bar{r} - \mathbb{E}[X \mid X < r_L]) \cdot \Pr\{X < r_L\} \\
&= \text{PoU} \cdot (\bar{r} - \mathbb{E}[X \mid X < r_L])
\end{aligned}
$$

The depth of the food deficit is the product of the prevalence of undernourishment and the difference between the average dietary energy requirement and the average dietary energy consumption, conditional on consumption being below the minimum requirement. Another expression is:

$$\text{FD} = \text{PoU} \cdot \mathbb{E}\left[(\bar{r} - X)_+ \mid X < r_L \right]$$

because $\bar{r} \geq r_L$. $\mathbb{E}\left[(\bar{r} - X)_+ \mid X < r_L \right]$ is the expected shortfall of food security.

(c) Following Roncalli (2020a, page 319), we introduce the notation $\Phi_c(x) = \Phi((x - \mu_x)/\sigma_x)$, and we calculate the conditional moment $\mu'_m(X) = \mathbb{E}[X^m \mid X < r_L]$ for $m \geq 1$ by using the change of variable $y = \ln x$:

$$
\begin{aligned}
\mu'_m(X) &= \frac{1}{\Phi_c(\ln r_L)} \int_0^{r_L} \frac{x^m}{x \sigma_x \sqrt{2\pi}} \exp\left(-\frac{1}{2} \left(\frac{\ln x - \mu_x}{\sigma_x} \right)^2 \right) dx \\
&= \frac{1}{\Phi_c(\ln r_L)} \int_{-\infty}^{\ln r_L} \frac{1}{\sigma_x \sqrt{2\pi}} \exp\left(-\frac{1}{2} \left(\frac{y - \mu_x}{\sigma_x} \right)^2 + my \right) dy
\end{aligned}
$$

We have:

$$
-\frac{1}{2}\left(\frac{y-\mu_x}{\sigma_x}\right)^2 + my = -\frac{1}{2}\left(\frac{y^2 - 2y\left(\mu_x + m\sigma_x^2\right) + \mu_x^2}{\sigma_x^2}\right)
$$

$$
= -\frac{1}{2}\left(\frac{y - \left(\mu_x + m\sigma_x^2\right)}{\sigma_x}\right)^2 + \left(m\mu_x + \frac{1}{2}m^2\sigma_x^2\right)
$$

We deduce that:

$$
\mu'_m(X) = \frac{\exp\left(m\mu_x + m^2\sigma_x^2/2\right)}{\Phi_c\left(\ln r_L\right)} \int_{-\infty}^{\ln r_L} \frac{1}{\sigma_x\sqrt{2\pi}} \exp\left(-\frac{1}{2}\left(\frac{y - \left(\mu_x + m\sigma_x^2\right)}{\sigma_x}\right)^2\right)\,\mathrm{d}y
$$

Using the change of variable $z = \dfrac{y - \left(\mu_x + m\sigma_x^2\right)}{\sigma_x}$, it follows that:

$$
\mu'_m(X) = \frac{\exp\left(m\mu_x + m^2\sigma_x^2/2\right)}{\Phi_c\left(\ln r_L\right)} \int_{-\infty}^{z_L} \frac{1}{\sqrt{2\pi}} \exp\left(-\frac{1}{2}z^2\right)\,\mathrm{d}z
$$

where:

$$
z_L = \frac{\ln r_L - \left(\mu_x + m\sigma_x^2\right)}{\sigma_x}
$$

Finally, we obtain:

$$
\mu'_m(X) = \frac{\Phi_c\left(\ln r_L - m\sigma_x^2\right)}{\Phi_c\left(\ln r_L\right)} \exp\left(m\mu_x + \frac{1}{2}m^2\sigma_x^2\right)
$$

and:

$$
\mathbb{E}\left[X \mid X < r_L\right] = \mu'_1(X) = \frac{\Phi\left(\dfrac{\ln r_L - \mu_x - \sigma_x^2}{\sigma_x}\right)}{\Phi\left(\dfrac{\ln r_L - \mu_x}{\sigma_x}\right)} \exp\left(\mu_x + \frac{1}{2}\sigma_x^2\right)
$$

The analytical expression of the depth of the food deficit is:

$$
\mathrm{FD} = \bar{r}\,\Phi\left(\frac{\ln r_L - \mu_x}{\sigma_x}\right) - e^{\mu_x + \frac{1}{2}\sigma_x^2}\,\Phi\left(\frac{\ln r_L - \mu_x - \sigma_x^2}{\sigma_x}\right)
$$

because:

$$
\mathrm{PoU} = \Pr\left\{X < r_L\right\} = \Phi\left(\frac{\ln r_L - \mu_x}{\sigma_x}\right)
$$

(d) The depth of the food deficit is equal to:

$$
\begin{aligned}
\mathrm{FD} &= 2\,500 \times \Phi\left(\frac{\ln 1\,850 - 7.7973}{0.2845}\right) - \\
&\quad \exp\left(7.7973 + \frac{1}{2}0.2845^2\right) \times \Phi\left(\frac{\ln 1\,850 - 7.7973 - 0.2845^2}{0.2845}\right) \\
&= 150.2968 \text{ kcal/capita/year}
\end{aligned}
$$

B.2 Calculating the species-area relationship using the theory of island biogeography

1. (a) We have:

$$
\begin{aligned}
f'(x) &= ae^{b(x/c)^d}bd\left(\frac{x}{c}\right)^{d-1}\frac{1}{c} \\
&= \frac{abd}{c}\left(\frac{x}{c}\right)^{d-1}e^{b(x/c)^d}
\end{aligned}
$$

and:

$$
\begin{aligned}
f''(x) &= \frac{abd}{c}(d-1)\left(\frac{x}{c}\right)^{d-2}\frac{1}{c}e^{b(x/c)^d} + \frac{abd}{c}\left(\frac{x}{c}\right)^{d-1}e^{b(x/c)^d}bd\left(\frac{x}{c}\right)^{d-1}\frac{1}{c} \\
&= \frac{abd(d-1)}{c^2}\left(\frac{x}{c}\right)^{d-2}e^{b(x/c)^d} + \frac{ab^2d^2}{c^2}\left(\frac{x}{c}\right)^{2d-2}e^{b(x/c)^d} \\
&= \frac{abd}{c^2}\left(\frac{x}{c}\right)^{d-2}\left(d-1+bd\left(\frac{x}{c}\right)^d\right)e^{b(x/c)^d}
\end{aligned}
$$

Since a, c and d are positive, we deduce that $\frac{x}{c} \geq 0$, $e^{b(x/c)^d} \geq 0$ and:

$$
f'(x) \geq 0 \Leftrightarrow b \geq 0
$$

$f(x)$ is an increasing function of x if the parameter b is positive, otherwise $f(x)$ is a decreasing function of x. We have:

$$
f''(x) \geq 0 \Leftrightarrow g(x;b) = \underbrace{b(d-1)}_{-/+} + \underbrace{b^2d\left(\frac{x}{c}\right)^d}_{+} \geq 0
$$

because we have:

$$
0 \leq b^2d\left(\frac{x}{c}\right)^d \leq b^2d
$$

We consider two cases:

i. $b = -1$
    If $d \leq 1$, then $g(x;-1) = 1 - d + d\left(\frac{x}{c}\right)^d$, $f''(x) \geq 0$ and the function is convex. If $d > 1$, the function is neither convex nor concave.

ii. $b = 1$
    If $d \geq 1$, then $g(x;1) = (d-1) + d\left(\frac{x}{c}\right)^d$, $f''(x) \geq 0$ and the function is convex. If $d \leq \frac{1}{2}$, then $g(0;1) = d - 1 < 0$, $g(c;1) = 2d - 1 \leq 0$, $f''(x) \leq 0$ and the function is concave. If $d \in \left(\frac{1}{2}, 1\right)$, the function is neither convex nor concave.

(b) We have[171]:

$$
\frac{\partial \lambda(t)}{\partial S(t)} = -\frac{\beta_1\lambda_0^2}{(1-e^{-1})S_s}\left(\frac{S(t)}{S_s}\right)^{\beta_1\lambda_0-1}e^{-\left(\frac{S(t)}{S_s}\right)^{\beta_1\lambda_0}} \leq 0
$$

with:

$$
\lambda(t_0) = \lambda_0\frac{e^{-0} - e^{-1}}{1 - e^{-1}} = \lambda_0
$$

---

[171]We set $a = \frac{\lambda_0}{1-e^{-1}}$, $b = -1$, $c = S_s$ and $d = \beta_1\lambda_0$.
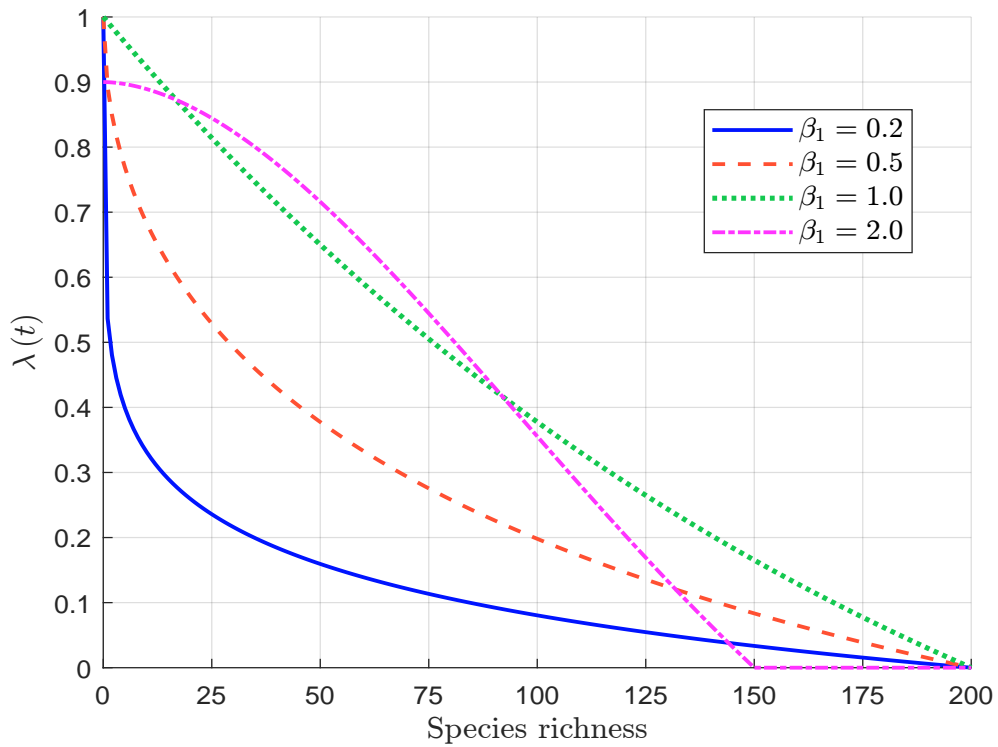
and:

$$\lambda(t_s) = \lambda_0 \frac{e^{-1} - e^{-1}}{1 - e^{-1}} = 0$$

The second-order derivative is:

$$\frac{\partial^2 \lambda(t)}{\partial S(t)^2} = -\frac{\beta_1 \lambda_0^2}{(1 - e^{-1}) S_s^2} \left(\frac{S(t)}{S_s}\right)^{\beta_1 \lambda_0 - 2} \left(\beta_1 \lambda_0 - 1 - \beta_1 \lambda_0 \left(\frac{S(t)}{S_s}\right)^{\beta_1 \lambda_0}\right) e^{-\left(\frac{S(t)}{S_s}\right)^{\beta_1 \lambda_0}}$$

$\lambda(t)$ is convex if and only if $\beta_1 \lambda_0 \leq 1$. The function $\lambda(t)$ is plotted in Figure 87. We verify that it is decreasing and convex for the first three sets of parameters because $\beta_1 \lambda_0 \leq 1$. For the last set of parameters, it is decreasing but not convex.

Figure 87: Immigrate rate function $\lambda(t)$

(c) We have[172]:

$$\frac{\partial \mu^{\text{long}}(t)}{\partial S(t)} = \frac{\beta_2 \mu_s^2}{(e^{-1} - 1) S_s} \left(\frac{S(t)}{S_s}\right)^{\beta_2 \mu_s - 1} e^{\left(\frac{S(t)}{S_s}\right)^{\beta_2 \mu_s}} \geq 0$$

with:

$$\mu^{\text{long}}(t_0) = \mu_s \frac{e^0 - 1}{e^1 - 1} = 0$$

and:

$$\mu^{\text{long}}(t_s) = \mu_s \frac{e^1 - 1}{e^1 - 1} = \mu_s$$

---

[172]We set $a = \frac{\mu_s}{e^{-1} - 1}$, $b = 1$, $c = S_s$ and $d = \beta_2 \mu_s$.

The second-order derivative is:

$$\frac{\partial^2 \mu^{\mathrm{long}}(t)}{\partial S(t)^2} = \frac{\beta_2 \mu_s^2}{(e^{-1}-1)S_s^2}\left(\frac{S(t)}{S_s}\right)^{\beta_2\mu_s-2}\left(\beta_2\mu_s - 1 + \beta_2\mu_s\left(\frac{S(t)}{S_s}\right)^{\beta_2\mu_s}\right)e^{\left(\frac{S(t)}{S_s}\right)^{\beta_2\mu_s}}$$

$\mu^{\mathrm{long}}(t)$ is convex if and only if $\beta_2\mu_s \geq 1$ and concave if and only if $\beta_2\mu_s \leq \frac{1}{2}$. The function $\mu^{\mathrm{long}}(t)$ is plotted in Figure 88. We verify that it is increasing and concave for the first two sets of parameters because $\beta_2\mu_s \leq \frac{1}{2}$. For the last two sets of parameters, it is increasing and convex.

Figure 88: Long-term extinction rate function $\mu^{\mathrm{long}}(t)$
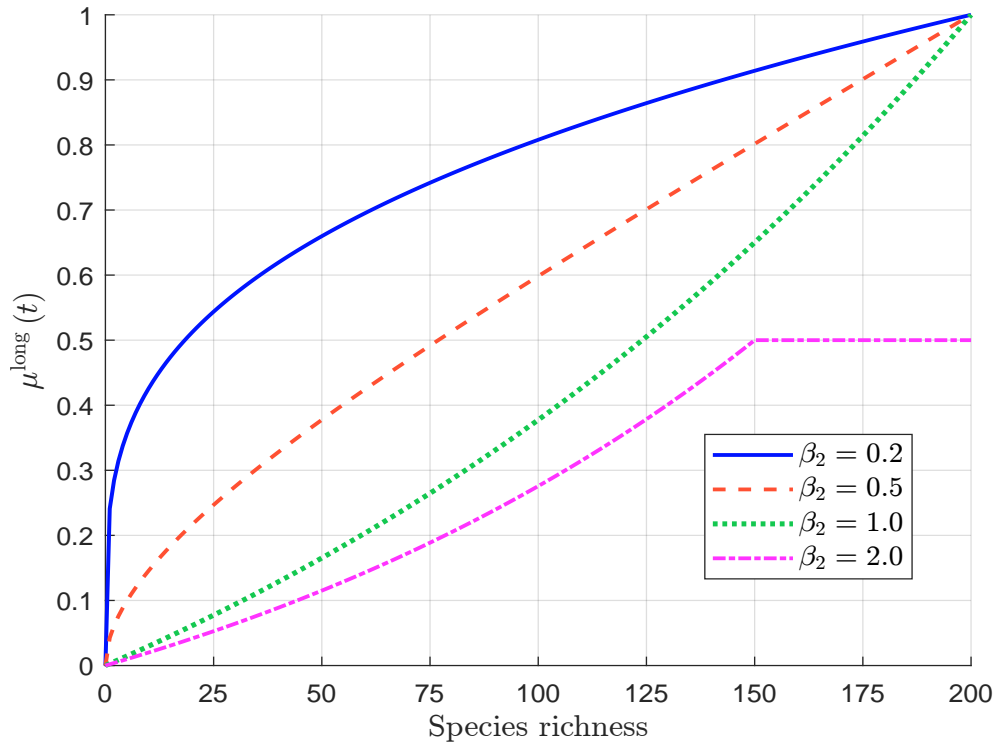
(d) $\mu^{\mathrm{short}}(t)$ is the product of two positive and decreasing functions: $\lambda(t)$ and $\beta_3\lambda(t)e^{-\beta_4 S(t)}$. We deduce that it is decreasing. We also have:

$$\mu^{\mathrm{short}}(t_0) = \beta_3\lambda_0 e^{-\beta_4 S_0} \leq \beta_3\lambda_0$$

and:

$$\mu^{\mathrm{short}}(t_s) = \beta_3\lambda_s e^{-\beta_4 S_s} = 0$$

The function $\mu^{\mathrm{short}}(t)$ is plotted in Figure 89.

(e) We have:

$$\mu(t_0) = \mu^{\mathrm{short}}(t_0) + \mu^{\mathrm{long}}(t_0) = \mu^{\mathrm{short}}(t_0) + 0 = \mu^{\mathrm{short}}(t_0)$$

and:

$$\mu(t_s) = \mu^{\mathrm{short}}(t_s) + \mu^{\mathrm{long}}(t_s) = 0 + \mu_s = \mu_s$$
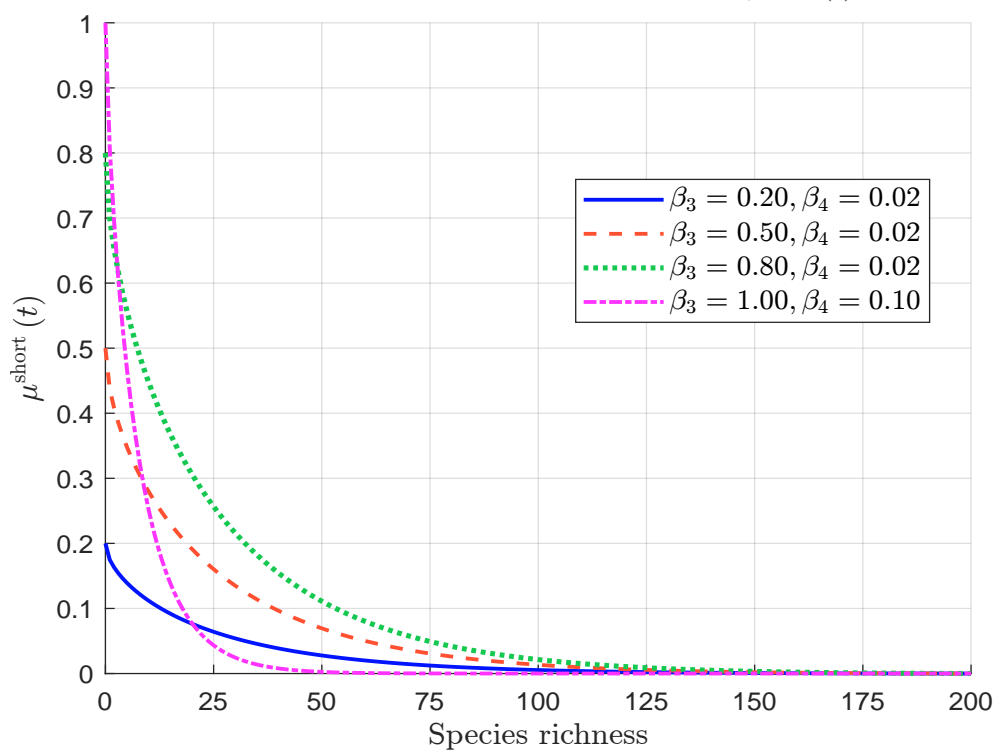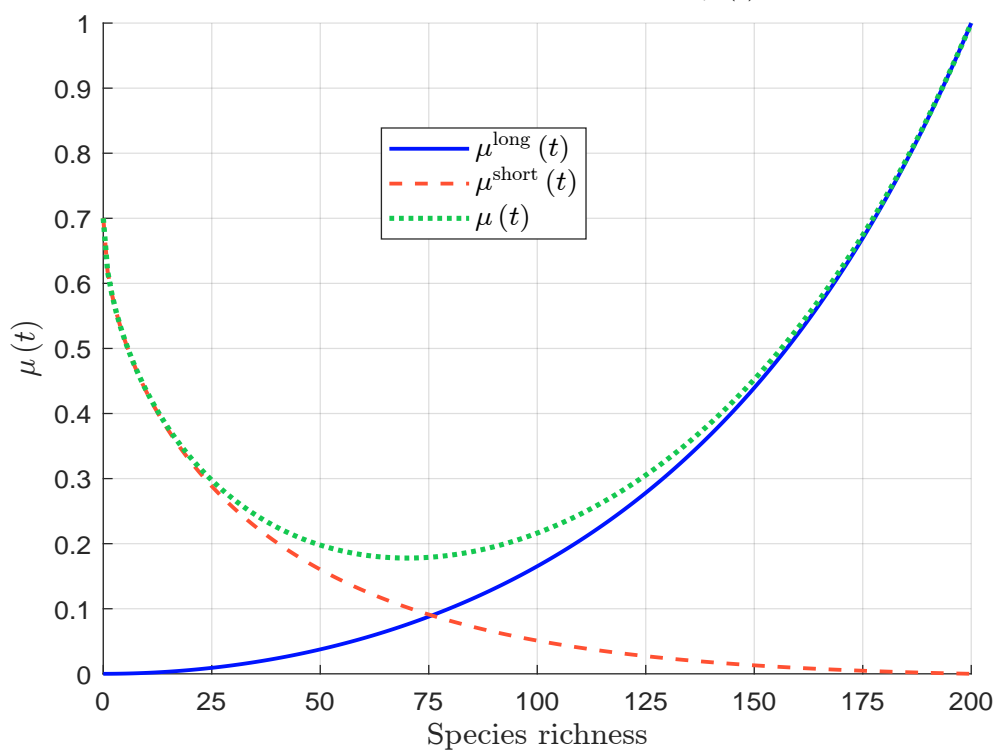
Figure 89: Short-term extinction rate function $\mu^{\text{short}}(t)$

Figure 90: Extinction rate function $\mu(t)$

Figure 90 illustrates the function $\mu(t)$. Since the extinction rate is the sum of two functions, $\mu^{\text{short}}(t)$ which is decreasing, and $\mu^{\text{long}}(t)$ which is increasing, $\mu(t)$ is not monotonic and can exhibit several shapes. However, for reasonable values of the parameters, we observe that $\mu(t)$ first decreases and then increases. This behavior arises because $\mu^{\text{short}}(t_0) > \mu^{\text{long}}(t_0)$ and $\mu^{\text{short}}(t_s) < \mu^{\text{long}}(t_s)$. Consequently, when $S(t)$ is low and close to zero, the short-term extinction rate dominates the long-term extinction rate, leading to a general decrease in $\mu(t)$. In contrast, when $S(t)$ is high and approaches the saturation state S_s, the long-term extinction rate becomes dominant, implying that $\mu(t)$ generally increases for high values of species richness. In summary, the extinction rate $\mu(t)$ has a U-shaped relationship with $S(t)$.

(f) An equilibrium occurs if and only if $\delta(t) = 0$ or $\lambda(t) = \mu(t)$. We deduce that such an equilibrium $S^\star$ is achieved if the following equation has at least one solution:

$$\lambda_0 \frac{e^{-\left(\frac{S^\star}{S_s}\right)^{\beta_1 \lambda_0}} - e^{-1}}{1 - e^{-1}} \left(1 - \beta_3 e^{-\beta_4 S^\star}\right) = \mu_s \frac{e^{\left(\frac{S^\star}{S_s}\right)^{\beta_2 \mu_s}} - 1}{e^1 - 1} \tag{38}$$

Figure 91 shows the functions $\lambda(t)$ and $\mu(t)$. Solving Equation (38) gives $S^\star = 96.472$. This equilibrium is stable, because $\dfrac{\mathrm{d}S(t)}{\mathrm{d}t} < 0$ when $S(t) > S^\star$ and $\dfrac{\mathrm{d}S(t)}{\mathrm{d}t} > 0$ when $S(t) < S^\star$. This implies that any perturbation from $S^\star$ will return to the steady state $S^\star$.

(g) In Table 61, we give the direction of variation of the functions $\lambda(t)$, $\mu^{\text{short}}(t)$, $\mu^{\text{long}}(t)$ and $\mu(t)$. We can then derive the table of variation of the net diversification rate $\delta(t) = \lambda(t) - \mu(t)$. When $\beta_3 = 0$, $\mu^{\text{short}}(t) = 0$ and $\delta(t)$ is a decreasing function with $\delta(t_0) = \delta_0 = \lambda_0 > 0$ and $\delta(t_s) = -\mu_s < 0$. We conclude that there is only one equilibrium. When $0 < \beta_3 \leq 1$, $\delta(t)$ increases up to a threshold S^* and then decreases. We have $\delta_0 = \lambda_0(1 - \beta_3) > 0$ and $\delta(t_s) = -\mu_s < 0$. We obtain the table of variation of the net diversification rate given in Table 62. When $\beta_3 > 1$, $\delta(t)$ has the same behavior as the previous case, but $\delta_0 = \lambda_0(1 - \beta_3) < 0$ and we obtain the table of variation of the net diversification rate given in Table 63. We deduce that there are two equilibria $S_1^\star$ and $S_2^\star$, with $S_1^\star \leq S_2^\star$. The equilibrium $S_1^\star$ is unstable because $\dfrac{\mathrm{d}S(t)}{\mathrm{d}t} < 0$ when $S(t) < S_1^\star$ and $\dfrac{\mathrm{d}S(t)}{\mathrm{d}t} > 0$ when $S(t) > S_1^\star$. Only $S_2^\star$ is a stable steady state. Furthermore, the net diversification rate is negative when $S(t) < S_1^\star$, which means that $S(t + \mathrm{d}t) < S(t)$ and $S(t)$ tends to the equilibrium $S_0^\star = 0$.

(h) The simulations of the species richness process are presented in Figures 93 and 94. In the one-equilibrium case, the process $S(t)$ converges to the equilibrium $S^\star = 96.47$, regardless of the initial state S_0. In the three-equilibrium case, the process $S(t)$ converges to either $S_0^\star = 0$ or $S_2^\star = 97.35$, depending on the initial state S_0. The equilibrium $S_1^\star = 27.65$ is reached only if $S_0 = S_1^\star$. Otherwise, we get the equilibrium $S_0^\star = 0$ if $S_0 < S_1^\star$, and the equilibrium $S_2^\star = 97.35$ if $S_0 > S_1^\star$.

2. (a) We have:

$$\frac{\partial \mu(t)}{\partial \beta_2} = \frac{\mu_s^2}{e^1 - 1} e^{\left(\frac{S(t)}{S_s}\right)^{\beta_2 \mu_s}} \left(\frac{S(t)}{S_s}\right)^{\beta_2 \mu_s} \ln\left(\frac{S(t)}{S_s}\right) \leq 0$$

This means that the relationship $\mu(t)$ shifts downward as β_2 increases. Figure 95 illustrates the equilibrium for the three values of β_2. From this, we deduce that if $\beta_2' \geq \beta_2$, then $S^\star(\beta_2') \geq S^\star(\beta_2)$.

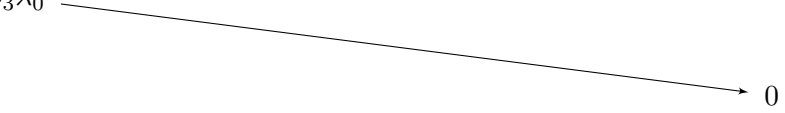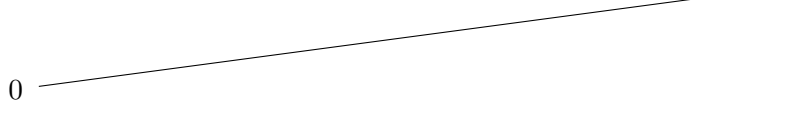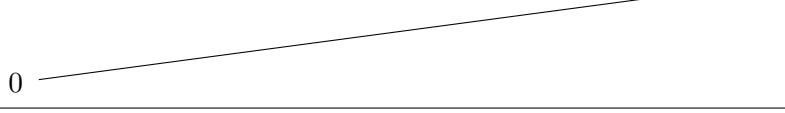Table 61: Table of variation for the immigration and extinction rates
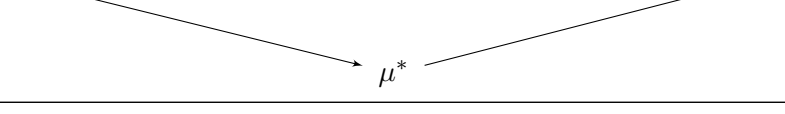
S	0	S^*	S_s
$\lambda(t)$	λ_0 ↘		0
$\mu^{\text{short}}(t)$	$\beta_3\lambda_0$ ↘		0
$\mu^{\text{long}}(t)$	0 ↗		μ_s
$\mu(t)$ $(\beta_3 = 0)$	0 ↗		μ_s
$\mu(t)$ $(\beta_3 > 0)$	$\beta_3\lambda_0$ ↘	μ^* ↗	μ_s

Table 62: Table of variation for the net diversification rate $\delta(t)$

S	0	S^*	$S^\star$	S_s
$\lambda(t) - \mu(t)$ $(0 < \beta_3 \leq 1)$	δ_0 ↗	δ^* ↘	0 ↘	$-\mu_s$
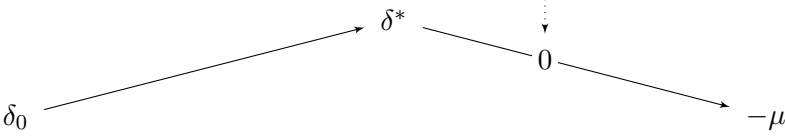
Table 63: Table of variation for the net diversification rate $\delta(t)$

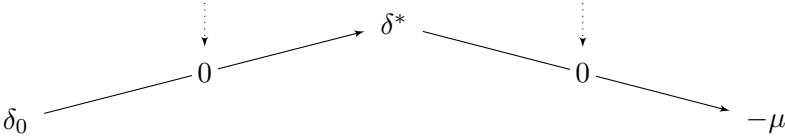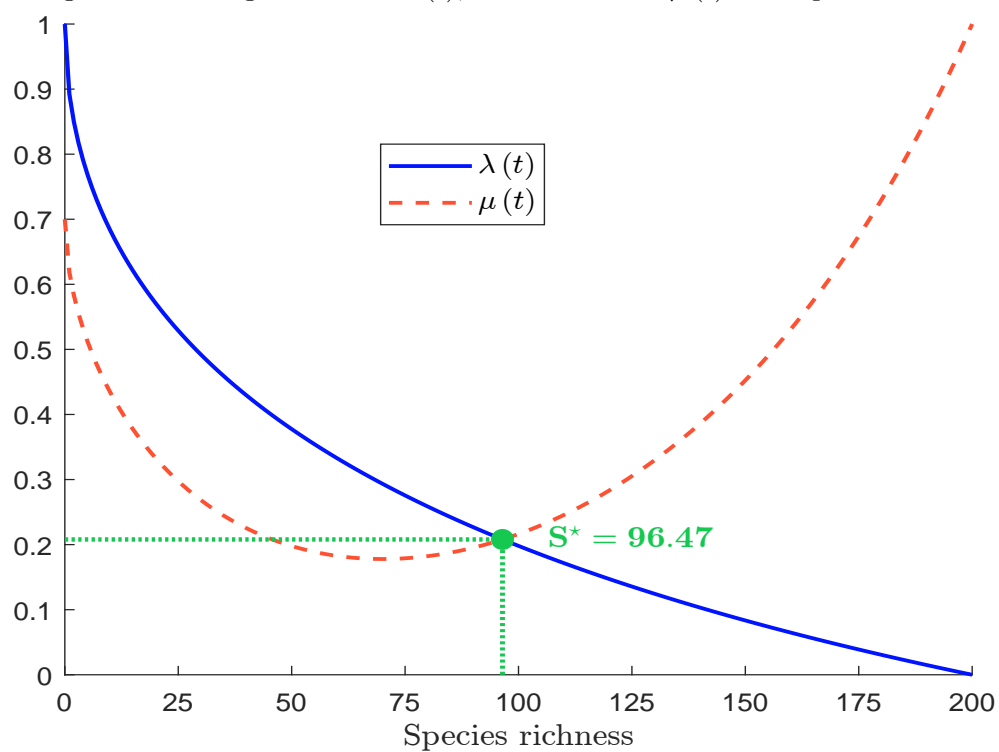| S	0	$S_1^\star$	S^*	$S_2^\star$	S_s
$\lambda(t) - \mu(t)$ $(\beta_3 > 1)$	δ_0 ↗	0 ↗	δ^* ↘	0 ↘	$-\mu_s$

Figure 91: Immigration rate $\lambda(t)$, extinction rate $\mu(t)$ and equilibrium $S^\star$

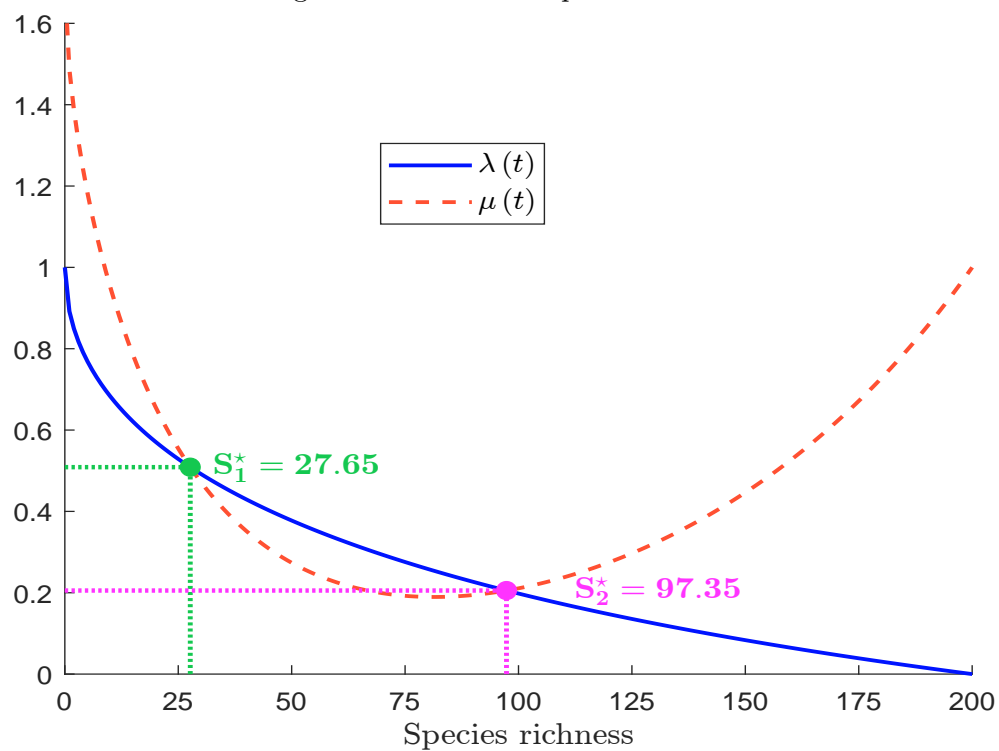Figure 92: The three-equilibrium case

Figure 93: Simulation of the species richness process under a one-equilibrium scenario
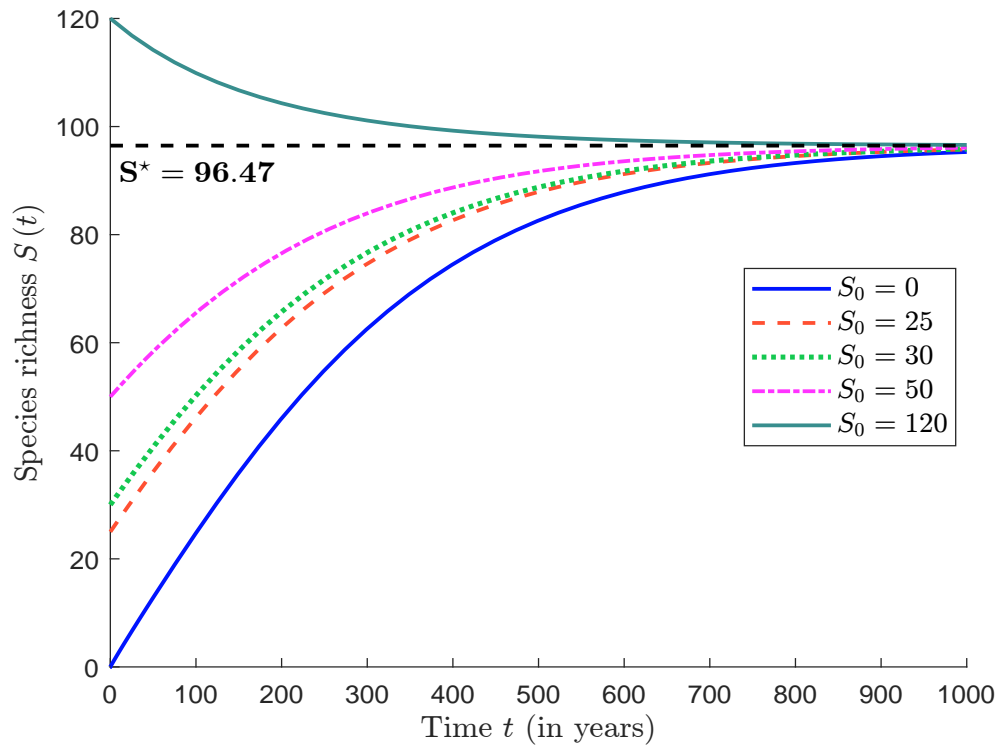

Figure 94: Simulation of the species richness process under a three-equilibrium scenario
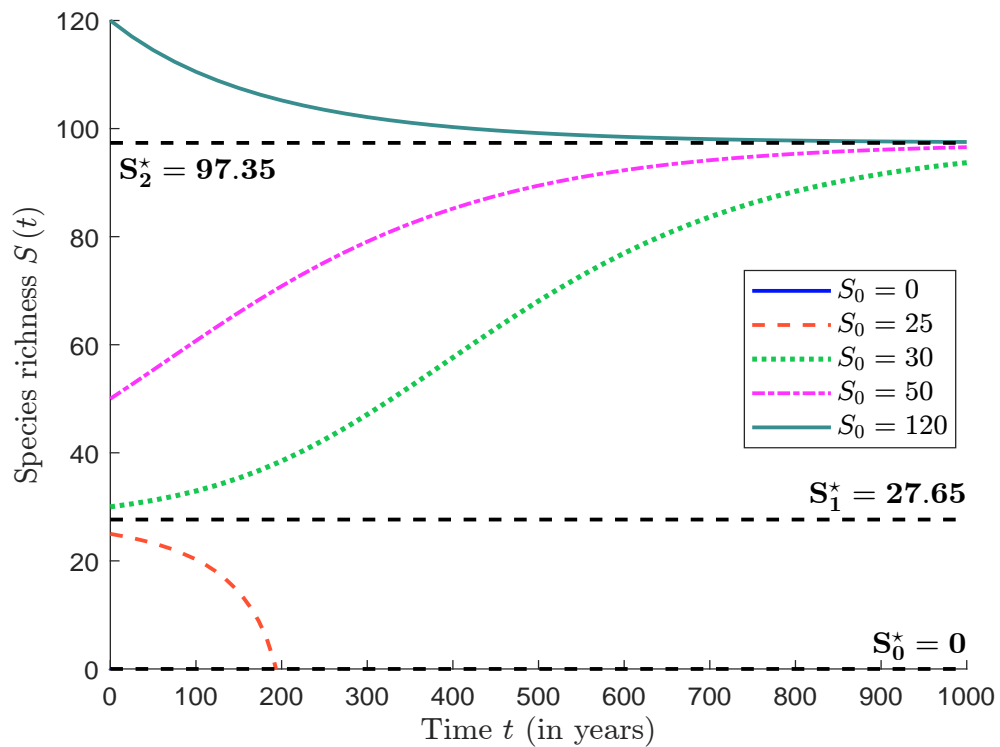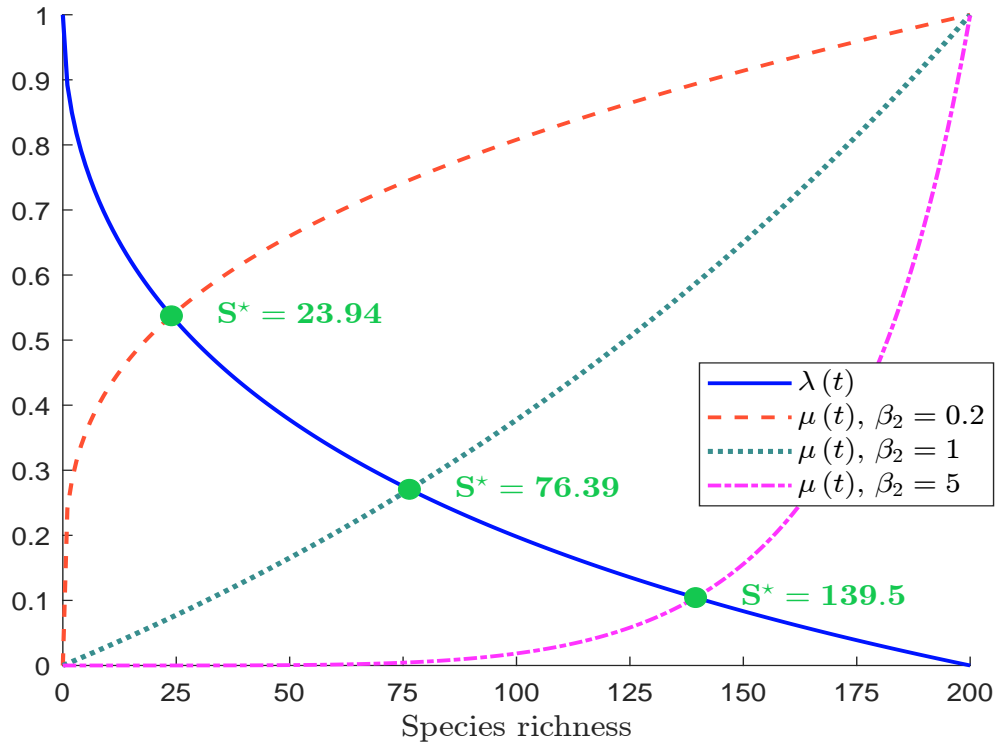
Figure 95: How the equilibrium shifts with the parameter β_2

(b) The relationship between β_2 and $S^\star$ is shown in Figure 96.

(c) We have:

$$\frac{\partial \mu(t)}{\partial \mu_s} = \frac{e^{\left(\frac{S(t)}{S_s}\right)^{\beta_2 \mu_s}} - 1}{e^1 - 1} + \frac{\beta_2 \mu_s}{e^1 - 1} e^{\left(\frac{S(t)}{S_s}\right)^{\beta_2 \mu_s}} \left(\frac{S(t)}{S_s}\right)^{\beta_2 \mu_s} \ln\left(\frac{S(t)}{S_s}\right)$$

Using the default parameter values and $S(t) = 100$, we find that $\partial_{\mu_s}\mu(t) = 0.045$ when $\mu_S = 1$ and $\partial_{\mu_s}\mu(t) = -0.047$ when $\mu_S = 5$. Since the derivative can be either positive or negative, we cannot determine the effect of μ_s on the equilibrium $S^\star$.

(d) The relationship between μ_s and $S^\star$ is shown in Figure 97.

(e) We can assume that the relationship between A and β_2 is increasing. In this case, we obtain the species-area relationship. We can also assume that the relationship between A and μ_s is increasing. In this case, we retrieve the species-area relationship only if μ_s is greater than a threshold.

(f) We obtain the following estimated values for the parameters:

Parameter	Power	Exponential	Kobayashi
c	74.513	82.098	73.539
z	0.562	45.199	1.797

The fitted models are displayed in Figure 98. We observe that the fitted curves closely align with the equilibrium curve predicted by the theory of island biogeography.
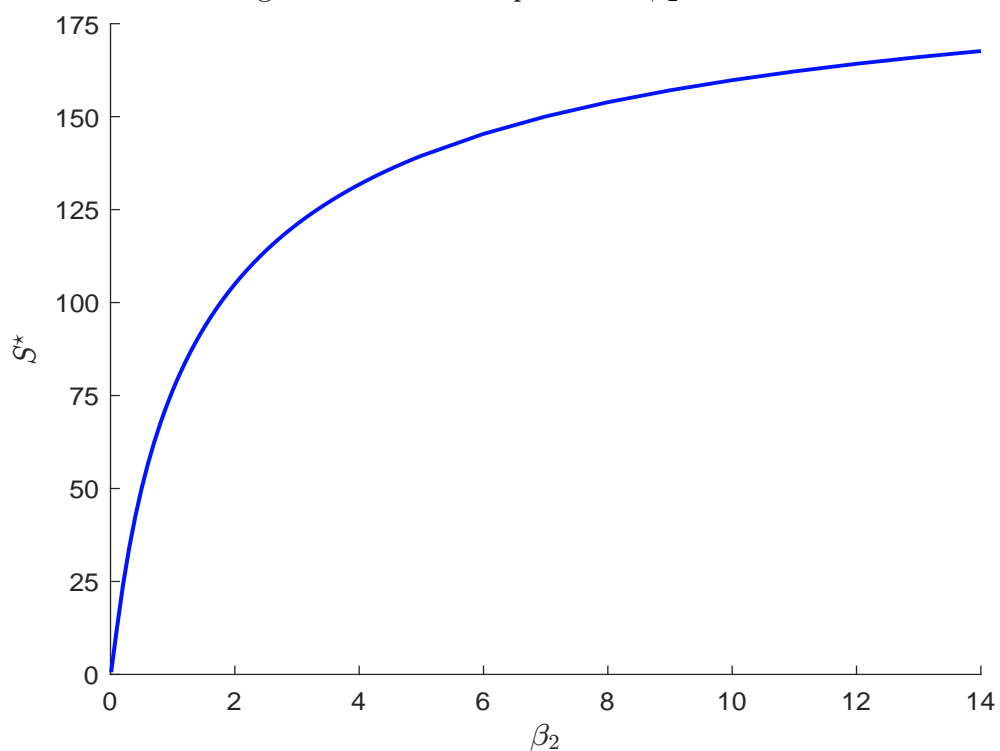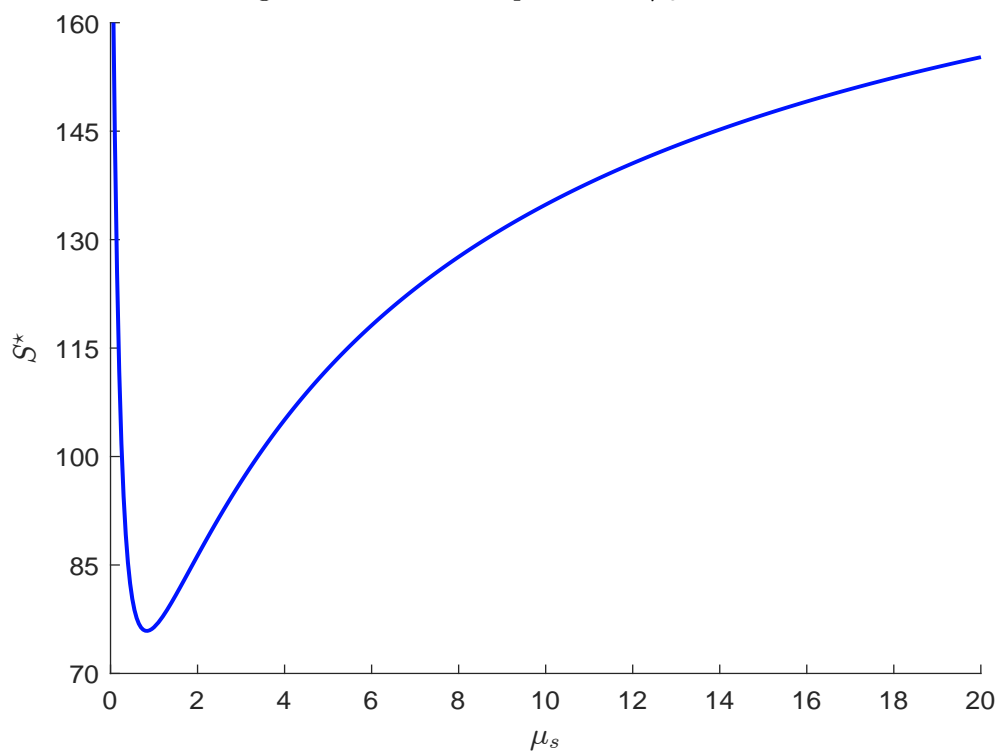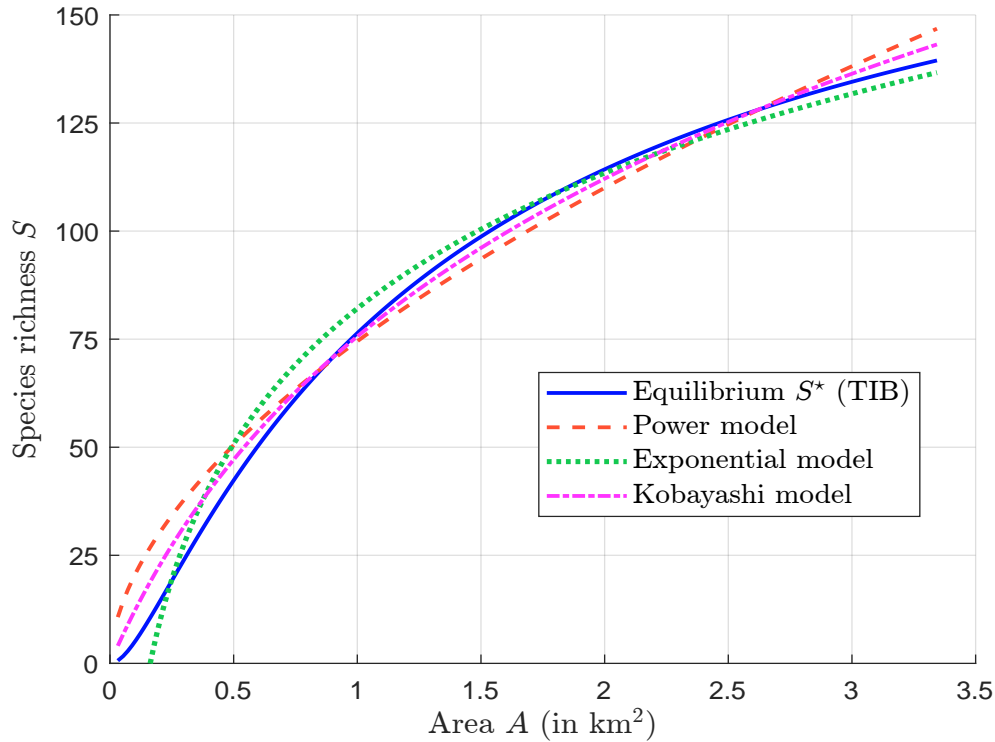
Figure 96: Relationship between β_2 and $S^\star$

Figure 97: Relationship between μ_s and $S^\star$

Figure 98: Species-area relationship (TIB, power, exponential and Kobayashi models)

B.3   Species abundance models

1. (a) We have:

$$\tilde{S}_a = \sum_{i=1}^{S} \tilde{S}_i$$

Assuming that the random variables $\tilde{S}_1, \ldots, \tilde{S}_S$ are independent, $\tilde{S}_a$ follows a Poisson binomial distribution:

$$\tilde{S}_a \sim \mathcal{PB}\left(p_1, \ldots, p_S\right)$$

The probability mass function is given by:

$$\Pr\left\{\tilde{S}_a = k\right\} = \sum_{\mathcal{E} \in \mathcal{F}_k} \prod_{i \in \mathcal{E}} p_i \prod_{j \in \mathcal{E}^c} (1 - p_j)$$

where $\mathcal{F}_k$ is the set of all subsets of k integers that can be selected from $\{1, \ldots, n\}$ and $\mathcal{E}^c$ denotes the complement of the subset $\mathcal{E}$. From this, we deduce the expected value:

$$S_a = \mathbb{E}\left[\tilde{S}_a\right] = \mathbb{E}\left[\sum_{i=1}^{S} \tilde{S}_i\right] = \sum_{i=1}^{S} p_i$$

Given $p = (20\%, 30\%, 10\%, 65\%, 10\%)$, we obtain the following probability mass function for $\tilde{S}_a$:

k	0	1	2	3	4	5
$\Pr\left\{\tilde{S}_a = k\right\}$	15.88%	43.79%	30.85%	8.48%	0.97%	0.04%

The expected number of species is $S_a = 1.35$.

(b) Let π be the probability that an individual occupies the subarea a. We have:

$$\pi = \frac{a}{A}$$

For example, if $A = 10\,\text{km}^2$, the occupancy probability is 20% when $a = 2\,\text{km}^2$. Let $\tilde{N}_i$ be the random variable indicating the number of individuals of species i present in the subarea a. $\tilde{N}_i$ follows a binomial distribution with parameters n_i (the total number of individuals of species i) and π. Thus, we have:

$$\Pr\left\{\tilde{N}_i = k\right\} = C_{n_i}^k \pi^k (1 - \pi)^{n_i - k}$$

The probability p_i of observing the species i on the subarea is then:

$$
\begin{aligned}
p_i = \Pr\left\{\tilde{S}_i = 1\right\} &= \Pr\left\{\tilde{N}_i > 0\right\} \\
&= 1 - \Pr\{N_i = 0\} \\
&= 1 - (1 - \pi)^{n_i} \\
&= 1 - \left(1 - \frac{a}{A}\right)^{n_i}
\end{aligned}
$$

Consequently, $\tilde{S}_a$ follows then a Poisson binomial distribution:

$$\tilde{S}_a \sim \mathcal{PB}\left(p_i = 1 - \left(1 - \frac{a}{A}\right)^{n_i}\right)$$

It follows that:

$$
\begin{aligned}
S_a &= \sum_{i=1}^{S} p_i \\
&= \sum_{i=1}^{S} \left(1 - \left(1 - \frac{a}{A}\right)^{n_i}\right) \\
&= S - \sum_{i=1}^{S} \left(1 - \frac{a}{A}\right)^{n_i}
\end{aligned}
$$

Given $(n_1, \ldots, n_5) = (10, 30, 25, 66, 8)$, $A = 10\,\text{km}^2$, and $a = 2\,\text{km}^2$, $\pi = 20\%$ and we obtain the following results:

k or i	0	1	2	3	4	5
p_i		89.26%	59.04%	99.62%	73.79%	83.22%
$\Pr\left\{\tilde{S}_a = k\right\}$	0.00%	0.21%	3.45%	19.78%	44.32%	32.34%

The expected number of species is $S_a = 4.05$.

(c) i. If the distribution is homogenous across species $(n_i = \frac{n}{S})$, we have:

$$p_i = 1 - \left(1 - \frac{a}{A}\right)^{\frac{n}{S}}$$

$\tilde{S}_a$ follows then a binomial distribution:

$$\tilde{S}_a \sim \mathcal{B}\left(S, p = 1 - \left(1 - \frac{a}{A}\right)^{\frac{n}{S}}\right)$$

The expected number of species is then equal to:

$$S_a = Sp = S\left(1 - \left(1 - \frac{a}{A}\right)^{\frac{n}{S}}\right)$$

ii. If the distribution is the most uneven ($n_i = 1$ for $i < S$ and $n_S = n - S + 1$), we have:

$$
\begin{aligned}
S_a &= S - \sum_{i=1}^{S-1}\left(1 - \frac{a}{A}\right)^{1} - \left(1 - \frac{a}{A}\right)^{n-S+1} \\
&= S - (S-1)\left(1 - \frac{a}{A}\right) - \left(1 - \frac{a}{A}\right)^{n-S+1} \\
&= 1 + (S-1)\frac{a}{A} - \left(1 - \frac{a}{A}\right)^{n-S+1}
\end{aligned}
$$

iii. We have:

$$
\begin{aligned}
S_a &= S - \sum_{i=1}^{s}\left(1 - \frac{a}{A}\right)^{1} - \sum_{i=s+1}^{S}\left(1 - \frac{a}{A}\right)^{n_s+1} \\
&= S - s\left(1 - \frac{a}{A}\right) - (S-s)\left(1 - \frac{a}{A}\right)^{n_s+1} \\
&= s\frac{a}{A} + (S-s)\left(1 - \left(1 - \frac{a}{A}\right)^{n_s+1}\right) \\
&= s\frac{a}{A} + (S-s)\left(1 - \left(1 - \frac{a}{A}\right)^{\frac{n-s}{S-s}}\right)
\end{aligned}
$$

If $s = 0$, we retrieve the most even model:

$$S_a = S\left(1 - \left(1 - \frac{a}{A}\right)^{\frac{n}{S}}\right)$$

If $s = S - 1$, we retrieve the most uneven model:

$$S_a = (S-1)\frac{a}{A} + \left(1 - \left(1 - \frac{a}{A}\right)^{\frac{n-S+1}{S-S+1}}\right) = 1 + (S-1)\frac{a}{A} - \left(1 - \frac{a}{A}\right)^{n-S+1}$$

iv. We have:

$$
\begin{aligned}
S_a &= \sum_{i=1}^{S}\left(1 - \left(1 - \frac{a}{A}\right)\left(1 + \frac{n_i a}{\kappa_i A}\right)^{-\kappa_i}\right) \\
&= S - \left(1 - \frac{a}{A}\right)\sum_{i=1}^{S}\left(1 + \frac{n_i a}{\kappa_i A}\right)^{-\kappa_i}
\end{aligned}
$$

v. We can approximate the harmonic sum by:

$$\sum_{k=i}^{S}\frac{1}{k} \approx \int_{i}^{S}\frac{1}{x}\,\mathrm{d}x = \ln\left(\frac{S}{i}\right)$$

We deduce that:

$$n_i = \frac{n}{S}\sum_{k=i}^{S}\frac{1}{k} \approx \frac{n}{S}\ln\left(\frac{S}{i}\right)$$

Lecture Notes on Biodiversity

We have:

$$\left(1 - \frac{a}{A}\right)^{n_i} = e^{\left(n_i \ln\left(1 - \frac{a}{A}\right)\right)} = \exp\left(\frac{n}{S} \ln\left(\frac{S}{i}\right) \ln\left(1 - \frac{a}{A}\right)\right) = \left(\frac{i}{S}\right)^{-\frac{n}{S} \ln\left(1 - \frac{a}{A}\right)}$$

and:

$$\sum_{i=1}^{S} \left(1 - \frac{a}{A}\right)^{n_i} = \sum_{i=1}^{S} \left(\frac{i}{S}\right)^{-\frac{n}{S} \ln\left(1 - \frac{a}{A}\right)} \approx \int_0^S \left(\frac{x}{S}\right)^{-\frac{n}{S} \ln\left(1 - \frac{a}{A}\right)} \mathrm{d}x$$

Using the change of variable $u = \dfrac{x}{S}$, we obtain:

$$
\begin{aligned}
\int_0^S \left(\frac{x}{S}\right)^{-\frac{n}{S} \ln\left(1 - \frac{a}{A}\right)} \mathrm{d}x &= S \int_0^1 u^{-\frac{n}{S} \ln\left(1 - \frac{a}{A}\right)} \mathrm{d}u \\
&= S \left[\frac{u^{-\frac{n}{S} \ln\left(1 - \frac{a}{A}\right) + 1}}{-\frac{n}{S} \ln\left(1 - \frac{a}{A}\right) + 1}\right]_0^1 \\
&= \frac{S}{-\frac{n}{S} \ln\left(1 - \frac{a}{A}\right) + 1} \\
&= \frac{S^2}{S - n \ln\left(1 - \frac{a}{A}\right)}
\end{aligned}
$$

Since we have:

$$S_a = S - \sum_{i=1}^{S} \left(1 - \frac{a}{A}\right)^{n_i} \approx S - \frac{S^2}{S - n \ln\left(1 - \frac{a}{A}\right)} = \frac{-Sn \ln\left(1 - \frac{a}{A}\right)}{S - n \ln\left(1 - \frac{a}{A}\right)}$$

we conclude that:

$$S_a = \frac{S \ln\left(1 - \dfrac{a}{A}\right)}{\ln\left(1 - \dfrac{a}{A}\right) - \dfrac{S}{n}}$$

(d) We have:

$$S_a = \sum_{i=1}^{S} p_i = \sum_j \sum_{i \in j} p_i = \sum_j s(j) p_j$$

where p_j is the probability that a species with abundance j is present in the subarea a. Since $p_j = 1 - \left(1 - \dfrac{a}{A}\right)^j$, we get:

$$S_a = \sum_j s(j) \left(1 - \left(1 - \frac{a}{A}\right)^j\right) = S - \sum_j s(j) \left(1 - \frac{a}{A}\right)^j$$

where $S = \sum_j s(j)$ is the total number of species. To calculate S_a for the log-series distribution, we use a preliminary result: $\sum_{j=1}^{\infty} x^j / j$ is the series expansion for $-\ln(1 - x)$ when $|x| < 1$. We have:

$$S = \sum_{j=1}^{\infty} s(j) = \alpha \sum_{j=1}^{\infty} \frac{x^j}{j} = -\alpha \ln(1 - x)$$

and:

$$\sum_{j=1}^{\infty} s\,(j)\left(1-\frac{a}{A}\right)^{j} = \alpha \sum_{j=1}^{\infty} \frac{x^{j}}{j}\left(1-\frac{a}{A}\right)^{j} = -\alpha \ln\left(1-x\left(1-\frac{a}{A}\right)\right)$$

We deduce that:

$$
\begin{aligned}
S_a &= -\alpha \ln\left(1-x\right) + \alpha \ln\left(1-x\left(1-\frac{a}{A}\right)\right) \\
&= \alpha \ln\left(\frac{1-x\left(1-\dfrac{a}{A}\right)}{1-x}\right) \\
&= \alpha \ln\left(1+\frac{x}{1-x}\frac{a}{A}\right)
\end{aligned}
$$

2. (a) Species i is locally endemic to subarea $a \subseteq A$ if all the individuals of this species are found in a. Let $E_i \sim \mathcal{B}\,(\breve{p}_i)$ be the Bernoulli random variable that takes the value 1 if species i is locally endemic to a. We have:

$$\breve{p}_i = \Pr\{E_i = 1\} = \prod_{k=1}^{n_i}\left(\frac{a}{A}\right) = \left(\frac{a}{A}\right)^{n_i}$$

(b) The expected number E_a of locally endemic species is equal to:

$$E_a = \mathbb{E}\left[E_1 + E_2 + \ldots + E_S\right] = \sum_{i=1}^{S}\mathbb{E}\left[E_i\right] = \sum_{i=1}^{S}\breve{p}_i = \sum_{i=1}^{S}\left(\frac{a}{A}\right)^{n_i}$$

(c) Since we have $S_a = S - \sum_{i=1}^{S}\left(1-\frac{a}{A}\right)^{n_i}$ and $E_a = \sum_{i=1}^{S}\left(\frac{a}{A}\right)^{n_i}$, we deduce that:

$$S_{A-a} = S - \sum_{i=1}^{S}\left(1-\frac{A-a}{A}\right)^{n_i} = S - \sum_{i=1}^{S}\left(\frac{a}{A}\right)^{n_i}$$

and:

$$E_{A-a} = \sum_{i=1}^{S}\left(\frac{A-a}{A}\right)^{n_i} = \sum_{i=1}^{S}\left(1-\frac{a}{A}\right)^{n_i}$$

It follows that:

$$S_{A-a} + E_a = S - \sum_{i=1}^{S}\left(\frac{a}{A}\right)^{n_i} + \sum_{i=1}^{S}\left(\frac{a}{A}\right)^{n_i} = S$$

(d) We have:

$$T_a = S_a + E_a = S - \sum_{i=1}^{S}\left(1-\frac{a}{A}\right)^{n_i} + \sum_{i=1}^{S}\left(\frac{a}{A}\right)^{n_i}$$

It follows that:

$$
\begin{aligned}
\frac{\partial T_a}{\partial a} &= -\sum_{i=1}^{S}n_i\left(1-\frac{a}{A}\right)^{n_i-1}\left(-\frac{1}{A}\right) + \sum_{i=1}^{S}n_i\left(\frac{a}{A}\right)^{n_i-1}\left(\frac{1}{A}\right) \\
&= \frac{1}{A}\left(\sum_{i=1}^{S}n_i\left(1-\frac{a}{A}\right)^{n_i-1} + \sum_{i=1}^{S}n_i\left(\frac{a}{A}\right)^{n_i-1}\right) \\
&\geq 0
\end{aligned}
$$

This implies that T_a is an increasing function of a. Moreover, we have:

$$T_\emptyset = S_\emptyset + E_\emptyset = S - \sum_{i=1}^{S} \left(1 - \frac{0}{A}\right)^{n_i} + \sum_{i=1}^{S} \left(\frac{0}{A}\right)^{n_i} = S - S + 0 = 0$$

and:

$$T_A = S_A + E_A = S - \sum_{i=1}^{S} \left(1 - \frac{A}{A}\right)^{n_i} + \sum_{i=1}^{S} \left(\frac{A}{A}\right)^{n_i} = S - 0 + S = 2S$$

We deduce that:

$$0 \le S_a + E_a \le 2S$$

B.4   Valuation of risks to life and health

1. Using Bayes theorem, we have:

$$\mathbf{S}(u \mid t) = \Pr\{\tau > u \mid \tau > t\} = \frac{\Pr\{\tau > u, \tau > t\}}{\Pr\{\tau > t\}} = \frac{\Pr\{\tau > u, t\}}{\Pr\{\tau > t\}} = \frac{\mathbf{S}(u)}{\mathbf{S}(t)}$$

2. Since $\mathrm{d}\mathbf{S}(t) = \partial \mathbf{S}(t)\, \mathrm{d}t = -f(t)\, \mathrm{d}t$, we can express the expected survival time as:

$$\mathbb{E}[\tau] = \int_0^\infty t f(t)\, \mathrm{d}t = -\int_0^\infty t\, \mathrm{d}\mathbf{S}(t)$$

Using integration by parts, we get:

$$\mathbb{E}[\tau] = -\left[t\mathbf{S}(t)\right]_0^\infty + \int_0^\infty \mathbf{S}(t)\, \mathrm{d}t = 0 + \int_0^\infty \mathbf{S}(t)\, \mathrm{d}t = \int_0^\infty \mathbf{S}(t)\, \mathrm{d}t$$

We deduce the conditional life expectancy for an individual alive at time t:

$$\mathrm{LE}(t) = \mathbb{E}[\tau \mid \tau > t] = \frac{\mathbb{E}[\mathbb{1}\{\tau > t\} \cdot \tau]}{\Pr\{\tau > t\}} = \frac{\int_t^\infty \mathbf{S}(u)\, \mathrm{d}u}{\mathbf{S}(t)} = \int_t^\infty \mathbf{S}(u \mid t)\, \mathrm{d}u$$

3. The expected present value of a payoff, taking into account the future lifetime, is given by:

$$\mathbb{E}[X; t, \varrho] = \int_t^\infty e^{-\varrho(u-t)} \mathbf{S}(u \mid t)\, X(u)\, \mathrm{d}u = \mathbb{E}[\delta(u) X(u)] \tag{39}$$

where $\delta(u) = B(t, u)\, \mathbf{S}(u \mid t)$ is the discount factor under uncertain lifetime and $B(t, u) = e^{-\varrho(u-t)}$ is the standard discount factor at time u. Therefore, we have:

$$\delta(u) = e^{-\varrho(u-t)} \Pr\{\tau > u \mid \tau > t\}$$

Equation (39) is the classical formula for the present value when the discount rate accounts for uncertainty about the individual's lifetime.

4. $\mathrm{DLE}(t; \varrho)$ is the mathematical expectation of the discounted survival time, given that the survival time exceeds t:

$$\mathrm{DLE}(t; \varrho) = \mathbb{E}\left[e^{-\varrho t}\tau \mid \tau > t\right]$$

Using integration by parts with $u = e^{-\varrho t}t$ and $v' = f(t)$, we can express the discounted life expectancy at $t = 0$ as:

$$
\begin{aligned}
\text{DLE}(0; \varrho) &= \int_0^\infty e^{-\varrho t}t f(t) \, \mathrm{d}t \\
&= \left[-e^{-\varrho t}t\mathbf{S}(t)\right]_0^\infty + \int_0^\infty \left(-\varrho e^{-\varrho t}t + e^{-\varrho t}\right)\mathbf{S}(t) \, \mathrm{d}t \\
&= \int_0^\infty e^{-\varrho t}\mathbf{S}(t) \, \mathrm{d}t - \varrho \int_0^\infty e^{-\varrho t}t\mathbf{S}(t) \, \mathrm{d}t
\end{aligned}
$$

because $u' = -\varrho e^{-\varrho t}t + e^{-\varrho t}$ and $v = -\mathbf{S}(t)$. We deduce that:

$$
\text{DLE}(0; \varrho) = \text{LE}(0; \varrho) - \underbrace{\varrho \int_0^\infty e^{-\varrho t}t\mathbf{S}(t) \, \mathrm{d}t}_{\geq 0}
$$

and:

$$
\text{LE}(0; \varrho) \geq \text{DLE}(0; \varrho) = \int_0^\infty e^{-\varrho t}t f(t) \, \mathrm{d}t
$$

The generalization to the case $t \neq 0$ is straightforward. Using the change of variable $x = u - t$, we obtain $\text{DLE}(t; \varrho) = \text{LE}(t; \varrho) - \varrho \int_0^\infty e^{-\varrho x}x\mathbf{S}(t + x) \, \mathrm{d}x$. Equality is achieved if and only if $\varrho = 0$.

5. Since $\mathbf{S}(t) = e^{-\lambda t}$, we have:

$$
\begin{aligned}
\text{LE}(t; \varrho) &= \frac{1}{e^{-\lambda t}} \int_t^\infty e^{-\varrho(u-t)}e^{-\lambda u} \, \mathrm{d}u \\
&= \int_t^\infty e^{-(\varrho+\lambda)(u-t)} \, \mathrm{d}u \\
&= \left[\frac{e^{-(\varrho+\lambda)(u-t)}}{(\varrho + \lambda)}\right]_t^\infty \\
&= \frac{1}{\varrho + \lambda}
\end{aligned}
$$

and:

$$
\begin{aligned}
\text{DLE}(t; \varrho) &= \int_t^\infty e^{-\varrho(u-t)}(u - t)f(u \mid t) \, \mathrm{d}u \\
&= \int_t^\infty e^{-\varrho(u-t)}(u - t)\lambda e^{-\lambda(u-t)} \, \mathrm{d}u \\
&= \int_0^\infty \lambda e^{-(\varrho+\lambda)s}s \, \mathrm{d}s \\
&= \left[-\lambda s\frac{e^{-(\varrho+\lambda)s}}{(\varrho + \lambda)}\right]_0^\infty + \lambda \int_0^\infty \frac{e^{-(\varrho+\lambda)s}}{(\varrho + \lambda)} \, \mathrm{d}s \\
&= \lambda\left[-\frac{e^{-(\varrho+\lambda)s}}{(\varrho + \lambda)^2}\right]_0^\infty \\
&= \frac{\lambda}{(\varrho + \lambda)^2}
\end{aligned}
$$

We verify that:

$$\mathrm{LE}\,(t;\varrho) = \left(1 + \frac{\varrho}{\lambda}\right)\mathrm{DLE}\,(t;\varrho) \geq \mathrm{DLE}\,(t;\varrho)$$

Moreover, we note that $\mathrm{LE}\,(t;\varrho)$ does not depend on time t because exponential survival times satisfy the property of lack of memory.

6. (a) In the case of exponential survival time, we have:

$$\mathbb{E}\,[\tau] = \frac{1}{\lambda}$$

It follows that:

$$\lambda = \frac{1}{\mathbb{E}\,[\tau]} = \frac{1}{70} = 0.01429$$

For the Weibull distribution, we have:

$$\mathbb{E}\,[\tau] = a\Gamma\left(1 + \frac{1}{b}\right)$$

We deduce that:

$$a = \frac{\mathbb{E}\,[\tau]}{\Gamma\left(1 + \dfrac{1}{b}\right)} = \frac{70}{\Gamma\left(1 + \dfrac{1}{5}\right)} = 76.23871$$

The survival functions $\mathbf{S}\,(t)$ and $\mathbf{S}\,(u \mid t = 50)$ are shown in Figure 99. It is evident that the exponential distribution is not suitable for modeling human lifetimes, as the probability of dying before reaching 50 years of age is approximately 50%. In contrast, the Weibull distribution provides a more realistic model for human lifetime.

(b) We have:

$$\mathrm{LE}\,(0;3\%) = \frac{1}{\varrho + \lambda} = \frac{1}{3\% + 1.43\%} = 22.58\,\text{years}$$

and:

$$\mathrm{DLE}\,(0;3\%) = \frac{\lambda}{(\varrho + \lambda)^2} = \frac{1.43\%}{(3\% + 1.43\%)^2} = 7.28\,\text{years}$$

The function $\mathrm{DLE}\,(t;\varrho)$ discounts lifetime too rapidly and is not a suitable approach for calculating present values while accounting for future lifetime.

(c) Figure 100 shows the results. We observe that $\mathrm{LE}\,(t;\varrho)$ is a decreasing function with respect to both time t and the discount rate ϱ. Using a standard discount rate of 3%, a life expectancy of 70 years corresponds to a discounted life expectancy of approximately 30 years at birth and 20 years at age 40.

7. (a) We have:

$$\begin{aligned}
\mathrm{QALE}\,(t;\varrho) &= \frac{1}{\mathbf{S}\,(t)} \int_t^\infty e^{-\varrho(u-t)}\mathbf{S}\,(u)\,Q\,(t)\,\mathrm{d}u \\
&= \left(\frac{1}{\mathbf{S}\,(t)} \int_t^\infty e^{-\varrho(u-t)}\mathbf{S}\,(u)\,\mathrm{d}u\right) \cdot Q\,(t) \\
&= \mathrm{LE}\,(t;\varrho) \cdot Q\,(t)
\end{aligned}$$

The quality-adjusted life expectancy is the product of the discounted life expectancy and the average quality of life weight.

Figure 99: Survival function $\mathbf{S}\left(u \mid t\right)$
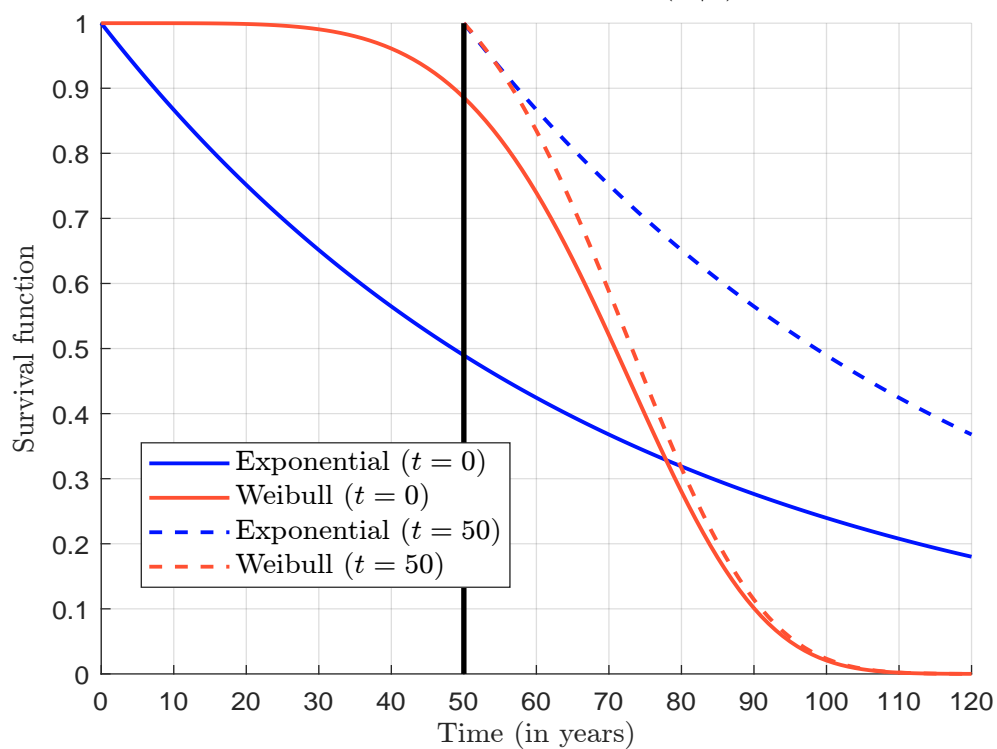
Figure 100: Discounted lifetime expectancy $\mathrm{LE}\left(t;\varrho\right)$
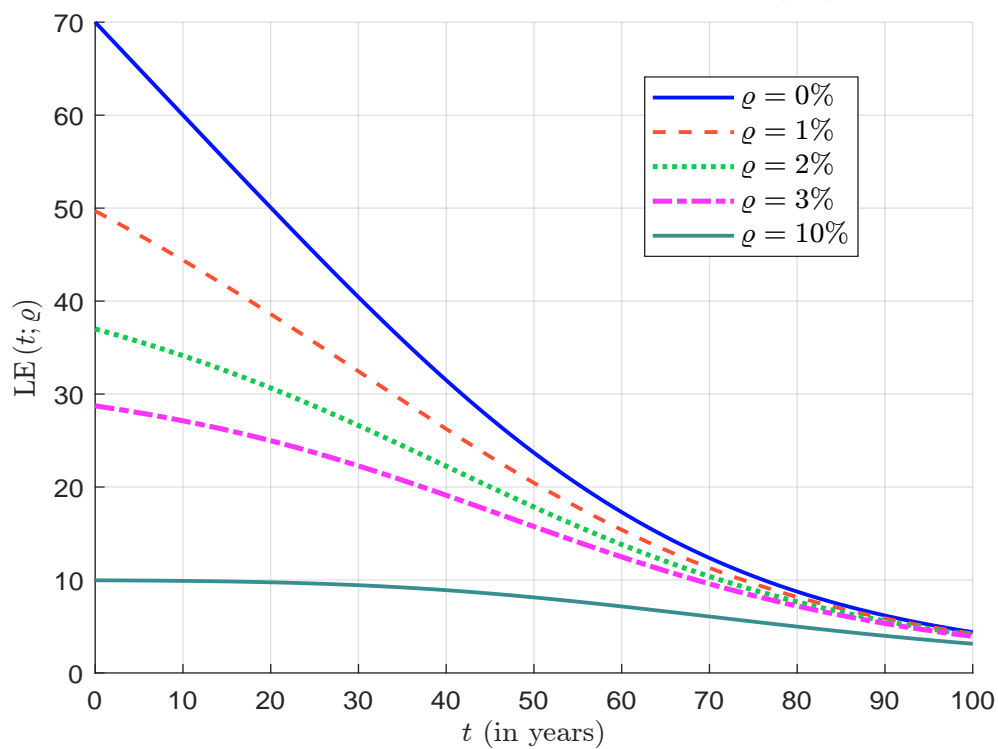
(b) Since $Q(t) \leq 1$, we deduce that:

$$0 \leq e^{-\varrho(u-t)} \frac{\mathbf{S}(u)}{\mathbf{S}(t)} Q(u) \leq e^{-\varrho(u-t)} \frac{\mathbf{S}(u)}{\mathbf{S}(t)}$$

and:

$$\int_t^\infty e^{-\varrho(u-t)} \frac{\mathbf{S}(u)}{\mathbf{S}(t)} Q(u) \, \mathrm{d}u \leq \int_t^\infty e^{-\varrho(u-t)} \frac{\mathbf{S}(u)}{\mathbf{S}(t)} \, \mathrm{d}u$$

We conclude that $\mathrm{QALE}(t; \varrho) \leq \mathrm{LE}(t; \varrho)$.

(c) $Q_1(t)$ is a piecewise linear function representing three phases of life. Before t_1, the quality of life is equal to 1. Between t_1 and t_2, the quality of life decreases linearly, reaching $1 - \kappa_1$ at $t = t_2$. The rate of decrease per year in this phase is $\kappa_1 / (t_2 - t_1)$. In the third phase, between t_2 and t_3, the quality of life continues to decline linearly at a rate of $\kappa_2 / (t_3 - t_2)$. Figure 101 shows the functions $\mathrm{LE}(t; \varrho)$, $\mathrm{QALE}_1(t; \varrho)$ calculated with $Q_1(t)$, and $\mathrm{QALE}_2(t; \varrho)$ calculated with $Q_2(t)$. The difference between $\mathrm{LE}(t; \varrho)$ and $\mathrm{QALE}_1(t; \varrho)$ is small, especially when $t \leq t_1$. It is more pronounced for large values of t because quality of life is strongly affected when people are old. In contrast, $\mathrm{QALE}_2(t; \varrho)$ is much lower than $\mathrm{LE}(t; \varrho)$, because the quality of life decreases exponentially 2% per year.

Figure 101: Discounted lifetime expectancy $\mathrm{LE}(t; \varrho)$
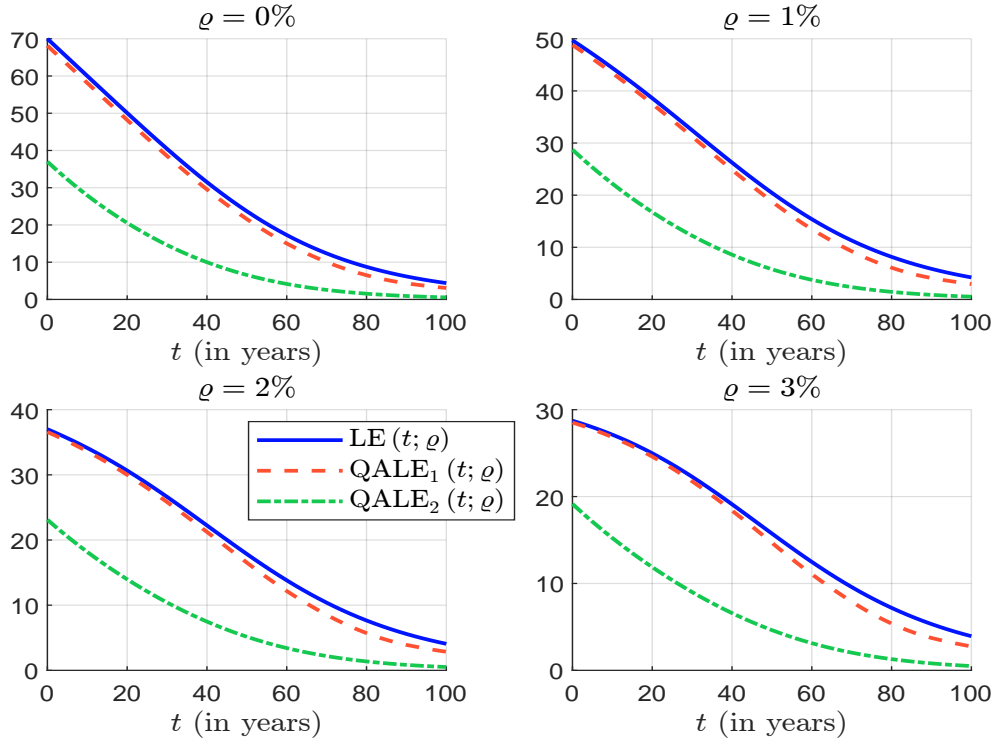
8. (a) We have:

$$\mathrm{VSL}(t) = \frac{v}{\Delta L(t)} = \frac{v}{\mathcal{R}(t) \cdot \Delta t}$$

We deduce that:

$$\mathrm{VSLY}(t) = \frac{\mathrm{VSL}(t) \cdot \Delta L}{\Delta \mathrm{LE}(t)} = \frac{\mathrm{VSL}(t)}{\mathrm{LE}(t; \varrho)}$$

and:
$$\text{VQALY}(t) = \frac{\text{VSL}(t) \cdot \Delta L}{\Delta \text{QALE}(t)} = \frac{\text{VSL}(t)}{\text{QALE}(t; \varrho)}$$

(b) Since $\Delta L(t) = \mathcal{R}(t) = \mathcal{I}(t)$ because $\Delta t = 1$ year, the associated payoff is:
$$X(t) = \text{VSL}(t) \cdot \mathcal{R}(t) = \text{VSL}(t) \cdot \Delta L(t)$$

It follows that:
$$X(t) = \text{VSLY}(t) \cdot \Delta \text{LE}(t) = \text{VQALY}(t) \cdot \Delta \text{QALE}(t)$$

(c) If $\text{VSL}(t)$ and $\mathcal{I}(t)$ are constant, we get:
$$
\begin{aligned}
\mathcal{G}(t; \varrho) &= \text{VSL} \cdot \left(\frac{1}{\mathbf{S}(t)} \int_t^\infty e^{-\varrho(u-t)} \mathbf{S}(u) \, \mathrm{d}u \right) \cdot \mathcal{I}(t) \\
&= \text{VSL} \cdot \text{LE}(t; \varrho) \cdot \Delta L
\end{aligned}
\tag{40}
$$

The economic gain is the value of a statistical life multiplied by the discounted life expectancy and the expected number of lives saved.

(d) In the case of air pollution, $\mathcal{I}(t)$ is negative and the economic cost becomes:
$$\mathcal{C}(t; \varrho) = -\mathcal{G}(t; \varrho) = \text{VSL} \cdot \text{LE}(t; \varrho) \cdot \Delta L$$

where ΔL is the expected number of deaths due to air pollution. If we compare with the formula:
$$\mathcal{C} = \text{VSLY} \cdot \text{YLL}$$

we can deduce that the years of life lost (YLL) is equal to:
$$\text{YLL} = \Delta L \cdot \text{LE}(t; \varrho)$$

In this model, years of life lost is the product of the expected number of deaths and the discounted life expectancy. The traditional formula is:
$$\text{YLL} = \Delta L \cdot \Delta \tau$$

where $\Delta \tau$ is the difference between life expectancy without air pollution and life expectancy with air pollution. Therefore, we assume that:
$$\Delta \tau = \text{LE}(t; \varrho) = \frac{1}{\mathbf{S}(t)} \int_t^\infty e^{-\varrho(u-t)} \mathbf{S}(u) \, \mathrm{d}u$$

This means that we take the discount rate into account when calculating years of life lost.

(e) Results are reported in Table 64. By construction, the life expectancy of an individual at age 0 is 70 years. Using a discount rate of 3%, the discounted life expectancy is 28.73 years. At age 40, the remaining life expectancy is 31.49 years, so the average lifetime of an individual alive at age 40 is 71.49 years. This corresponds to a discounted life expectancy of 19.11 years. At age 80, the remaining life expectancy is 8.74 years, so the average lifetime of an individual alive at age 80 is 88.74 years. The impact of the quality-of-life weight is shown in the second row. The estimated value of a statistical life is calculated as:
$$\text{VSL}(t) = \frac{\$1\,000}{1/10\,000} = \$10\,\text{mn}$$

Table 64: Calculation of the economic gain $\mathcal{G}\left(t;\varrho\right)$

Discount rate	$\varrho = 0\%$			$\varrho = 3\%$			Unit
Age	Birth	40 years	80 years	0	40 years	80 years	
LE $(t;\varrho)$	70.00	31.49	8.74	28.73	19.11	7.19	years
QALE $(t;\varrho)$	68.13	29.54	6.50	28.52	18.39	5.38	
VSL (t)	10 000						
VSLY (t)	143	318	1 144	348	523	1 390	$1 000
VQALY (t)	147	339	1 538	351	544	1 858	
VSL (t)	10 500	4 723	1 312	4 310	2 867	1 079	
VSLY (t)	150						$ 1000
VQALY (t)	154	160	202	151	156	200	
$\mathcal{G}\left(t;\varrho\right)$	36 750	7 437	573	6 191	2 740	388	$

We can then compute the value of a statistical life year. Assuming an age of 40 years and a discount rate of 3%, we obtain:

$$\text{VSLY}\left(40\right) = \frac{\text{VSL}\left(40\right)}{\text{LE}\left(40;3\%\right)} = \frac{\$10\,\text{mn}}{19.11} = \$523\,206$$

and:

$$\text{VQALY}\left(40\right) = \frac{\text{VSL}\left(40\right)}{\text{QALE}\left(40;3\%\right)} = \frac{\$10\,\text{mn}}{18.39} = \$543\,817$$

The assumption that VSL (t) is constant is not realistic. For instance, the value per statistical life year for a newborn is $142\,857$, while for an 80-year-old individual it is $1\,390\,448$. On the other hand, the assumption that VSLY (t) is constant is more realistic, even if it does not fully match reality. In fact, we can expect VSLY $(40) \geq$ VSLY (0) and VSLY $(40) \geq$ VSLY (80). Finally, we calculate the economic gain using Equation (40). For example, assuming an age of 40 years and a discount rate of 3%, the economic gain is:

$$\mathcal{G}\left(40;3\%\right) = \$2\,866\,938 \times 19.11 \times \frac{5}{100\,000} = \$2\,740$$

We observe that the economic gain is greater for newborns than for older individuals.